

Gulf of Mexico Circulation Modeling Study

Annual Progress Report: Years 3 and 4

Gulf of Mexico Circulation Modeling Study

Annual Progress Report: Years 3 and 4

Author

Alan J. Wallcraft
JAYCOR

Prepared under MMS Contract
~~14-12-0001-30073~~
by
JAYCOR
1608 Spring Hill Road
Vienna, VA 22182-2270

Published by

U.S. Department of the Interior
Minerals Management Service
Gulf of Mexico OCS Region

**New Orleans
March 1991**

DISCLAIMER

This report was prepared under contract between the Minerals Management Service (MMS) and Geo-Marine, Inc. This report has been technically reviewed by the MMS and approved for publication. Approval does not signify that contents necessarily reflect the views and policies of the Service, nor does the mention of trade names or commercial products constitute endorsement or recommendation for use. It is, however, exempt from review and compliance with MMS editorial standards.

REPORT AVAILABILITY

Preparation of this report was conducted under contract between the MMS and Geo-Marine, Inc. Extra copies of this report may be obtained from the Public Information Unit (Mail Stop MS 5034) at the following address:

U.S. Department of the Interior
Minerals Management Service
Gulf of Mexico **OCS** Regional Office
1201 **Elmwood** Park Boulevard
New Orleans, LA 70123-2394

Attention: Public Information Unit (MS 5034)
(Telephone Number: 504-736-2519)
(FTS Number: 686-2519)

CITATION

Wallcraft, A.J., Gulf of Mexico Circulation Modeling Study, Annual Progress Report: Years 3 and 4, Prepared by JAYCOR, OCS Study MMS 90-0008, **U.S.** Department of the Interior, Minerals Management Service, New Orleans, LA, **pp.214**, 1990.

ABSTRACT

This is the final report of a four-year numerical ocean circulation modeling program for the Gulf of Mexico. The aim of the program was to progressively upgrade an existing model of the Gulf of Mexico to provide the most realistic long-term simulation possible of Gulf circulation. The **NOARL/JAYCOR** multi-layer hydrodynamic and thermodynamic primitive equation circulation models of the Gulf of Mexico on a 0.2 degree and a 0.1 degree grid were used in the program. They were forced by constant inflow through the Yucatan Straits compensated by outflow through the Florida Straits, and by wind stresses from the Navy Corrected Geostrophic Wind data set for the Gulf of Mexico. The most **realistic** simulation produced by the program was a blending of **one-layer** and two-layer experiments, augmented by a perturbation analysis to extract surface currents from the vertically averaged ocean model velocities. Actual wind stresses from 1967 to 1982 were used to force the simulation, but the resulting currents are intended to be representative of Gulf circulation rather than a **hindcast** of the actual state of the Gulf over this time period. Wind stress, surface current, and geostrophic surface current fields from this simulation, sampled every three days for 10 years, have been delivered to MMS. Current fields at 100,300,750, and 1,600 meter depths, sampled every six days for the same 10-year period, have also been delivered. As have detailed vertical current profiles at the locations of 16 moored buoys used in Years 1 through 5 of **MMS's** recently concluded **Gulf** of Mexico Physical Oceanography Program.

TABLE OF CONTENTS

<u>SECTION</u>	<hr/>	<u>PAGE</u>
	Disclaimer.....	iii
	Abstract.....	iv
	Table of Contents.....	v
	List of Figures.....	vi
	Table of Model Notation.....	xi
I	INTRODUCTION	1
II	SUMMARY OF YEARS 1 AND 2	2
III	YEAR 3.....	15
IV	YEAR 4.....	27
V	CONCLUSIONS.....	82
VI	REFERENCES.....	212
	REPORT DOCUMENTATION PAGE.....	213

LIST OF FIGURES

FIGURE		PAGE
1	a. Instantaneous view of the interface deviation in a two-layer simulation of the Gulf of Mexico driven from rest to statistical equilibrium solely by inflow through the Yucatan Straits (Experiment 9). b. Depth of the 22 degree isothermal surface, 4-18 August 1966 (Alarninos cruise 66-A-11), from Leipper (1970).....	3
2	Instantaneous view of upper-layer averaged velocities from Experiment 68 on model Day 3918	5
3	Instantaneous view of upper-layer averaged velocities from Experiment 68 on model Day 4038	6
4	Instantaneous view of upper-layer averaged velocities from Experiment 68 on model Day 4158	7
5	Instantaneous view of upper-layer averaged velocities from Experiment 68 on model Day 4218	8
6	Instantaneous view of upper-layer averaged velocities from Experiment 201/16.0 on model Days (a) 2880 and (b) 2970	9
7	Instantaneous view of upper-layer averaged velocities from Experiment 201/16.0 on model Days (a) 3060 and (b) 3150	10
8	Instantaneous view of upper-layer averaged velocities from Experiment 201/16.0 on model Days (a) 3240 and (b) 3330	11
9	Instantaneous view of upper-layer averaged velocities from Experiment 201/16.0 on model Days (a) 3420 and (b) 2510	12
10	Instantaneous view of upper-layer averaged velocities from Experiment 201/16.0 on model Days (a) 3600 and (b) 3690	13
11	Kinetic energy spectra at 40 m depth for (solid) Experiment 201/13.0 at Location Z and (dashed) Mooring F	14
12	Layer depths for a two-dimensional two-layer hydrodynamic model with full-scale bottom topography that uses Flux Corrected Transport to allow the layer interface to 'intersect' the topography.....	17
13	Layer depths on (a) Day 0 and (b) Day 3 for a two-dimensional two-layer hydrodynamic simulation that uses Flux Corrected Transport to allow the layer interface to 'intersect' the topography.....	18
14	Layer depths on (a) Day 6 and (b) Day 12 for a two-dimensional two-layer hydrodynamic simulation that uses Flux Corrected Transport to allow the layer interface to 'intersect' the topography.....	19
15	Sea surface temperature and the corresponding calculated upper-layer density for January from a monthly climatology based on historical ship observation data	24

LIST OF FIGURES (CONT'D.)

<u>FIGURE</u>		<u>PAGE</u>
16	Instantaneous (a) free surface deviation and (b) upper-layer density from a thermodynamic model of the Gulf with no wind forcing..	25
17	Instantaneous (a) free surface deviation and (b) upper-layer density from the same simulation as Figure 16..	26
18	Instantaneous view of the (a) free surface deviation and (b) upper-layer density deviation from Experiment 212/83.1 on wind Day 093/1971	32
19	Instantaneous view of the (a) free surface deviation and (b) upper-layer density deviation from Experiment 212/83.1 on wind Day 183/1971	33
20	Instantaneous view of the (a) free surface deviation and (b) upper-layer density deviation from Experiment 212/83.1 on wind Day 273/1971	34
21	Instantaneous view of the (a) free surface deviation and (b) upper-layer density deviation from Experiment 212/83.1 on wind Day 004/1972. ...	35
22	Instantaneous view of the (a) free surface deviation and (b) upper-layer density deviation from Experiment 212/83.1 on wind Day 094/1972	36
23	Instantaneous view of the (a) free surface deviation and (b) upper-layer density deviation from Experiment 212/83.1 on wind Day 184/1972	37
24	Instantaneous view of the (a) free surface deviation and (b) upper-layer density deviation from Experiment 212/83.1 on wind Day 274/1972	38
25	Instantaneous view of the (a) free surface deviation and (b) upper-layer density deviation from Experiment 212/83.1 on wind Day 004/1973. ...	39
26	Instantaneous view of the free surface deviation from Experiment 212/83.1 on wind Days (a) 005/1974 and (b) 095/1974	40
27	Instantaneous view of the free surface deviation from Experiment 212/83.1 on wind Days (a) 185/1974 and (b) 275/1974	41
28	Annual climatology from 10 years of Experiment 212/83.1 (a) interface deviation and (b) upper-layer density deviation.....	43
29	Monthly climatology for January from 10 years of Experiment 212/83.1 (a) interface deviation and (b) upper-layer density deviation..	44
30	Monthly climatology for April from 10 years of Experiment 212/83.1 (a) interface deviation and (b) upper-layer density deviation..	45
31	Monthly climatology for July from 10 years of Experiment 212/83.1 (a) interface deviation and (b) upper-layer density deviation..	46
32	Monthly climatology for October from 10 years of Experiment 212/83.1 (a) interface deviation and (b) upper-layer density deviation..	47

LIST OF FIGURES (CONT'D.)

<u>FIGURE</u>		<u>PAGE</u>
33	Upper-layer current vectors and bottom topography contours for the Texas shelf on wind Day 001/1969 for (a) one-layer Experiment 2121/80.0 and (b) two-layer Experiment 212/83.1.	48
34	Merged current vectors and bottom topography contours for the Texas shelf on wind Day 001/1969 for (a) "geostrophic" surface currents and (b) surface currents	49
35	Merged current vectors and bottom topography contours for the Texas shelf on wind Day 091/1969 for (a) "geostrophic" surface currents and (b) surface currents	51
36	Merged current vectors and bottom topography contours for the Texas shelf on wind Day 181/1969 for (a) "geostrophic" surface currents and (b) surface currents	52
37	Merged current vectors and bottom topography contours for the Texas shelf on wind Day 271/1969 for (a) "geostrophic" surface currents and (b) surface currents.....	53
38	Merged current vectors and bottom topography contours for the Texas shelf on wind Day 002/1970 for (a) "geostrophic" surface currents and (b) surface currents	54
39	Merged current vectors and bottom topography contours for the Texas shelf on wind Day 092/1970 for (a) "geostrophic" surface currents and (b) surface currents	55
40	Merged current vectors and bottom topography contours for the Texas shelf on wind Day 001/1969 for (a) surface currents and (b) surface currents using the 3.5% rule..	56
41	(a) Wind Stresses and (b) local wind induced currents for the Texas shelf on wind Day 001/1969..	57
42	(a) Wind Stresses and (b) local wind induced currents from the 3.5% rule for the Texas shelf on wind Day 001/1969	58
43	Merged current vectors and bottom topography contours for the Texas shelf on wind Day 091/1969 for (a) surface currents and (b) surface currents using the 3.5% rule	59
44	(a) Wind Stresses and (b) local wind induced currents for the Texas shelf on wind Day 091/1969..	60
45	(a) Wind Stresses and (b) local wind induced currents from the 3.5% rule for the Texas shelf on wind Day 091/1969	61
46	Upper-layer current vectors and bottom topography contours for the Florida shelf on wind Day 001/1969 for (a) ane-layer Experiment 213/80.0 and (b) two-layer Experiment 212/83.1..	62

LIST OF FIGURES (CONT'D.)

FIGURE		PAGE
47	Merged current vectors and bottom topography contours for the Florida shelf on wind Day 001/1969 for (a) "geostrophic" surface currents and (b) surface currents	63
48	Merged current vectors and bottom topography contours for the Florida shelf on wind Day 091/1969 for (a) "geostrophic" surface currents and (b) surface currents	64
49	Merged current vectors and bottom topography contours for the Florida shelf on wind Day 181/1969 for (a) "geostrophic" surface currents and (b) surface currents	65
50	Merged current vectors and bottom topography contours for the Florida shelf on wind Day 271/1969 for (a) "geostrophic" surface currents and (b) surface currents	66
51	Merged current vectors and bottom topography contours for the Florida shelf on wind Day 003/1970 for (a) "geostrophic" surface currents and (b) surface currents	67
52	Merged current vectors and bottom topography contours for the Florida shelf on wind Day 093/1970 for (a) "geostrophic" surface currents and (b) surface currents	68
53	Annual surface current climatology (a) from the 10-year merged simulation and (b) from historical observations..	69
54	Annual surface current climatology (a) from the 10-year merged simulation and (b) "geostrophic" climatology from the merged simulation... ..	71
55	Winter surface current climatology (a) from the 10-year merged simulation and (b) from historical observations	72
56	Spring surface current climatology (a) from the 10-year merged simulation and (b) from historical observations..	73
57	Summer surface current climatology (a) from the 10-year merged simulation and (b) from historical observations..	74
58	Fall surface current climatology (a) from the 10-year merged simulation and (b) from historical observations	75
59	On wind Day 001/1969 (a) surface current from the merged simulation and (b) surface current anomaly vs the winter climatology.....	76
60	On wind Day 091/1969 (a) surface current from the merged simulation and (b) surface current anomaly vs the spring climatology.....	77
61	On wind Day 181/1969 (a) surface current from the merged simulation and (b) surface current anomaly vs the summer.	78

LIST OF FIGURES (CONT'D.)

FIGURE		PAGE
62	On wind Day 271/1969 (a) surface current from the merged simulation and (b) surface current anomaly vs the fall climatology	79
63	Map of the Gulf of Mexico showing the locations of current meter arrays from the Gulf of Mexico Physical Oceanography Program.	80
64	Velocity component spectra for 10 years from the simulation at location MOF (a) u component and (b) v component..	81
65	Velocity component spectra for 362 days from the observations at location MOD (a) u component at 60 m and (b) v component at 60 m.....	83
66	Velocity component spectra for one year from the simulation at location MOD (a) u component and (b) v component..	84
67	Velocity component spectra for 1,090 days from the observations at location MOE (a) u component at 100 m and (b) v component at 100 m.	85
68	Velocity component spectra for 10 years from the simulation at location MOE (a) u component and (b) v component	86
69	Velocity component spectra for 10 years from the simulation at location MOA (a) u component and (b) v component..	87
70	Velocity component spectra for 10 years from the simulation at location MOC (a) u component and (b) v component..	88
71	Velocity component spectra for 10 years from the simulation at location MF (a) u component and (b) v component	89
72	Velocity component spectra for 10 years from the simulation at location MGG (a) u component and (b) v component	90
73-193	Surface currents from the merged simulation, every three days for a full Loop Current eddy cycle. The wind day for each figure is given by the "DATE" in the top right-hand corner of each plot..	91

TABLE OF MODEL NOTATION

L1	Results from a one-layer model. Currents are vertically averaged over the layer depth, i.e., are barotropic. The currents over the continental shelf can be taken as "geostrophic" surface currents.
L2	Results from a two-layer model. Currents in each layer are vertically averaged over the layer depth. The upper-layer currents can be taken as "geostrophic" surface currents.
L2+L1	Merged L1 and L2 results using L1 in shallow water and L2 in deep water. Currents are still vertically averaged over layer depths. The upper-layer currents can be taken as "geostrophic" surface currents.
L2+L1+P	L2+L1 with the addition of a perturbation analysis that converts the layer averaged currents into a full vertical profile. The actual surface currents and the currents at fixed depths can be obtained.
L2+L1+3.5%	L2+L1 with MMS's "3.5%" of wind speed rule. An alternative to L2+L1+P , but for surface currents only.
P only	(L2+L1+P) - (L2+L1) at the surface.
3.5% only	(L2+L1+3.5%) - (L2+L1) at the surface.
FCT2D	A two-dimensional (x-z) version of the layered model that used the technique of "Flux Corrected Transports" to allow layer interfaces to effectively intersect the bottom topography.
FCT3D	A three-dimensional version of FCT2D . This model was never completed.
N	Climatological currents from historical ship drift data.

I. INTRODUCTION

This report gives details of the third and fourth years of a four-year numerical ocean circulation modeling program for the Gulf of Mexico. The aim of the program was to progressively upgrade, in modest increments, an existing numerical ocean circulation model of the Gulf so that the final model has a horizontal resolution of about 10 km and a vertical resolution approaching 1-10 m in the mixed layer, 10 m at the thermocline, and 100 m in the deep water. Throughout the four-year period, the validity of the upgraded model was continuously tested and velocity field time series were delivered periodically based on the most realistic simulation of Gulf circulation available.

Experiments in the first year were with the existing Naval Oceanographic and Atmospheric Research Laboratory* and JAYCOR (**NOARL/JAYCOR**) two-layer hydrodynamic primitive equation ocean circulation model of the Gulf on a 0.2 degree grid. They concentrated on correctly specifying the coastline and bottom topography for maximum realism in circulation simulation and on how best to include wind forcing.

Experiments in the second year were also with the existing **NOARL/JAYCOR** hydrodynamic model, but most were on a 0.1 degree, rather than 0.2 degree grid. **Wind-forced-only**, **port-forced-only**, and **wind-plus-port-forced** simulations were generated. The major limitation of layered models is that bathymetry is **confined** to the lowest layer, so multilayer models are not generally realistic in shallow water. Detailed comparisons between the model results and observations on the Florida Shelf demonstrated that this limitation was severe enough to **warrant** a change of approach.

An attempt was made in the third year to modify the layered model to allow bathymetry to be in any layer, and hence, more realistically represent shelf regions. A two-dimensional prototype was successfully demonstrated, but the three-dimensional version was not functional by the end of the third year.

Rather **than** continue the development of this new model design, the Year 4 effort concentrated on producing the best possible surface currents with the existing thermodynamic model. This involved running a one-layer version of the model to obtain realistic results over the shelf and blending them with two-layer model results that were more realistic in deep water. A

* **NOARL** was previously known as the **Naval Ocean Research and Development Activity (NORDA)**.

perturbation analysis technique was then used to obtain vertical profiles from the blended layer averaged fields.

Simulated surface currents sampled every three days for more than 10 years were delivered to MMS from the blended and perturbed fields, which represents the best simulation available from the entire four-year effort. Corresponding currents at selected **fixed** depths sampled every six days were also delivered, as were detailed vertical profiles of currents sampled every three days at 16 locations where MMS has collected current meter time series in the Gulf.

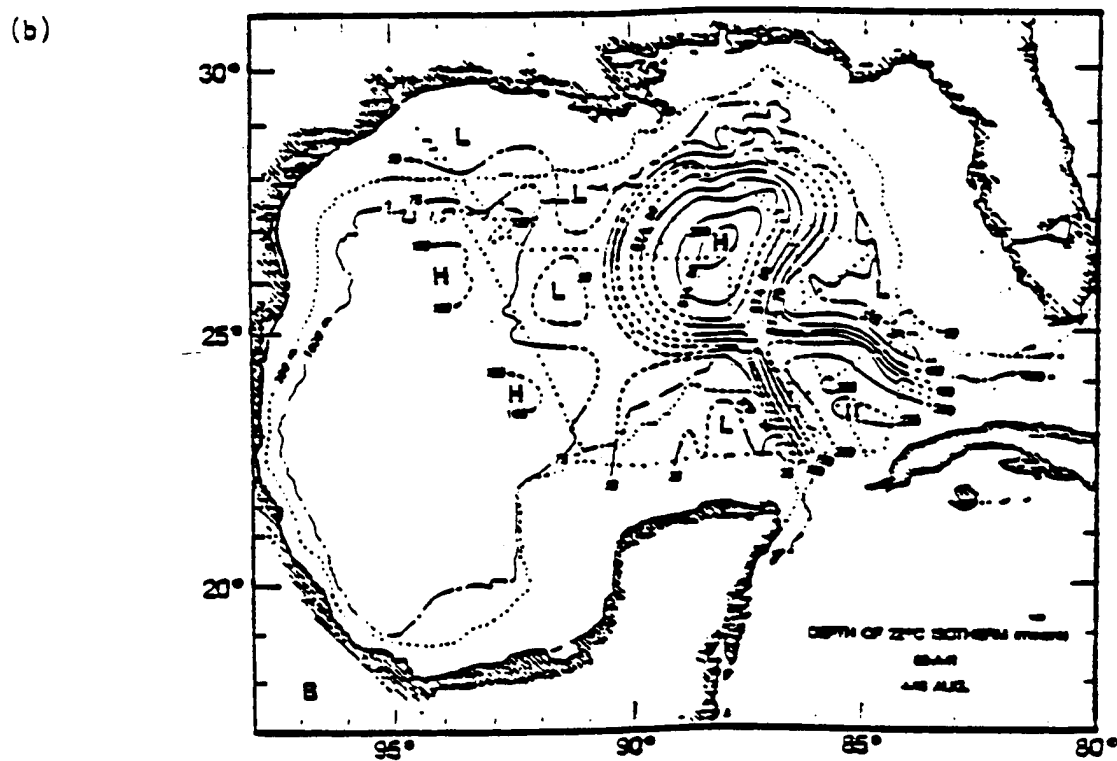
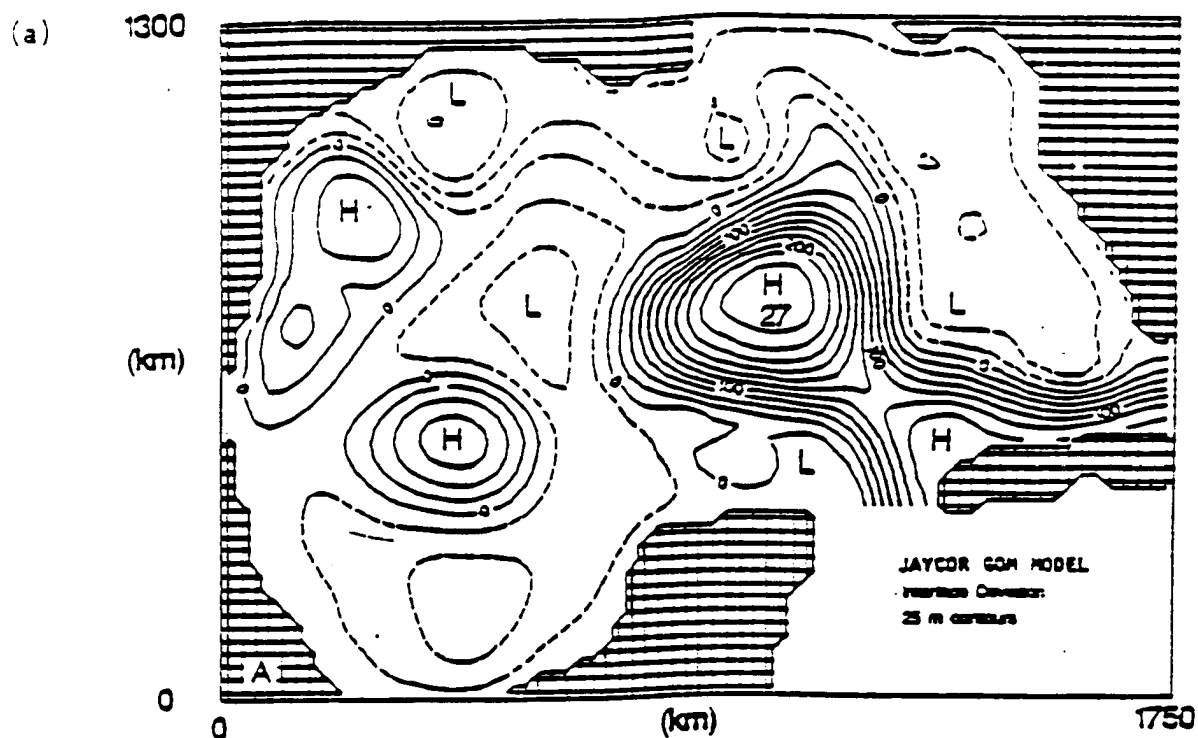
II. SUMMARY OF YEARS 1 AND 2

The hydrodynamic ocean model, used for Years 1 and 2, contained many innovative features and the reader is referred to its detailed discussion in Hurlburt and Thompson (1980). In particular, Section 2 (pp.1613-1614) gives the model equations and Appendix B (pp.1647-1650) describes the numerical design of the model. Since 1980, the code has been completely rewritten by JAYCOR and the capability to handle general basin geometry had been added, but this does not affect the description in any major way. Wind forcing is treated identically to interfacial and bottom stress terms, *i.e.*, wind stress appears directly as an additive term in the momentum equation [p. 1614 of Hurlburt and Thompson (1980)].

In terms of 'realism' Experiment 9 (Wallcraft, 1984) was the most successful Gulf of Mexico numerical simulation prior to the start of this project. The model was driven from rest to statistical equilibrium solely by a steady inflow through the Yucatan Straits that was compensated by outflow through the Florida Straits. Figure 1 compares 'instantaneous' upper-ocean flow patterns just before an eddy is shed by the Loop current (a) from the numerical model and (b) from observations by Leipper (1970). The ability of the model to simulate observed features is clearly demonstrated by this comparison, which is remarkable given the simplicity of the model forcing. However some discrepancies remain; for example, the eddy has not penetrated as far into the Gulf and is more intense than that shown in the observations. Waves can be seen moving around the wall of the Loop in the observations, but in the model they are at the limit of resolution and therefore unrealistically large. Moreover in the Gulf the waves are more pronounced on the eastern wall of the Loop and can form strong cold intrusions that may contribute to the eddy-shedding process (Vukovitch and Maul, 1984).

Experiment 68 (Wallcraft, 1984) is the most realistic simulation produced in Year 1. It has two layers on a 0.2 degree grid and is forced by transport through the Yucatan Strait and by winds

Figure 1. (a) Instantaneous view of the interface deviation in a two-layer simulation of the Gulf of Mexico driven from rest to statistical equilibrium solely by inflow through the Yucatan Straits (Experiment 9). The contour interval is 25 m with solid contours representing downward deviations. (b) Depth of the 22-degree isothermal surface, 4-18 August 1966 (Alaminos cruise 66-A-11), from Leipper (1970). The contour interval is 25 m.



from the Navy Corrected Geostrophic Wind data set for the Gulf of Mexico, which is based on the Navy's 12-hour surface pressure analysis from 1967-1982 (Rhodes et al., 1986). Figures 2-5 show upper-layer currents (*i.e.*, vertically averaged currents above the thermocline) every 60-120 days for 300 days. Vectors are only drawn at every second point (*i.e.*, every 0.4 degrees) to improve readability. Figure 2 shows the furthest northward penetration of the Loop Current ever attained by the ocean model, which is often seen in the Gulf. After the eddy breaks off, the Loop Current intrudes onto the Florida Shelf and some of the flow splits off to the north for a brief time (Figure 3). Similar intrusions have been observed in the Gulf, but the model's inadequate representation of shelf topography makes it likely that the simulated currents in shallow areas (less than 100 m) are too energetic. A persistent anticyclonic gyre in the northwest Gulf has been a feature of almost all Gulf simulations performed to date. The addition of wind forcing in Experiment 68 has increased its average size and its effect on incoming Loop Current eddies (Figure 4). The presence of a gyre in this position is explainable by the northward migration of anticyclonic eddies along the coast of Mexico until the continental slope bends eastward and they can go no further, which magnifies the effect because the winds also tend to produce an anticyclonic gyre at the same spot. However, in the Gulf the gyre probably dissipates relatively rapidly against the shallow shelf area.

Simulations in Year 2 (Wallcraft, 1986) were on a 0.1, rather than 0.2 degree grid. Experiment 201116.0 is the most realistic of these and it is forced by winds and Yucatan transports very similar to those used in Experiment 68. Figures 6-10 show upper-layer currents every 90 days for two Loop Current eddy shedding cycles with winds from 1968 and 1969. When compared with similar simulations without wind forcing, this simulation has higher maximum currents and significantly more variability; for example, in Loop Current eddy shedding cycle times. However, the anticyclonic gyre off the Texas coast is generally larger, as is expected from the wind stress curl patterns.

The major limitation of layered models is that bathymetry is confined to the lowest layer, so multilayer models, in general, are not realistic in shallow water. In order to quantify how well the ocean model was performing in shelf areas, three years of hydrographic data obtained at fixed moorings on the Florida Shelf (as part of a 1986 MMS-sponsored Gulf of Mexico Physical Oceanography Study done by SAIC) was compared to 1,080 days of simulated current meter data at approximately the same 1/13.0. In all cases the currents were significantly **stronger** in the simulation than in the observations. Figure 11 shows a comparison of observed and simulated

Figure 2. Instantaneous view of upper-layer averaged velocities from Experiment 68 on model Day 3918. Vectors are only plotted at every second model grid point, i.e., every 0.4 degrees.

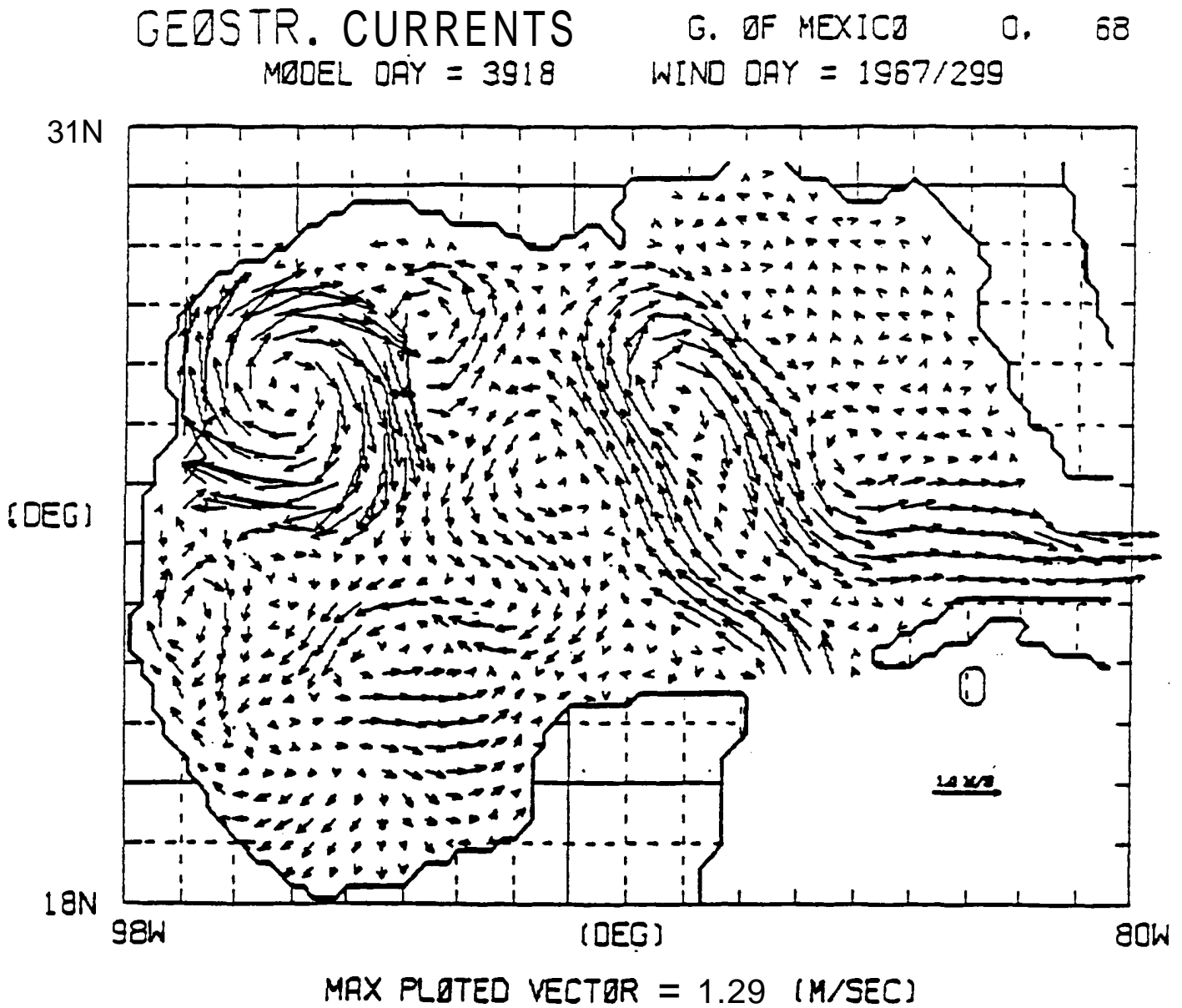


Figure 4. Instantaneous view of upper-layer averaged velocities from Experiment 68 on model Day 4158. Vectors are only plotted at every second model grid point, i.e., every 0.4 degrees.

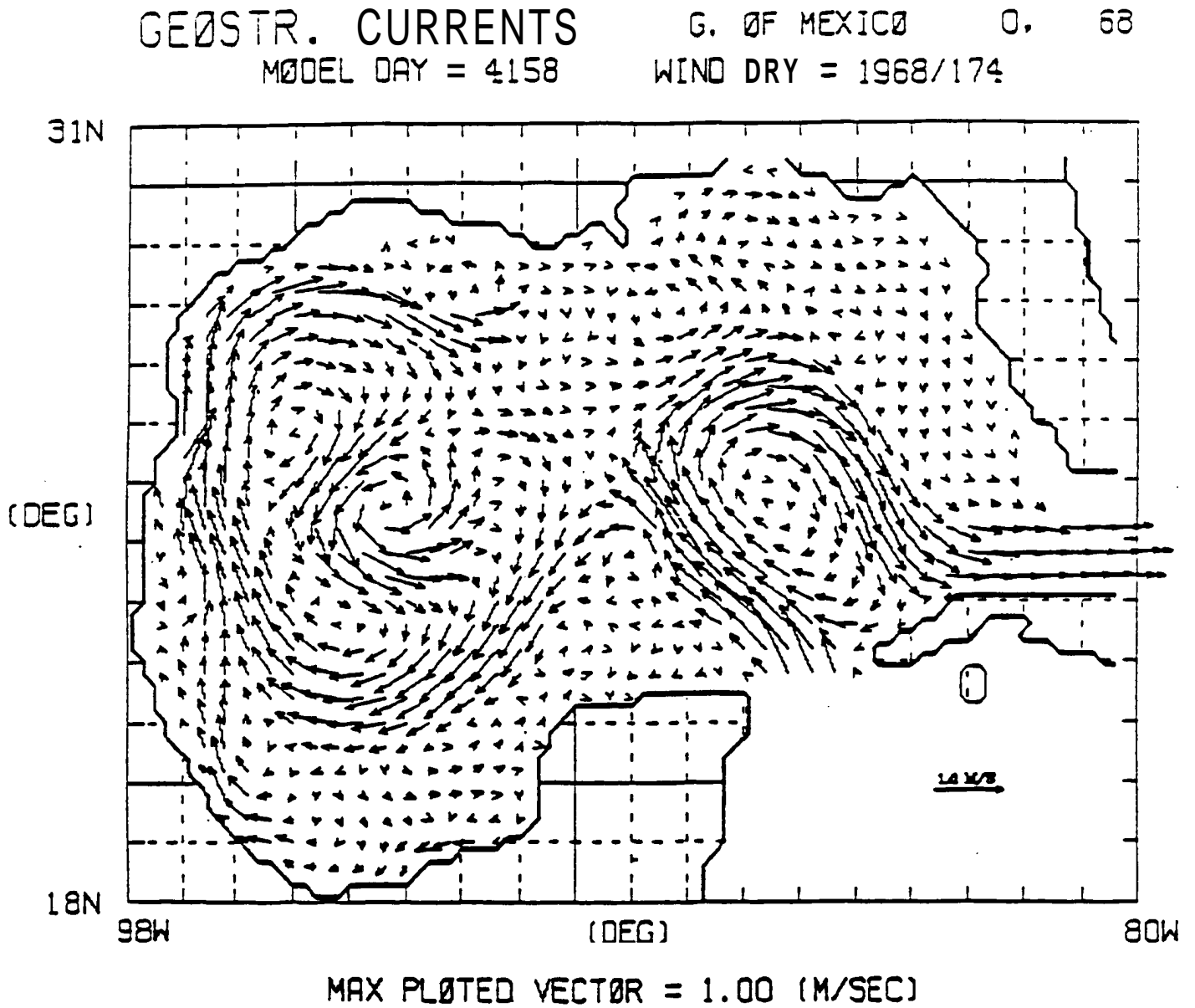


Figure 5. Instantaneous view of upper-layer averaged velocities from Experiment 68 on model Day 4218. Vectors are only plotted at every second model grid point, i.e., every 0.4 degrees.

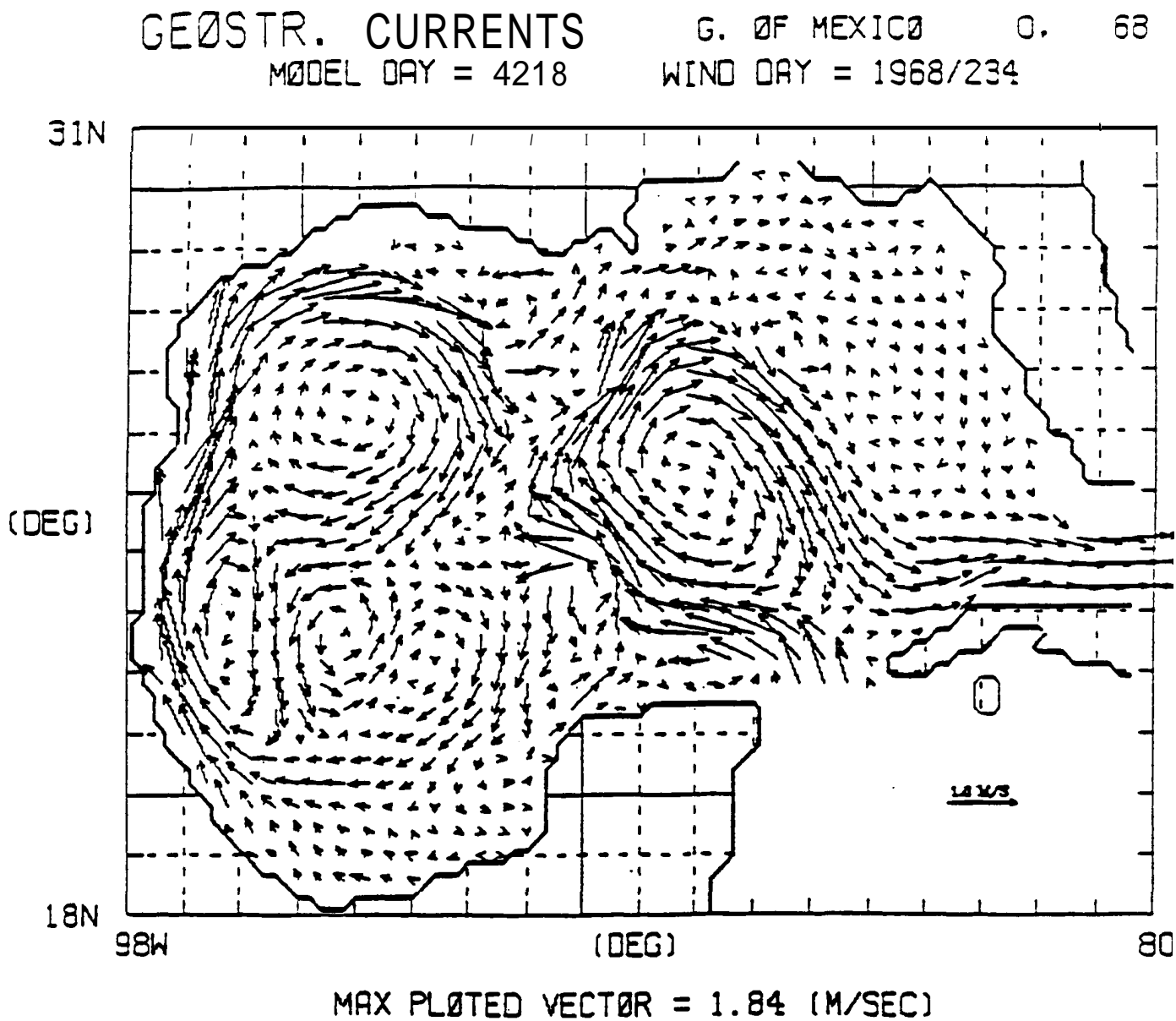


Figure 6. Instantaneous view of the upper-layer averaged velocities from Experiment 201/16.0 on model days (a) 2880 and (b) 2970. The assigned dates (344/1967 and 069/1968) indicate the applied wind forcing, but the experiment was not a hindcast and the ocean currents in the Gulf on that date might have been quite different from those shown. Vectors are only plotted at every second model grid point, i.e., every 0.2 degrees, and all velocities greater than 50 cm/sec are plotted as 50 cm/sec.

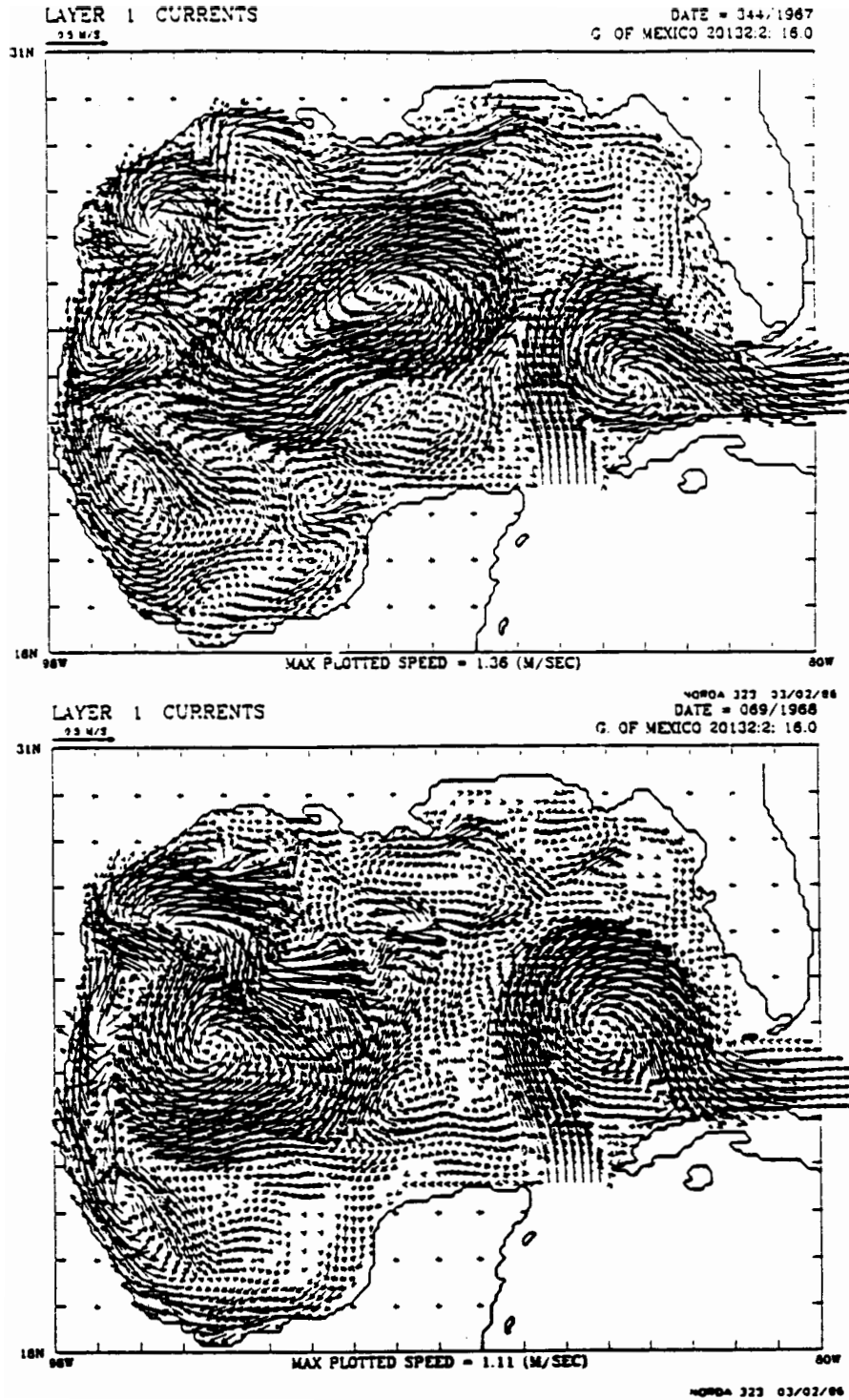
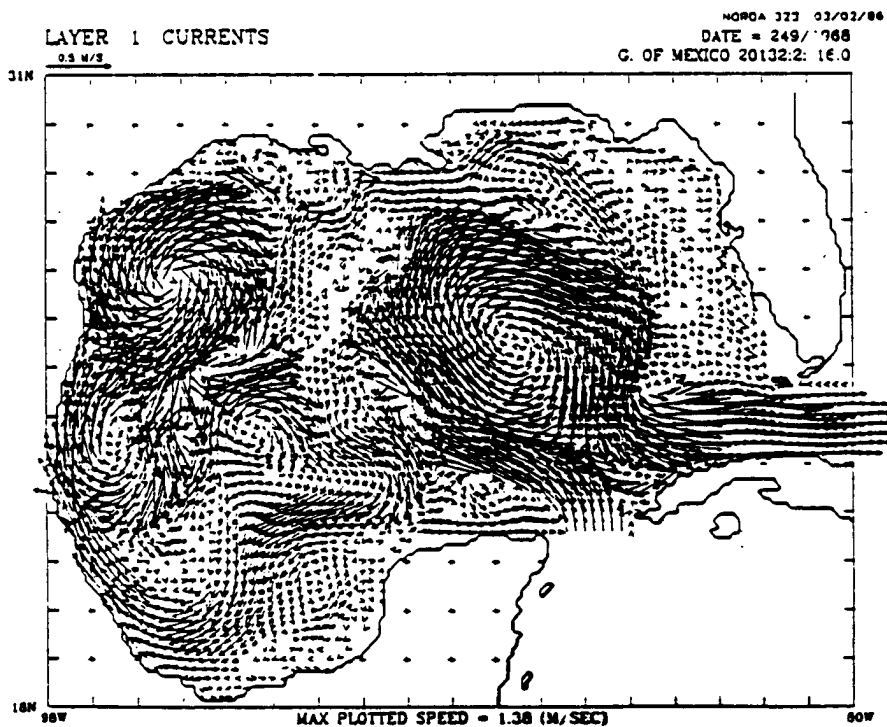
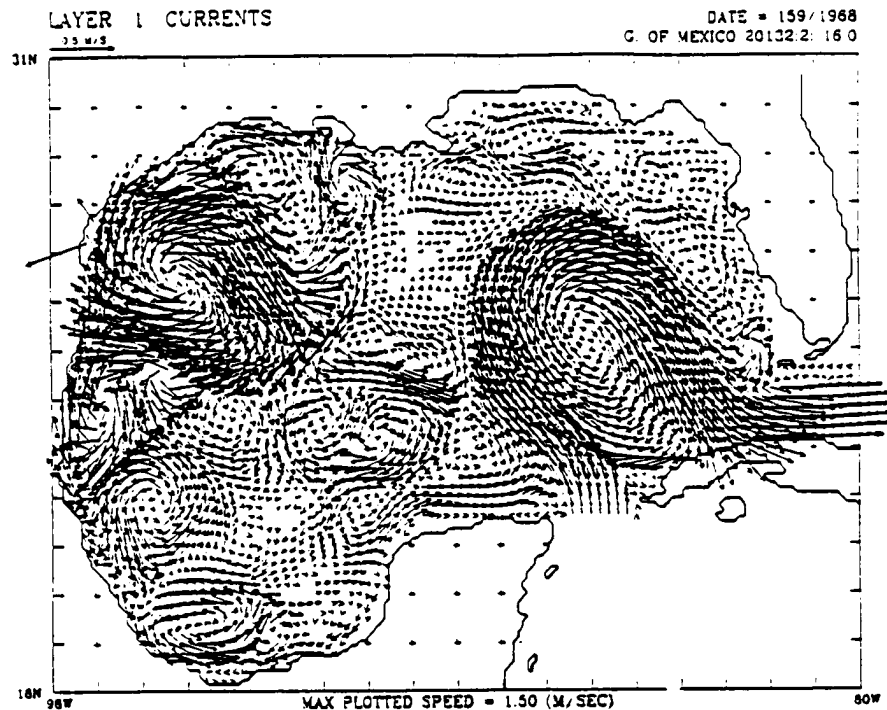


Figure 7. Instantaneous view of the **upper-layer** averaged velocities from Experiment 201/16.0 on model days (a) 3060 and (b) 3150. The assigned dates (159/1968 and 249/1968) indicate the applied wind forcing, but the experiment was not a **hindcast** and the ocean currents in the Gulf on that date might have been quite different from those shown. Vectors are only plotted at every second model grid point, i.e., every 0.2 degrees and all velocities greater than 50 cm/sec are plotted as 50 cm/sec.



NOPOA 323 03/02/86

Figure 8. Instantaneous view of the upper layer averaged velocities from Experiment 201/16.0 on model Days (a) 3240 and (b) 3330. The assigned dates (339/1968 and 063/1969) indicate the applied wind forcing, but the experiment was not a hindcast and the ocean currents in the Gulf on that date might have been quite different from those shown. Vectors are only plotted at every second model grid point, i.e., every 0.2 degrees and all velocities greater than 50 cm/sec are plotted as 50 cm/sec.

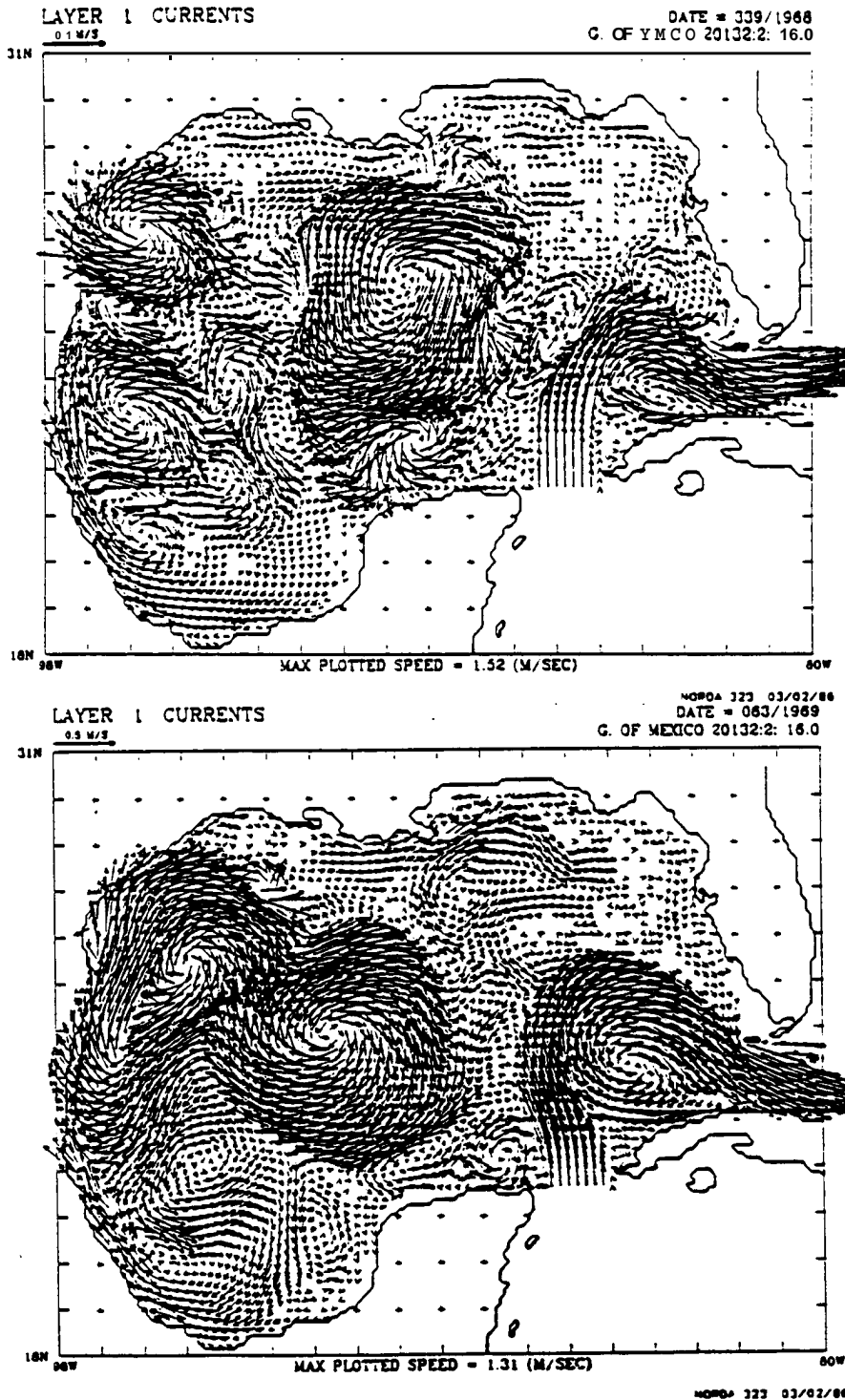


Figure 9. Instantaneous view of the upper layer averaged velocities from Experiment 201/16.0 on model Days (a) 3420 and (b) 2510. The assigned dates (153/1969 and 243/1969) indicate the applied wind forcing, but the experiment was not a hindcast and the ocean currents in the Gulf on that date might have been quite different from those shown. Vectors are only plotted at every second model grid point, i.e., every 0.2 degrees and all velocities greater than 50 cm/sec are plotted as 50 cm/sec.

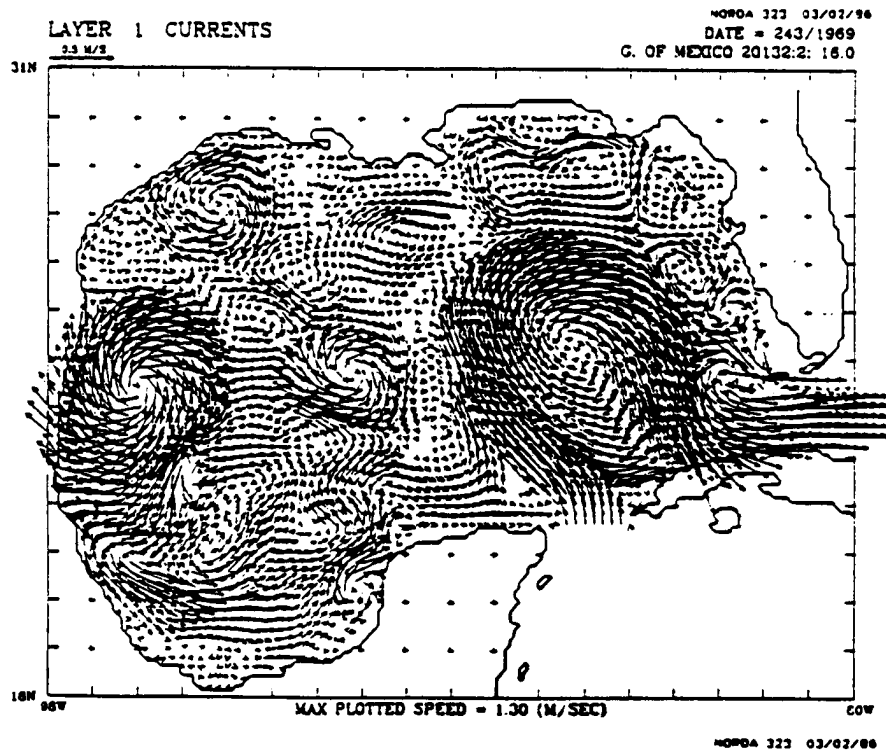
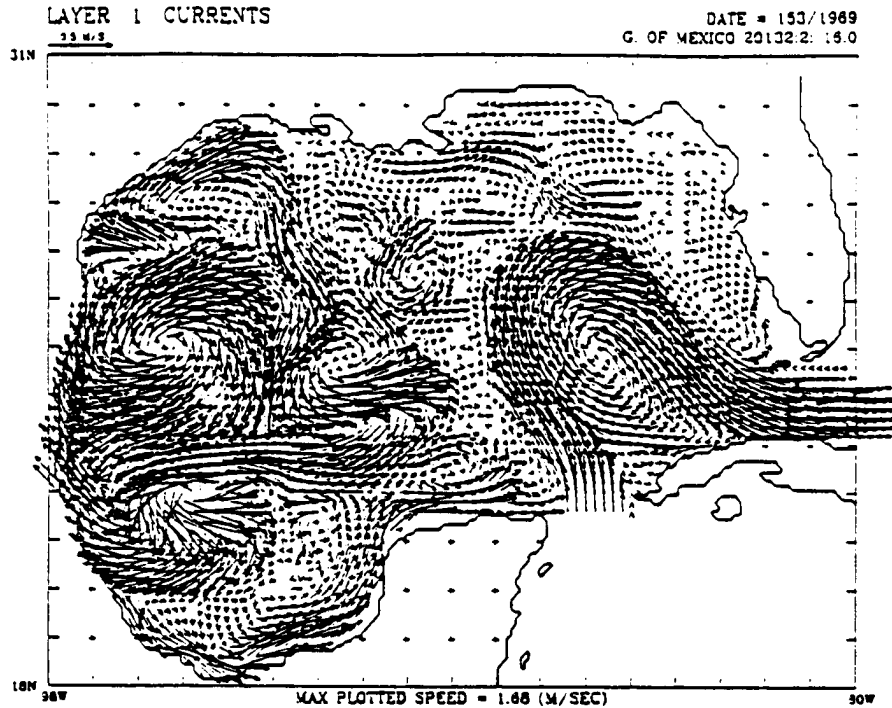


Figure 10. Instantaneous view of the upper layer averaged velocities from Experiment 201/16.0 on model Days (a) 3600 and (b) 3690. The assigned dates (333/1969 and 058/1970) indicate the applied wind forcing, but the experiment was not a hindcast and the ocean currents in the Gulf on that date might have been quite different from those shown. Vectors are only plotted at every second model grid point, i.e., every 0.2 degrees and all velocities greater than 50 cm/sec are plotted as 50 cm/sec.

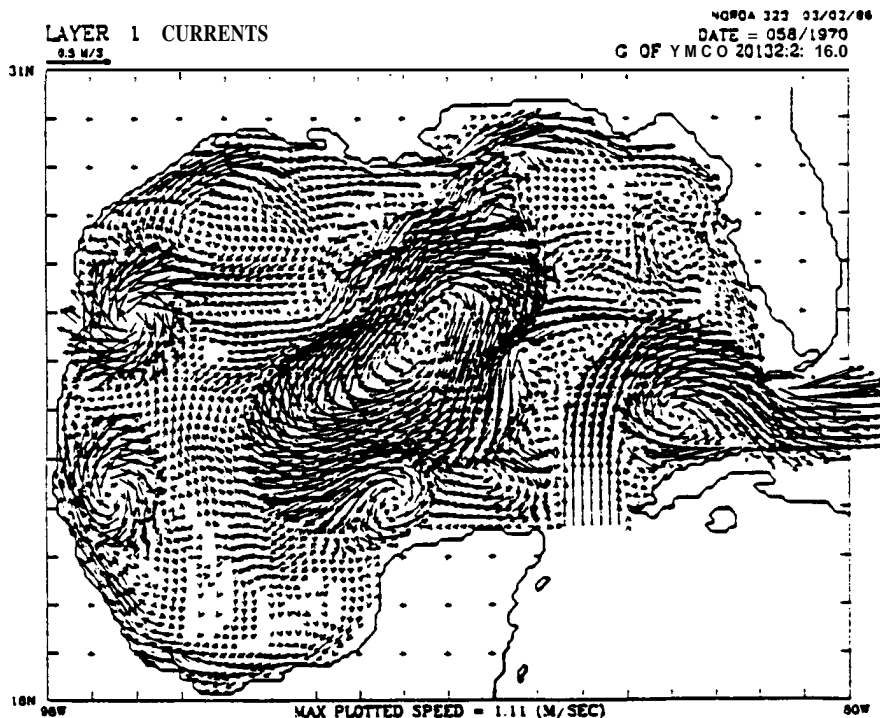
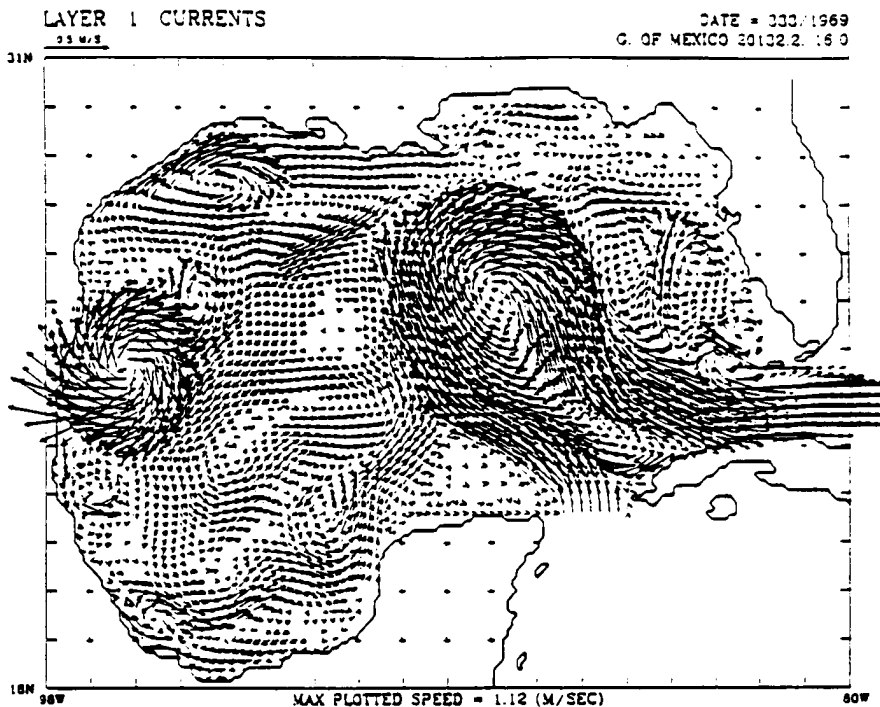
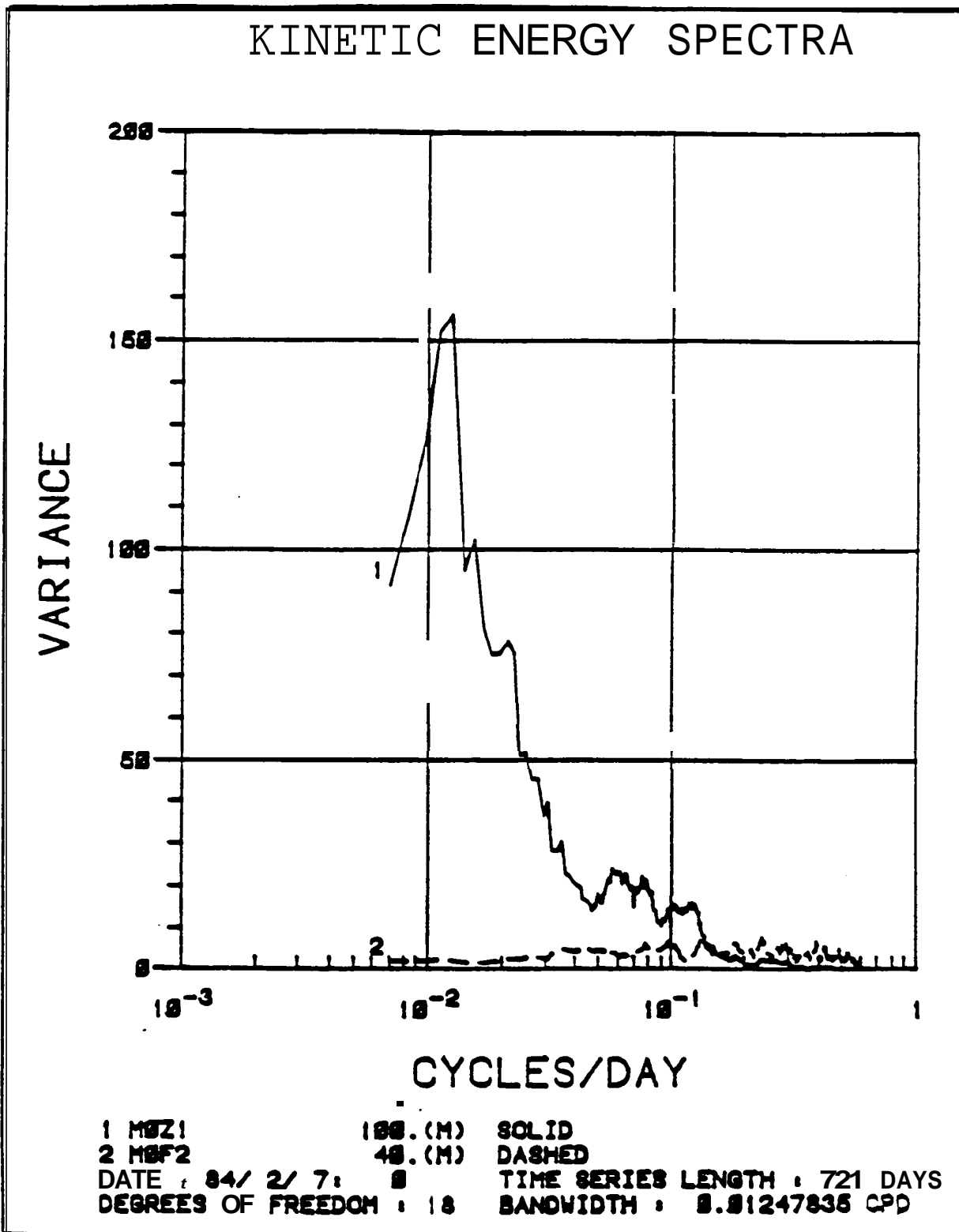


Figure 11. Kinetic energy spectra at 40 m depth for (solid) Experiment 201/13.0 at location Z and (dashed) Mooring F.



kinetic energy spectra at mooring MOF, which was located on the inner shelf in 50 m of water. The simulation is far too energetic and still shows a strong influence from the Loop Current that is completely absent from the observations.

III. YEAR 3

A major thrust of the third-year program was an attempt to produce improved simulations in shelf areas by developing a version of the layered-ocean model that would allow layer interfaces to, in effect, intersect the bottom topography. When intersection occurs in a conventional layer model the layer thickness becomes negative, which is clearly unphysical and leads to unrealistic results and, if the situation persists, catastrophic failure of the model run due to undamped instabilities. The obvious solution of setting a minimum layer thickness at or about zero does not work because: (a) it leads to loss of mass and (b) clamping the layer thickness induces dispersive ripples in the interface at the intersection point (i.e., we have an unresolved boundary layer). In a study of the effects of **hurricanes** in the Gulf, Cooper and Thompson (1989) used a multilayer model in which each layer interface intersects with a different artificial vertical step in the topography that acts as a solid wall boundary to that interface. This technique proved effective for short-term simulations of hurricane forcing with the simplifying assumption that the Gulf was at rest before the **hurricane** occurred. The technique is not generally applicable to simulations that include the Loop Current. In this case, the variations in each layer interface depth across the Gulf, which makes it impossible to design a stepped topography that guarantees that each interface will be everywhere and intersect the topography on the vertical face of a step at all times. The most promising approach to the layer intersection problem is to insure positive layer thicknesses via 'Flux Corrected Transport,' a technique that was originally developed for fluid problems with shocks (Book et al., 1981). In this method the continuity equation is solved for layer thickness using two different sets of transports; one obtained via a low-order (highly dispersive) scheme, guaranteed to give monotonic results; and, the other via a standard (ripple prone) high order scheme. The low-order scheme, used alone, would prevent layer intersection, but it very rapidly damps out circulation features and would not produce realistic simulations. Instead, the final layer thickness at each point is a linear combination of the two solutions chosen to be as close as possible to the high-order solution. Away from areas of layer intersection, the high-order scheme is used alone and the solution is identical to that without FCT, but near intersections just sufficient contribution from the low-order scheme is used to **ensure** a positive layer thickness. In other words, bottom topography is still confined to the lowest layer, but that layer can get very thin so

there is effectively no contribution from the deep layer over the shelf and no limit on how shallow the bottom topography can be. This method has been used with some success in a similar layered ocean model, both for interfaces that intersect the surface and for layers that intersect the topography (Bleck et al., 1983). The major problem with the method is that FCT is an inherently explicit scheme in contrast to the existing ocean model that treats gravity waves implicitly (to allow much larger timesteps). A fully explicit model's **timestep** would be controlled by the external gravity wave speed (about 150 m/s), but the depth averaged flow can still be treated implicitly in a model with FCT, so the **timestep** depends on the internal gravity wave speed (about three m/s). The ocean model without FCT, on the other hand, treats both external and internal gravity waves implicitly and can use a **timestep** three-to-five **times** longer **than** the **FCT** code.

Two-dimensional (x-z) versions of a two-layer hydrodynamic model that uses **FCT** to allow layers to intersect the bottom were developed and tested on sections across the Gulf of Mexico (**FCT2D**) (Figure 12). The position of each model grid point is indicated by a vertical line below the topography contour. Data is only available at grid points and straight lines are used to connect data values in the plot. The upper-layer rest depth is 300 m over deep water, but is less near 98W and 82W, where the continental shelf is shallower than 300 m deep. The lower layer is set to be at least 10 cm thick across the entire region, so there is a lower layer over the continental shelf although it is too thin to be seen in the plot. Figure 12 is for two days into an experiment to test the ocean model with no applied forcing. The layers are in exactly the same position as at the initial time and the velocities are zero everywhere. This demonstrates that the model does not deviate from an initial rest state without applied forcing.

Figures 13 and 14 show only the upper 450 m of the water column for a gravity wave sloshing experiment, where there is no applied forcing, but the layer interface is initialized with a single-period cosine profile across the region. Figure 13(a) shows the initial state with about 100 m variation in the depth of the interface from east to west (note that the lower layer is again 10 cm thick where the topography is shallower than the expected interface depth). Figure 13(b) is for Day 3 of the simulation, where the layer interface is now almost level. Figure 14(a) is for Day 6. The layer interface has moved up or down about 100 m at each end to reverse the profile; however, it is no longer exactly sinusoidal because gravity waves travel slower in shallow water than they do in deep water. The interface is level again between Days 9 and 10. Figure 14(b) is for Day 12, where the interface is again shallower to the west as it was on Day 0, but the wave is almost square

Figure 12. Layer depths for a two-dimensional two-layer hydrodynamic model with full-scale bottom topography that uses Flux Corrected Transport to allow the layer interface to 'intersect' the topography. The figure is for Day 2 of an experiment testing the stability of the rest configuration in the absence of external forcing. There has been no change over the two days. The lower layer is 10 cm thick at all points where the topography appears to intrude into the upper layer.

LAYER DEPTHS

G.O.M. FCT 22052:2: 71.0

Y = 26.00N

DAY = 2.000

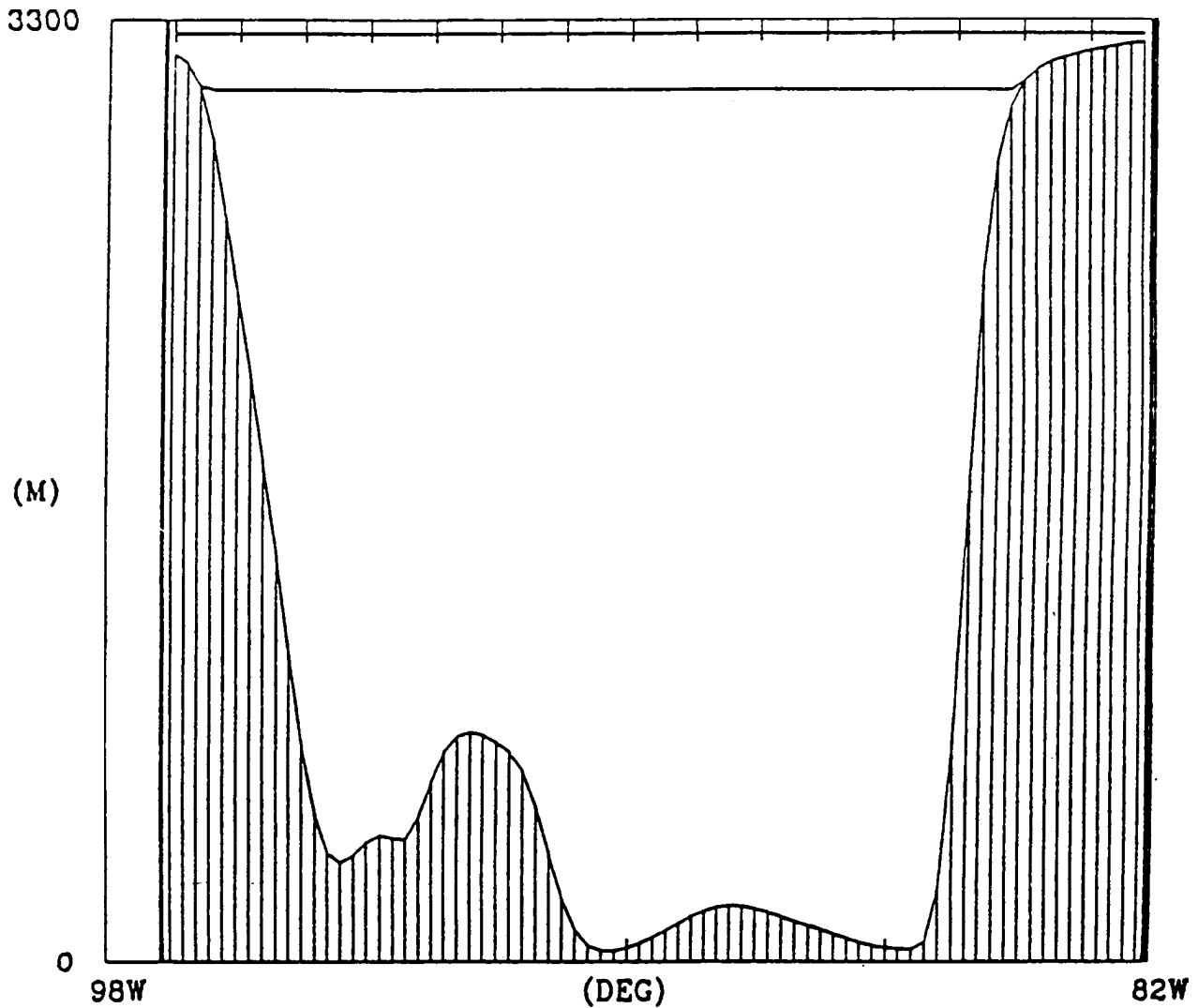
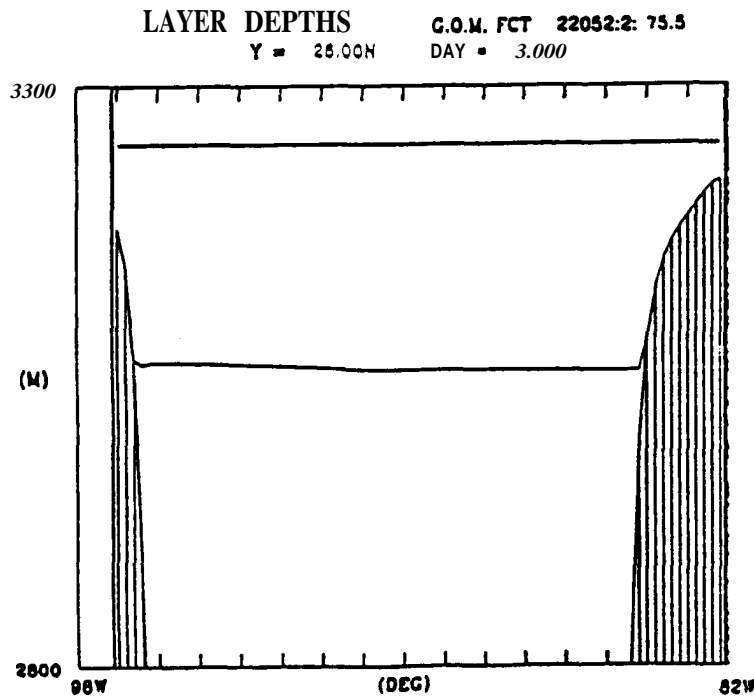
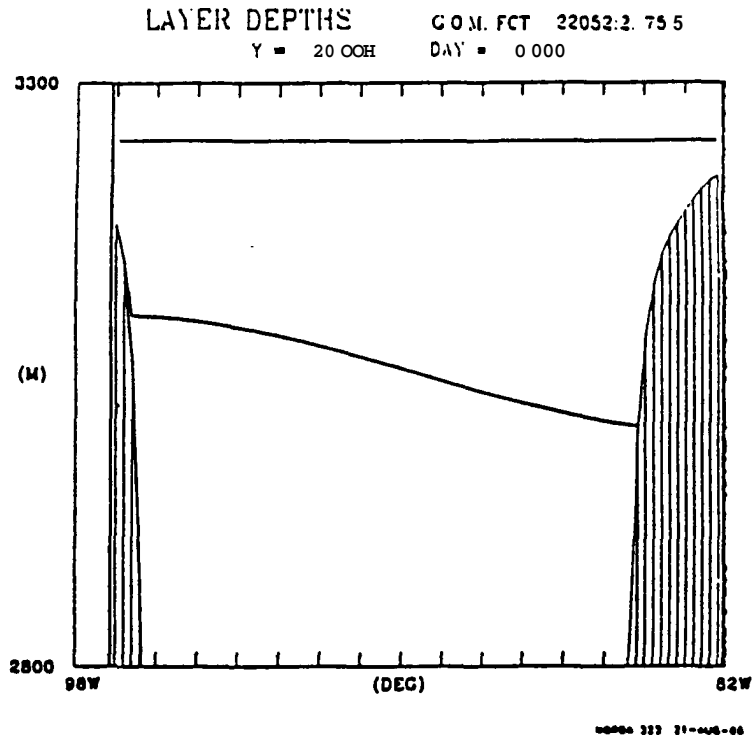


Figure 13. Layer depths on Days (a)0 and (b) 3 for a two-dimensional two-layer hydrodynamic simulation that uses Flux Corrected Transport to allow the layer interface to 'intersect' the topography. Only the upper 450 m of the water column is shown.



and the model blows up at Day 15 as the wave 'breaks.' The conversion of the original wave into a breaking wave is to be expected, given than gravity waves travel slower in shallow water.

The extension of **FCT2D** to three dimensions (**FCT3D**) was still under development at the end of Year 3. The only difficulty encountered was the practical one of the time and expense involved in debugging the code. There is no reason to suppose that a model of this kind could not work in the Gulf of Mexico; however, there is no guarantee that it could produce acceptable simulations. One obvious area of concern with such a model would be the accuracy of the simulation in the zone where the model goes from one layer to two. However, any single model that tried to accurately simulate on- and off-shelf flow at the same time would have problems in this shelf slope region. Models like **FCT3D** are at least one, and perhaps two, orders of magnitude less expensive than all other model designs that might be able to provide similar simulations.

The second major element of the third-year program was the addition of bulk-layer thermodynamics to the model. The existing model was 'hydrodynamic' (i.e., the density in each layer was constant and fixed for all time) with the fixed densities and the density difference between layers set to realistic mean values for the Gulf of Mexico. With the addition of thermodynamics, the density is allowed to vary in space and evolve with time under the control of an equation of state and a temperature equation forced by heat fluxes (or by relaxation back to a density **climatology**) and the density of inflow water. Mixing of denser fluid from the layer below into each layer is also allowed and this can prevent the layer interface surfacing due to upwelling, i.e., the layer gets denser rather than getting thinner. In hydrodynamic models there is no exchange of fluid between layers.

The vertically integrated equations of motion used in the n-layer finite depth thermodynamic model are, for $k=1\dots n$:

$$\begin{aligned} \frac{\partial \vec{V}_k}{\partial t} + (\nabla \cdot \vec{V}_k + \vec{V}_k \cdot \nabla) \vec{v}_k + \hat{k} \times f \vec{V}_k = & \\ \max(0, \omega_k) \vec{v}_{k+1} - (\max(0, -\omega_k) + \max(0, \omega_{k-1})) \vec{v}_k + \max(0, -\omega_{k-1}) \vec{v}_{k-1} & \\ - h_k \sum_{l=1}^n (G_{kl} \nabla (h_l - H_l) + h_l \nabla G_{kl}) - \frac{g}{\rho_o} h_k \left(\frac{1}{2} h_k + \sum_{l=1}^{k-1} h_l \right) \nabla \rho_k & \\ + (\bar{\tau}_{k-1} - \bar{\tau}_k) / \rho_o + A_H \nabla^2 \vec{v}_k & \\ \frac{\partial \rho_k}{\partial t} + \vec{v}_k \cdot \nabla \rho_k = & \\ \max(0, \omega_k) \frac{\rho_{k+1} - \rho_k}{h_k} + \max(0, -\omega_{k-1}) \frac{\rho_{k-1} - \rho_k}{h_k} & \end{aligned}$$

$$\begin{aligned}
& -\frac{\bar{\rho}_k H_k}{\rho_k \bar{h}_k} \sigma_\rho (\rho_k - \hat{\rho}_k) - \delta_{1k} \frac{\gamma Q}{\rho_1 c_p \bar{h}_1} + K_H \nabla^2 \rho_k \\
\frac{\partial h_k}{\partial t} + \nabla \cdot \vec{V}_k = & \\
\omega_k - \omega_{k-1} + \frac{h_k}{\rho_k} \left(\frac{\bar{\rho}_k H_k}{\rho_k \bar{h}_k} \sigma_\rho (\rho_k - \hat{\rho}_k) + \delta_{1k} \frac{\gamma Q}{\rho_1 c_p \bar{h}_1} \right) &
\end{aligned}$$

where

$$\begin{aligned}
\vec{V}_k &= h_k \vec{v}_k \\
D &= \text{actual water depth} \\
\tilde{D} &= \text{model water depth, } \tilde{D} \geq D \\
H_k &= \text{k-th layer thickness at rest} \\
H_n &= \tilde{D}(x, y) - \sum_{i=1}^{n-1} H_i \\
\bar{h}_k &= \min(h_k, D) \\
\bar{\rho}_k &= \text{k-th layer (constant) density at rest} \\
\hat{\rho}_k &= \text{k-th layer density climatology} \\
Q &= \text{surface heat flux}
\end{aligned}$$

The above equations are only valid provided the layer thicknesses are always positive, and the density fields are always stably **stratified**. Stable stratification is not generally a problem in the Gulf, and mixing can be used to prevent a layer becoming thin due to upwelling, but the model depth, \tilde{D} , must be made deeper than the **actual** Gulf depth, D , over the continental shelf in order to insure that the lowest layer interface never intersects the bottom.

The model is always initialized from rest, with zero velocities, level layer interfaces, and constant density fields, **i.e.**, at time $t=0$:

$$\begin{aligned}
\vec{V}_k &= 0 \\
\rho_k &= \bar{\rho}_k \\
h_k &= H_k
\end{aligned}$$

In the absence of external density forcing and mixing, the density in each layer remains constant for all time and the above equations are equivalent to those for the hydrodynamic model (Hurlburt and Thompson, 1980). External density forcing can take the form of atmospheric heat flux, Q , or relaxation back to a density climatology, $\hat{\rho}_k$, or the inflow through a port can be at a different density. Mixing is the process of entraining or detaining mass **from** one layer to the next. Mixing cannot be applied to a hydrodynamic model because it causes a change in the layer

averaged density. In a layered model, the "physics" of mixing is controlled by the calculation of the vertical mixing velocity at the layer interfaces, $\hat{\omega}_k$. Since in this case the layer interface represents the thermocline depth, rather than the mixed layer depth, very simple mixing physics is used to effectively constrain the layer thickness to tend to stay in the range h_k^- to h_k^+ . This form of mixing is primarily designed to prevent the layer interface surfacing due to upwelling, i.e., the layer gets denser rather than getting thinner. Mixing is also balanced, by $\hat{\omega}_k$, so that there is no net exchange of mass between the layers over the region as a whole.

The surface heat flux fields, Q , used to drive an ocean model must be of high quality, otherwise they will cause climate drift in the model by applying too much heating or cooling. Since there are no data sets of sufficient quality for heat fluxes in the Gulf of Mexico, the model was instead required to relax back to a monthly density climatology, $\hat{\rho}_1$, based on sea surface temperature maps from historical ship observations. One way to look at relaxation to climatology is as a heat flux that always drives the model's instantaneous density field back towards a reference density field, i.e.,

$$\frac{\bar{\rho}_1 H_1}{\rho_1 \bar{h}_1} \sigma_\rho (\rho_1 - \hat{\rho}_1) = \frac{\gamma \bar{Q}}{\rho_1 c_p \bar{h}_1}$$

where

$$\bar{Q} = \frac{\bar{\rho}_1 c_p H_1 \sigma_\rho}{\gamma} (\rho_1 - \hat{\rho}_1)$$

The e-folding time for the relaxation, $\rho_1 \tilde{h}_1 / \bar{\rho}_1 H_1 \sigma_\rho$, was chosen to be about 360 days in the center of a Loop Current eddy, but only 90 days over the continental shelf. The use of the smaller of the layer thicknesses and the actual water depth, \tilde{h}_1 , ensures rapid relaxation over the continental shelf where rapid winter cooling is important. The model can be forced by sufficiently accurate heat flux fields; however, because of the problem of climate drift, it would probably always be wise to **include** a relaxation term that forced the model's density field to stay close to the climatological mean field. This relaxation term is, in effect, a parameterization of the mean heat flux forcing. The additional heat fluxes, applied to a model that includes such a relaxation term, should represent the perturbations in heat fluxes about the long-term mean. The present model is forced by relaxation to a monthly density climatology. The alternative, should heat fluxes of sufficient quality be available, would be to relax to a mean density climatology and in addition

force the model with heat flux anomalies about the mean heat flux field. The mean density climatology would simply be the average of the existing monthly density fields.

Figure 15 shows the sea surface and corresponding density fields for January. The density ranges from 25.8 sigma-t over the shelf to 24.0 sigma-t in the Yucatan Straits. The model sets the density of the Loop Current inflow through the straits to agree with the density climatology there month by month. Figure 16 shows contour maps of sea surface height and of density for an experiment without wind forcing and with a constant inflow transport of 20 Sv in the upper layer. It is for a day in December and so the shelf areas are cool (note the strong density front between the large anticyclonic and the smaller cyclonic eddies in the northwest Gulf). In this case, a new eddy is in the process of developing on the Loop Current as it extends into the Gulf. Figure 17 is for 180 days later in the summer. The anticyclonic eddy has detached from the Loop Current and is in the central Gulf, which is already cooler than the Loop Current. The shelf areas are significantly less dense than they were during the winter.

A detailed study of the appropriate model parameters to use for this layered model in the Gulf of Mexico was performed by Hurlburt and Thompson (1980 and 1982). Their results were for a simplified Gulf of Mexico geometry, but they carry over to the more realistic geometry used here. Many of the parameters are constrained to be physically realistic for the Gulf of Mexico. The Coriolis parameter and the beta used in the **beta-plane** approximation are set by the Gulf's location and the acceleration due to gravity is set at 9.8 meters per second for obvious reasons. The mean upper-layer thickness, **H1**, is set to 200 m in **all** two-layer simulations because this is the approximate average depth of the **thermocline** in the Gulf. Similarly the value of reduced gravity, g' , is chosen based on the average contrast between the vertically averaged density above and below the thermocline. The allowable range is from 0.02 to 0.03 meters per second and 0.025 is typically used here. The reference thickness of the lower layer, **H2**, in two-layer simulations is chosen to be slightly larger than the actual rest thickness everywhere when allowing for bottom topography. Since the bottom topography used is never deeper than 3,650 meters, a value of 3,450 meters is used for **H2** (allowing for an **H1** of 200 meters). The actual rest thickness of the lowest layer depends on the bottom topography. Following Hurlburt and Thompson (1980), the total transport through the Yucatan Straits is held fixed in all multilayer experiments at 30 Sv; however, the distribution of transport between layers is **difficult** to estimate from observations and different simulations have allocated as much **as** 26 Sv and **as** little **as** 20 Sv of the total to the upper layer. Allocating more transport to the upper layer increases the speed of the Loop **Current**; **how-**

Figure 15. Sea surface temperature and the corresponding calculated upper-layer density for January from a monthly climatology based on historical ship observation data.

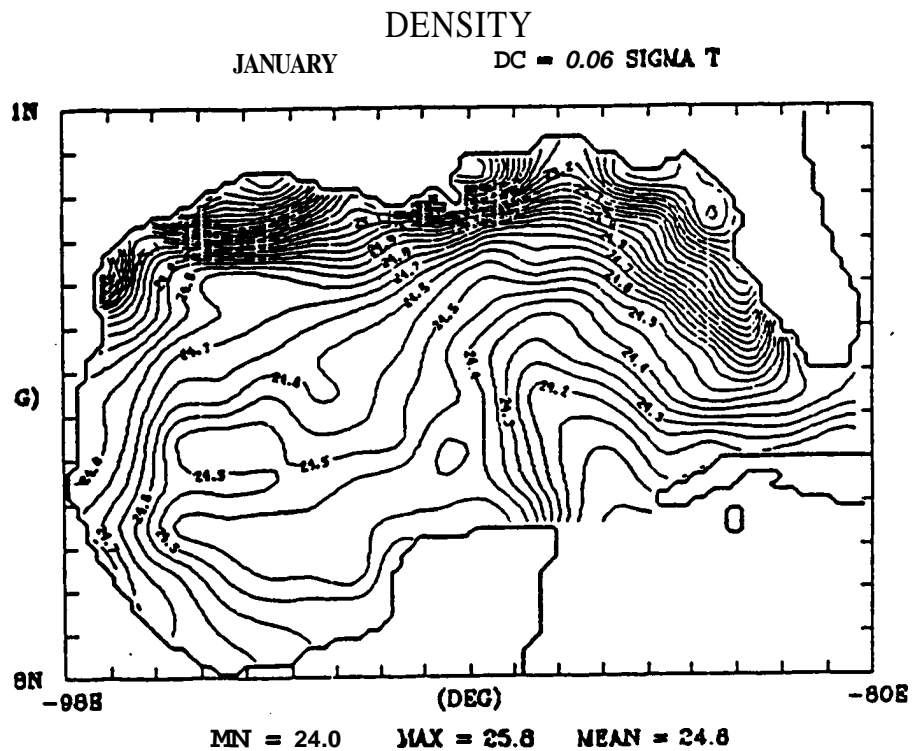
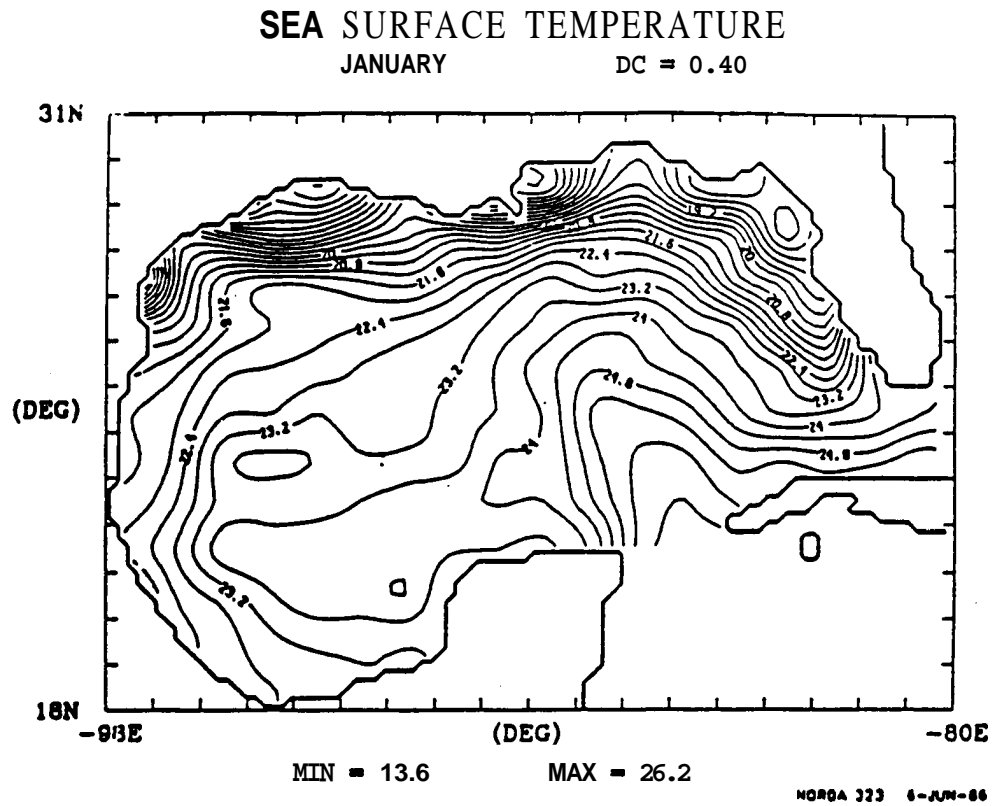


Figure 16. Instantaneous (a) free surface deviation and (b) upper-layer density from a thermodynamic model of the Gulf with no wind forcing. Snapshots are for December 26 after four years of spin up from rest.

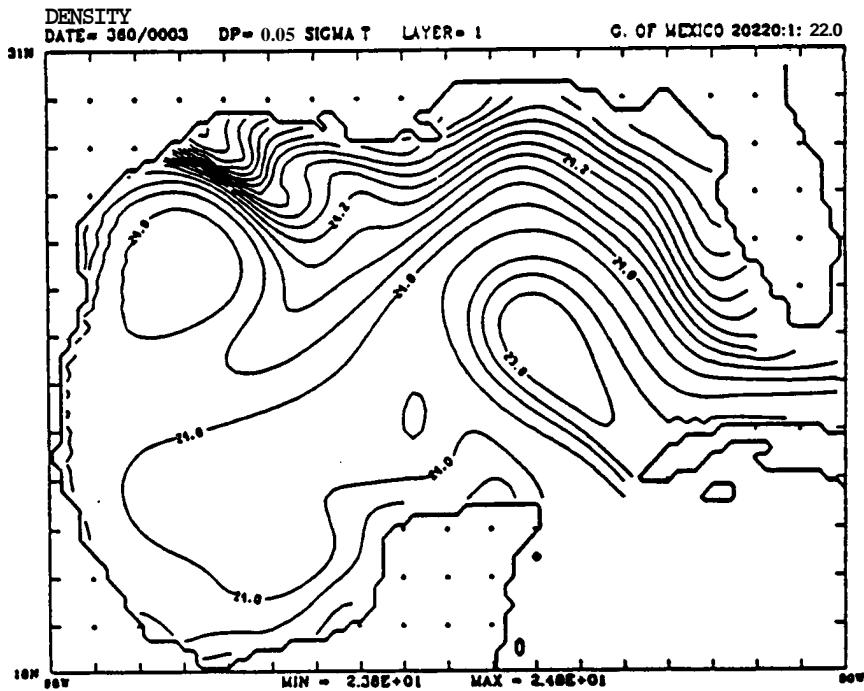
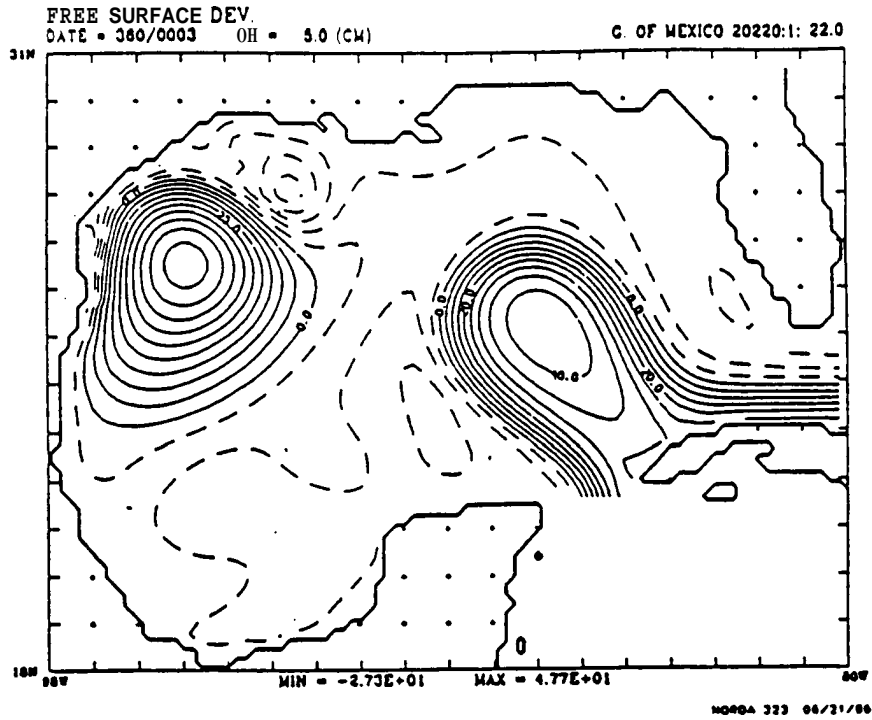
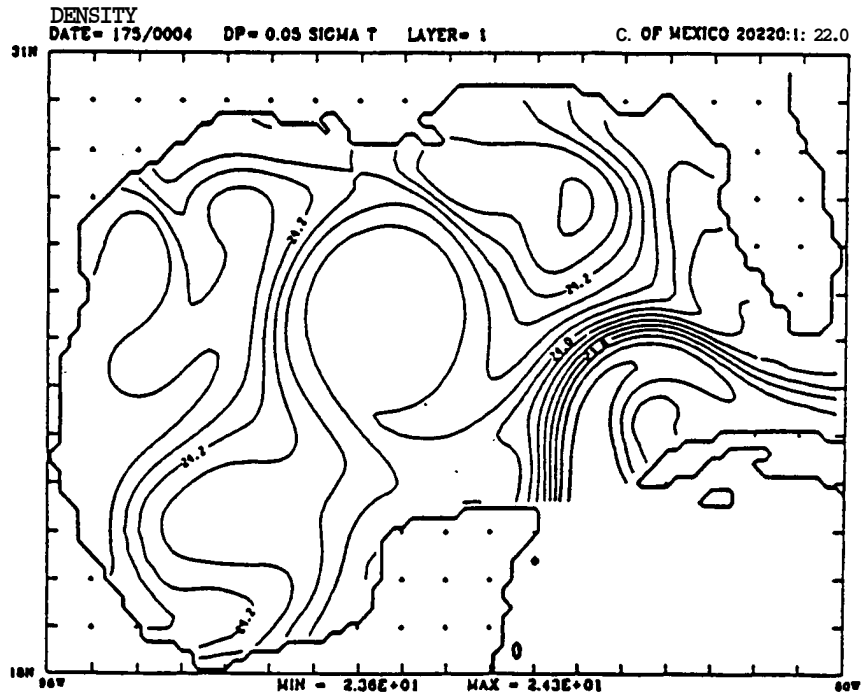
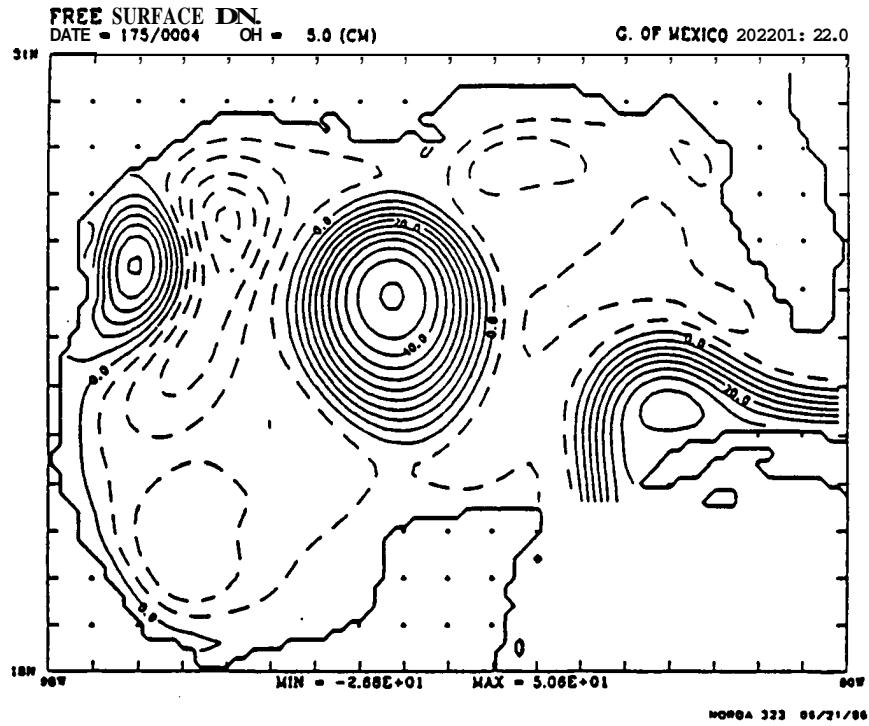


Figure 17. Instantaneous (a) free surface deviation and (b) upper layer density from the same simulation as Figure 16. Snapshots are for 180 days later than Figure 16, i.e., for a day in the summer.



ever, allocating more transport to the lower layer tends to prevent the Loop Current from intruding onto the Florida Shelf. The horizontal grid spacing is chosen to resolve the features of interest. A good rule of thumb is that 10 grid points are required across an eddy and five grid points across a jet in order for their dynamics to be resolved by the model. Twenty kilometers is sufficient to resolve the Loop Current and Loop Current eddies, but 10 kilometers is required to resolve some associated features that have smaller horizontal scales. The actual grid spacing is specified in degrees at the center of the Gulf and is either 0.2 degrees (20 km by 22 km) or 0.1 degrees (10 km by 11 km). The model parameterizes **subgrid** scale processes using Laplacian eddy viscosity and density diffusivity. The appropriate coefficients are primarily controlled by the horizontal grid spacing and less viscosity is required on a finer grid. Density diffusivity is only required in thermodynamic models, since hydrodynamic models have no horizontal variation in density. Density diffusivity has typically been set five times larger than eddy viscosity. A quadratic formulation has been used for bottom stress with a typical coefficient of 0.002, although some simulations have used 0.003.

IV. YEAR 4

The thermodynamic simulations started in Year 3 were continued into Year 4; however, no further attempt was made to develop a three-dimensional model with flux-corrected transport. Instead, the best possible simulation was generated using the existing multilayer thermodynamic model. Similar barotropic models have been used by others (O'Brien, 1971). The NOARL/JAYCOR-layered ocean model is designed to run with one or more layers. The one-layer Gulf of Mexico simulations use the same model code on the same grid over the same region as the two-layer simulations. The only difference is that there is just one layer and the topography does not need to be scaled back as it does in multilayer simulations.

The model equations apply equally well to a one-layer barotropic model as to a two- or three-layer model. In fact, the original Gulf of Mexico simulations with a very early version of the model included barotropic experiments (Hurlburt and Thompson, 1980). The advantage of one-layer simulations is that the standard requirement, rather than bottom topography confined to the lowest layer, is not a limitation (since the only layer is the lowest layer). The disadvantage of such a model is that one vertically-averaged layer is a very poor approximation to the ocean's structure in deep water since it cannot include a thermocline. So a one-layer model does well over the shelf,

but less well over deep water; and a two- or three-layer model does well over deep water, but not as well over the shelf.

To obtain the "best" simulation, the results from two independent model runs (one layer (L1) and two layers (L2) using the same forcing) were merged (L2+L1). The barotropic fields were used in water shallower than 100 meters, the two-layer fields were used in water deeper than 200 meters, and a linear combination of the two sets of fields weighted by water depth were used in the fairly narrow zone at the shelf break between these regions. In particular, the merged layer thicknesses and transports are given by:

$$\begin{aligned}\vec{v}_1^{(L_1+L_2)} &= \alpha \vec{v}_1^{(L_1)} + (1 - \alpha) \vec{v}_1^{(L_2)} \\ \vec{v}_2^{(L_1+L_2)} &= \begin{cases} 0 & \text{for } D \leq h_1^{(L_2)} \\ \vec{v}_2^{(L_2)} & \text{for } D > h_1^{(L_2)} \end{cases}\end{aligned}$$

where

$$\alpha = \begin{cases} 1 & \text{for } D \leq 100 \\ 0 & \text{for } D \geq 200 \\ (200 - D)/100 & \text{otherwise} \end{cases}$$

and the merged layer thicknesses are given by:

$$\begin{aligned}h_1^{(L_1+L_2)} &= \min(h_1^{(L_2)}, D) \\ h_2^{(L_1+L_2)} &= \begin{cases} 0 & \text{for } D \leq h_1^{(L_2)} \\ h_2^{(L_2)} & \text{for } D > h_1^{(L_2)} \end{cases}\end{aligned}$$

The choice of 100 m as the cutoff depth, at which L1 starts merging with L2, was chosen based on current meter data on the Florida shelf (SAIC, 1986) that indicated that there was no discernable effect of the Loop **Current** in water shallower than this depth. The choice of 200 m as the cutoff depth, at which L2 starts merging with L1, was based on the average depth of L2 layer interface across the entire Gulf at this depth. Any value between 200 m and 500 m would have had very little effect on the final result since the horizontal distance between these depths is very small in the Gulf.

This approach does not guarantee that currents in the blending zone will be physically **realistic**. For example, an attempt to merge Experiment 210/16.0 from Year 2 (Figures 6-10) with a barotropic experiment would give poor results since modeled deep water features often intrude to a

significant degree onto the inner shelf. These features, such as an anticyclonic eddy off the Texas coast and the Loop Current on the Florida shelf just after an eddy is shed (Figure 7) would be sheared off in the merged fields. Merging the fields only makes sense if the multilayer simulation confines deep water circulation features primarily to deep water. Three-layer models have difficulty keeping circulation off the shelf because there is insufficient connection between the topography confined to the lowest layer and the upper-layer circulation. Two-layer models typically do better than three-layer versions at confining flow to deep water, but conventional two-layer simulations are not good enough to allow merging of the one- and two-layer fields. A new two-layer version of the model was used with a modified **mixing** term that holds the layer interface close to the rest depth of 200 meters over the shelf for the entire simulation. Major eddies and jets cause significant deformation of the layer interface, so these features cannot get over the shelf if the interface is held rigid. The advantages of this approach are that the minimum topography depth can be raised from 500-300 meters and the simulation is much improved in the shelf and shelf break regions. The disadvantages are that only two layers can be used (to maximize shelf realism) and the strong mixing over the shelf must be balanced region wide to maintain a constant-layer thickness that adds friction to the deep water circulation. In the Gulf, there are occasional intrusions of eddies onto the outer shelf and more frequent entrainment of fluid off the shelf into deep water. The former are excluded from the merged simulation, but the latter can occur since the two-layer component includes the full shelf region. A major advantage of blending two independent simulations is that either one can be replaced by an improved simulation at a later date. In this case, the shelf circulation is more likely to be upgraded in this way. In fact, each major shelf region (*i.e.*, the Texas and Florida shelves) could be upgraded with different models at different times.

Layered models provide current fields representing the vertical average over their instantaneous layer depths. Upper-layer currents are very similar to geostrophic surface currents. In order to obtain actual surface currents and currents at **fixed** depths throughout the water column, an analytic perturbation analysis is used (Thompson, 1974). By subtracting the vertically-averaged equations from the Navier-Stokes equations, differentiating the result with respect to the vertical, employing the hydrostatic relation, and assuming small **Rosby** number and quasi-equilibrium conditions, the following lowest order perturbation equation results:

$$\begin{aligned}
 a &= \bar{a}(x, y, t) + a'(x, y, z, t) \\
 \hat{k} \times f \frac{\partial \vec{v}'}{\partial z} &= \frac{g}{\rho_0} \nabla \rho + A_v \frac{\partial^3 \vec{v}'}{\partial z^3}
 \end{aligned}$$

Define

$$w_k = (\bar{u}_k + u'_k) + i(\bar{v}_k + v'_k) \quad 0 \leq z \leq b_k = -h_k$$

Then

$$\begin{aligned} \frac{\partial^3 w_k}{\partial z^3} - s^2 \frac{\partial w_k}{\partial z} &= G_k \quad 0 \leq z \leq b_k \\ G_k &= \frac{-g}{\rho_o A_v} \left(\frac{\partial \rho_k}{\partial x} + i \frac{\partial \rho_k}{\partial y} \right) \\ s &= \sqrt{\frac{f}{2A_v}} + i \sqrt{\frac{f}{2A_v}} \end{aligned}$$

with integral constraints

$$\int_{b_k}^0 w_k dz = -b_k \bar{w}_k$$

and boundary conditions

$$\begin{aligned} \left. \frac{\partial w_1}{\partial z} \right|_{z=0} &= \frac{\tau_x^w}{\rho_o a_v} + i \frac{\tau_y^w}{\rho_o a_v} = Q_1 \\ \left. \frac{\partial w_k}{\partial z} \right|_{z=0} &= \left. \frac{\partial w_{k-1}}{\partial z} \right|_{z=b_{k-1}} = Q_k \quad k = 2 \dots n \\ w_k|_{z=b_k} &= w_{k+1}|_{z=b_n} = J_k \quad k = 1 \dots n-1 \\ w_n|_{z=b_n} &= \frac{A_v}{C_D} \left. \frac{\partial w_n}{\partial z} \right|_{z=b_n} = J_n \end{aligned}$$

The boundary conditions match both stress and velocity across each internal interface and linear friction is applied at the bottom, i.e., $A_v \partial \omega / \partial z = C_D \omega$.

If all the Q_k s and J_k s were known, the solution would be:

$$\begin{aligned} w_k &= \frac{A_k e^{sz}}{s} - \frac{B_k e^{-sz}}{s} - \frac{G_k z}{s^2} + C_k \\ A_k &= Q_k - B_k + G_k/s^2 \\ B_k &= Q_k \left(\frac{(sb_k - 1)e^{sb_k} + 1}{sb_k} \right) \\ &\quad + G_k \left(\frac{(s^2 b_k - 1)e^{sb_k} + 1}{s^3 b_k} - \frac{3b_k}{2s} \right) + s(\bar{w}_k - J_k) \\ C_k &= \frac{A_k}{s^2 b_k} (1 - e^{sb_k}) + \frac{B_k}{s^2 b_k} (1 - e^{-sb_k}) - \frac{G_k b_k}{2s^2} + \bar{w}_k \end{aligned}$$

The boundary values $Q_2 \dots Q_n$ and $J_1 \dots J_n$ can be found by solving (numerically) an appropriate set of simultaneous linear equations formed by expressing A, B, and C in terms of Q and J, and expanding the boundary condition equations.

The resulting currents (**L2+L1+P**) have the same vertical average as the layered fields (**L2+L1**), but include an Ekman component and a contribution from horizontal variations in

mass. The major disadvantage of this approach is the assumption that the model is at quasi-equilibrium, and in particular, that wind stresses are steady. So the winds used in both L1 and L2 models, consisting of a seven-day running average of the Navy Corrected Geostrophic Winds (Rhodes et al., 1986 and 1989), are sampled every three days with linear interpolation used in time between samples. As in the Year 3 simulations, heat fluxes are represented by relaxation to a monthly density climatology.

Experiment 212183.1 has been selected as the best two-layer simulation (L2). Model parameters are:

- Upper-layer inflow transport = $26 \times 10^6 \text{ m}^3 \text{ sec}^{-1}$ (26 Sv),
- Lower-layer inflow transport = $5 \times 10^6 \text{ m}^3 \text{ sec}^{-1}$ (5 Sv),
- Wind stress = seven day Navy Winds,
- Heat flux = relaxation to monthly density climatology,
- Horizontal eddy viscosity, $A = 200 \text{ m}^2/\text{sec}$,
- Horizontal density diffusivity, $ARHO = 1000 \text{ m}^2/\text{sec}$,
- Grid spacing = 20 by 22 km (0.2 by 0.2 degrees),
- Upper-layer reference thickness, $H1 = 200 \text{ m}$,
- Lower-layer reference thickness, $H2 = 3,450 \text{ m}$,
- Minimum depth of bottom topography = 300 m,
- Beta, $d\text{fldy} = 2 \times 10^{-11} \text{ m}^{-1} \text{ sec}^{-1}$,
- Coriolis parameter at the southern boundary, $f = 4.5 \times 10^{-5} \text{ sec}^{-1}$,
- Gravitational acceleration, $g = 9.8 \text{ m}/\text{sec}^2$,
- Reference reduced gravity, $g' = .025 \text{ m}/\text{sec}^2$,
- Interfacial stress = 0,
- Coefficient of quadratic bottom stress = .002, and
- Time step = 0.5 hours.

The simulation was spun up from rest for 10 years to reach statistical equilibrium and then run for another 10 years. All results are from the last 10 years. Figures 18-25 show free surface deviation and upper-layer density deviation every 90 days for a typical Loop Current eddy cycle. This sequence was forced by winds from 1971 and 1972, but the simulation is not intended to be a hindcast, *i.e.*, the circulation is typical of the Gulf, but does not represent the actual Gulf in 1971 and 1972. The path of the Loop Current eddy, into the southwest Gulf and then north to the Texas coast, is typical of large eddies. The simulation includes smaller **Loop** Current eddies that take a path due west, rather than southwest. Figures 26 and 27 show free surface deviation every 90 days for a typical cycle that includes **the reabsorption** of an eddy by the Loop Current. Over the 10-

Figure 18. Instantaneous view of (a) the free surface deviation and (b) the upper-layer density deviation from Experiment 212/83.1 on wind Date 093/1971.

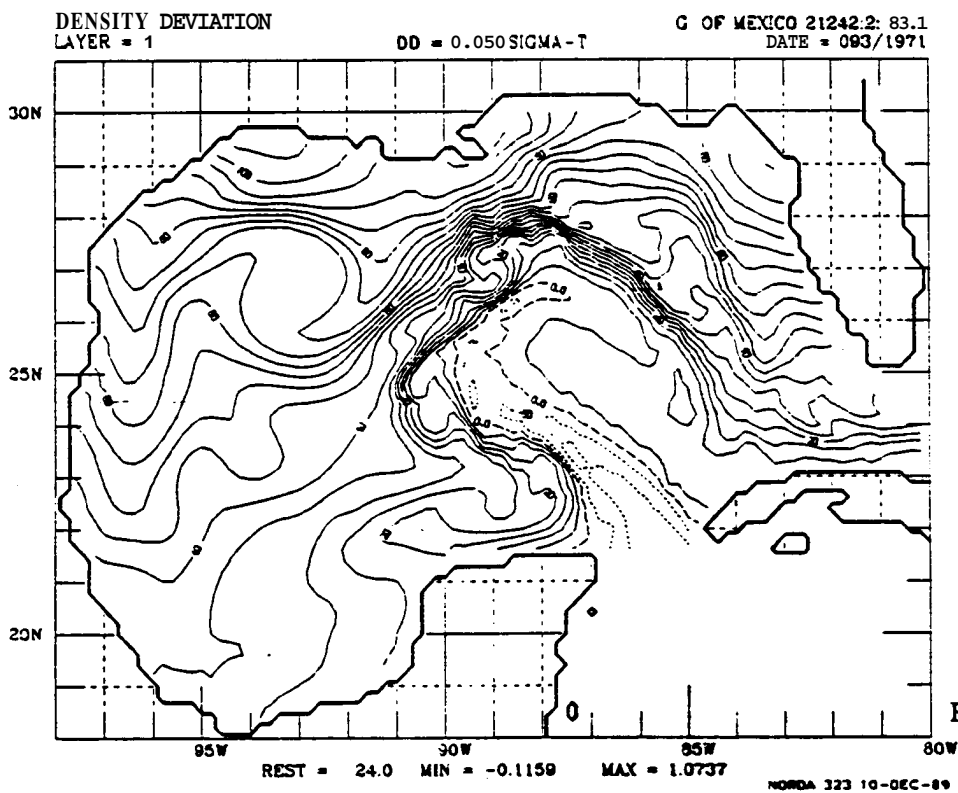
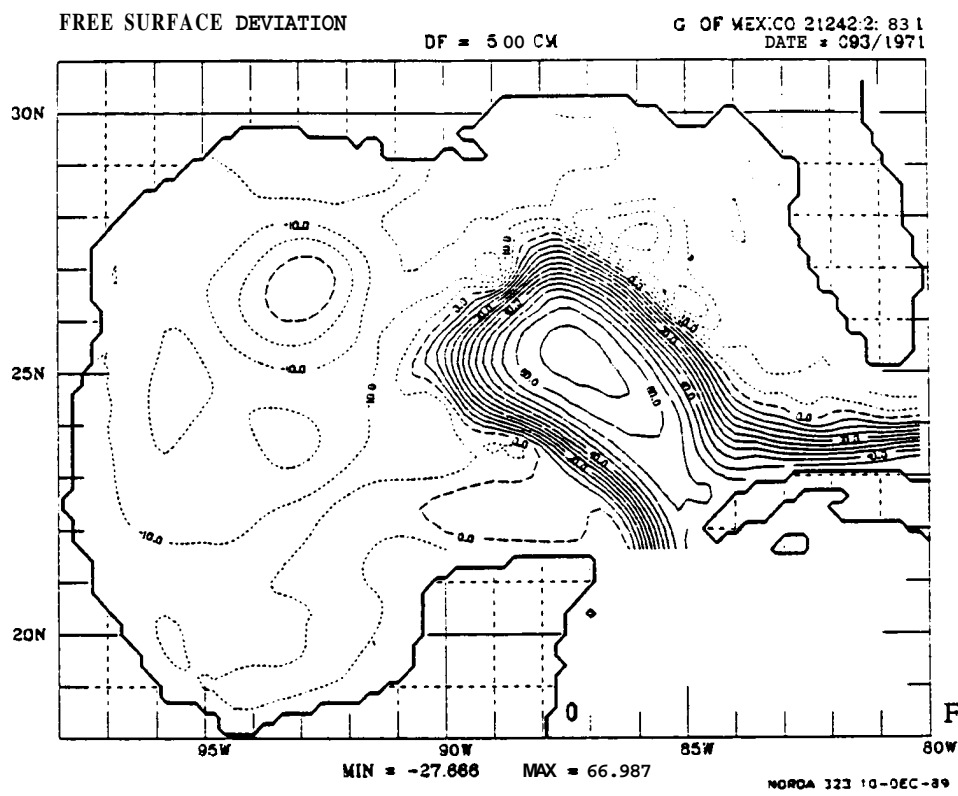


Figure 19. Instantaneous view of (a) the free surface deviation and (b) the upper-layer density deviation from Experiment 212/83.1 on wind Date 183/1971.

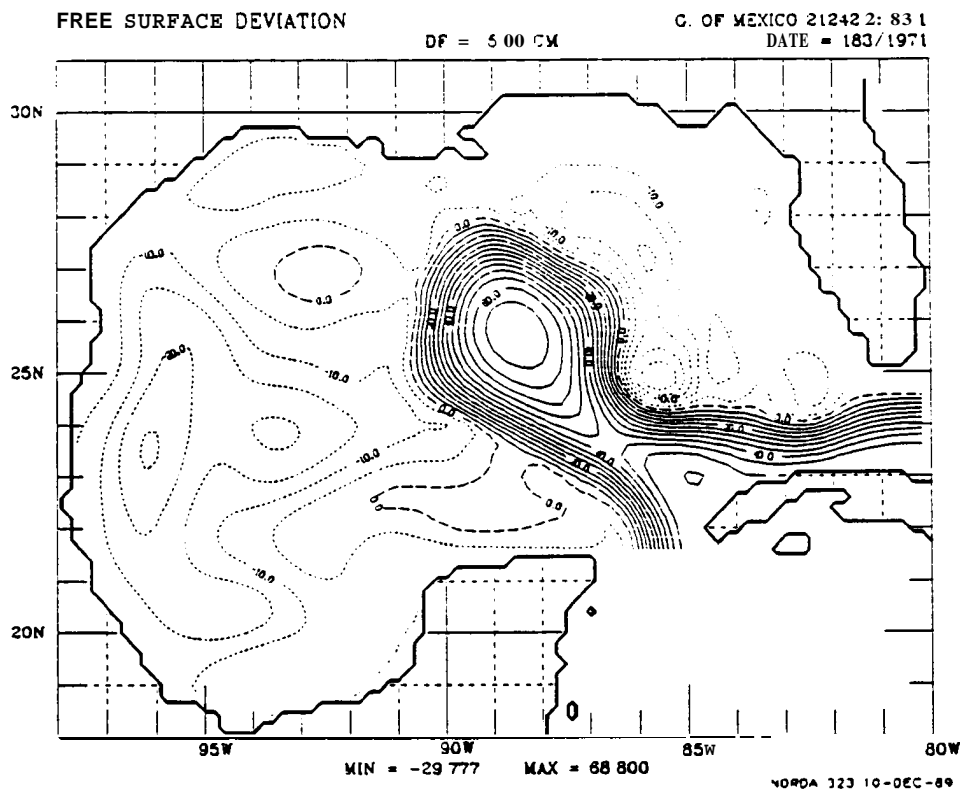


FIGURE 19b

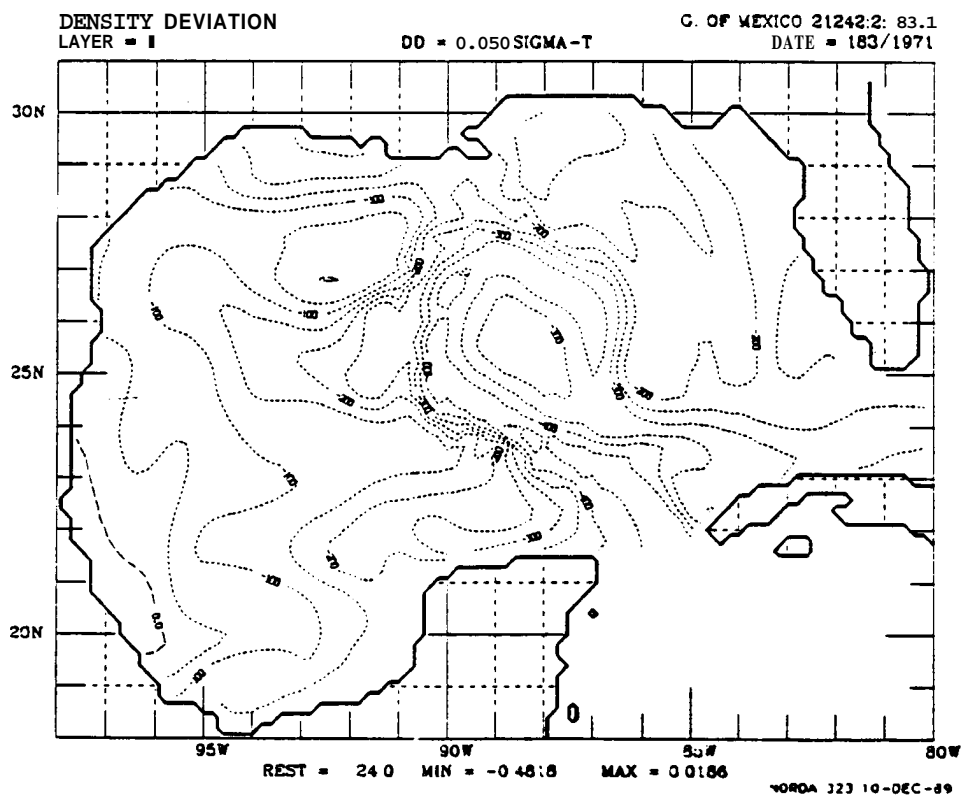


FIGURE 19a

Figure 20. Instantaneous view of (a) the free surface deviation and (b) the upper-layer density deviation from Experiment 212/83.1 on wind Date 273/1971.

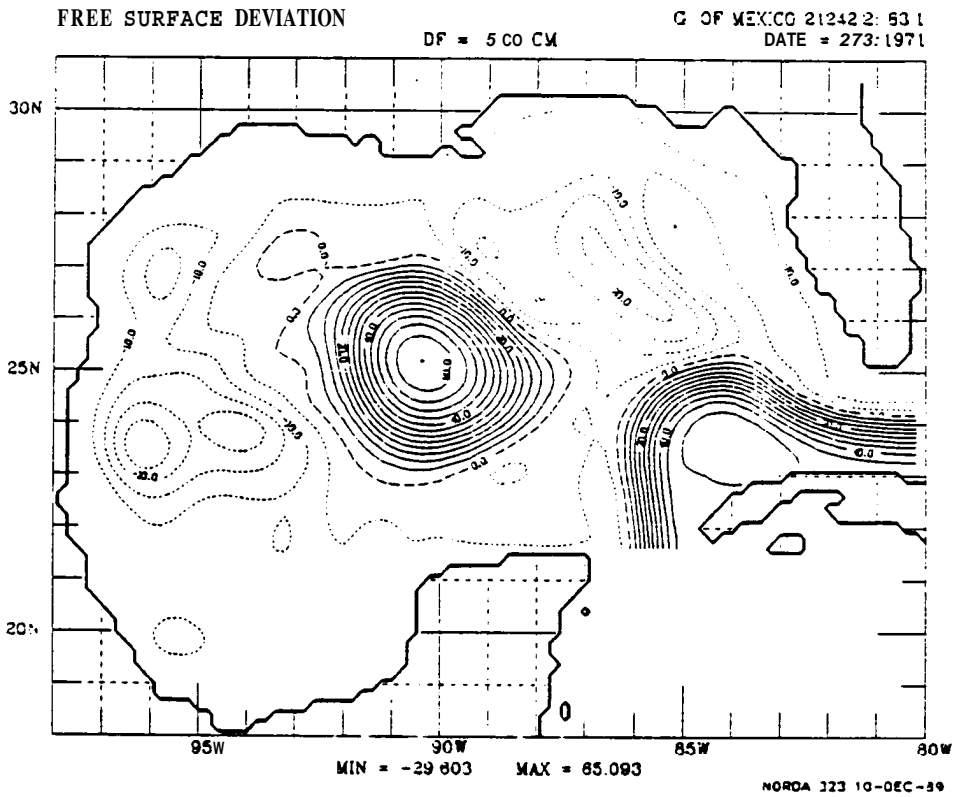


FIGURE 20a

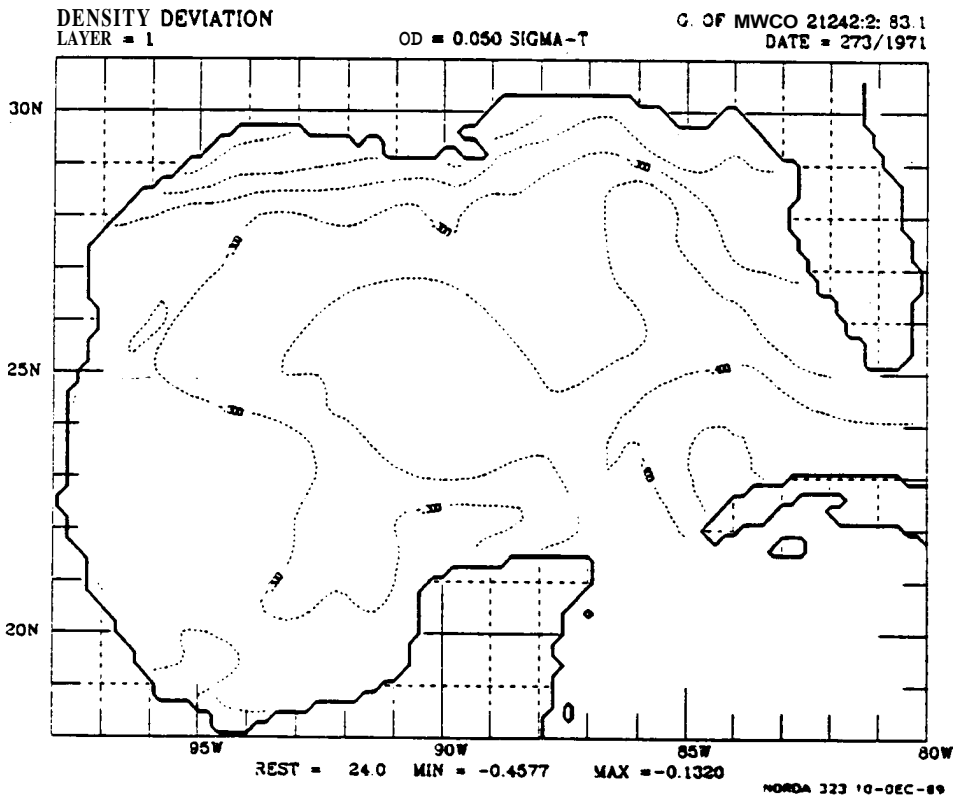


FIGURE 20b

Figure 21. Instantaneous view of (a) the free surface deviation and (b) the upper-layer density deviation from Experiment 212/83.1 on wind Date 004/1972.

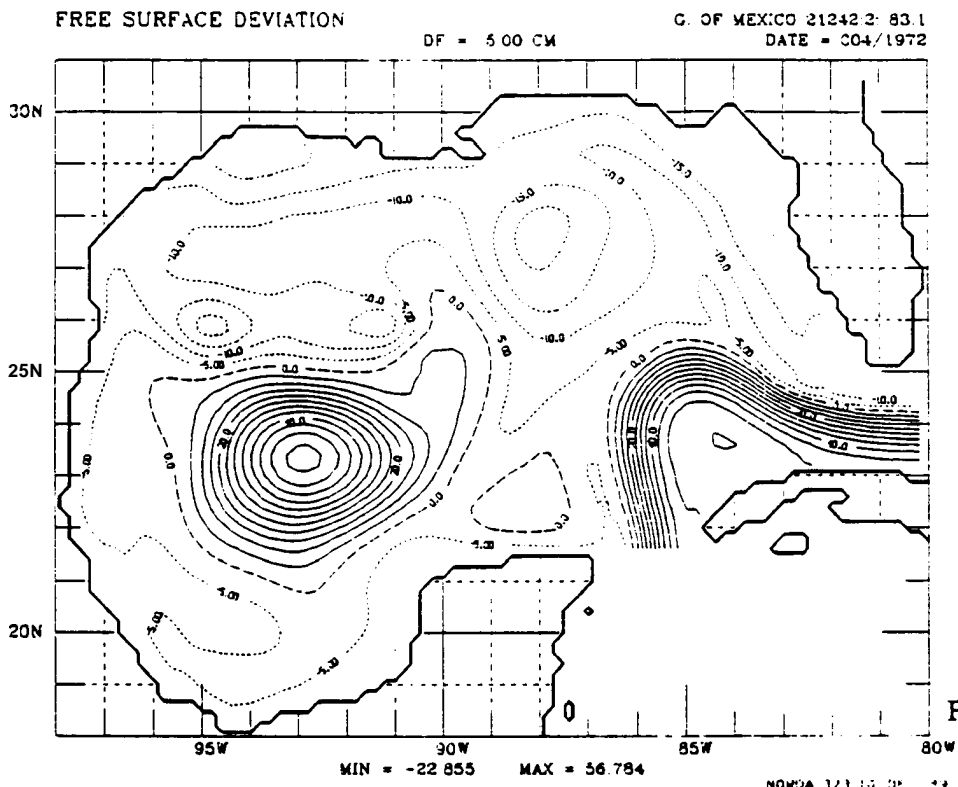


FIGURE 21a

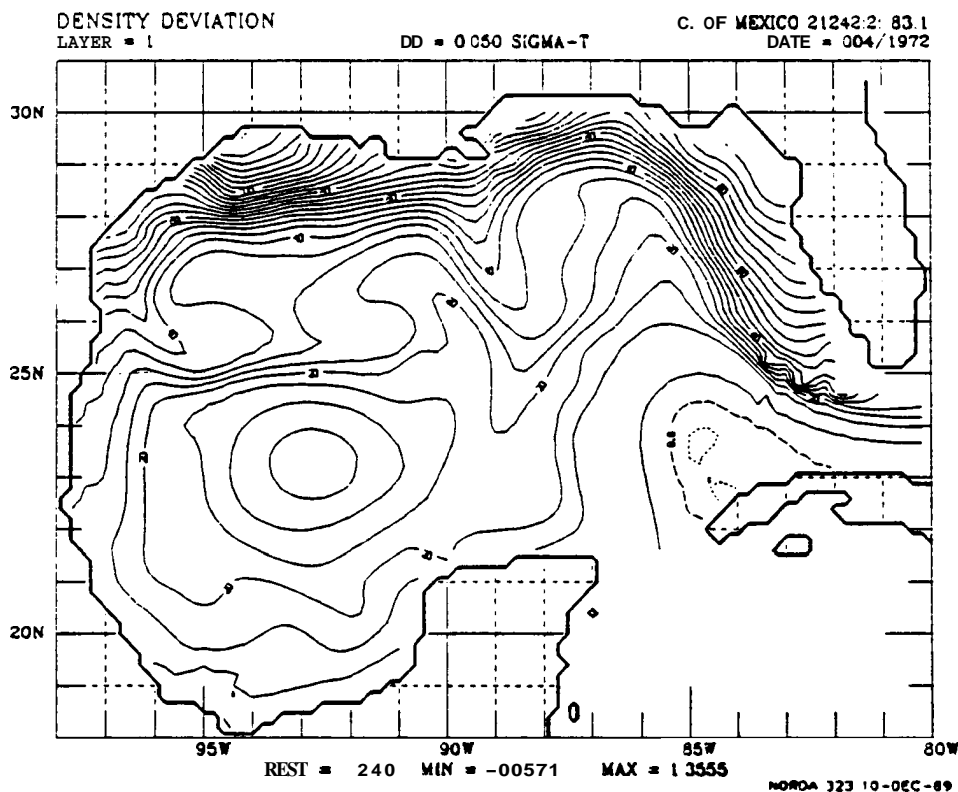


FIGURE 21b

Figure 22. Instantaneous view of (a) the free surface deviation and (b) the upper-layer density deviation from Experiment 212/83.1 on wind Date 094/1972.

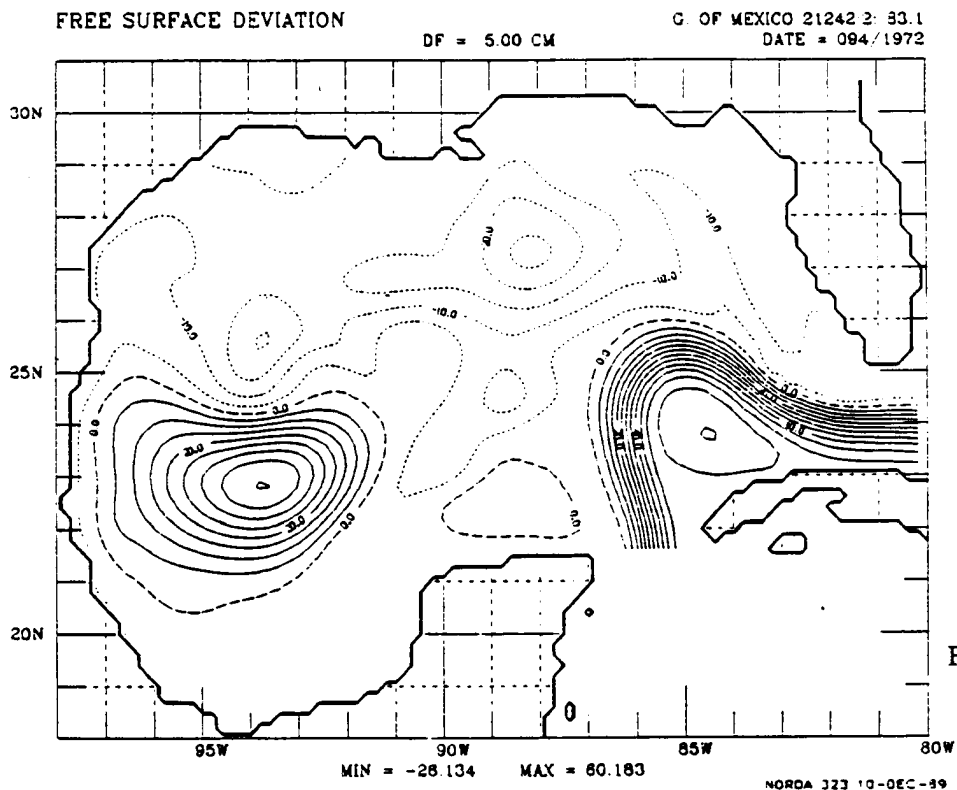


FIGURE 22a

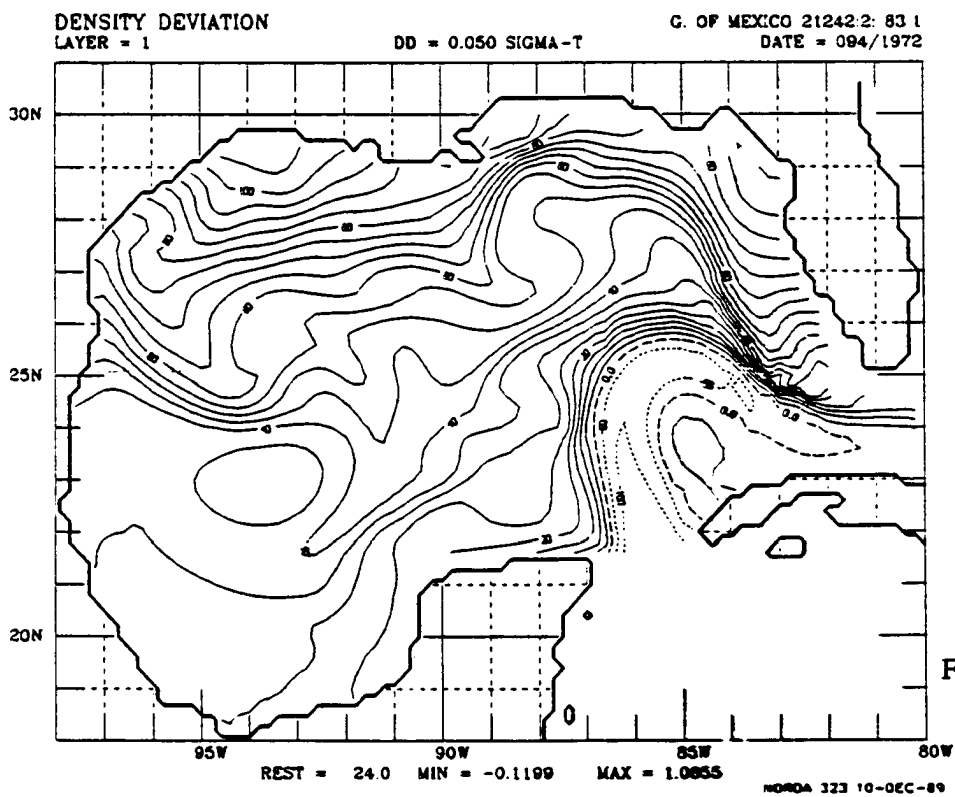


FIGURE 22b

Figure 23. Instantaneous view of (a) the free surface deviation and (b) the upper-layer density deviation from Experiment 212/83.1 on wind Date 184/1972.

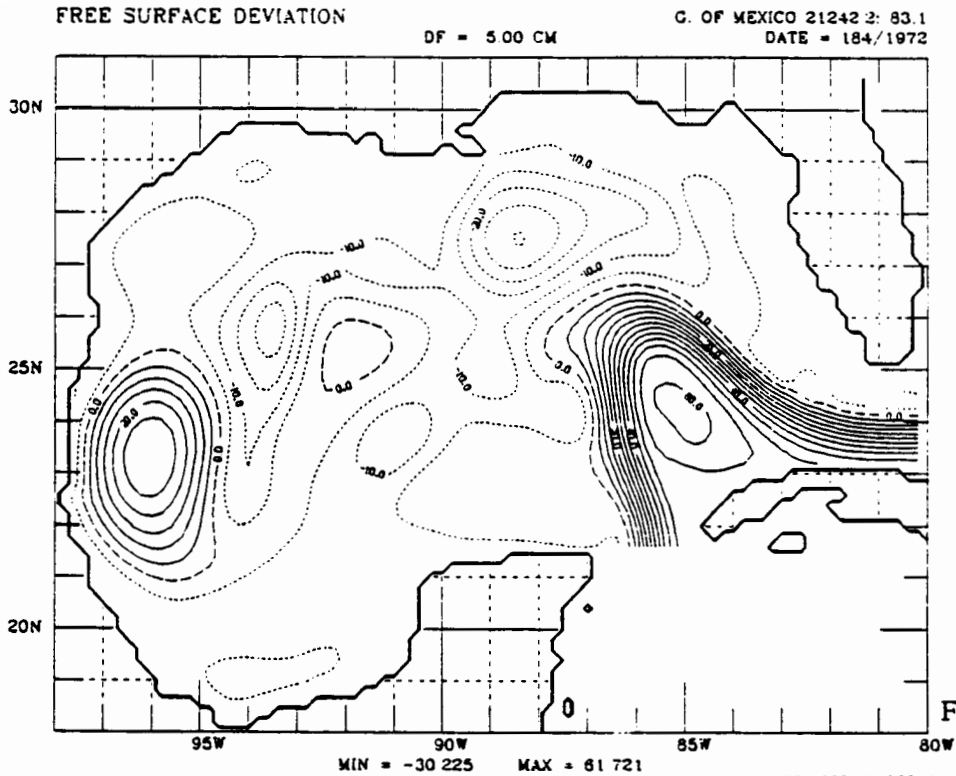


FIGURE 23a

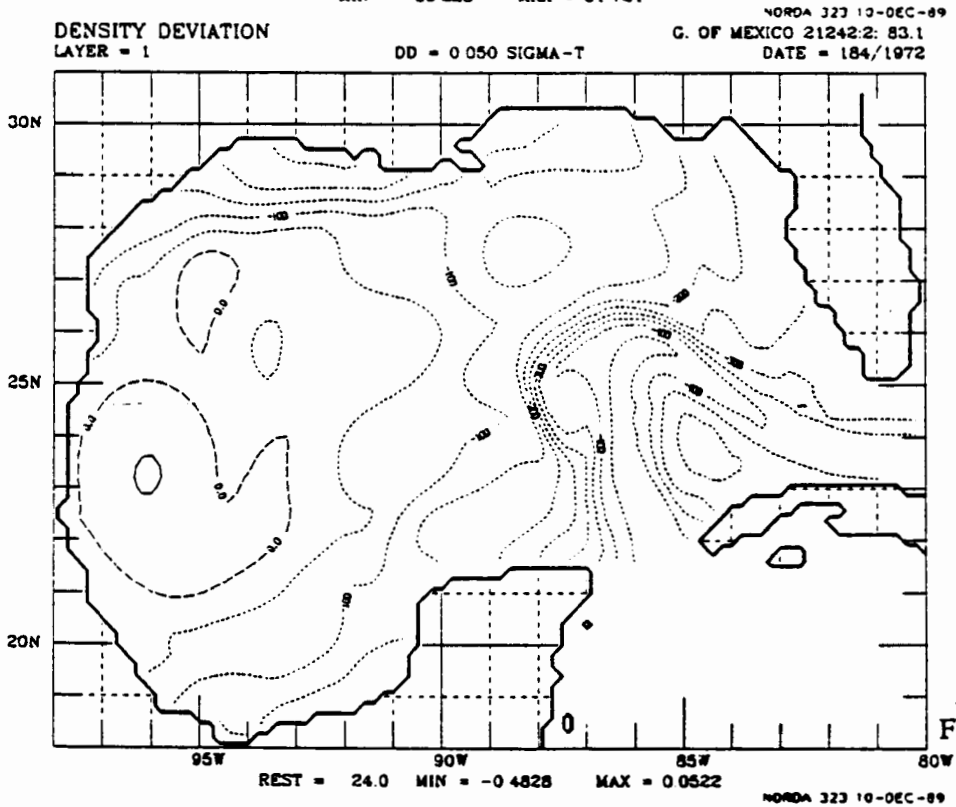


FIGURE 23b

Figure 24. Instantaneous view of (a) the free surface deviation and (b) the upper-layer density deviation from Experiment 212/83.1 on wind Date 274/1972.

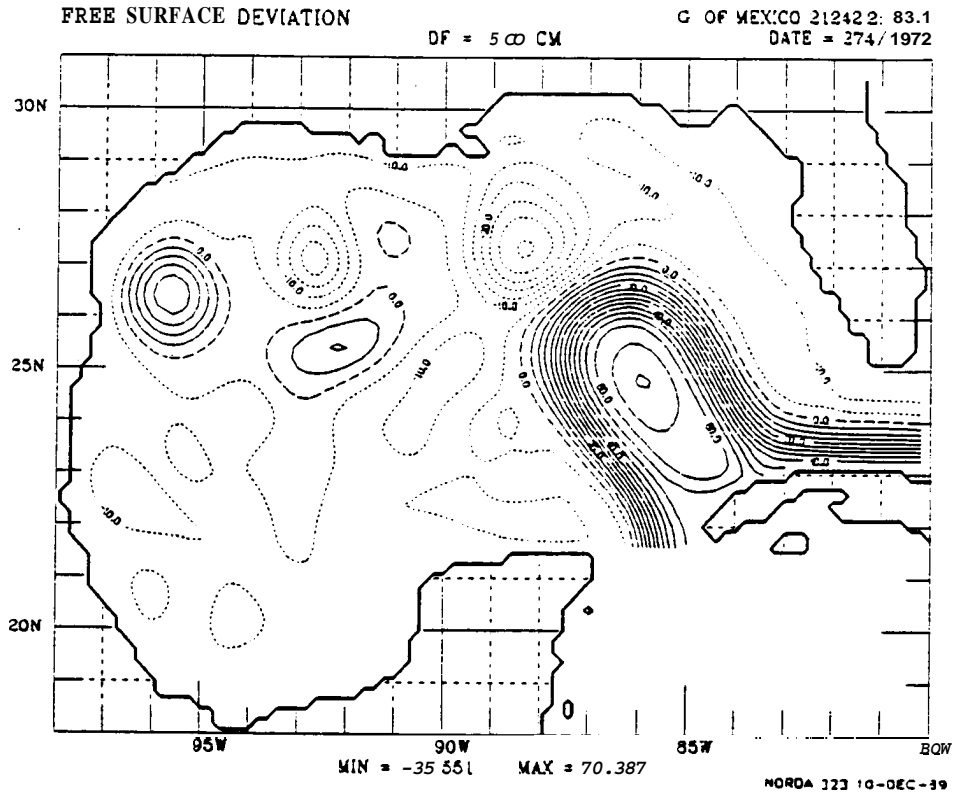


FIGURE 24a

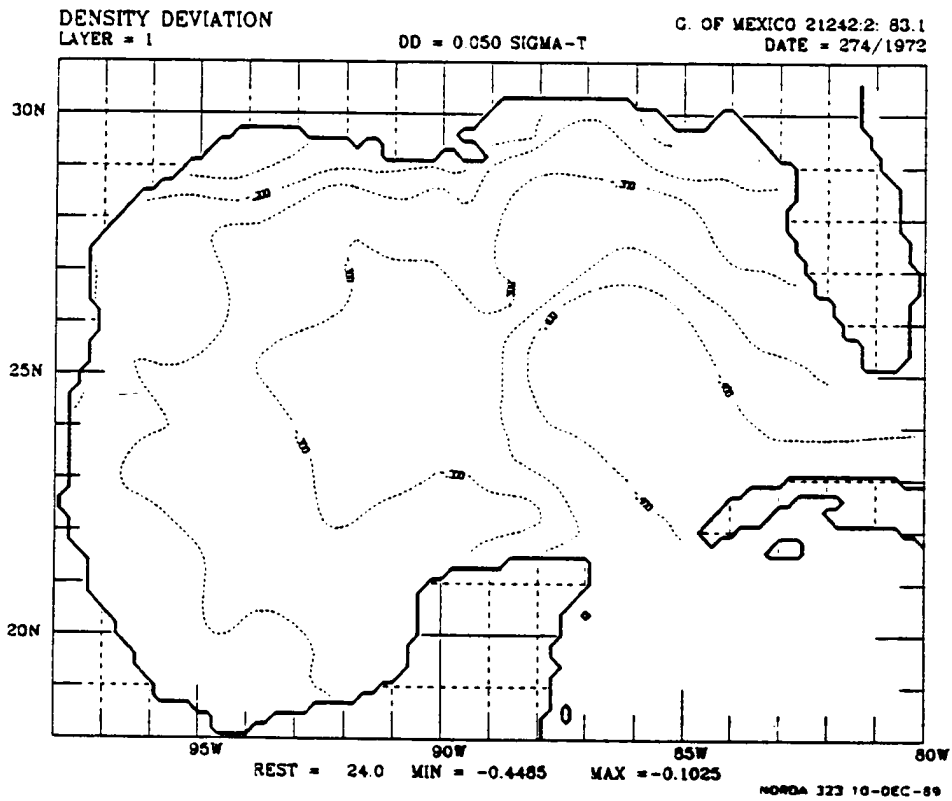


FIGURE 24b

Figure 25. Instantaneous view of (a) the free surface deviation and (b) the upper-layer density deviation from Experiment 212/83.1 on wind Date 004/1973.

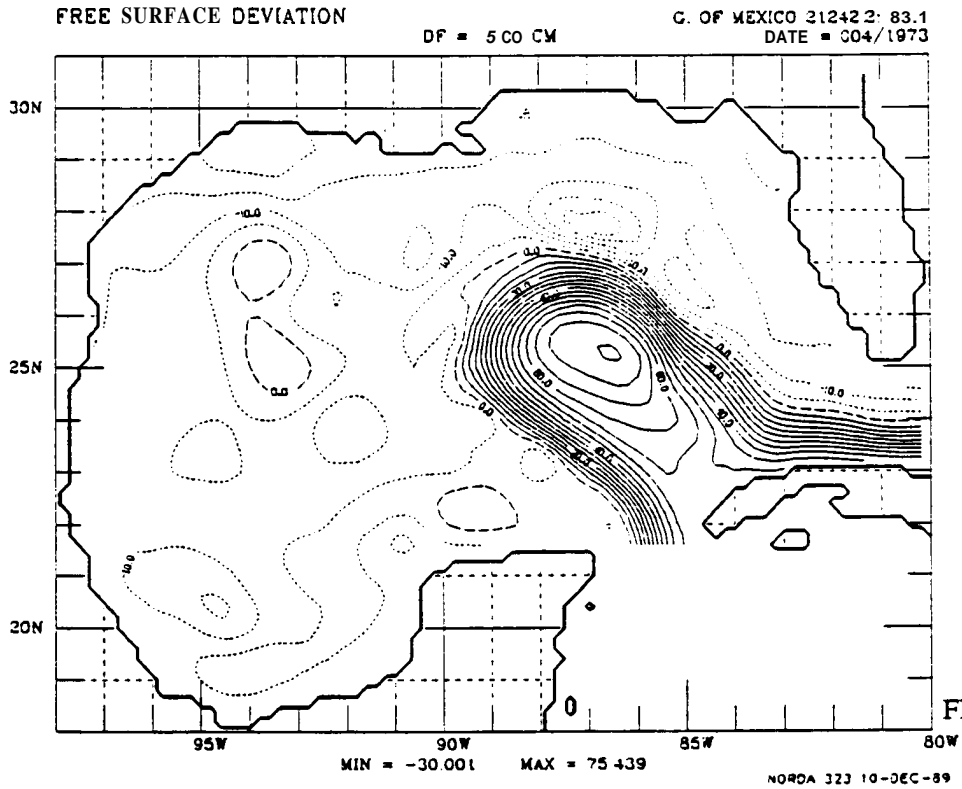


FIGURE 25a

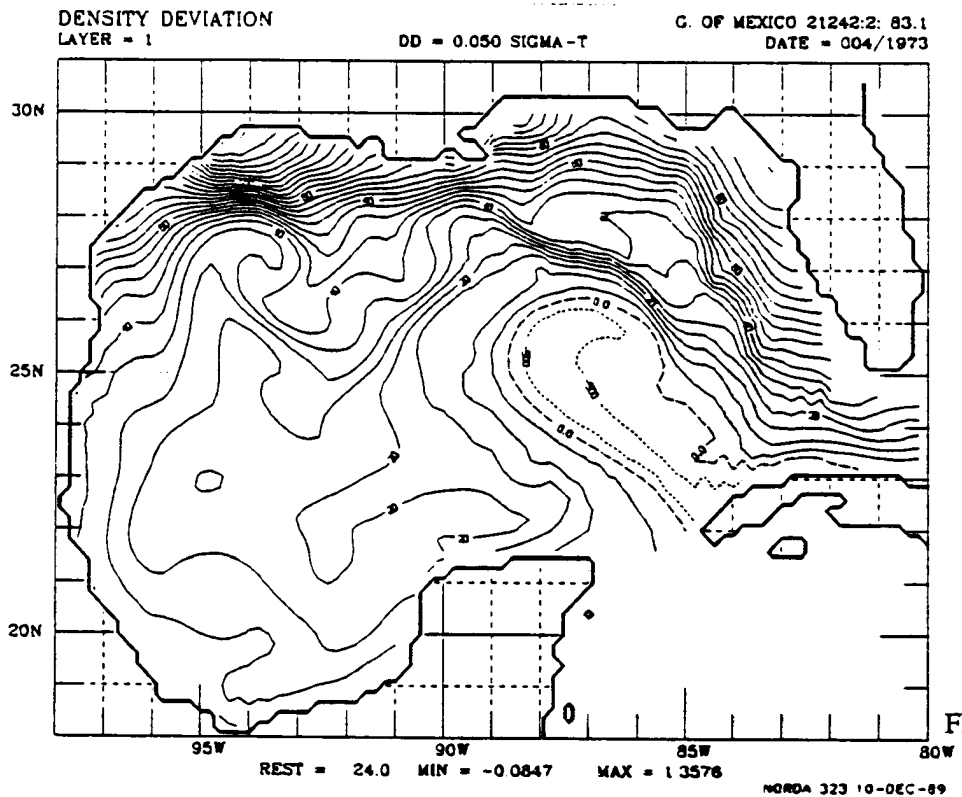


FIGURE 25b

Figure 26. Instantaneous view of the free surface deviation from Experiment 212/83.1 on wind Dates (a) 005/1974 and (b) 095/1974.

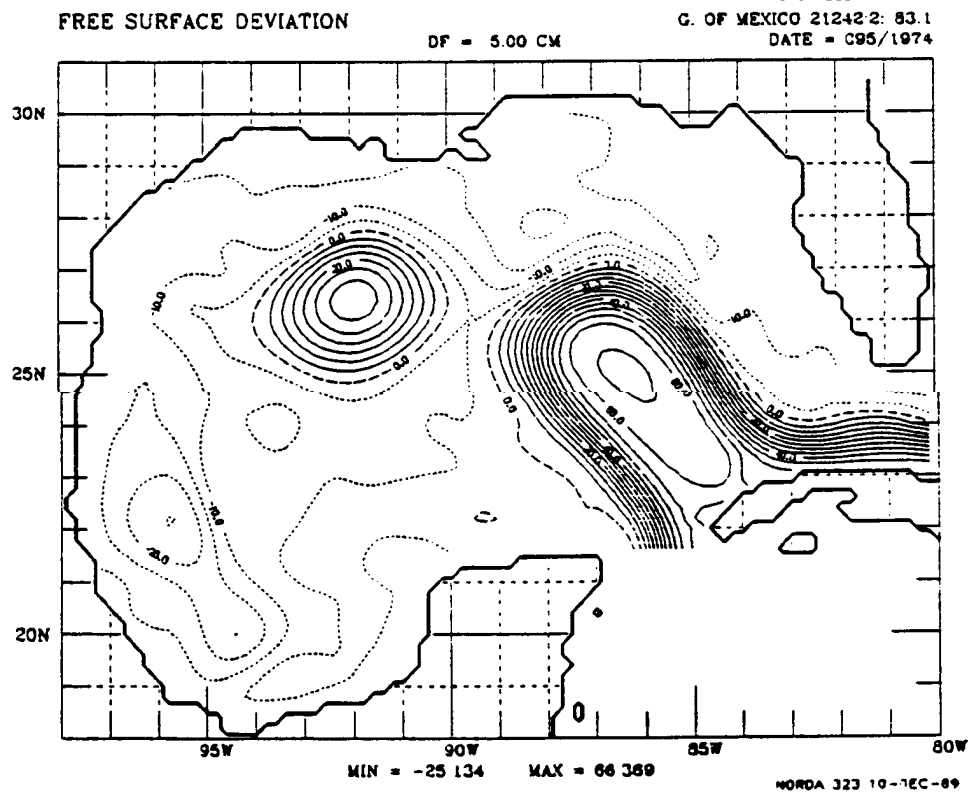
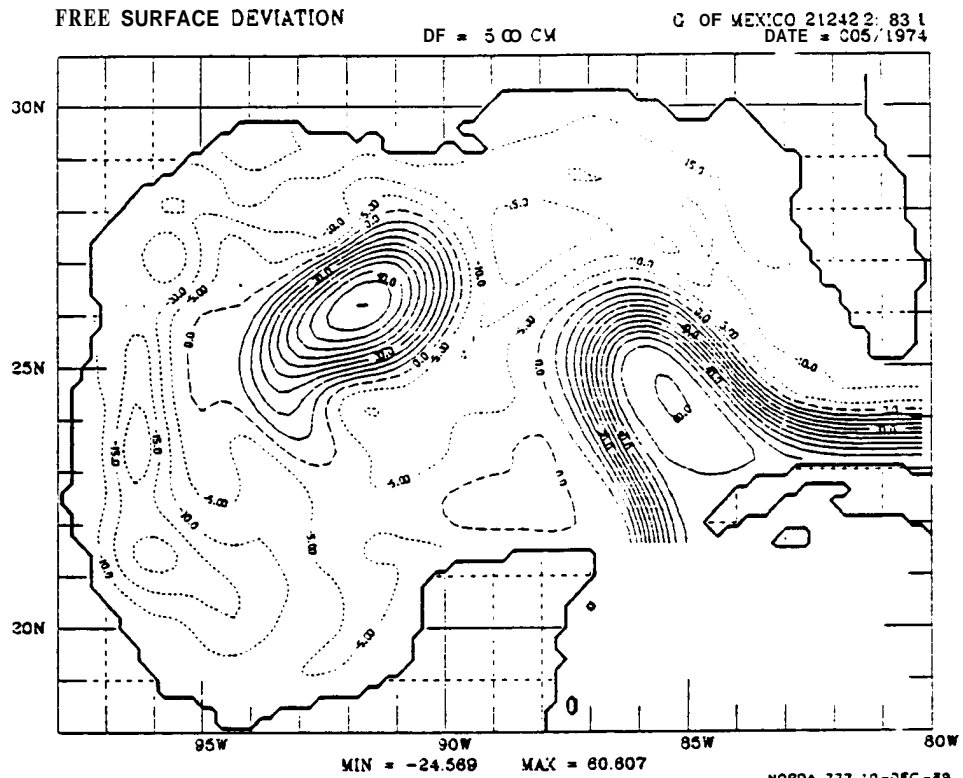
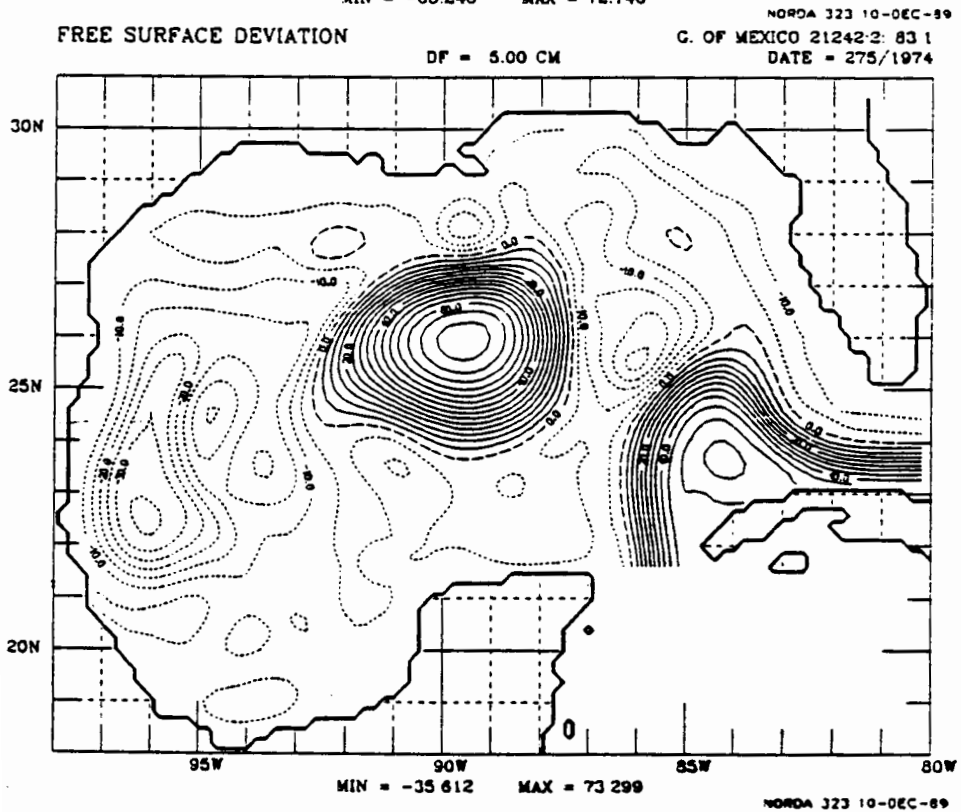
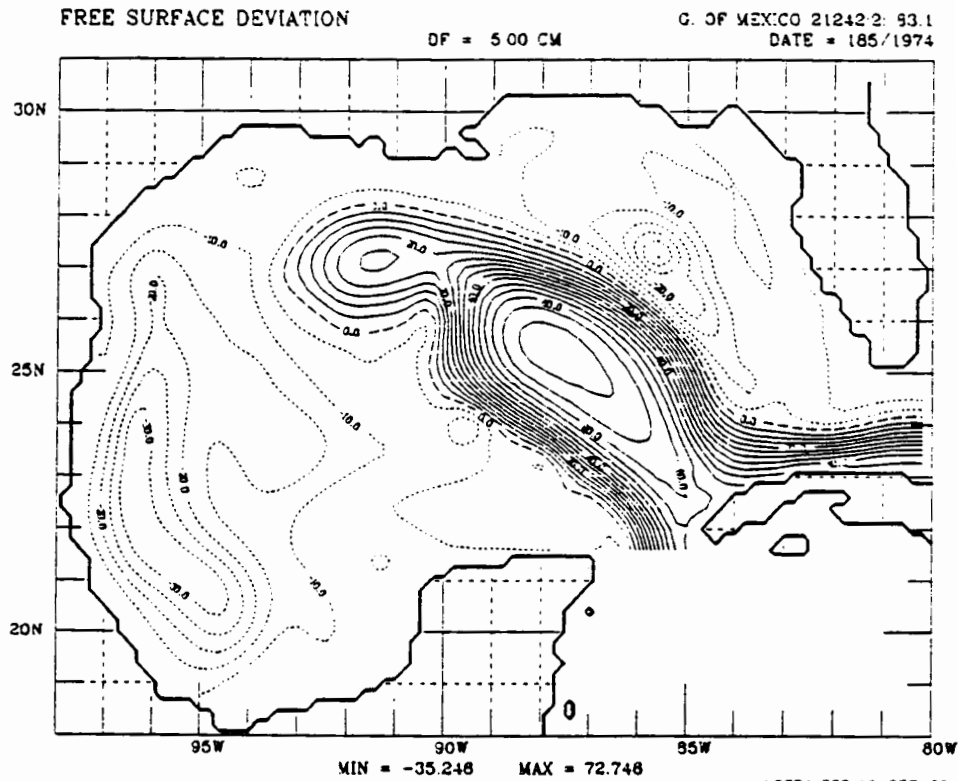


Figure 27. Instantaneous view of the free surface deviation from Experiment 212/83.1 on wind Dates (a) 185/1974 and (b) 275/1974.



year period, six eddies are shed from the **Loop** Current. The average Loop Current eddy shedding cycle in the simulation is perhaps as much as twice that of the actual Gulf. This may be partly due to the additional friction from the shelf mixing. The effective distance between the Yucatan and Florida Straits is also reduced by the shelf mixing and has also been shown to have the effect of increasing the shedding period in the case of highly idealized Gulf of Mexico geometries (Hurlburt and Thompson, 1980).

Figure 28 shows interface deviation and upper-layer density deviation annual climatologies over the 10 years for Experiment **121/83.1**. These fields are comparable to the depth of the thermocline and the temperature at that depth (*i.e.*, Robinson, 1973). Figures 29-32 show monthly climatologies for January, April, July, and October. There is a clear seasonal cycle in the density climatology, but a 10-year sample length is too short for any significance to be placed in most of the differences in the interface deviation fields.

Experiment **212/80.0** has been selected as the best one-layer simulation (**L1**). Model parameters are:

- Upper-layer inflow transport = $10 \times 10^6 \text{ m}^3 \text{ sec}^{-1}$ (10 Sv),
- Wind stress = seven-day Navy winds,
- Horizontal eddy viscosity, $A = 200 \text{ m}^2/\text{sec}$,
- Grid spacing = 20 by 22 km (0.2 by 0.2 degrees),
- Upper-layer reference thickness, $H1 = 3,650 \text{ m}$,
- Minimum depth of bottom topography = 30 m,
- Beta, $df/dy = 2 \times 10^{-11} \text{ m}^{-1} \text{ sec}^{-1}$,
- Coriolis parameter at the southern boundary, $f = 4.5 \times 10^{-5} \text{ sec}^{-1}$,
- Gravitational acceleration, $g = 9.8 \text{ m}/\text{sec}^2$,
- Coefficient of quadratic bottom stress = **.002**, and
- Time step = 0.5 hours.

The simulation was spun up from rest for six years to reach statistical equilibrium and then run for another 10 years. All results are from the last 10 years. The forcing fields are identical to those used in Experiment **121/83.1**. The final 10 years of the two simulations have been merged as described above (**L2+L1**). Figure 33 shows upper-layer currents from both experiments (**L2** and **L1**) on the same day for the Texas shelf region. The 100 and 200 meter topography depth contours are included to show the blending region. Figure 34 shows the corresponding merged

Figure 28. Annual climatology, from 10 years of Experiment 212/83.1 (a) interface deviation and (b) upper-layer density deviation.

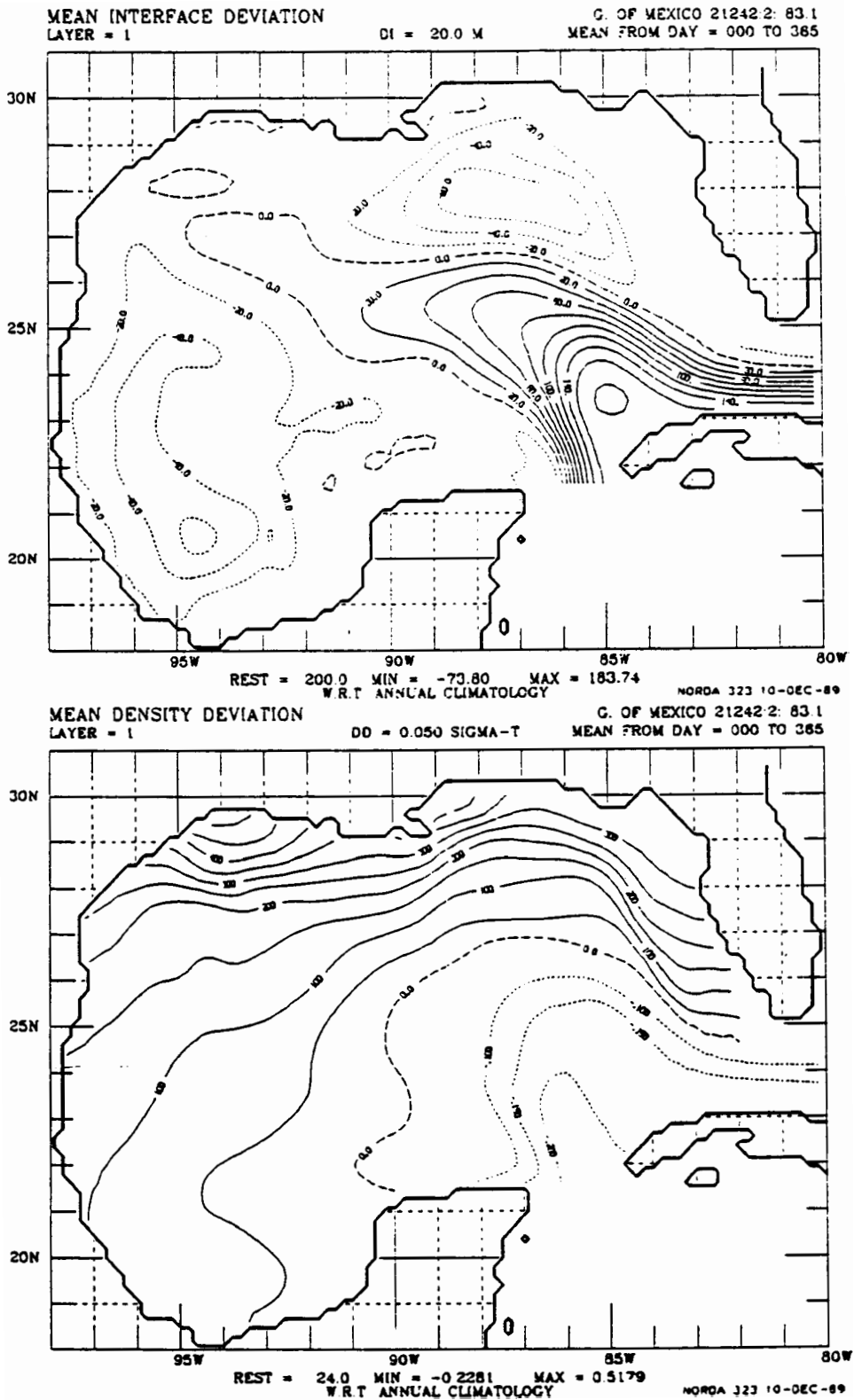


Figure 29. Monthly climatology for January from 10 years of Experiment 212/83.1 (a) interface deviation and (b) upper-layer density deviation.

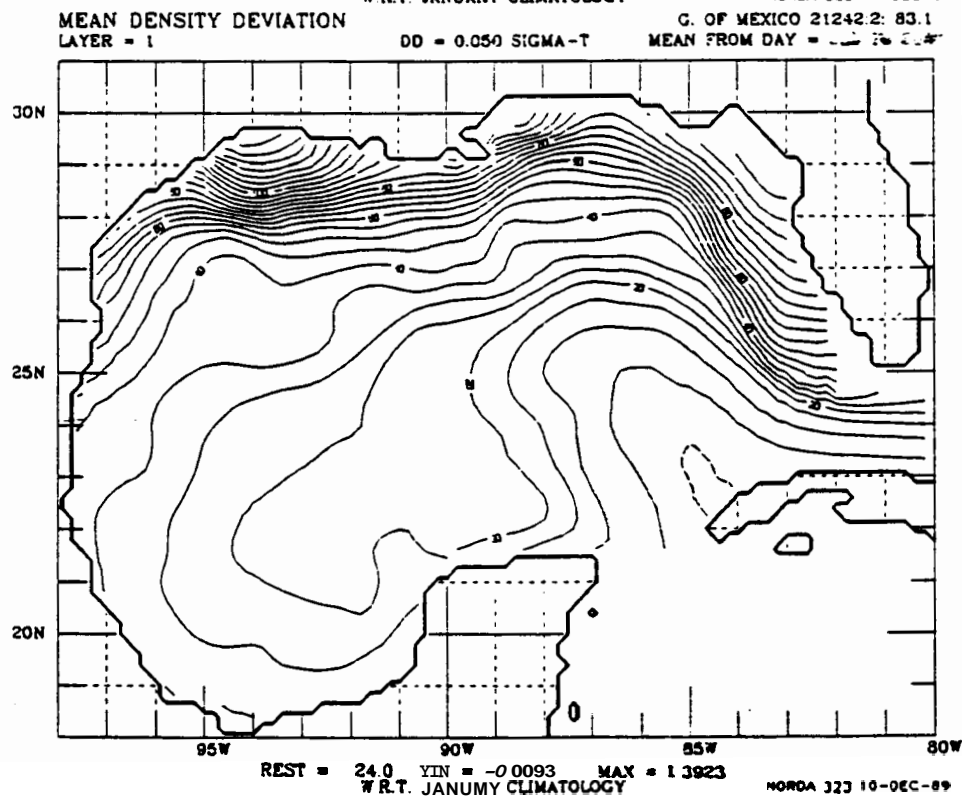
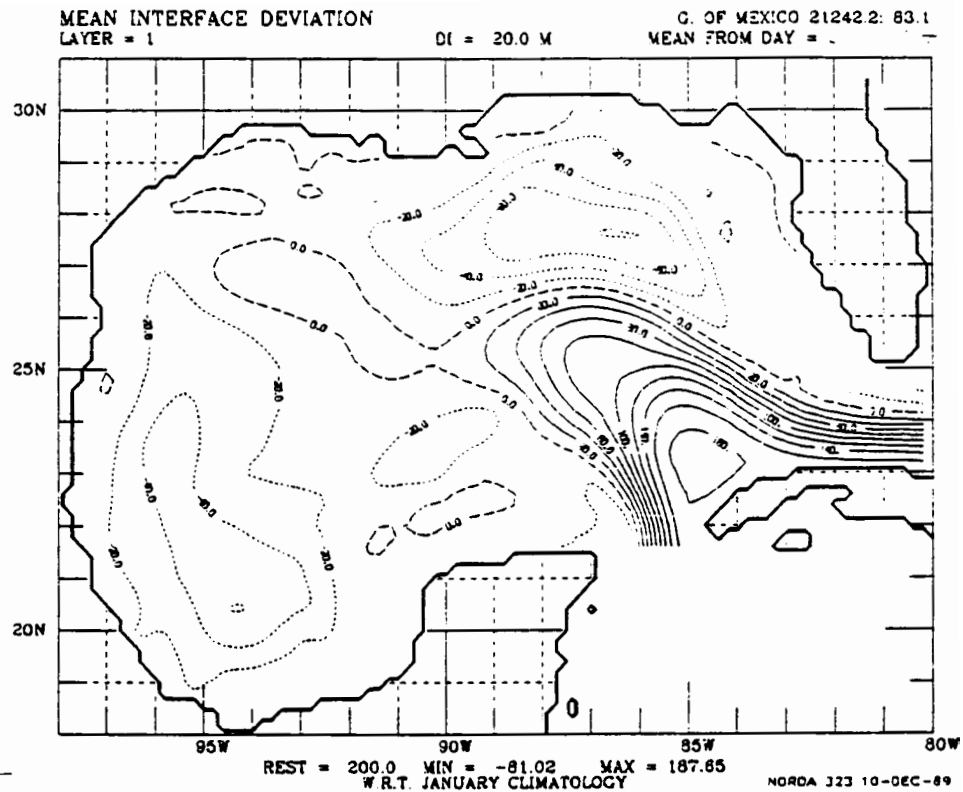


Figure 30. Monthly climatology for April from 10 years of Experiment 212/83.1 (a) interface deviation and (b) upper-layer density deviation.

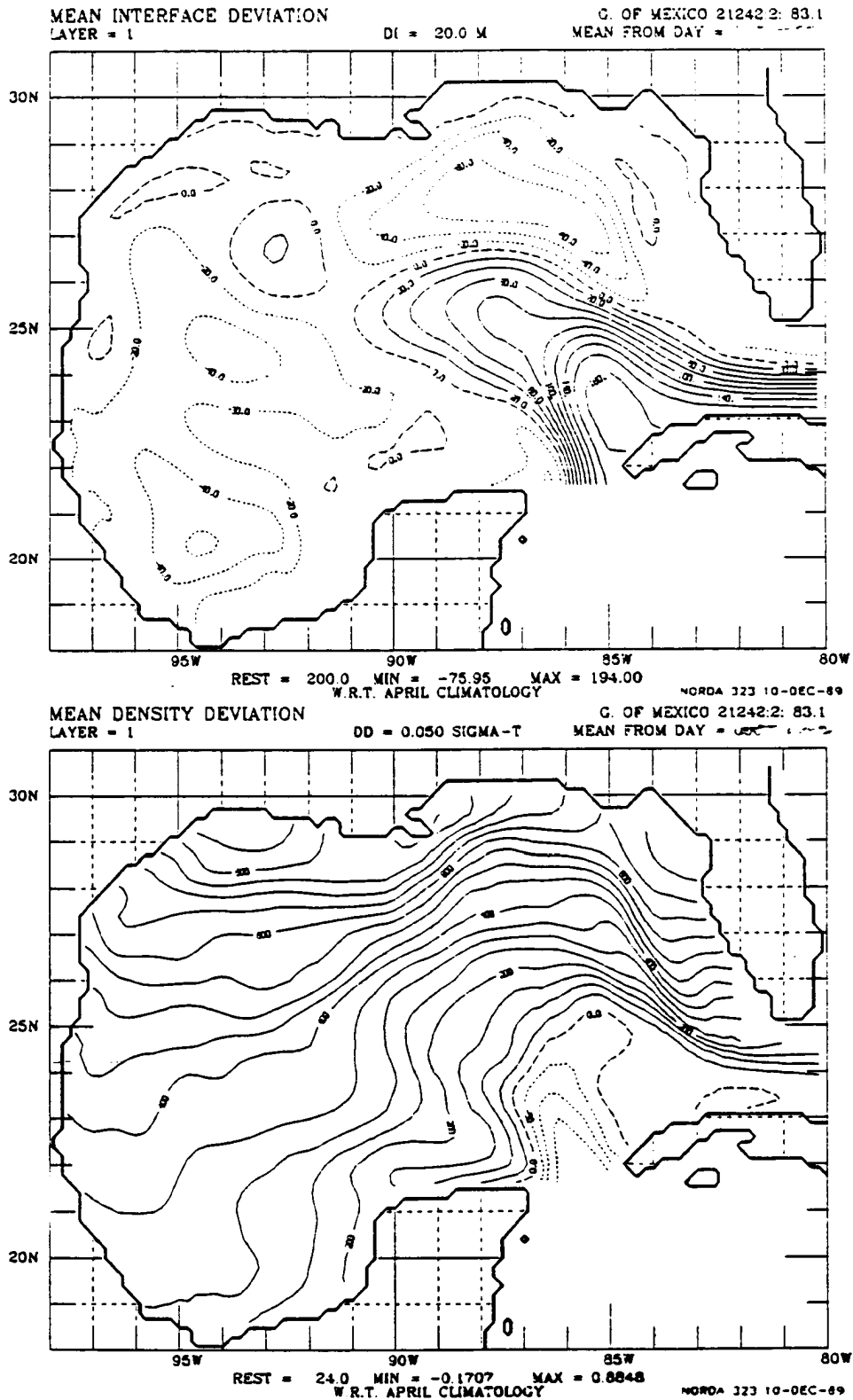


Figure 31. Monthly climatology for July from 10 years of Experiment 212/83.1 (a) interface deviation and (b) upper-layer density deviation.

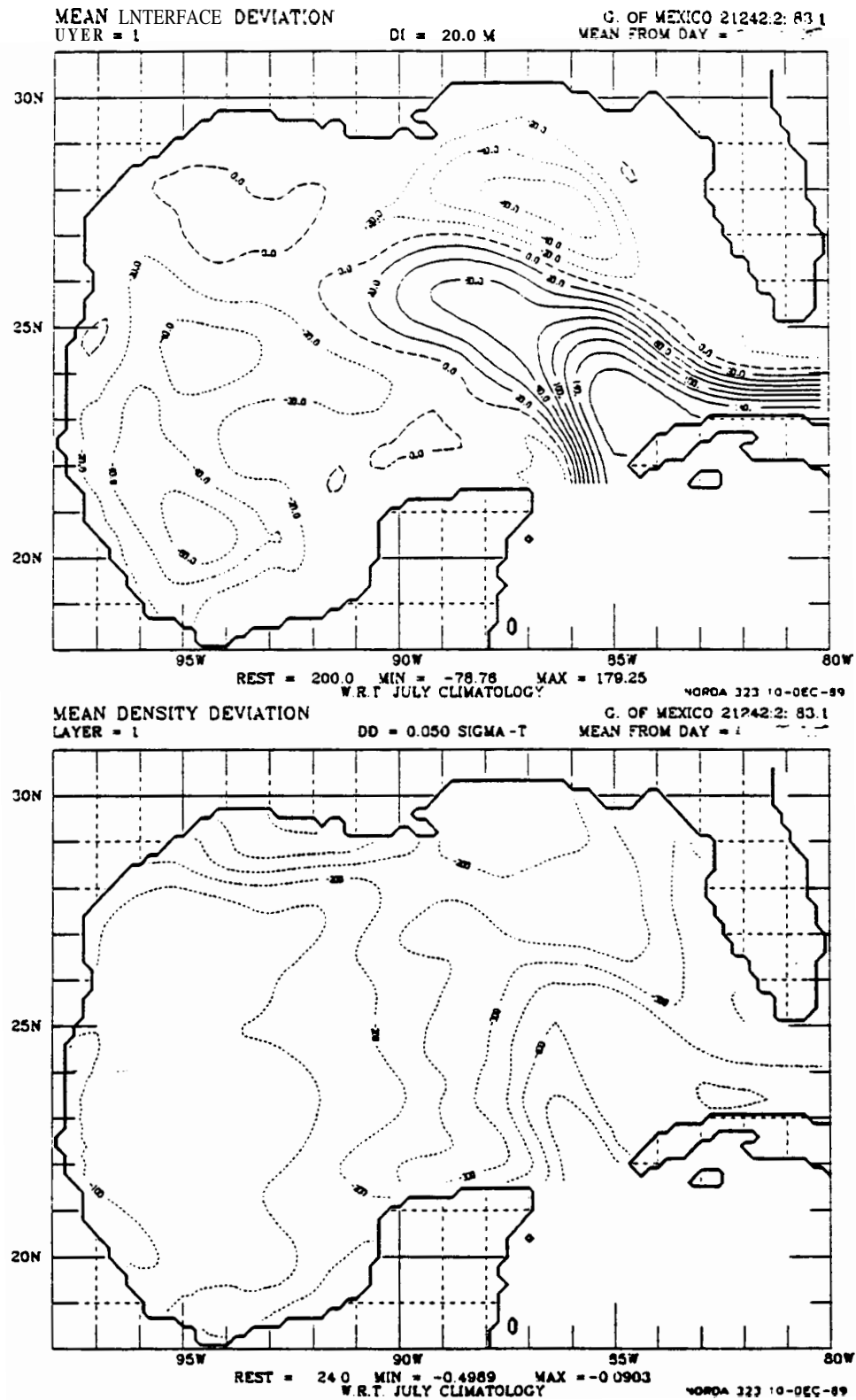


Figure 32. Monthly climatology for October from 10 years of Experiment 212/83.1 (a) interface deviation and (b) upper-layer density deviation.

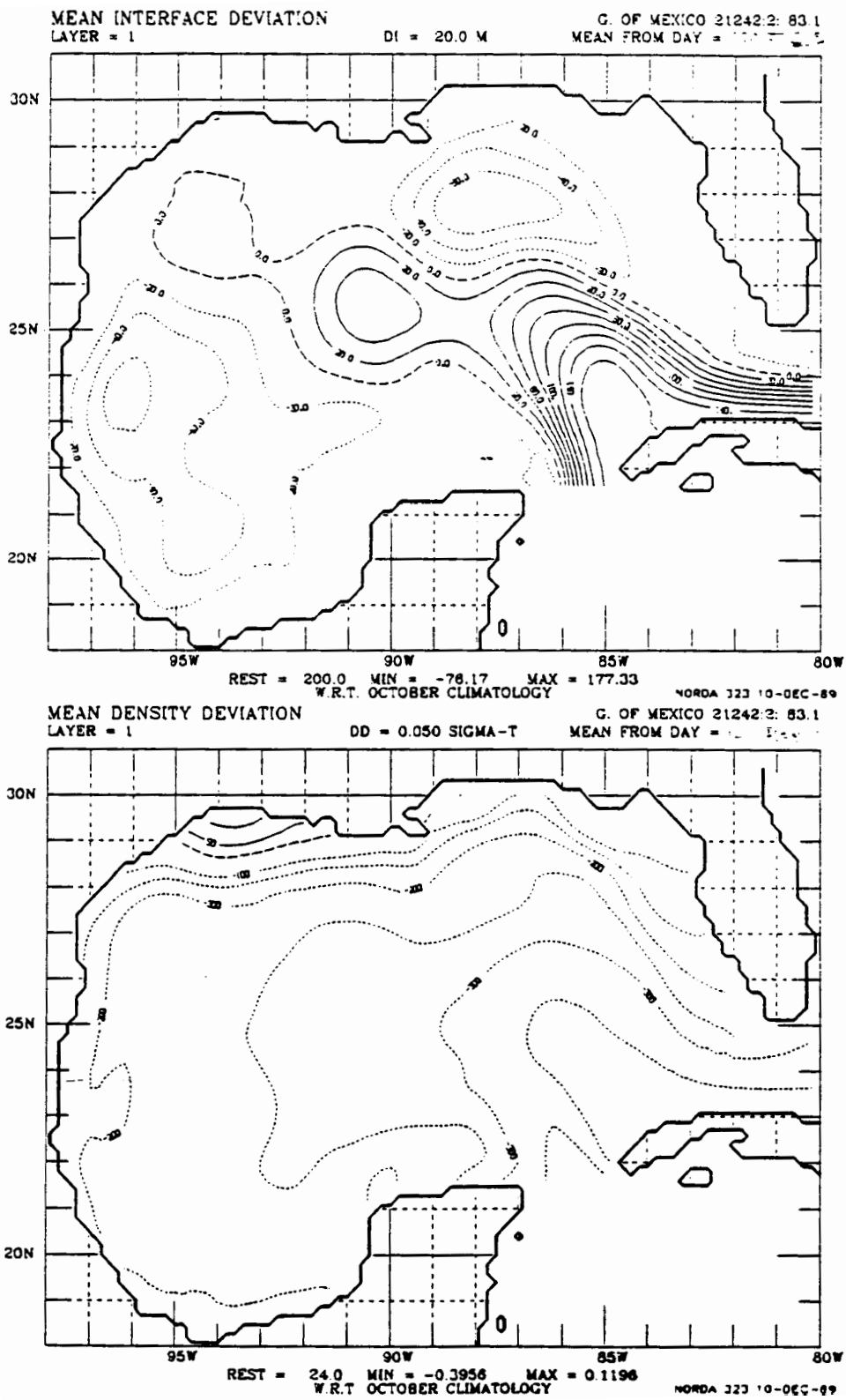


Figure 33. Upper-layer current vectors and bottom topography contours for the Texas shelf on wind Day 001/1969 for (a) one-layer Experiment 212/80.0 and (b) two-layer Experiment 212/83.1.

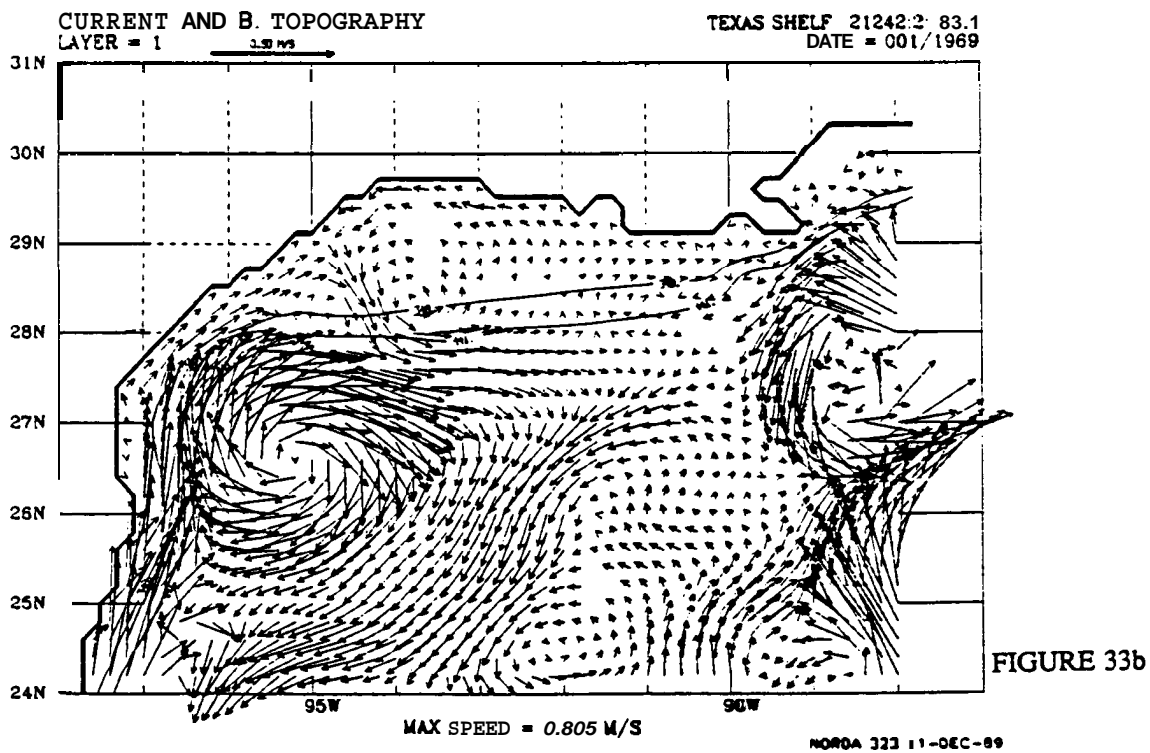
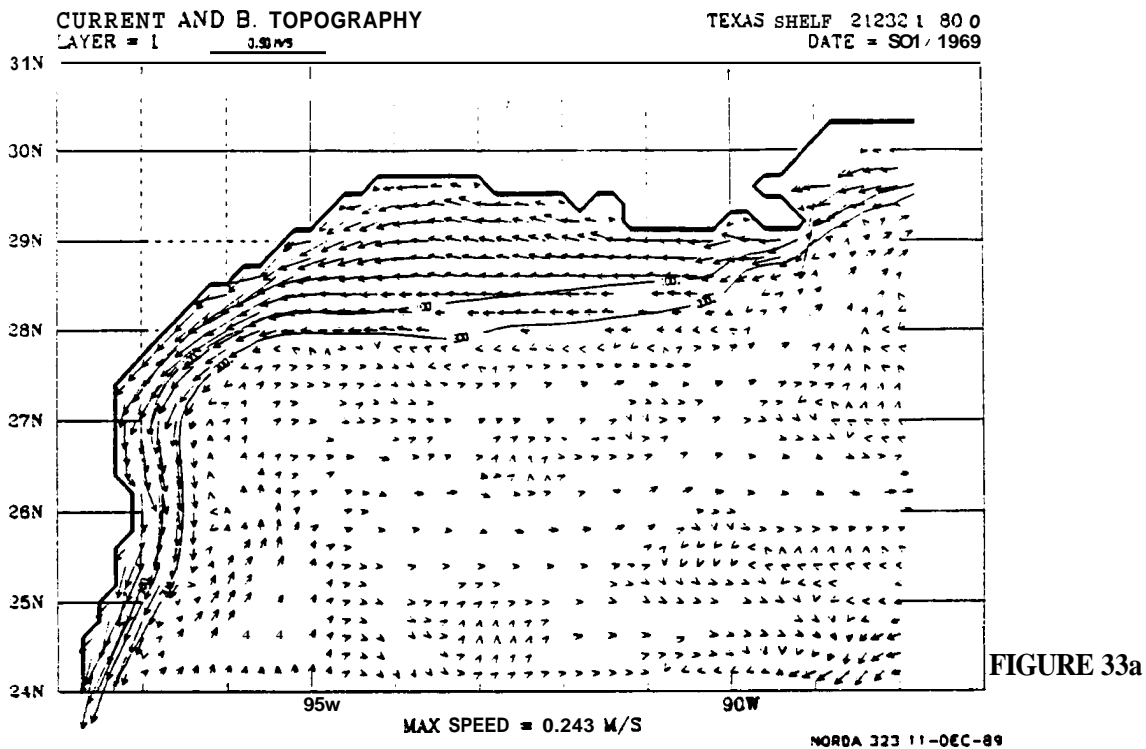
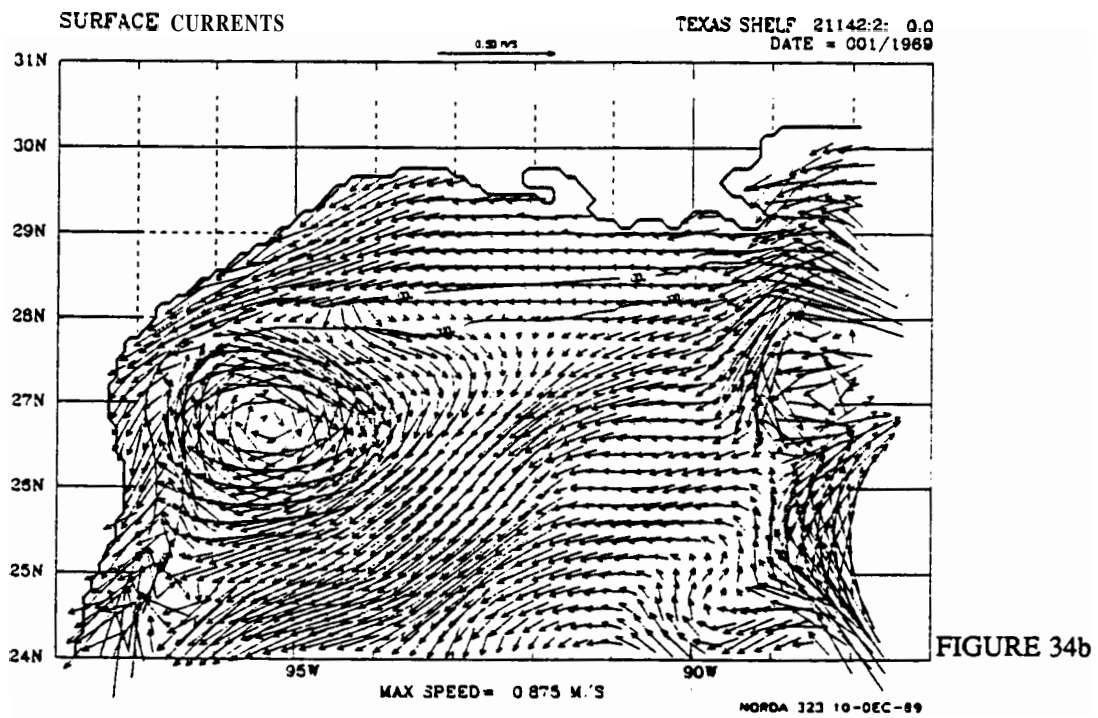
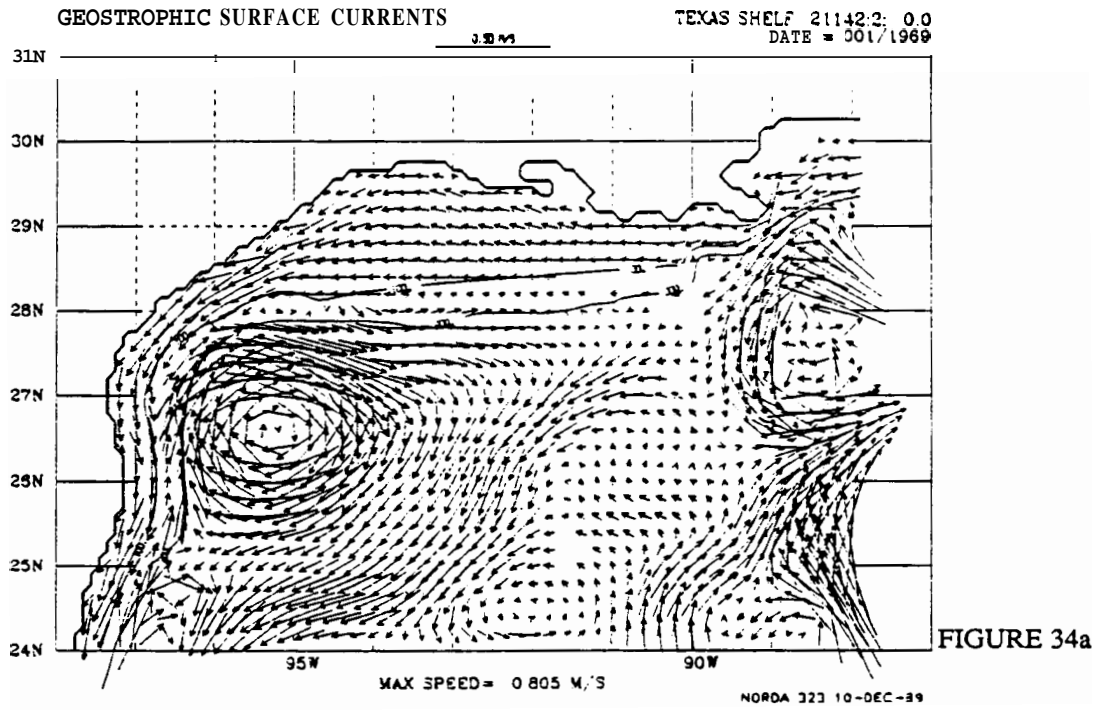


Figure 34. Merged current vectors and bottom topography contours for the Texas shelf on wind Day 001/1969: (a) "geostrophic" surface currents and (b) surface currents.



field (**L2+L1**), labeled as "geostrophic" surface current, and the surface current obtained after applying the perturbation analysis to obtain a detailed vertical profile (**L2+L1+P**). Figures 35-37 show the same merged fields at 90-day time intervals to illustrate the seasonal cycle on the shelf. Figures 38 and 39 are one year later than Figures 34 and 35 respectively, illustrating interannual variability.

The present Oil Spill Risk Analysis system at Minerals Management Service calculates the surface current due to local wind forcing by taking 3.5% of the wind speed at an angle to the right of the wind of between 0 and 30 degrees depending on wind speed (Samuels et al., 1982). This current is then added to the geostrophic component to obtain the total surface current. Figure 40 shows the surface current for a day in January calculated via the perturbation analysis and by the 3.5% rule (**L2+L1+P** vs. **L2+L1+3.5%**). Figures 41 and 42 show the corresponding wind stresses and the surface currents minus the geostrophic component (**P** only versus 3.5% only). Figures 43-45 show the same fields for a day in April. The perturbation analysis typically generates a current component that is about 45 degrees to the right of the local wind, which is further to the right than the 3.5% rule. This is consistent with the **Ekman** spiral produced by the analytic analysis and is appropriate for a steady wind. The different angles, and the fact that the perturbation analysis gives smaller magnitudes, is partly due to the absence of the Stoke's drift current component from the analysis. The perturbation analysis is also sensitive to the drag coefficient used to convert wind speeds to stresses. In this case, the drag coefficient is 0.00012 [see **Rhodes** et al. (1989)]. These winds were not generated as part of this contract; if they were, it is likely that greater attention would have been paid to what drag coefficient to use. The geostrophic surface currents (**L2+L1**) and the wind stresses have been made available, in addition to the surface currents from the perturbation analysis (**L2+L1+P**). So the 3.5% rule, or some other alternative technique, can be used to obtain the currents due to local wind effects. Figures 46-52 cover the same period as Figures 33-39, but for the Florida shelf. Obviously, this brief comparison is not sufficient to decide on the relative merits of the two approaches. In any case, both are very gross approximations to the actual effect of **winds** on the surface current.

Figure 53 shows the annual surface current climatology for the full 10-year simulation (**L2+L1+P**) and a corresponding climatology based on historical ship drift data (N) provided by the Naval Oceanographic Office. The observational climatology bins data into one-degree squares, so the full resolution of this data set is shown. The model currents have been subsampled in space to improve plot clarity. Given the wide variation in horizontal resolution between these two data sets,

Figure 35. Merged current vectors and bottom topography contours for the Texas shelf on wind Day 091/1969: (a) "geostrophic" surface currents and (b) surface currents.

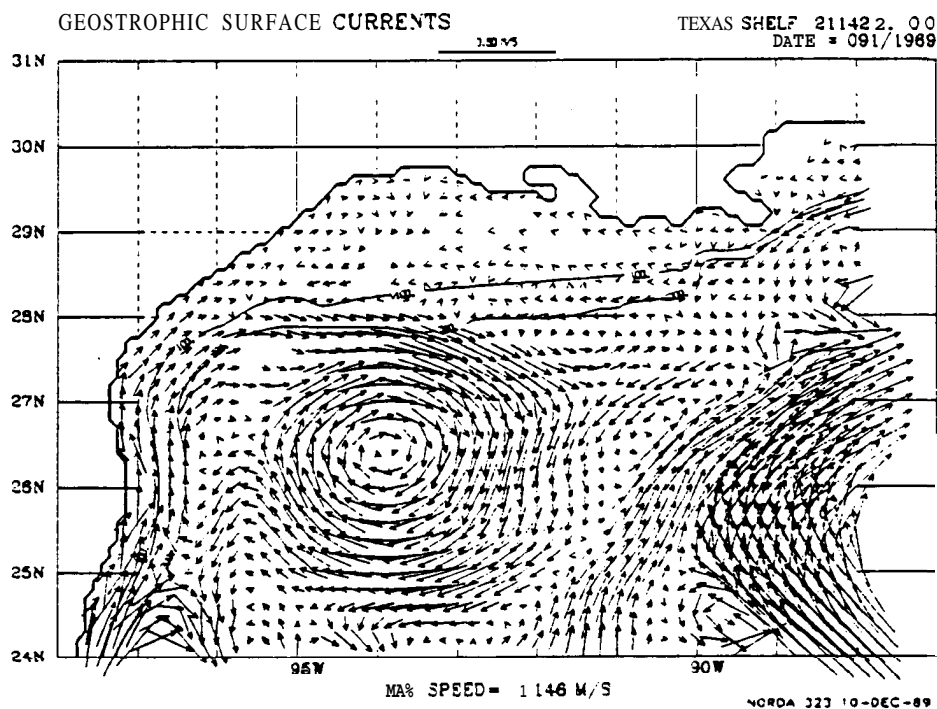


FIGURE 35a

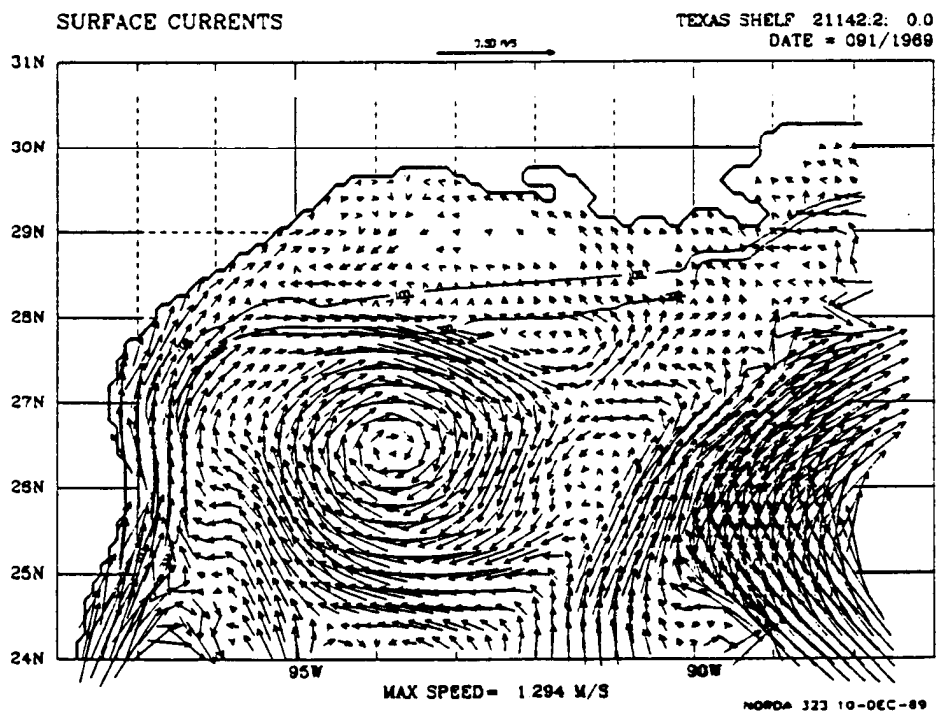


FIGURE 35b

Figure 36. Merged current vectors and bottom topography contours for the Texas shelf on wind Day 181/1969: (a) "geostrophic" surface currents and (b) surface currents.

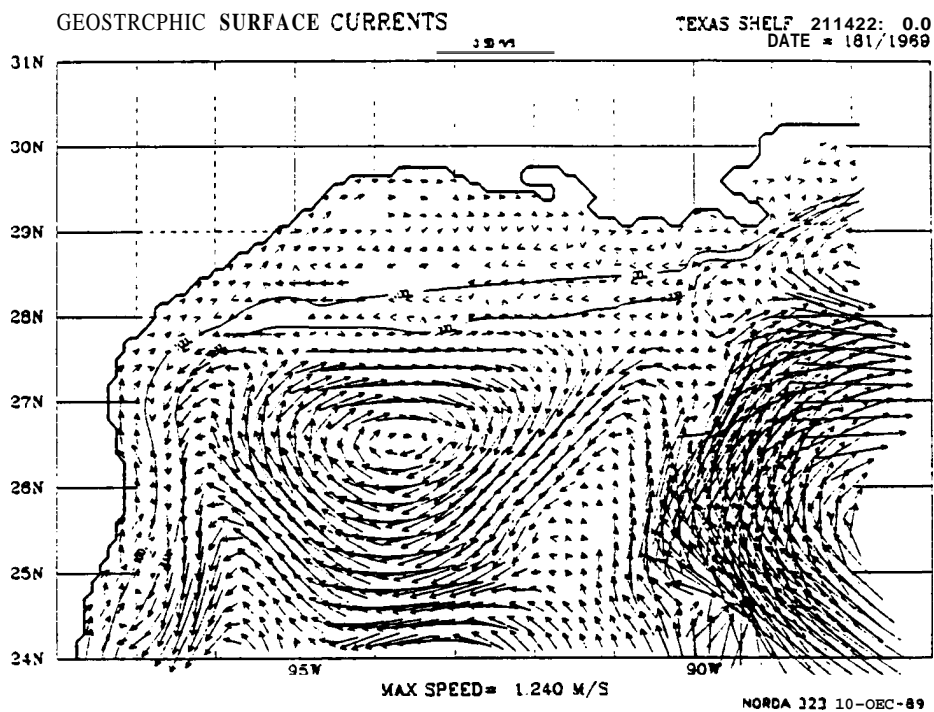


FIGURE 36a

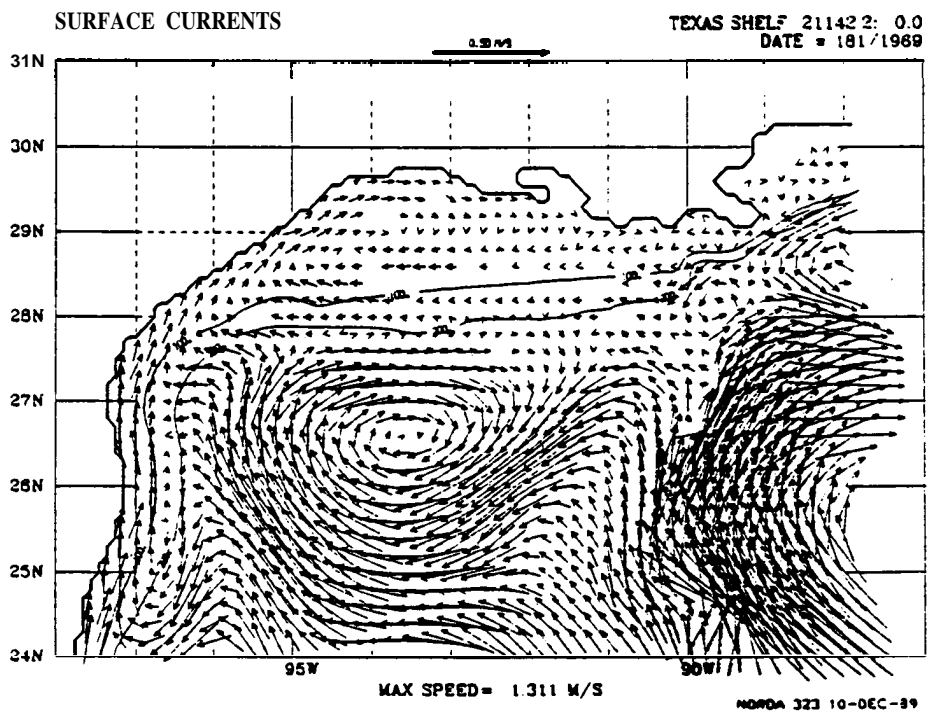


FIGURE 36b

Figure 37. Merged current vectors and bottom topography contours for the Texas shelf on wind Day 271/1969: (a) "geostrophic" surface currents and (b) surface currents.

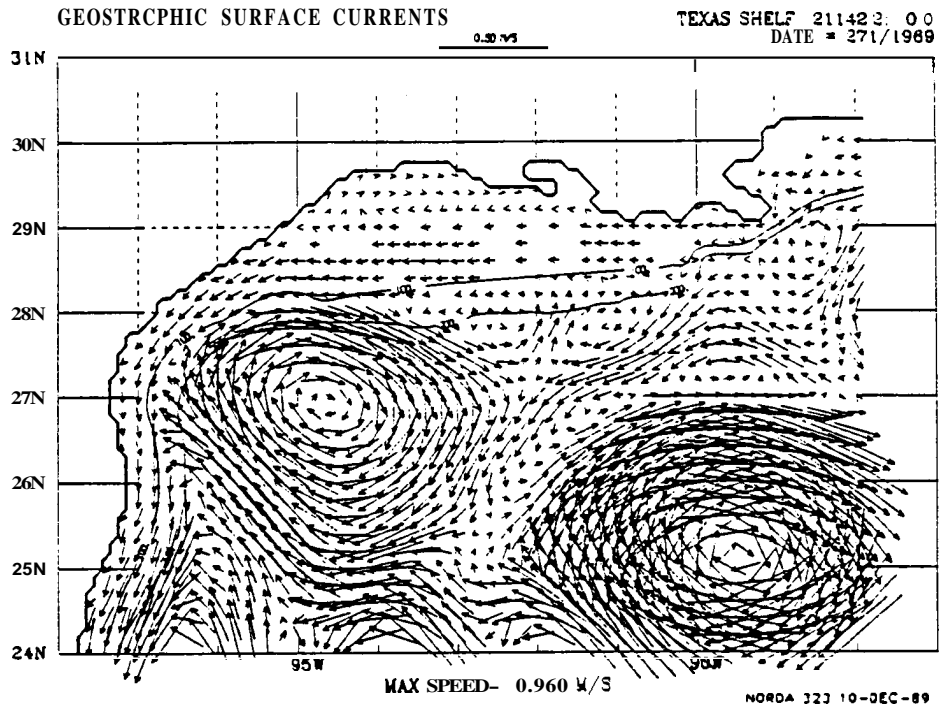


FIGURE 37a

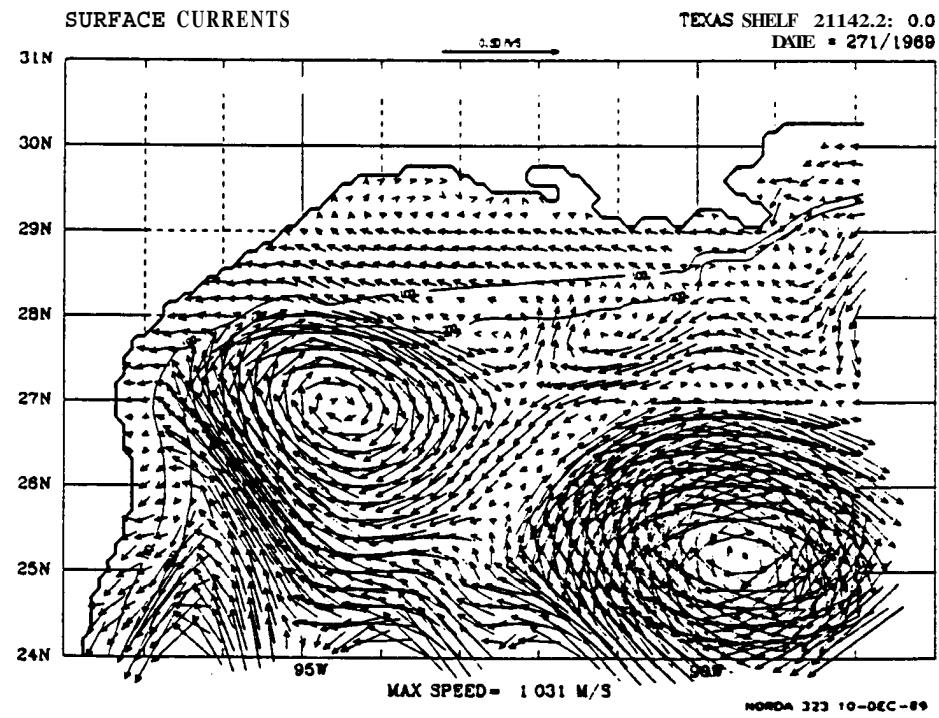


FIGURE 37b

Figure 38. Merged current vectors and bottom topography contours for the Texas shelf on wind Day 002/1970: (a) "geostrophic" surface currents and (b) surface currents.

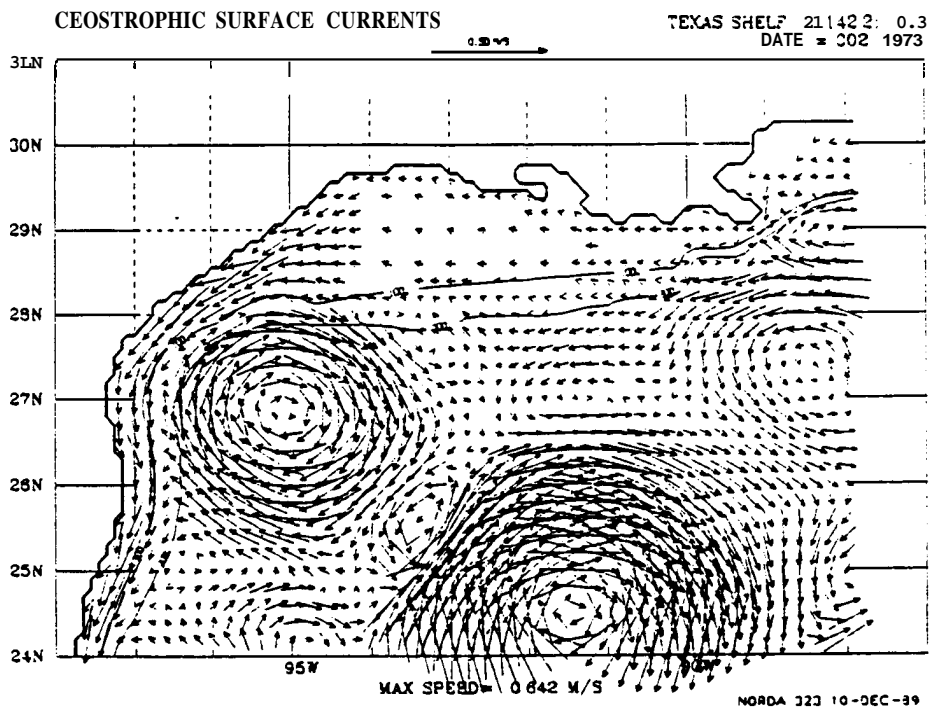


FIGURE 38a

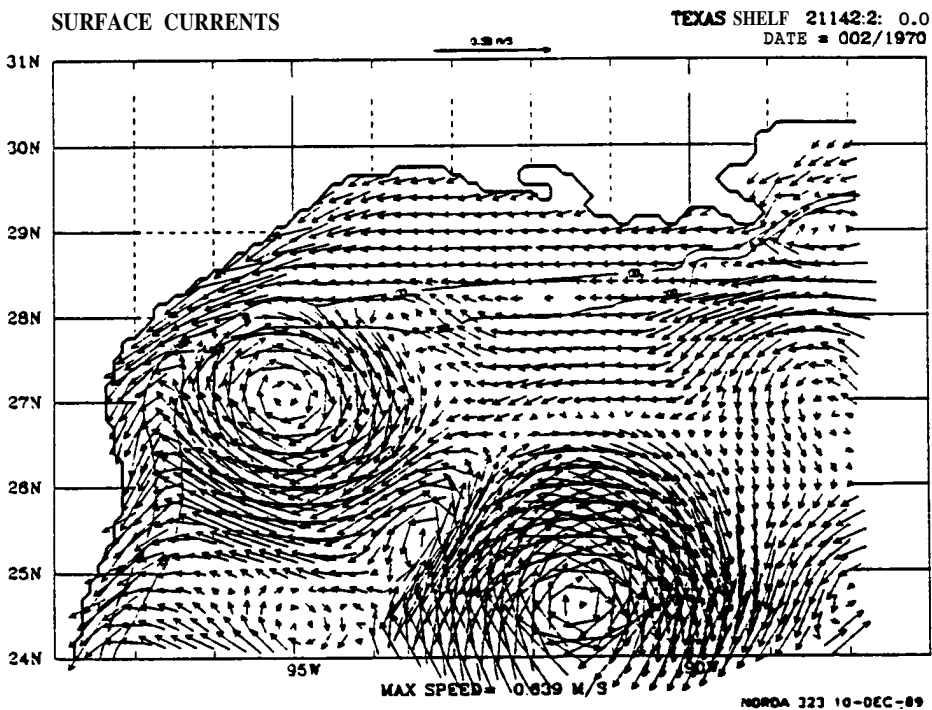


FIGURE 38b

Figure 39. Merged current vectors and bottom topography contours for the Texas shelf on wind Day 092/1970: (a) "geostrophic" surface currents and (b) surface currents.

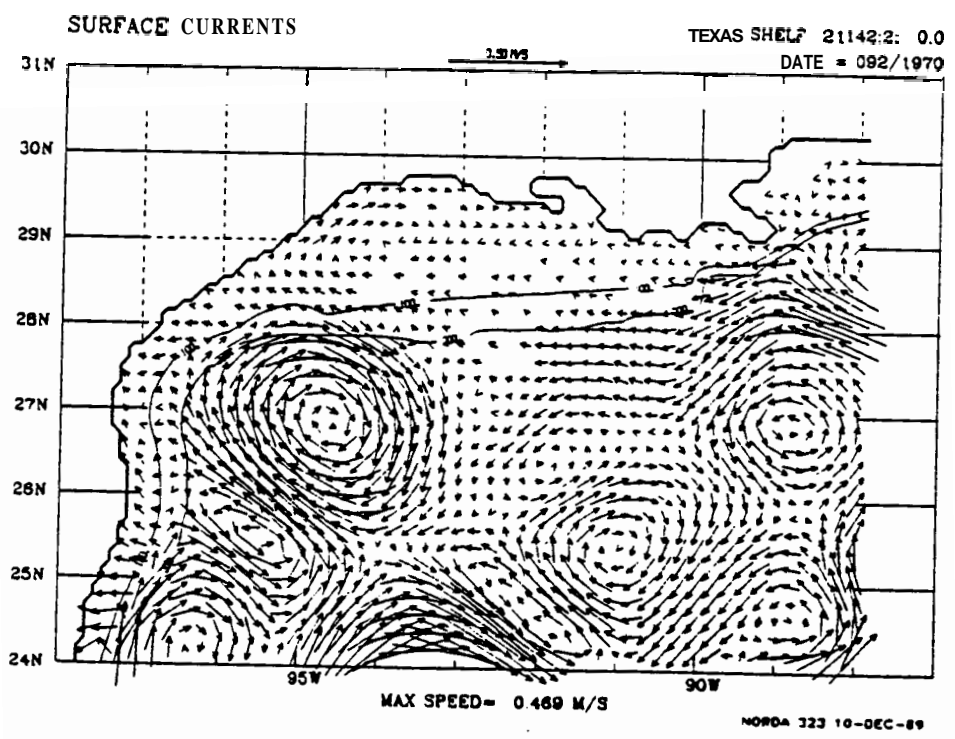
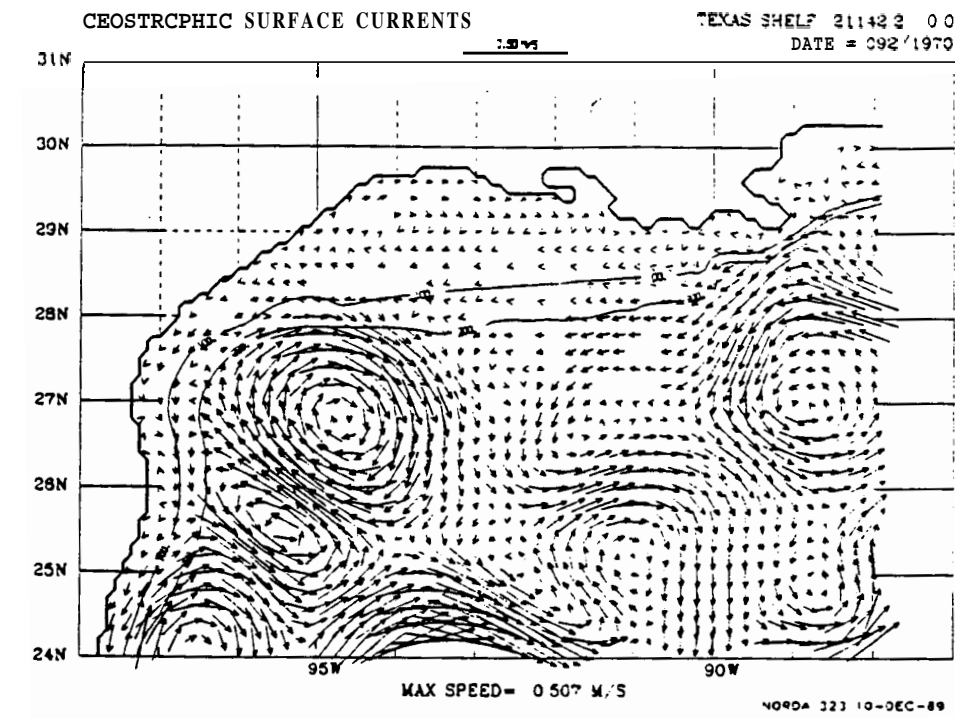


Figure 40. Merged current vectors and bottom topography contours for the Texas shelf on wind Day 001/1969: (a) surface currents and (b) surface currents using the 3.5% rule.

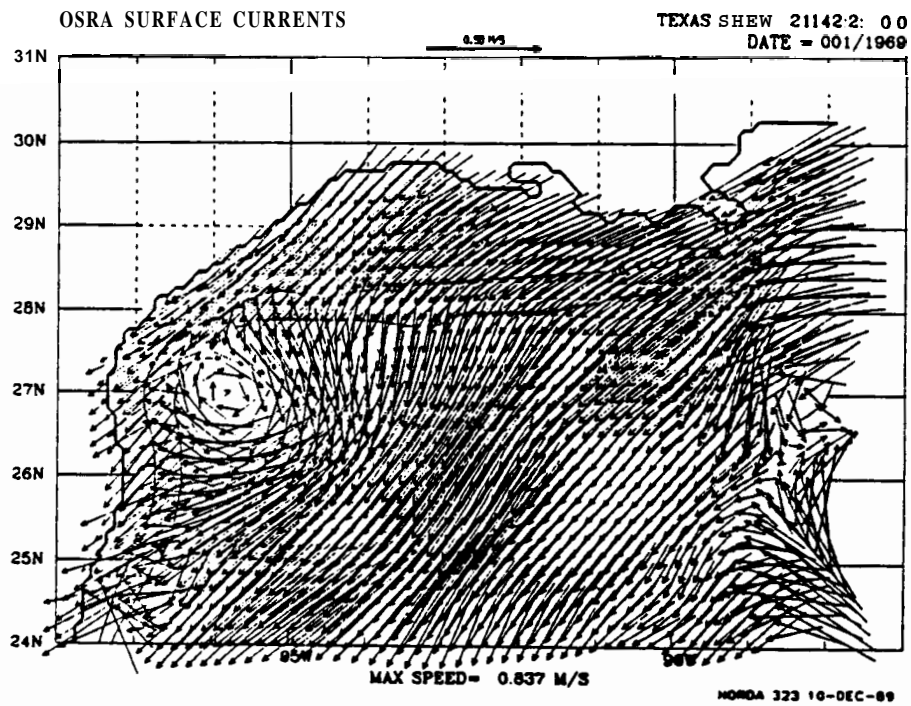
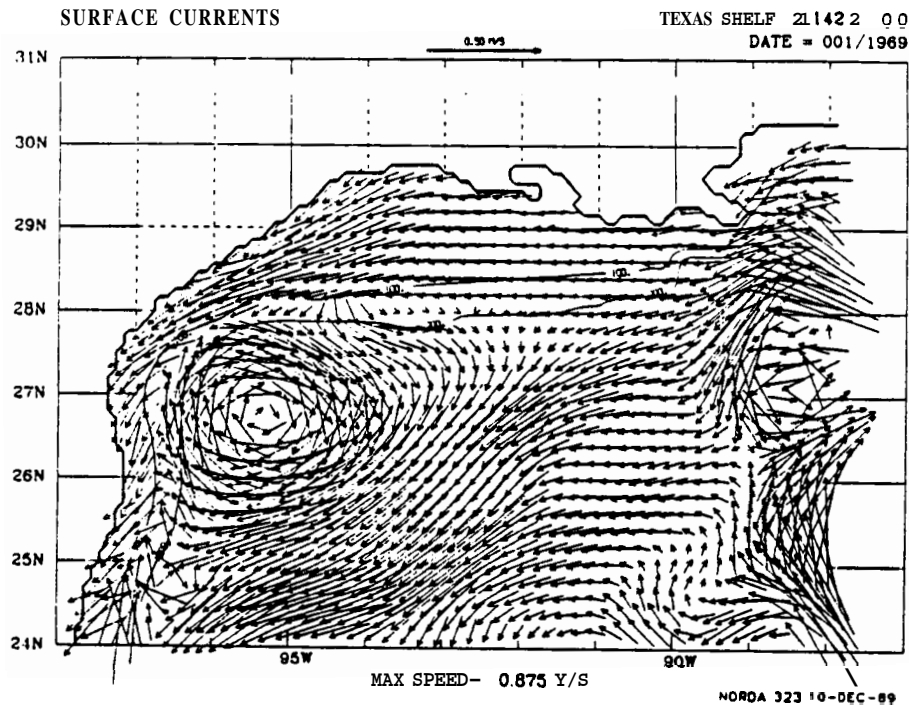


Figure 41. (a) Wind stresses and (b) local wind-induced currents for the Texas shelf on wind Day 001/1969.

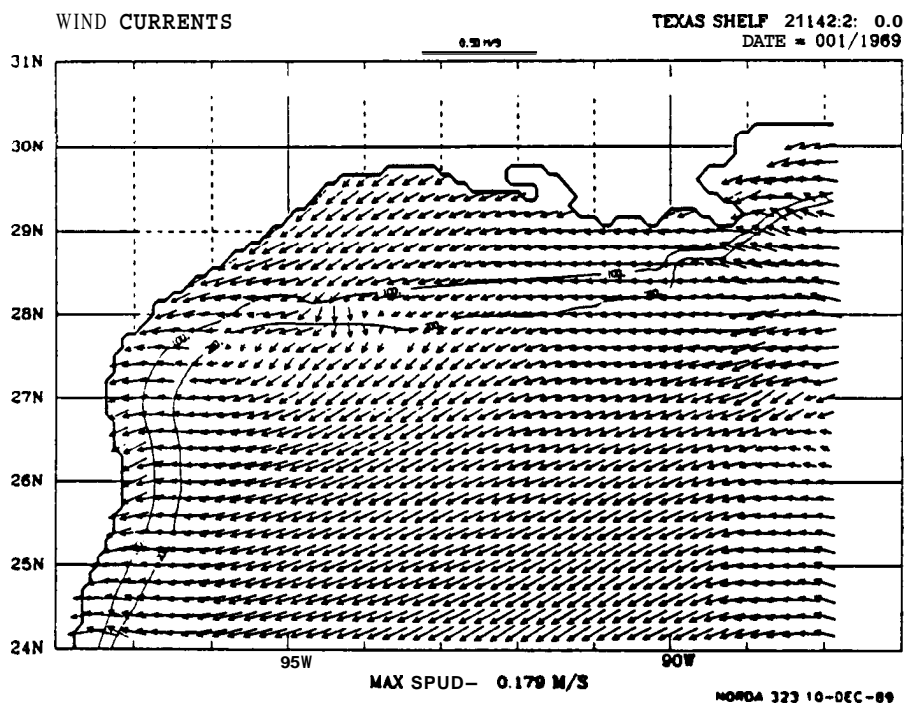
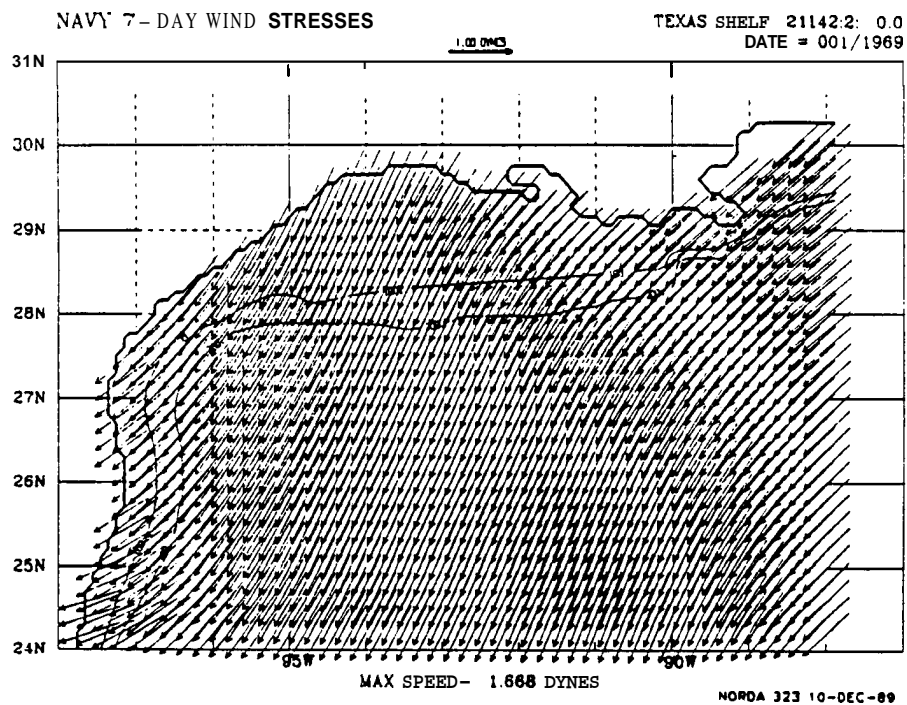


Figure 42. (a) Wind stresses and (b) local wind-induced currents from the 3.5% rule for the Texas shelf on wind Day 001/1969.

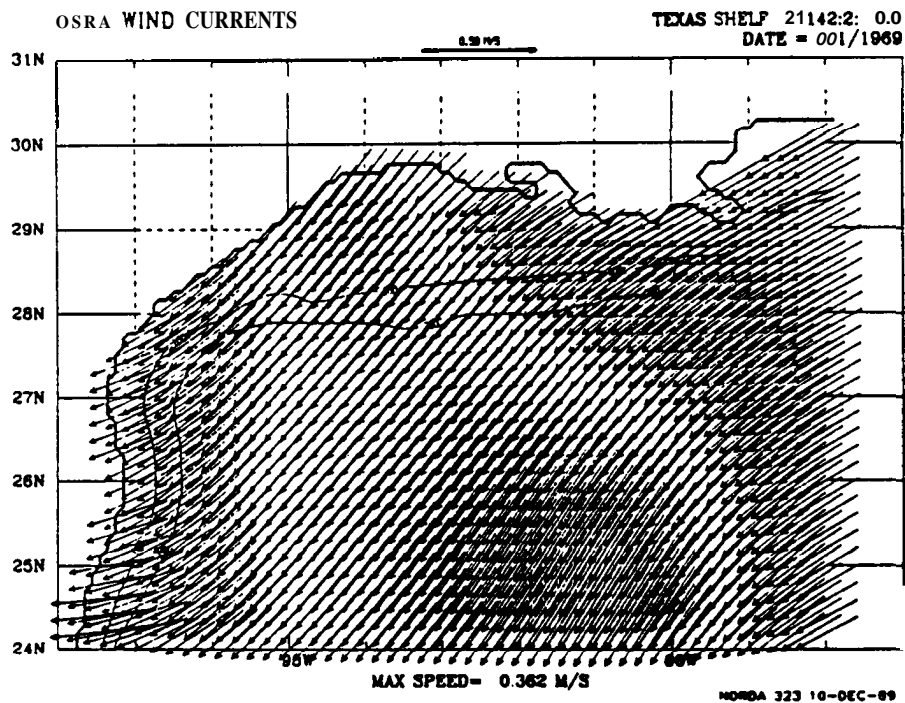
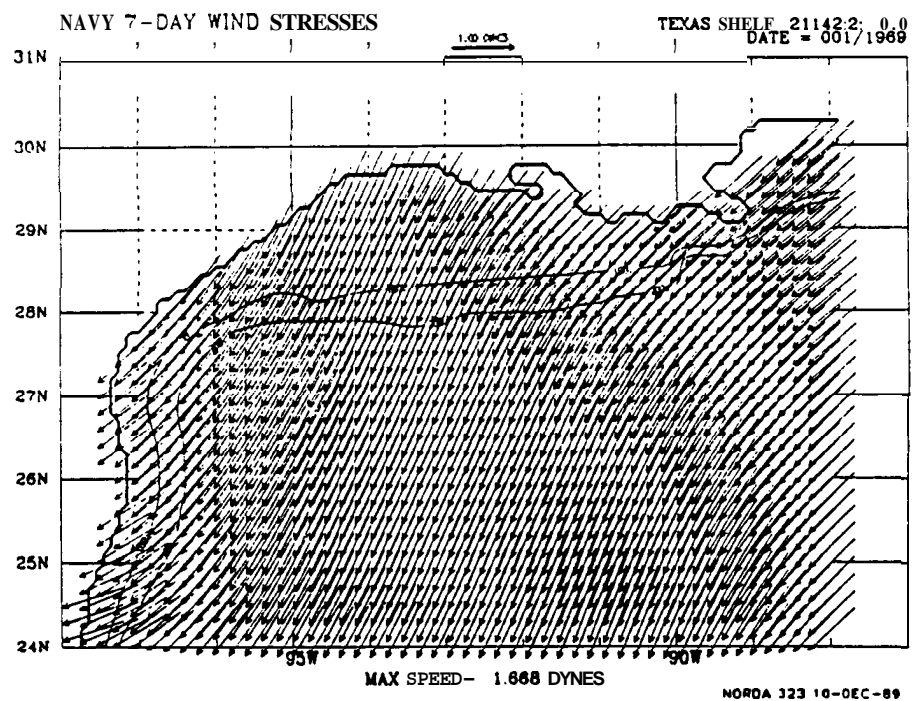


Figure 43. Merged current vectors and bottom topography contours for the Texas shelf on wind Day 091/1969: (a) surface currents and (b) surface currents using the 3.5% rule.

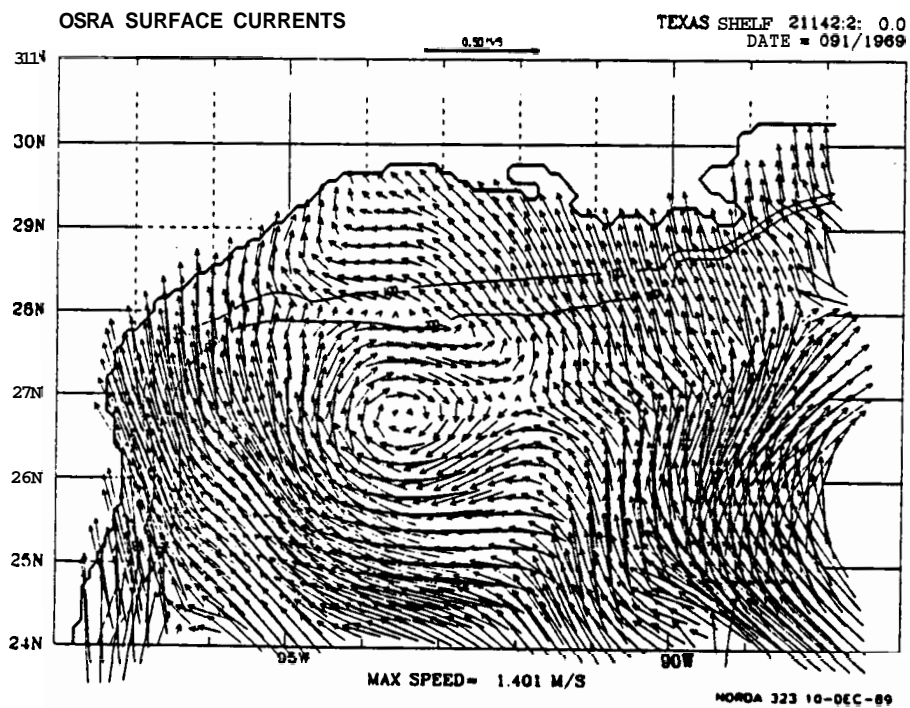
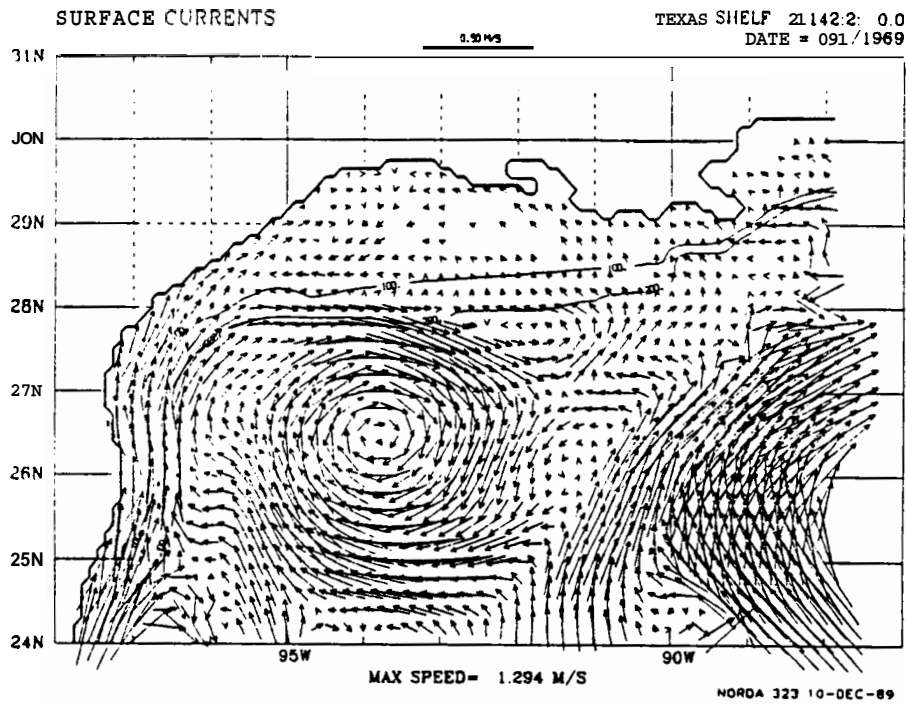


Figure 44. (a) Wind stresses and (b) local wind-induced currents for the Texas shelf on wind Day 0911/969.

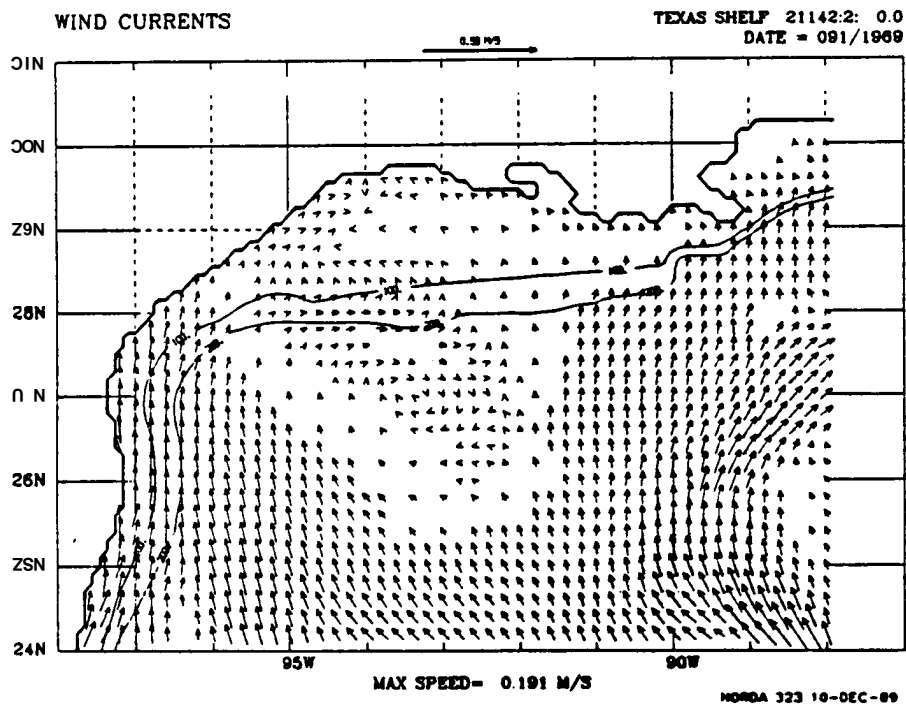
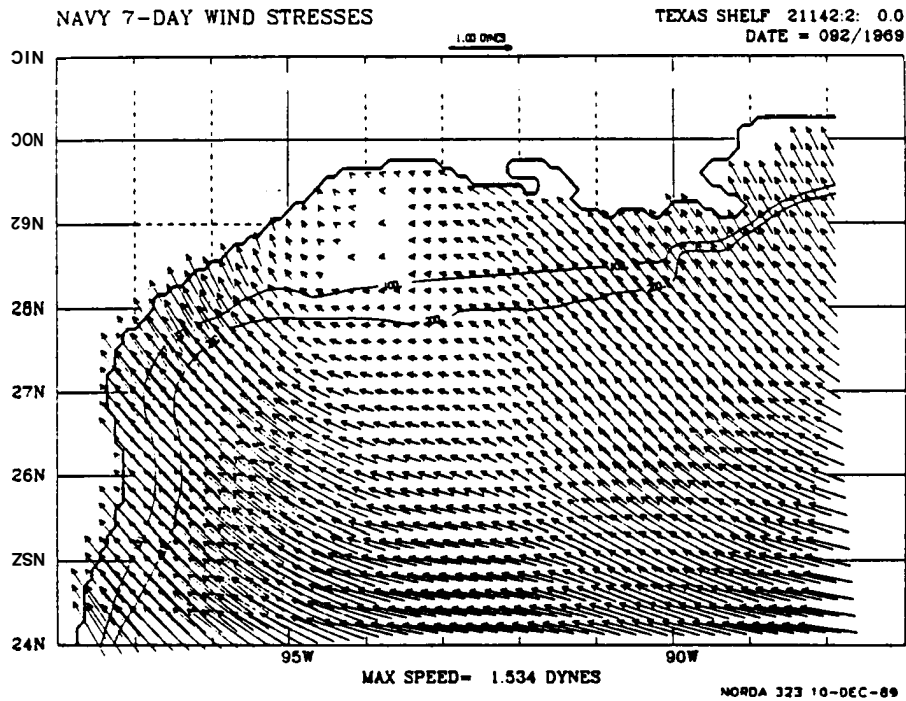


Figure 45. (a) Wind stresses and (b) local wind-induced currents from the 3.5% rule for the Texas shelf on wind Day 091/1969.

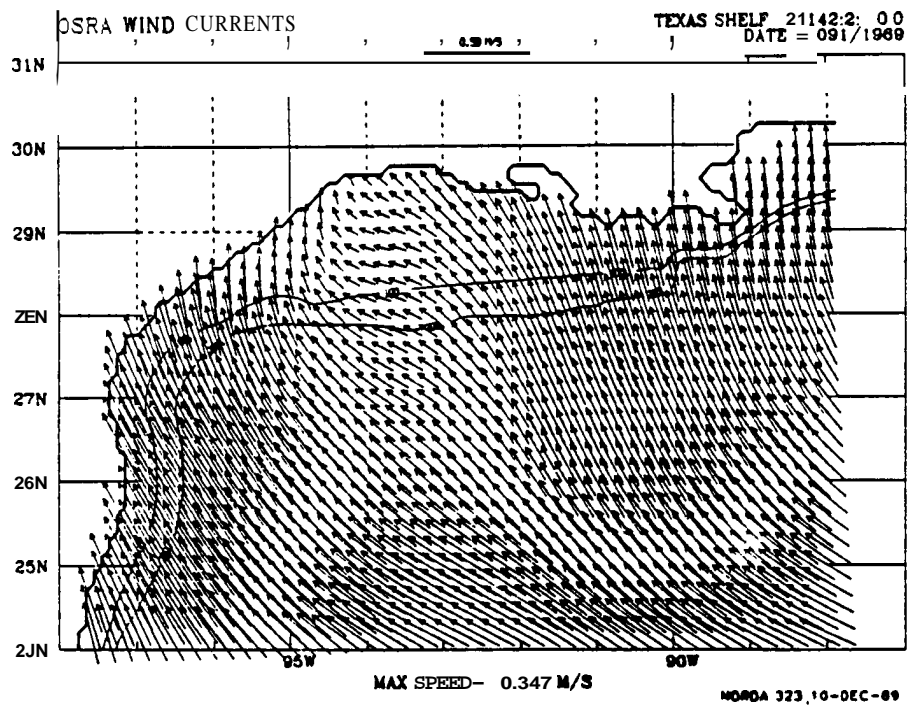
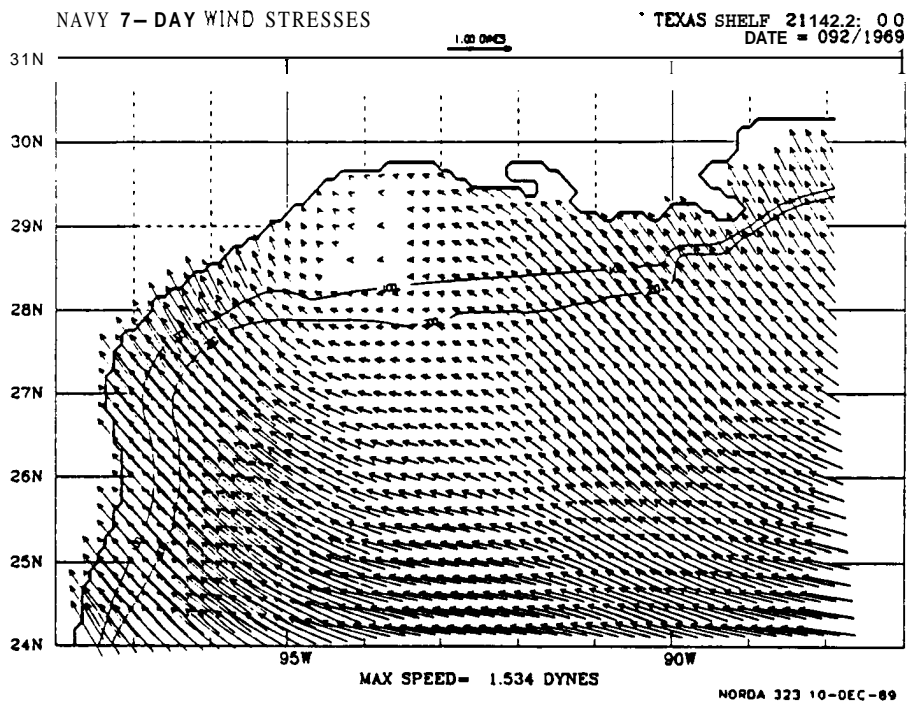


Figure 46. Upper layer current vectors and bottom topography contours for the Florida shelf on wind Day 001/1969 for: (a) one-layer Experiment 212/80.0 and (b) two-layer Experiment 212/83.1.

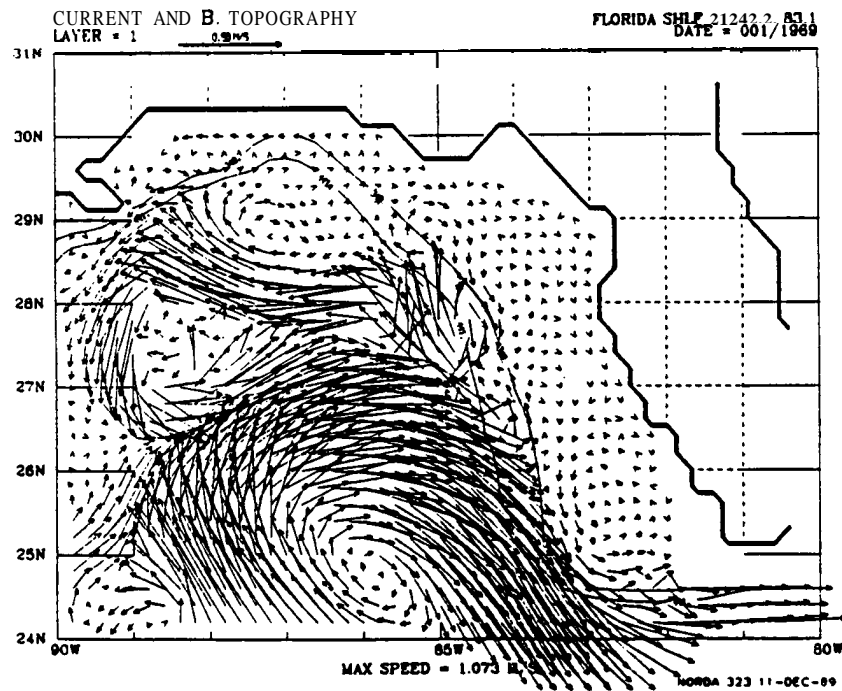
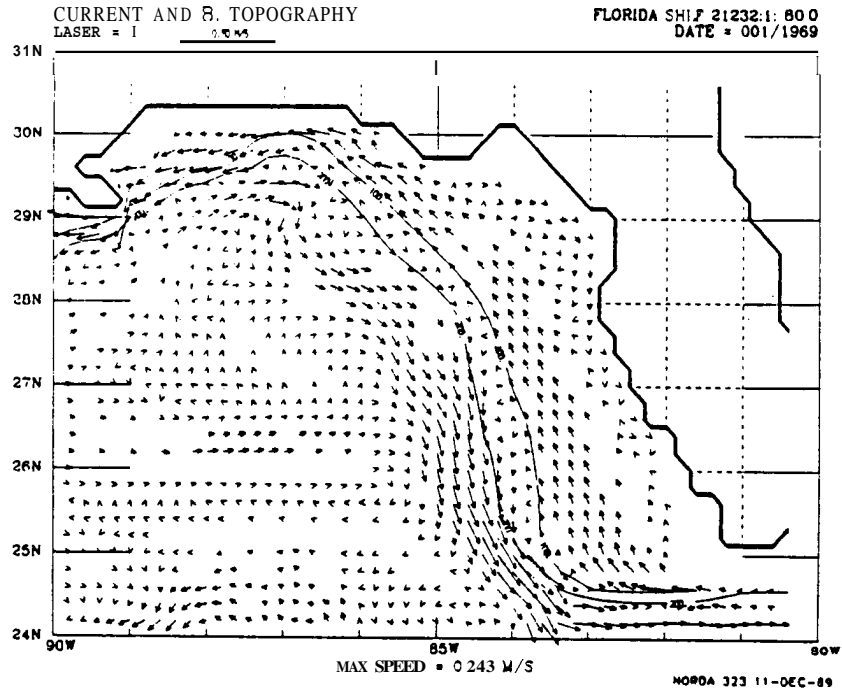


Figure 47. Merged current vectors and bottom topography contours for the Florida shelf on wind Day 001/1969: (a) "geostrophic" surface currents and (b) surface currents.

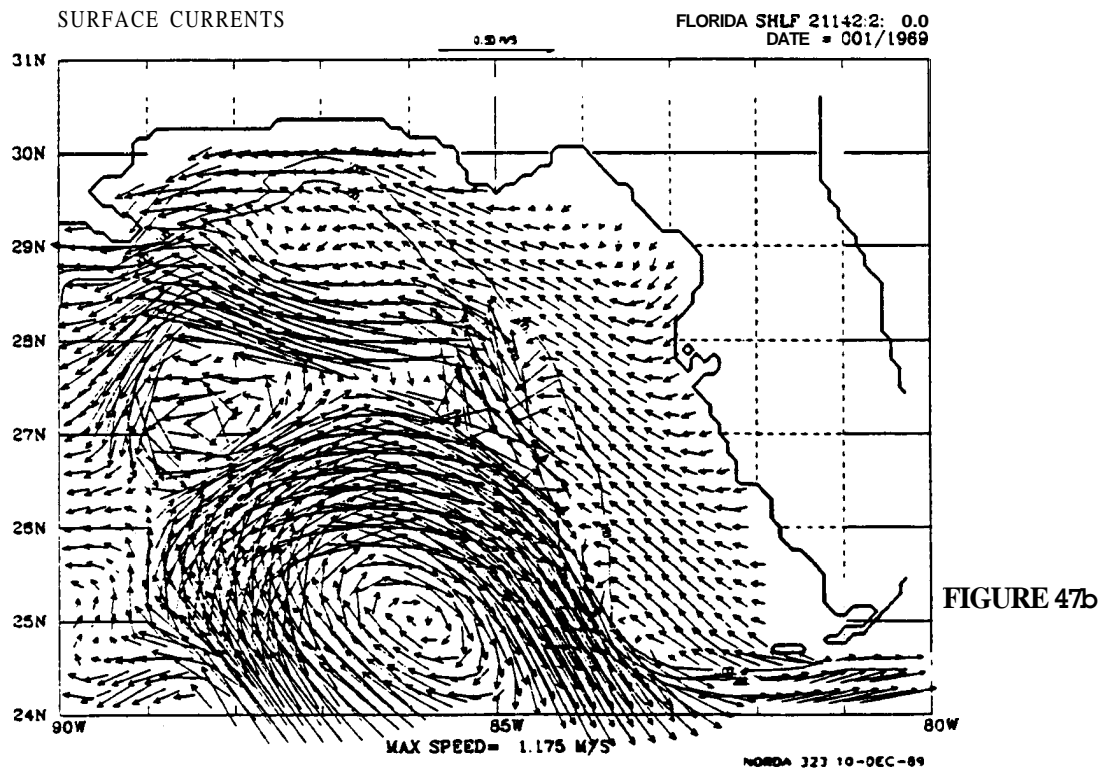
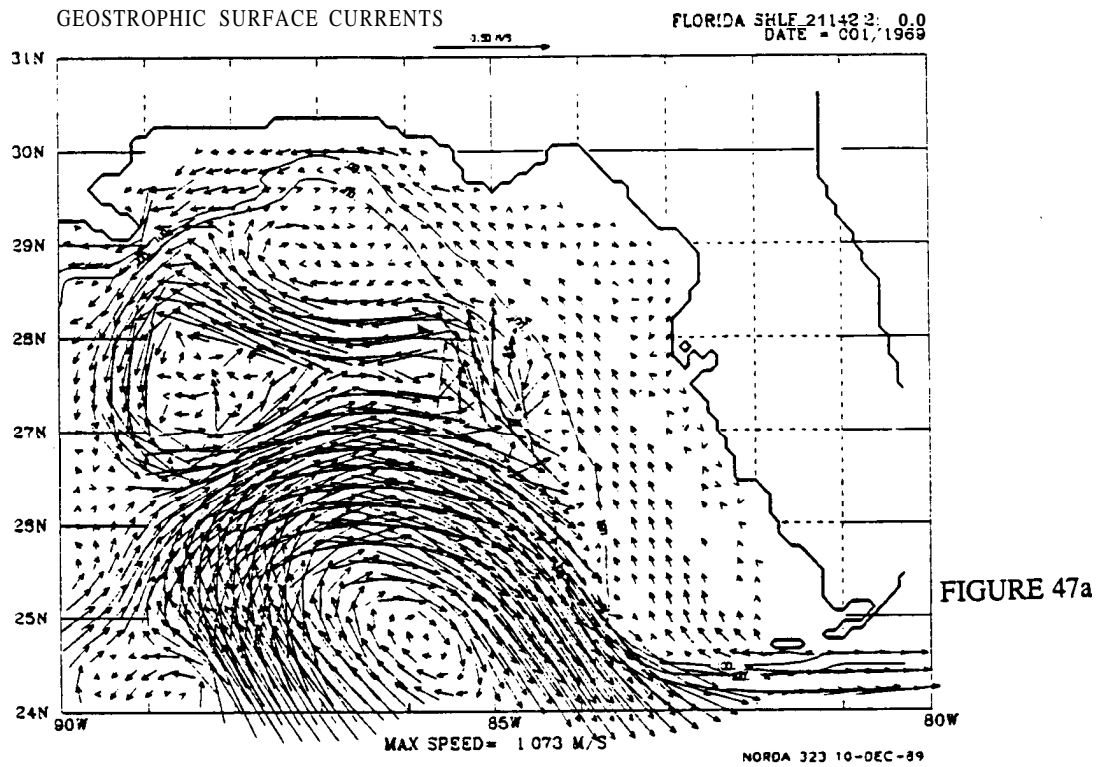


Figure 48. Merged current vectors and bottom topography contours for the Florida shelf on wind Day 091/1969: (a) "geostrophic" surface currents and (b) surface currents.

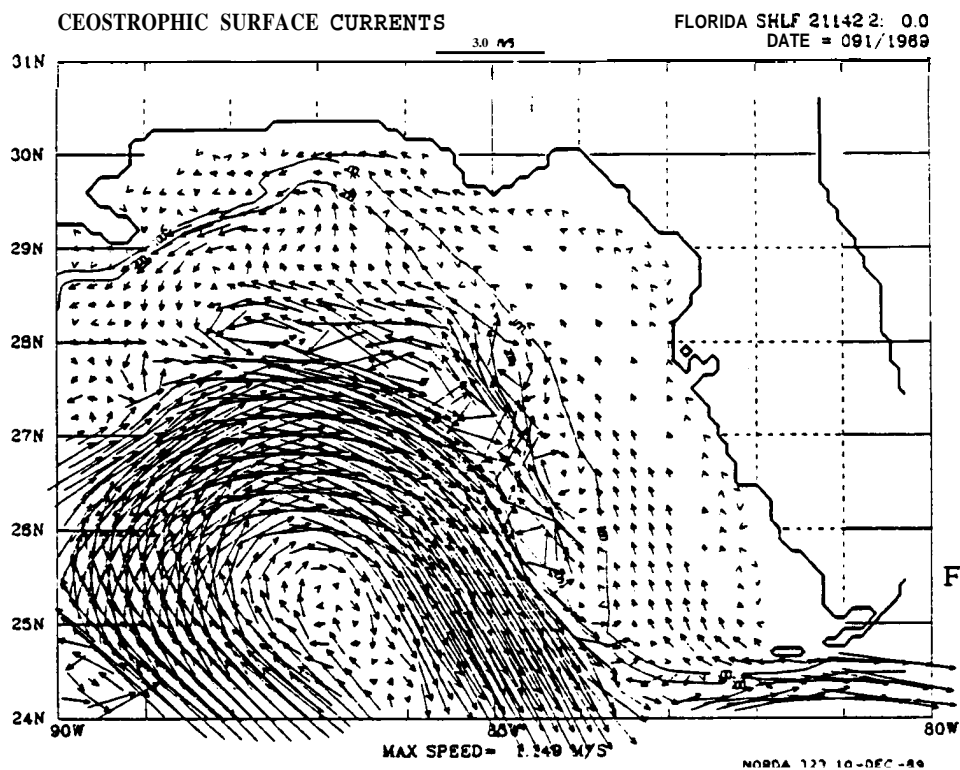


FIGURE 48a

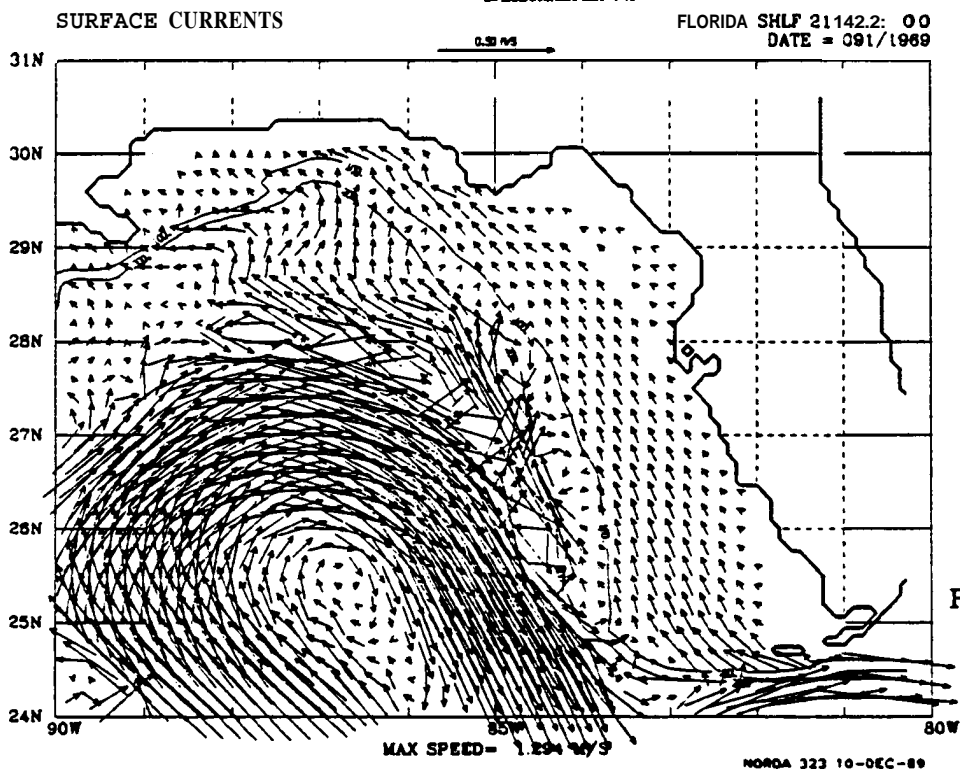


FIGURE 48b

Figure 49. Merged current vectors and bottom topography contours for the Florida shelf on wind Day 181/1969: (a) "geostrophic" surface currents and (b) surface currents.

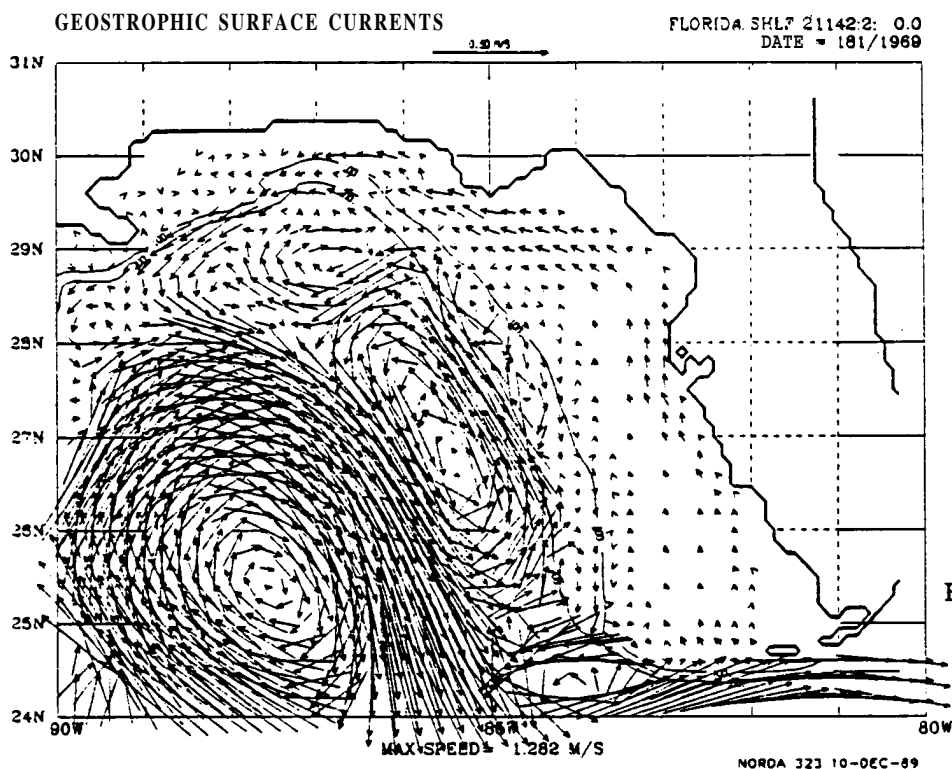


FIGURE 49a

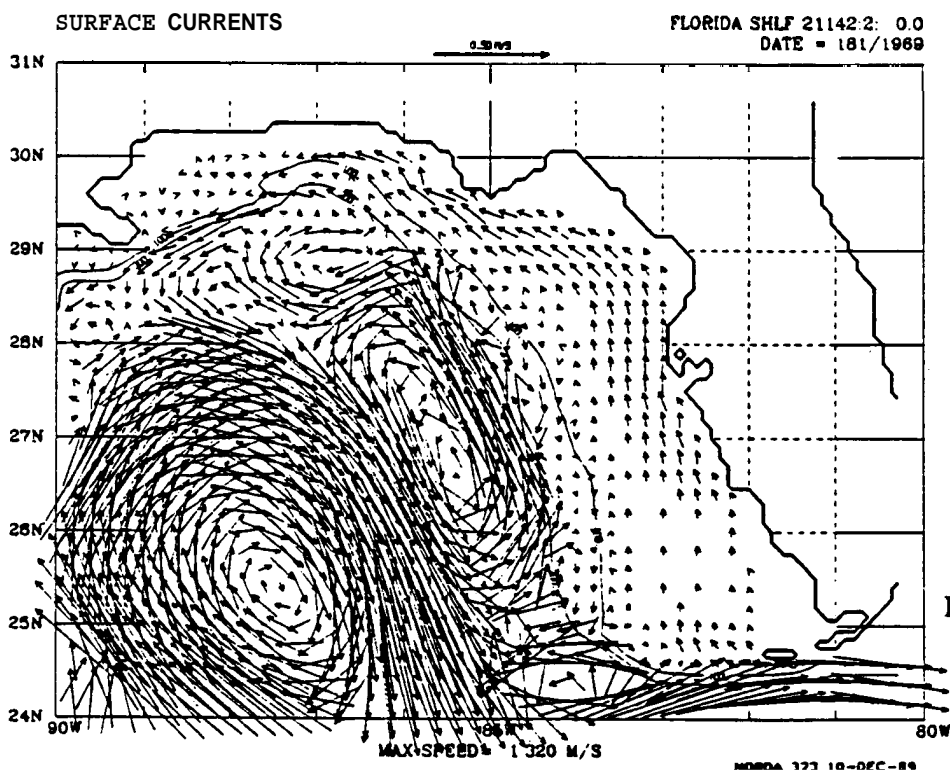


FIGURE 49b

Figure 50. Merged current vectors and bottom topography contours for the Florida shelf on wind Day 271/1969: (a) "geostrophic" surface currents and (b) surface currents.

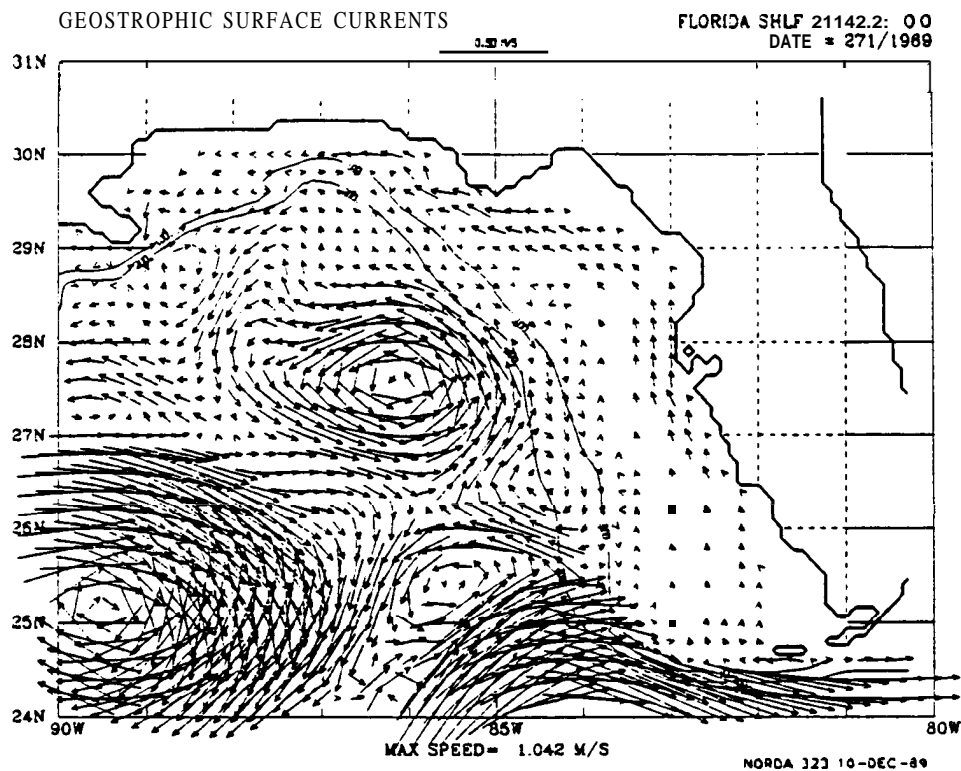


FIGURE 50a

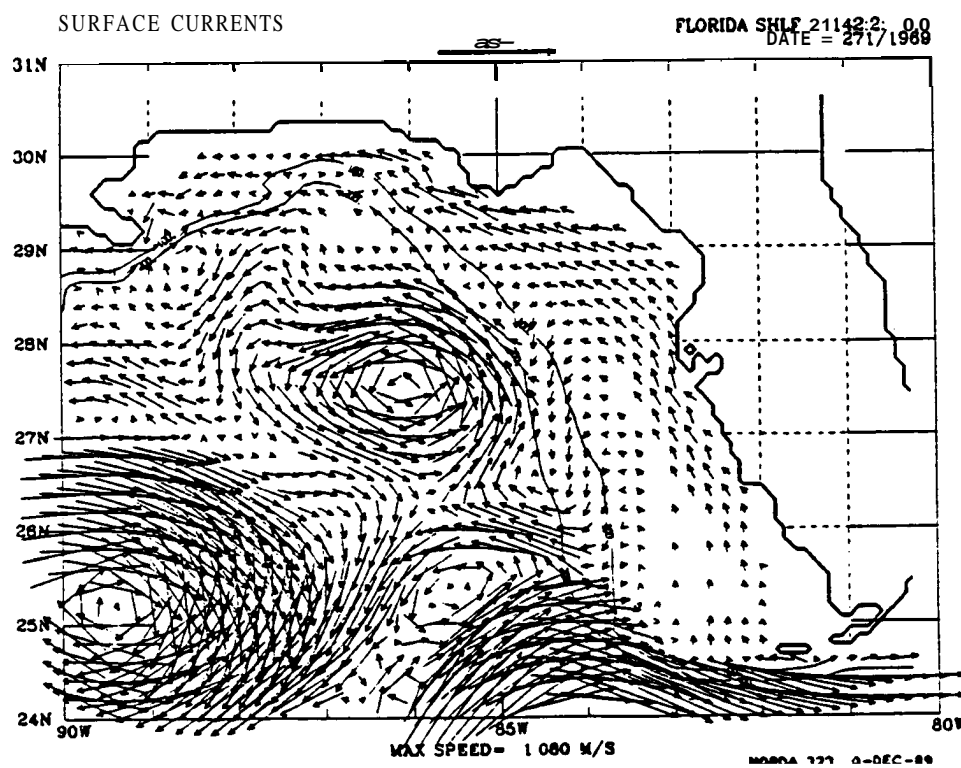


FIGURE 50b

Figure 51. Merged current vectors and bottom topography contours for the Florida shelf on wind Day 002/1970: (a) "geostrophic" surface currents and (b) surface currents.

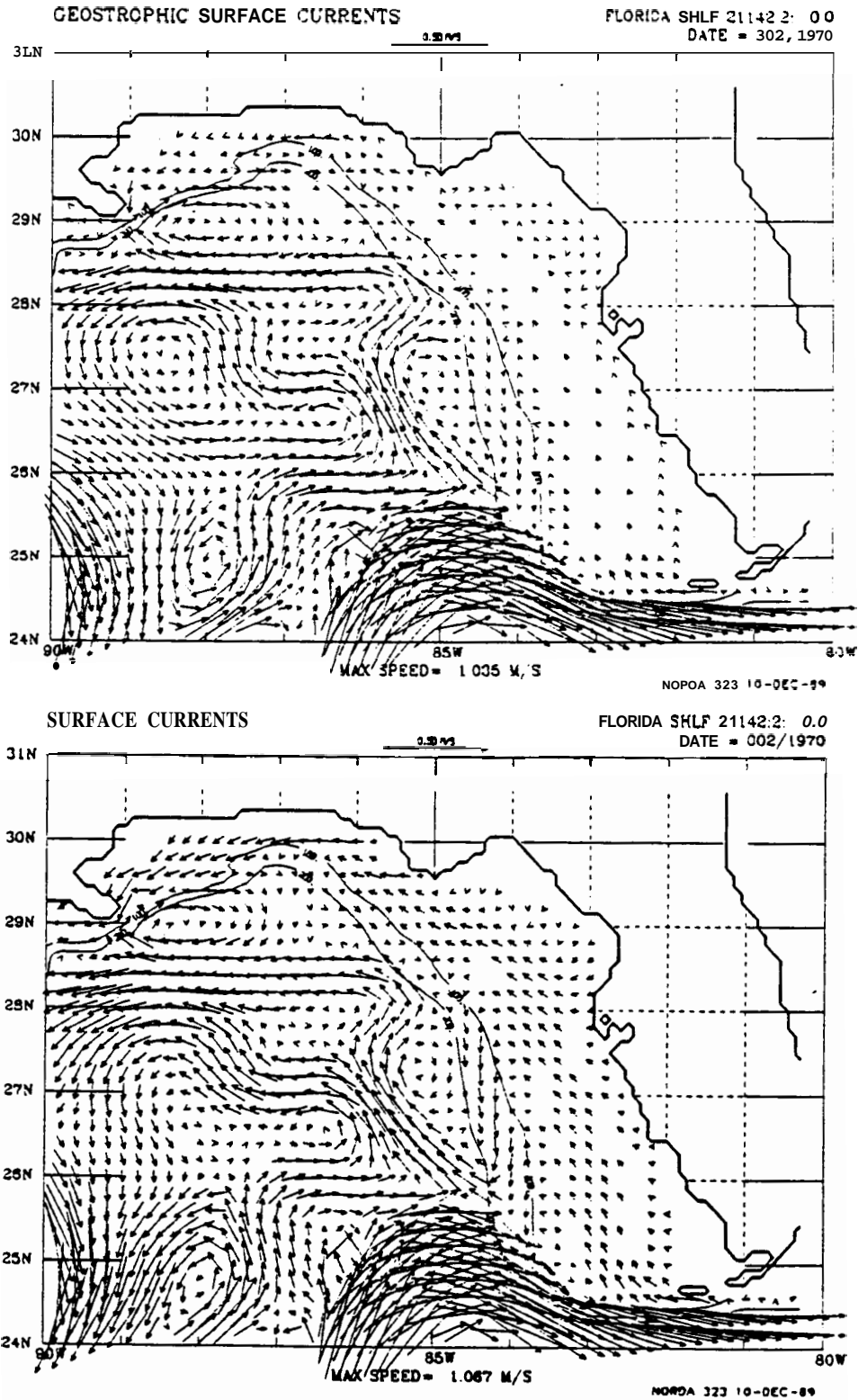


Figure 52. Merged current vectors and bottom topography contours for the Florida shelf on wind Day 092/1970: (a) "geostrophic" surface currents and (b) surface currents.

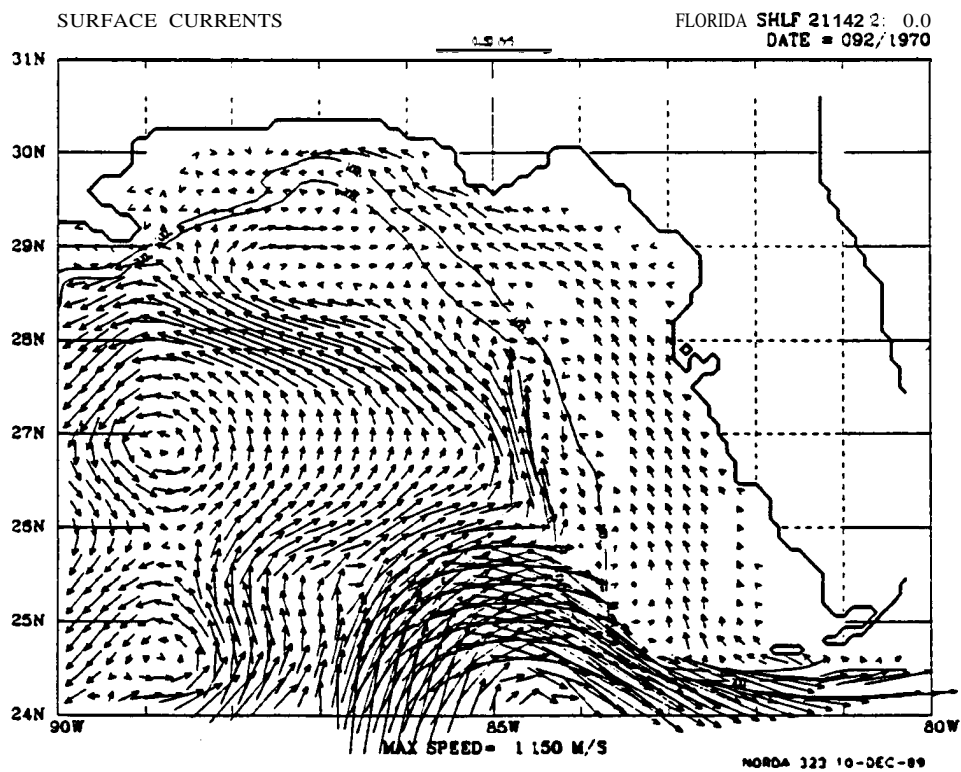
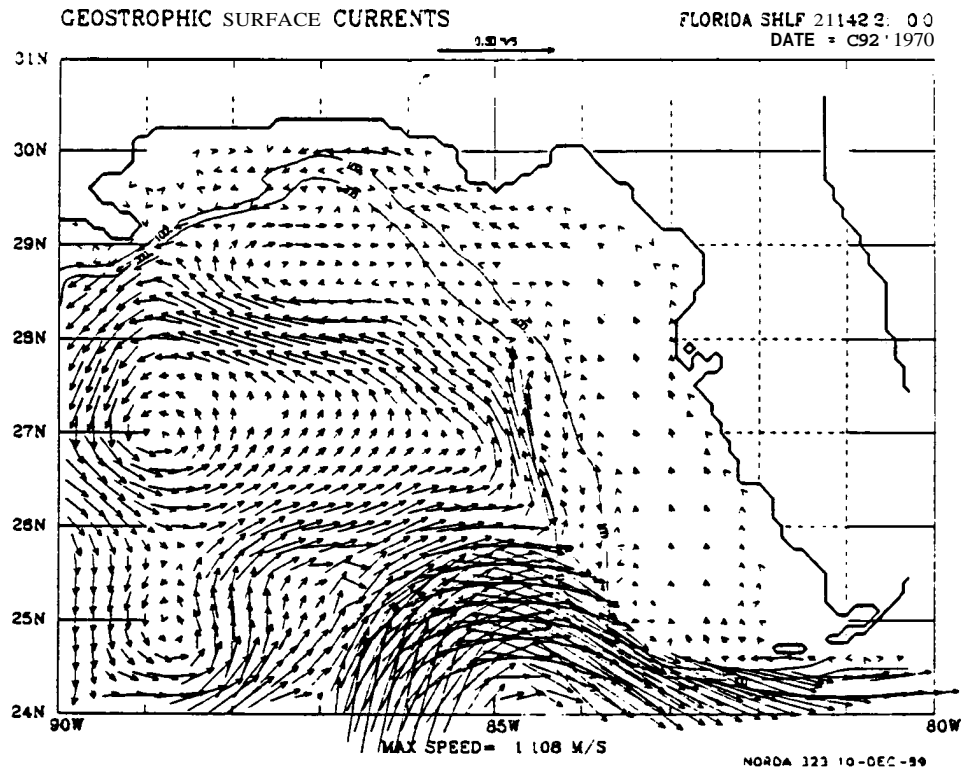
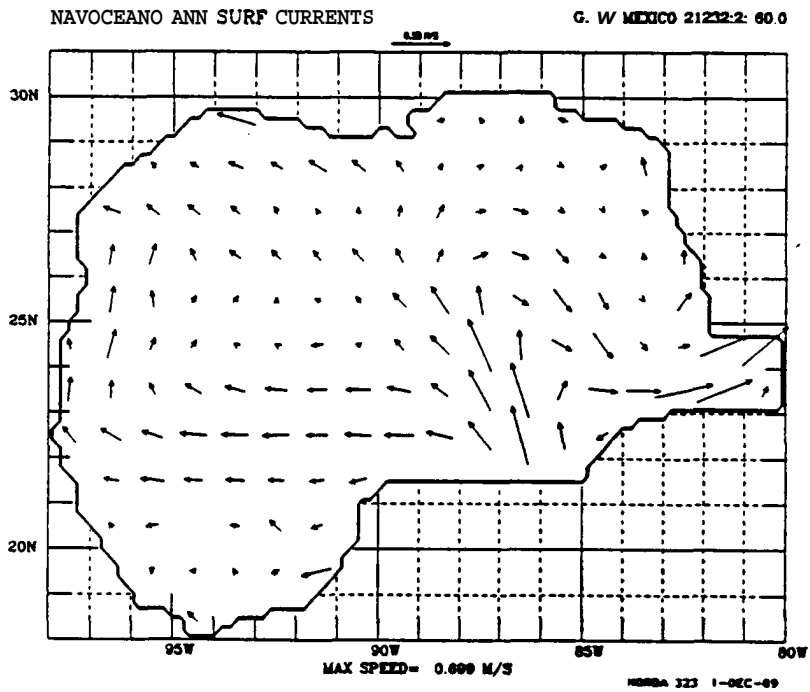
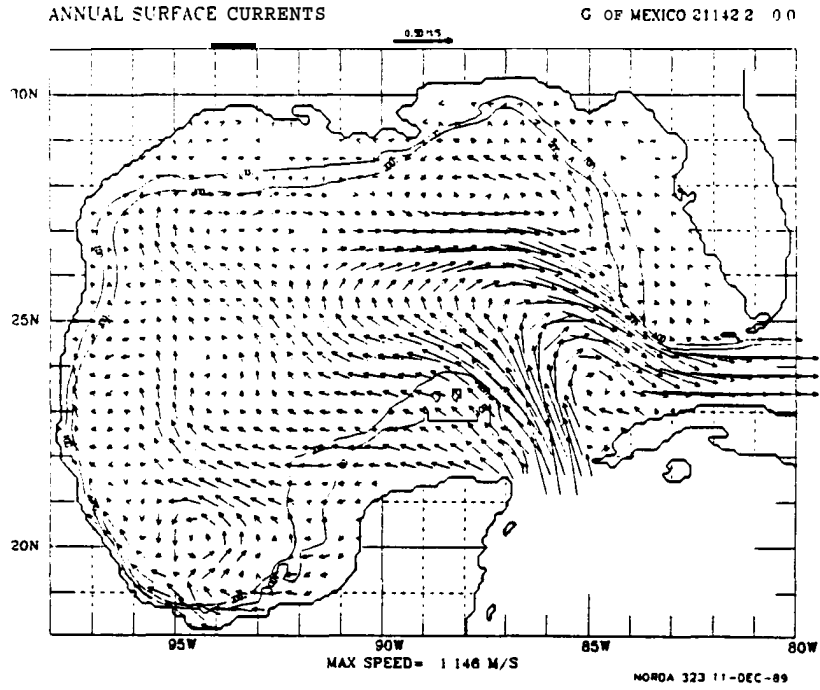


Figure 53. Annual surface current climatology (a) from the 10-year merged simulation and (b) from historical observations.



a side-by-side comparison is more appropriate than a plot of the two fields differenced together. Both fields include a mean Loop Current, but it bends further westward in the simulation. Both show westward zonal flow at 22N to 23N bending northward near the **Mexico/Texas** coast. These currents are stronger in the observations, but the simulation only includes seven-day wind stress averages and the simulated mean flow might be stronger with 12 hourly winds. Figure 54 compares the annual surface current and annual geostrophic surface current climatologies. The zonal flow at 22N is weaker in the geostrophic case, suggesting this is largely a wind driven response. Figures 55-58 show seasonal climatologies. In all seasons the simulation shows a cyclonic **gyre** in the far southwest Gulf. This feature is not seen in the observations; however, it would be barely resolvable on a one-degree grid and there **are** probably relatively few observations in the region. On the other hand, the wind stresses used by the model are also open to question in that region (**Rhodes** et al., 1989). Figures 59-62 show a representative instantaneous field and its difference from the seasonal mean for each season. The differences are taken with respect to the model mean, rather than the mean from observations because of the wide variation in horizontal resolution between these two data sets. The size of the anomaly is comparable to that of the original field particularly in deep water.

The comparisons, begun in Year 2 (**Wallcraft, 1986**), between statistical measures of the simulated currents and those from actual field measurements have been continued. The ocean model simulation is not a **hindcast** (i.e., it does not claim to represent the actual situation in the Gulf over any given time period), so direct day-by-day comparison with observations would be inappropriate. This is unfortunate since a direct comparison would provide far more information on the quality of the simulation than the statistical measures used here. Figure 63 shows the locations of moored current meter arrays deployed as part of **MMS's** Gulf of Mexico Physical Oceanography Program (**SAIC, 1986**). Very good data has been obtained from these moorings, but statistical comparisons **are** made more difficult by the fact that the data record at many moorings extends for no longer than one year. The average Loop **Current** eddy shedding period is about one year, but it can vary from 6-18 months. So a one-year data record is too short to obtain reliable statistics about Loop **Current** related phenomena, which means in practice that the only place where the data record is likely to be long enough for good **long-term** statistics is over the shelf. Figure 64 shows the full **10-year** velocity component spectra from the simulation at mooring MOF, which is on the inner shelf so the one-layer model (**L1**) results apply. There is very little energy below 10 days, as would be expected from seven-day averaged wind stress forcing, and there is a strong

Figure 54. Annual surface current climatology (a) from the 10-year merged simulation and (b) "geostrophic" climatology from the merged simulation.

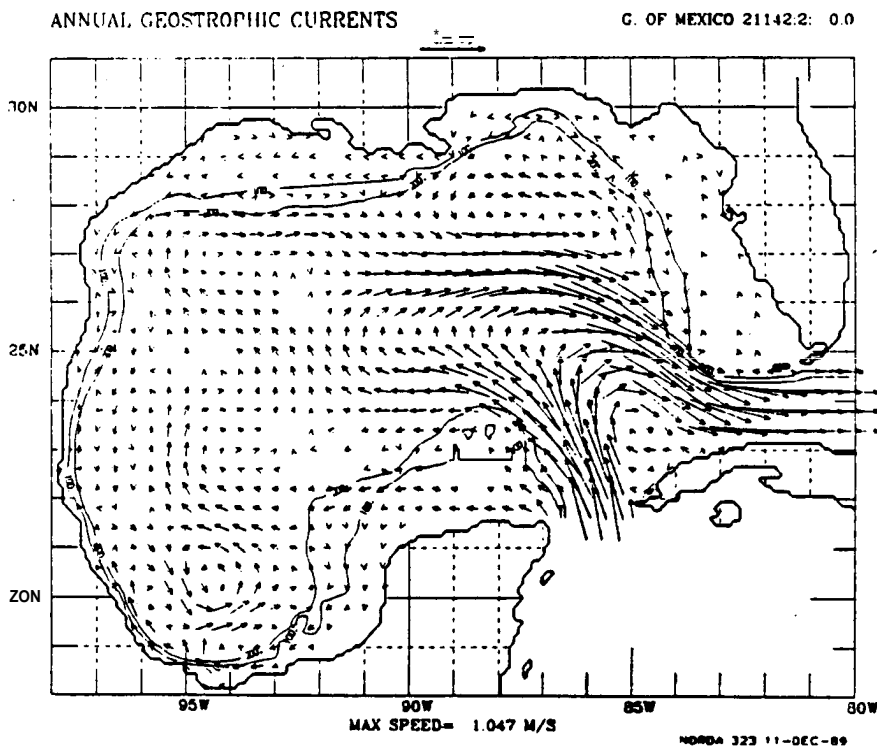
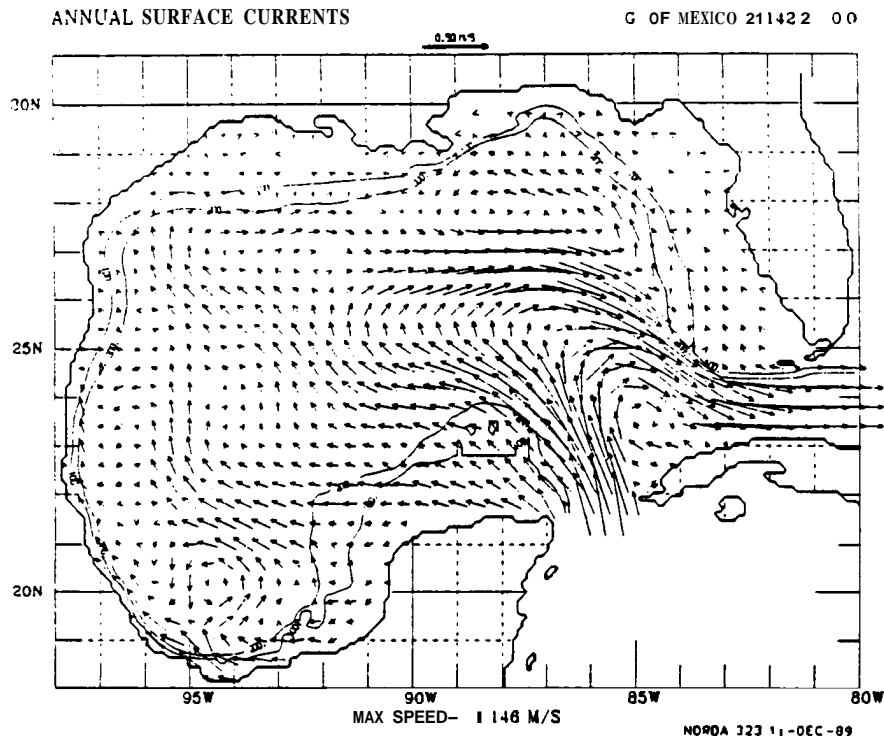


Figure 55. Winter surface current climatology (a) from the 10-year merged simulation and (b) from historical observations.

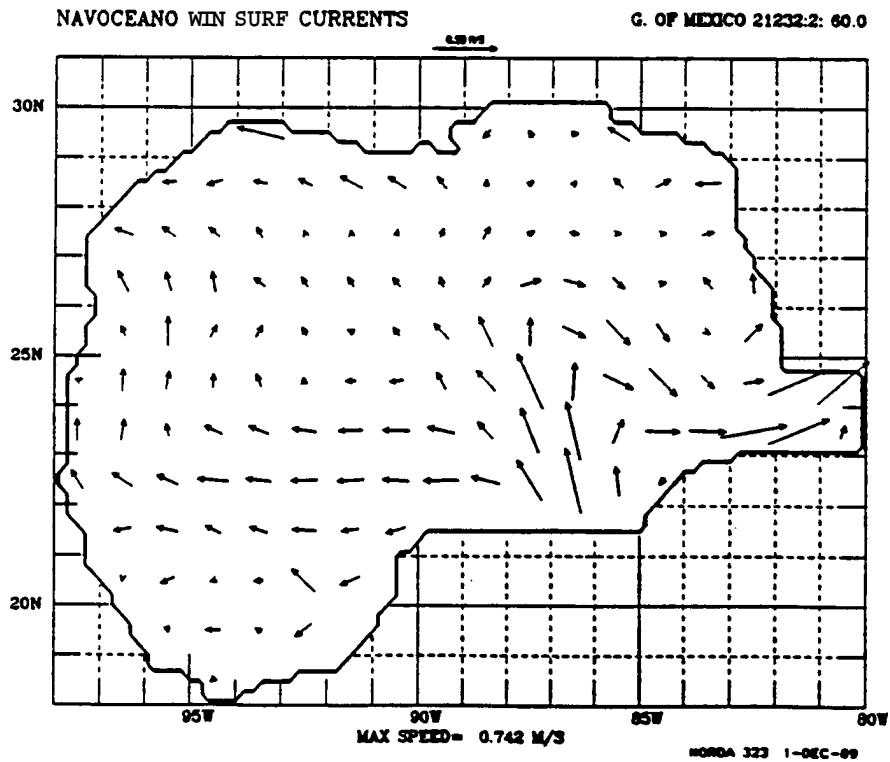
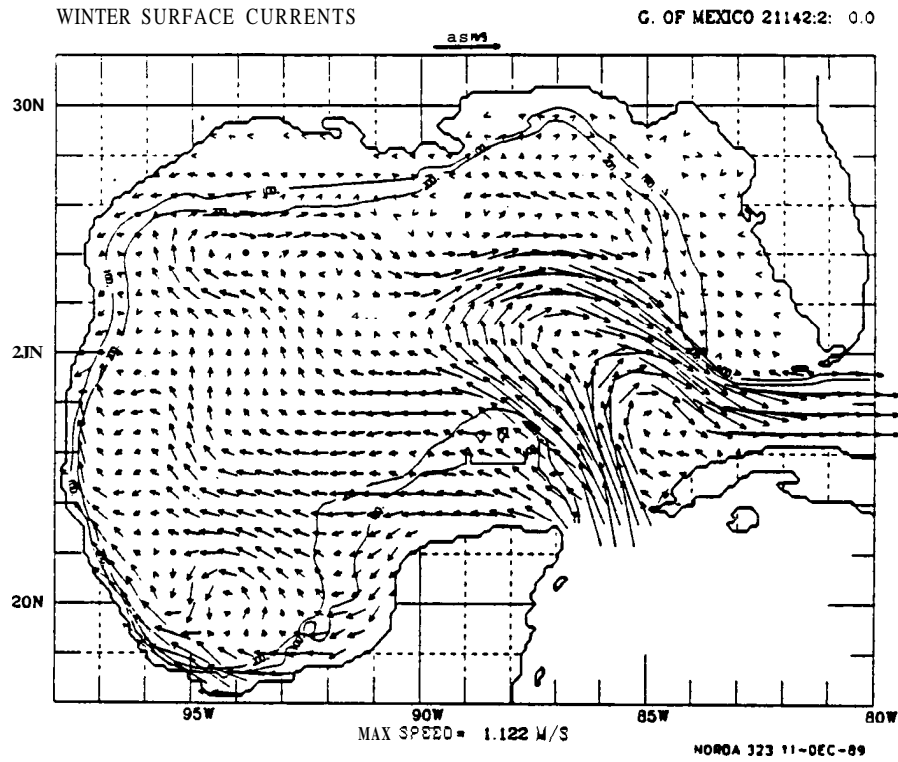


Figure 56. Spring surface current climatology (a) from the 10-year merged simulation and (b) from historical observations.

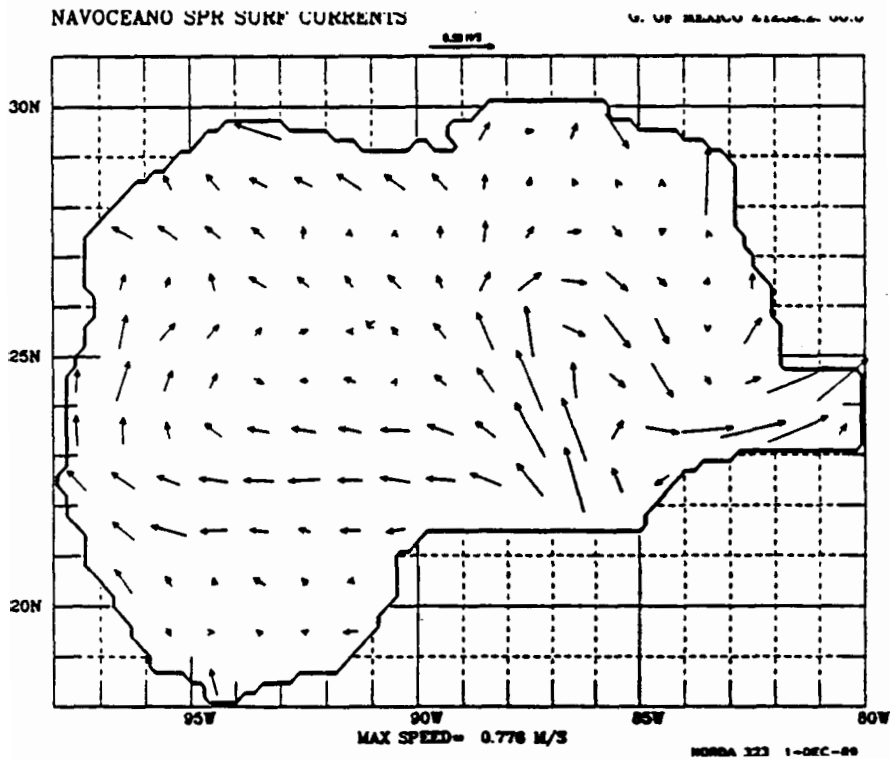
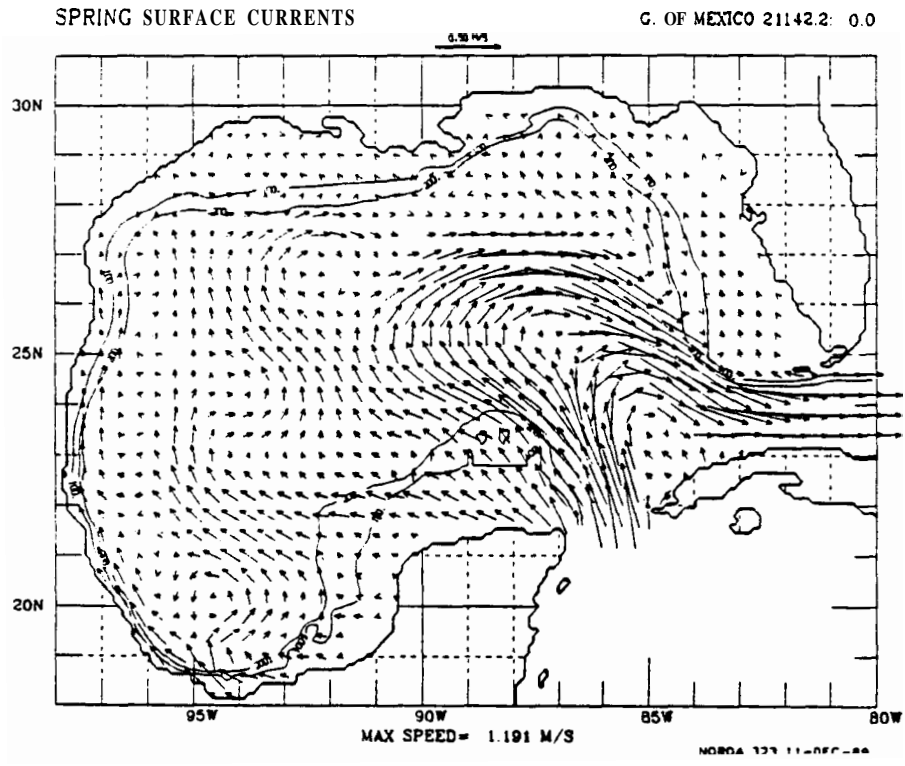


Figure 57. Summer surface current climatology (a) from the 10-year merged simulation and (b) from historical observations.

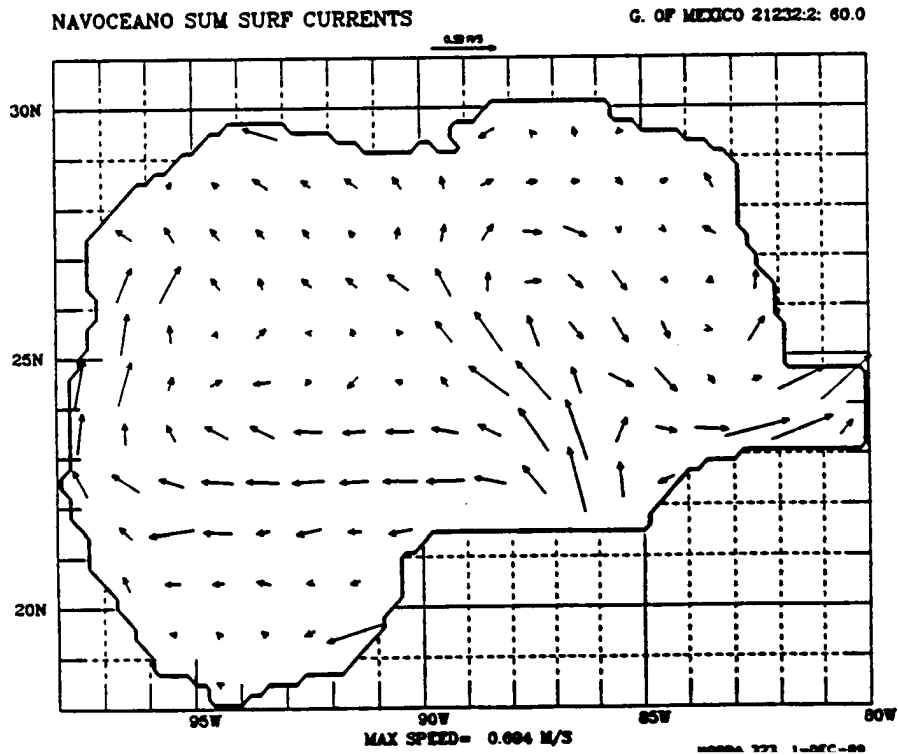
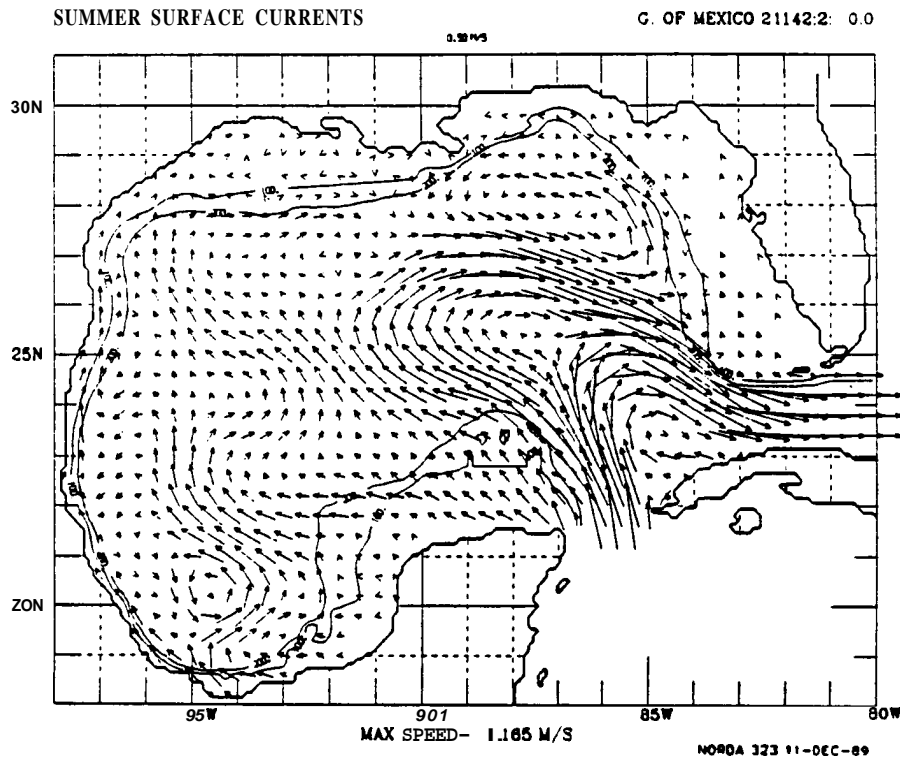


Figure 58. Fall surface current climatology (a) from the 10-year merged simulation and (b) from historical observations.

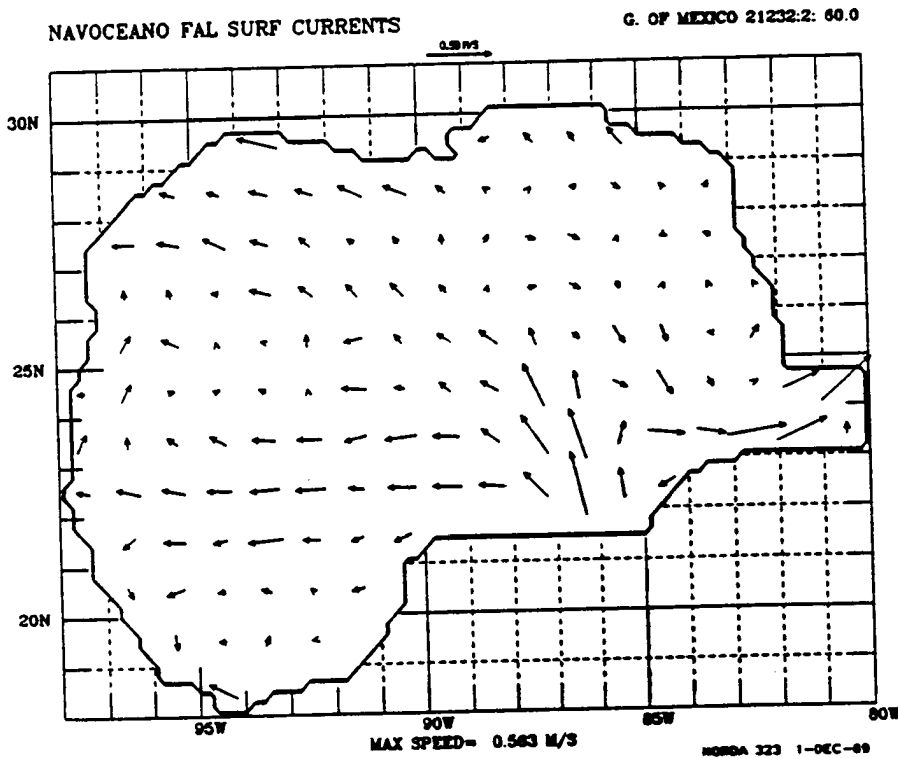
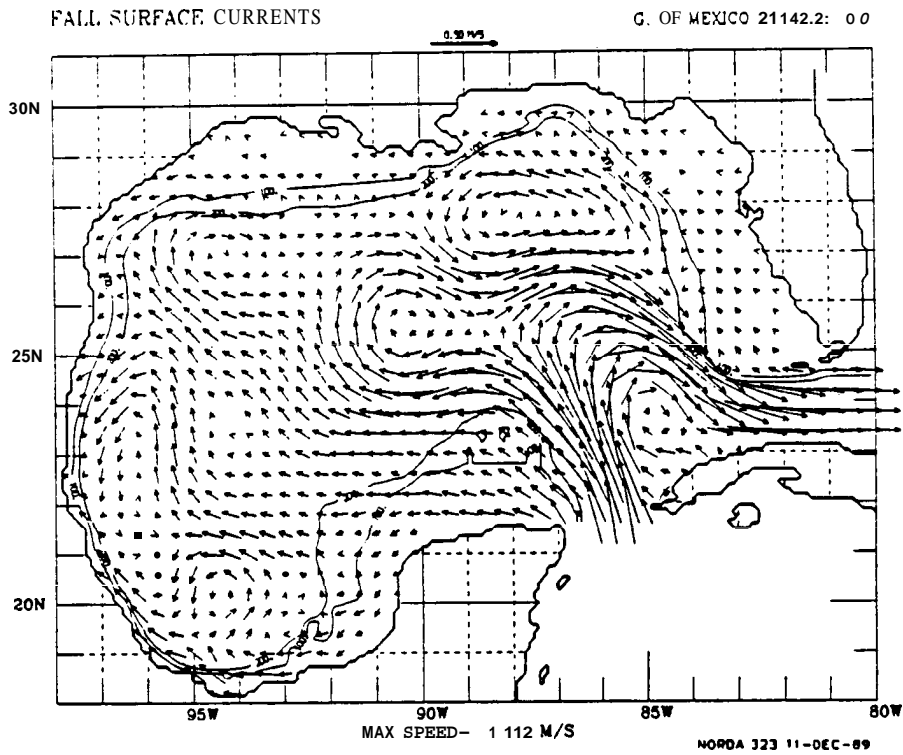


Figure 59. On wind Day 001/1969 (a) surface current from the merged simulation and (b) surface current anomaly versus the winter climatology.

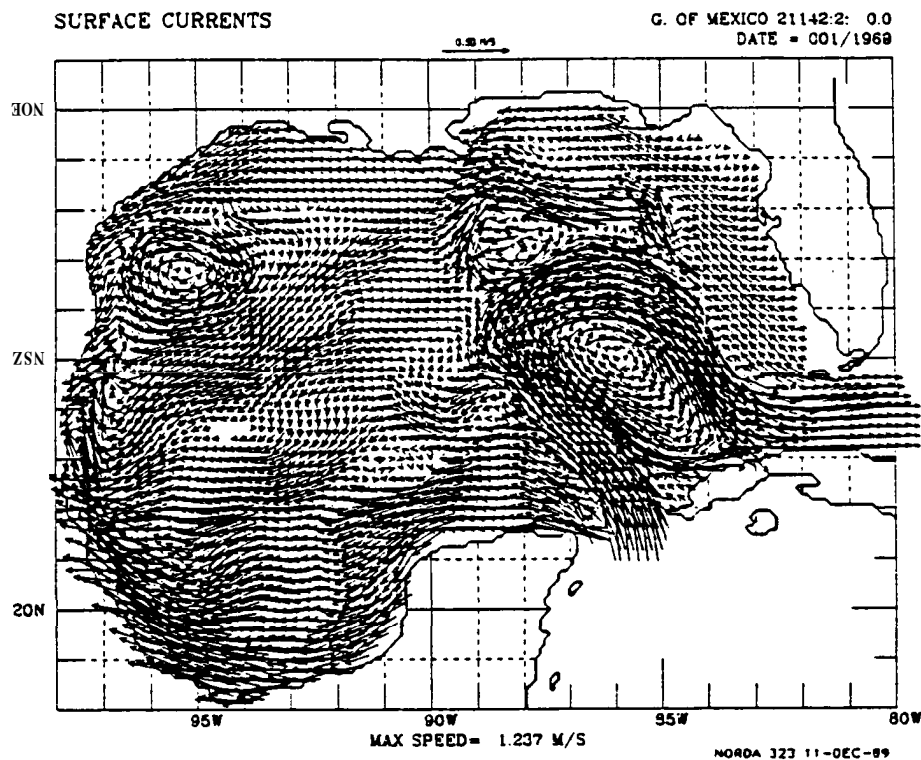


FIGURE 59a

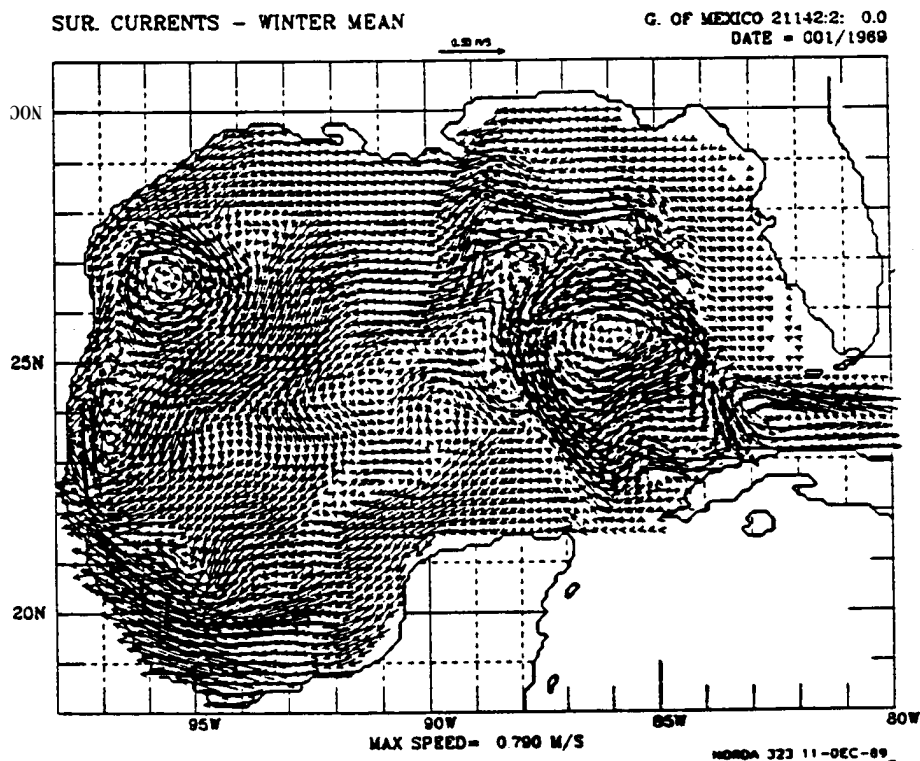


FIGURE 59b

Figure 60. **On** wind Day 091/1969 (a) surface current from the merged simulation and (b) surface current anomaly versus the spring climatology.

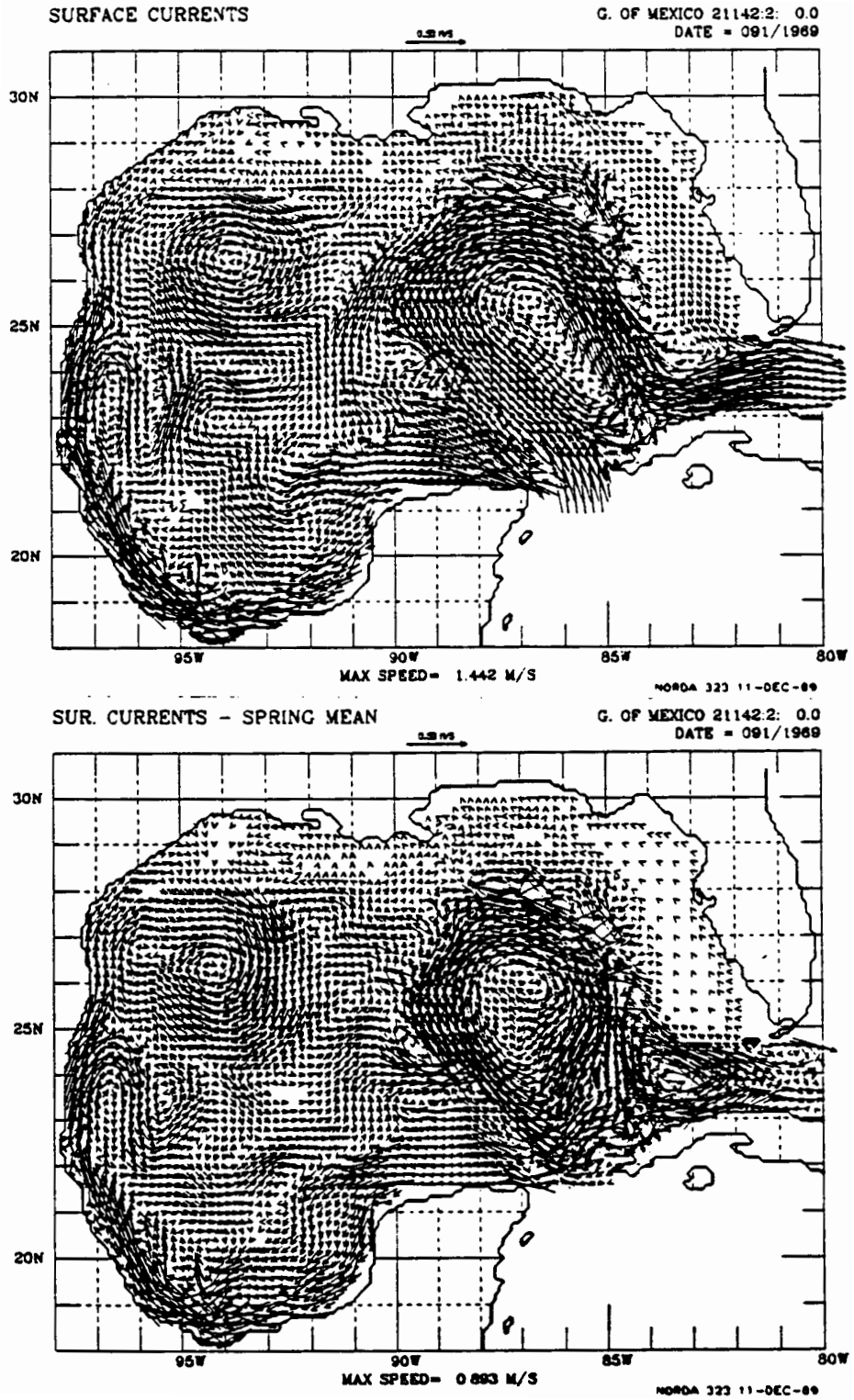


Figure 61. On wind Day 181/1969 (a) surface current from the merged simulation and (b) surface current anomaly versus the summer.

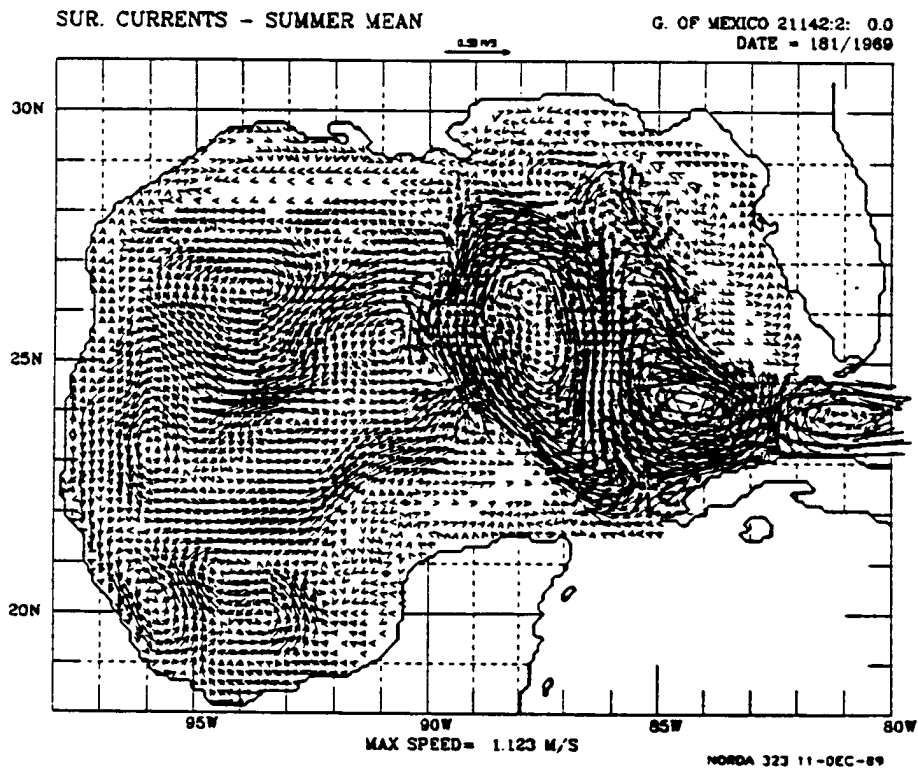
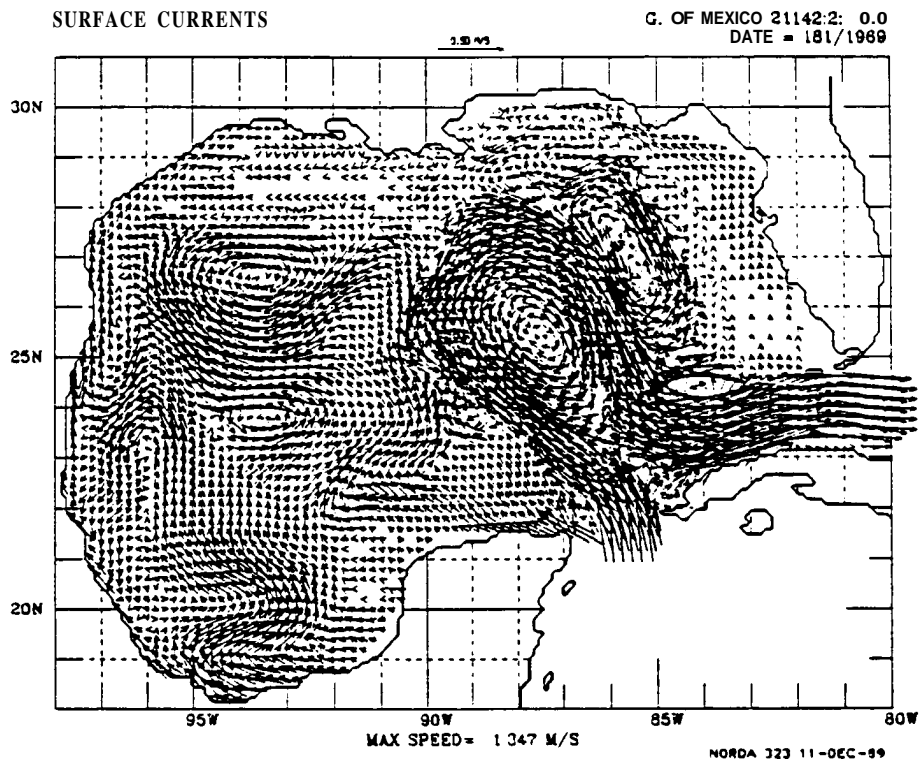


Figure 62. On wind Day 271/1969 (a) surface current from the merged simulation and (b) surface current anomaly versus the fall climatology.

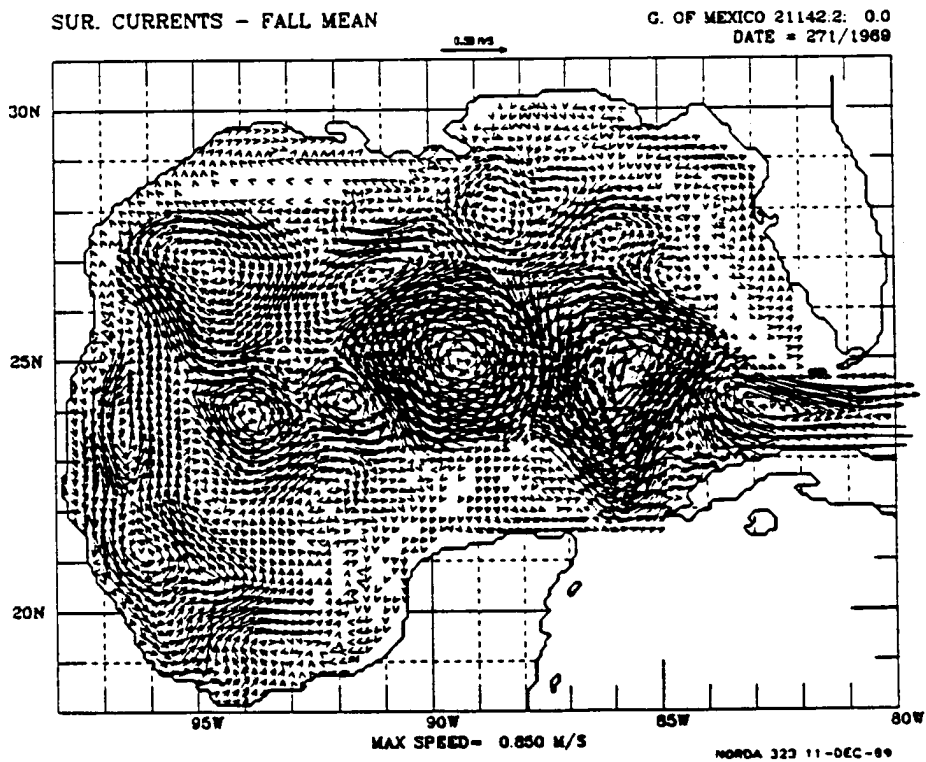
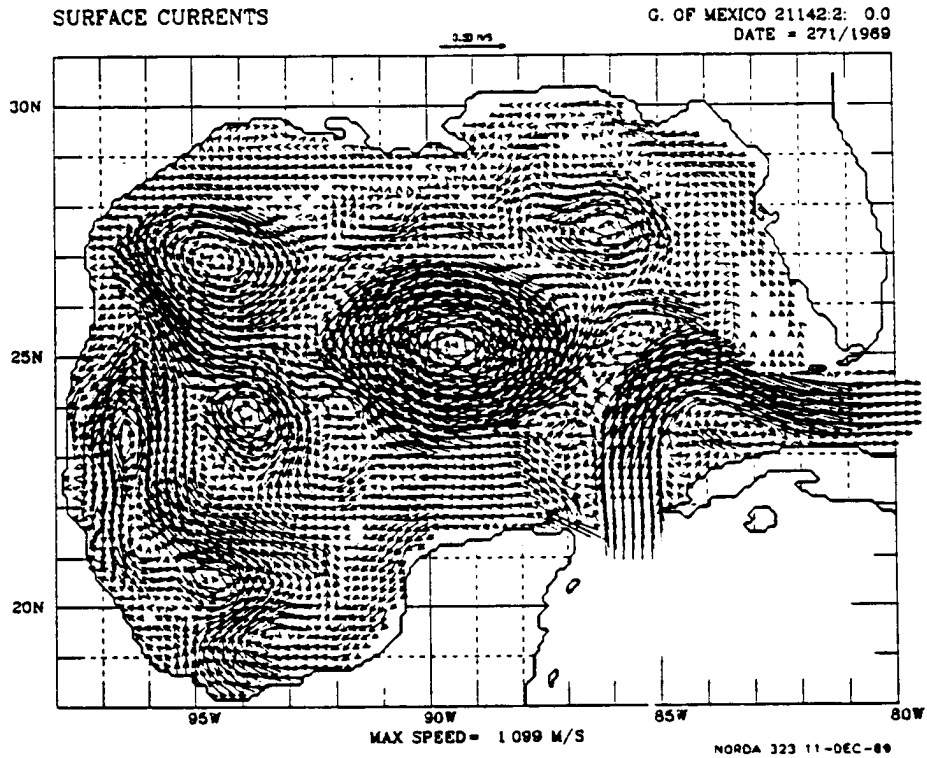


Figure 63. Map of the Gulf of Mexico showing the locations of current meter arrays from the Gulf of Mexico Physical Oceanography Program.

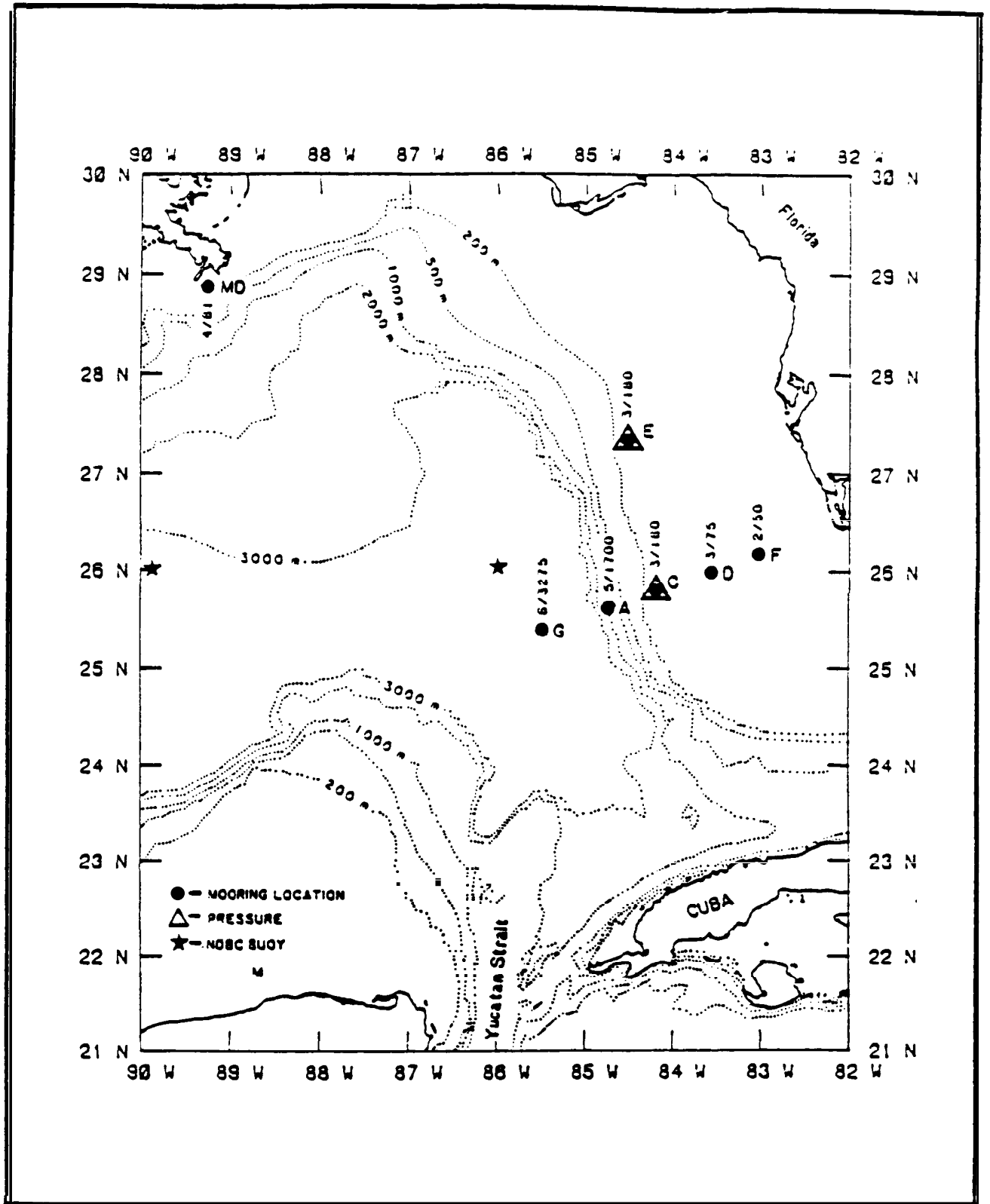
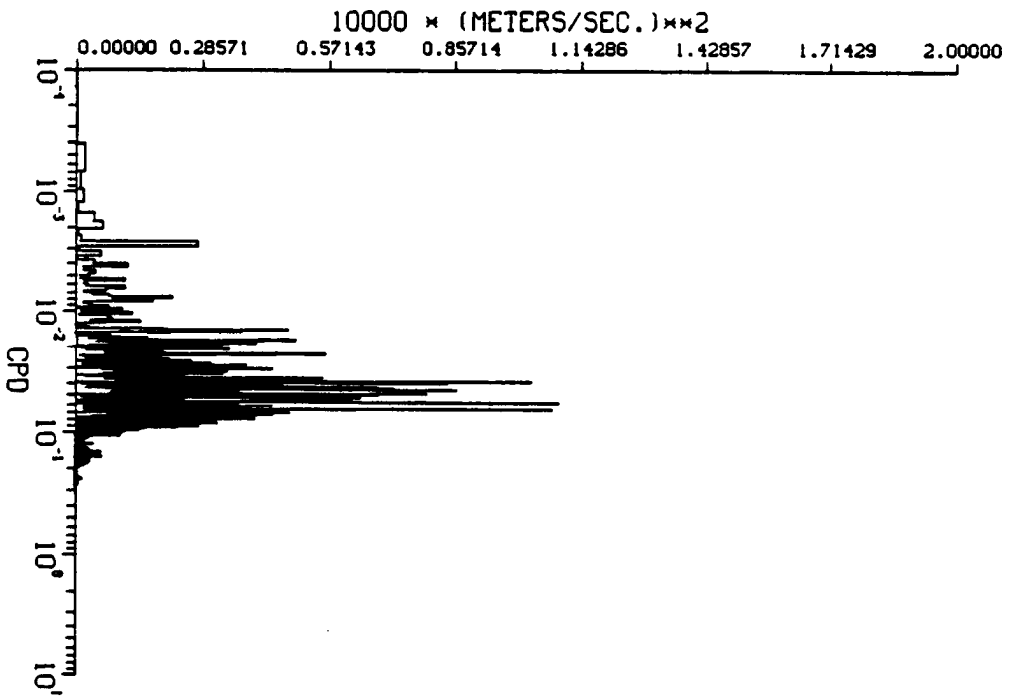
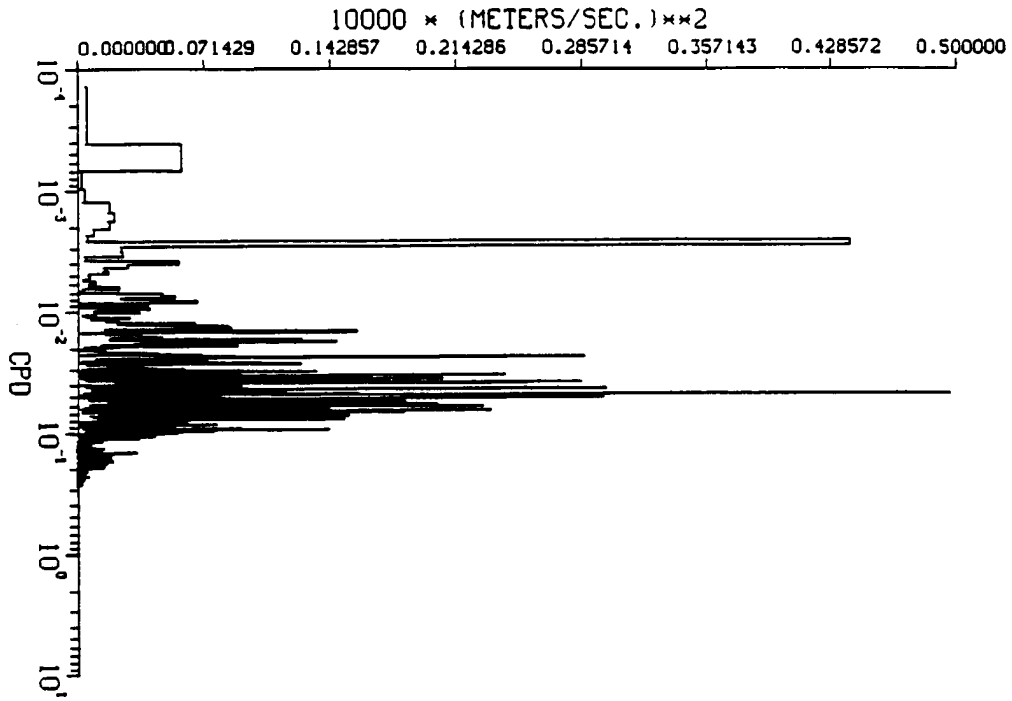


Figure 64. Velocity component spectra for 10 years from the simulation at location MOF (a) u component and (b) v component.



annual signal in the cross shelf, but not the the long shelf direction. In contrast to the case studied in the second year (Wallcraft, 1986) comparison (Figure 11), there is no peak at about 100 days in the latest simulation. This is additional evidence that the original signal was due to Loop Current effects that cannot be present in the merged simulation at this location. Figures 65 and 66 show velocity component spectra at location **MOD** for the observations and the simulation. As in all cases, there is very little energy below seven days in the simulation. Both show a peak at about 50-100 days, but the simulation shows a strong peak at 20 days that is not present in the observations. Figures 67 and 68 are for location MOE that has one of the longest set of observations (1,090 days). The observations and simulation are in good agreement although the 10-year simulation shows energy at multiyear periods that is not present in the observations.

Figures 69 and 70 are for the simulation only at locations MOA and MOC. They show a strong peak at about two years, which is the signature of the Loop Current cycle in this simulation (six eddies shed in 10 years). Figures 71 and 72 are again for the simulation only, but this time for locations **MEF** and MGG in the central Gulf. A strong Loop Current eddy signature can be seen here too.

Wind stress, surface current (**L2+L1+P**), and geostrophic surface current (**L2+L1**) fields from the merged simulation (sampled every three days for 10,750 and 1,600 meter depths, sampled every six days for the same 10-year period) have also been delivered, as have detailed vertical current profiles (**L2+L1+P**) at the locations of all the moored buoys used in Years 1-5 of **MMS's** recently concluded Gulf of Mexico Physical Oceanography Program. Figures 73-193 show all the surface current fields (**L2+L1+P**) delivered for one full Loop Current eddy cycle, which is about 20% of the surface current fields in the full 10 years.

V. CONCLUSIONS

This project was designed from the outset to be modest in scope. The limitations of the original layered model were known from the beginning (**JAYCOR, 1983**), but the fact that the shelf circulation is vital to the success of any simulation used in oil spill risk analysis was not fully appreciated at **first**. Attempts to improve the multilayered model's skill over the shelf, while maintaining the project's modest funding level, have proved largely unsuccessful. The final product does not have several of the major enhancements to the model that were originally proposed; and instead, uses two related models with the same forcing, but with no other coupling between them for the shelf and deep water circulation. If a **more** ambitious project were to choose

Figure 65. Velocity component spectra for 362 days from the observations at location MOD (a) u component at 60 m and (b) v component at 60 m.

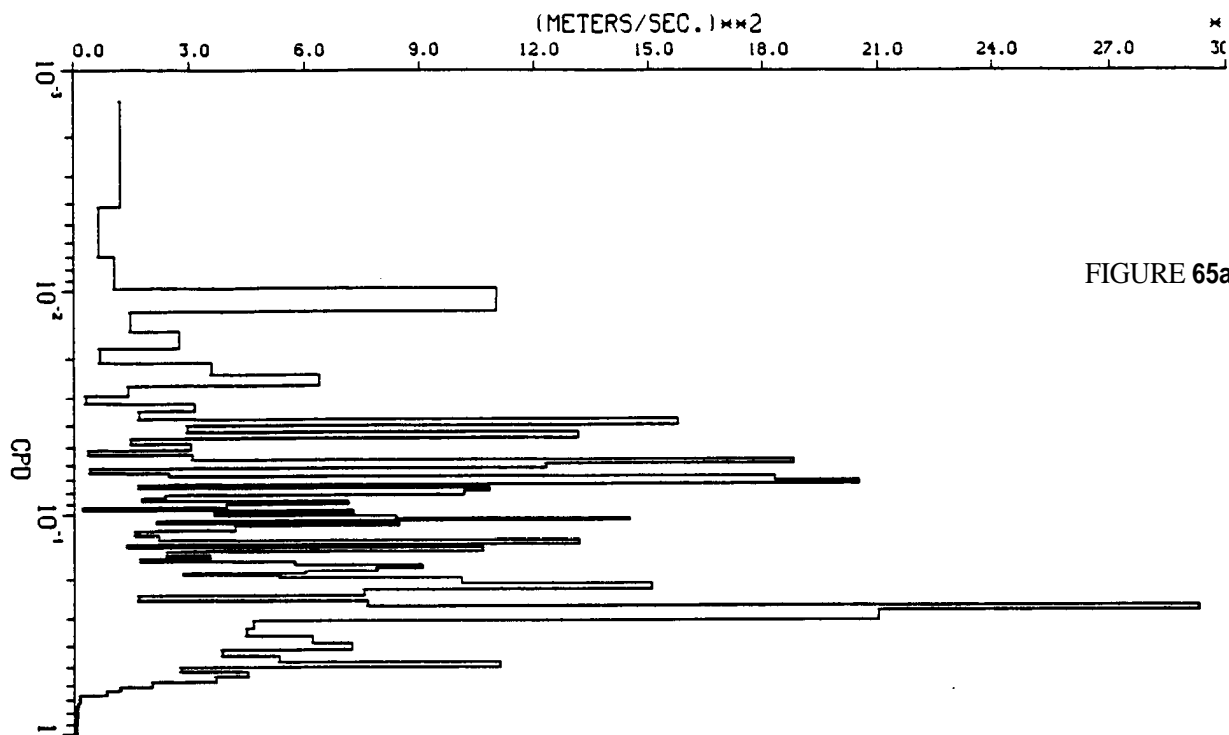


FIGURE 65a

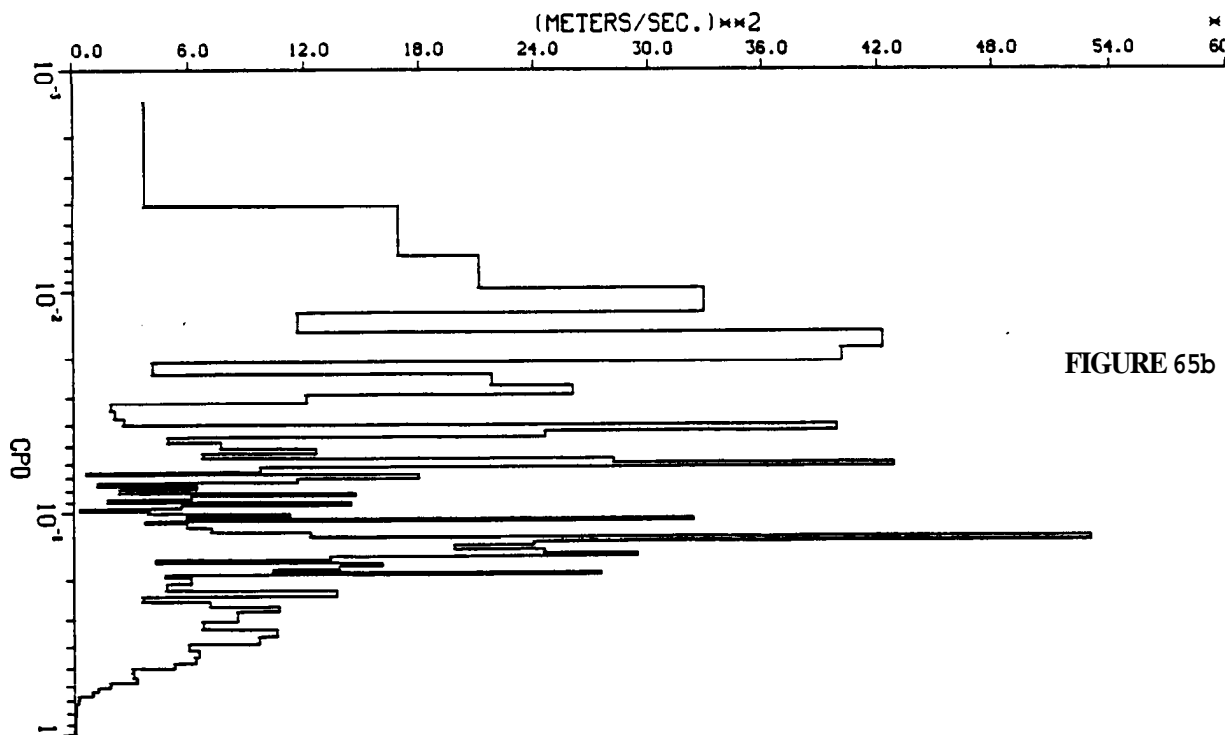


FIGURE 65b

Figure 66. Velocity component spectra for one year from the simulation at location MOD (a) u component and (b) v component.

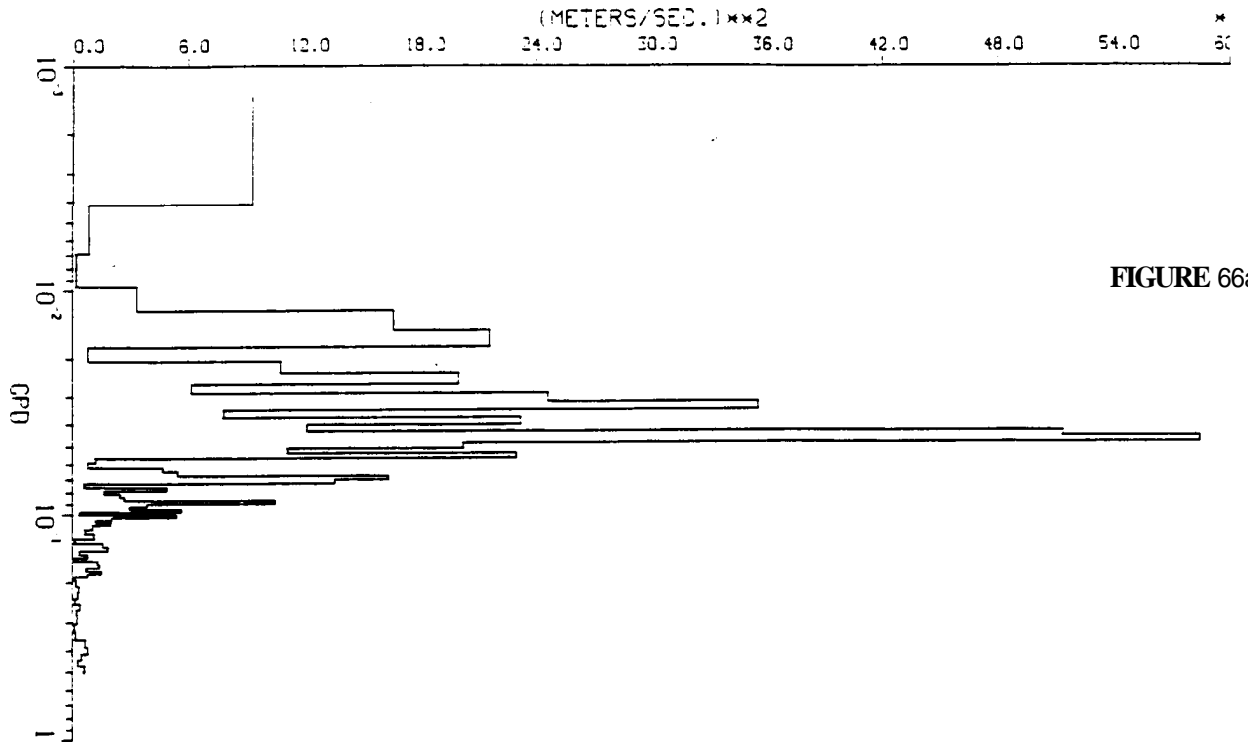


FIGURE 66a

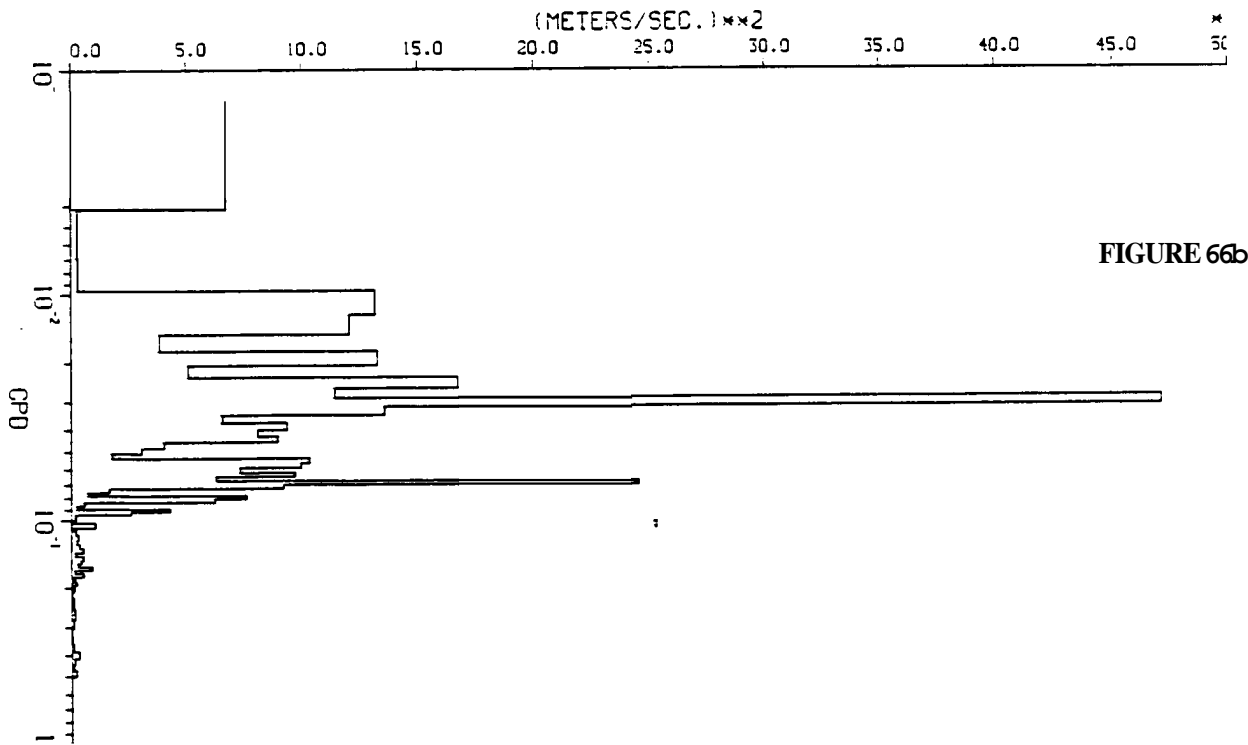


FIGURE 66b

Figure 67. Velocity component spectra for 1090 days from the observations at location MOE (a) u component at 100 m and (b) v component at 100 m.

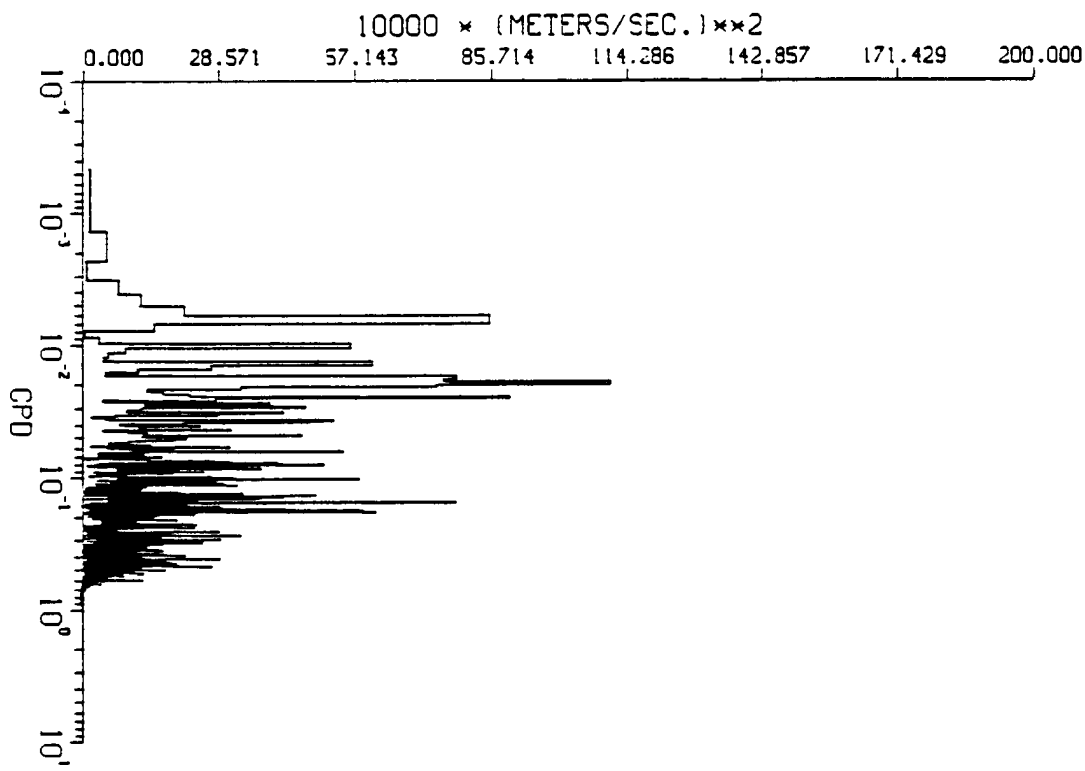
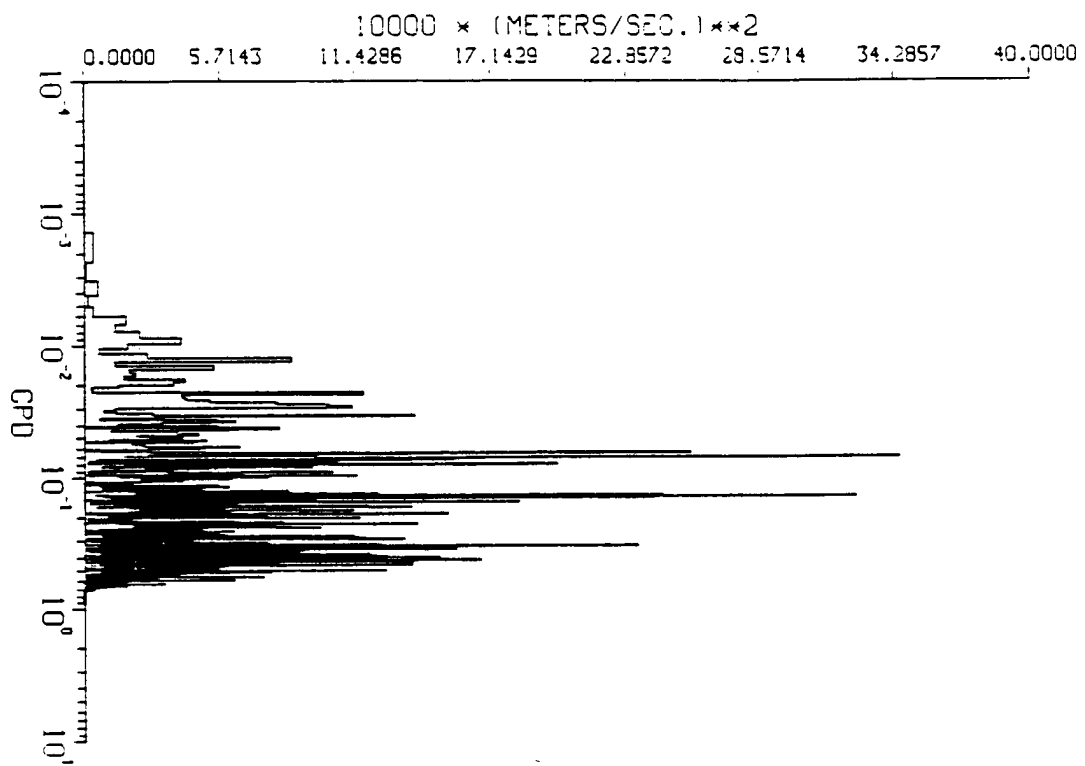


Figure 68. Velocity component spectra for 10 years from the simulation at location MOE (a) u component and (b) v component.

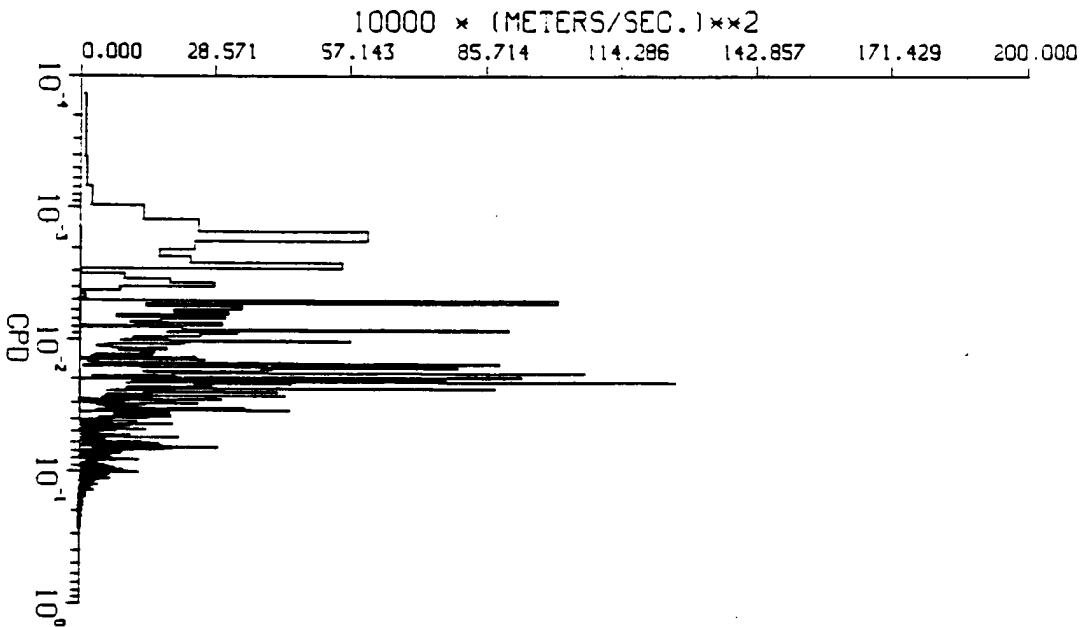
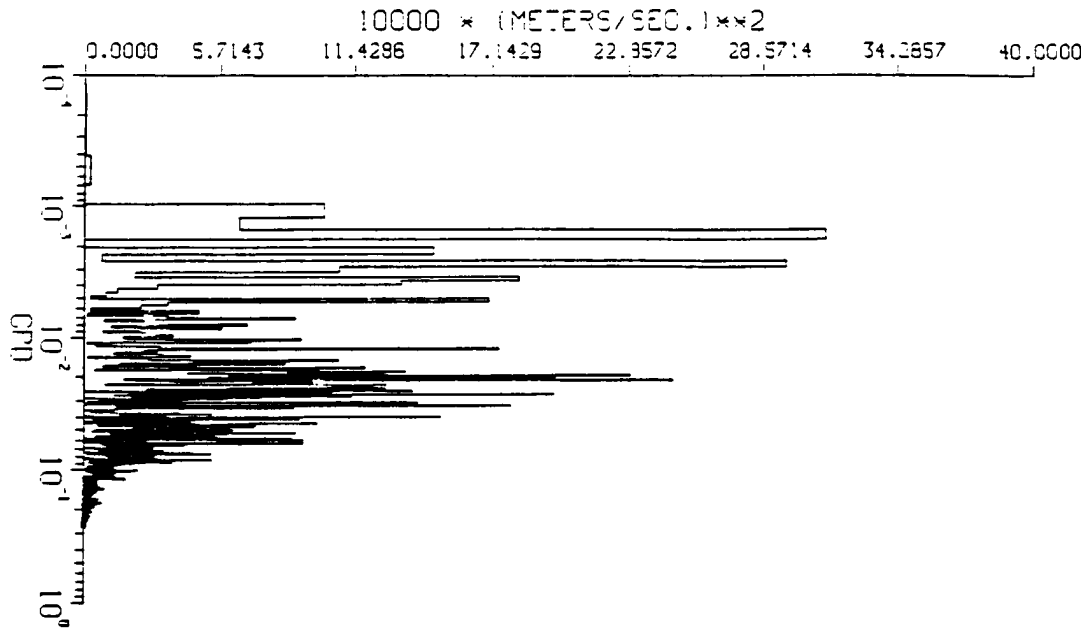


Figure 69. Velocity component spectra for 10 years from the simulation at location MOA (a) u component and (b) v component.

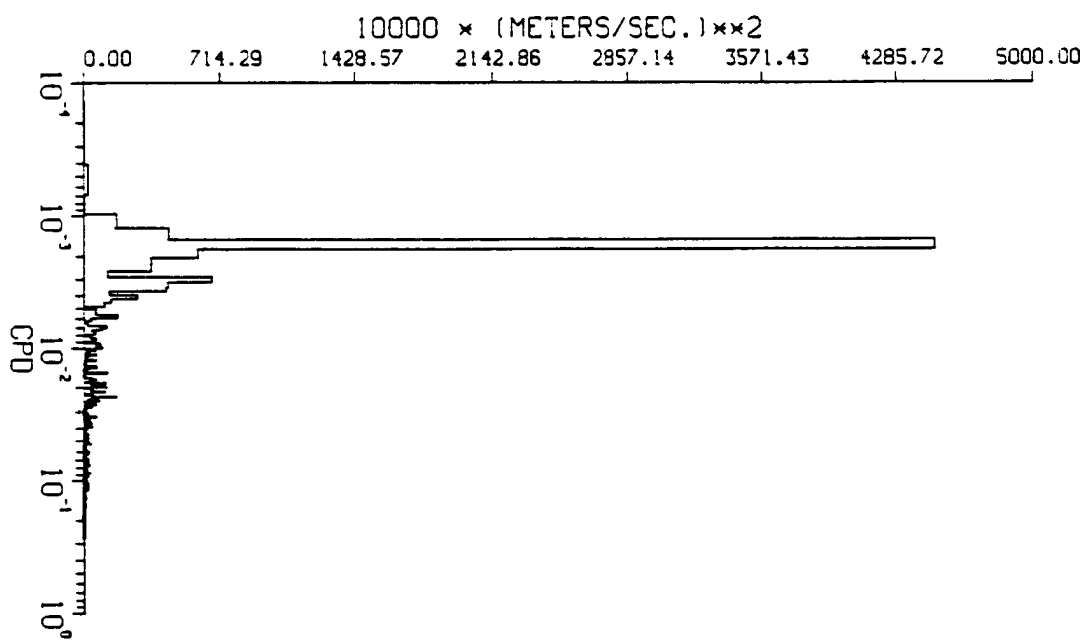
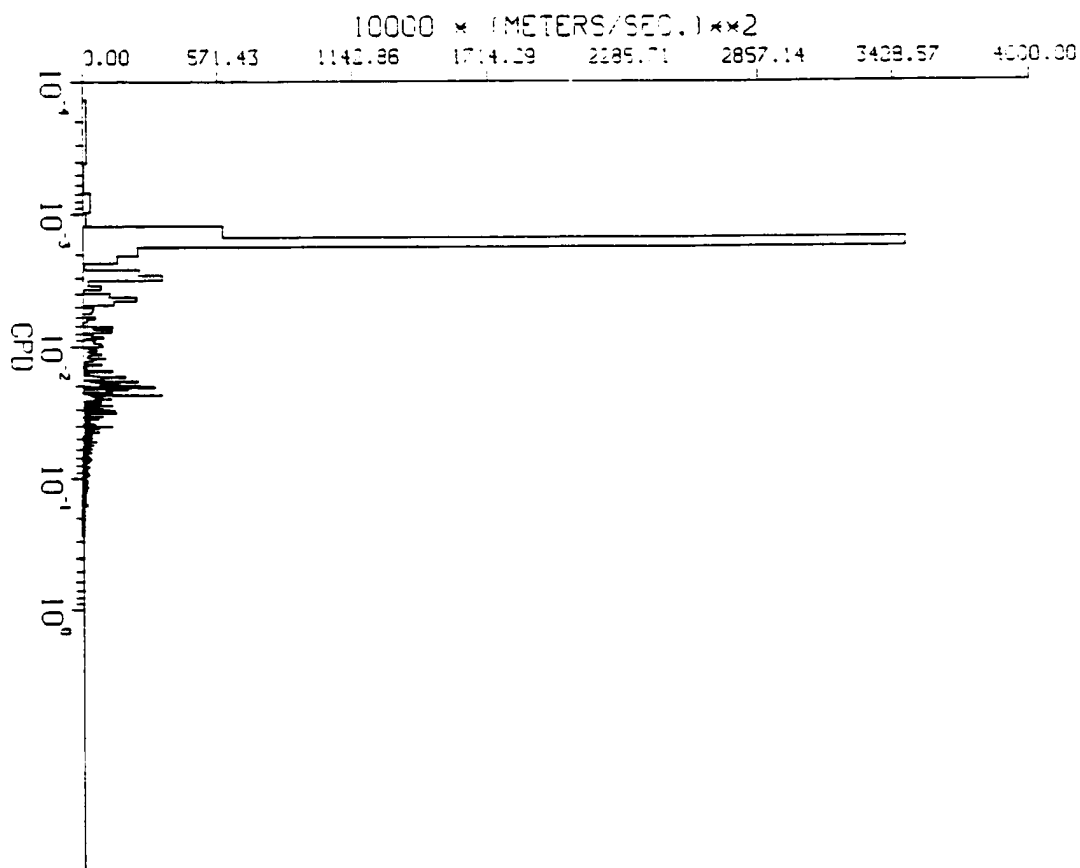


Figure 70. Velocity component spectra for 10 years from the simulation at location MOC (a) u component and (b) v component.

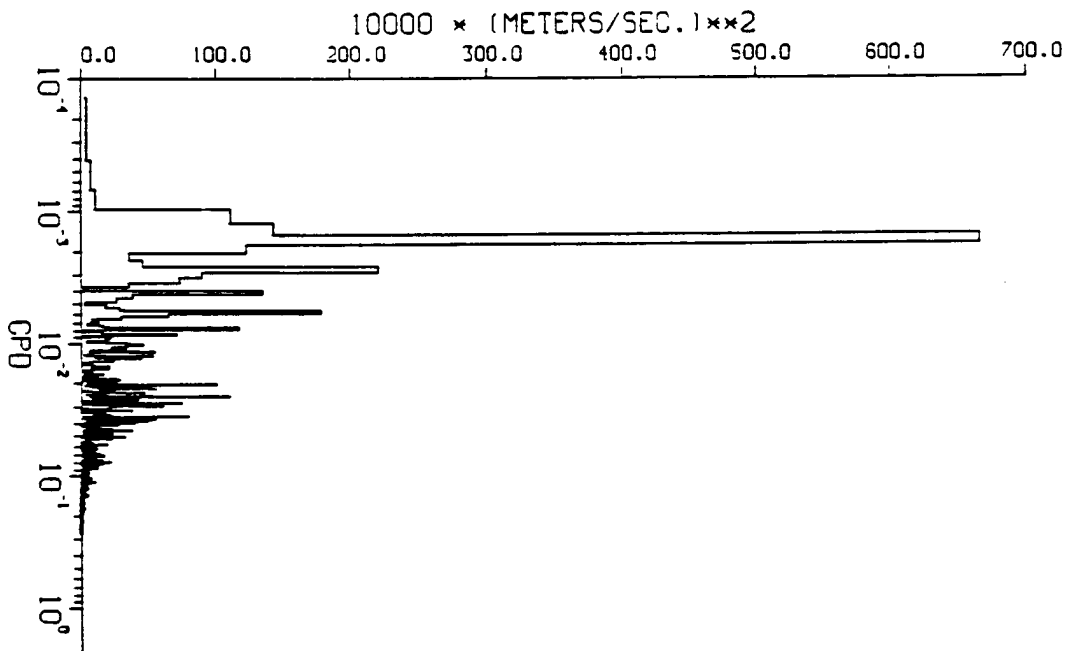
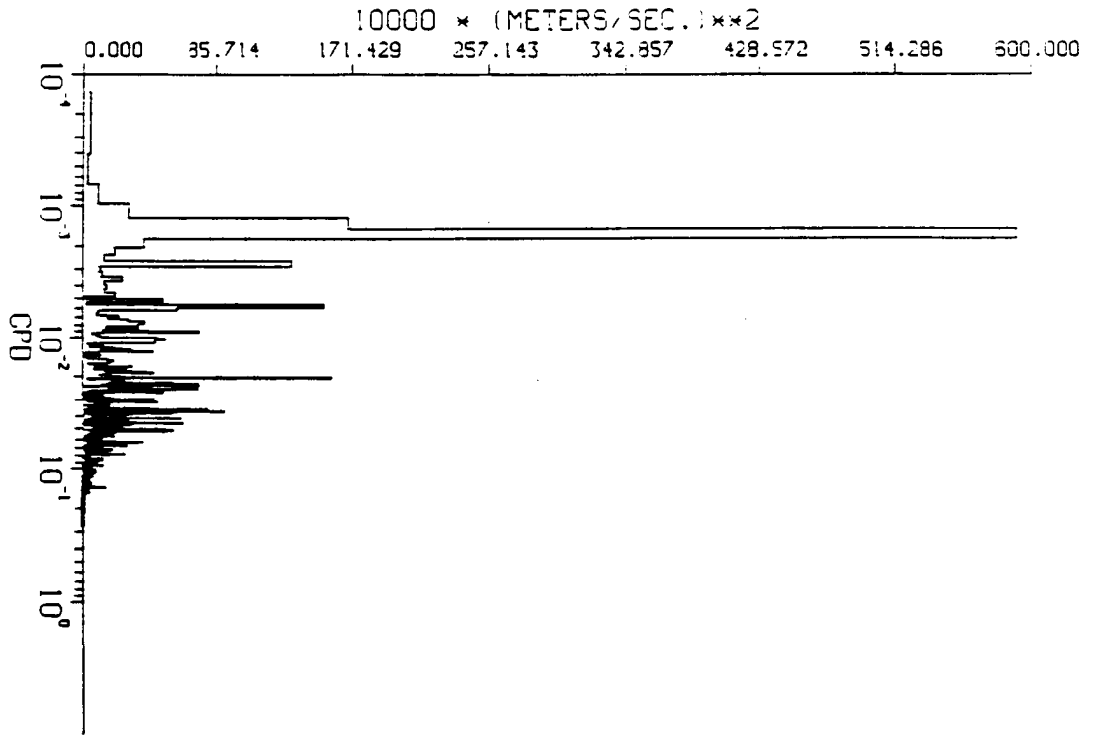


Figure 71. Velocity component spectra for 10 years from the simulation at location MFF (a) u component and (b) v component.

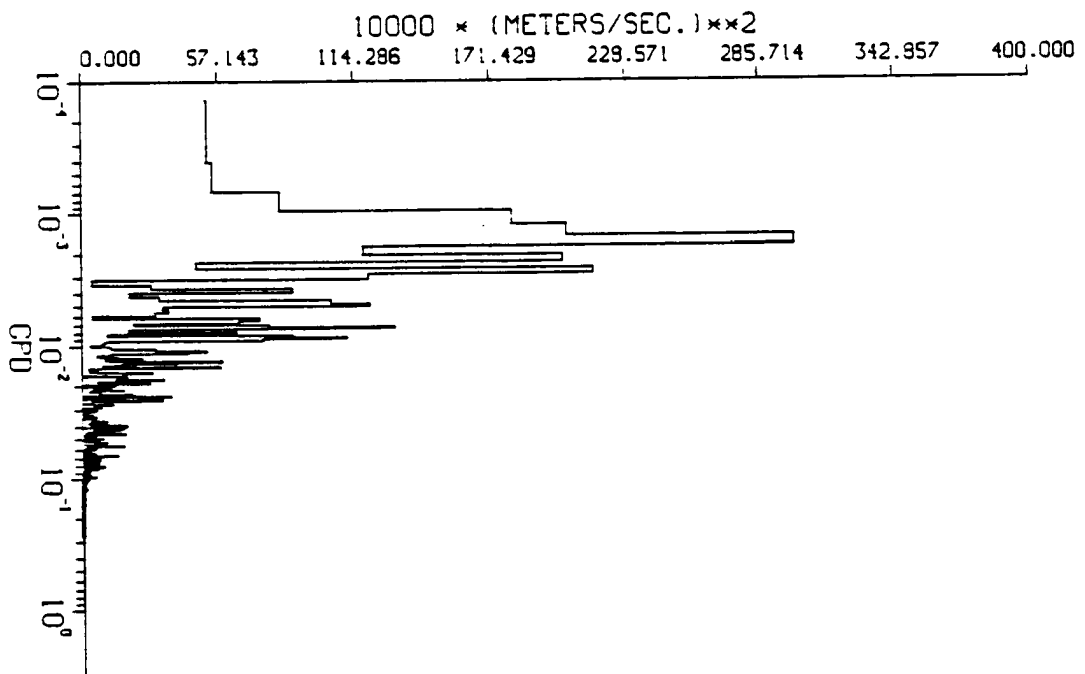
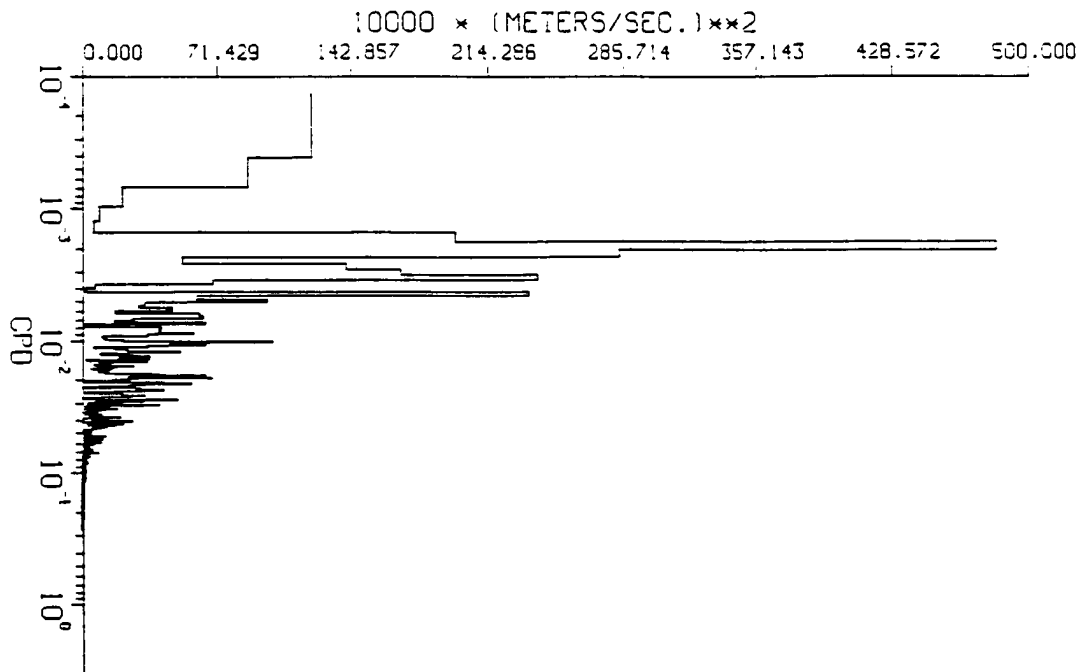
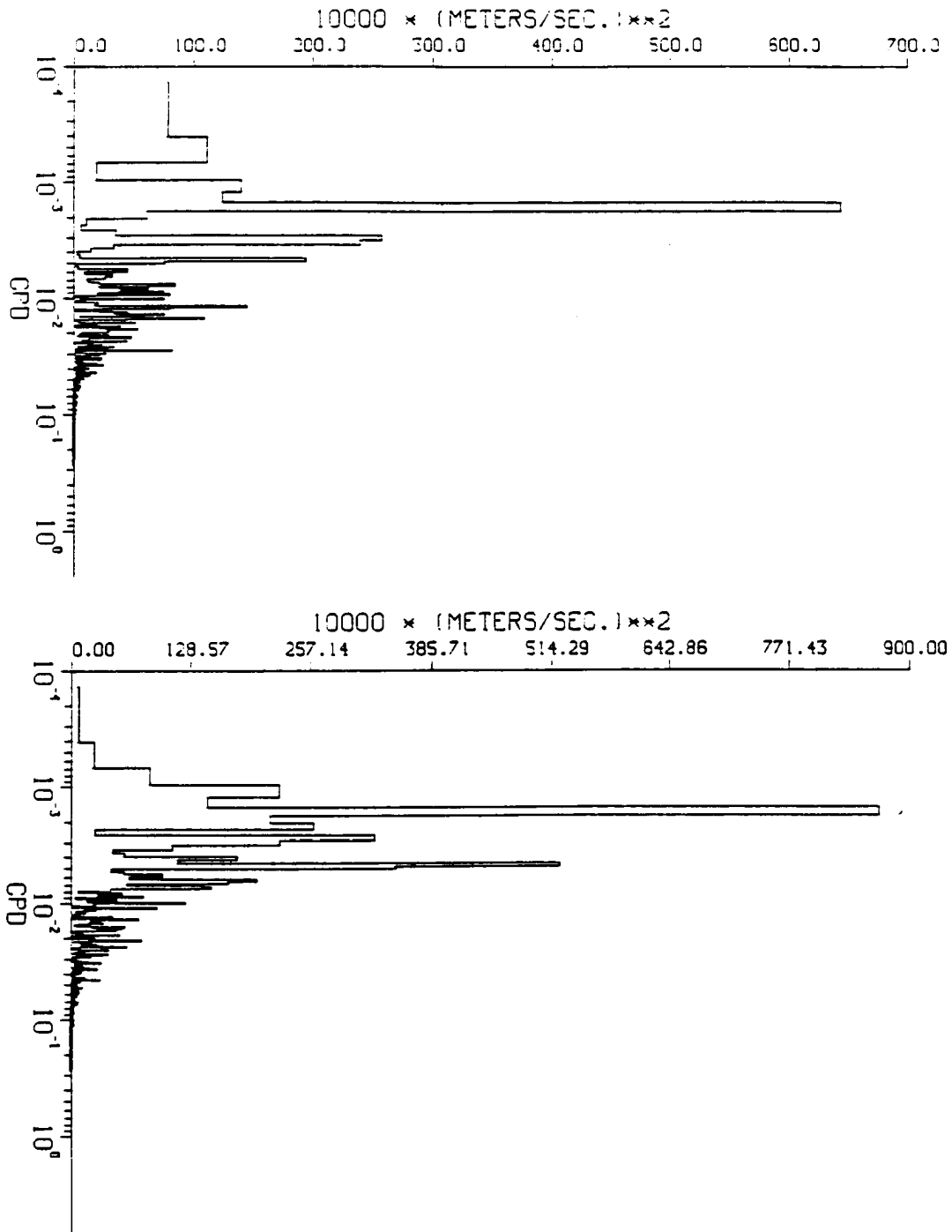


Figure 72. Velocity component spectra for 10 years from the simulation at location MGG (a) u component and (b) v component.



Figures 73-193. Surface currents from the merged simulation every three days for a full Loop Current eddy cycle. The wind day for each figure is given by the "DATE" in the top right-hand corner of each plot.

FIGURE 73

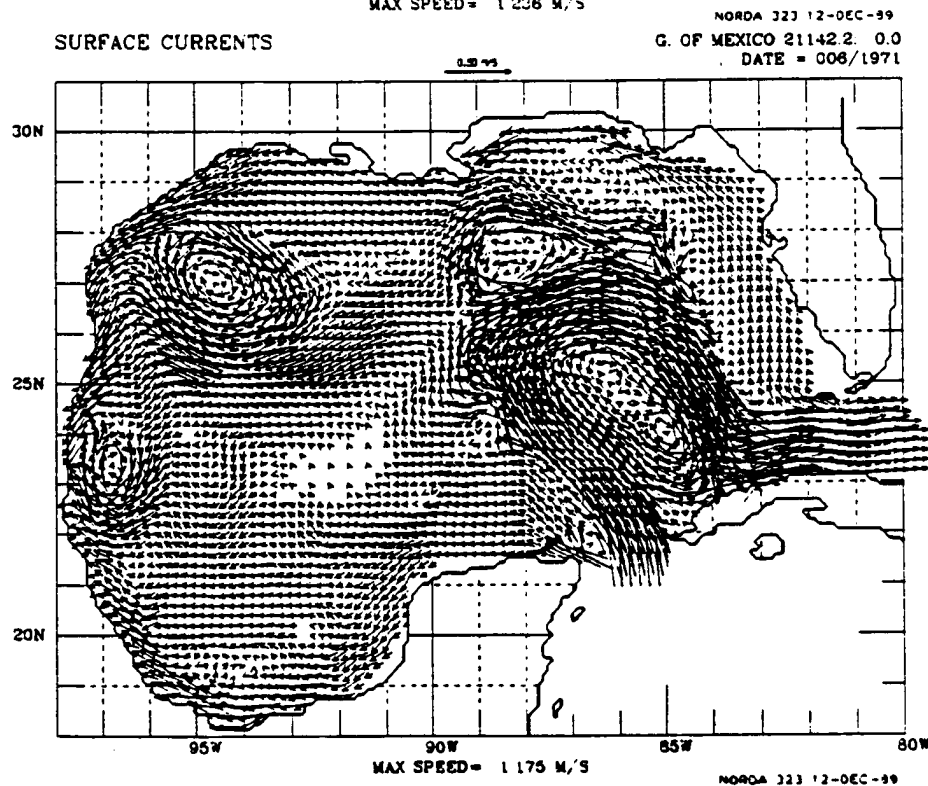
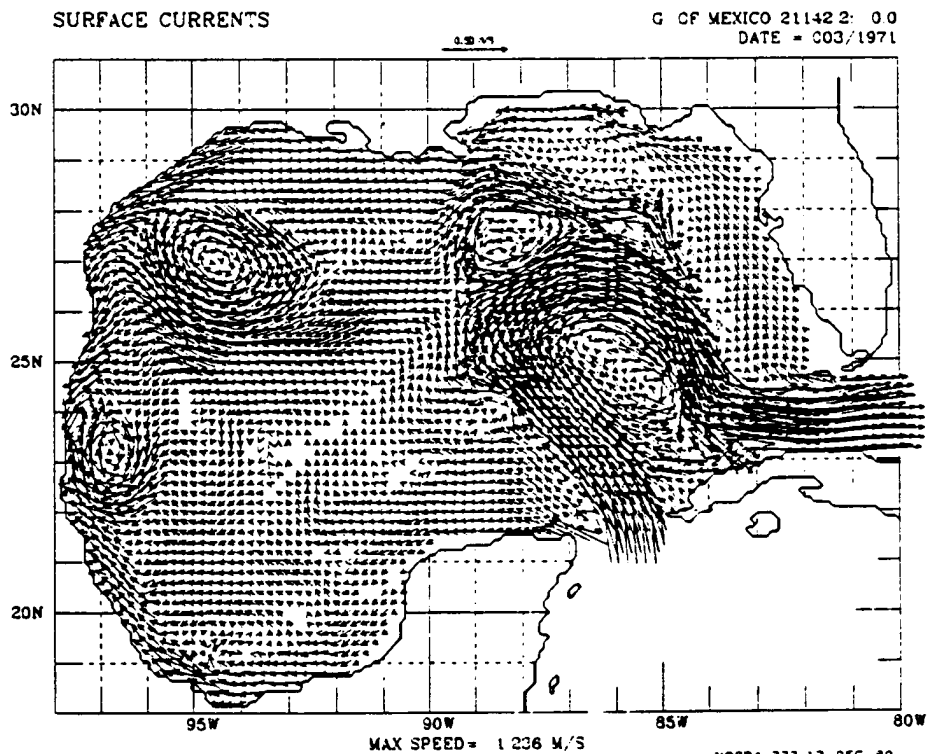
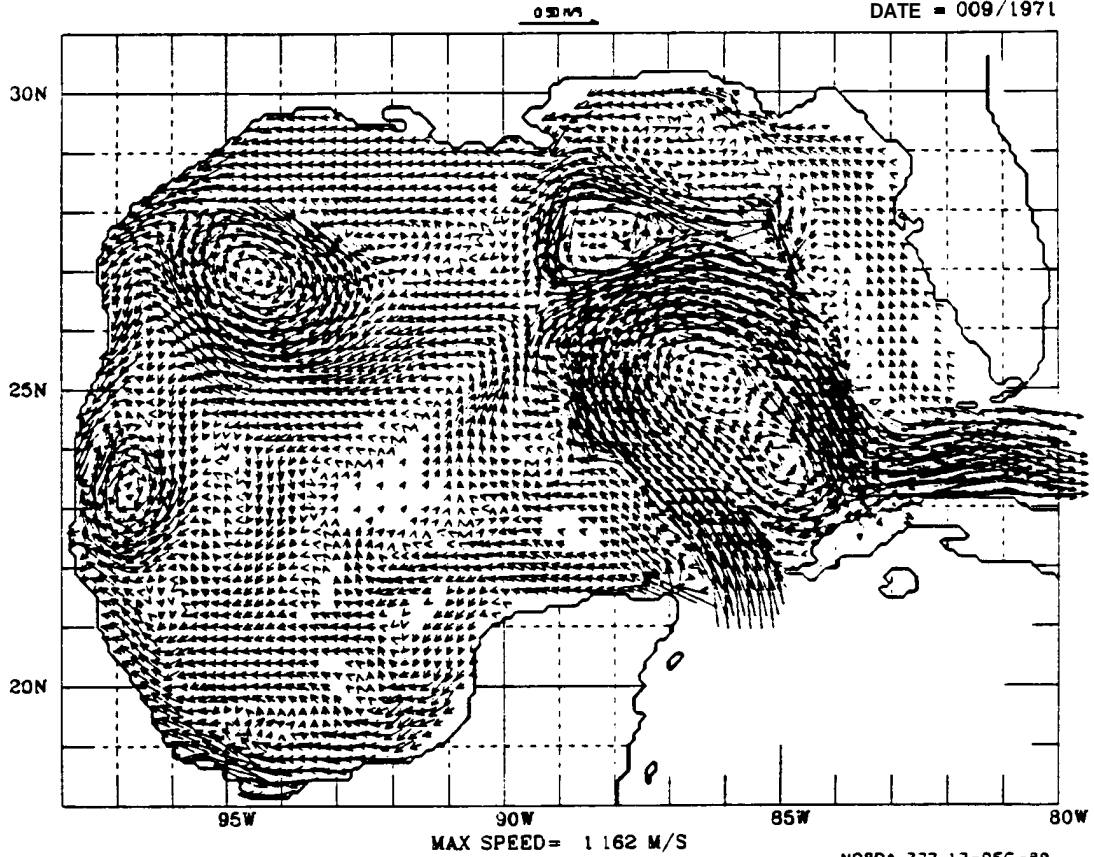


FIGURE 74

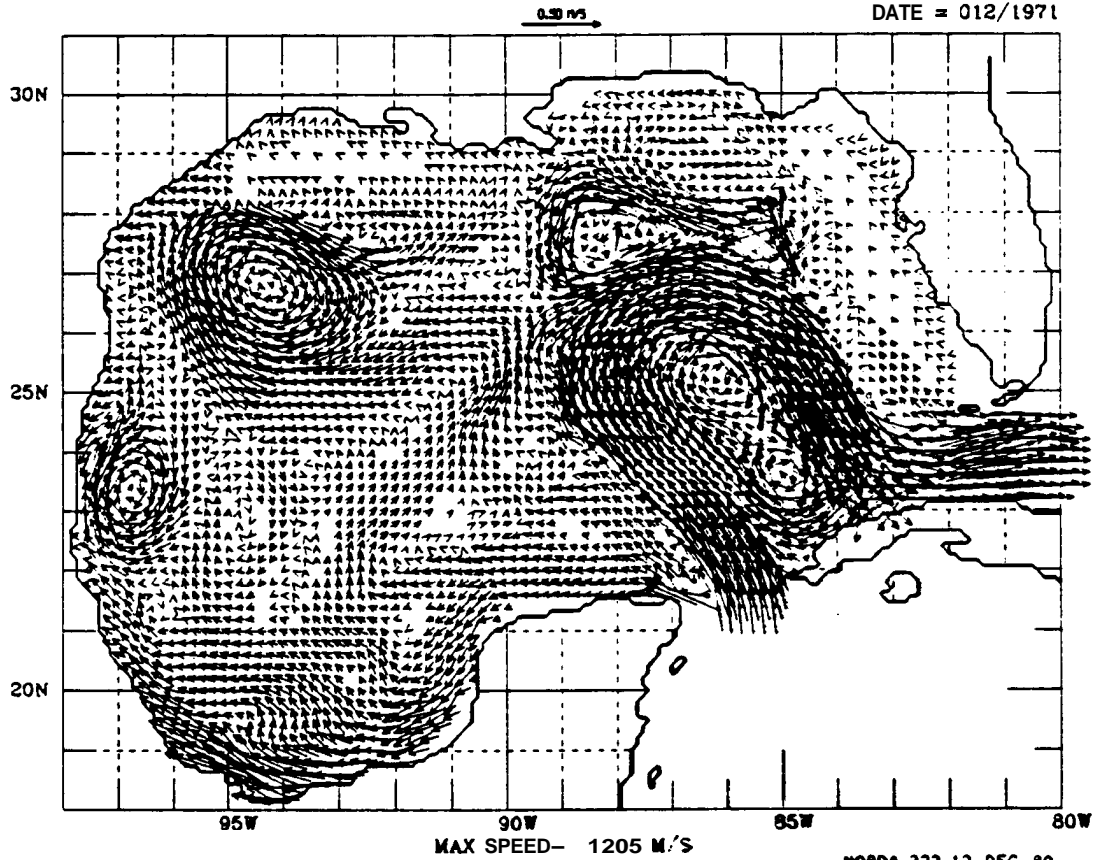
SURFACE CURRENTS

G. OF MEXICO 21142.2: 03
DATE = 009/1971



SURFACE CURRENTS

NORDA 323 12-DEC-89
G. OF MEXICO 21142.2: 0.0
DATE = 012/1971

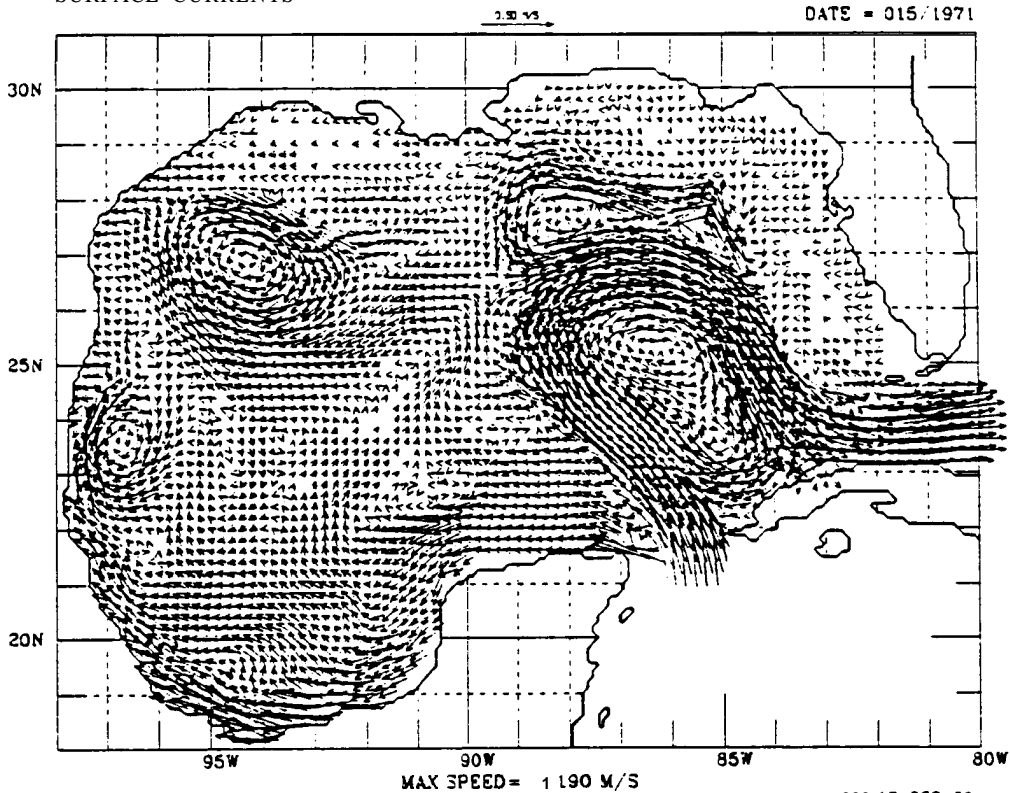


NORDA 323 12-DEC-89

FIGURE 75

SURFACE CURRENTS

G. OF MEXICO 21142.2: 0.3
DATE = 015/1971



SURFACE CURRENTS

NOROA 323 12-DEC-89
G. OF MEXICO 21142.2: 0.0
DATE = 018/1971

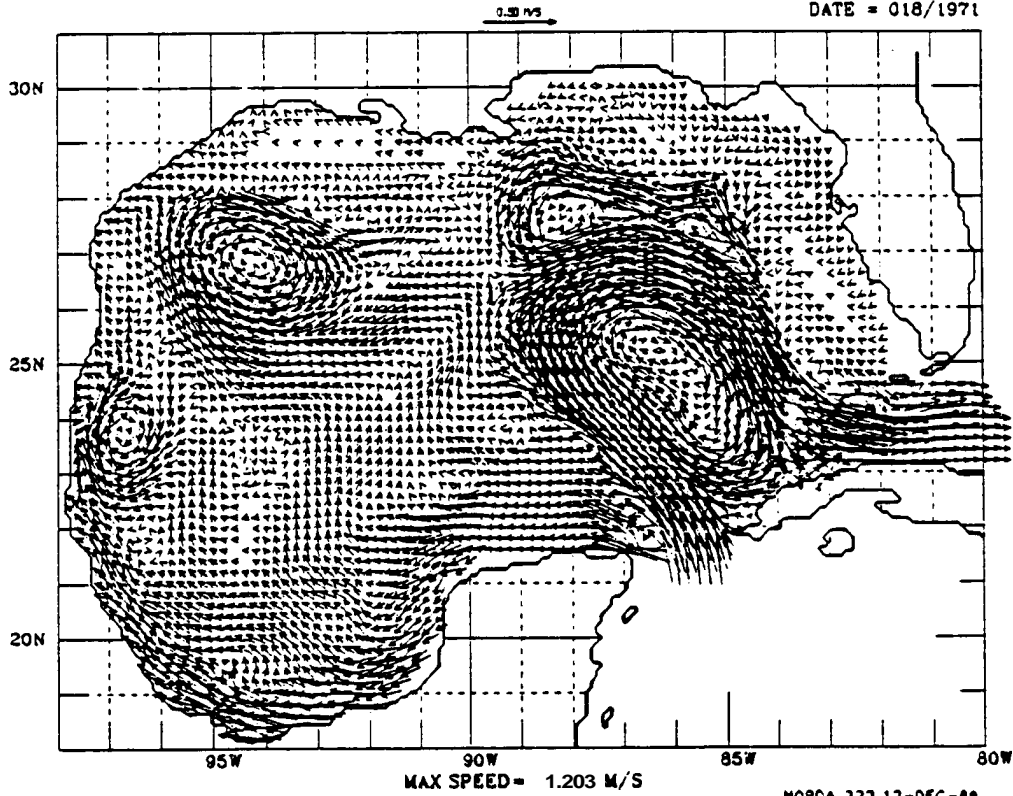
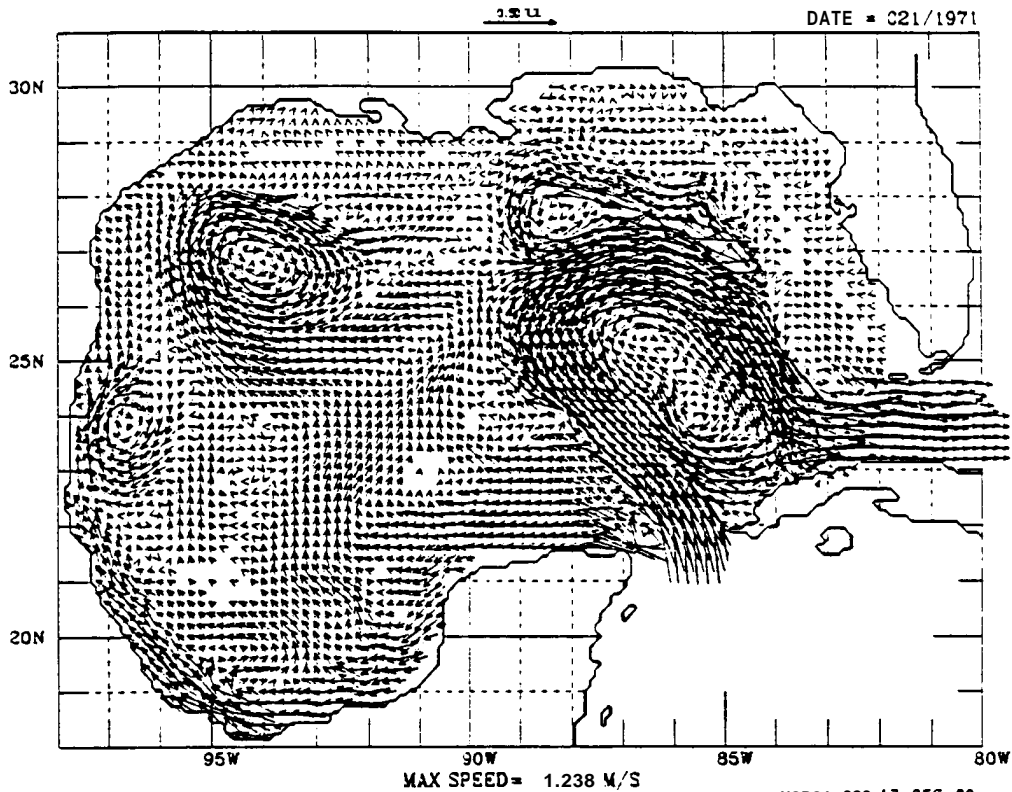


FIGURE 76

SURFACE CURRENTS

G. OF MEXICO 21142:2: 0.3

DATE = 021/1971



SURFACE CURRENTS

NOROA 323 12-DEC-89
G. OF MEXICO 21142:2: 0.0

DATE = 024/1971

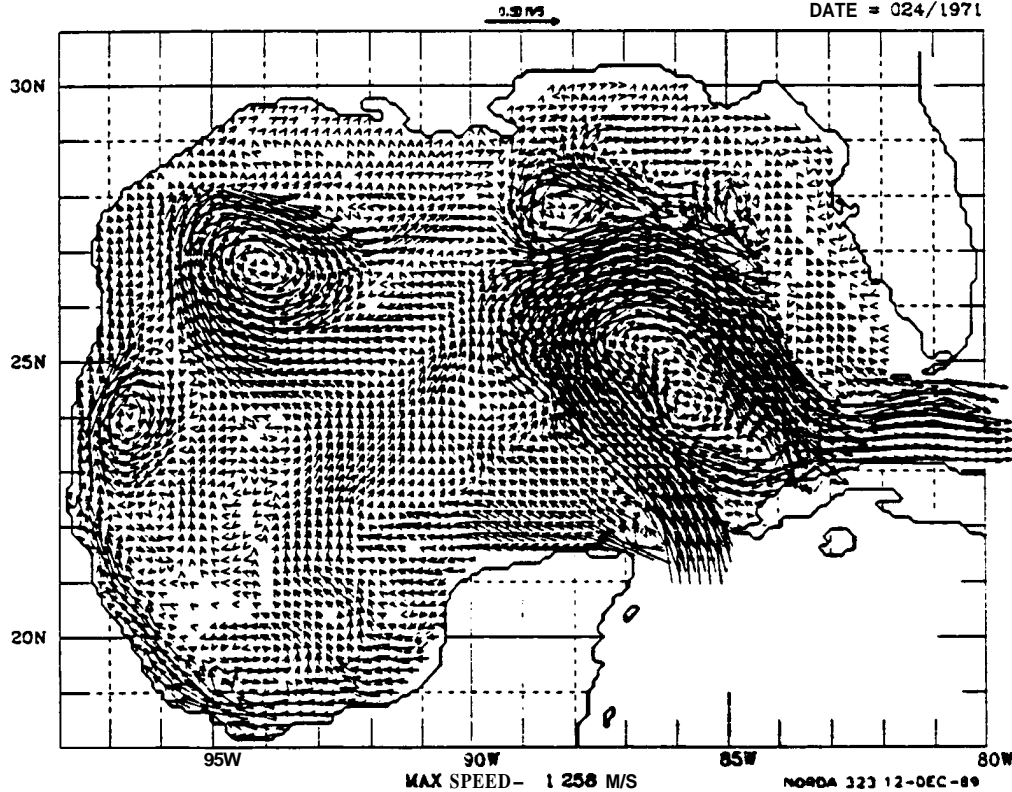
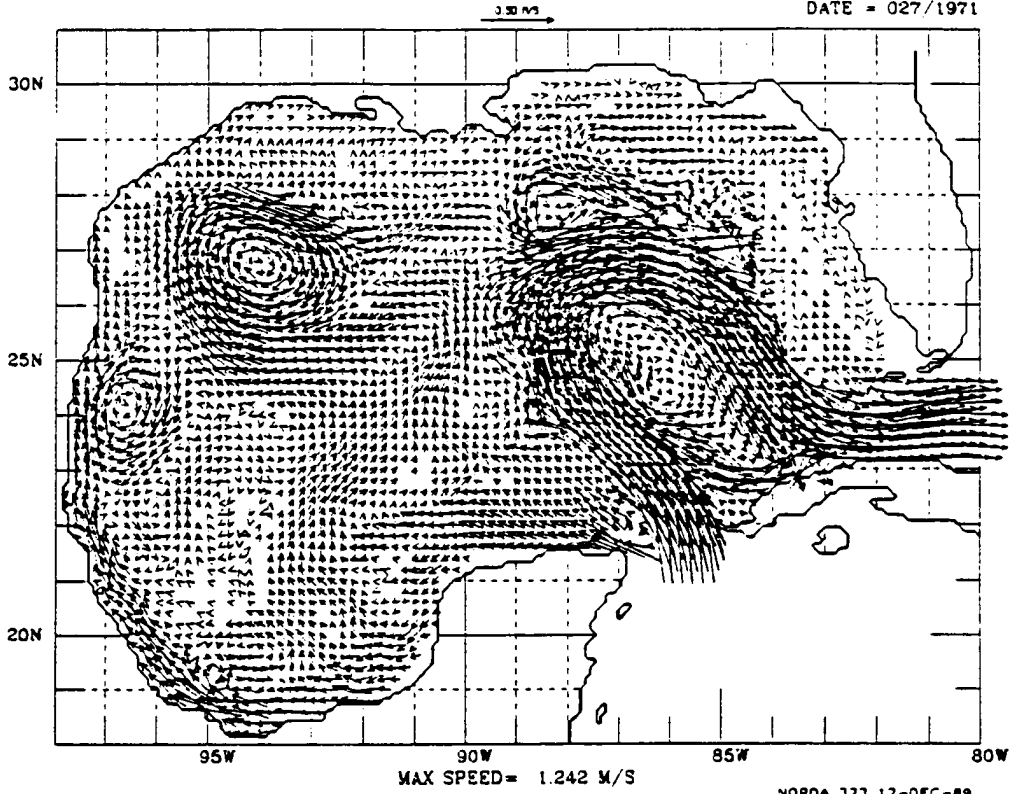


FIGURE 77

SURFACE CURRENTS

G. OF MEXICO 21142:2: 0.0
DATE = 027/1971



SURFACE CURRENTS

NORDA 323 12-DEC-89
G. OF MEXICO 21142:2: 0.0
DATE = 030/1971

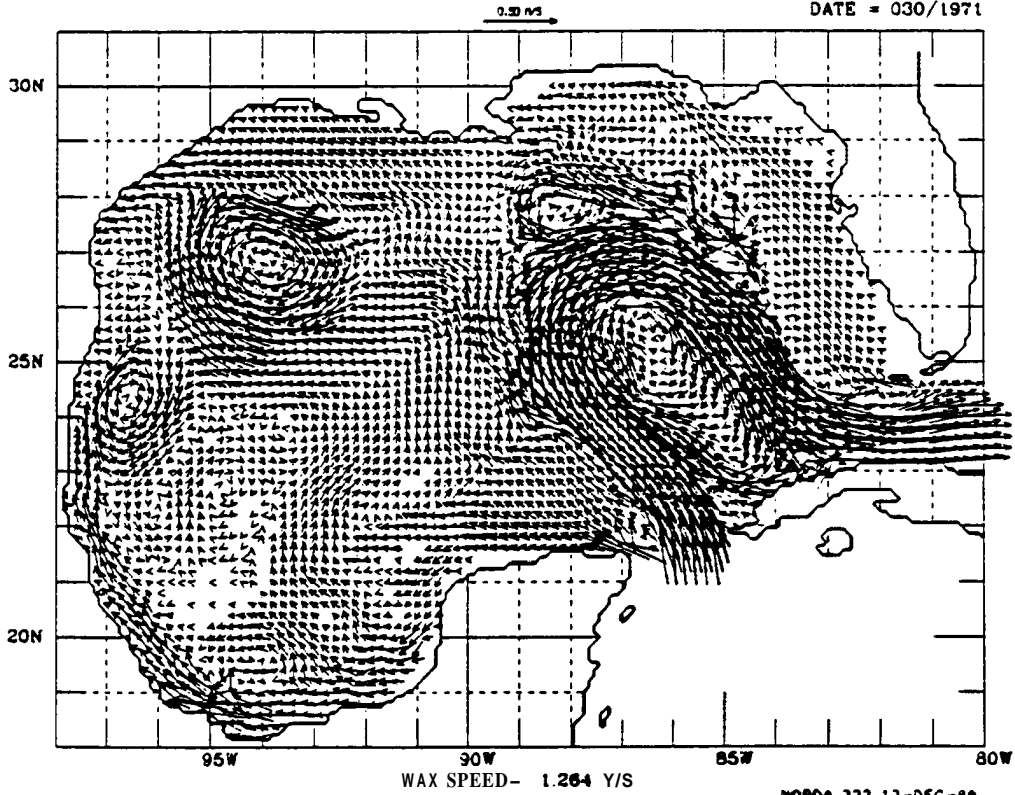
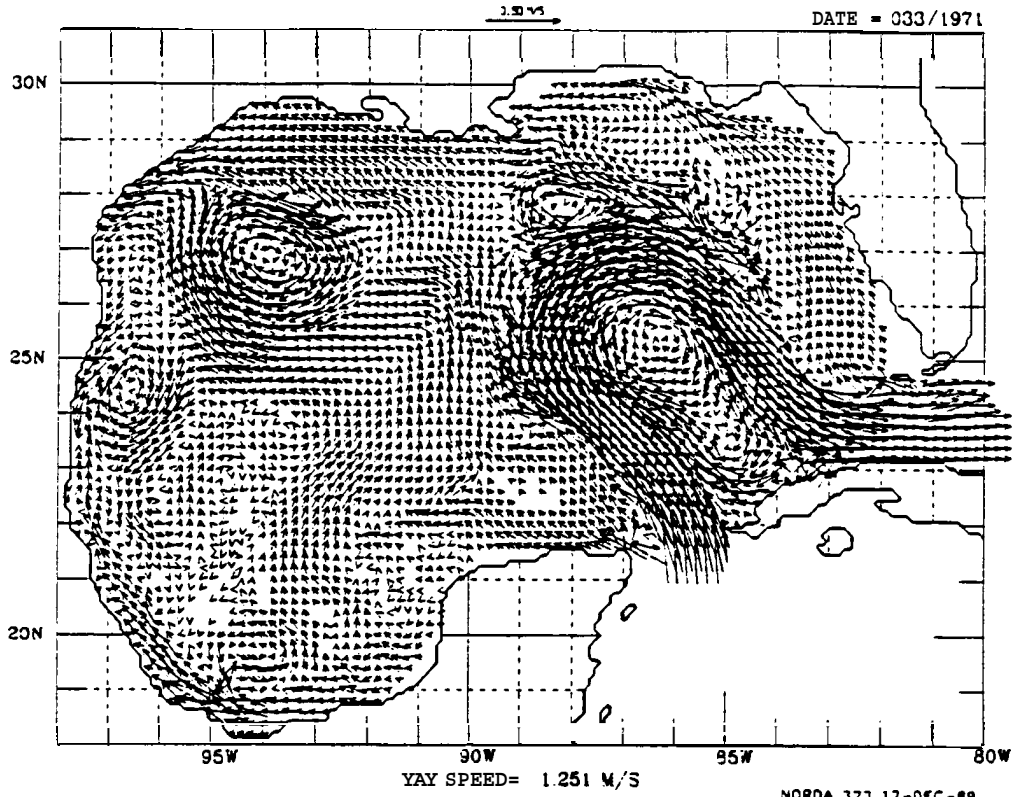


FIGURE 78

SURFACE CURRENTS

G. OF MEXICO 21142:2: 00

DATE = 033/1971



SURFACE CURRENTS

G. OF MEXICO 21142:2: 00

DATE = 036/1971

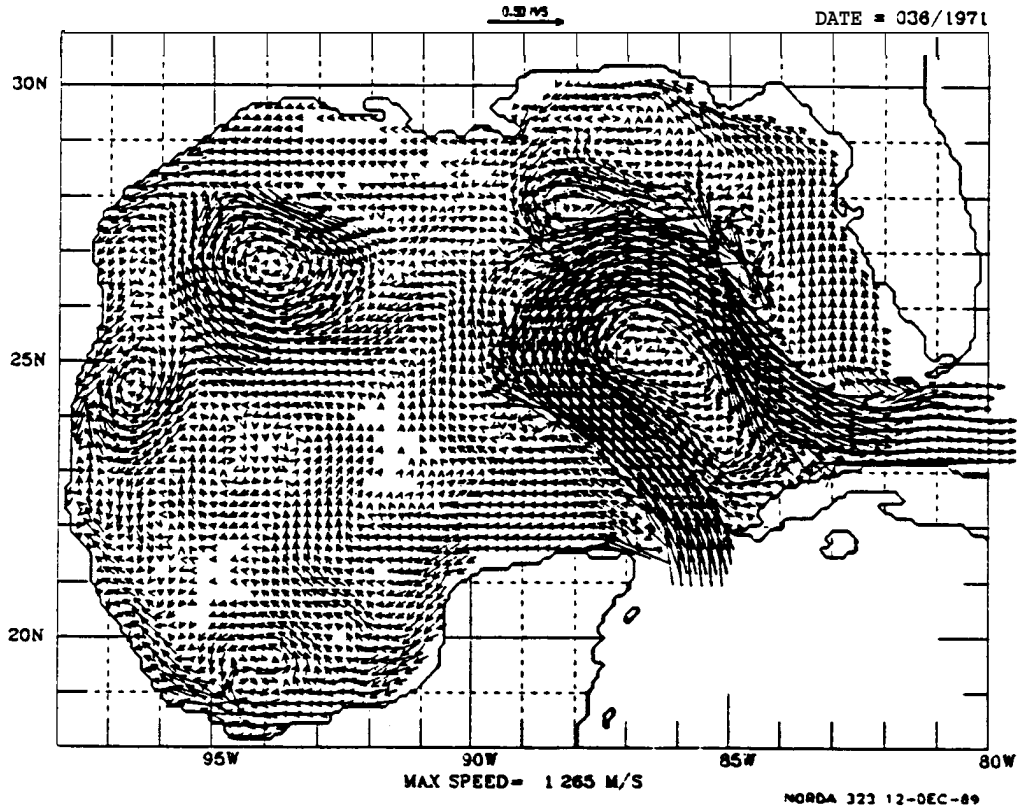
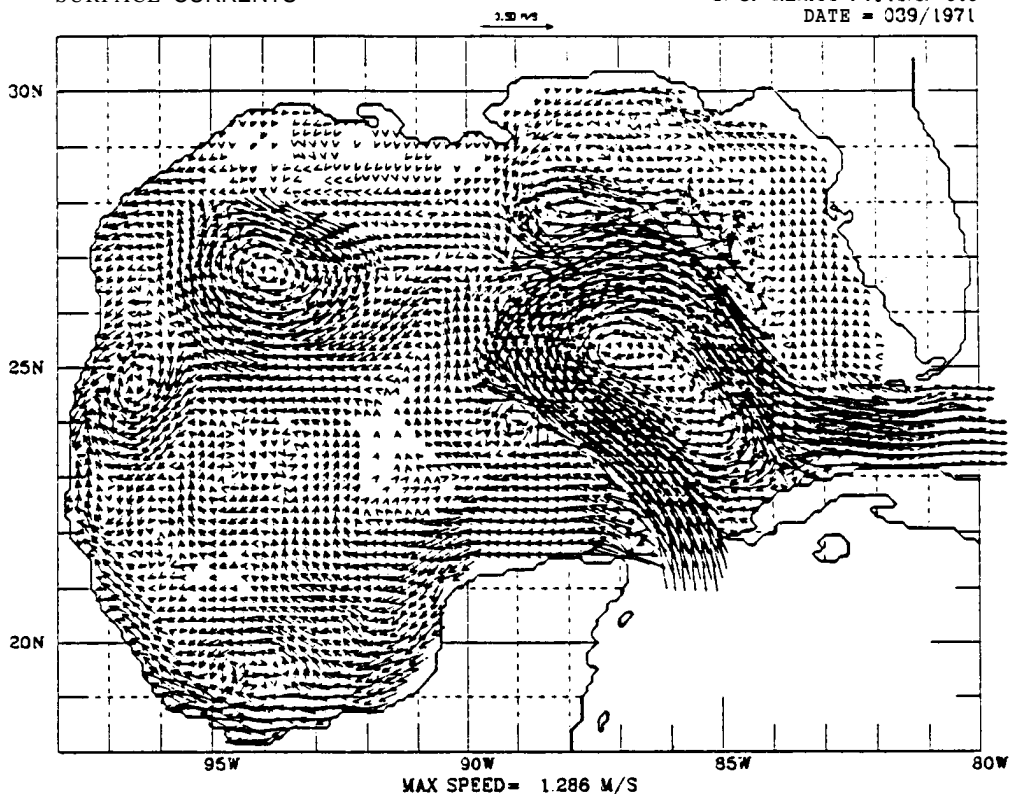


FIGURE 79

SURFACE CURRENTS

G. OF MEXICO 71142:2: 0.0
DATE = 039/1971



SURFACE CURRENTS

NORDA 323 12-DEC-89
G. OF MEXICO 21142:2: 0.0
DATE = 042/1971

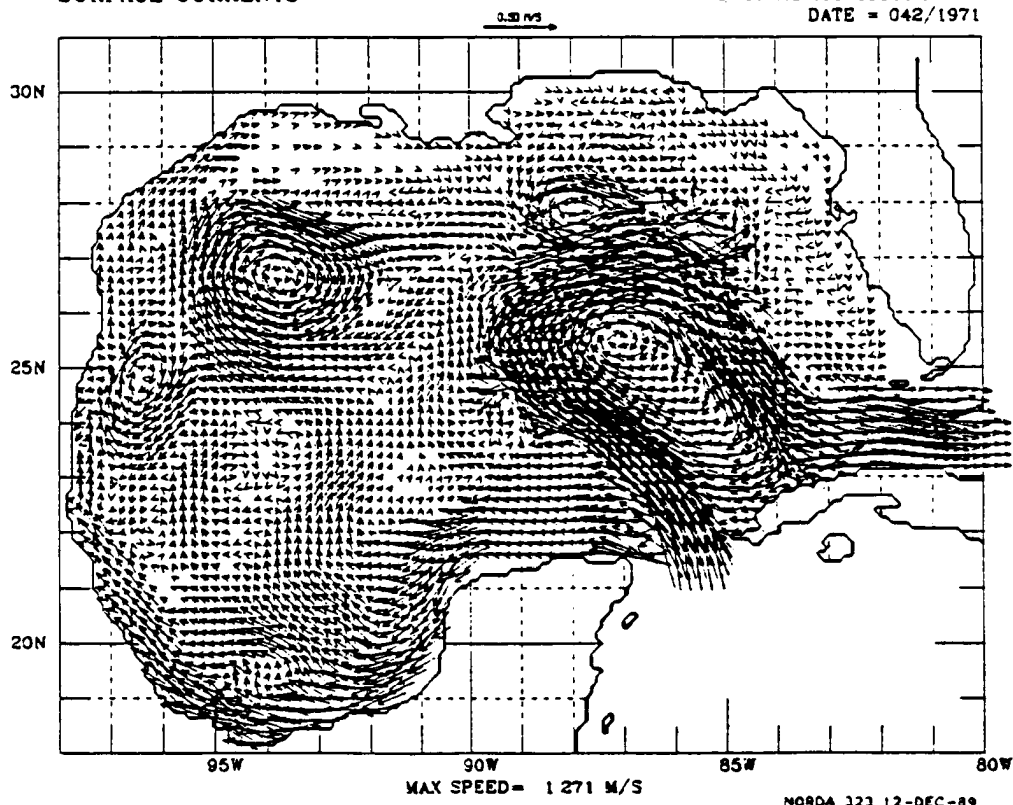
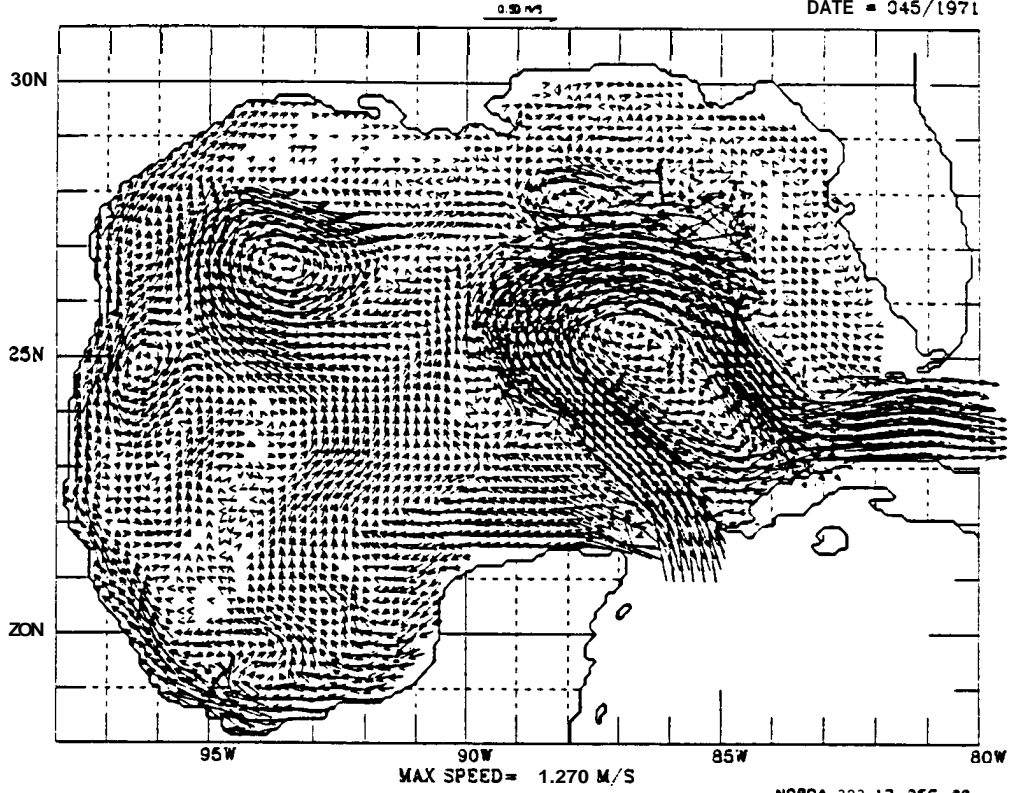


FIGURE 80

SURFACE CURRENTS

G. OF MEXICO 21142:2: 0.3
DATE = 045/1971



SURFACE CURRENTS

NORDA 323 12-DEC-89
G. OF MEXICO 21142:2: 0.3
DATE = 048/1971

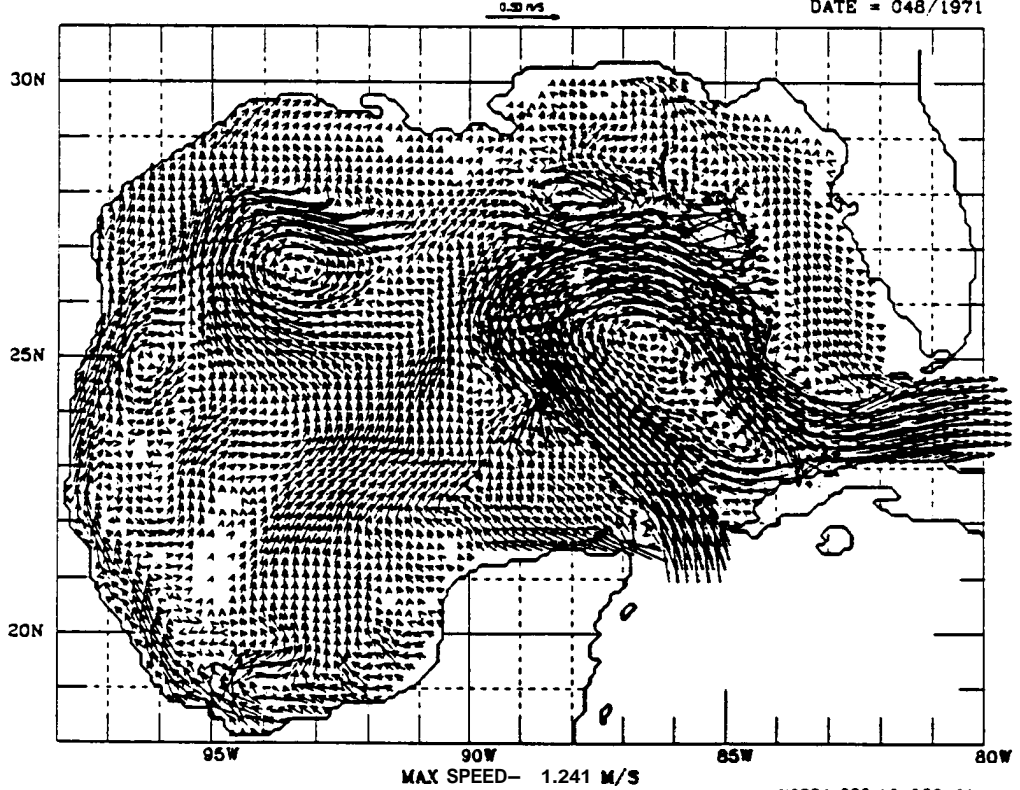


FIGURE 81

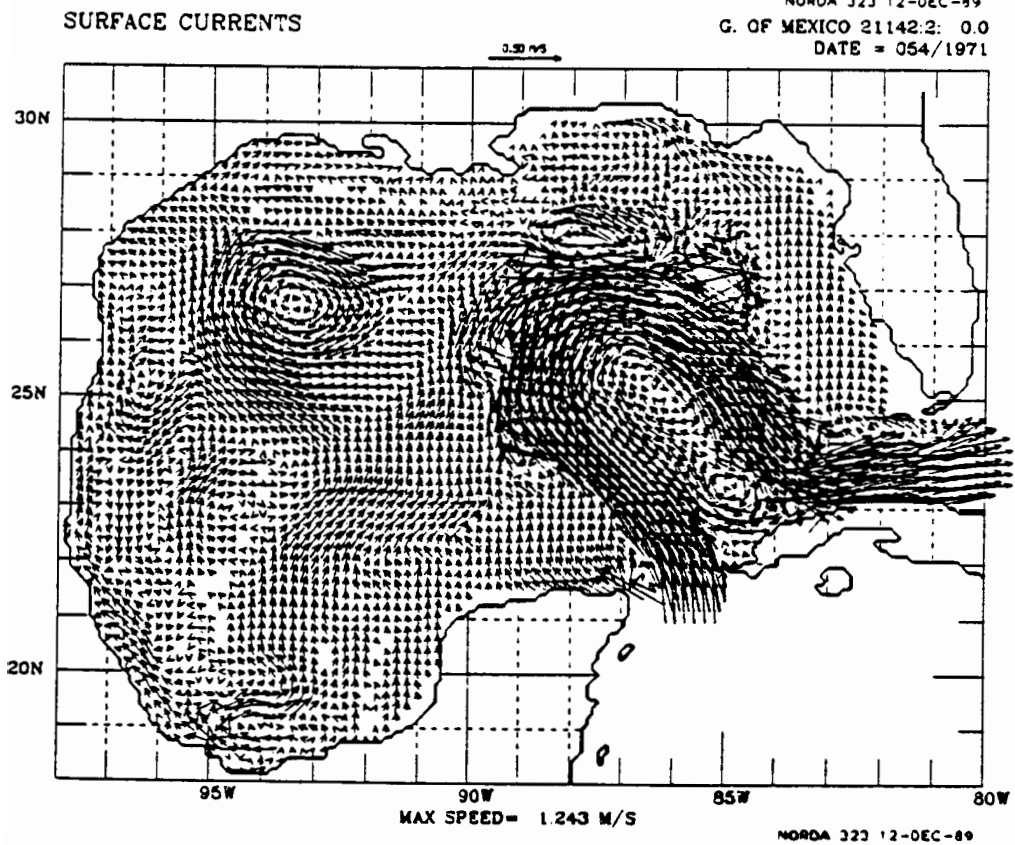
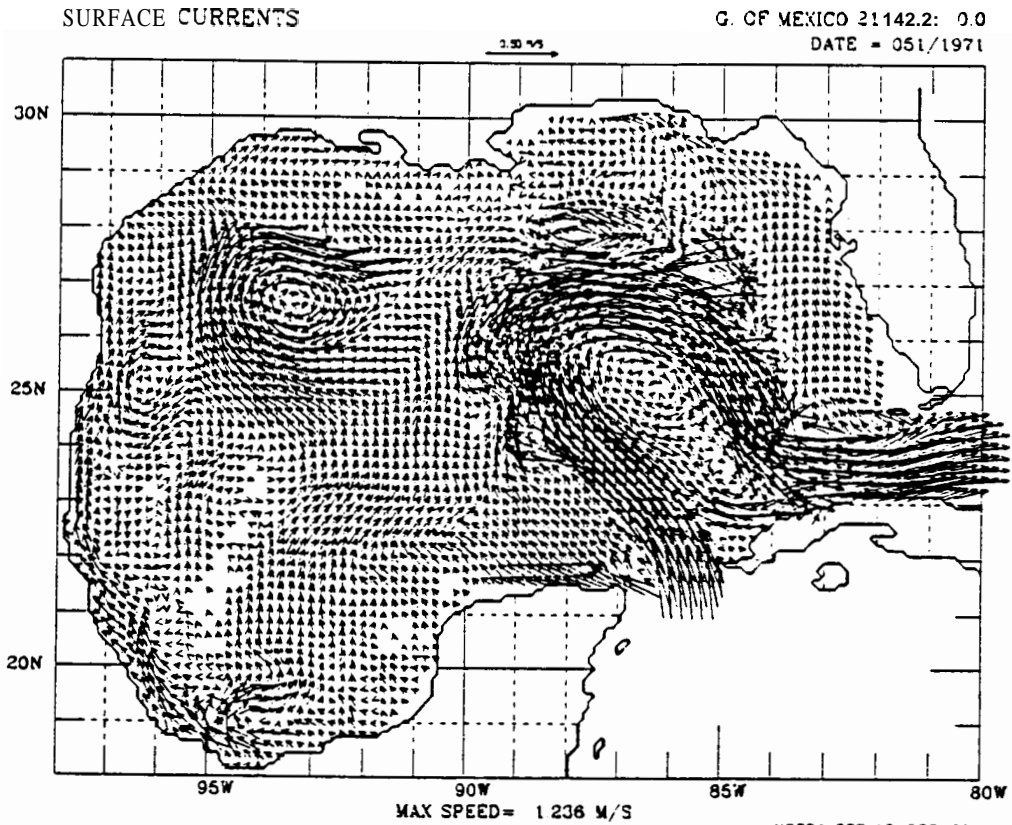
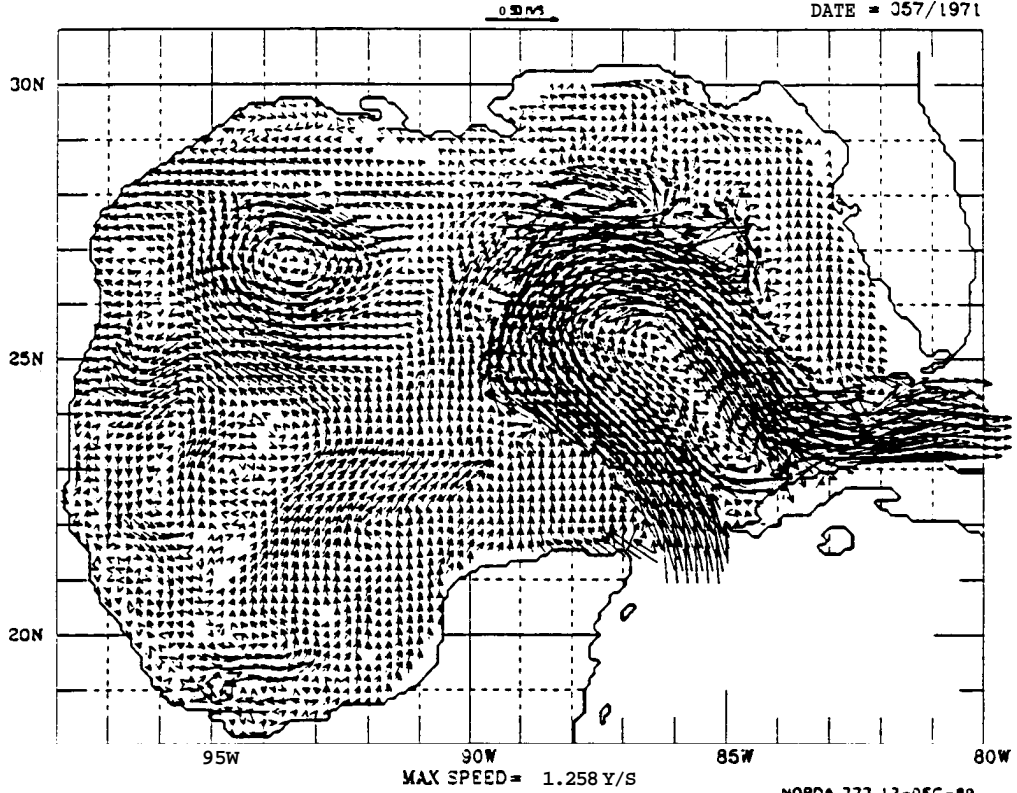


FIGURE 82

SURFACE CURRENTS

G. OF MEXICO 21142:2: 0.0
DATE = 357/1971



SURFACE CURRENTS

NORDA 323 12-DEC-89
G. OF MEXICO 21142:2: 0.0
DATE = 060/1971

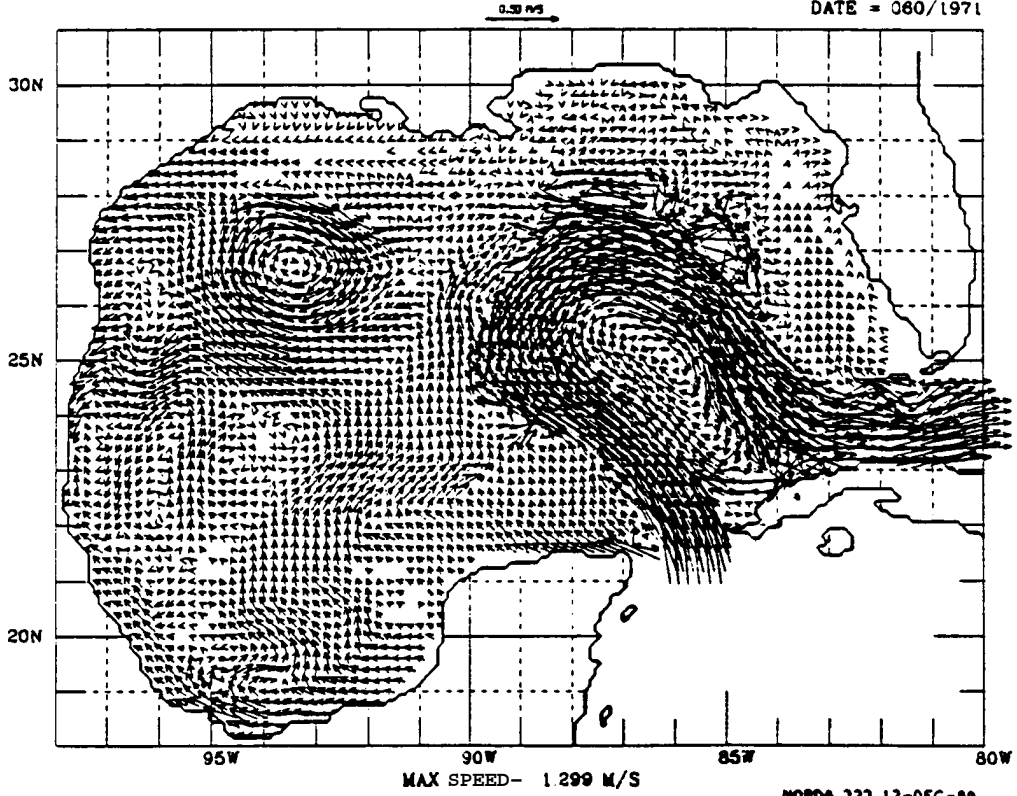


FIGURE 83

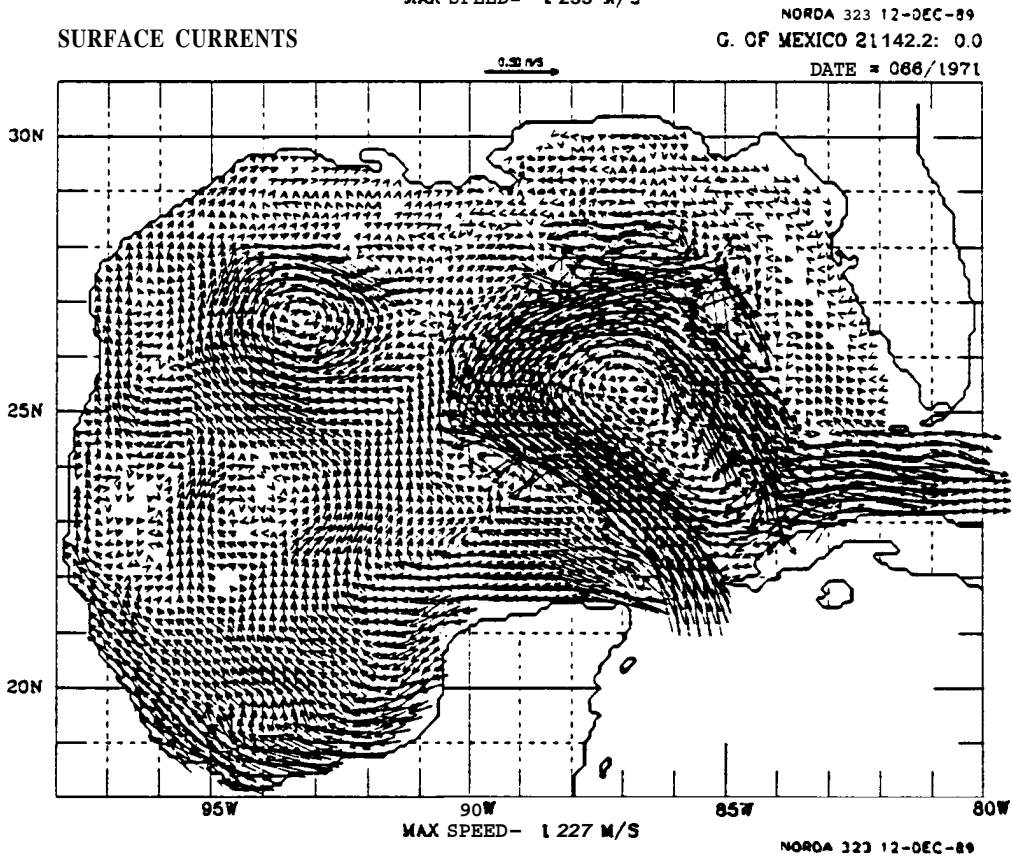
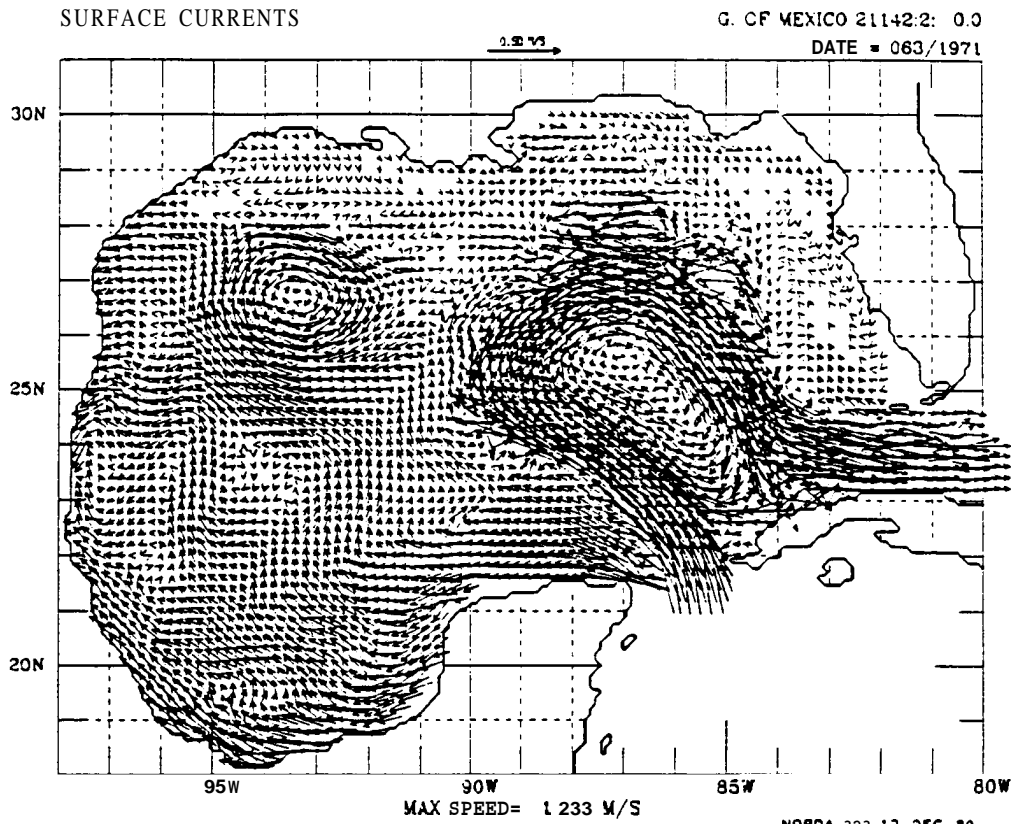


FIGURE 84

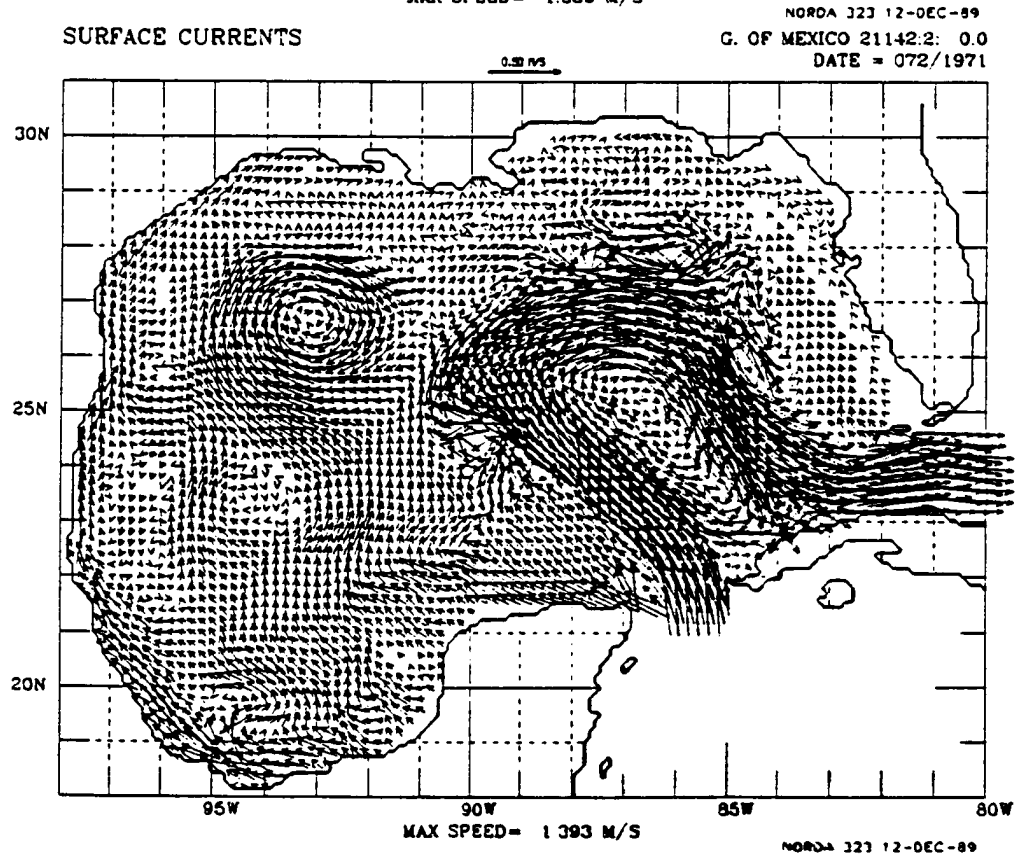
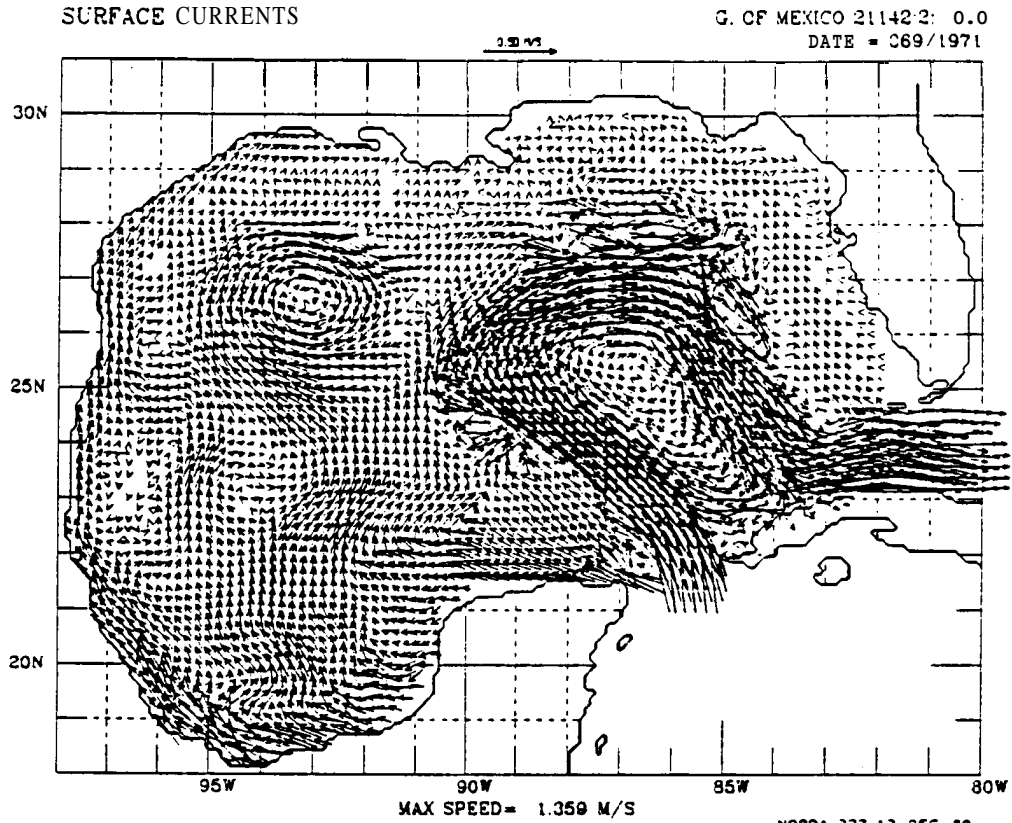
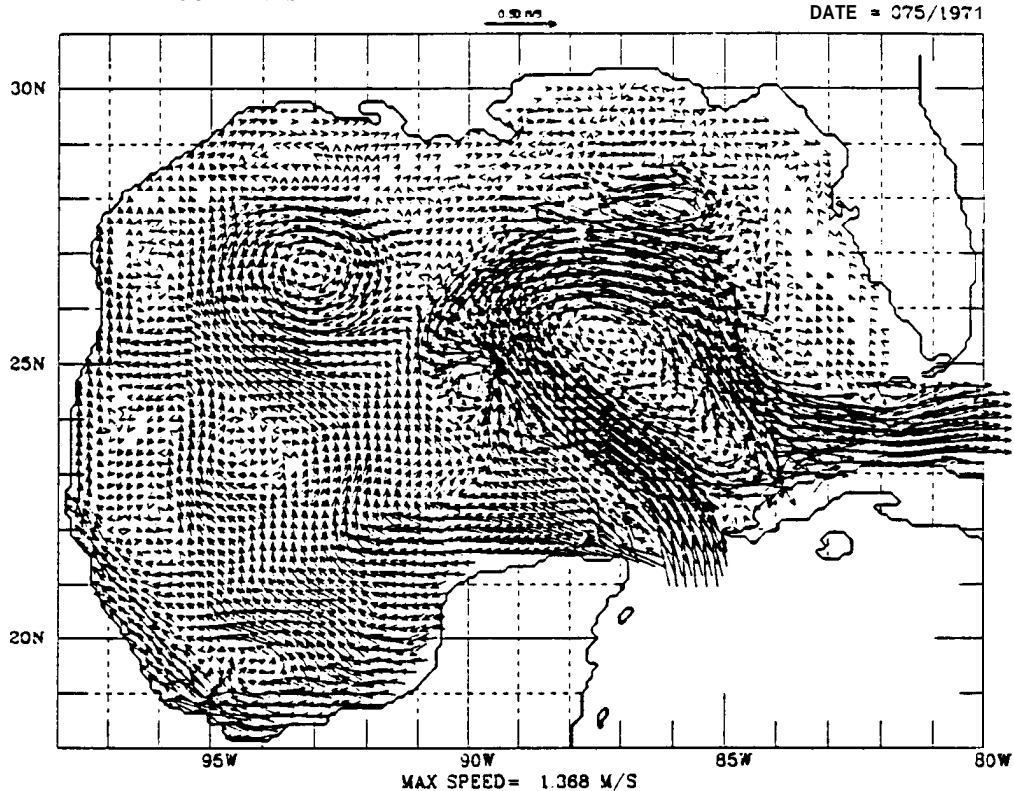


FIGURE 85

SURFACE CURRENTS

G. OF MEXICO 21142:2: 0.0
DATE = 075/1971



SURFACE CURRENTS

NORDA 323 12-DEC-89
G. OF MEXICO 21142 2: 0.0
DATE = 078/1971

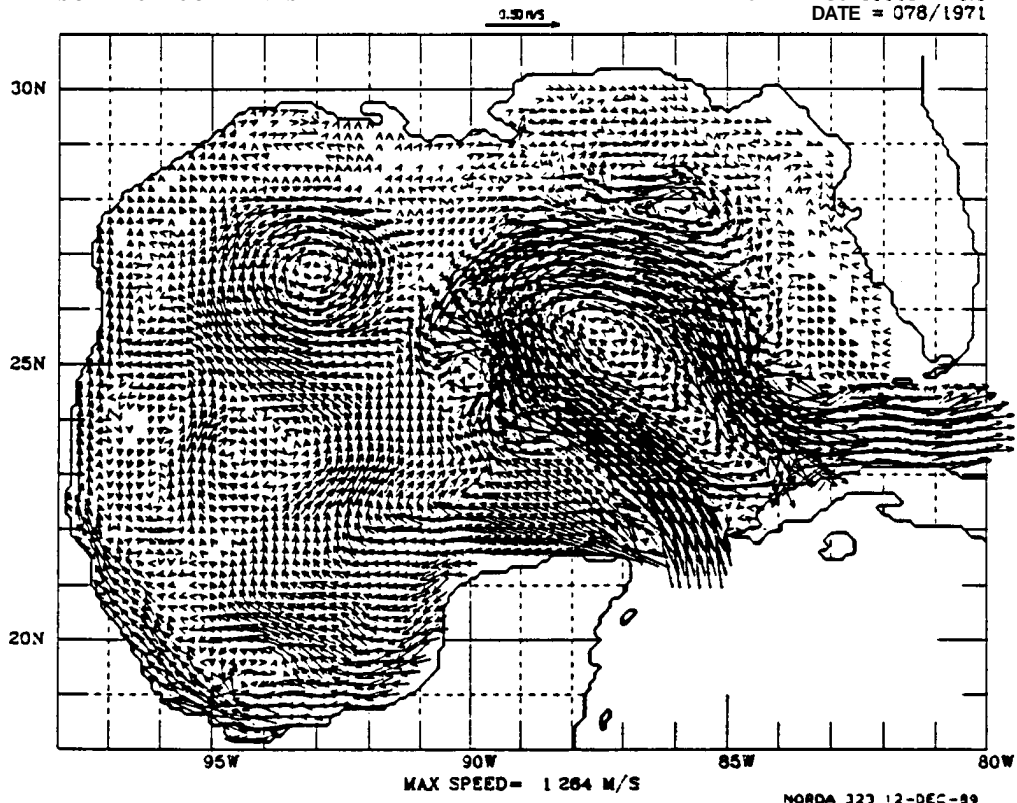
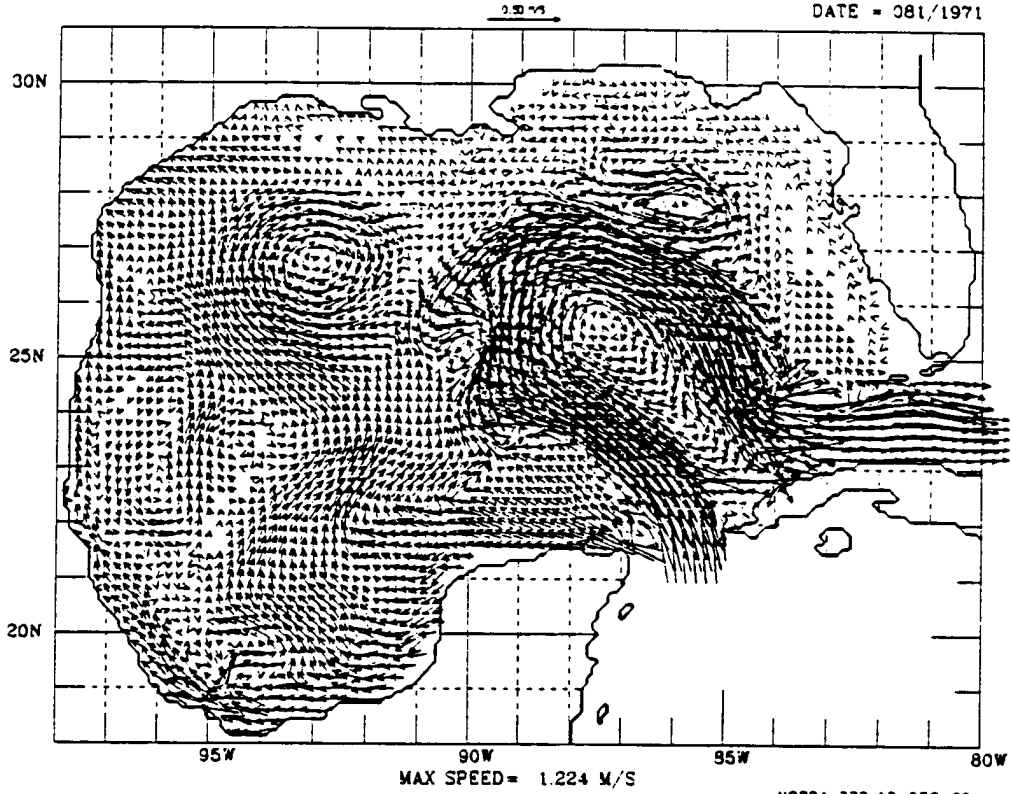


FIGURE 86

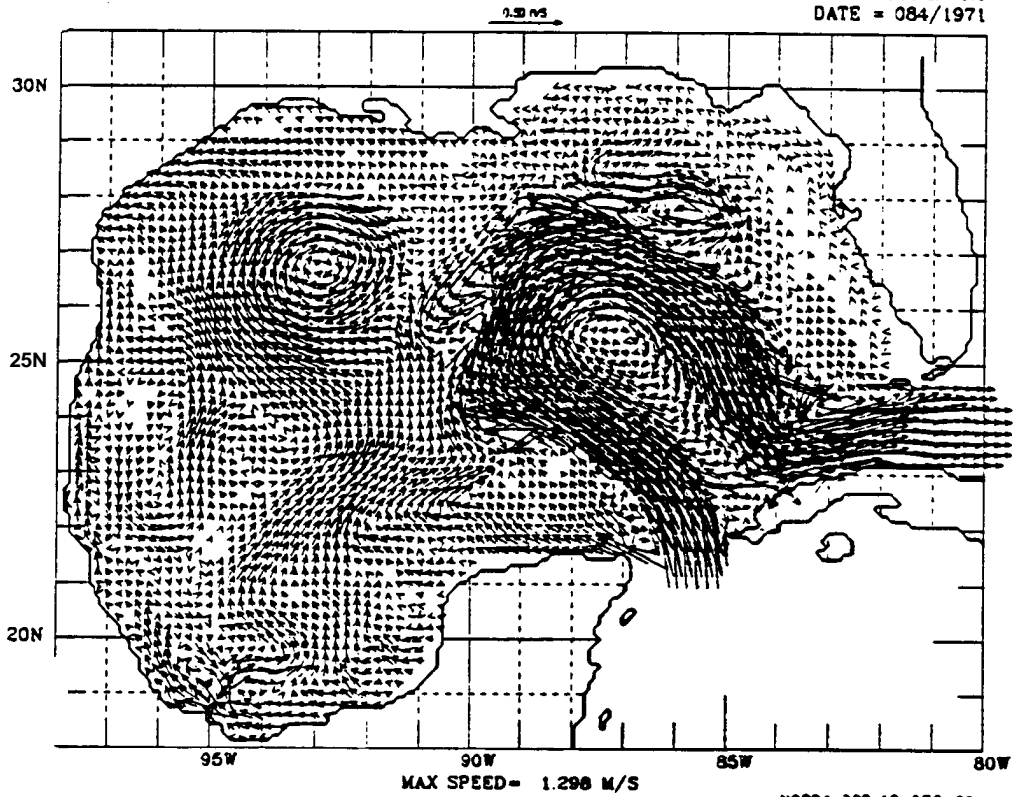
SURFACE CURRENTS

G. OF MEXICO 21142-2: 0.0
DATE = 081/1971



SURFACE CURRENTS

NORDA 323 12-DEC-89
G. OF MEXICO 21142-2: 0.0
DATE = 084/1971

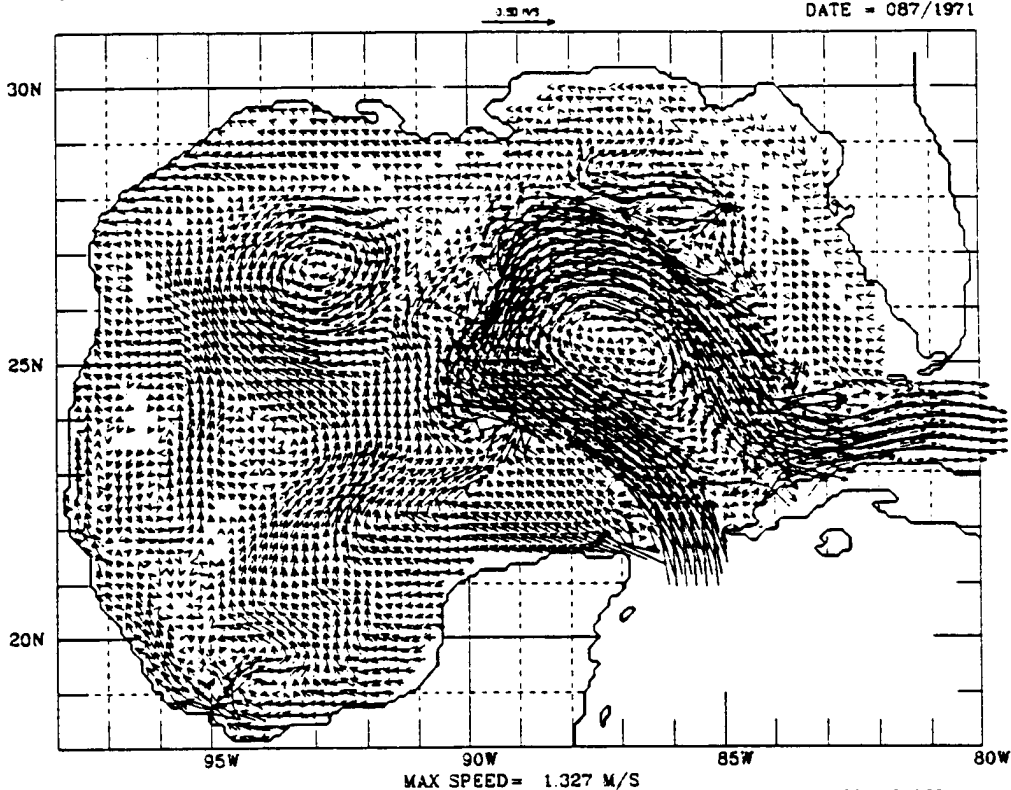


NORDA 323 12-DEC-89

FIGURE 87

SURFACE CURRENTS

G. OF MEXICO 21142.2: 0.0
DATE = 087/1971



SURFACE CURRENTS

NORDA 323 12-DEC-89
G. OF MEXICO 21142.2: 0.0
DATE = 090/1971

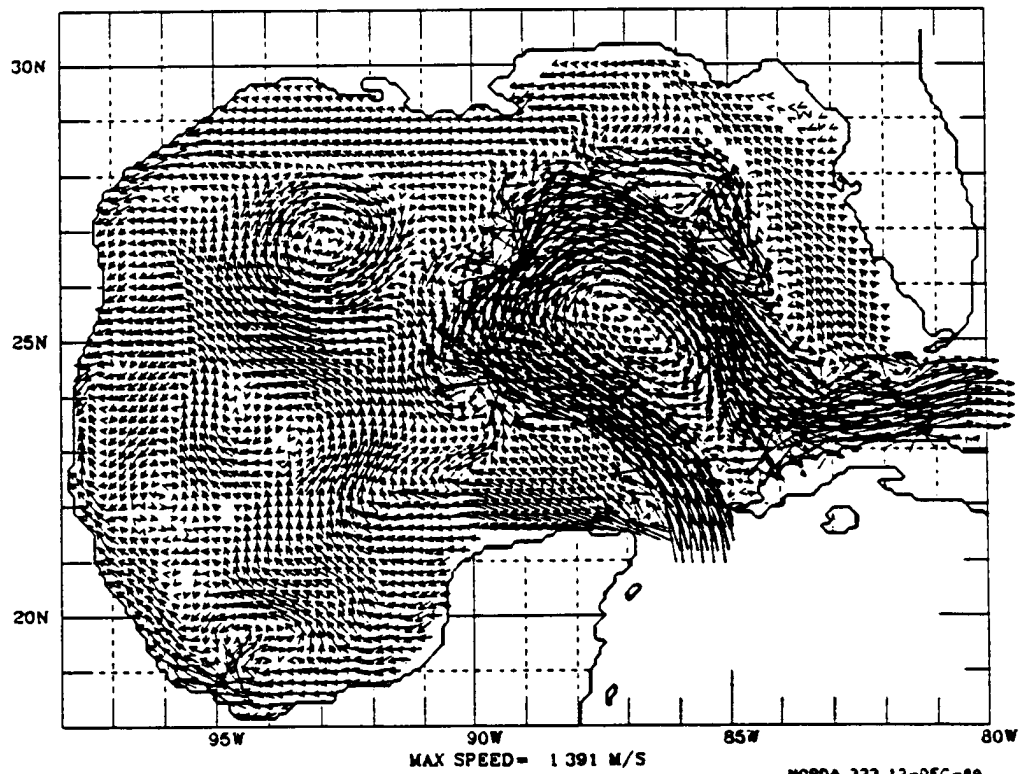
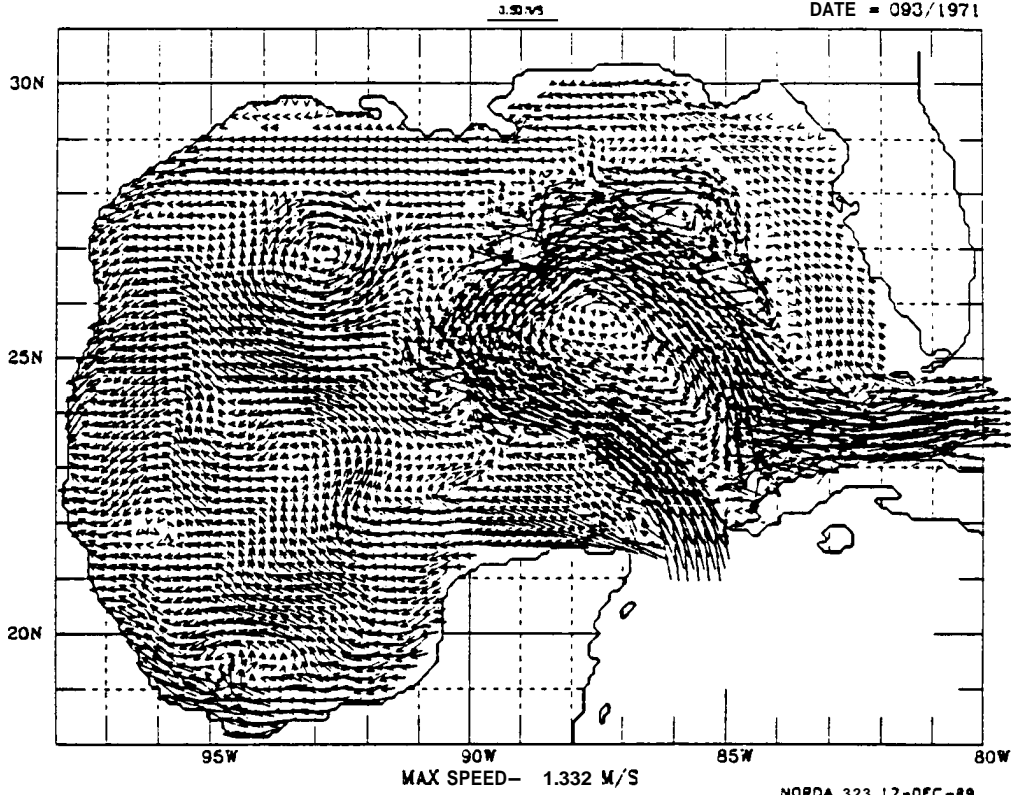


FIGURE 88

SURFACE CURRENTS

G. OF MEXICO 21142.2: 0.0
DATE = 093/1971



SURFACE CURRENTS

NORDA 323 12-DEC-89
G. OF MEXICO 21142.2: 0.0
DATE = 096/1971

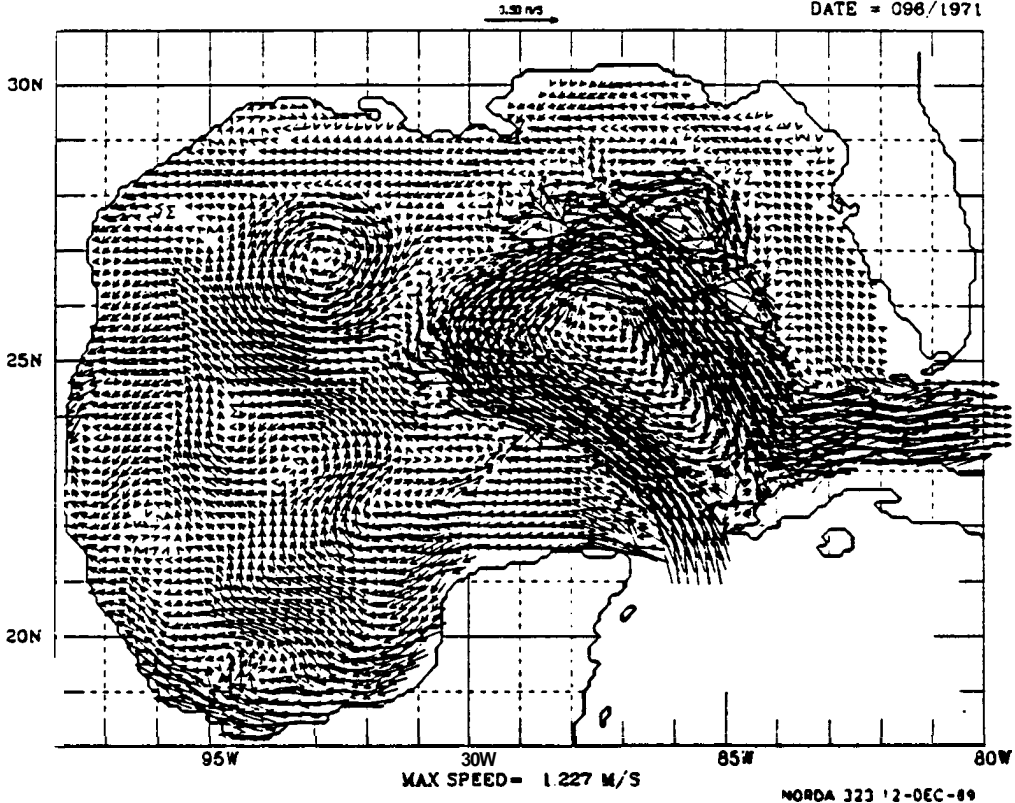


FIGURE 89

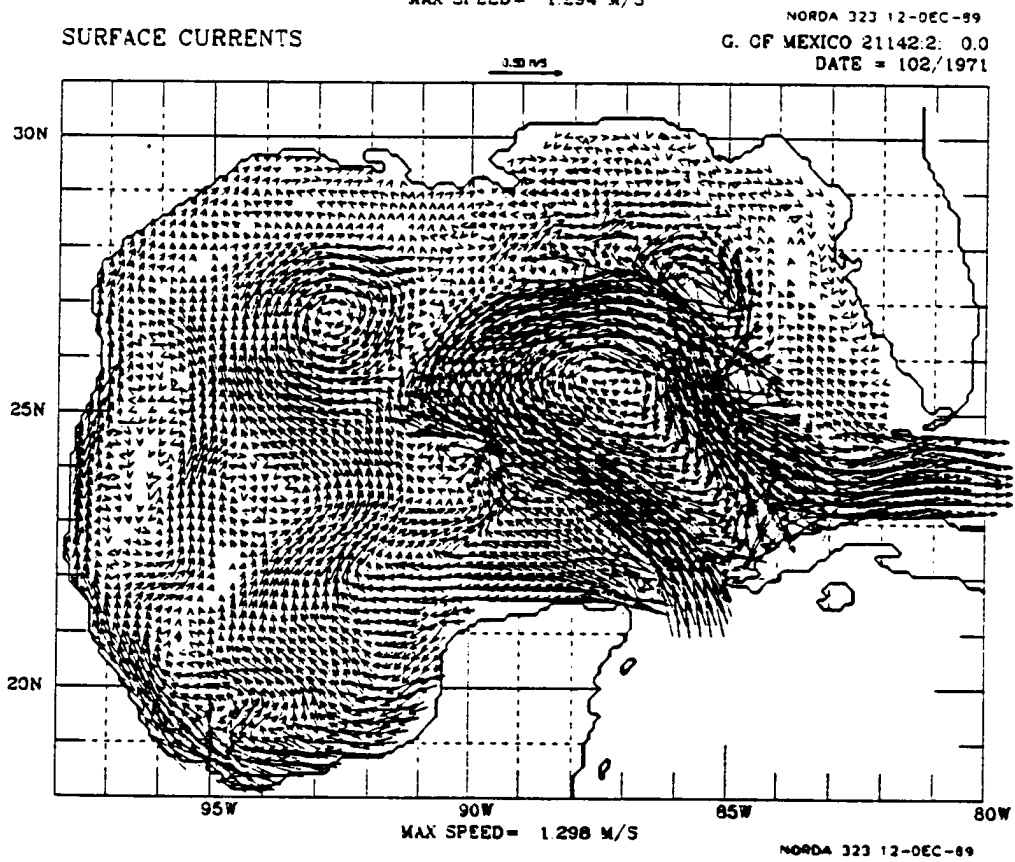
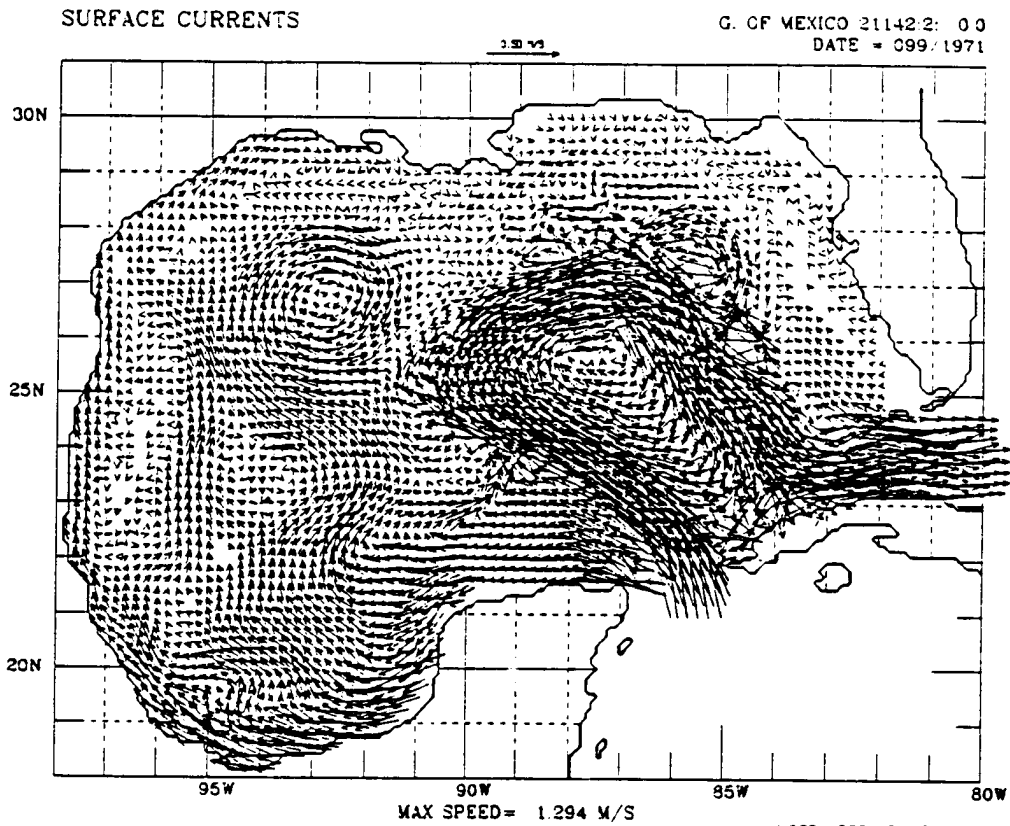
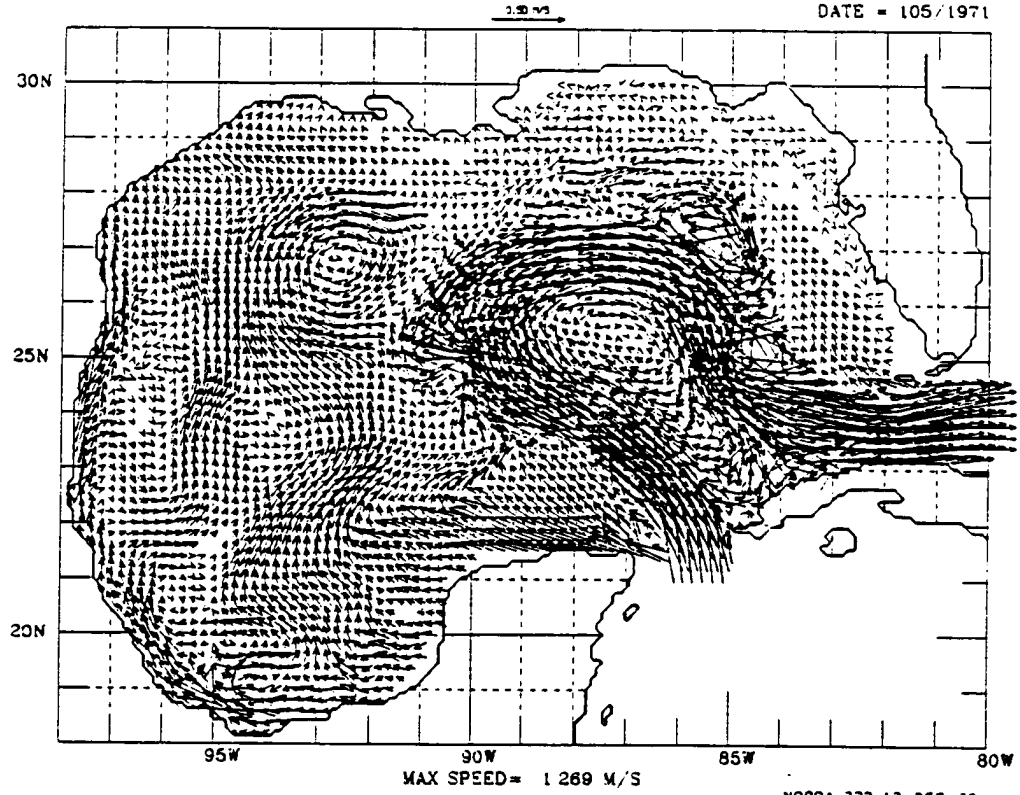


FIGURE 90

SURFACE CURRENTS

G. OF MEXICO 21142.2: 0.0
DATE = 105/1971



SURFACE CURRENTS

NORDA 323 12-DEC-89
G. OF MEXICO 21142.2: 0.0
DATE = 108/1971

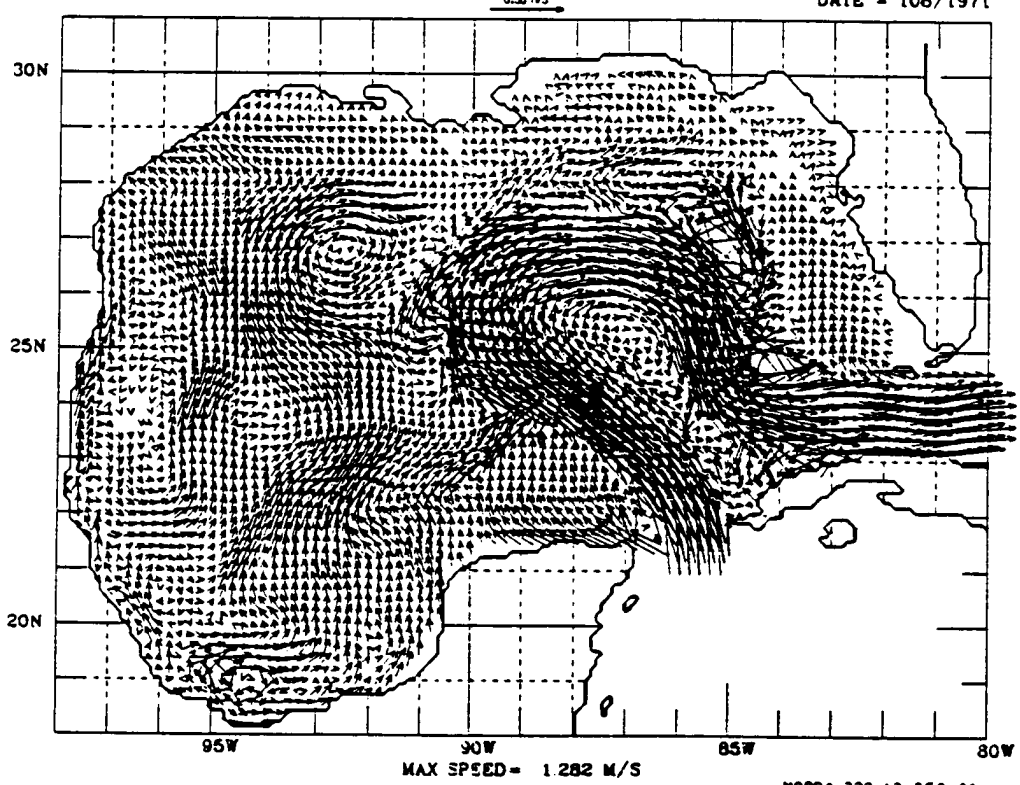
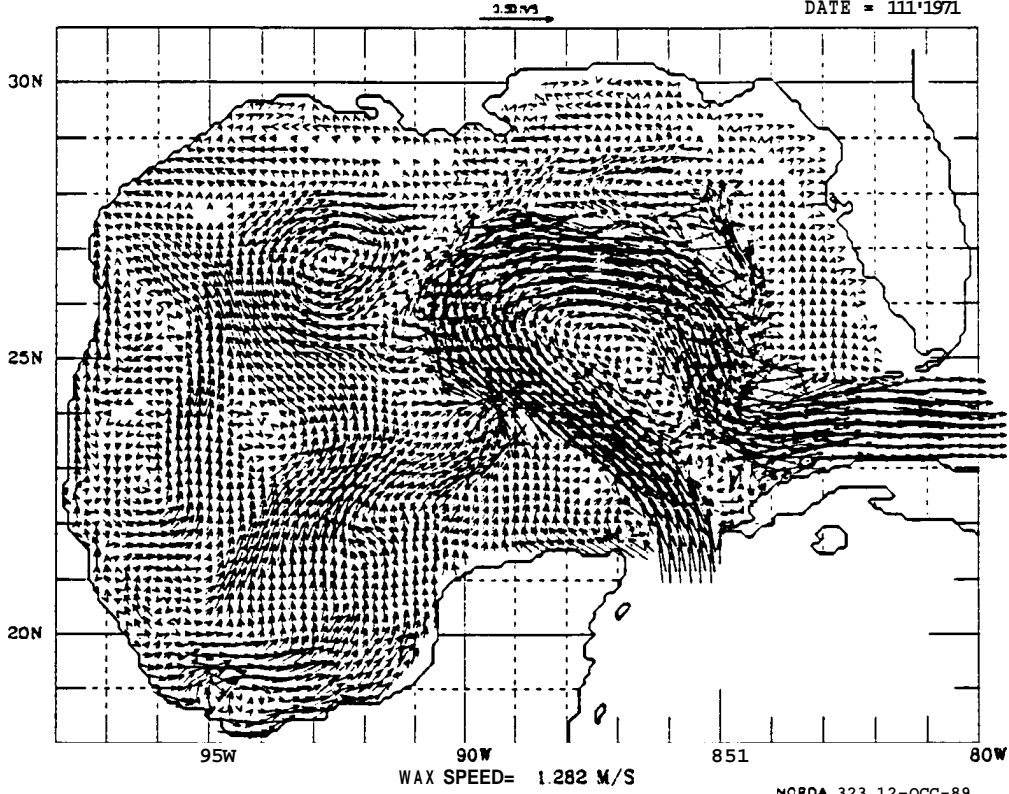


FIGURE 91

SURFACE CURRENTS

G. OF MEXICO 211422: 00
DATE = 111/1971



SURFACE CURRENTS

G. OF MEXICO 211422: 00
DATE = 114/1971

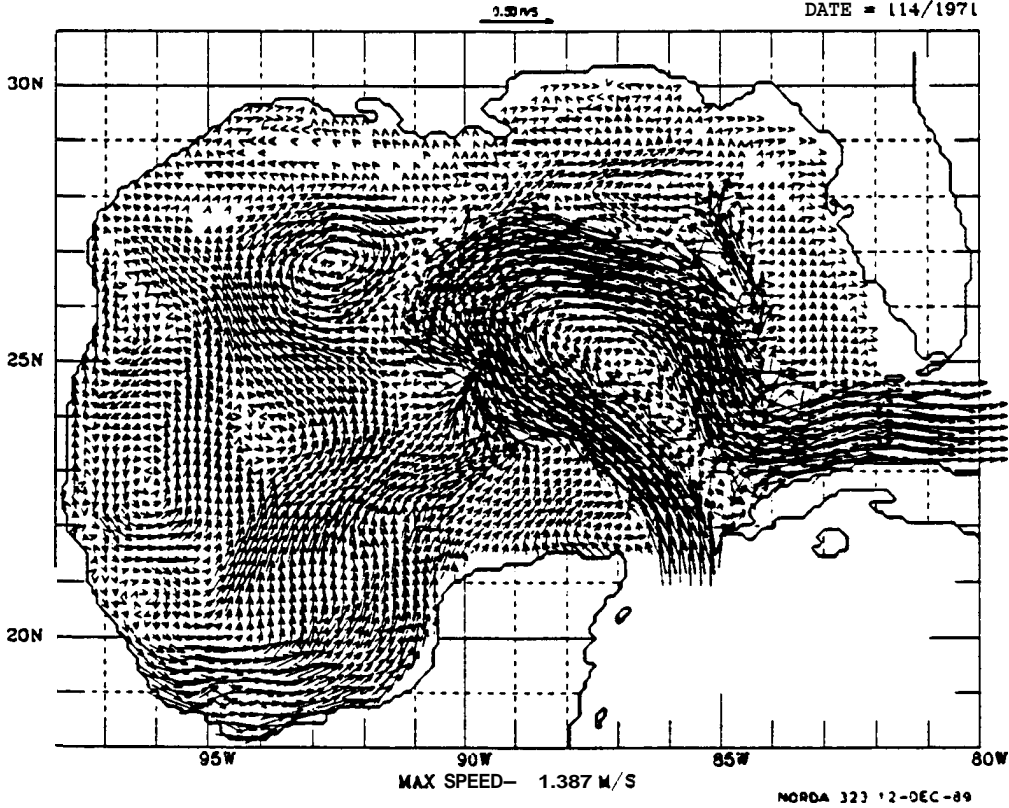
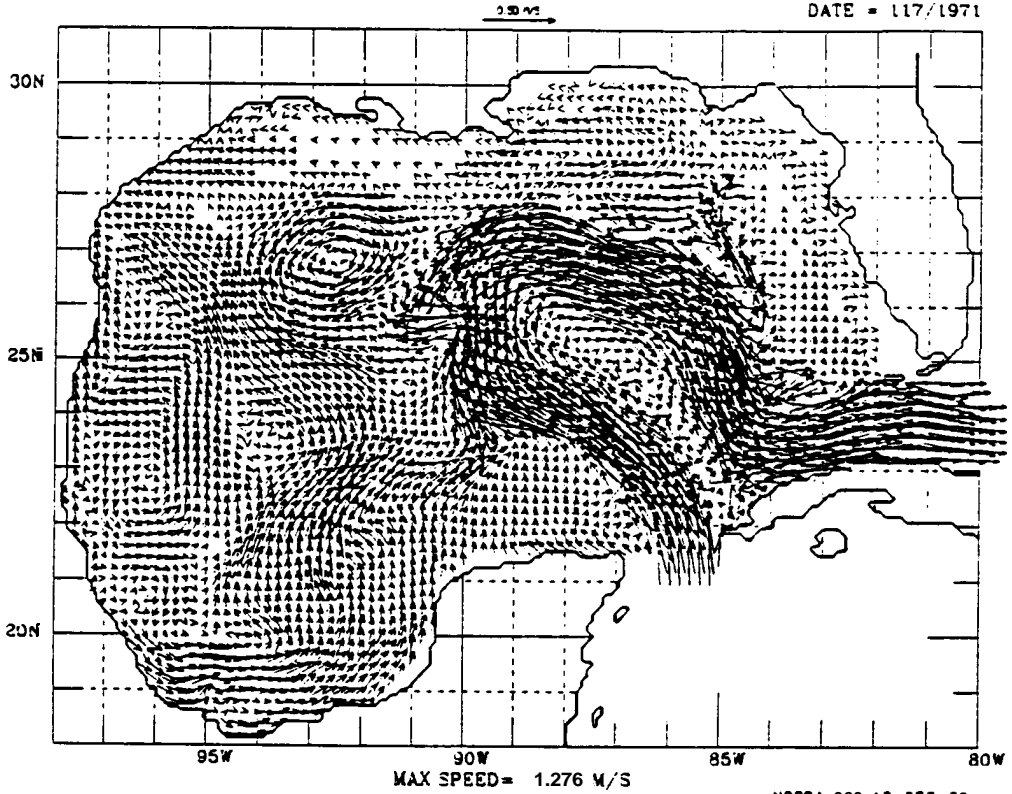


FIGURE 92

SURFACE CURRENTS

G. OF MEXICO 21142.2: 0.3
DATE = 117/1971



SURFACE CURRENTS

NORDA 323 12-DEC-89
G. OF MEXICO 21142.2: 0.0
DATE = 120/1971

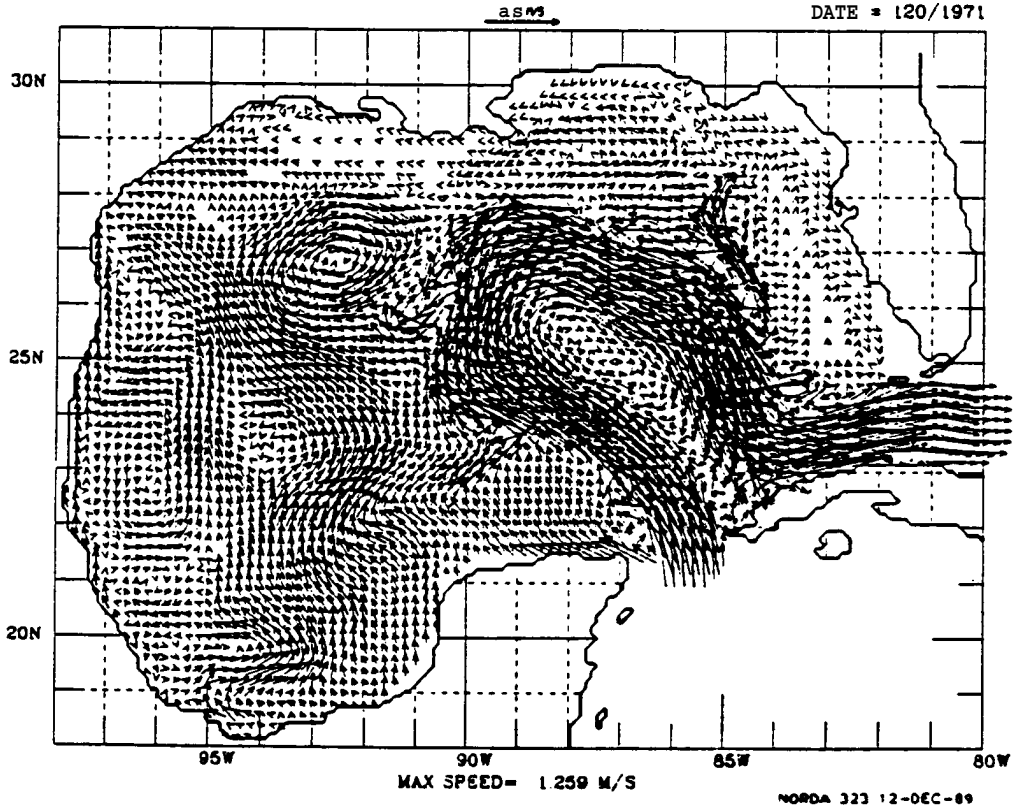
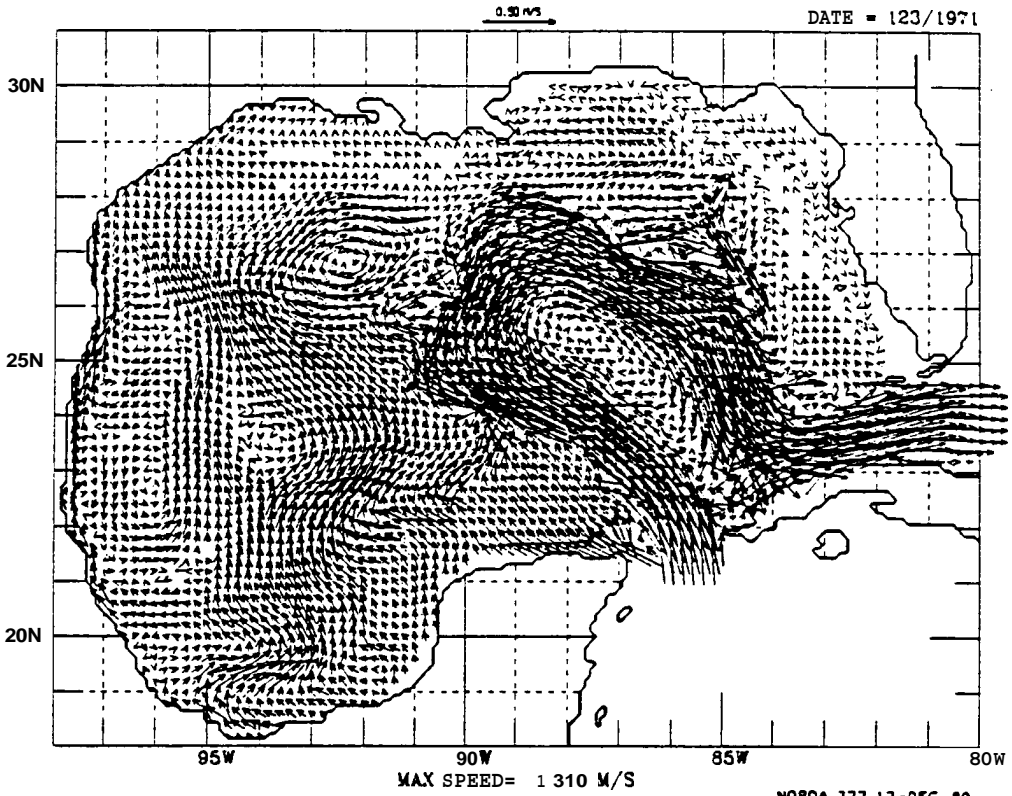


FIGURE 93

SURFACE CURRENTS

G. OF MEXICO 21142.2: 0.0

DATE = 123/1971



SURFACE CURRENTS

NORDA 323 12-DEC-89

G. OF MEXICO 21142.2: 0.0

DATE = 126/1971

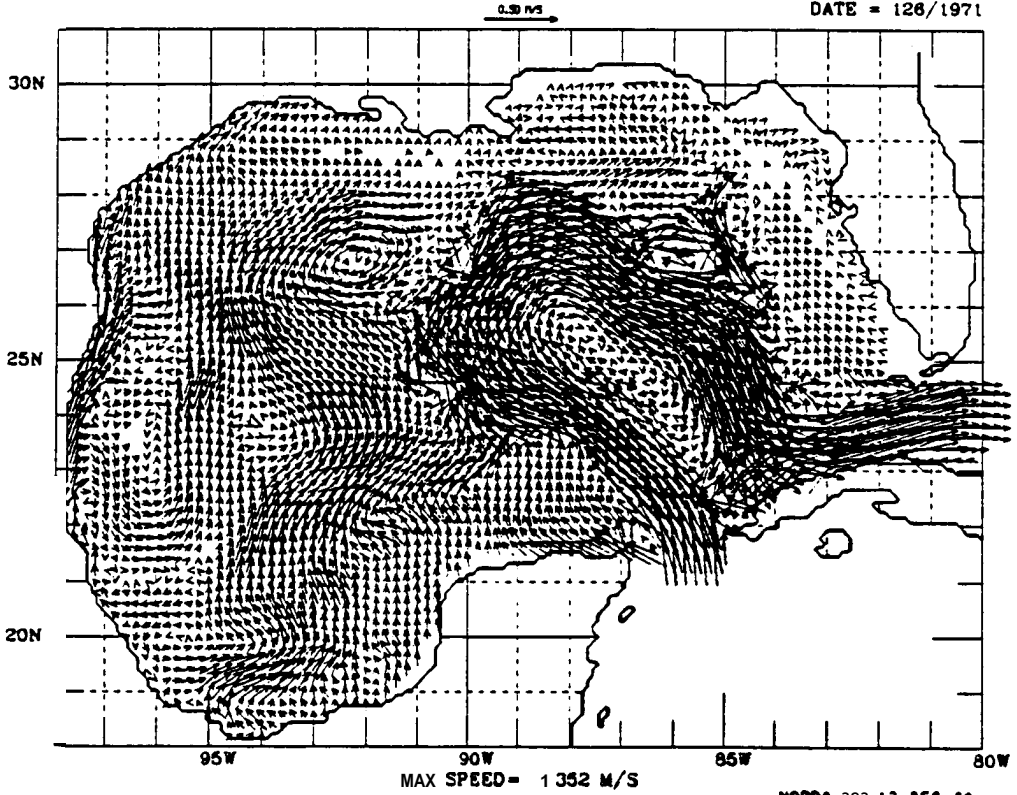


FIGURE 94

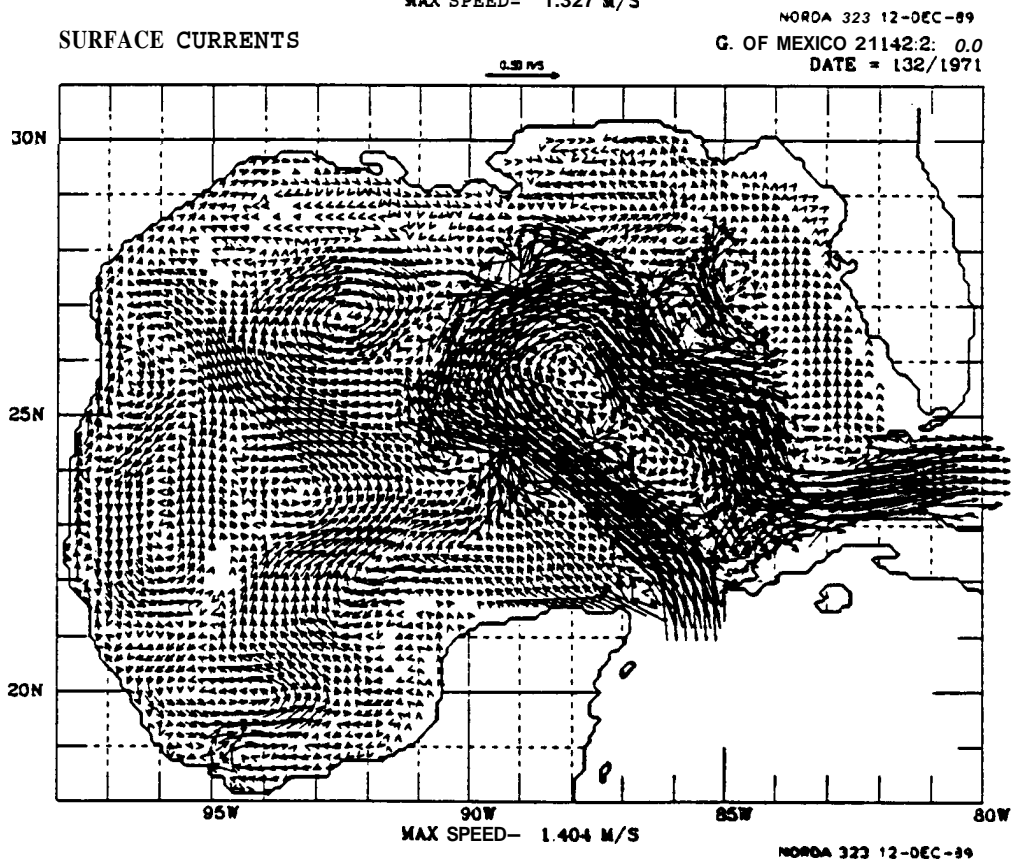
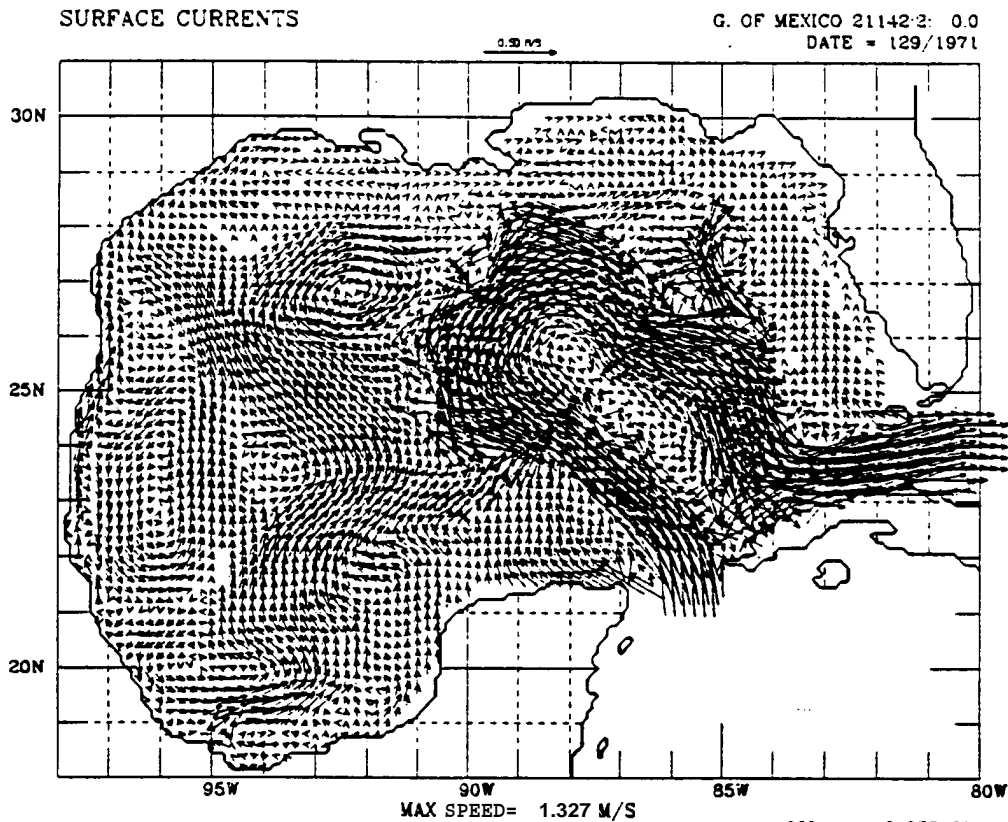
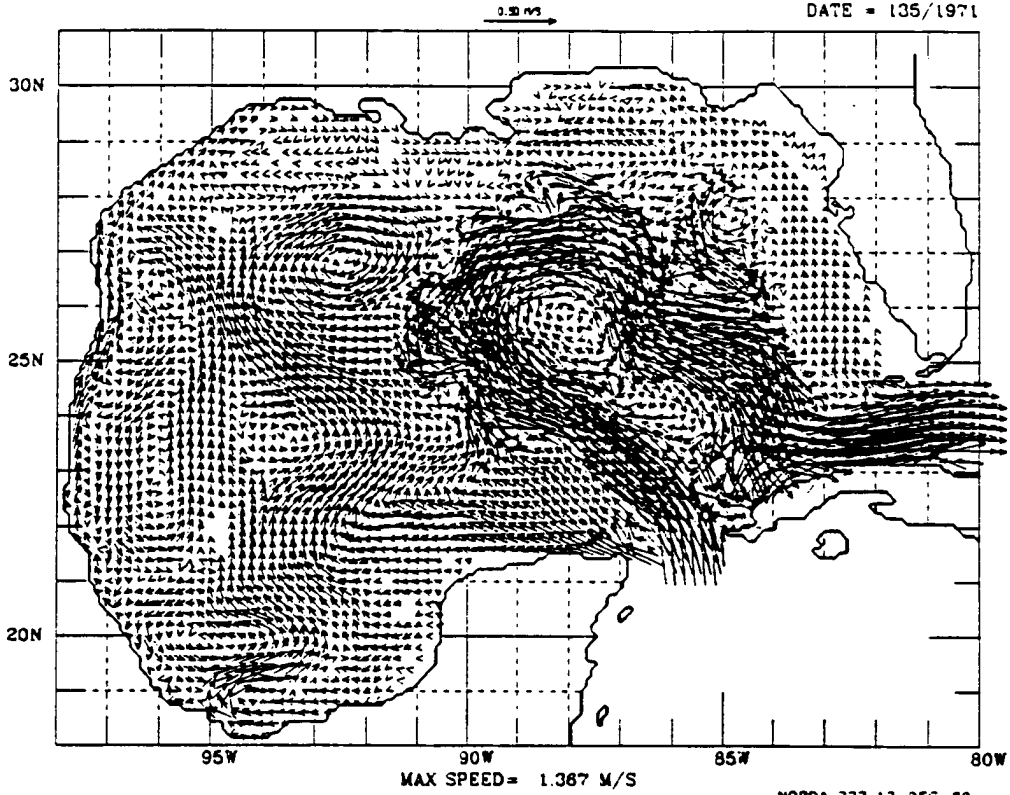


FIGURE 95

SURFACE CURRENTS

G. OF MEXICO 21142-2: 0.0
DATE = 135/1971



SURFACE CURRENTS

NORDA 323 12-DEC-89
G. OF MEXICO 21142-2: 0.0
DATE = 138/1971

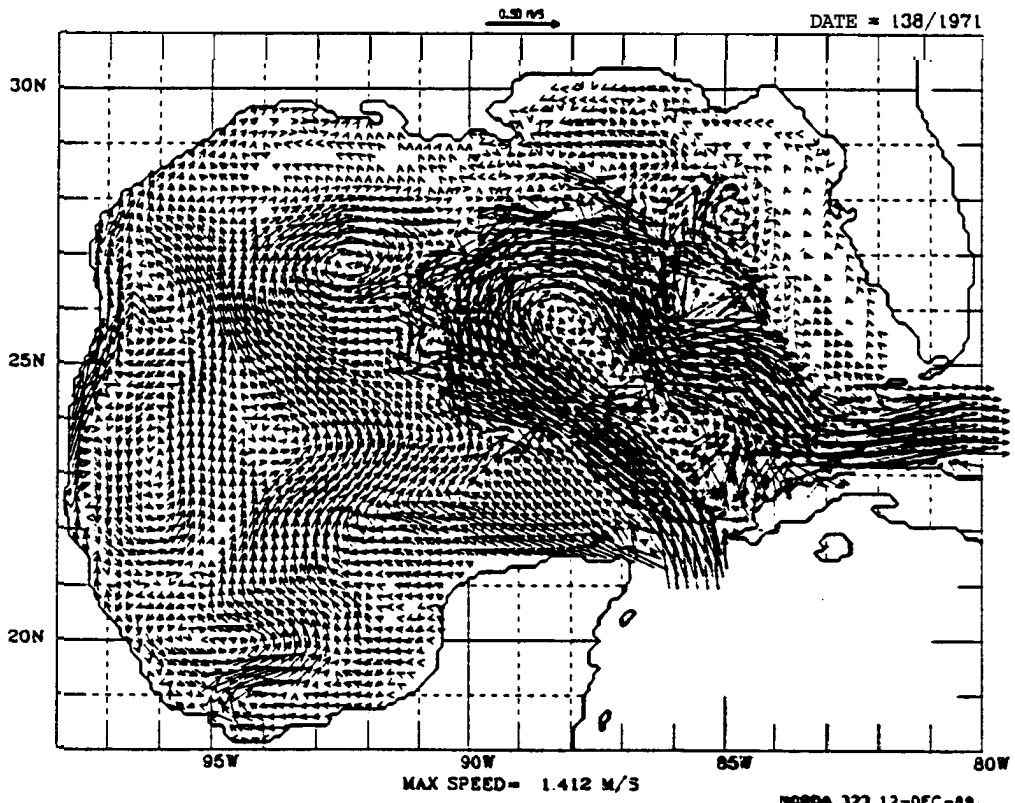
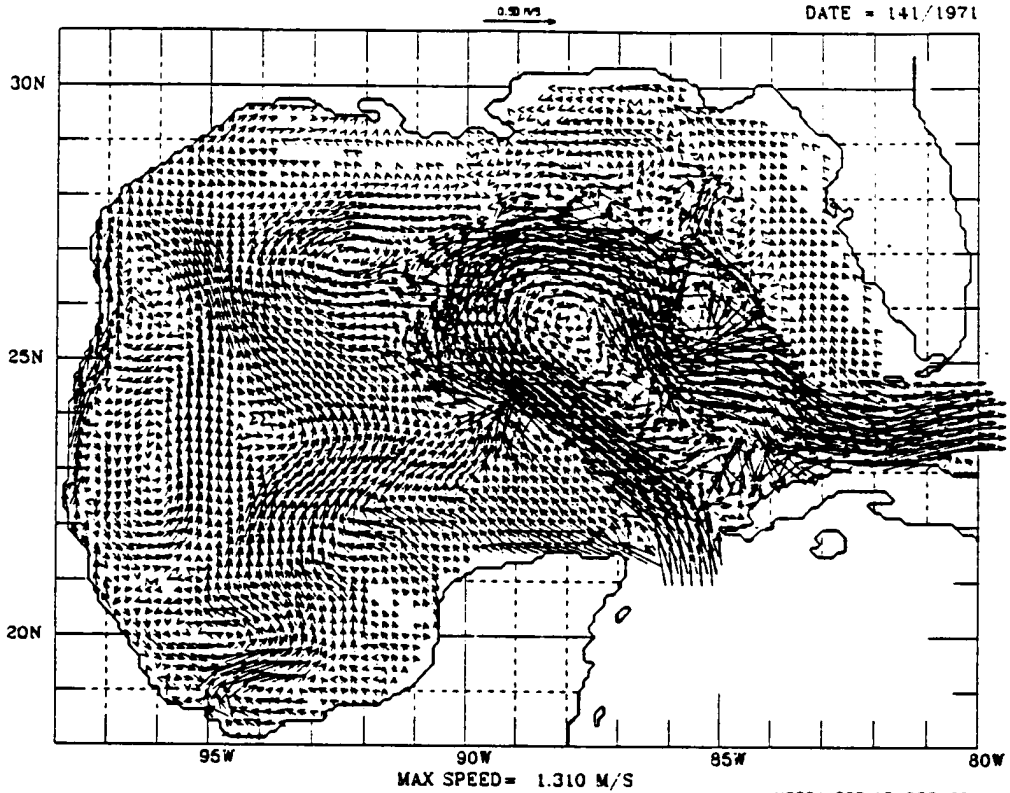


FIGURE 96

SURFACE CURRENTS

G. OF MEXICO 21142:2: 0.0
DATE = 141/1971



SURFACE CURRENTS

NORDA 323 12-DEC-89
G. OF MEXICO 21142:2: 0.0
DATE = 144/1971

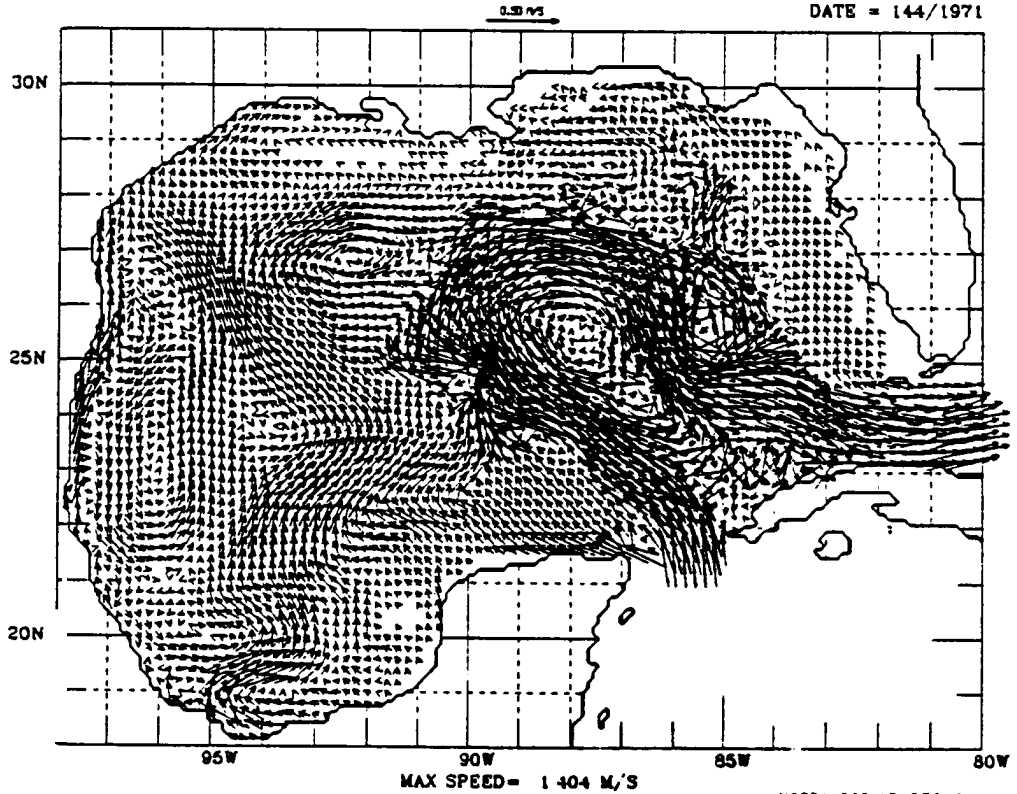
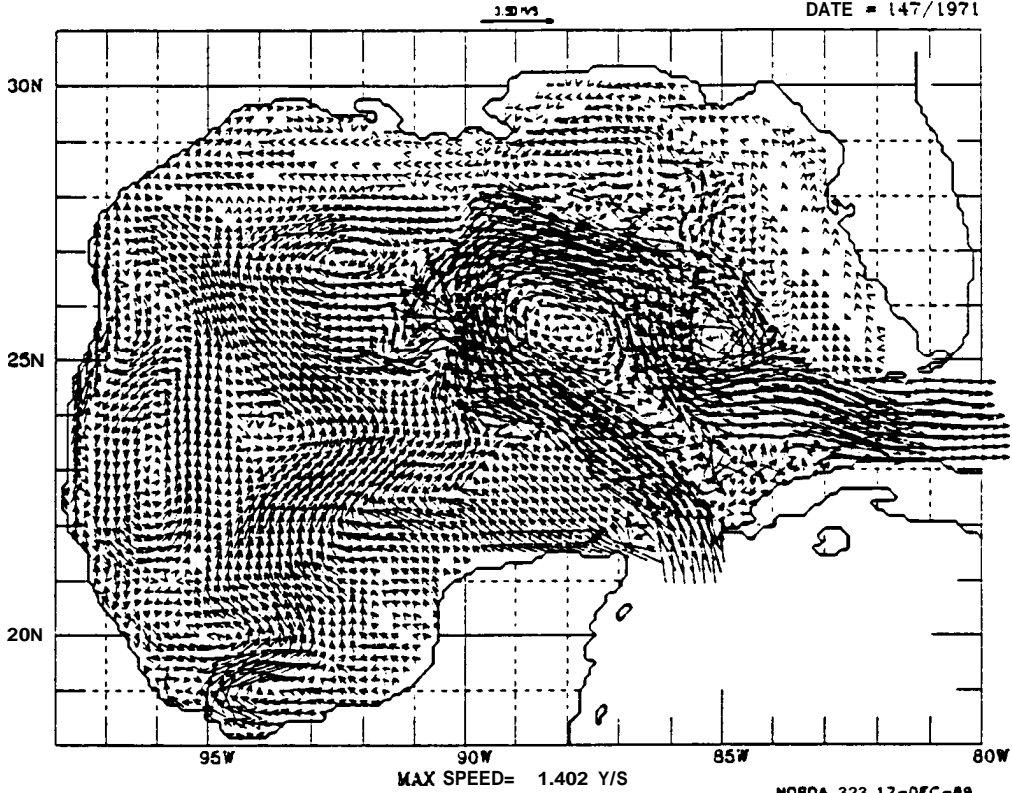


FIGURE 97

SURFACE CURRENTS

G. OF MEXICO 21142:2: 0.3
DATE = 147/1971



SURFACE CURRENTS

NORDA 323 12-DEC-89
G. OF MEXICO 21142:2: 0.0
DATE = 150/1971

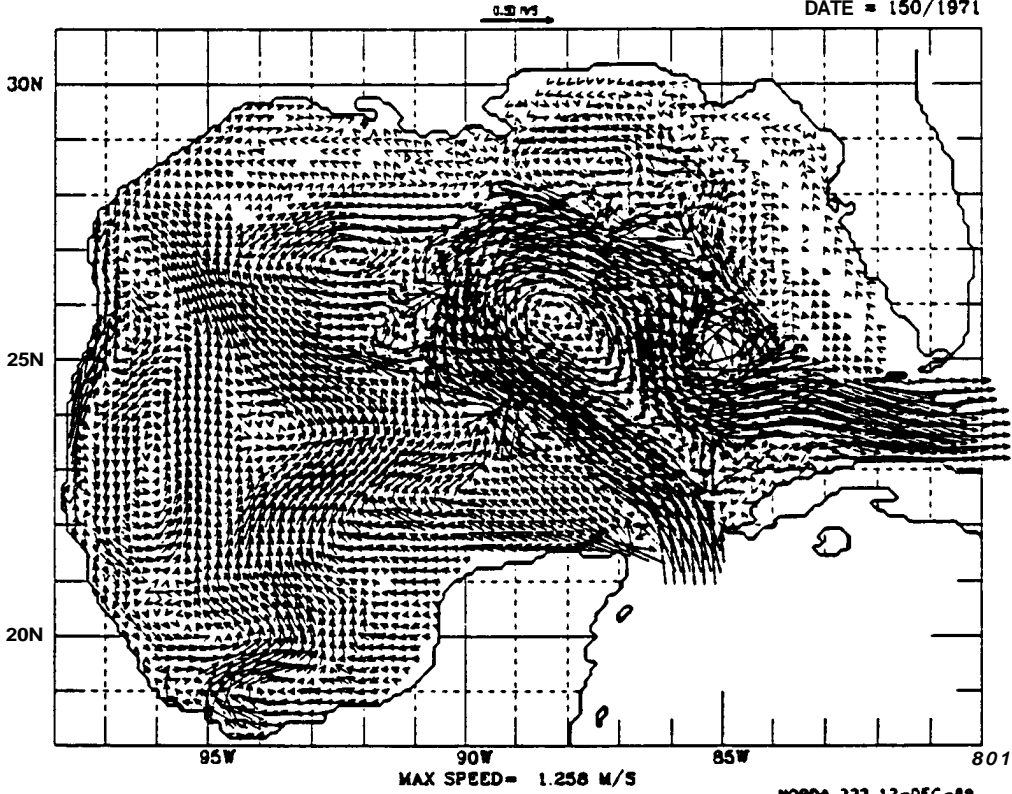
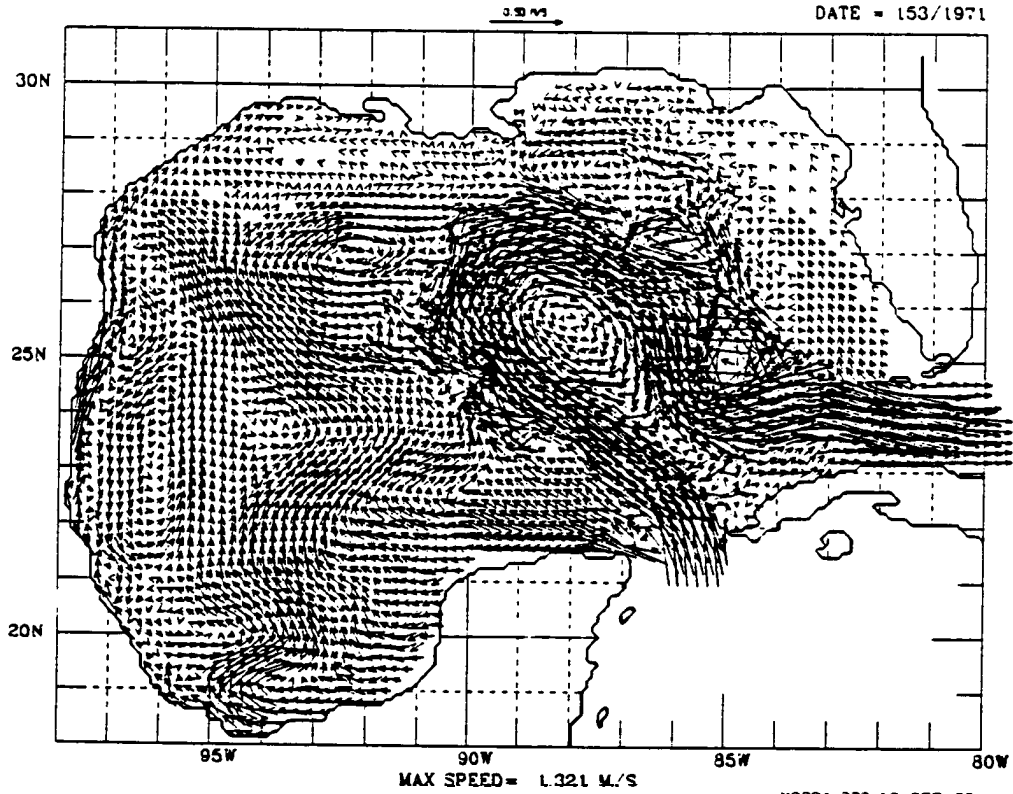


FIGURE 98

SURFACE CURRENTS

G. OF MEXICO 21142:2: 0.0
DATE = 153/1971



SURFACE CURRENTS

NORDA 323 12-DEC-89
G. OF MEXICO 21142:2: 0.0
DATE = 156/1971

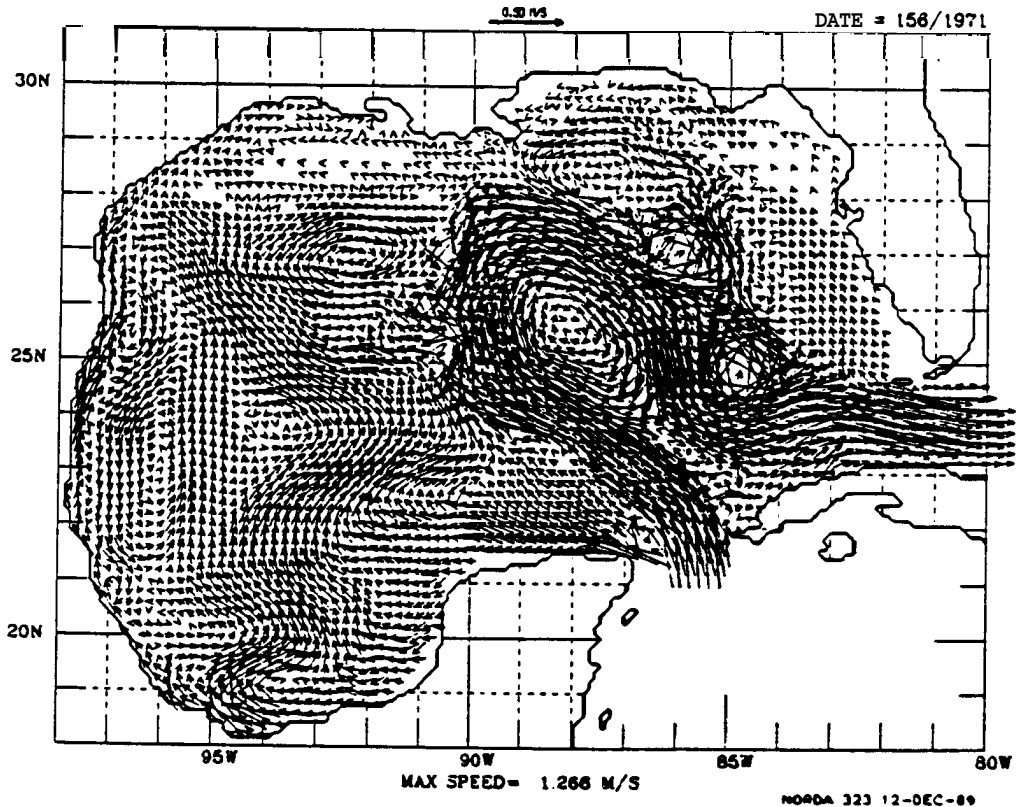


FIGURE 99

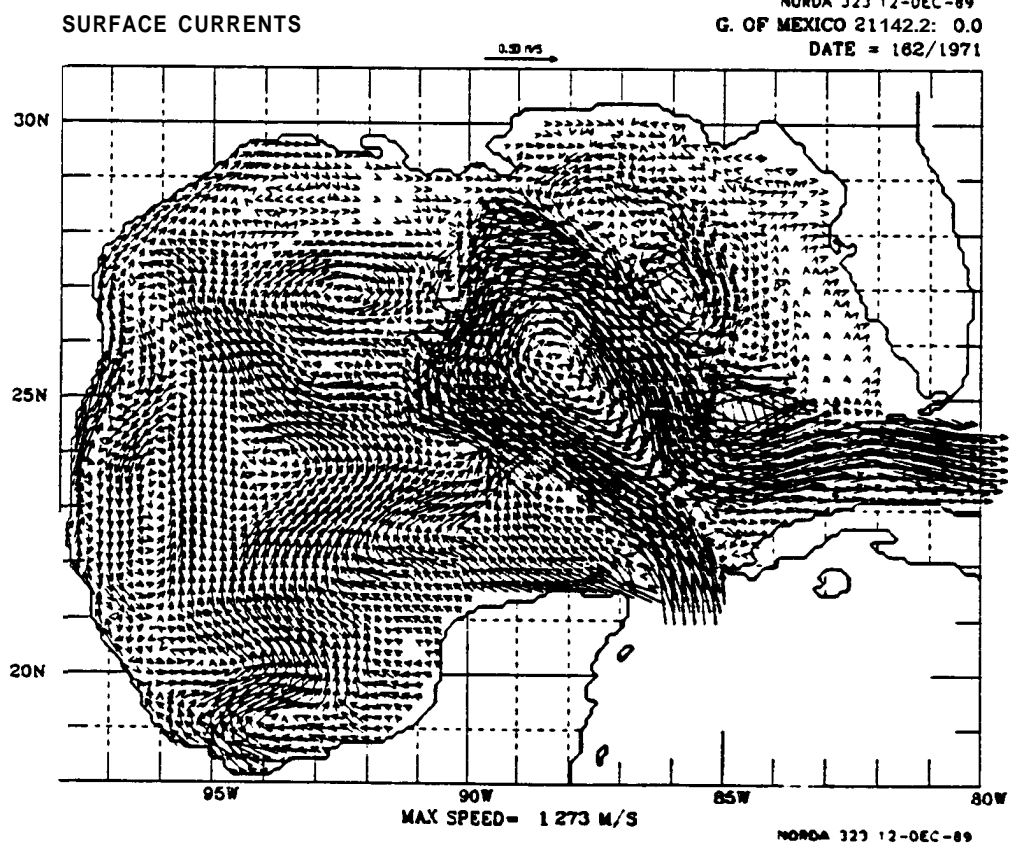
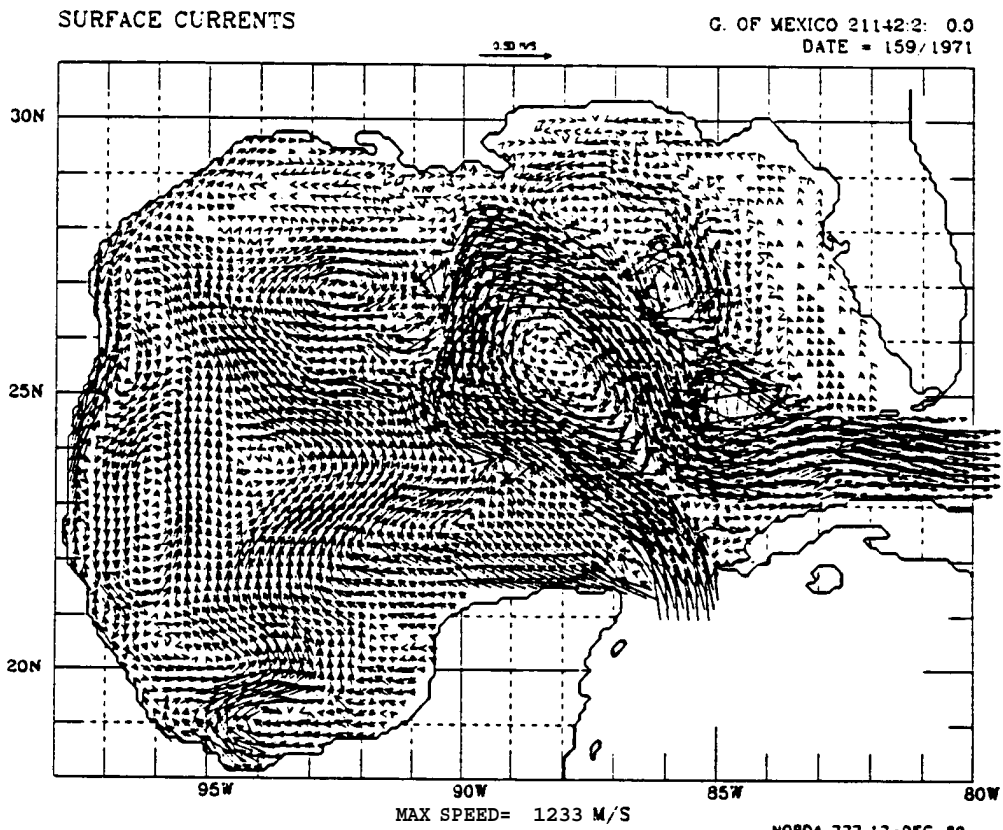


FIGURE 100

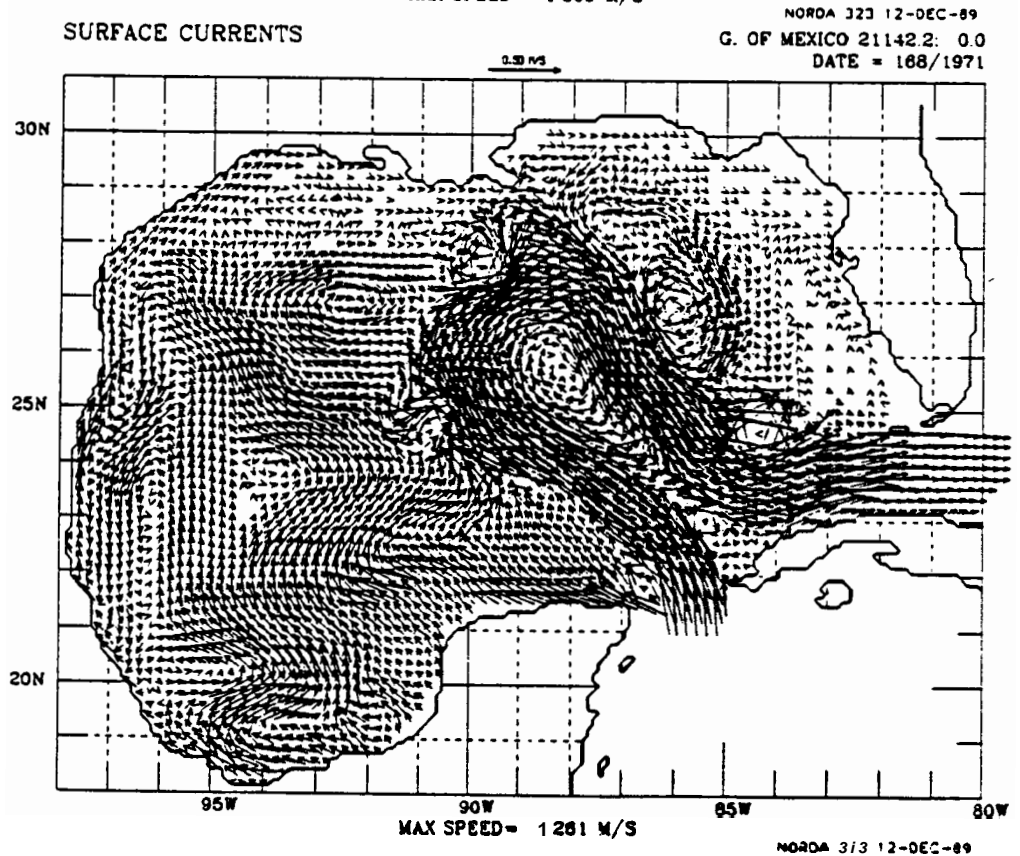
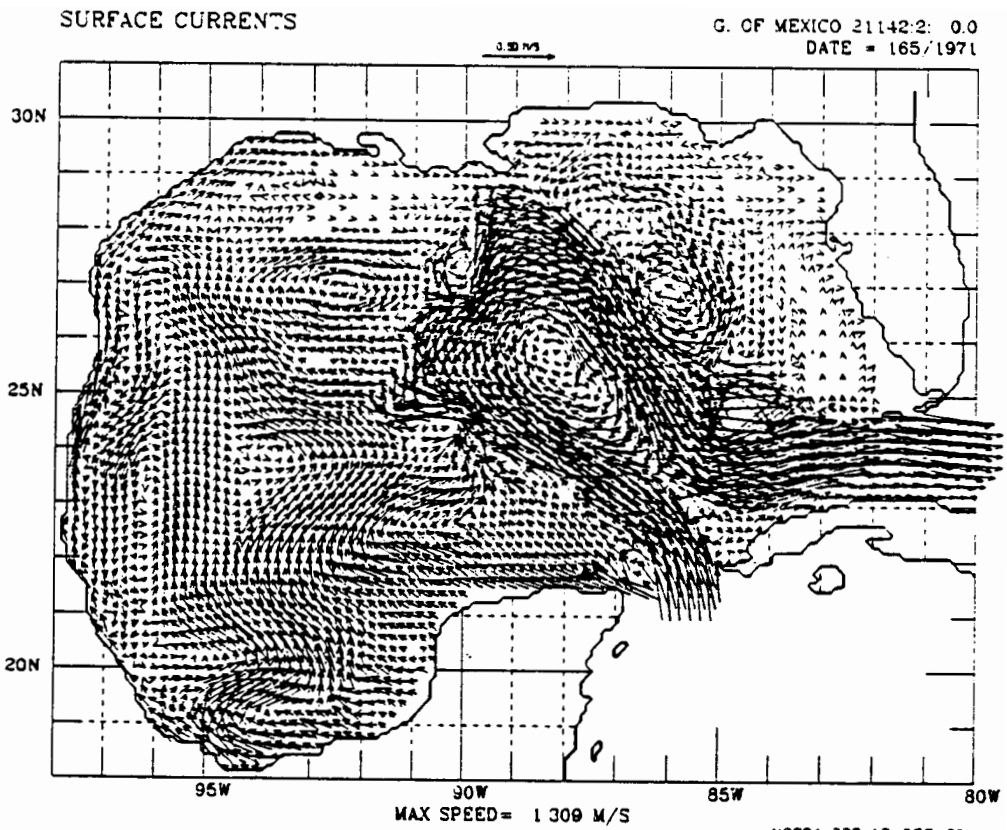
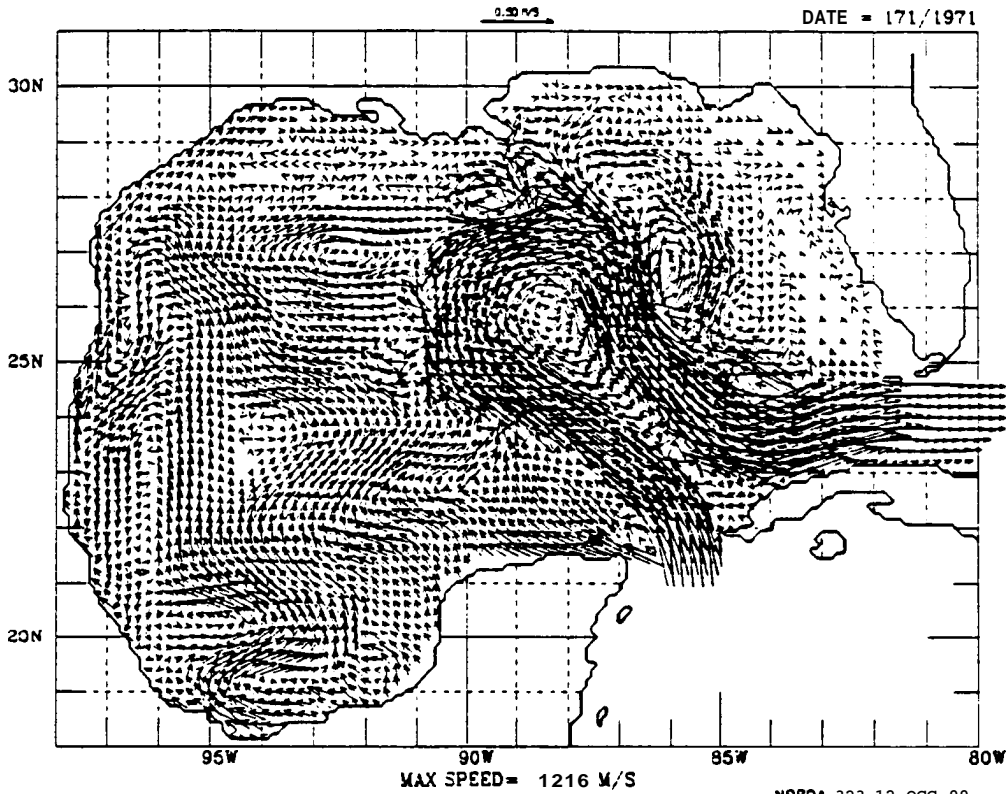


FIGURE 101

SURFACE CURRENTS

G. OF MEXICO 21142.2: 0.3
DATE = 171/1971



SURFACE CURRENTS

NORDA 323 12-OCC-99
G. OF MEXICO 21142.2: 0.0
DATE = 174/1971

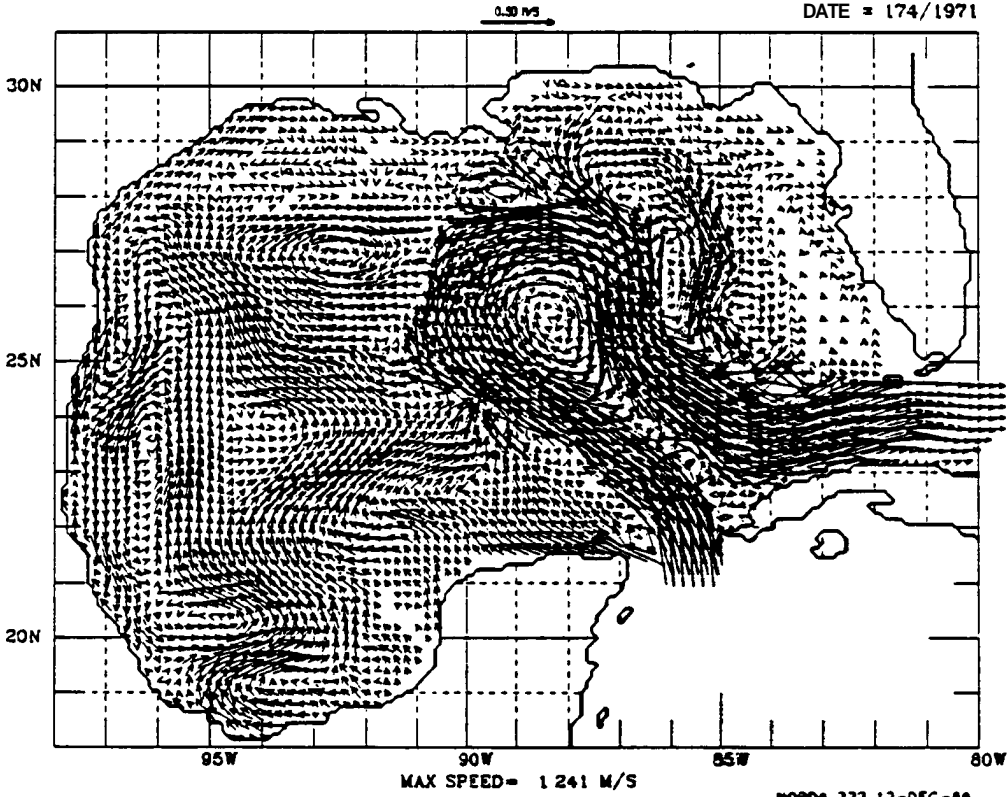


FIGURE 102

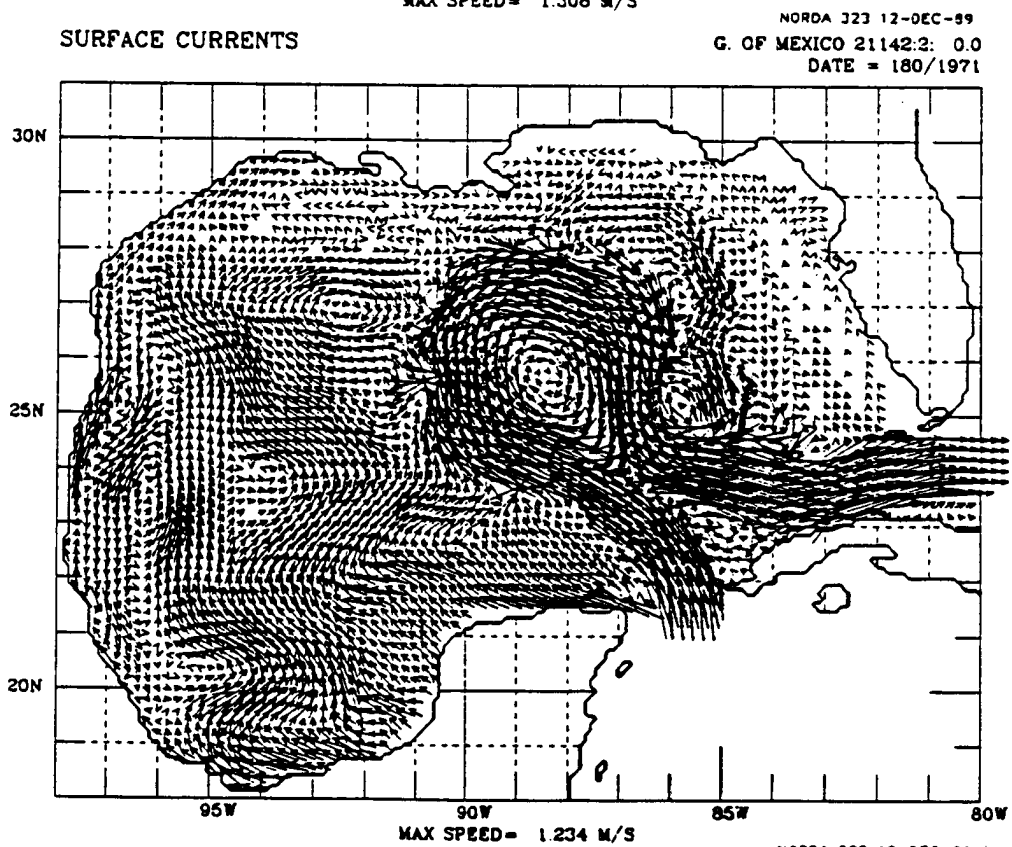
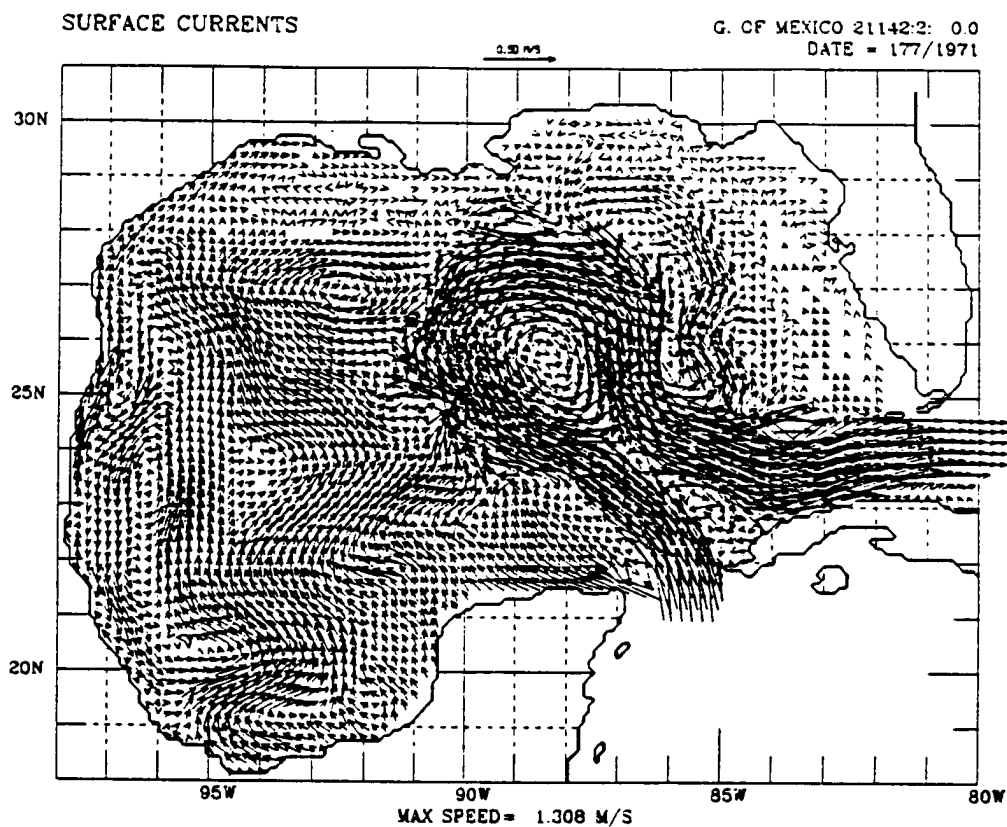


FIGURE 103

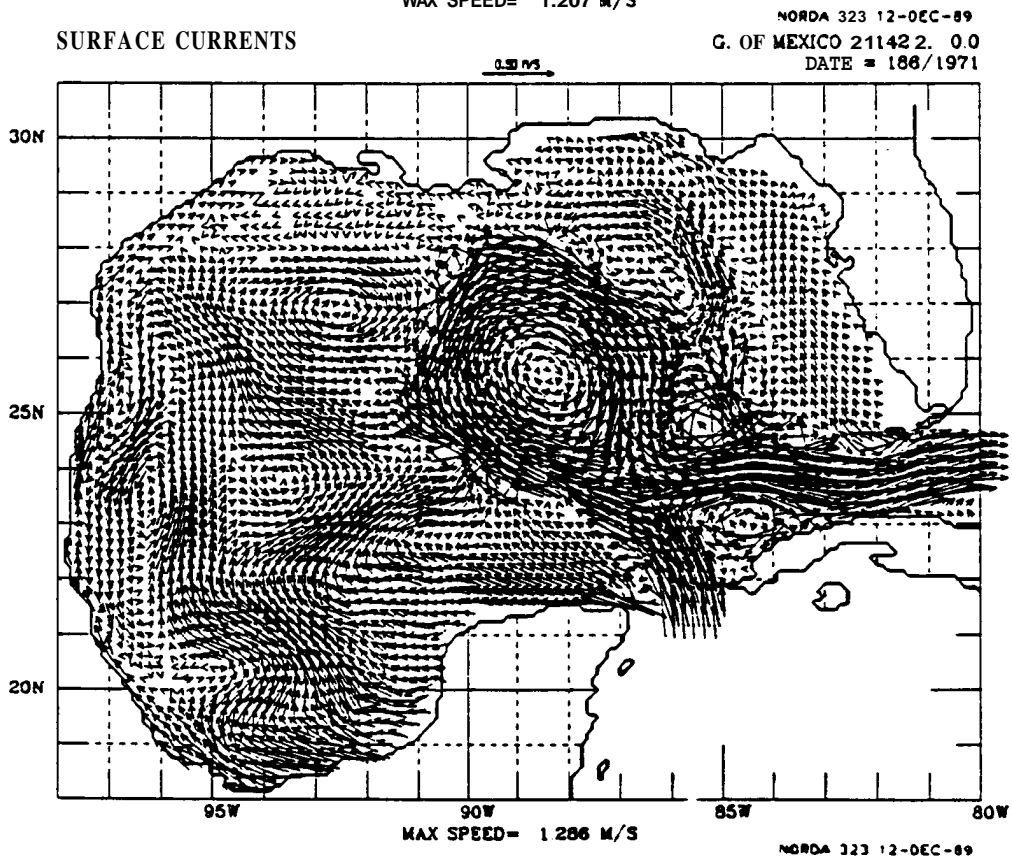
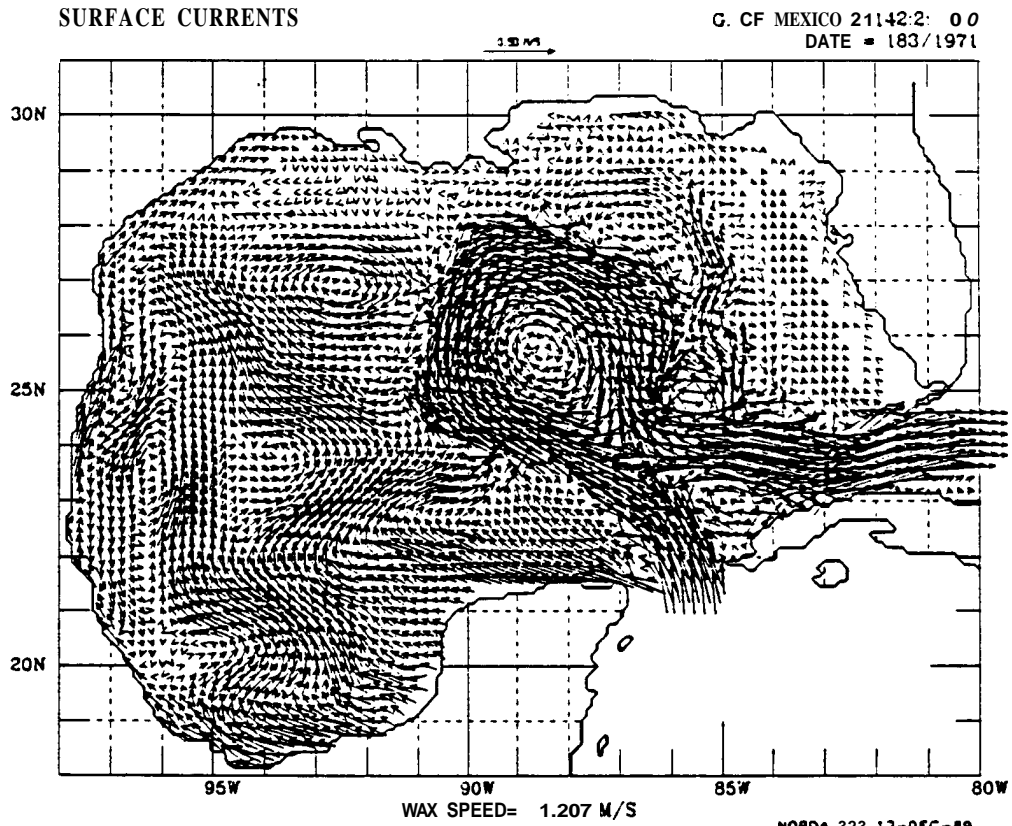
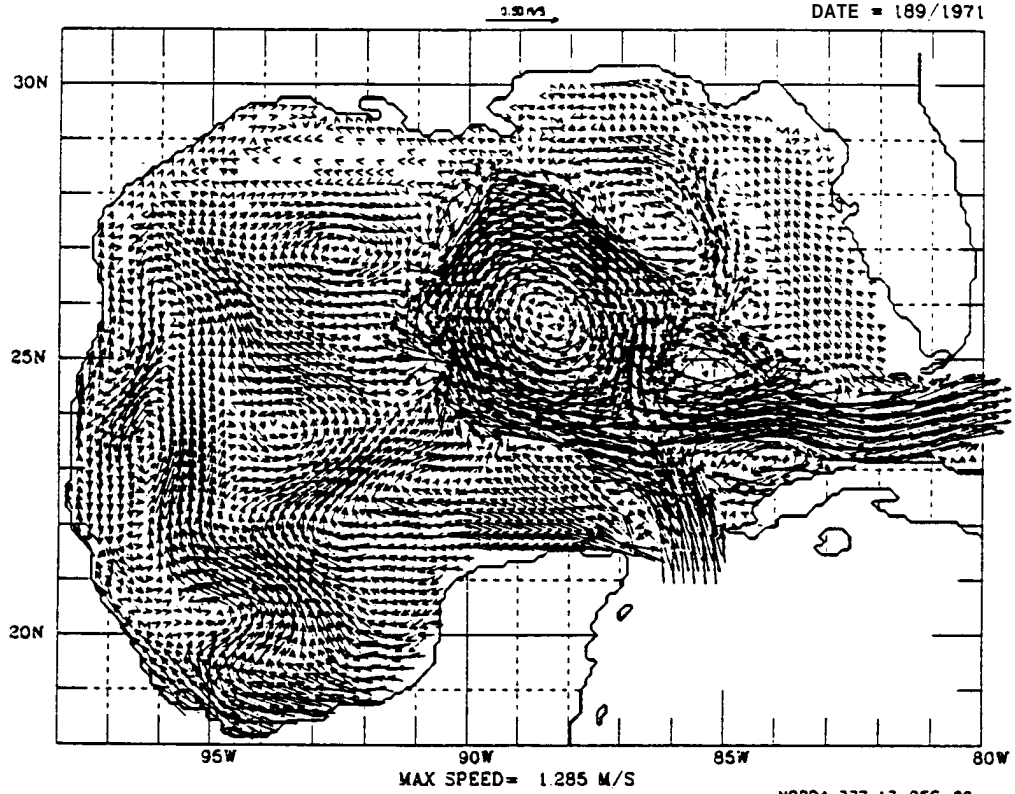


FIGURE 104

SURFACE CURRENTS

G. OF MEXICO 21142:2: 0.0
DATE = 189/1971



SURFACE CURRENTS

NORDA 323 12-DEC-89
G. OF MEXICO 21142:2: 0.0
DATE = 192/1971

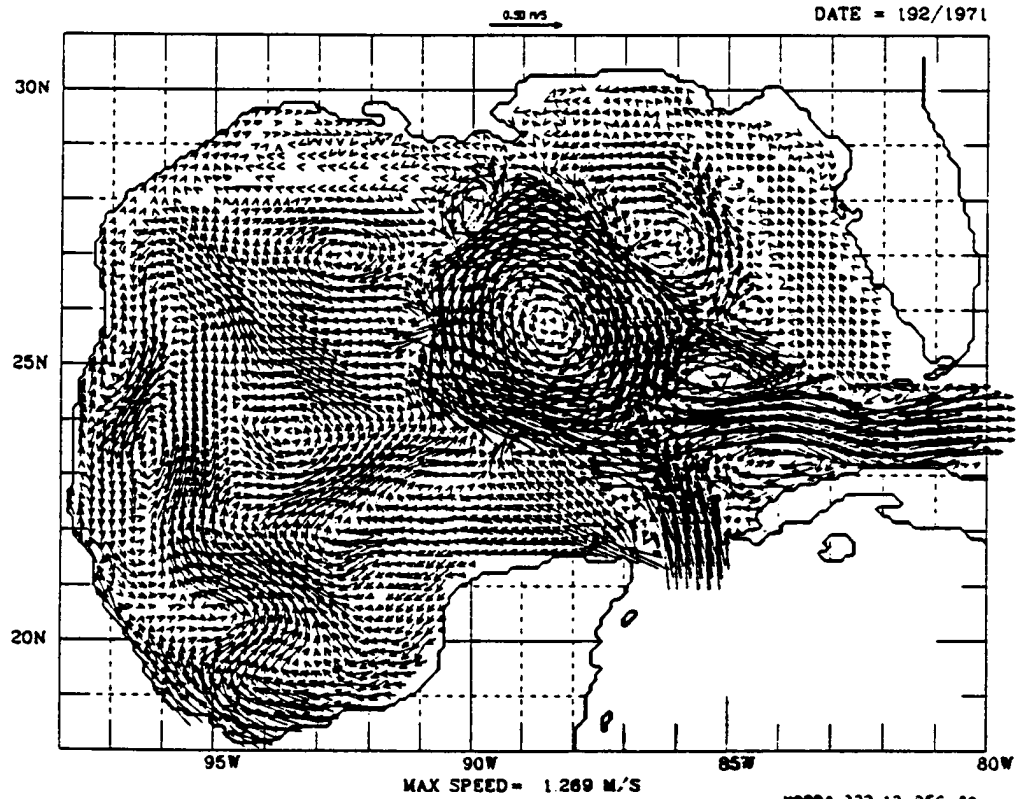
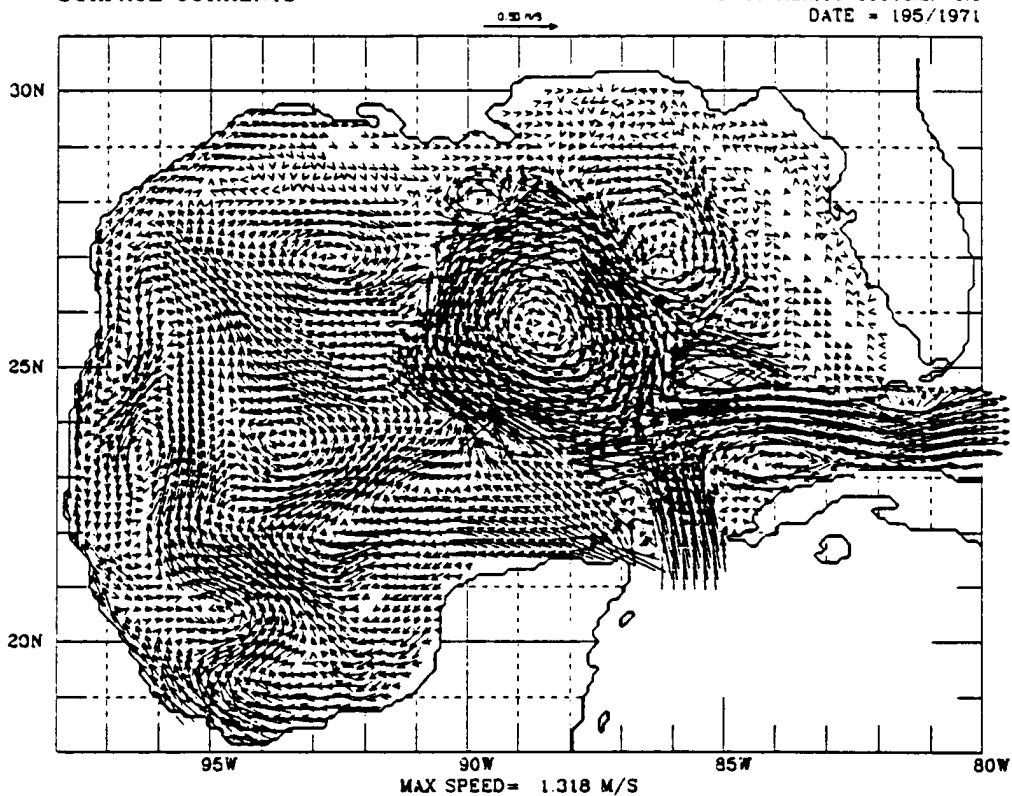


FIGURE 105

SURFACE CURRENTS

G. OF MEXICO 21142:2: 0.0
DATE = 195/1971



SURFACE CURRENTS

NORDA 323 12-OEC-89
G. OF MEXICO 21142:2: 0.0
DATE = 198/1971

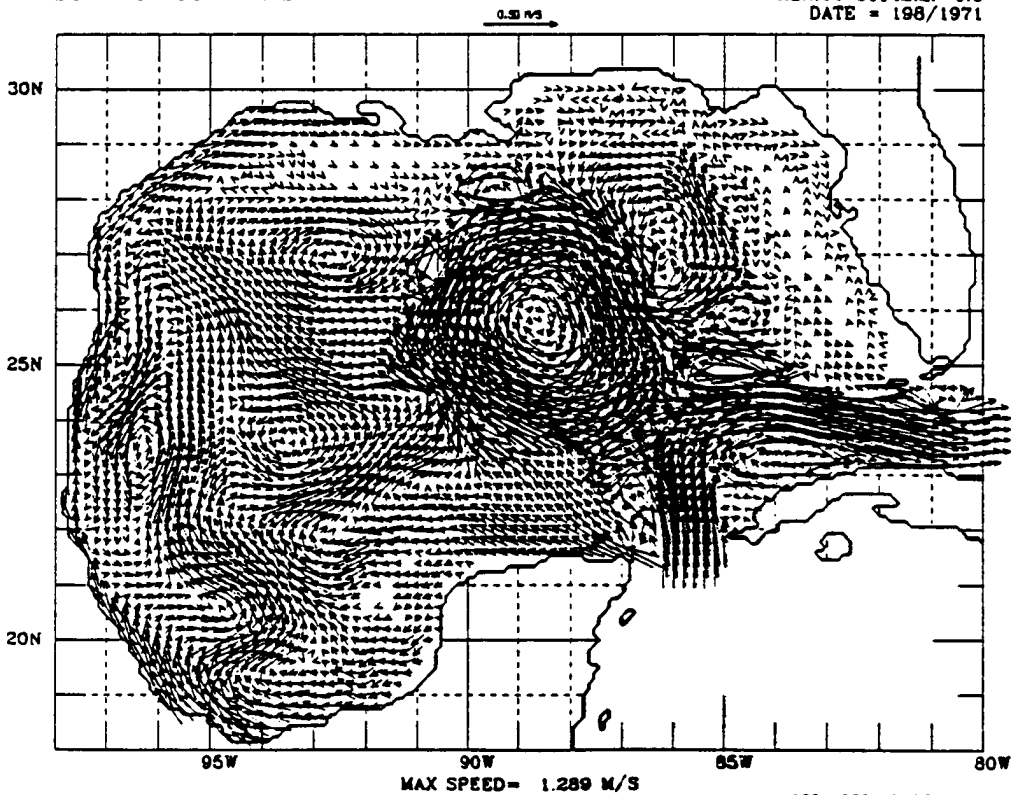
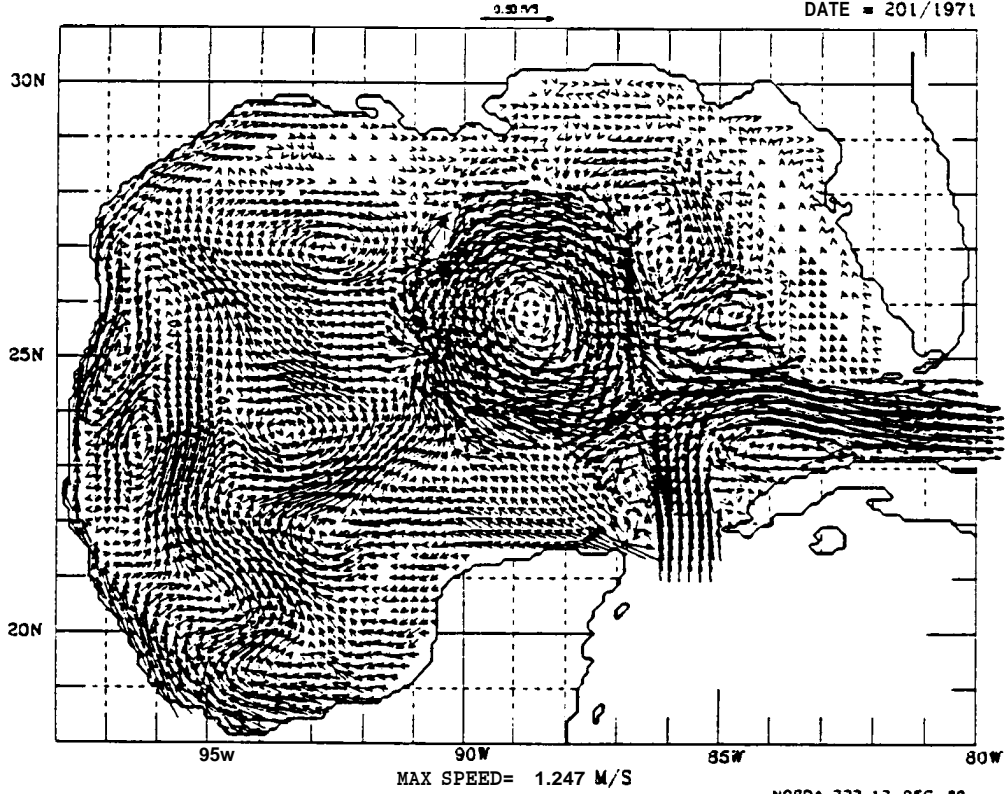


FIGURE 106

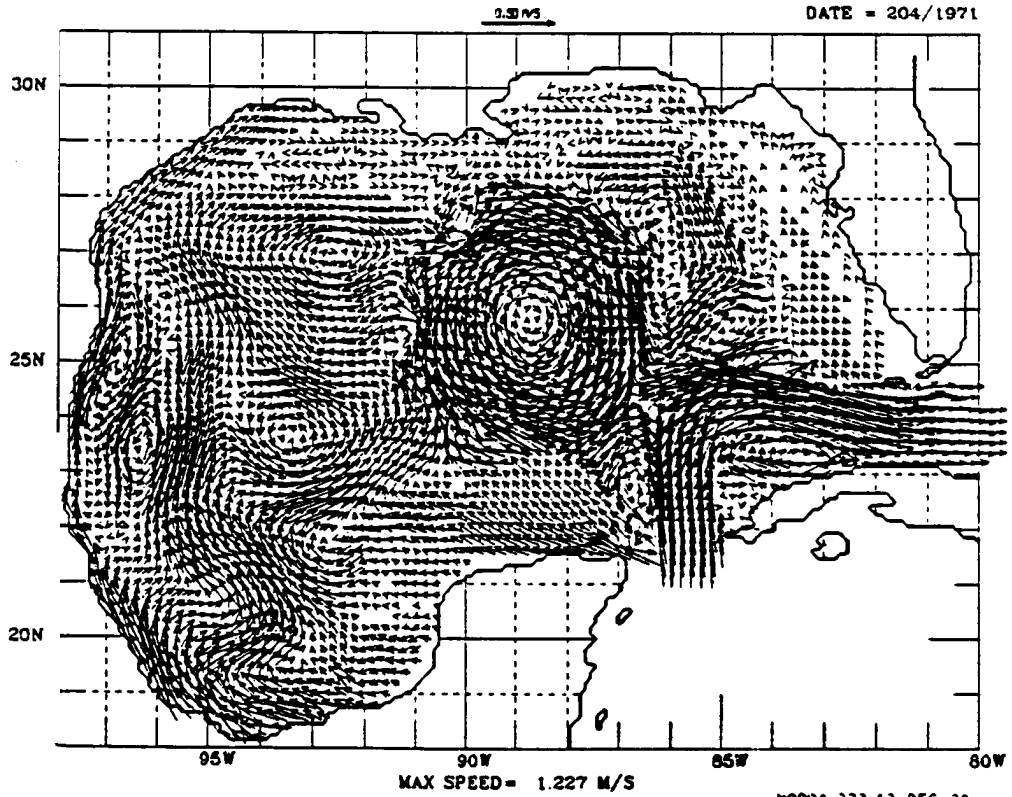
SURFACE CURRENTS

G. OF MEXICO 21142:2: 0.0
DATE = 201/1971



SURFACE CURRENTS

NORDA 323 12-DEC-89
G. OF MEXICO 21142:2: 0.0
DATE = 204/1971

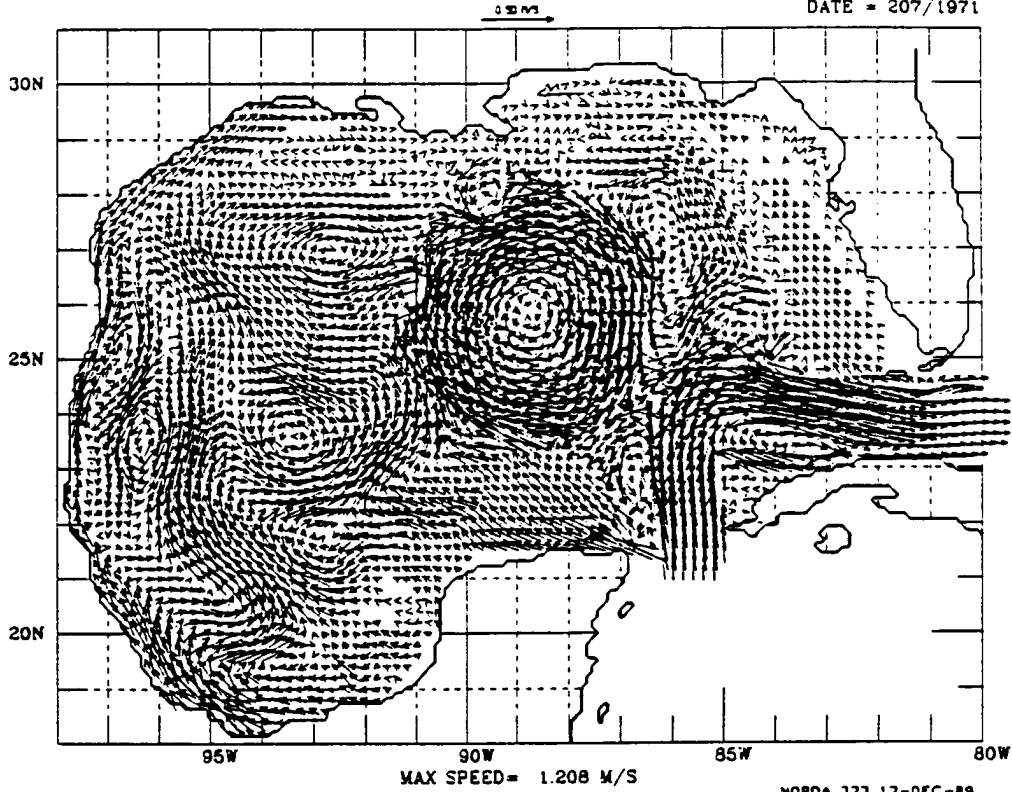


NORDA 323 12-DEC-89

FIGURE 107

SURFACE CURRENTS

G. OF MEXICO 21142:2: 0.0
DATE = 207/1971



SURFACE CURRENTS

NORDA 323 12-DEC-89
G. OF MEXICO 21142:2: 0.0
DATE = 210/1971

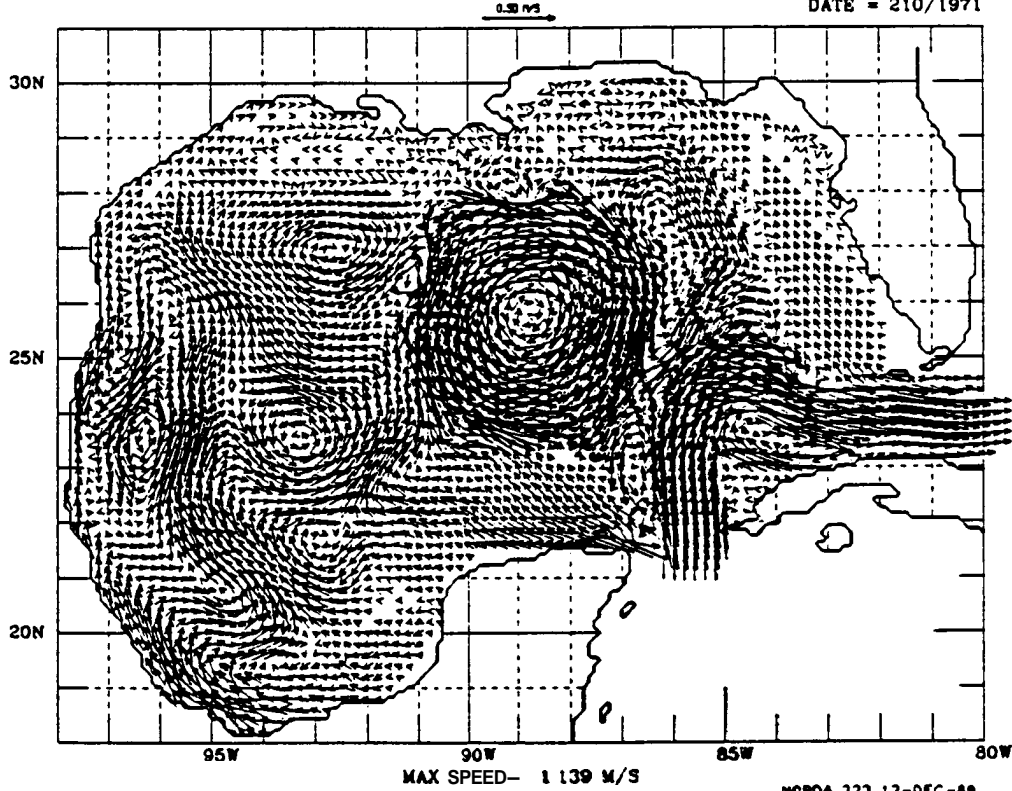
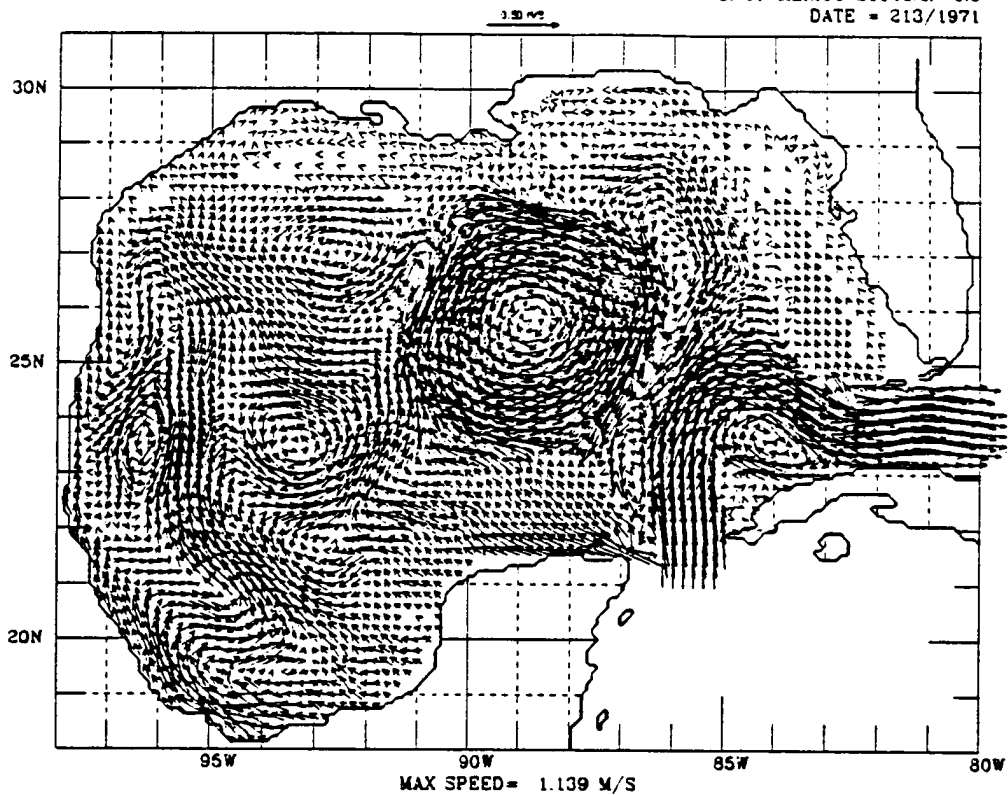


FIGURE 108

SURFACE CURRENTS

G. OF MEXICO 21142.2: 0.0
DATE = 213/1971



SURFACE CURRENTS

NORDA 323 12-DEC-89
G. OF MEXICO 21142.2: 0.0
DATE = 216/1971

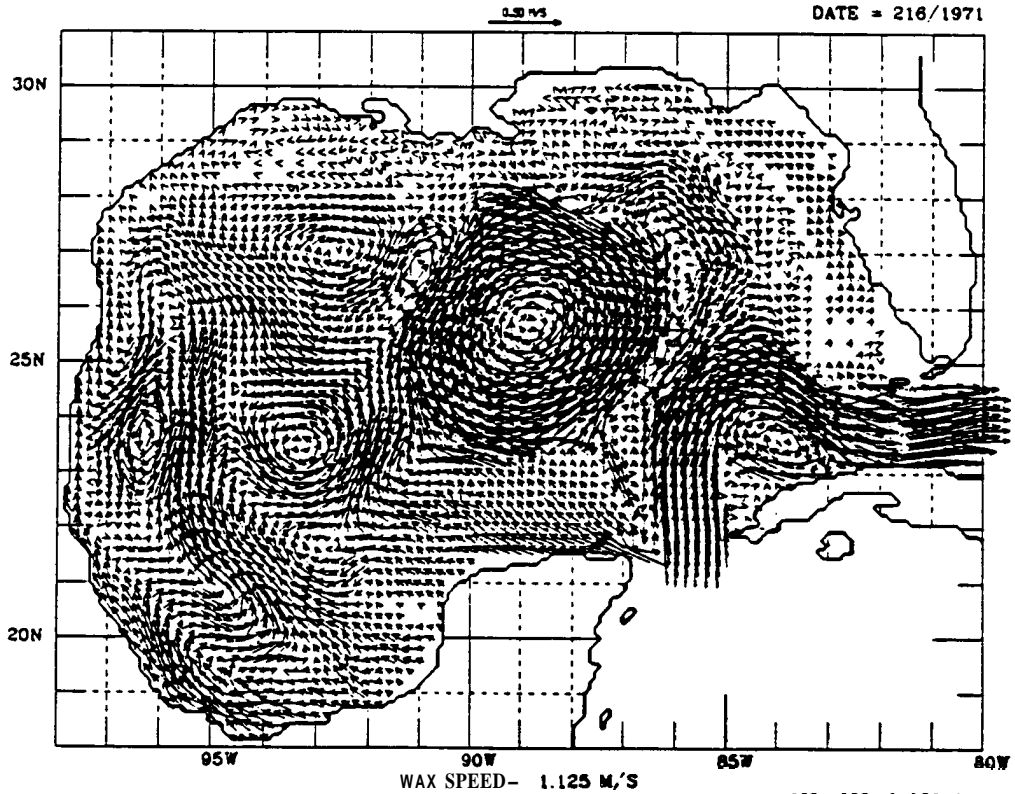
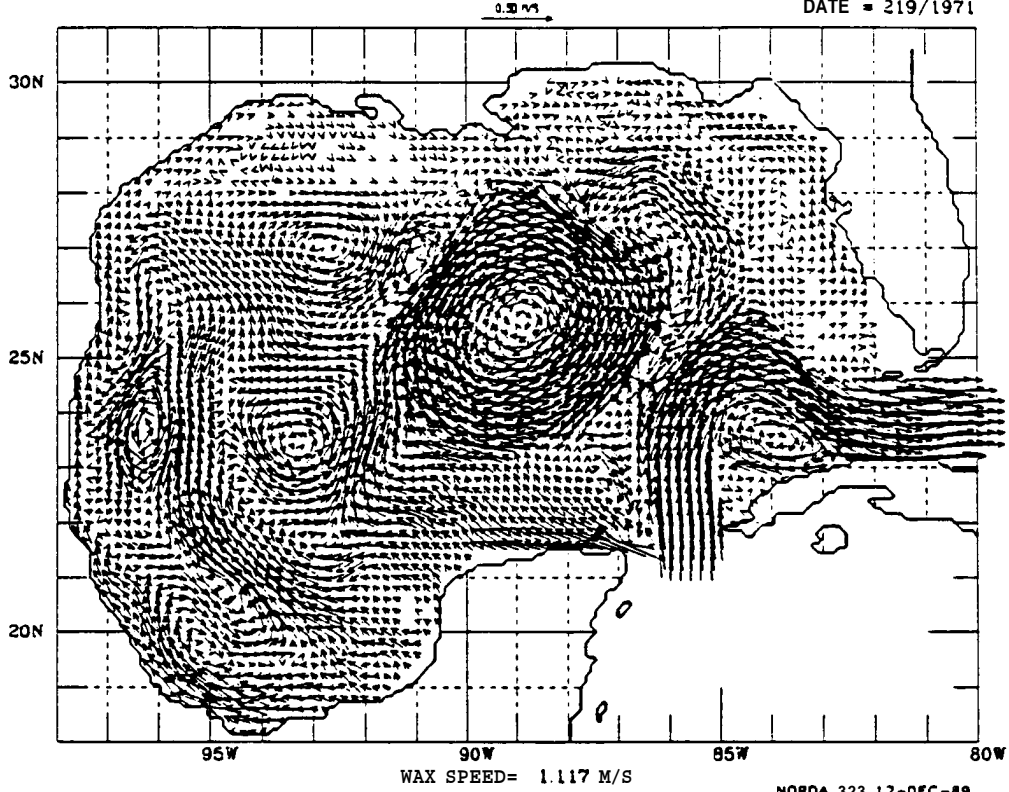


FIGURE 109

SURFACE CURRENTS

G. OF MEXICO 21142:2: 0.3
DATE = 219/1971



SURFACE CURRENTS

G. OF MEXICO 21142:2: 0.0
DATE = 222/1971

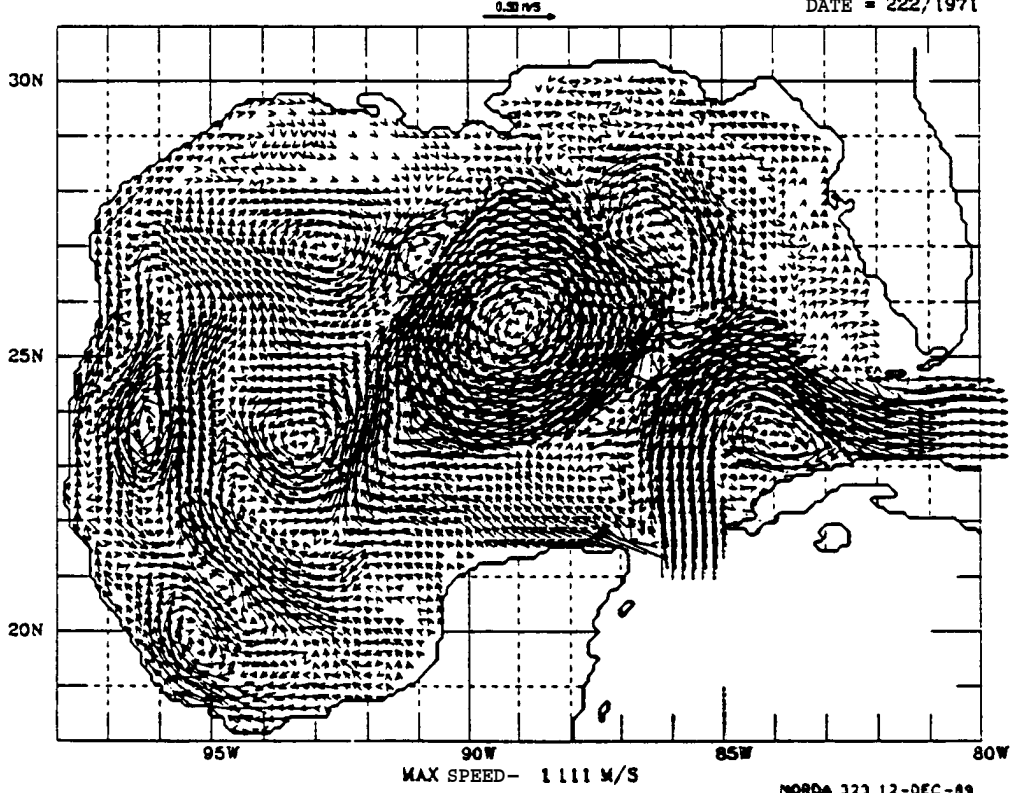
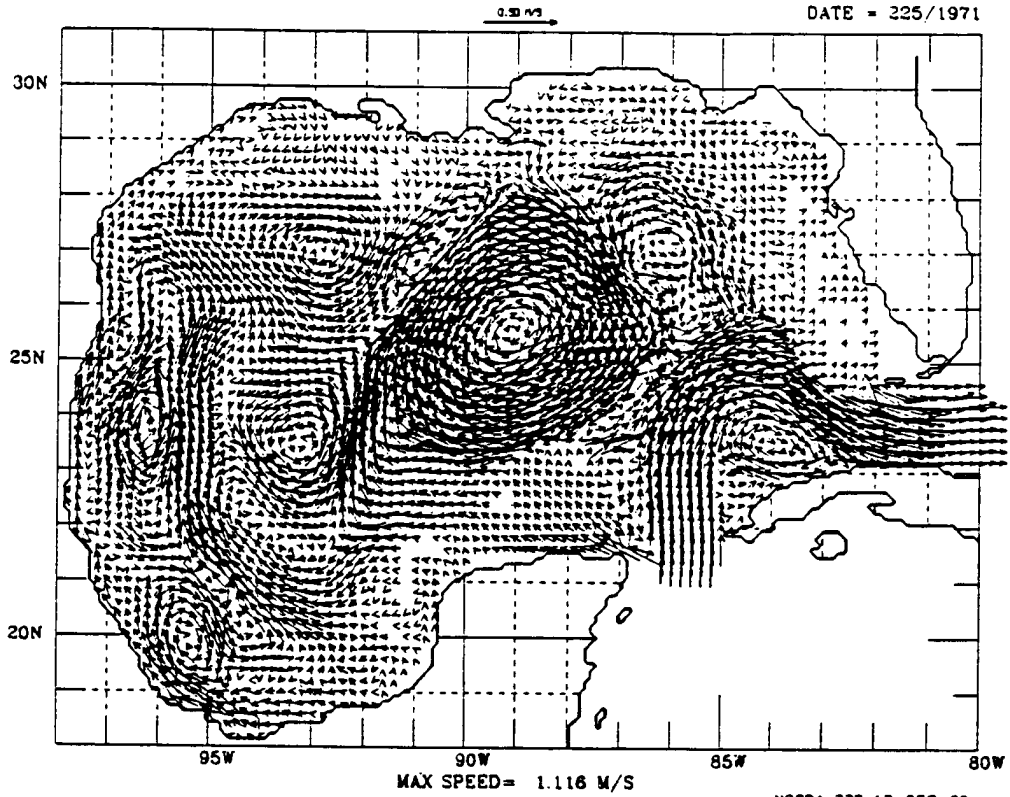


FIGURE 110

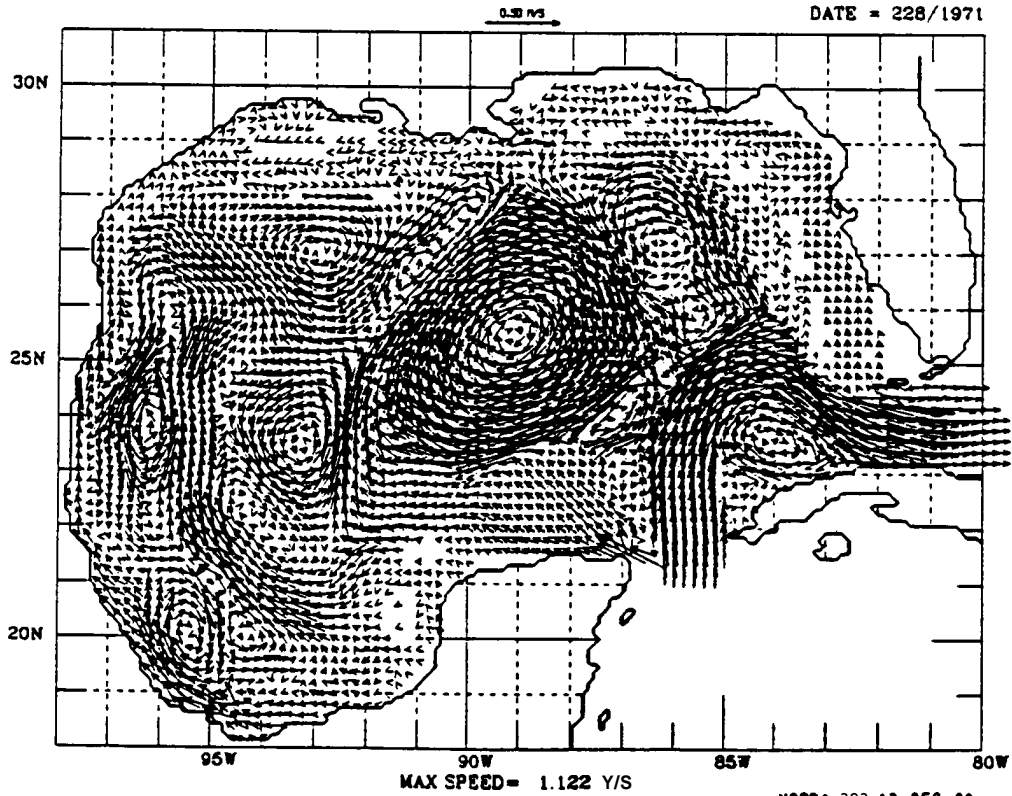
SURFACE CURRENTS

G. OF MEXICO 21142:2: 0.0
DATE = 225/1971



SURFACE CURRENTS

NORDA 323 12-DEC-89
G. OF MEXICO 21142:2: 0.0
DATE = 228/1971



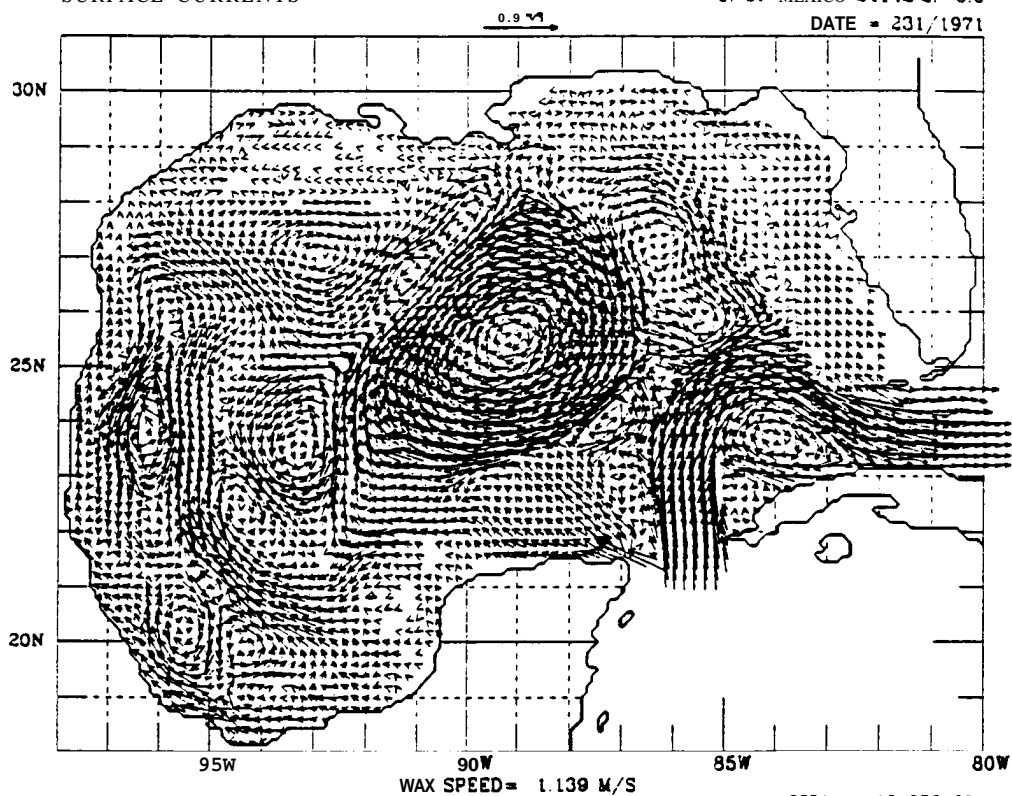
NORDA 323 12-DEC-89

FIGURE 111

SURFACE CURRENTS

G. OF MEXICO 21142-2: 0.0

DATE = 231/1971

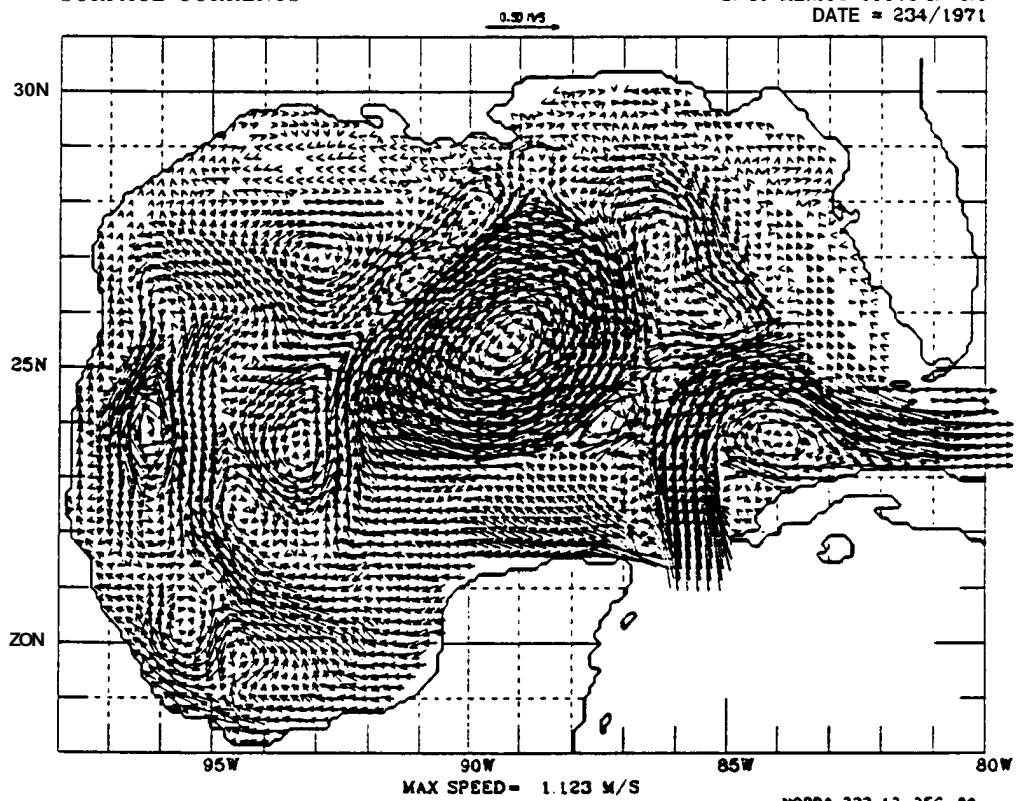


SURFACE CURRENTS

NORDA 323 12-DEC-89

G. OF MEXICO 21142-2: 0.0

DATE = 234/1971



NORDA 323 12-DEC-89

FIGURE 112

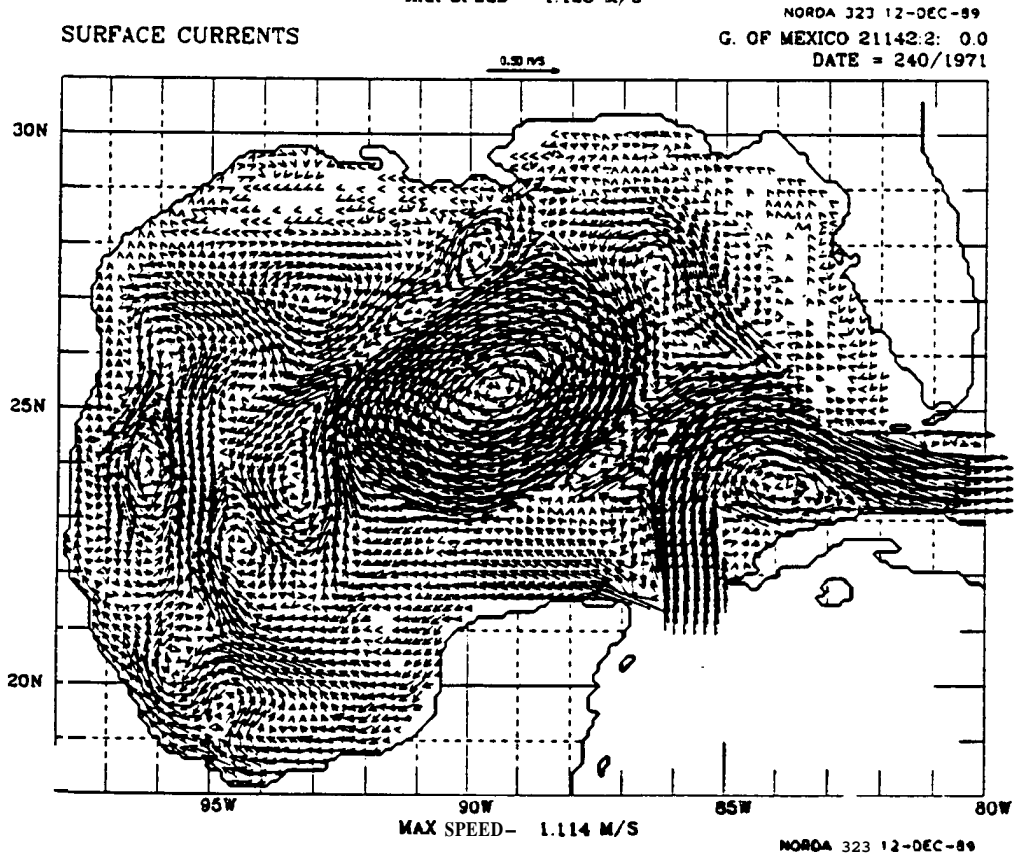
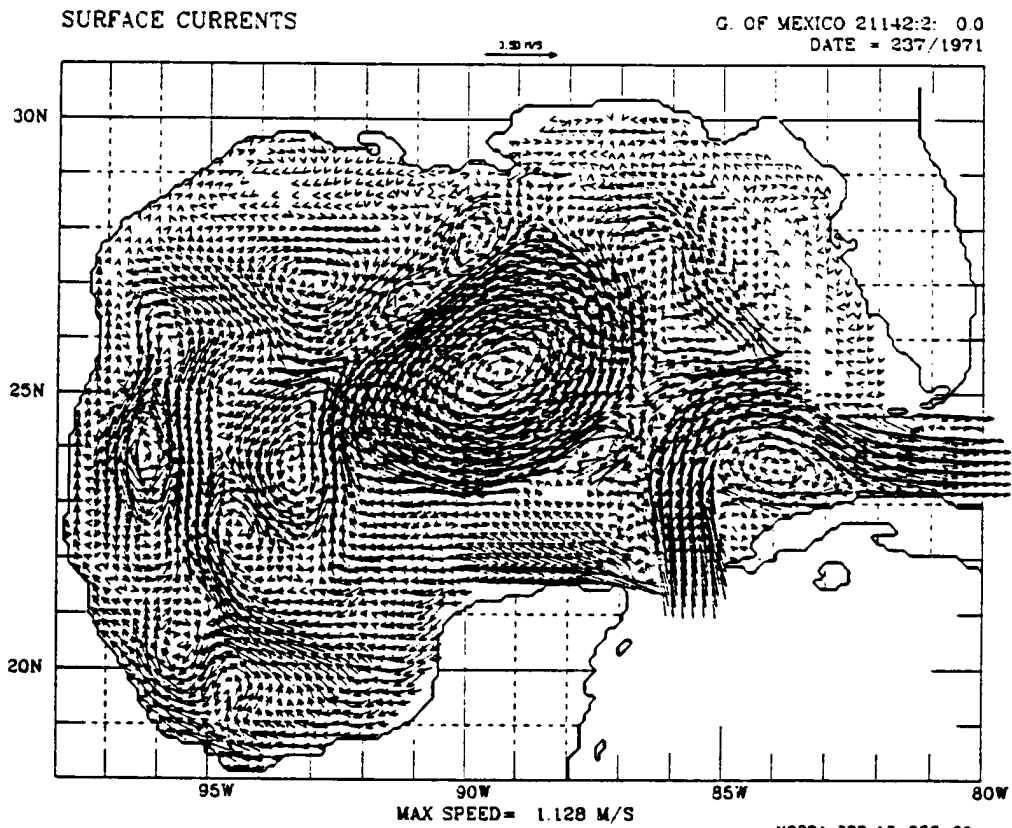
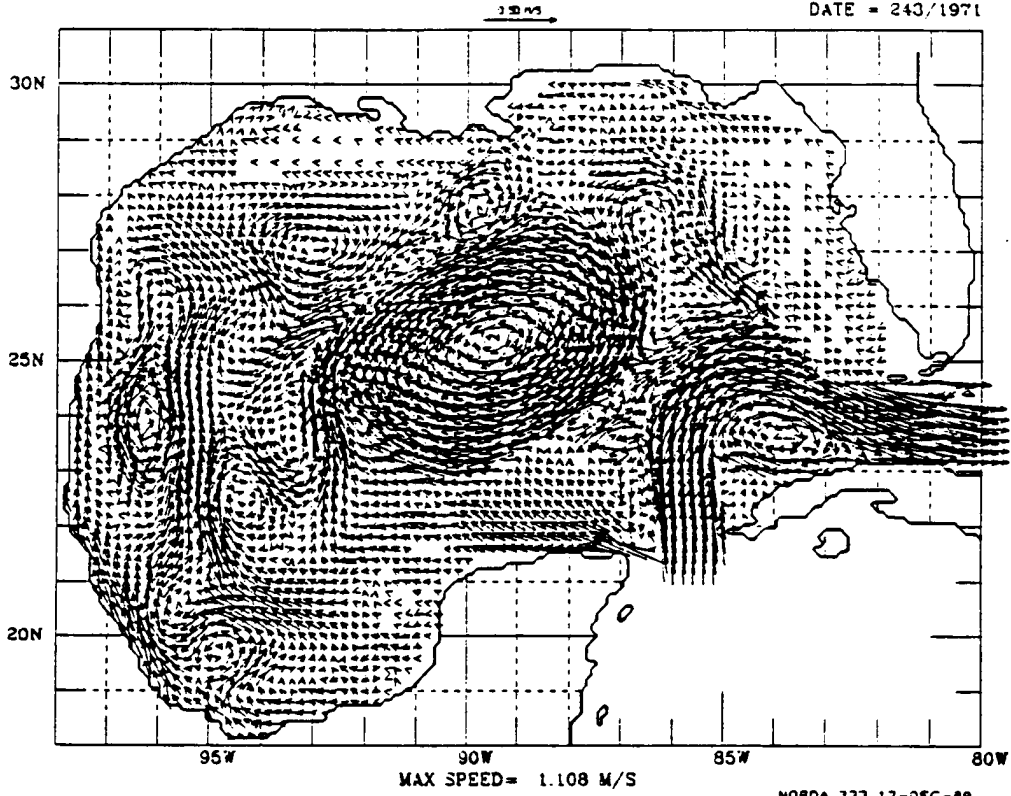


FIGURE 113

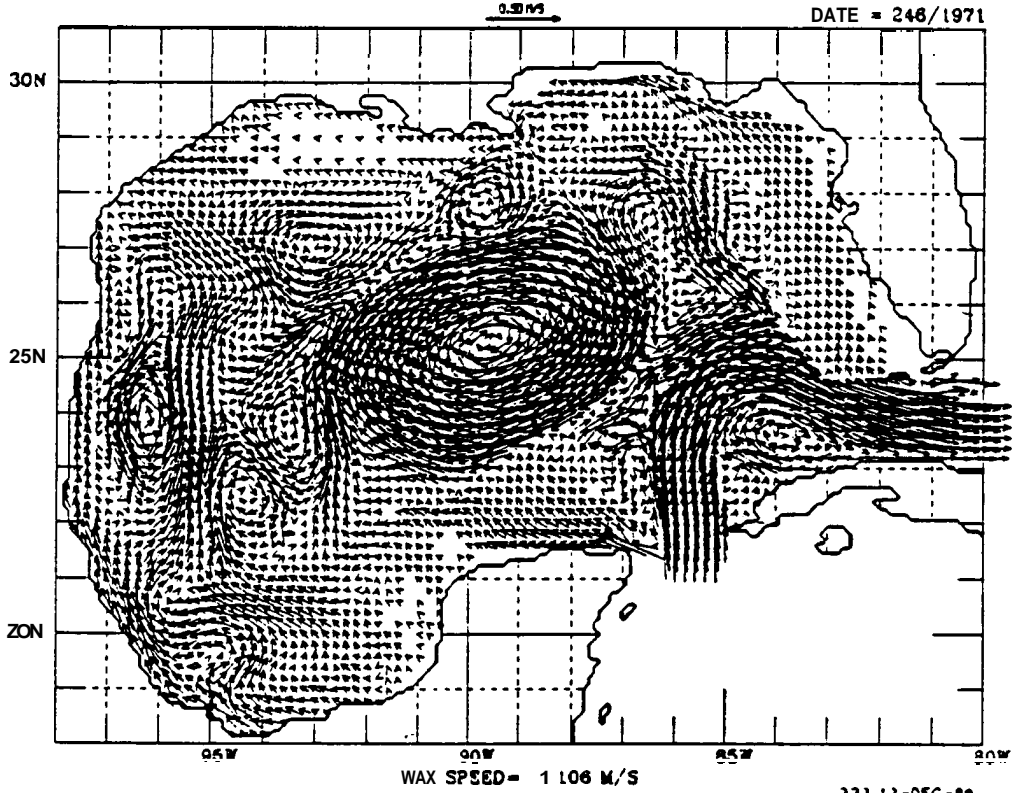
SURFACE CURRENTS

G. OF MEXICO 21142:2: 0.0
DATE = 243/1971



SURFACE CURRENTS

NORDA 323 12-DEC-89
G. OF MEXICO 21142:2: 0.0
DATE = 246/1971



323 12-DEC-89

FIGURE 114

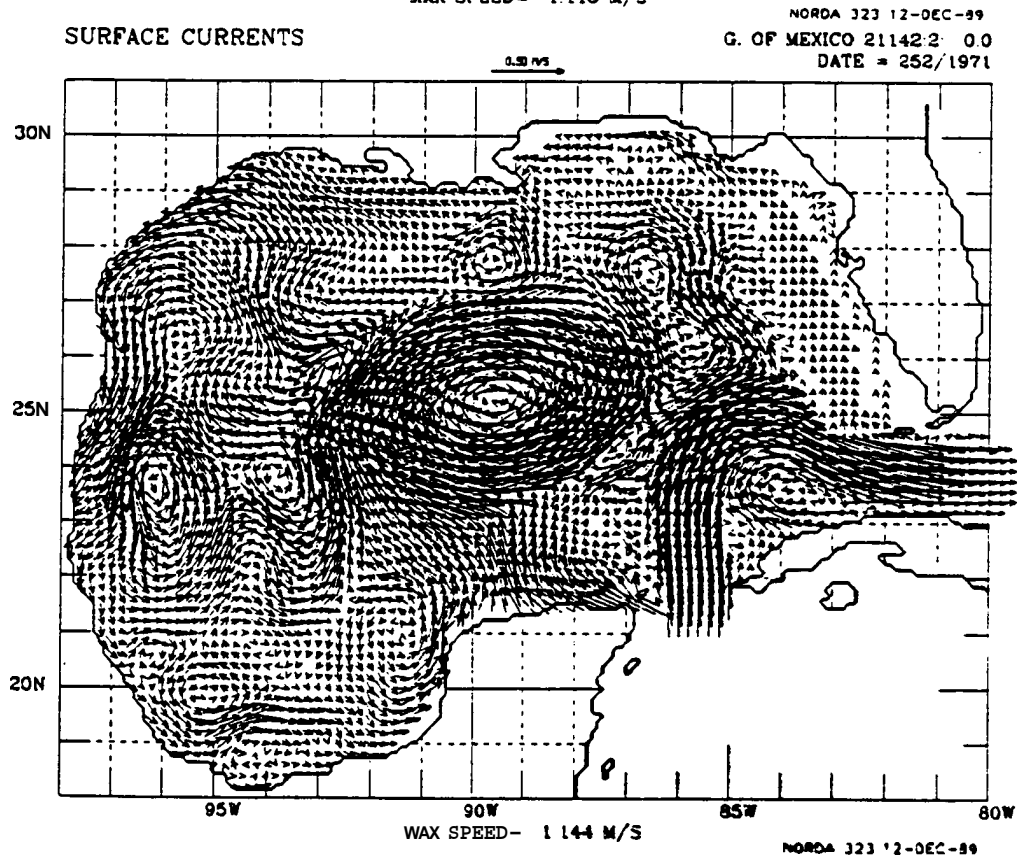
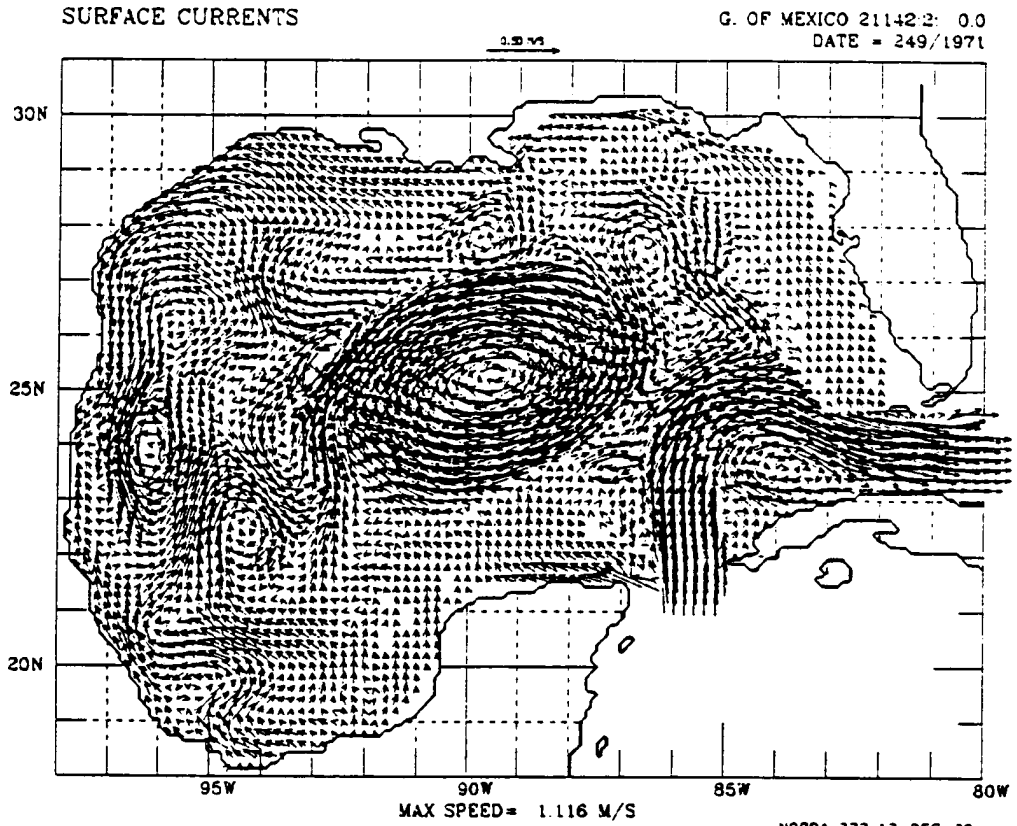
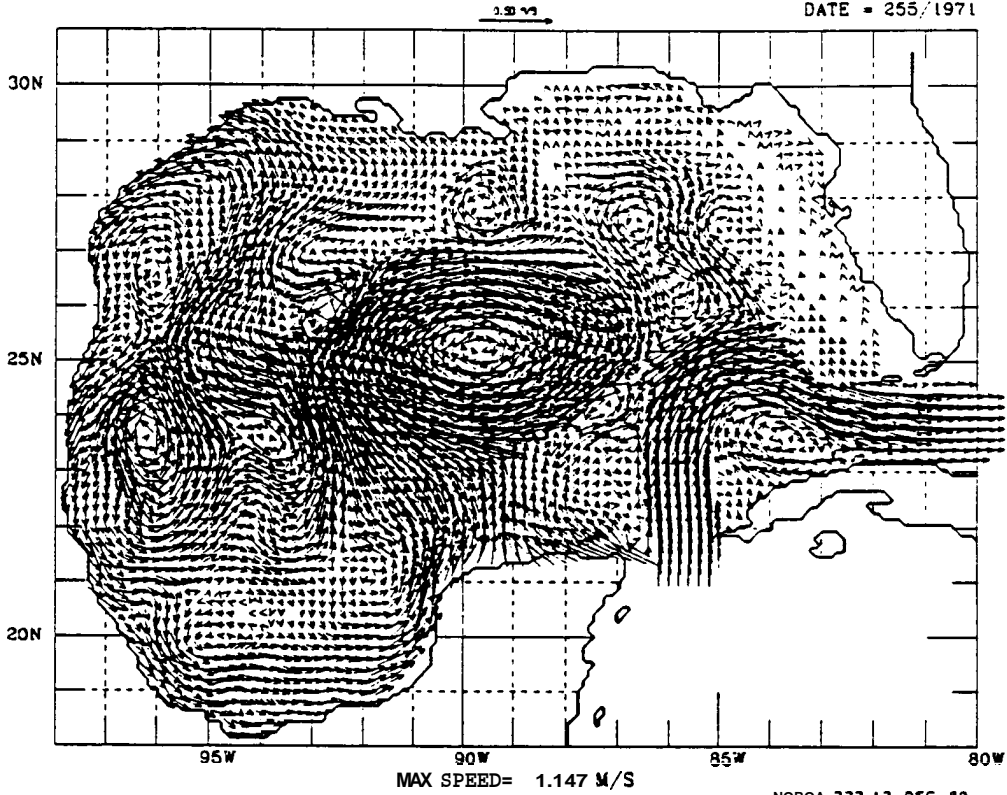


FIGURE 115

SURFACE CURRENTS

G. OF MEXICO 21142-2: 0.0
DATE = 255/1971



SURFACE CURRENTS

NORCA 323 12-DEC-89
G. OF MEXICO 21142-2: 0.0
DATE = 258/1971

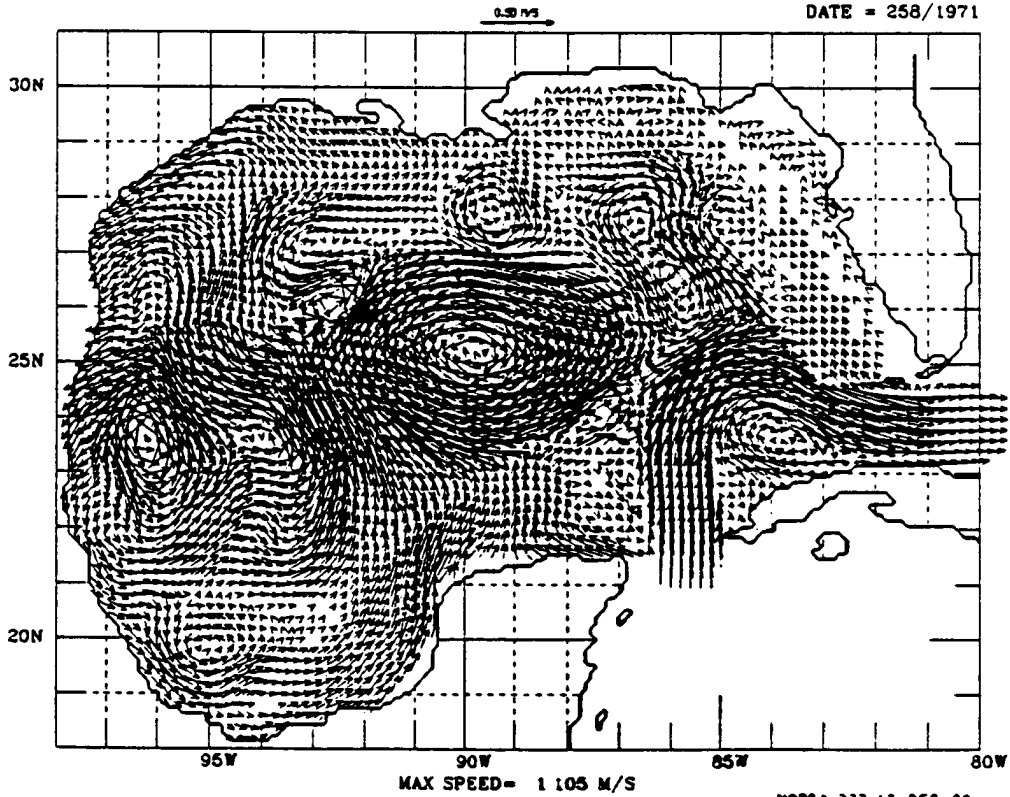
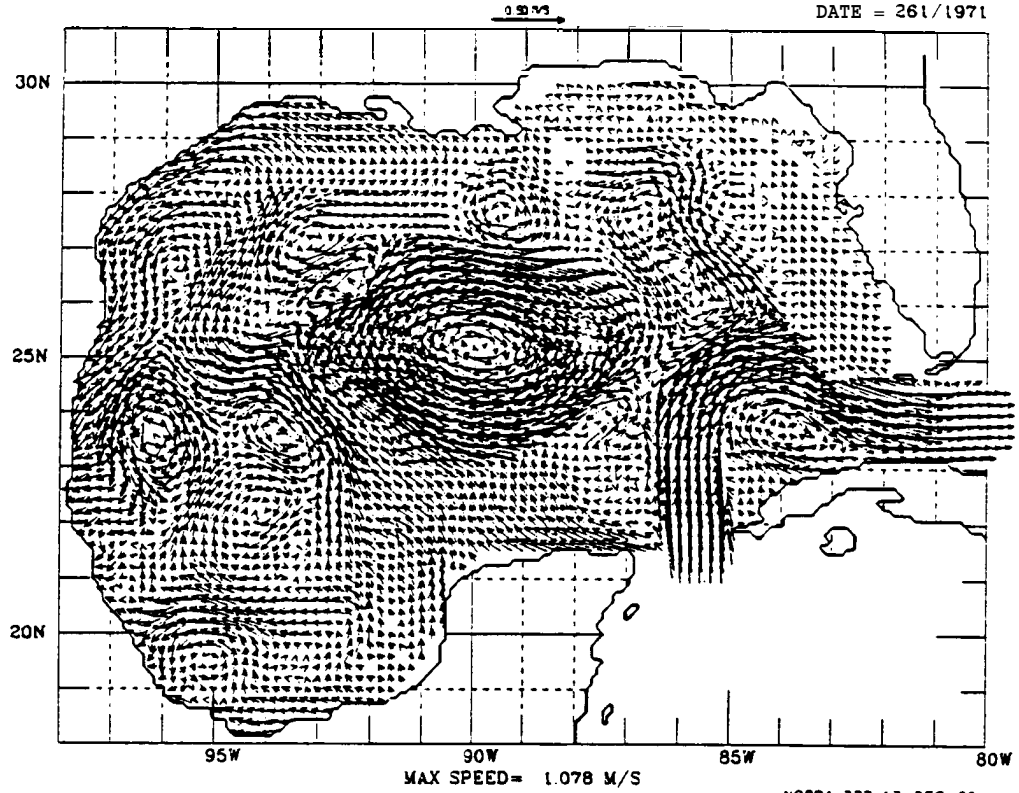


FIGURE 116

SURFACE CURRENTS

G. OF MEXICO 21142.2: 0.0
DATE = 261/1971



SURFACE CURRENTS

NORDA 323 12-DEC-89
G. OF MEXICO 21142.2: 0.0
DATE = 284/1971

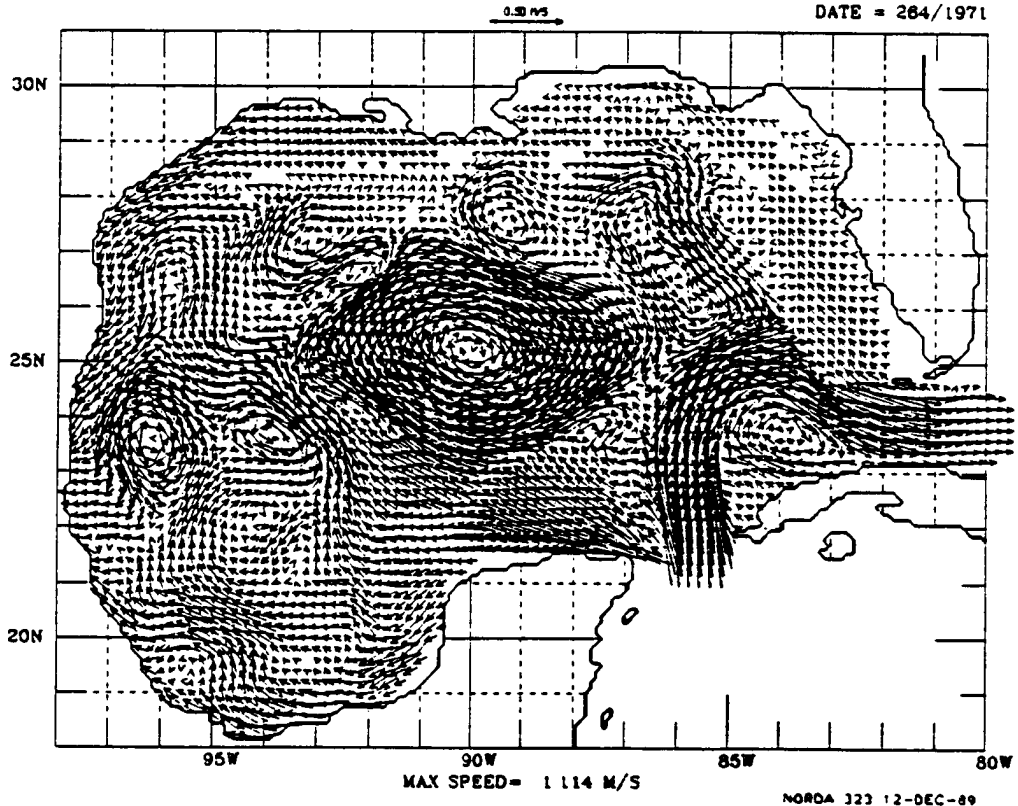


FIGURE 117

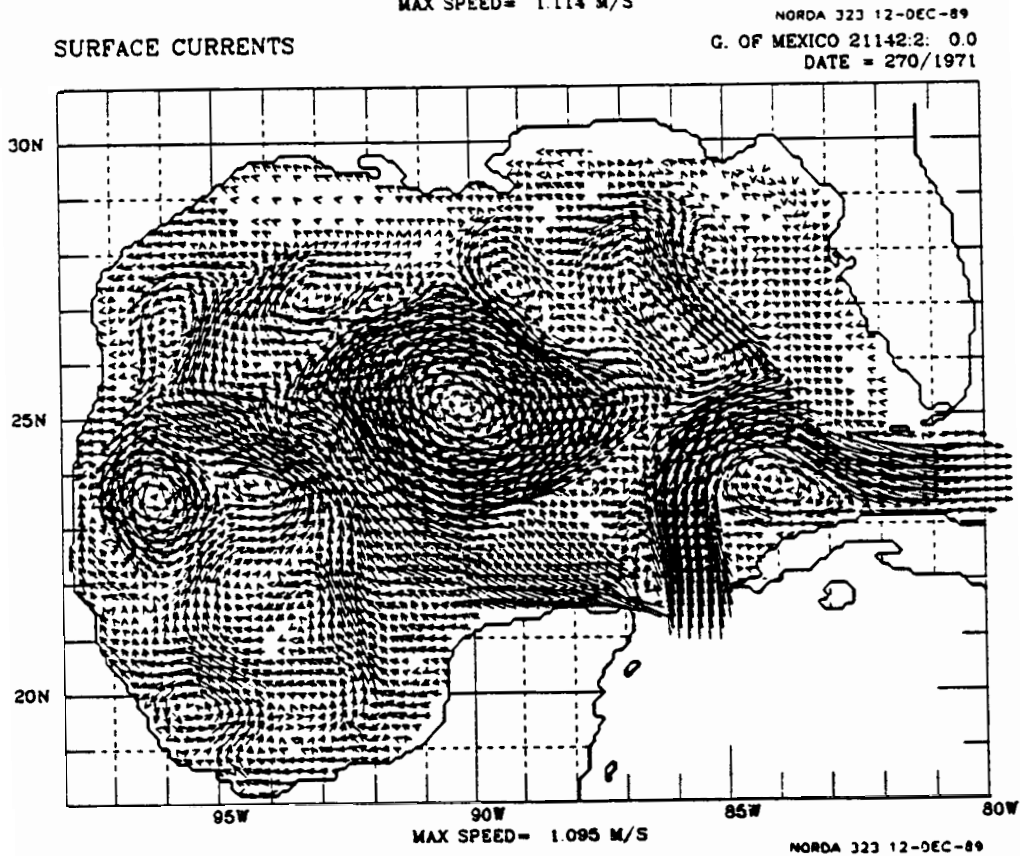
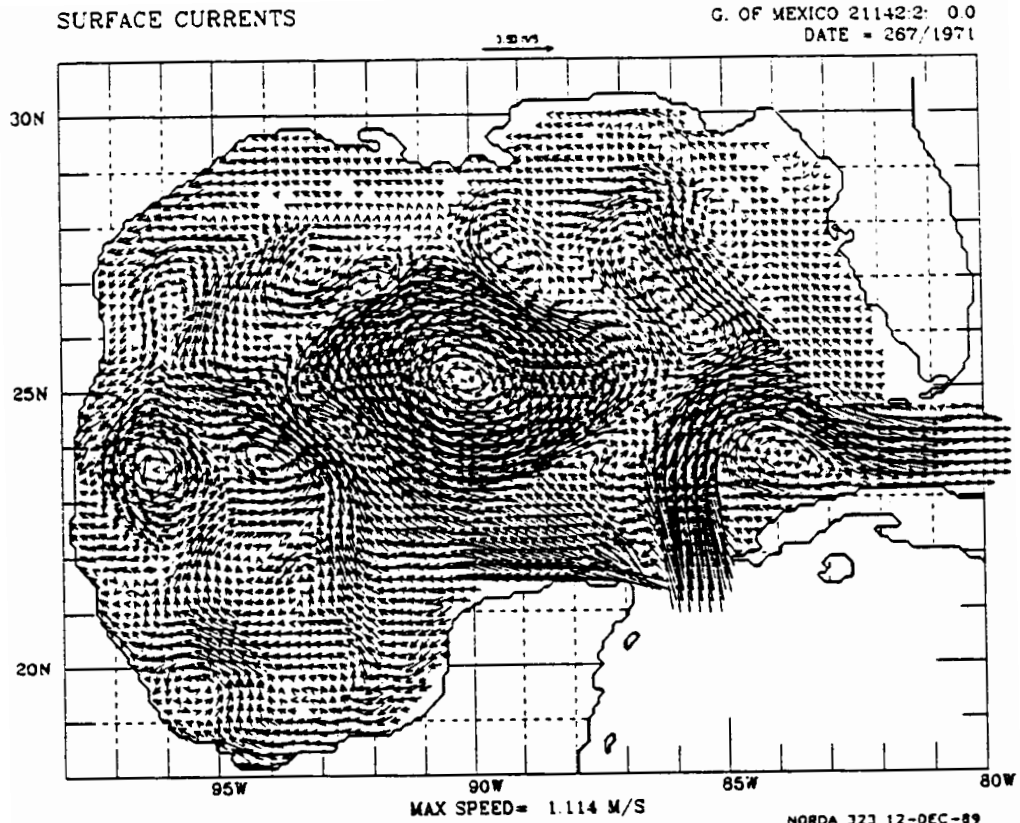
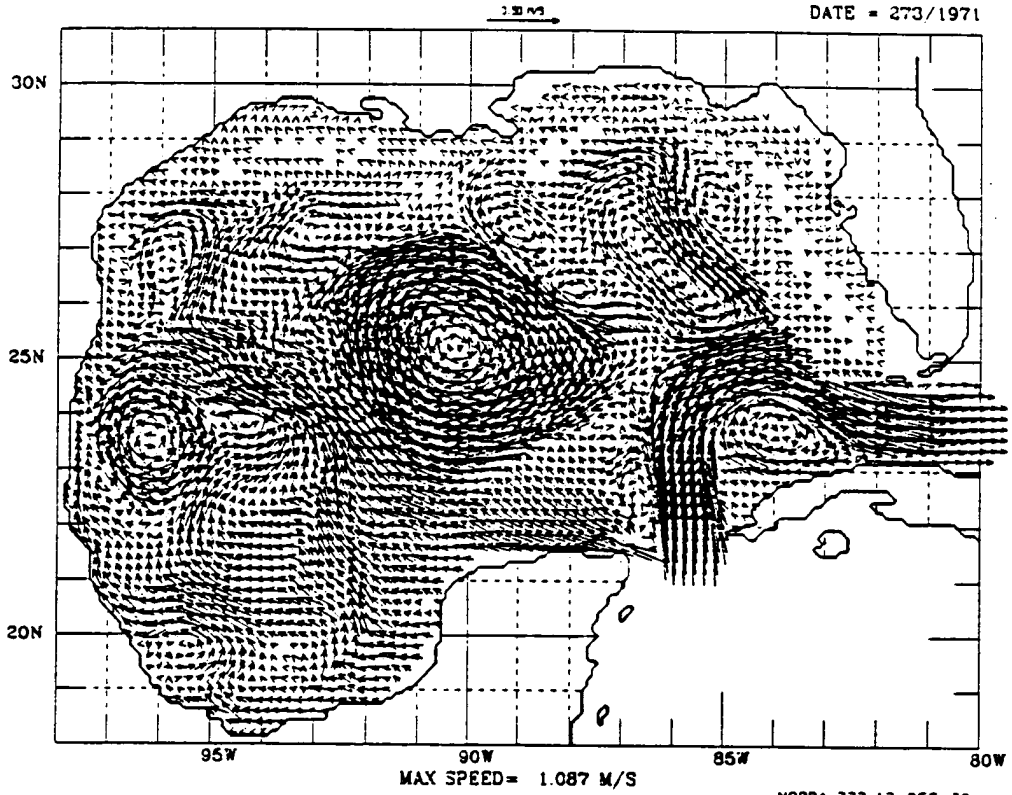


FIGURE 118

SURFACE CURRENTS

G. OF MEXICO 21142:2: 00
DATE = 273/1971



SURFACE CURRENTS

NORDA 323 12-DEC-89
G. OF MEXICO 21142:2: 00
DATE = 276/1971

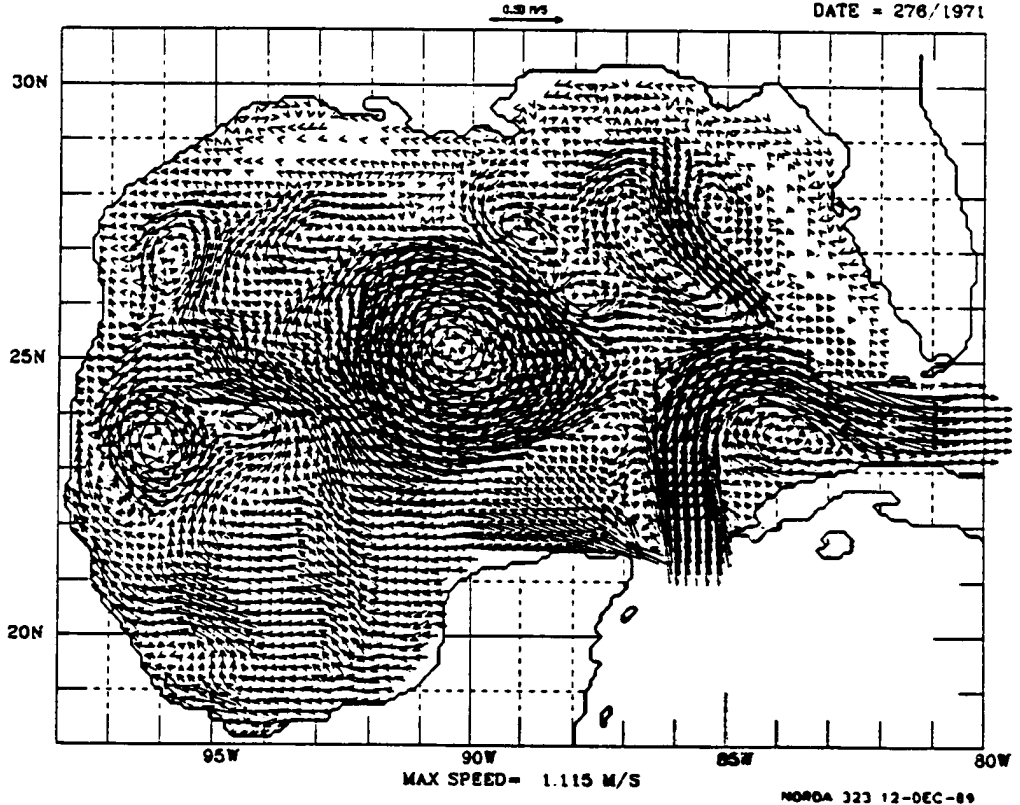
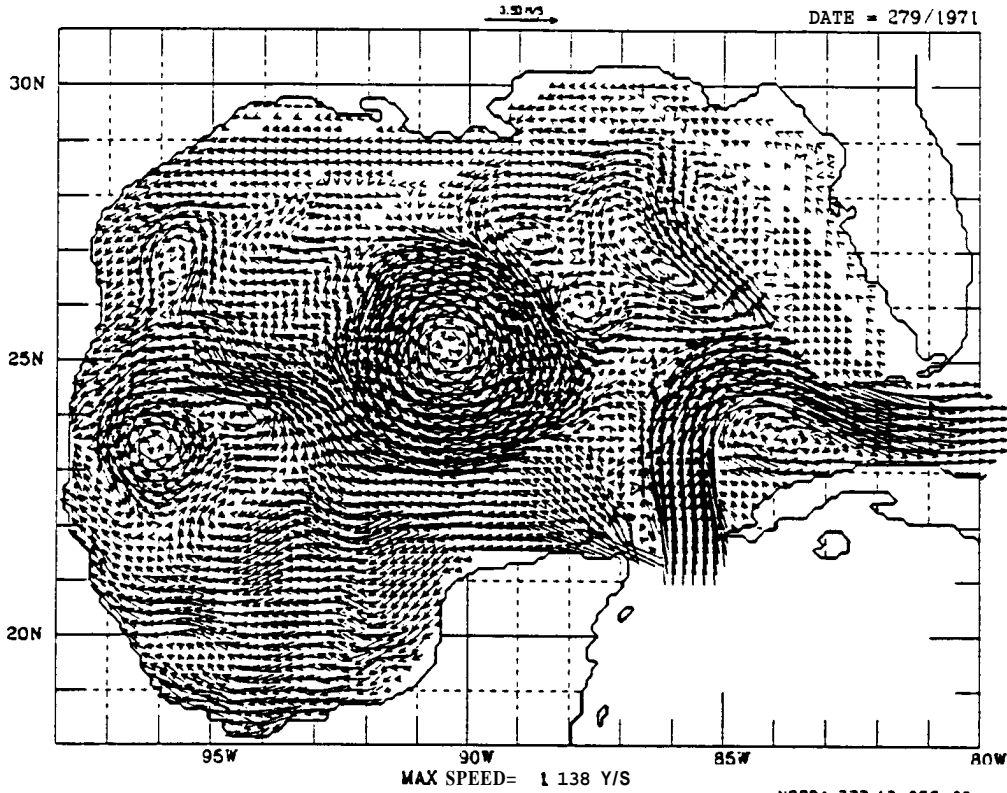


FIGURE 119

SURFACE CURRENTS

G. OF MEXICO 21142:2: 00

DATE = 279/1971



SURFACE CURRENTS

NORDA 323 12-OEC-89
G. OF MEXICO 21142:2: 00
DATE = 282/1971

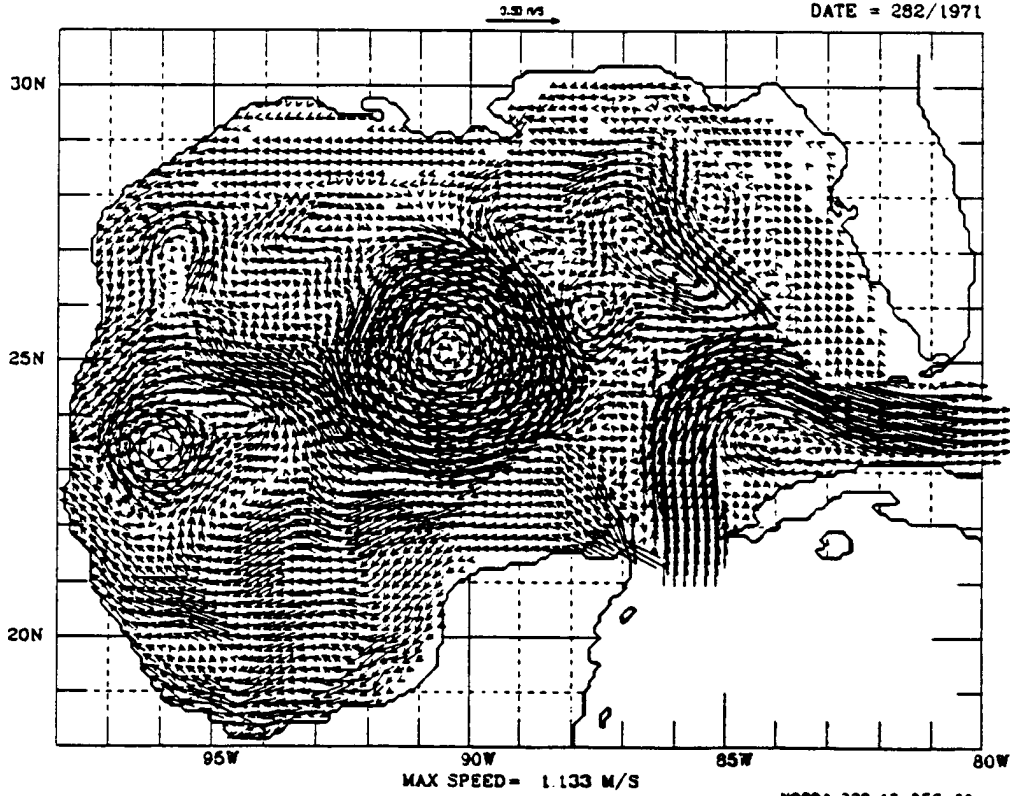
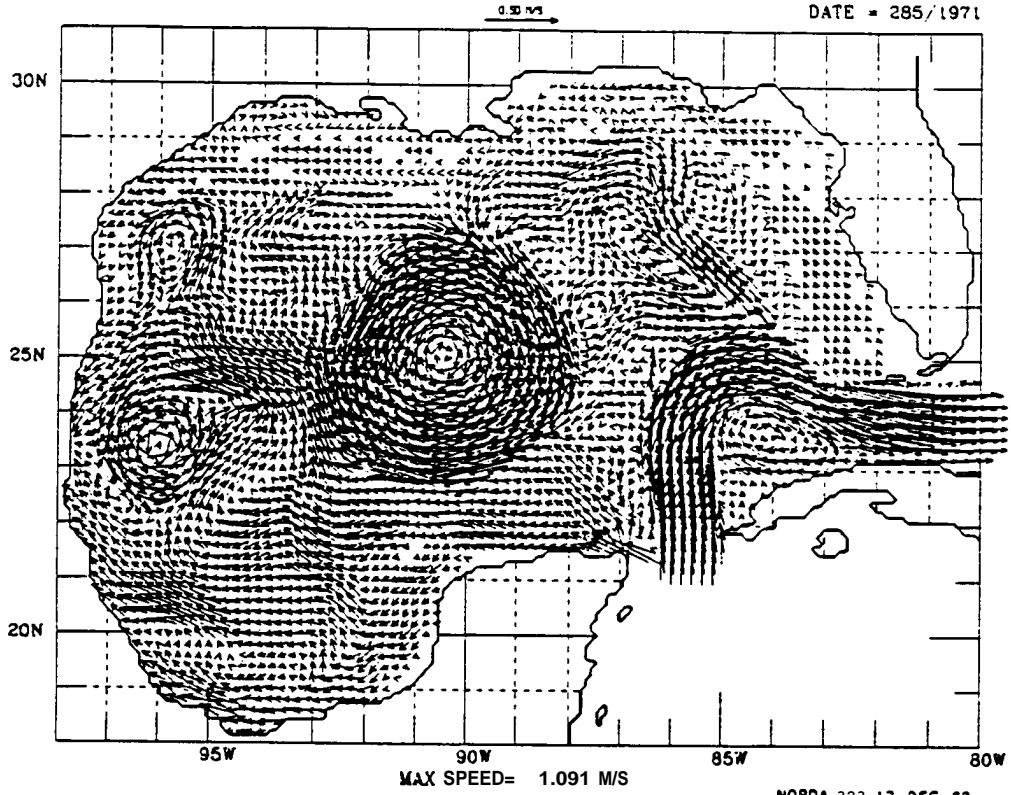


FIGURE 120

SURFACE CURRENTS

G. OF MEXICO 21142.2: 00

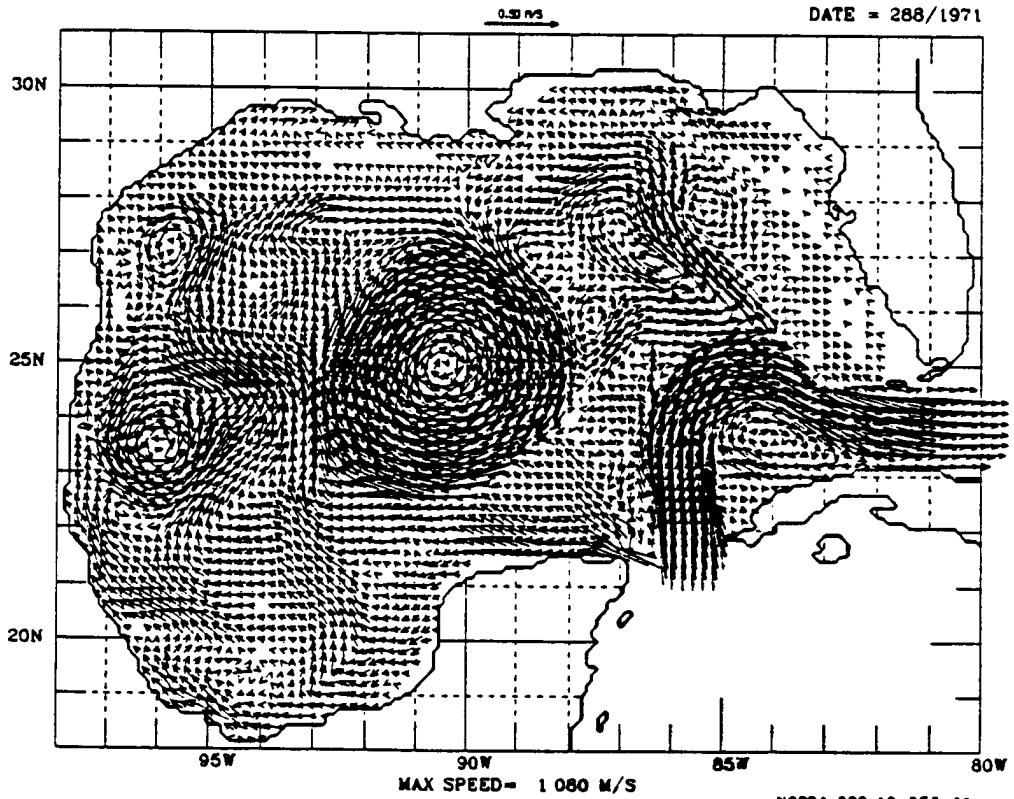
DATE = 285/1971



SURFACE CURRENTS

NORDA 323 12-DEC-89
G. OF MEXICO 21142.2: 00

DATE = 288/1971

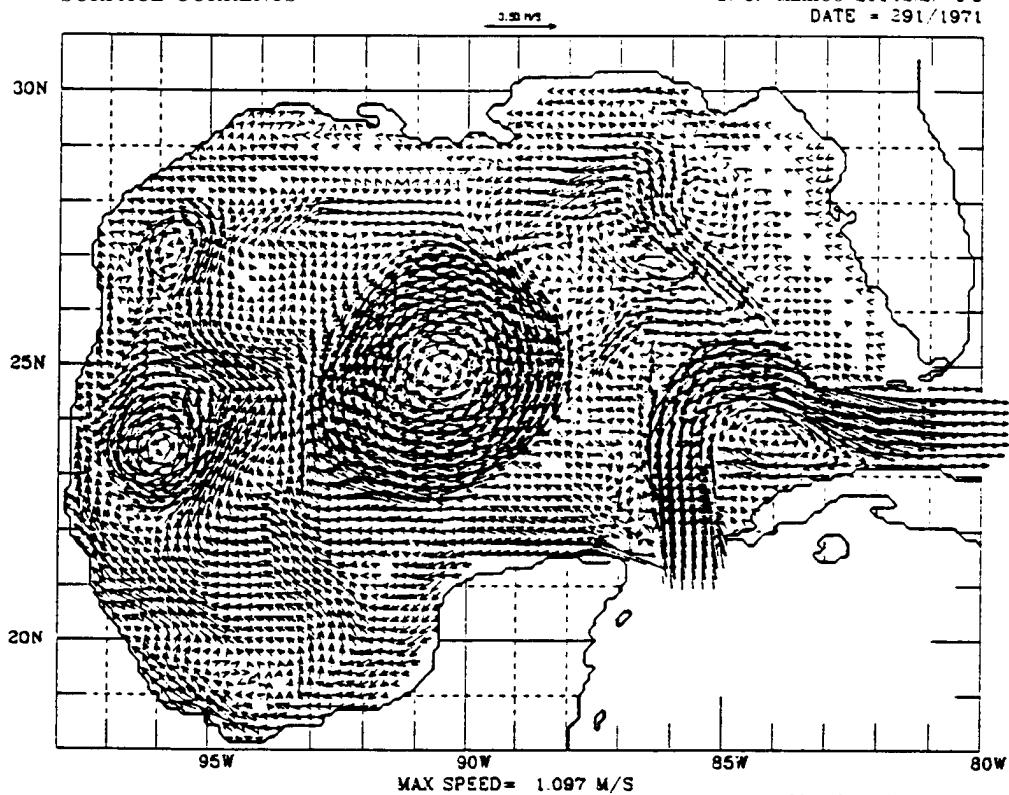


NORDA 323 12-DEC-89

FIGURE 121

SURFACE CURRENTS

G. OF MEXICO 21142:2: 0.0
DATE = 291/1971



SURFACE CURRENTS

NORDA 323 12-DEC-89
G. OF MEXICO 21142:2: 0.0
DATE = 294/1971

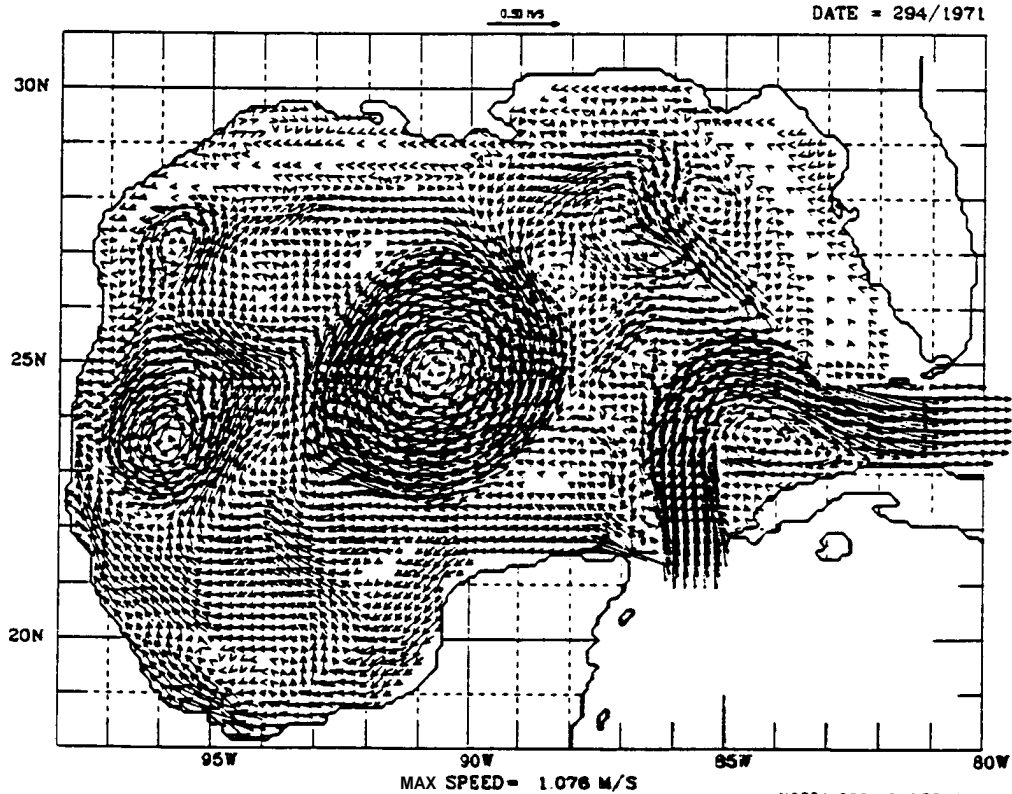
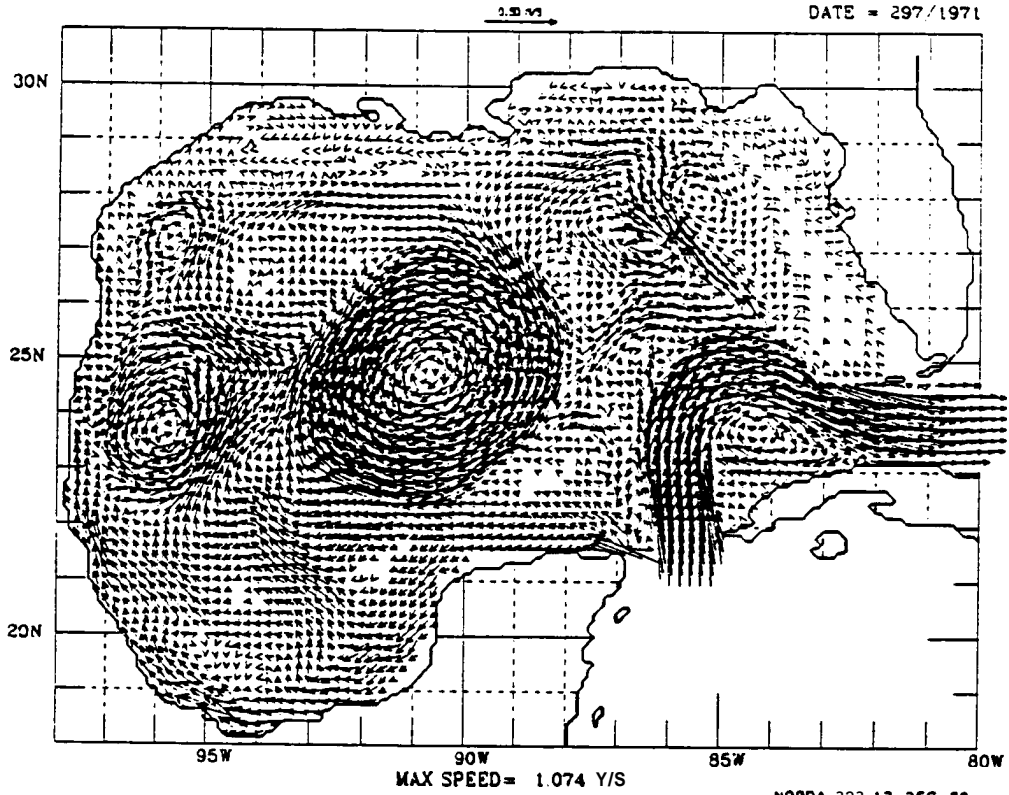


FIGURE 122

SURFACE CURRENTS

G. OF MEXICO 21142:2: 0.0
DATE = 297/1971



SURFACE CURRENTS

NORDA 323 12-DEC-89
G. OF MEXICO 21142:2: 0.0
DATE = 300/1971

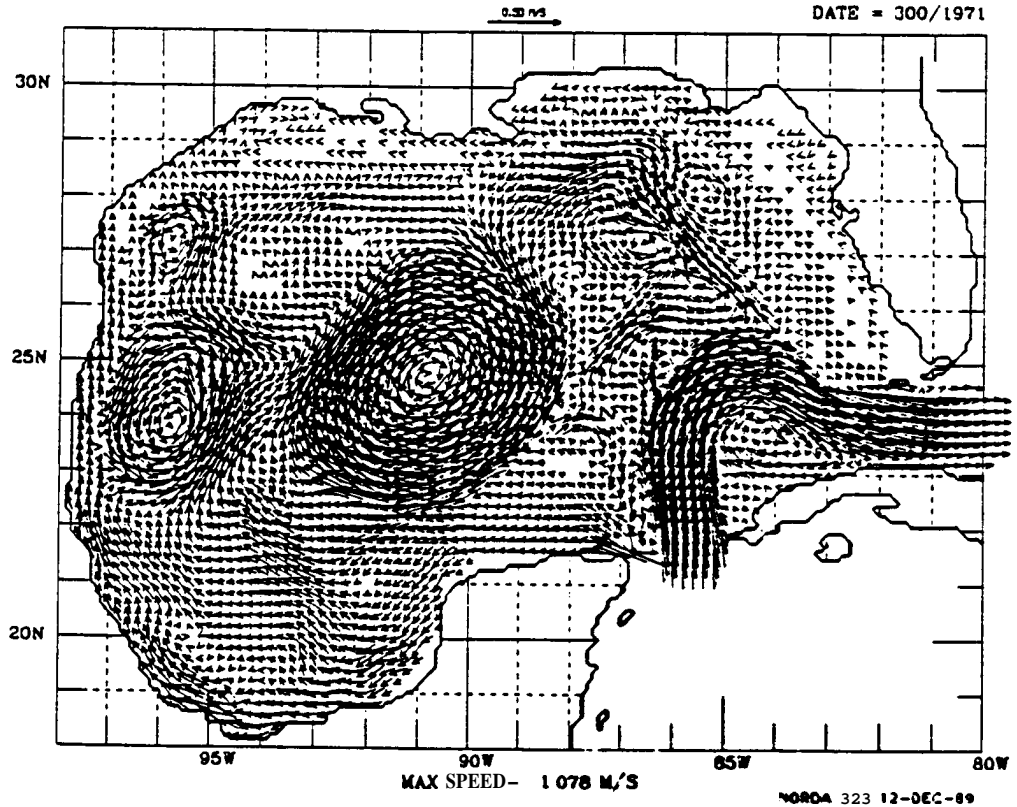
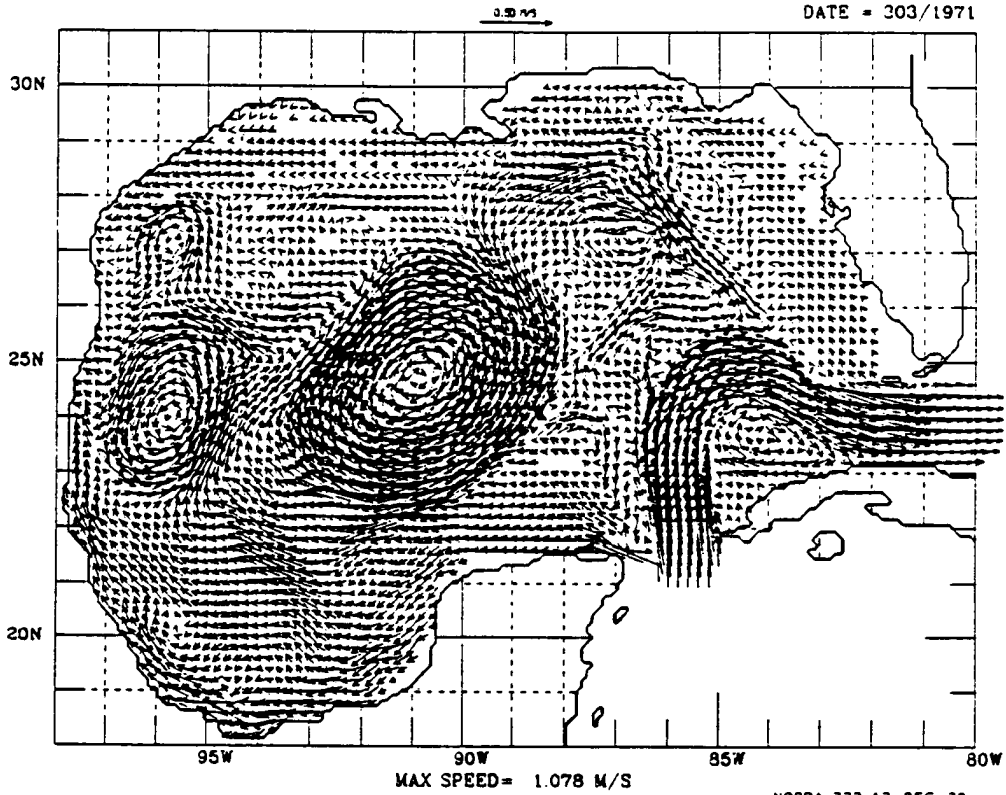


FIGURE 123

SURFACE CURRENTS

G. OF MEXICO 21142:2: 0.0
DATE = 303/1971



SURFACE CURRENTS

NORDA 323 12-DEC-89
G. OF MEXICO 21142:2: 0.0
DATE = 306/1971

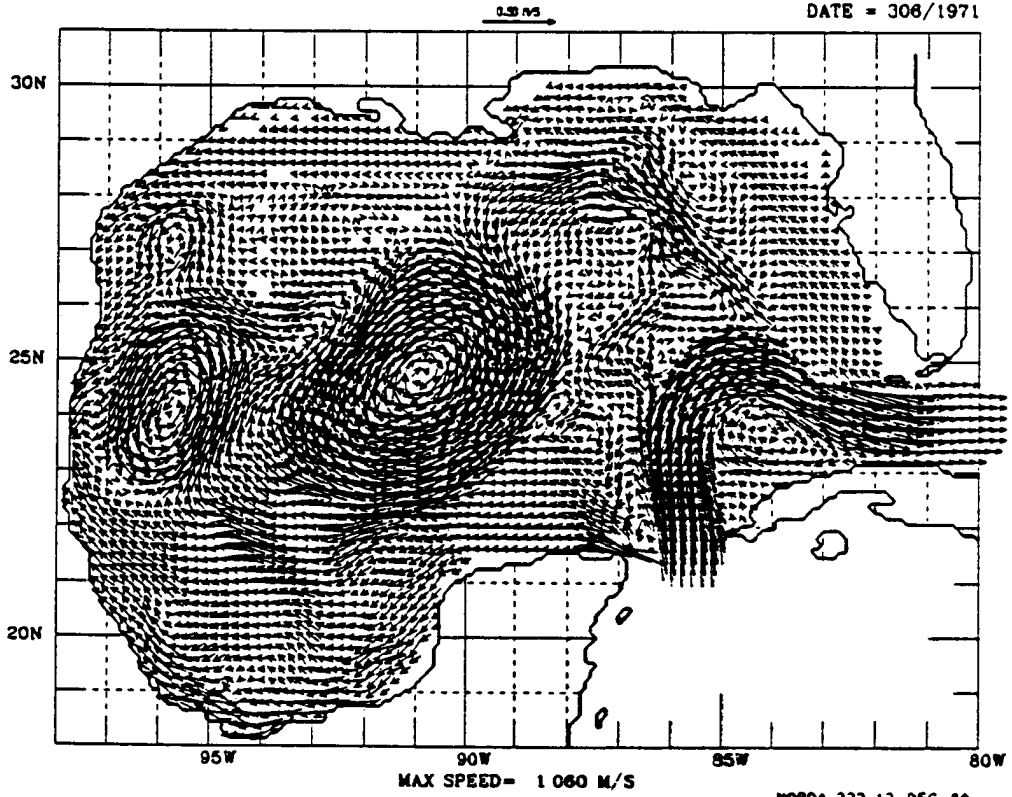
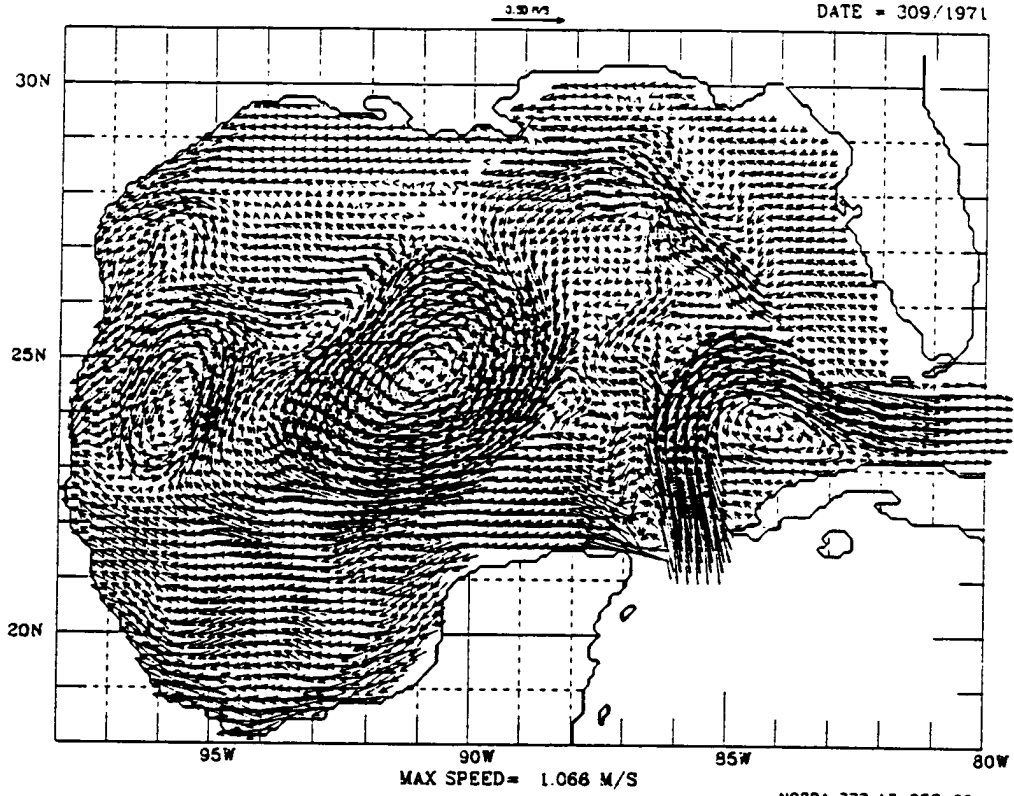


FIGURE 124

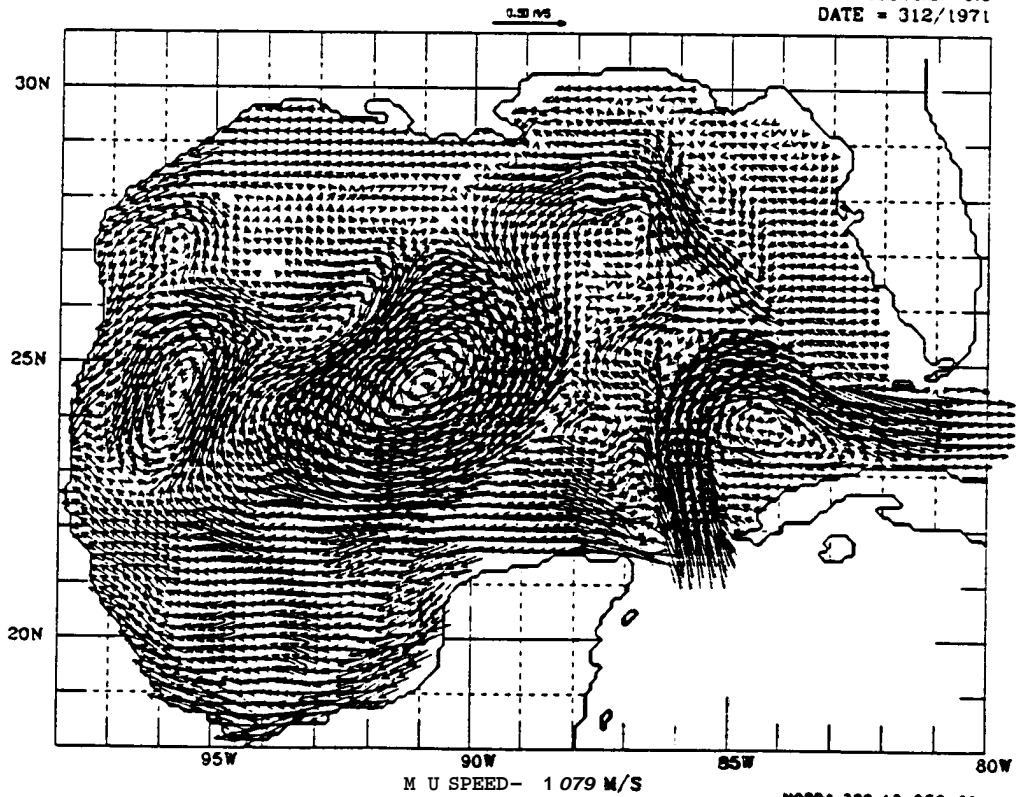
SURFACE CURRENTS

G. OF MEXICO 21142:2: 0.0
DATE = 309/1971



SURFACE CURRENTS

NORDA 323 12-DEC-89
G. OF MEXICO 21142:2: 0.0
DATE = 312/1971

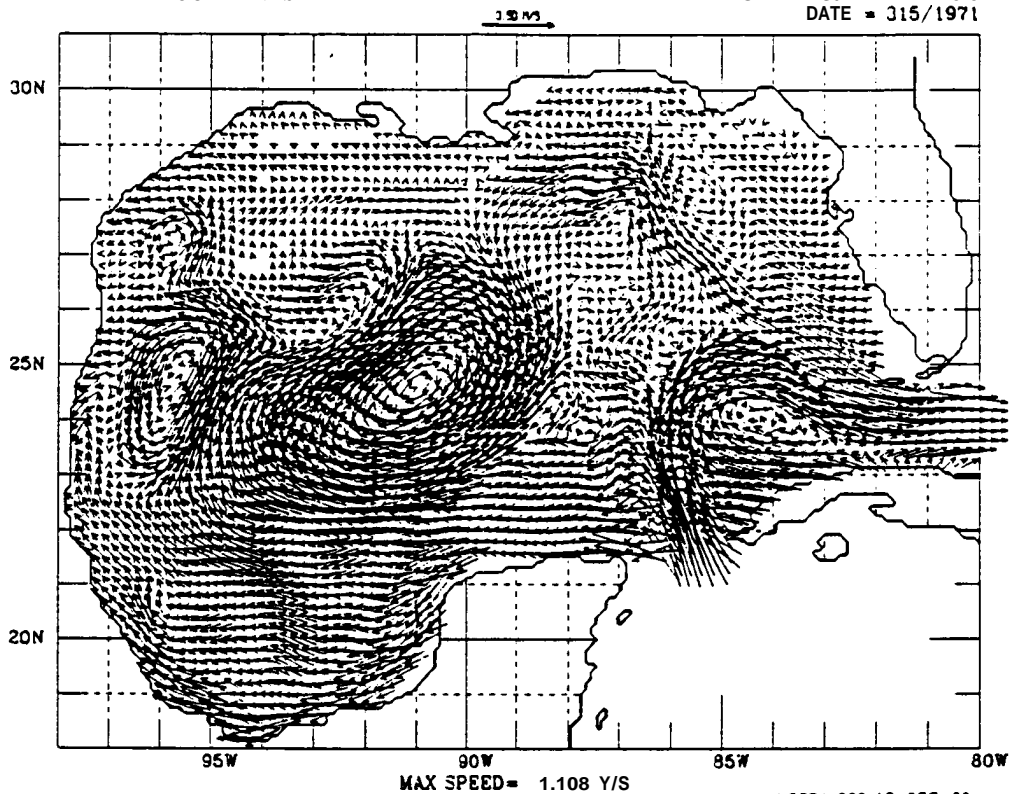


NORDA 323 12-DEC-89

FIGURE 125

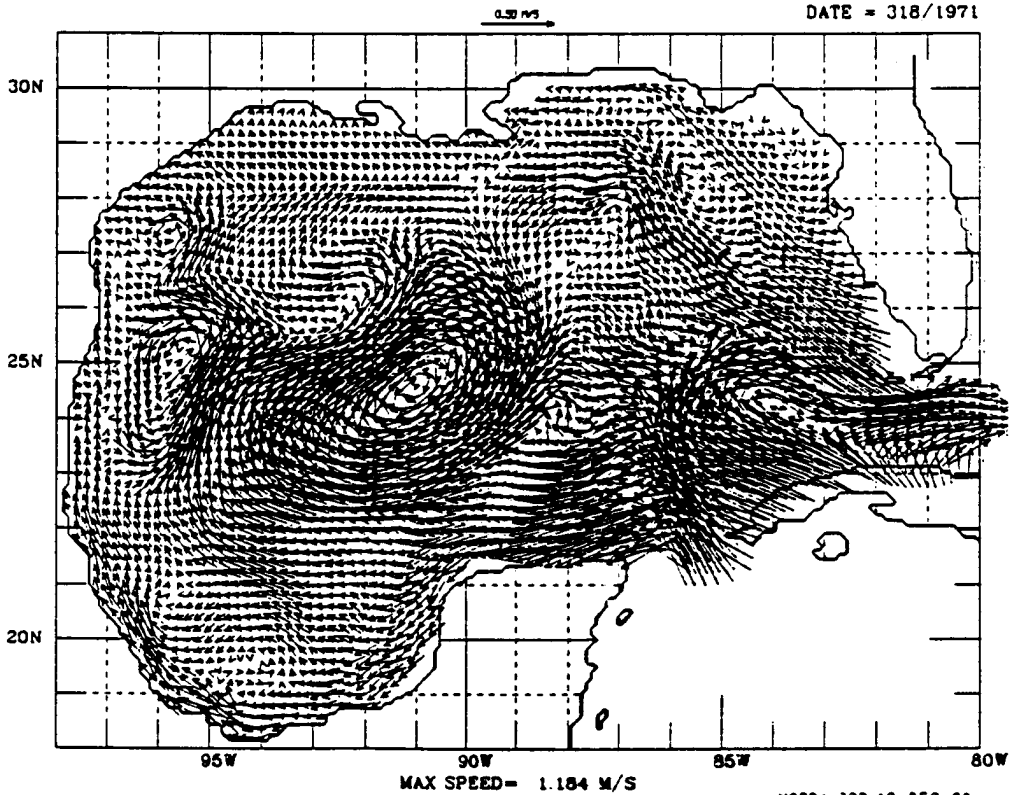
SURFACE CURRENTS

G. OF MEXICO 21142:2: 0.0
DATE = 315/1971



SURFACE CURRENTS

NORDA 323 12-DEC-69
G. OF MEXICO 21142:2: 0.0
DATE = 318/1971



NORDA 323 12-DEC-69

FIGURE 126

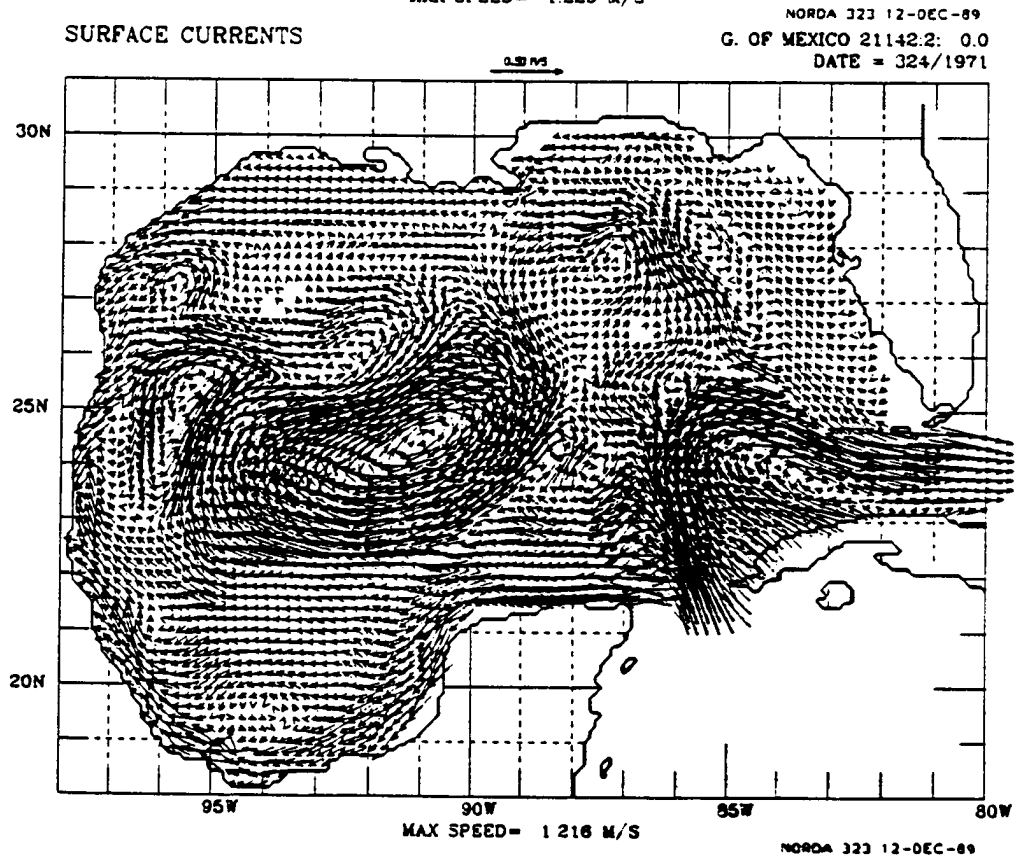
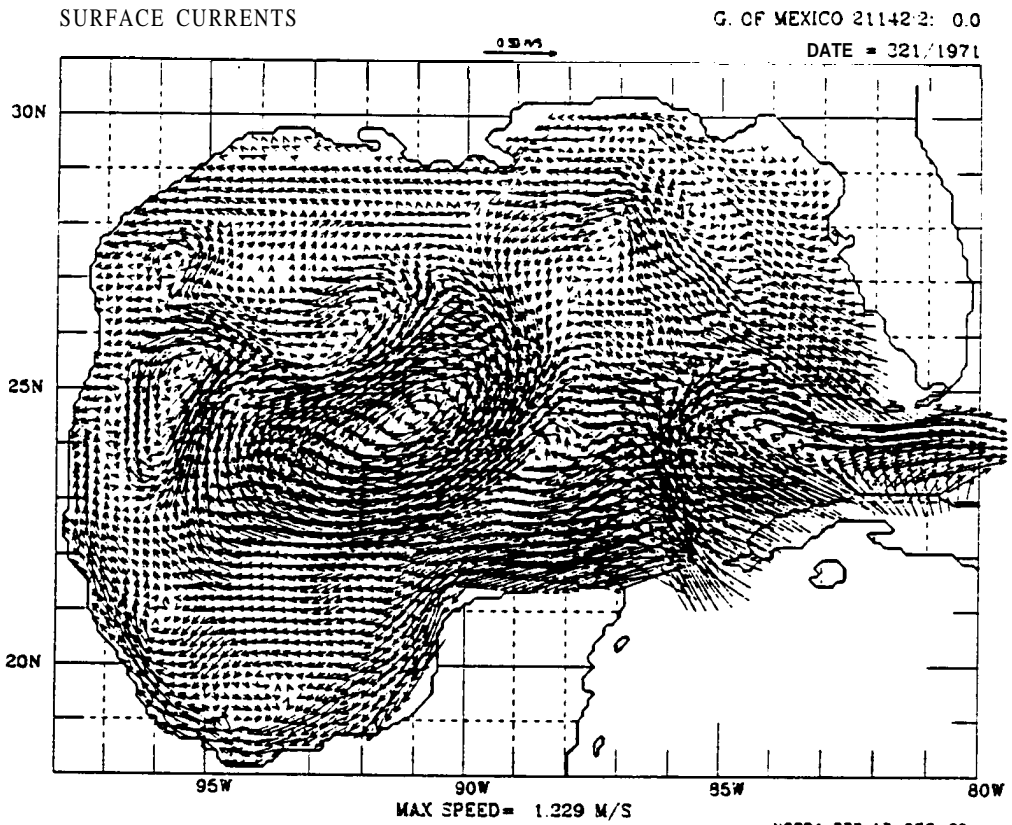
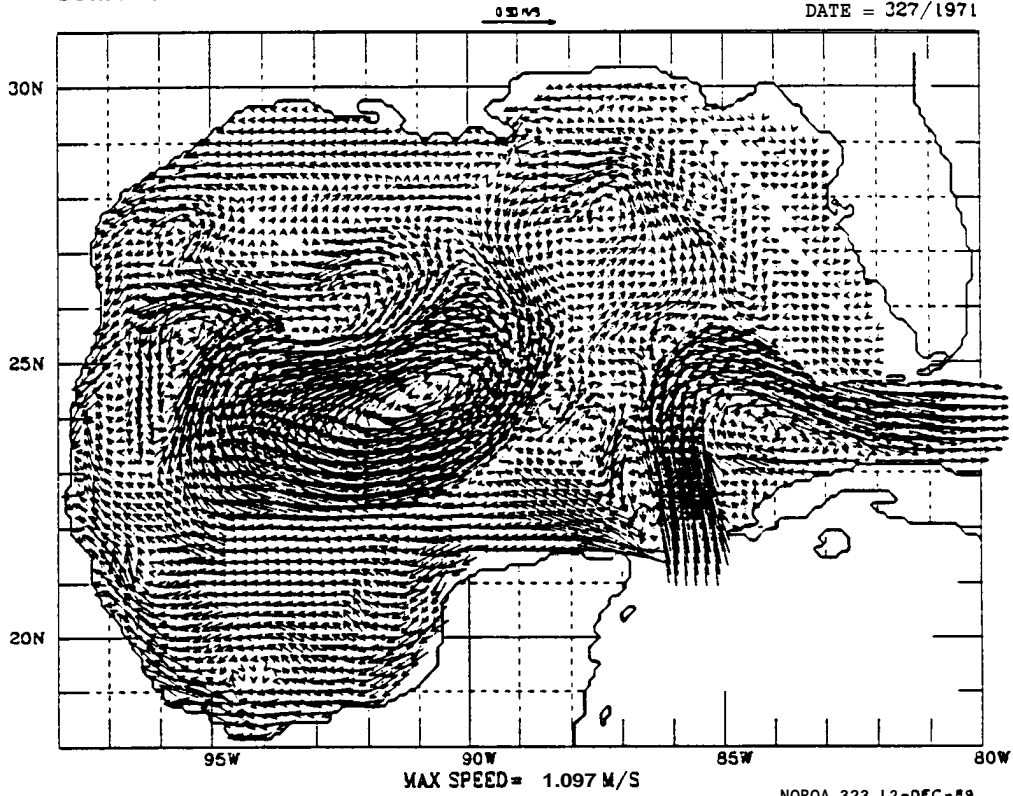


FIGURE 127

SURFACE CURRENTS

G. OF MEXICO 21142.2: 0.0
DATE = 327/1971



SURFACE CURRENTS

G. OF MEXICO 21142.2: 0.0
DATE = 330/1971

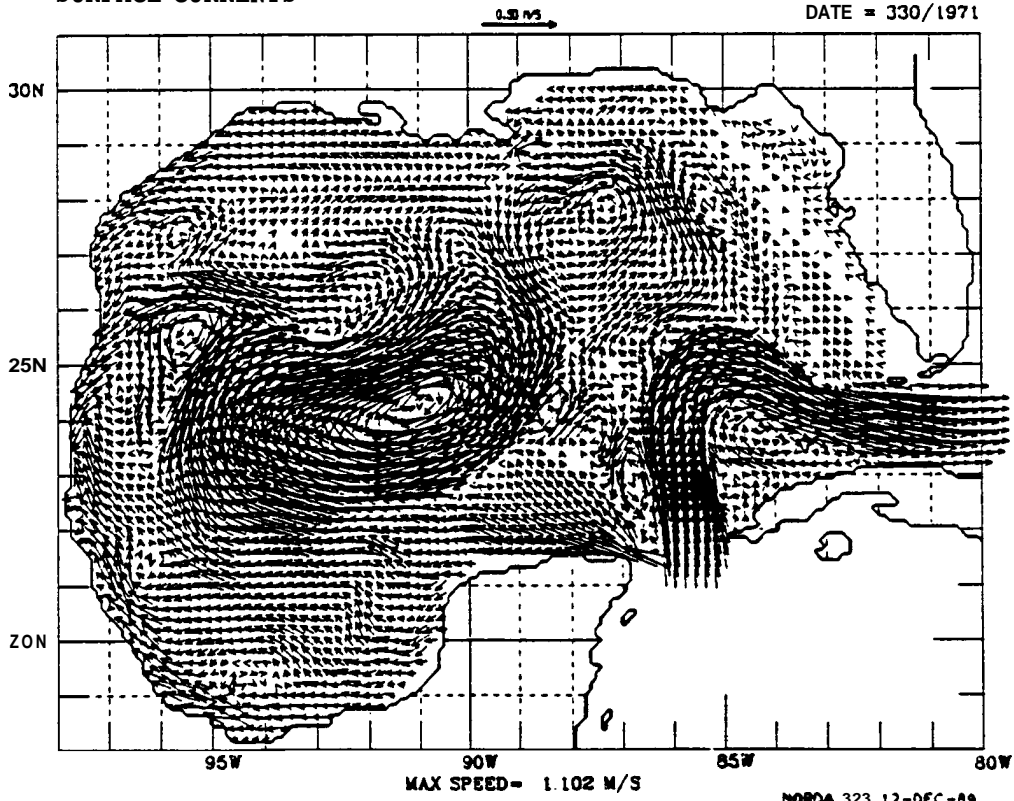
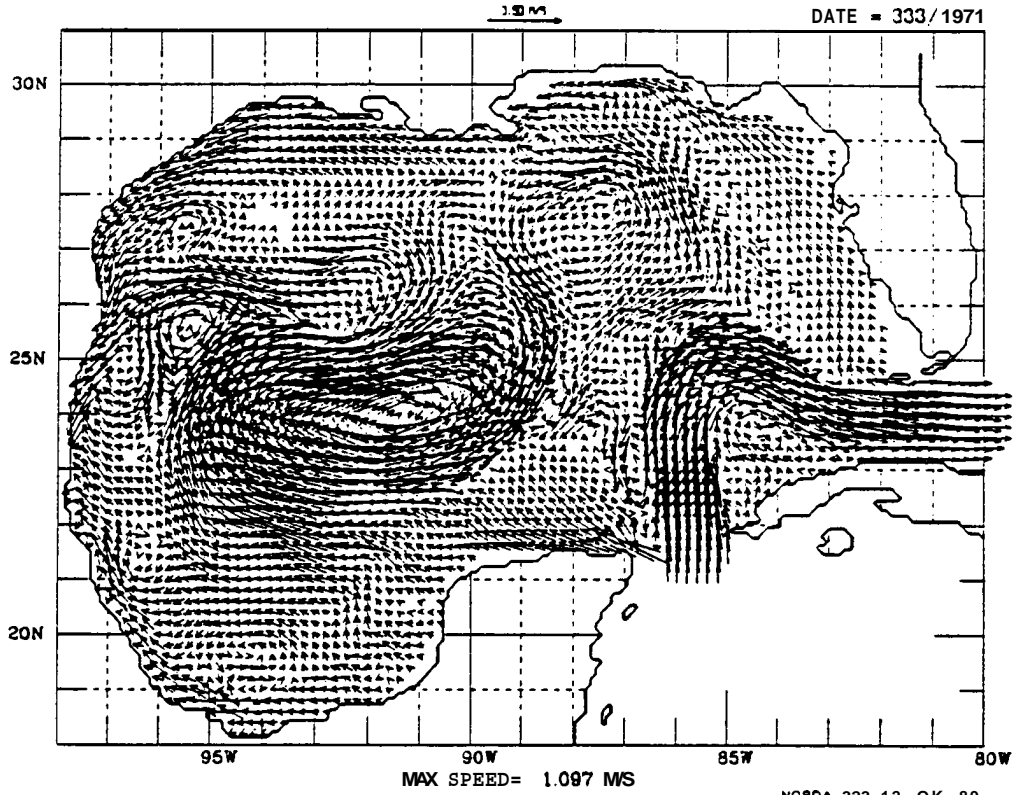


FIGURE 128

SURFACE CURRENTS

G. OF MEXICO 211-42:2: 0.0
DATE = 333/1971



SURFACE CURRENTS

NORDA 323 12-OK-89
G. OF MEXICO 211-42:2: 0.0
DATE = 338/1971

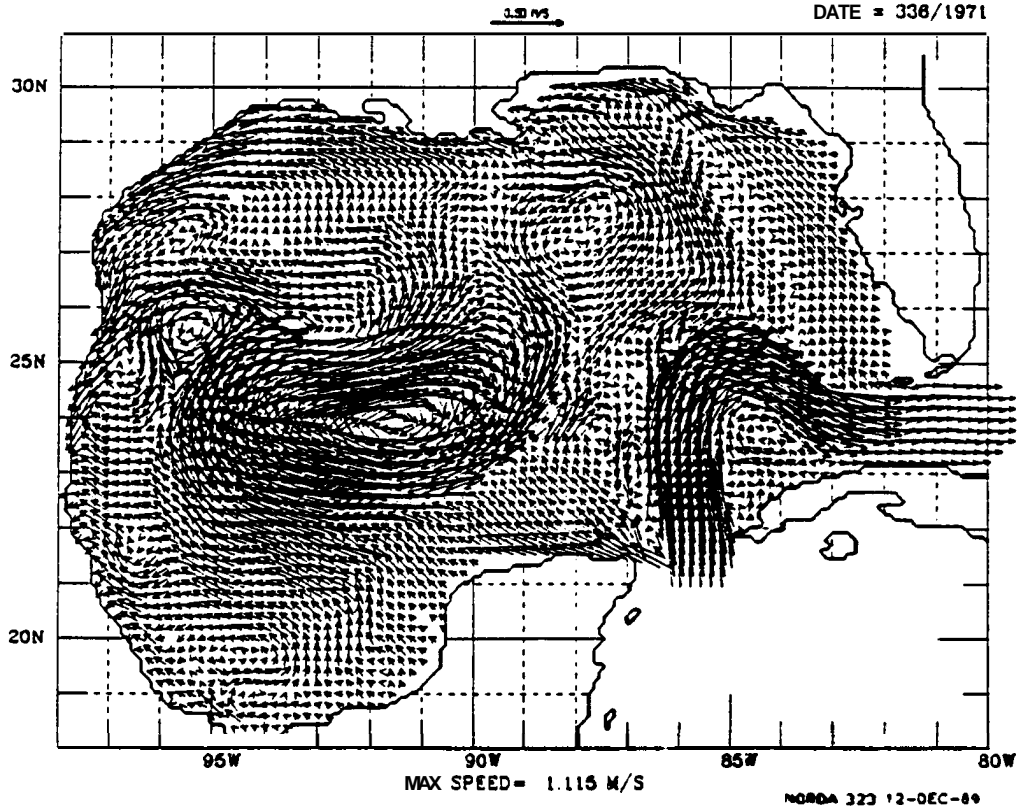
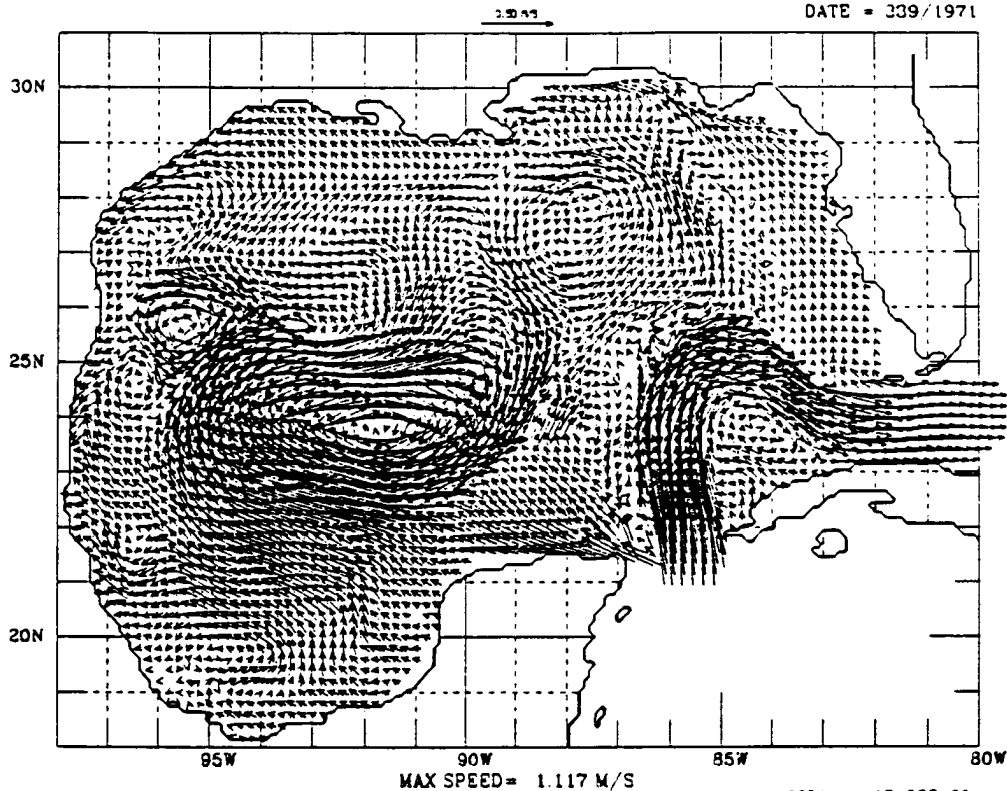


FIGURE 129

SURFACE CURRENTS

G. OF MEXICO 21142:2: 0.0
DATE = 339/1971



SURFACE CURRENTS

NORDA 323 12-DEC-89
G. OF MEXICO 21142:2: 0.0
DATE = 342/1971

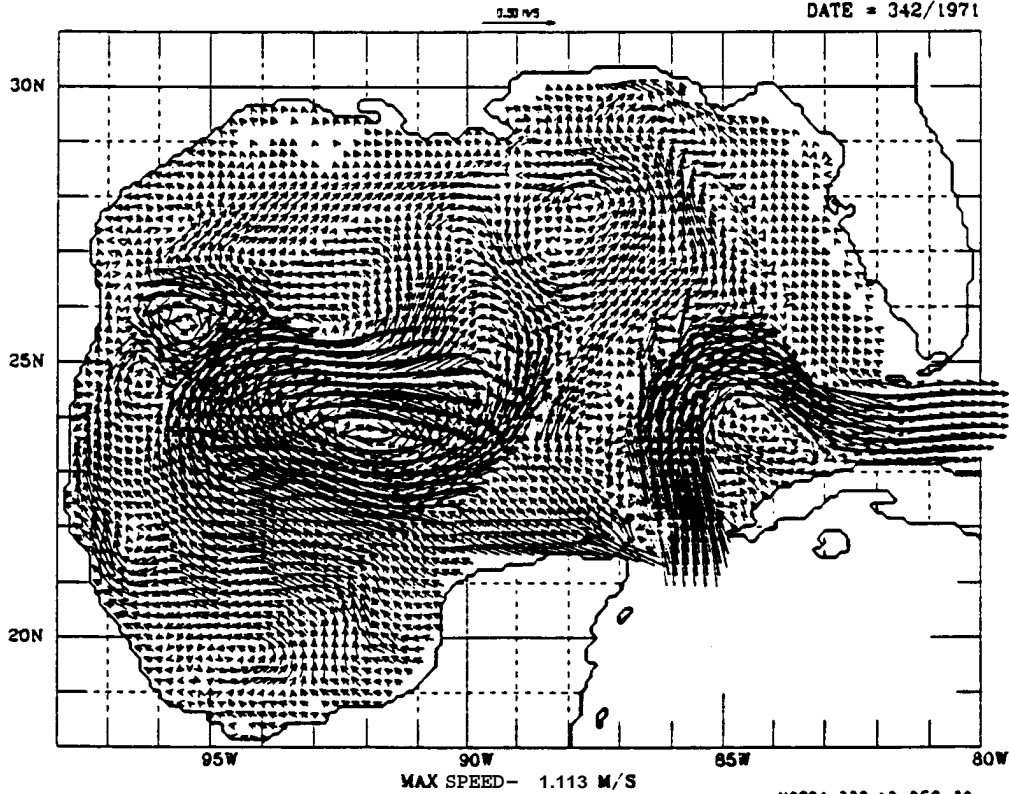
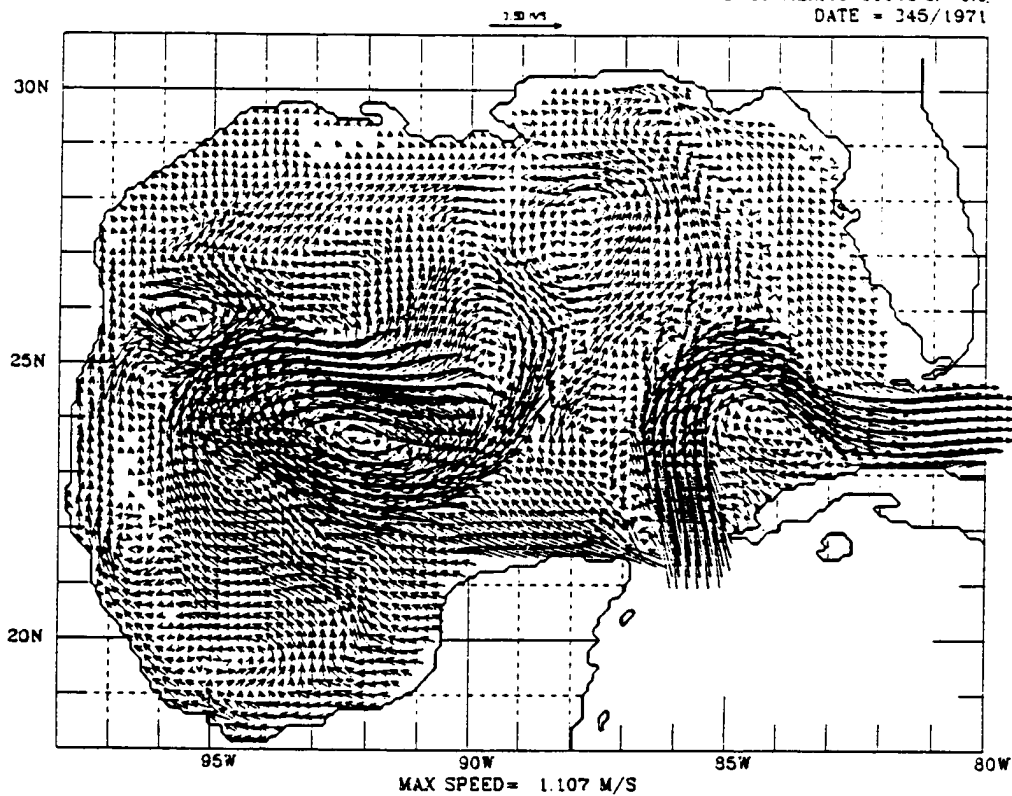


FIGURE 130

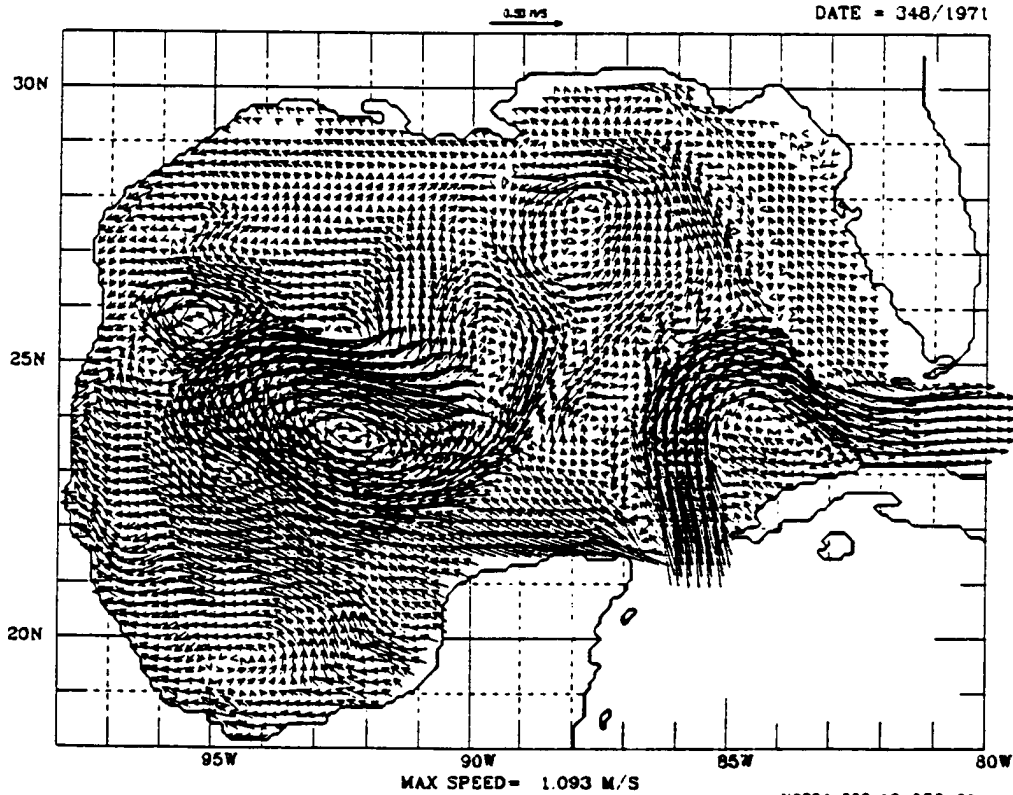
SURFACE CURRENTS

G. OF MEXICO 21142.2: 0.0
DATE = 345/1971



SURFACE CURRENTS

NORDA 323 12-DEC-89
G. OF MEXICO 21142.2: 0.0
DATE = 348/1971

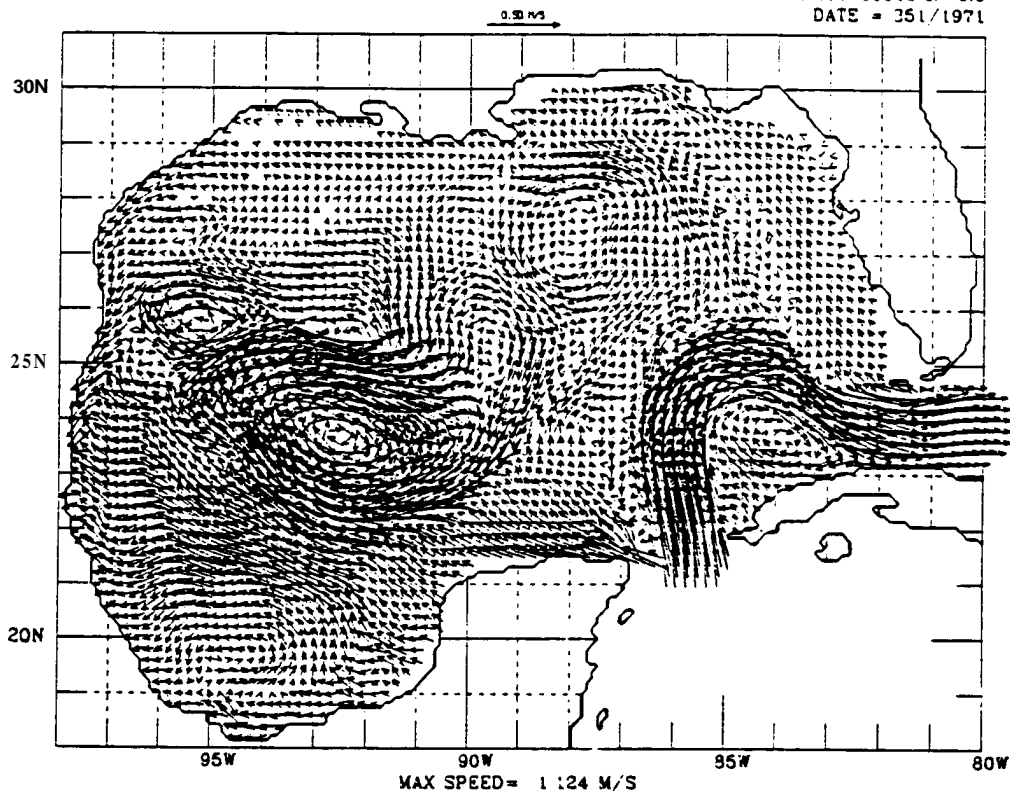


NORDA 323 12-DEC-89

FIGURE 131

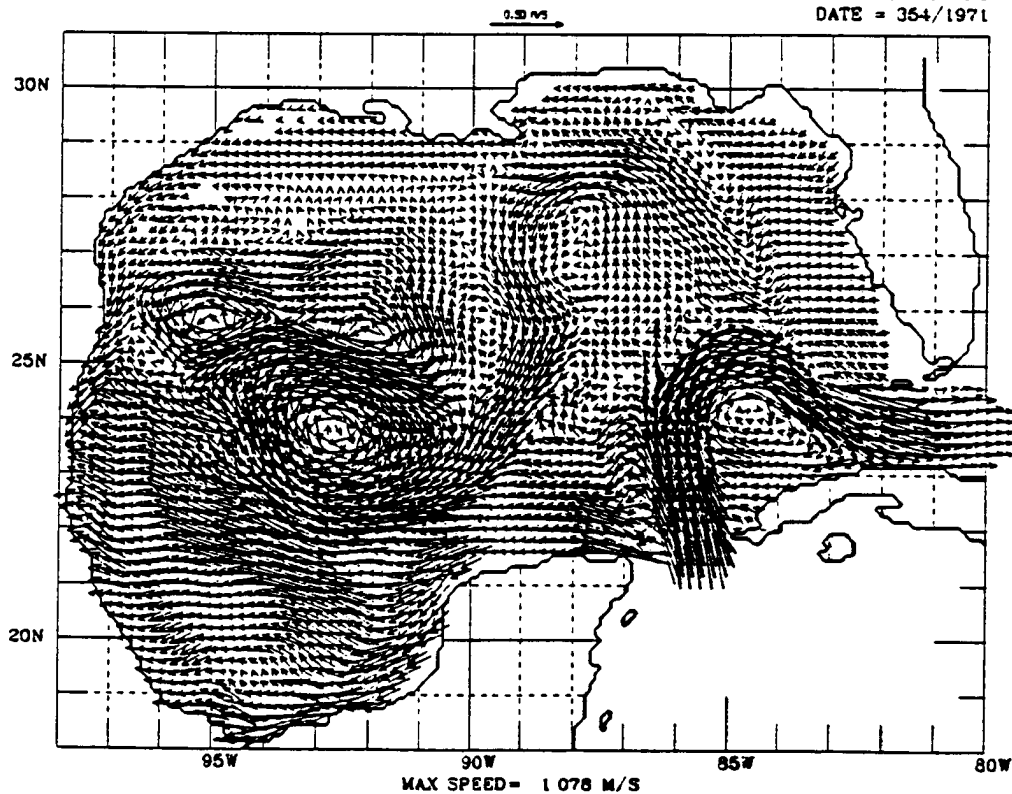
SURFACE CURRENTS

G. OF MEXICO 21142:2: 0.0
DATE = 351/1971



SURFACE CURRENTS

NORDA 323 12-DEC-89
G. OF MEXICO 21142:2: 0.0
DATE = 354/1971



NORDA 323 12-DEC-89

FIGURE 132

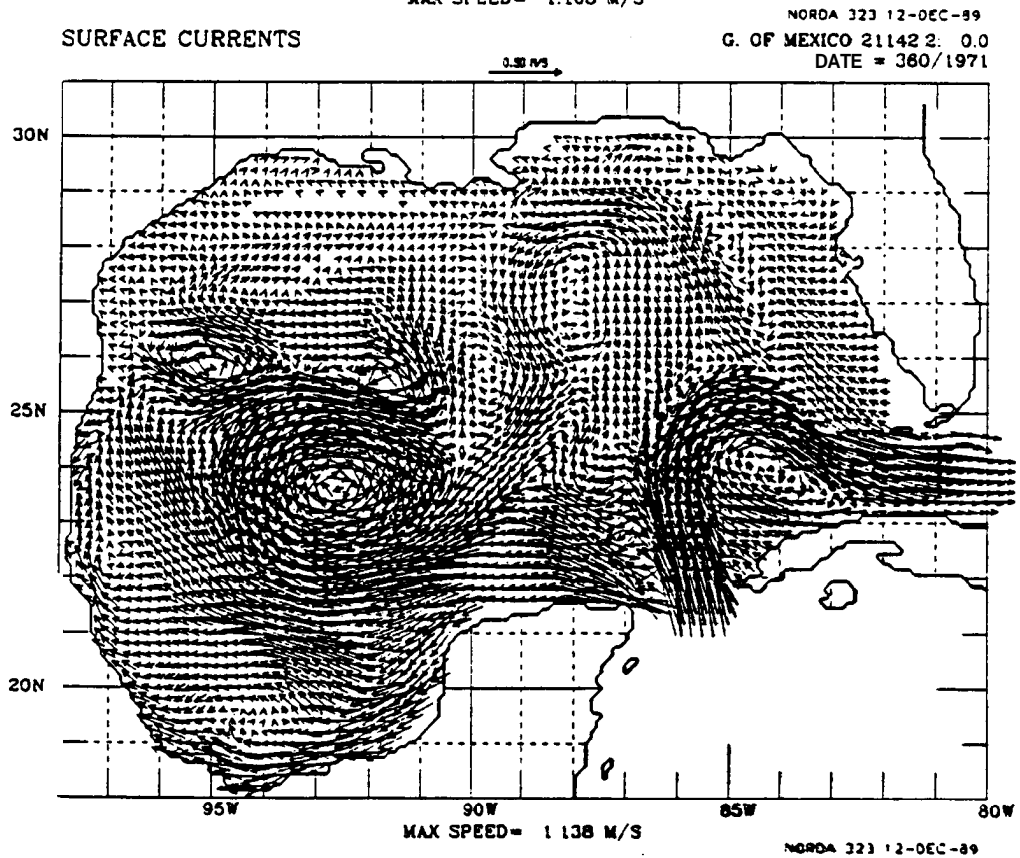
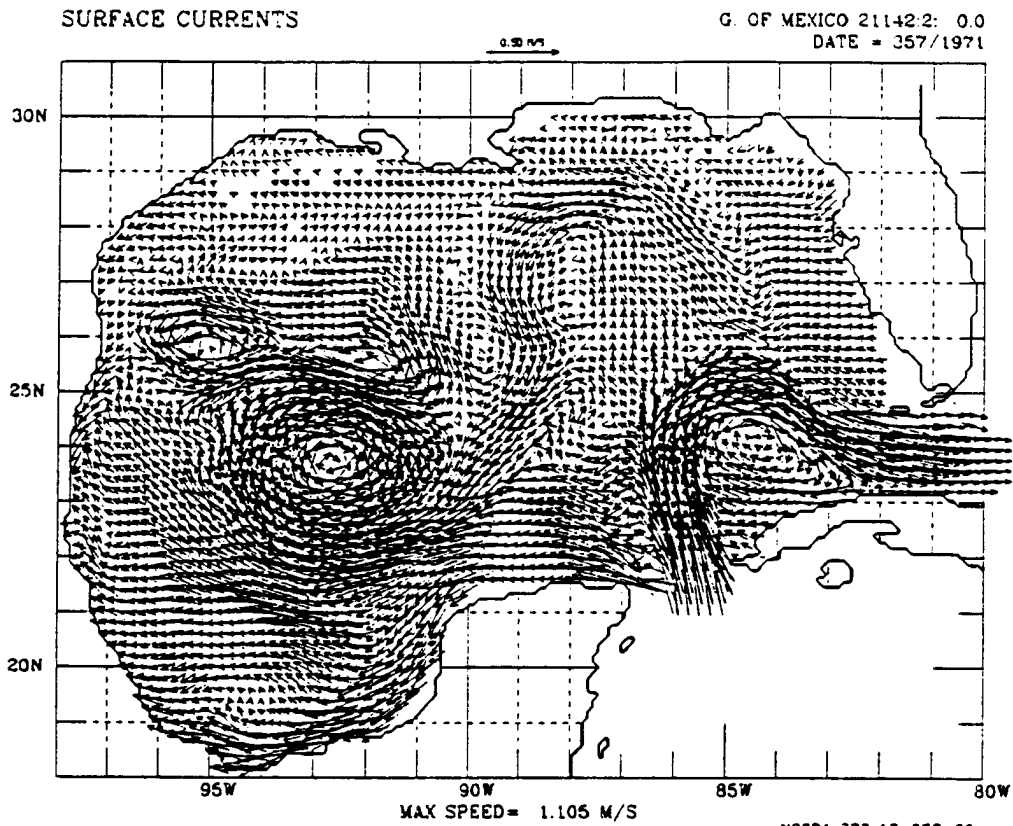
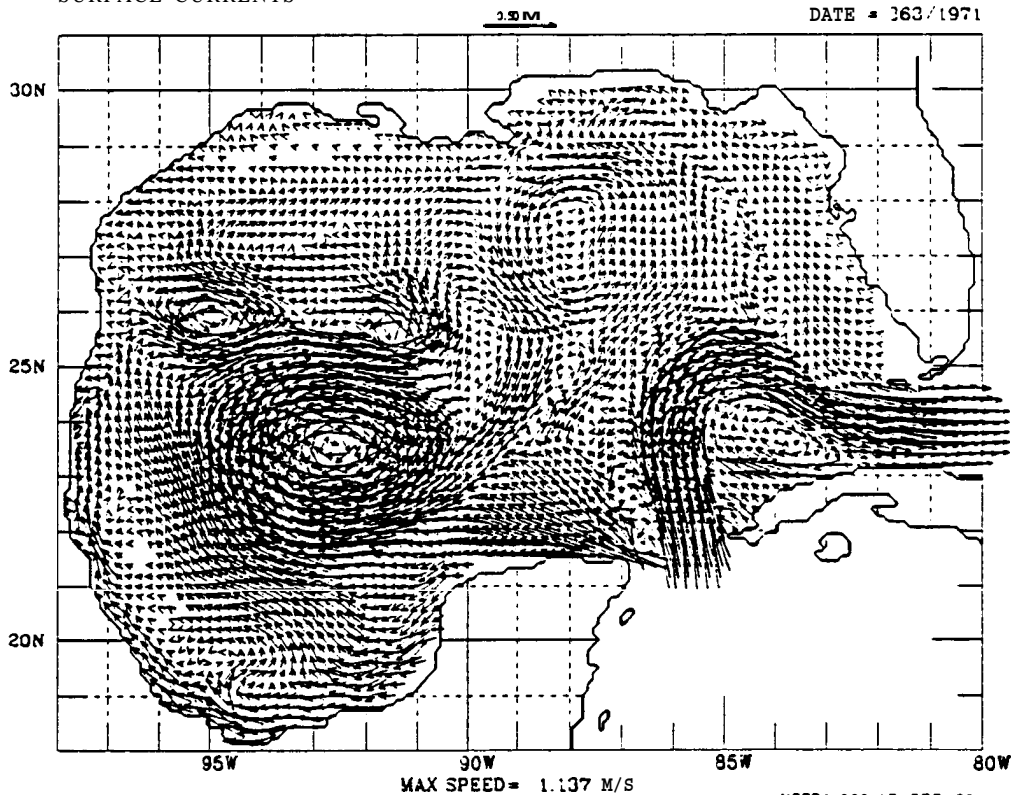


FIGURE 133

SURFACE CURRENTS

G. OF MEXICO 21142.2: 0.0
DATE = 363/1971



SURFACE CURRENTS

NORDA 323 12-DEC-89
G. OF MEXICO 21142.2: 0.0
DATE = 301/1972

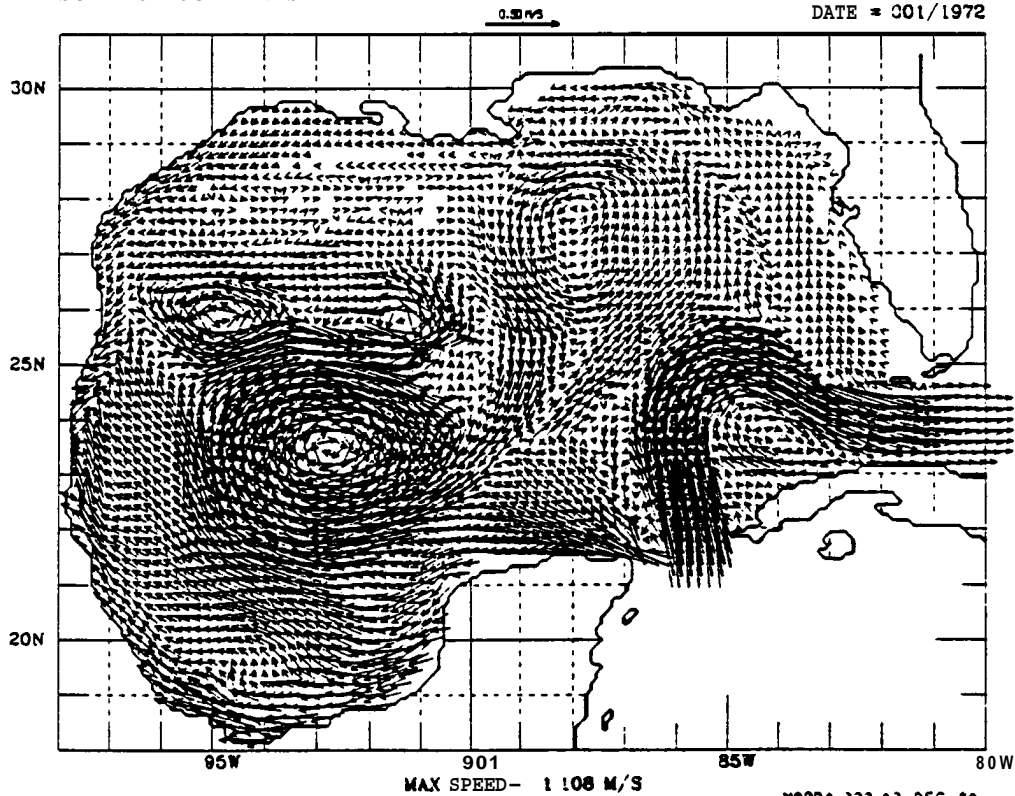
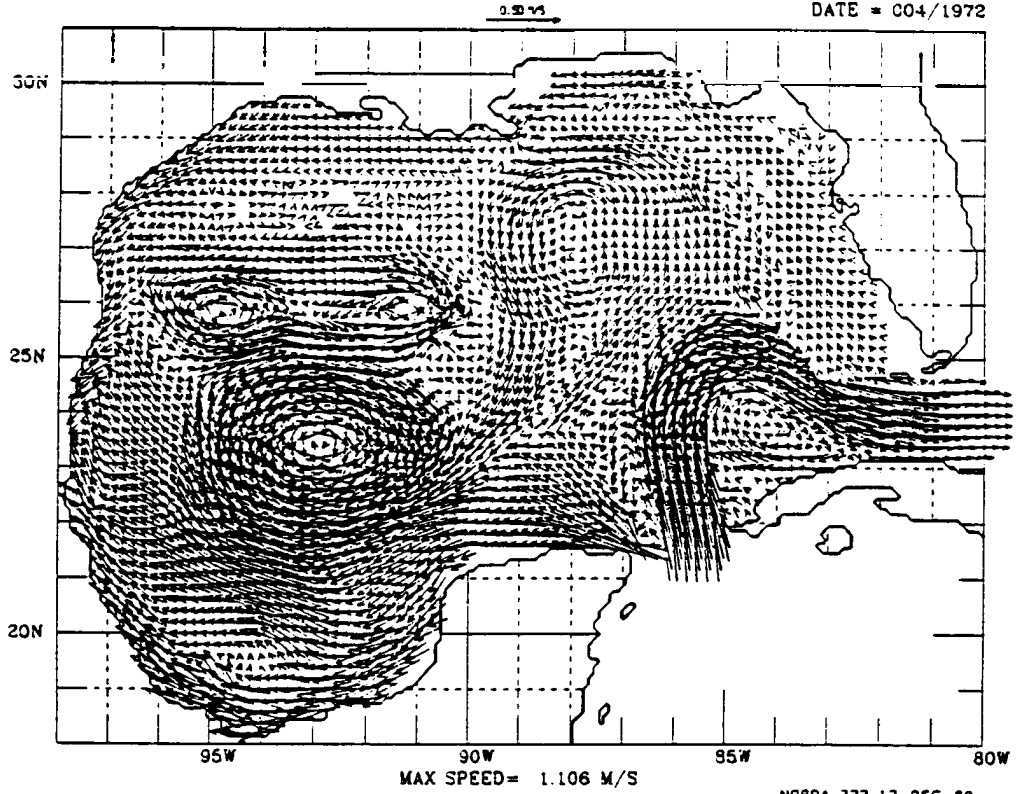


FIGURE 134

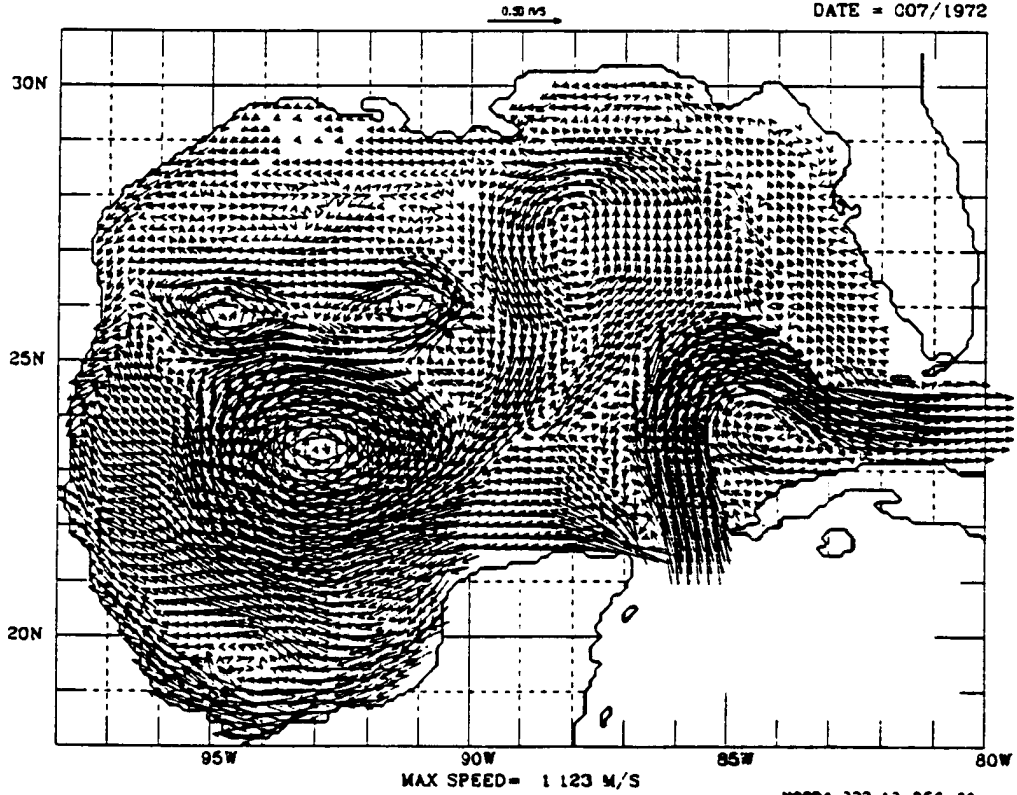
SURFACE CURRENTS

G. OF MEXICO 21142:2: 0.0
DATE = 004/1972



SURFACE CURRENTS

NORDA 323 12-DEC-89
G. OF MEXICO 21142:2: 0.0
DATE = 007/1972



NORDA 323 12-DEC-89

FIGURE 135

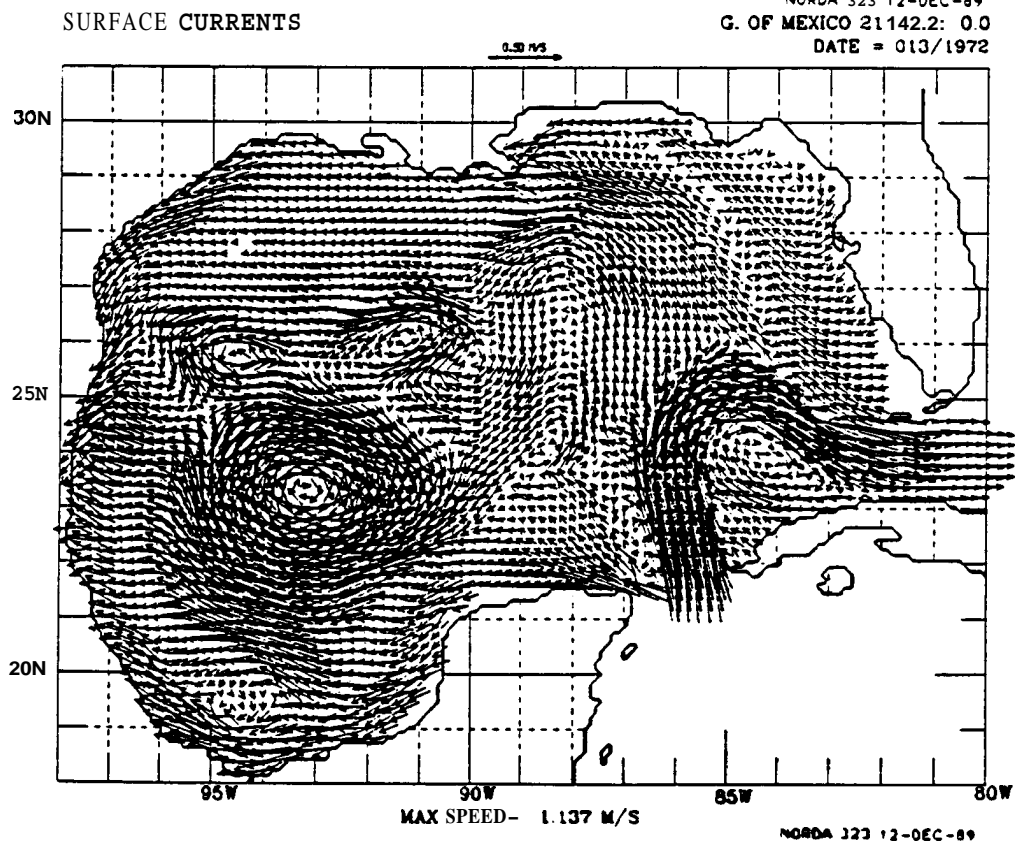
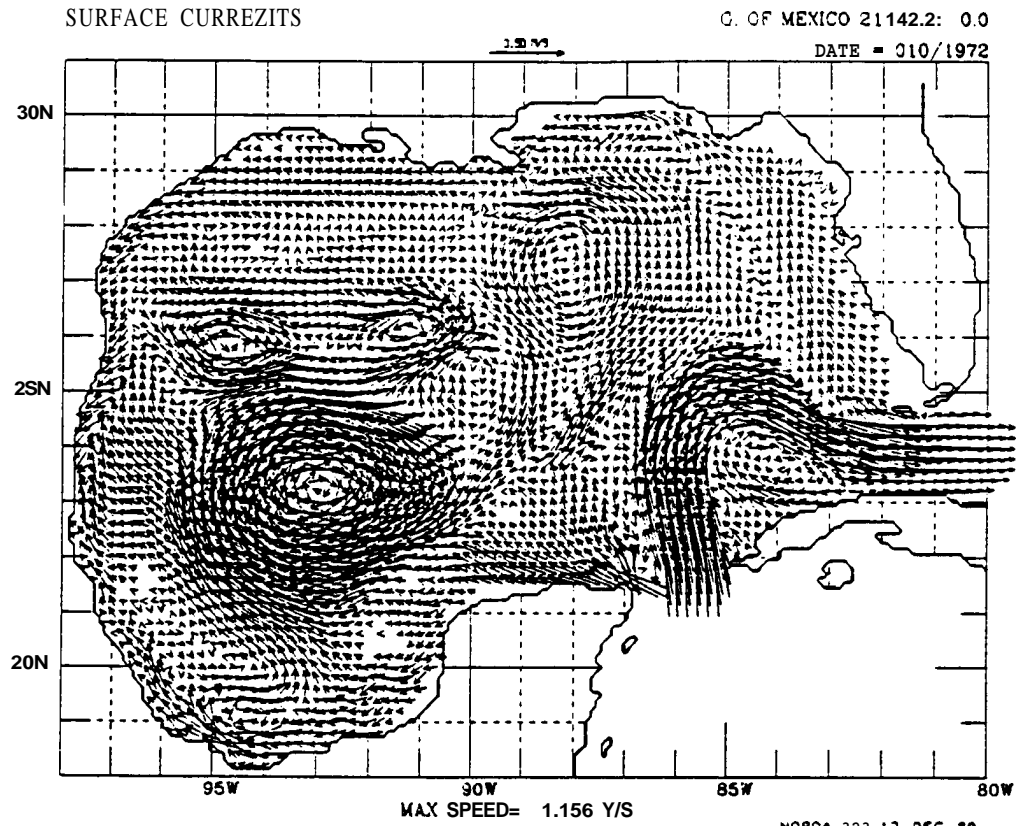


FIGURE 136

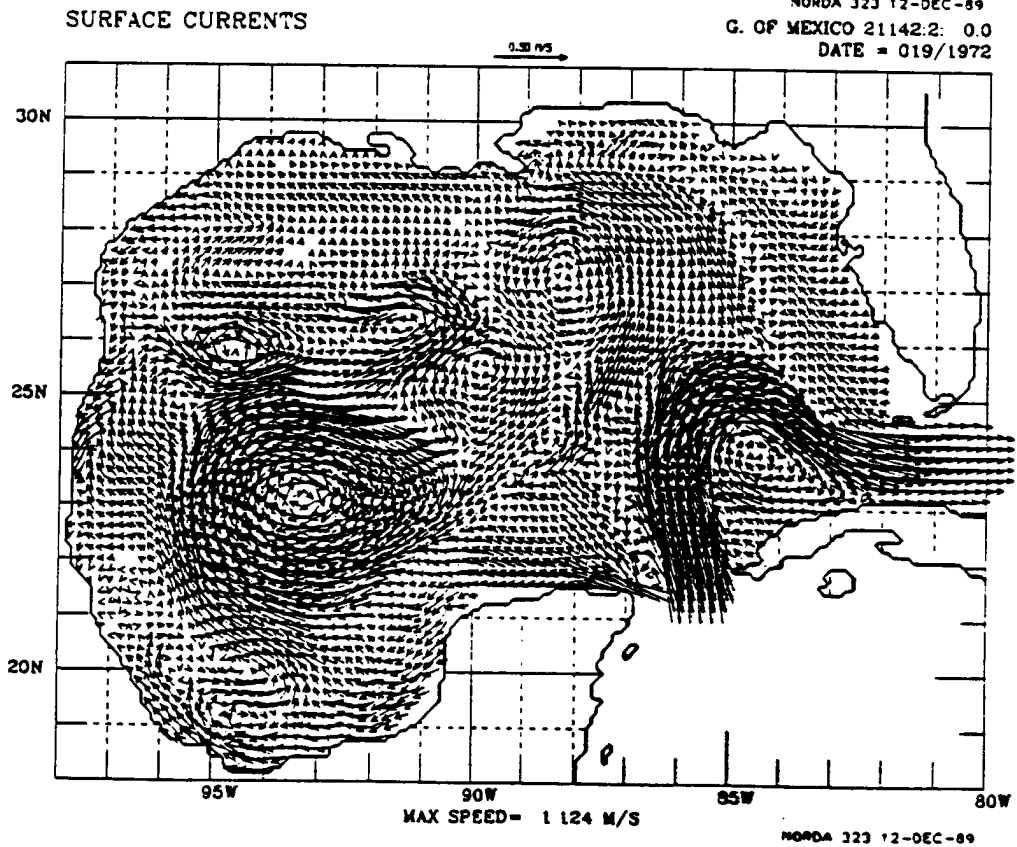
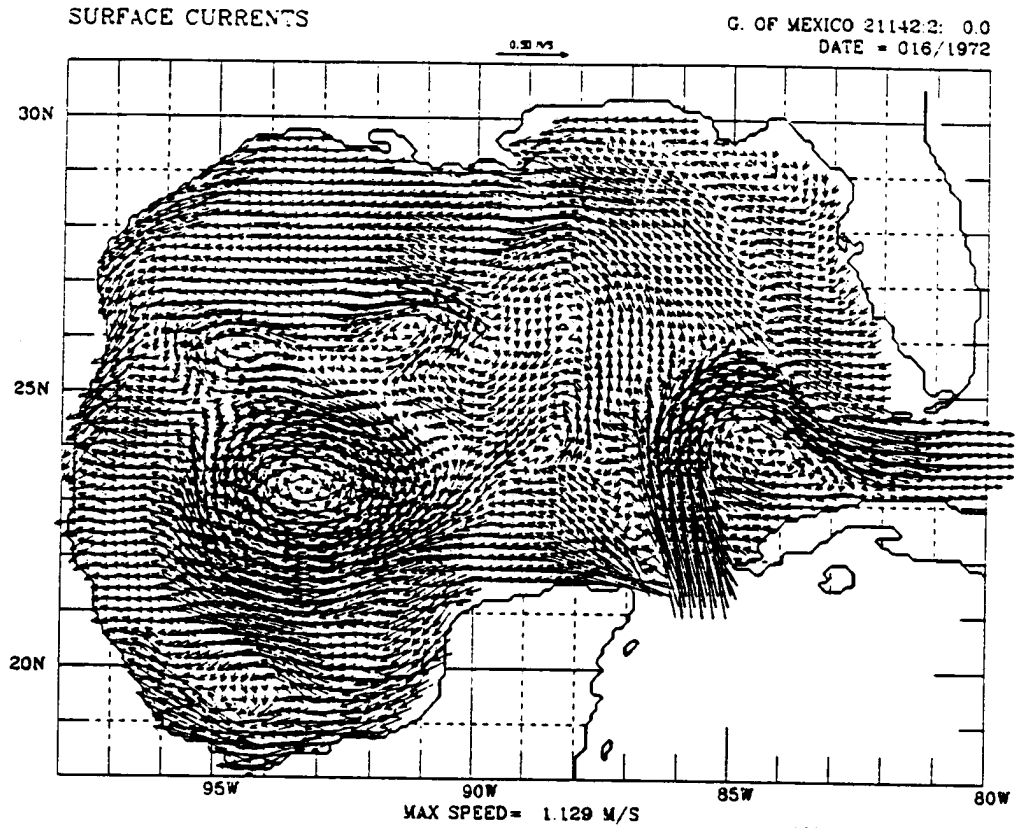
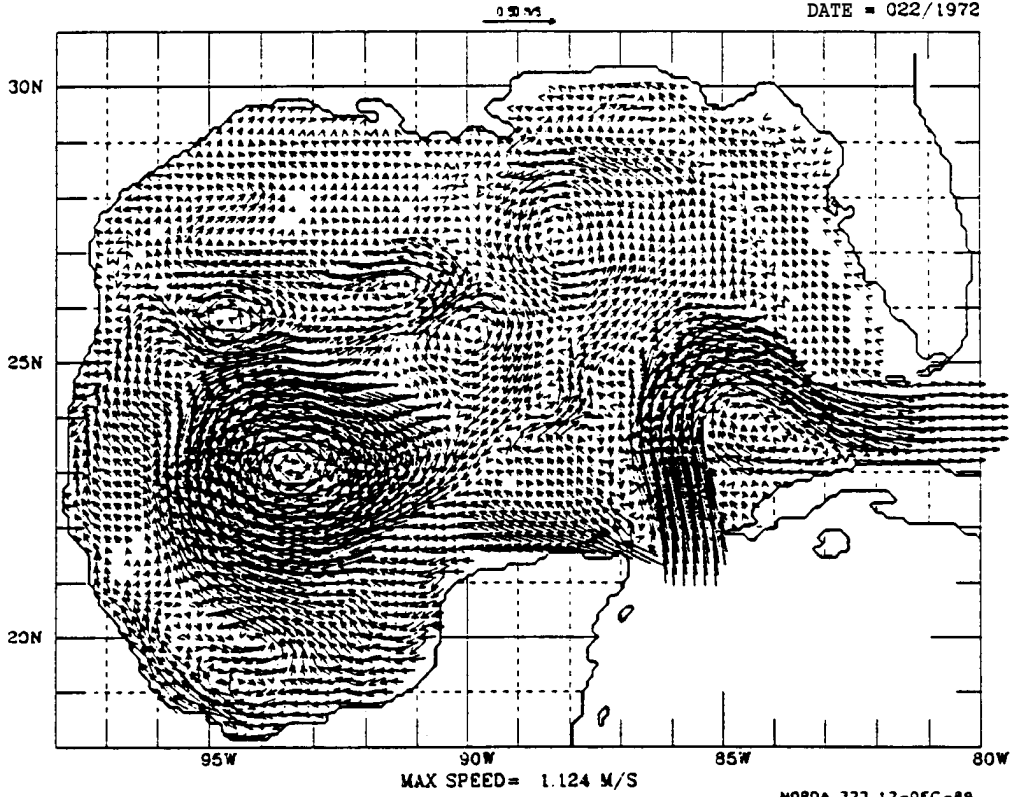


FIGURE 137

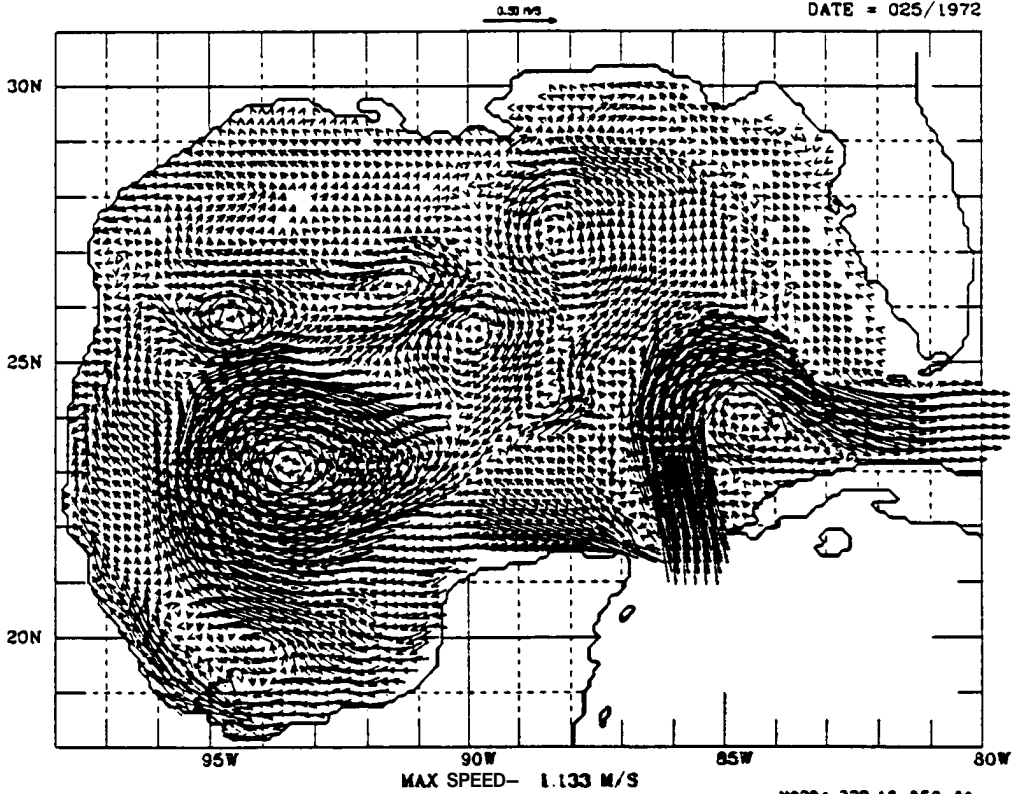
SURFACE CURRENTS

G. OF MEXICO 21142:2: 0.0
DATE = 022/1972



SURFACE CURRENTS

NORDA 323 12-DEC-89
G. OF MEXICO 21142:2: 0.0
DATE = 025/1972

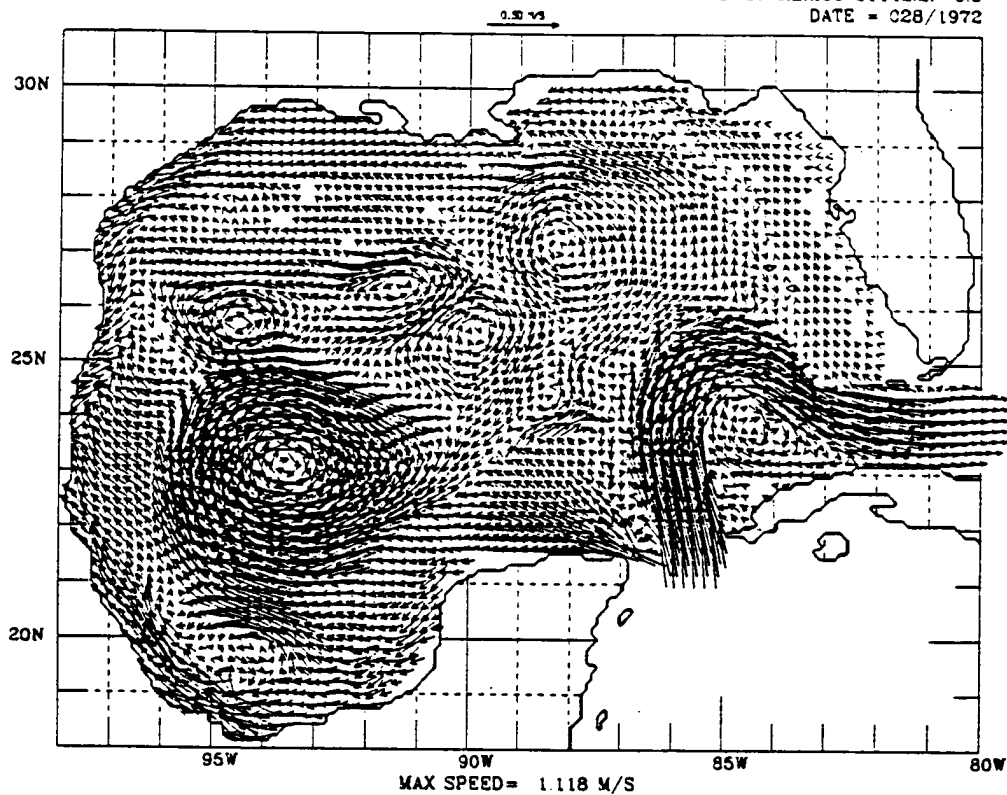


NORDA 323 12-DEC-89

FIGURE 138

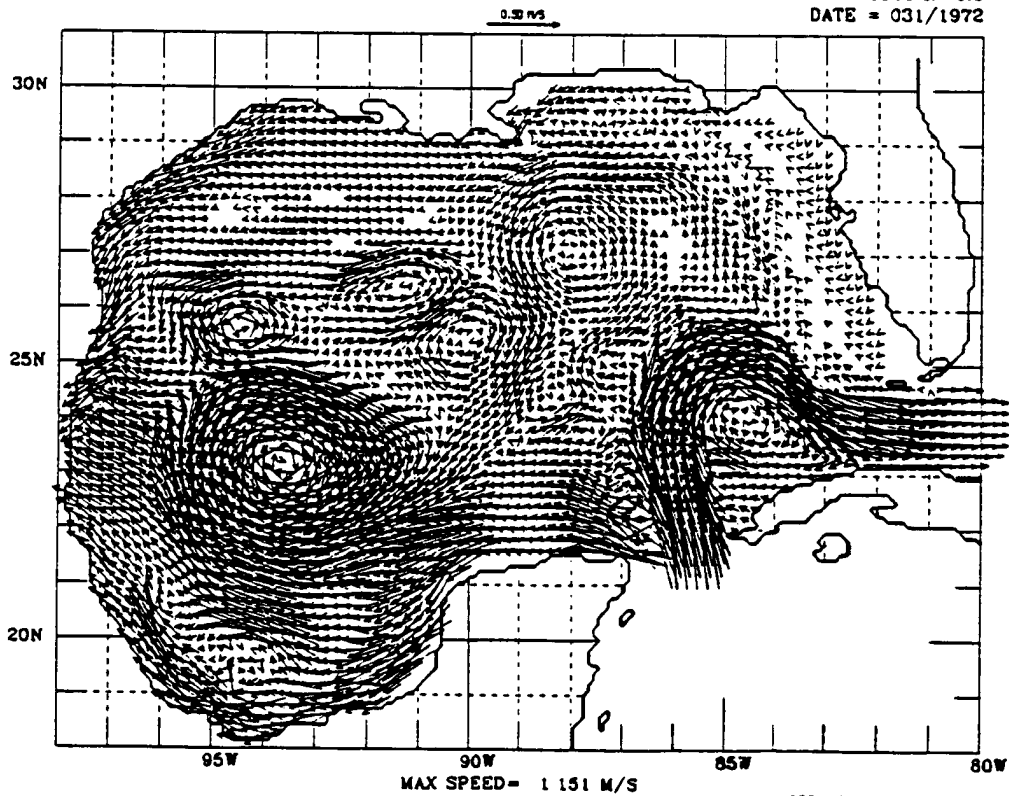
SURFACE CURRENTS

G. OF MEXICO 21142.2: 0.0
DATE = 028/1972



SURFACE CURRENTS

NORDA 323 12-DEC-89
G. OF MEXICO 21142.2: 0.0
DATE = 031/1972



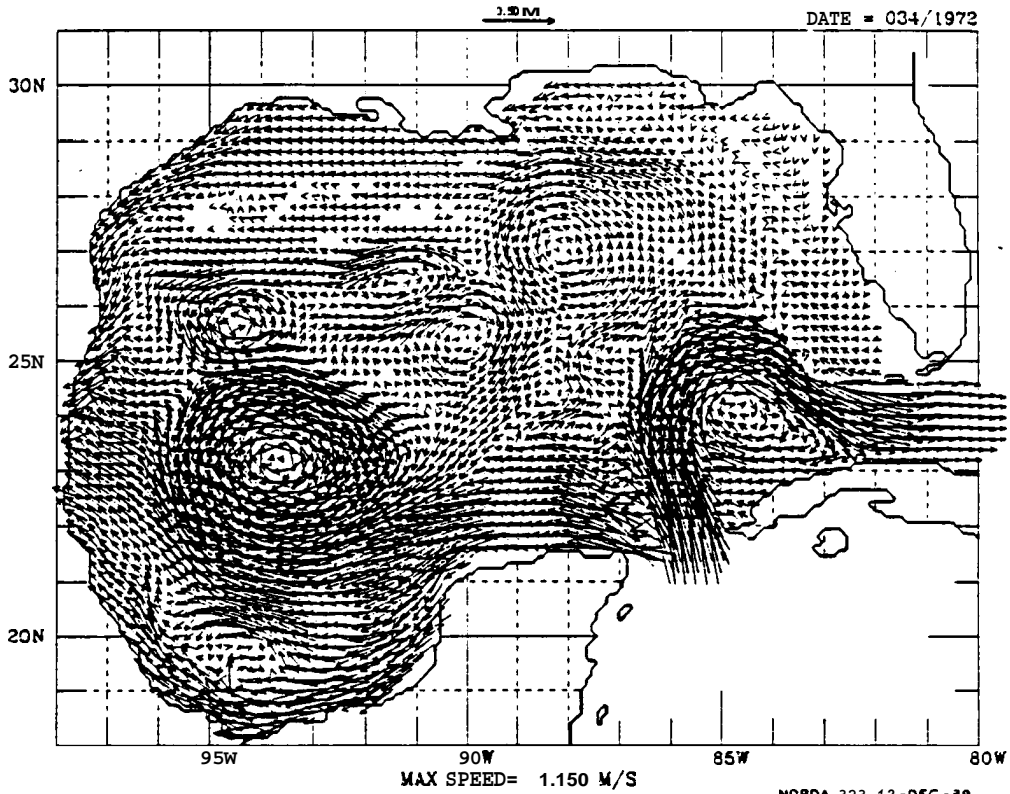
NORDA 323 12-DEC-89

FIGURE 139

SURFACE CURRENTS

G. OF MEXICO 21142.2: 0.3

DATE = 034/1972



SURFACE CURRENTS

G. OF MEXICO 21142.2: 0.0

DATE = 037/1972

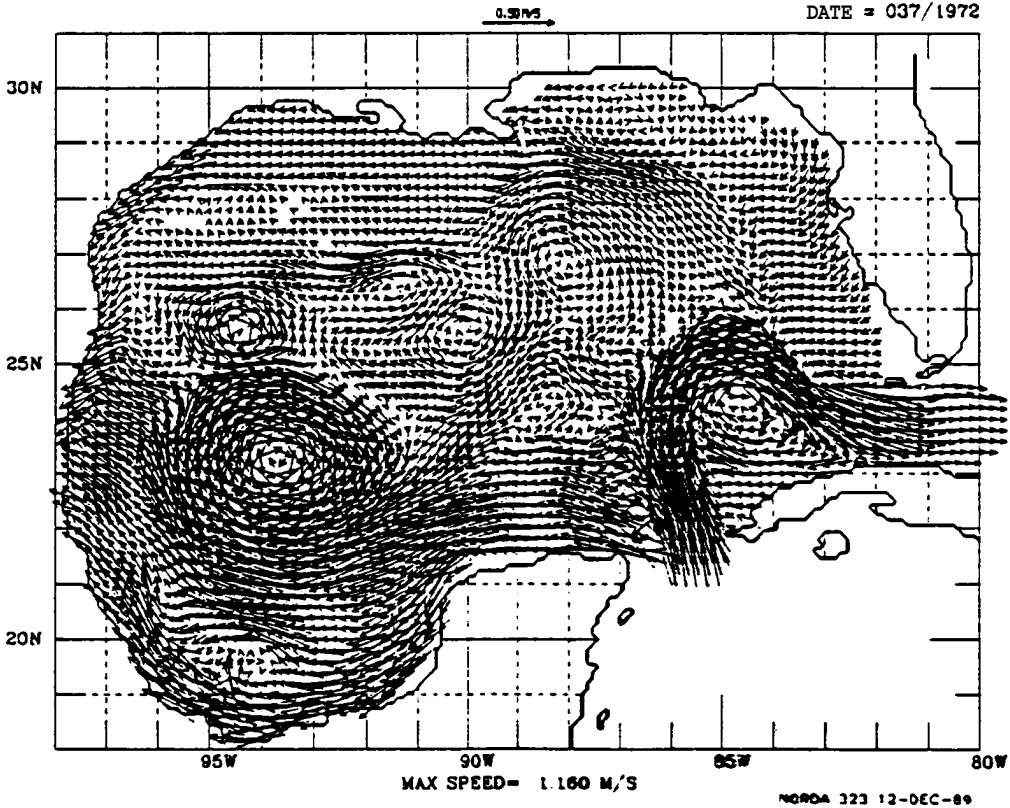
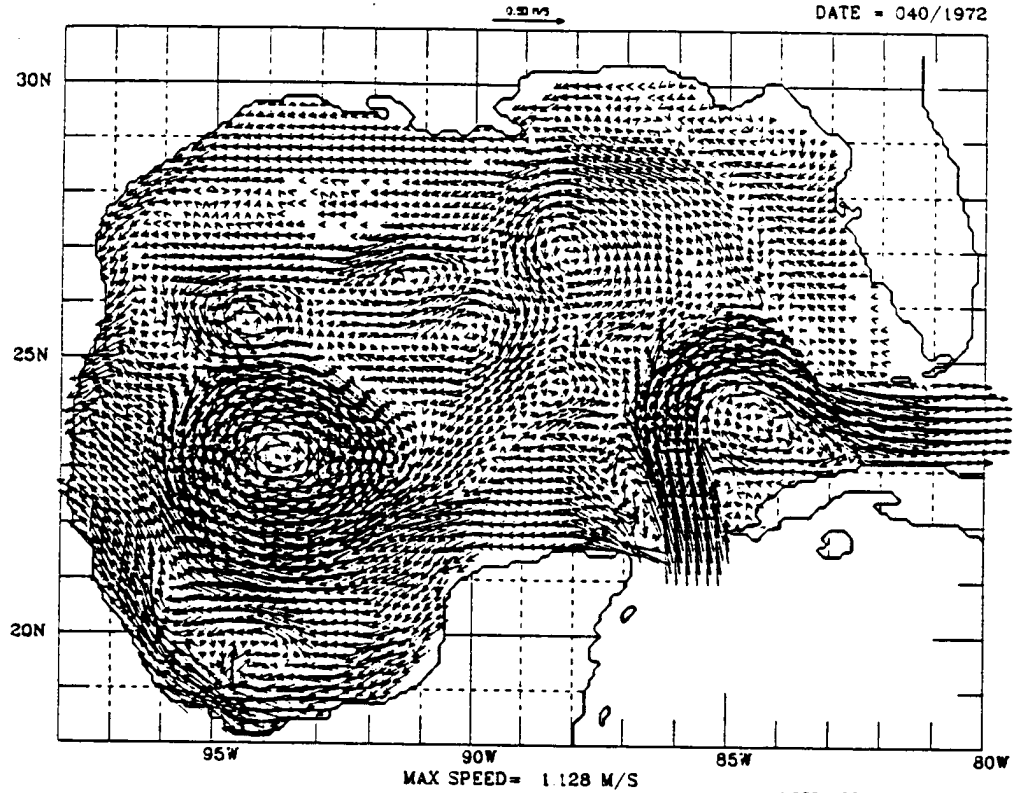


FIGURE 140

SURFACE CURRENTS

G. OF MEXICO 21142:2: 0.0
DATE = 040/1972



SURFACE CURRENTS

NORDA 323 12-DEC-89
G. OF MEXICO 21142:2: 0.0
DATE = 043/1972

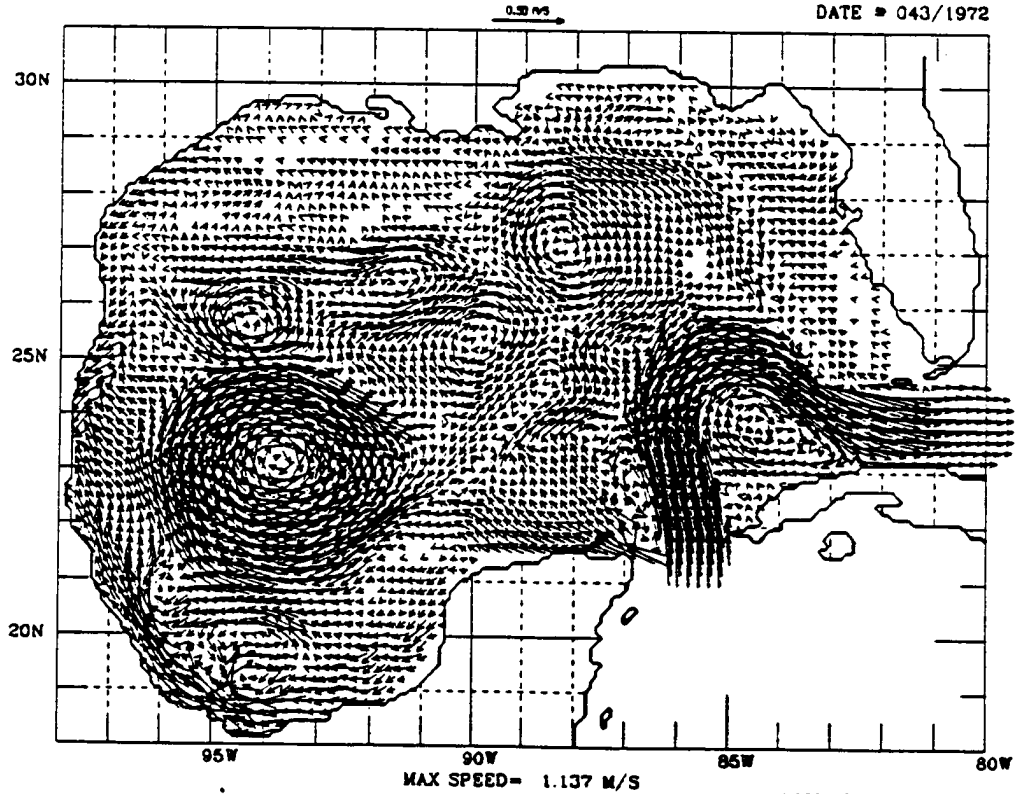


FIGURE 141

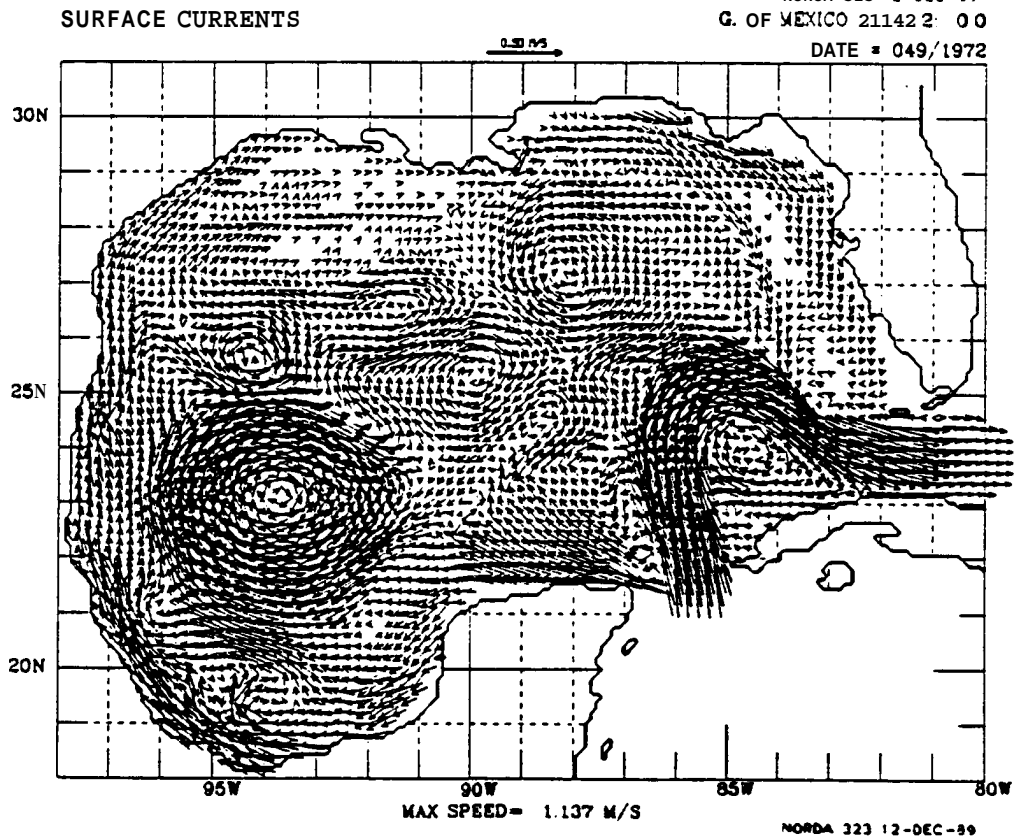
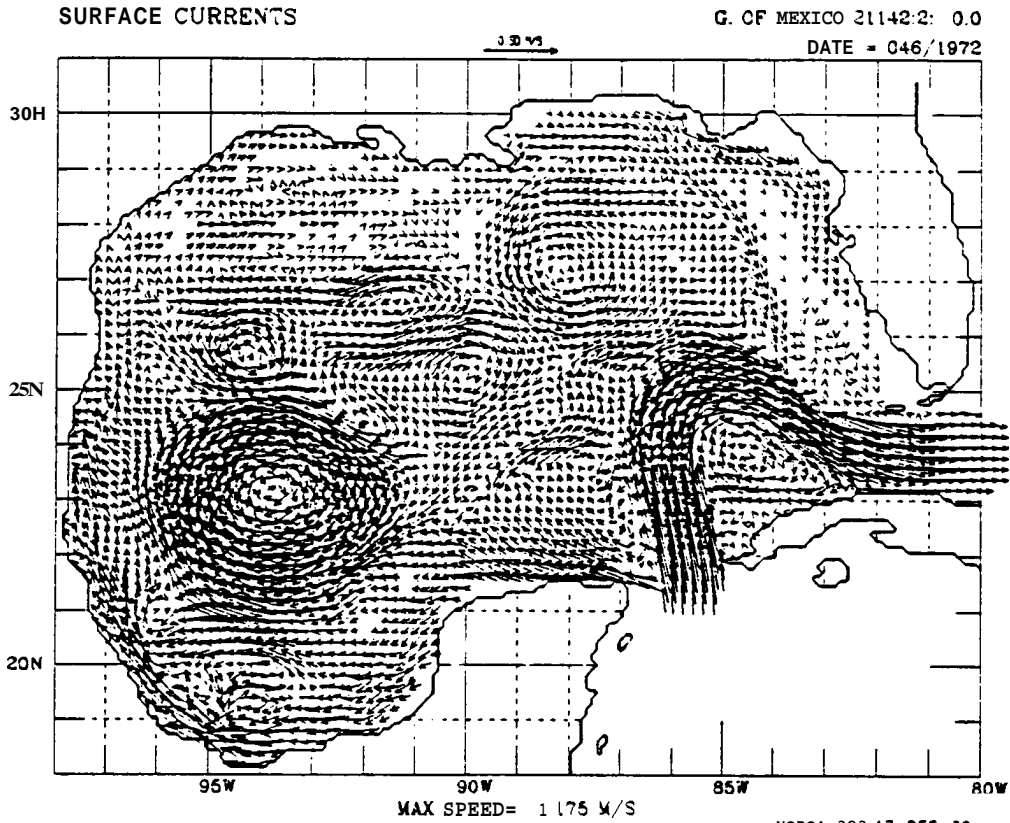


FIGURE 142

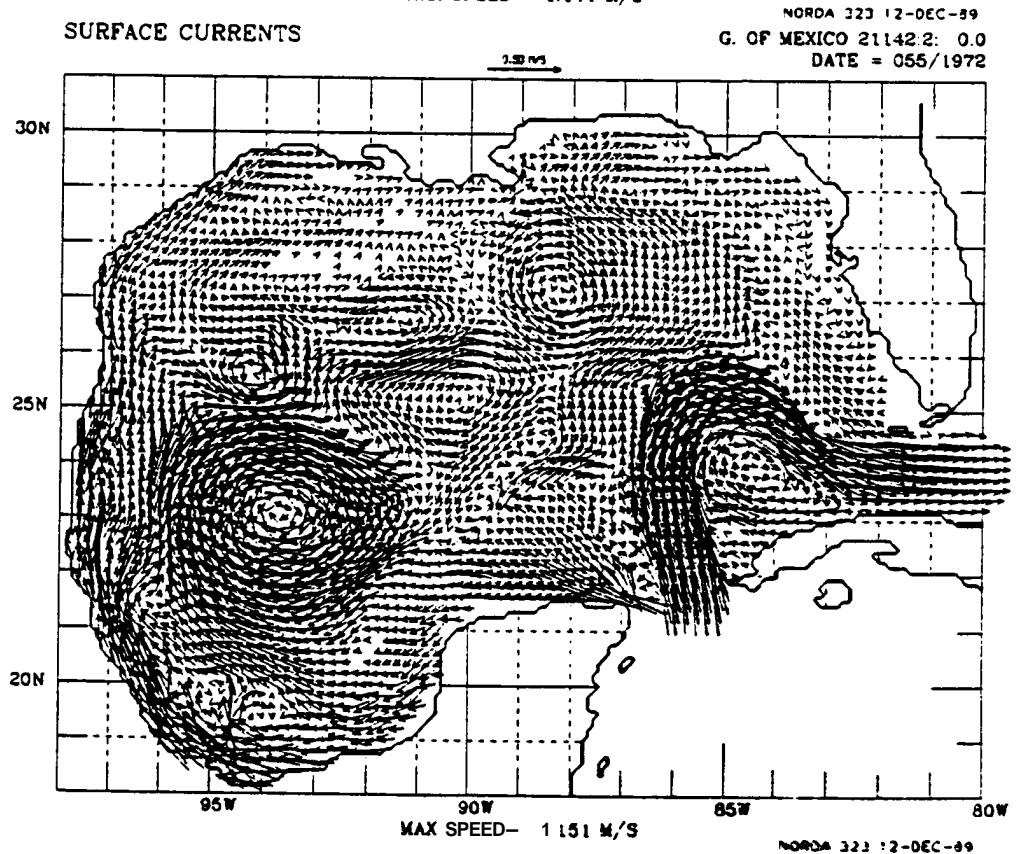
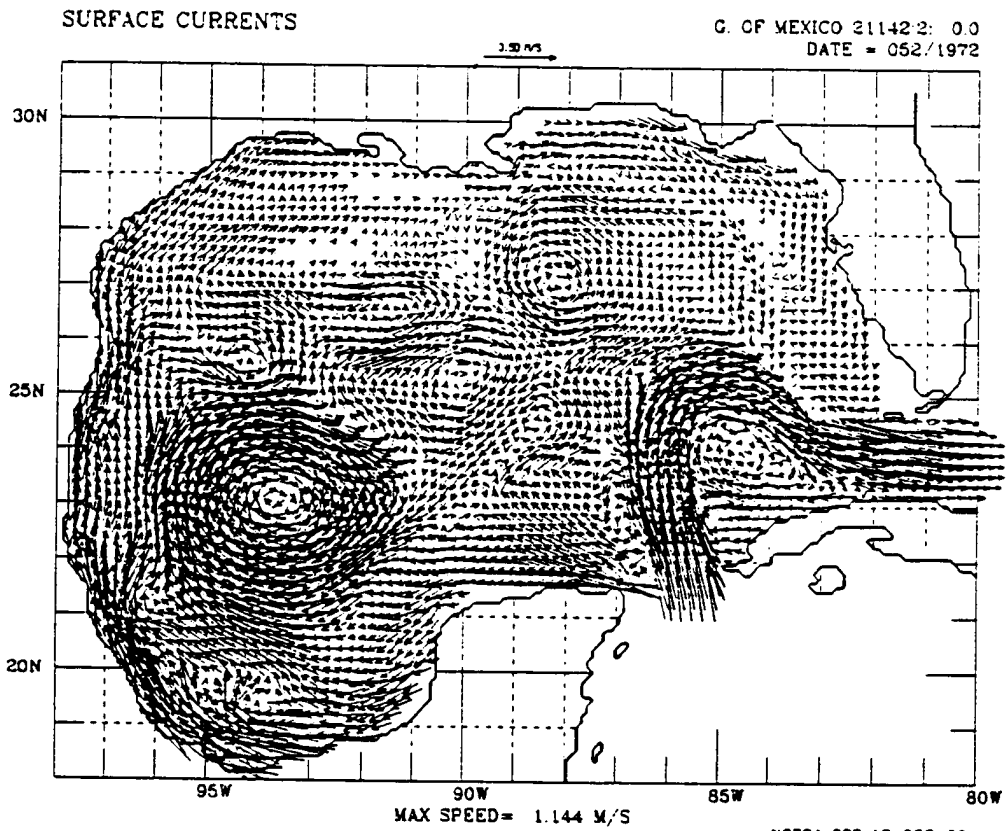


FIGURE 143

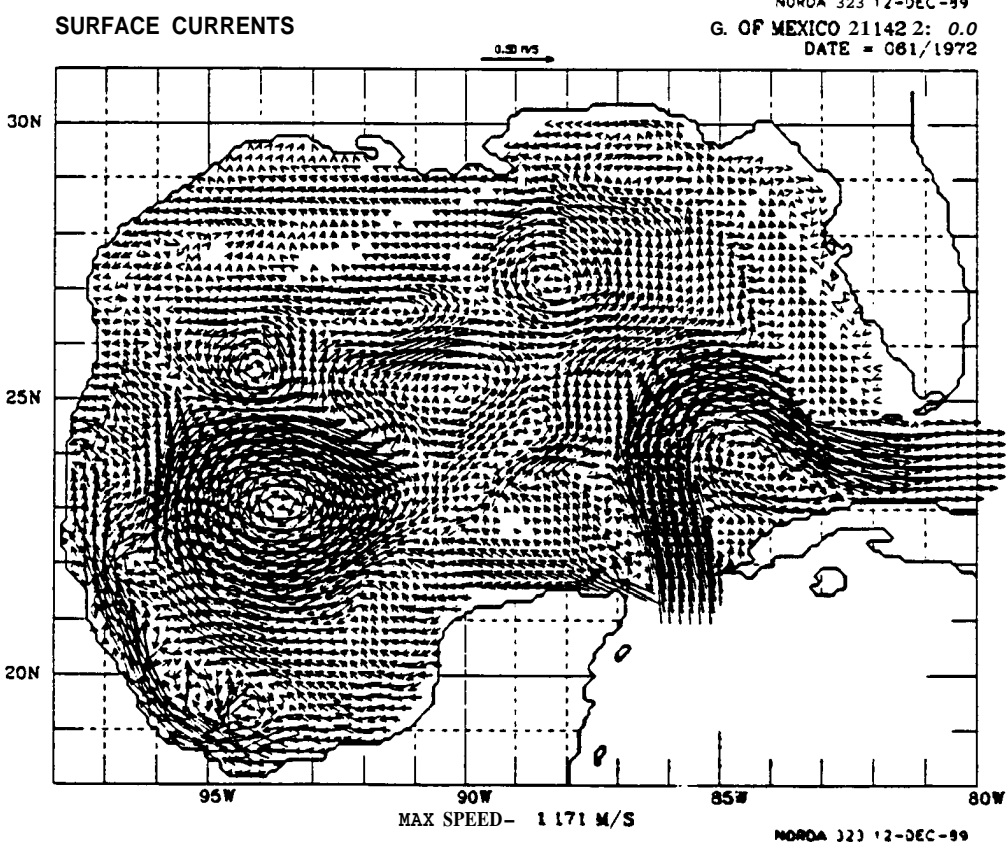
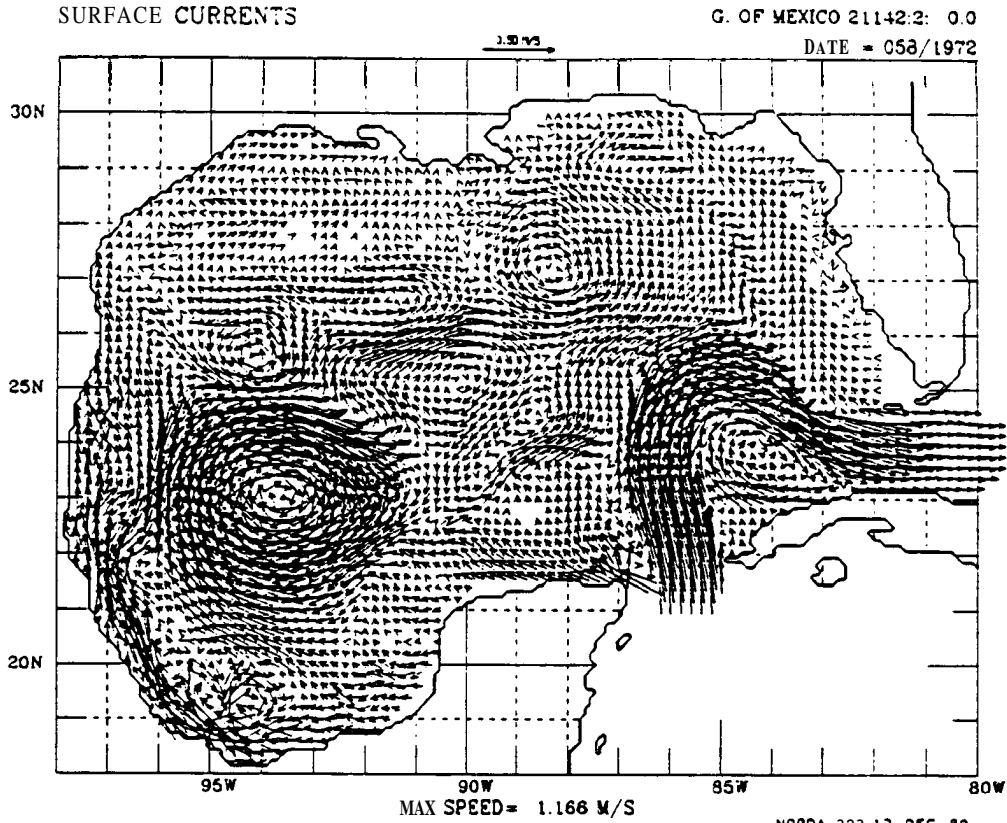


FIGURE 144

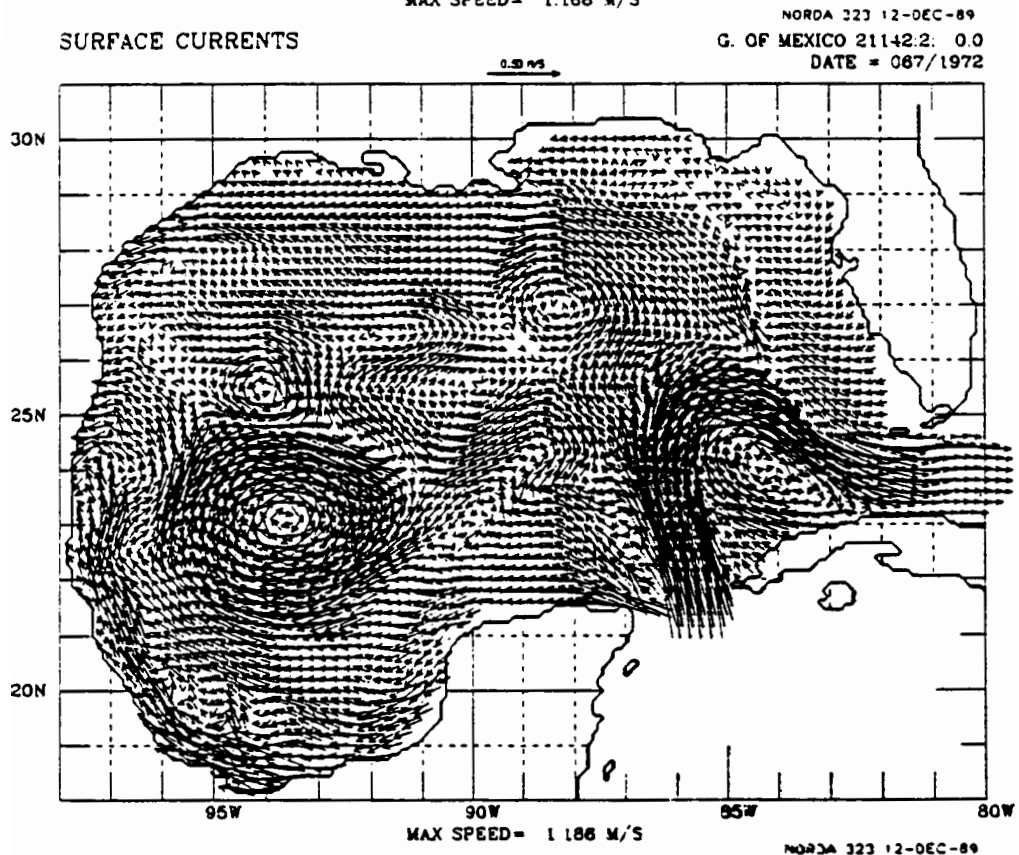
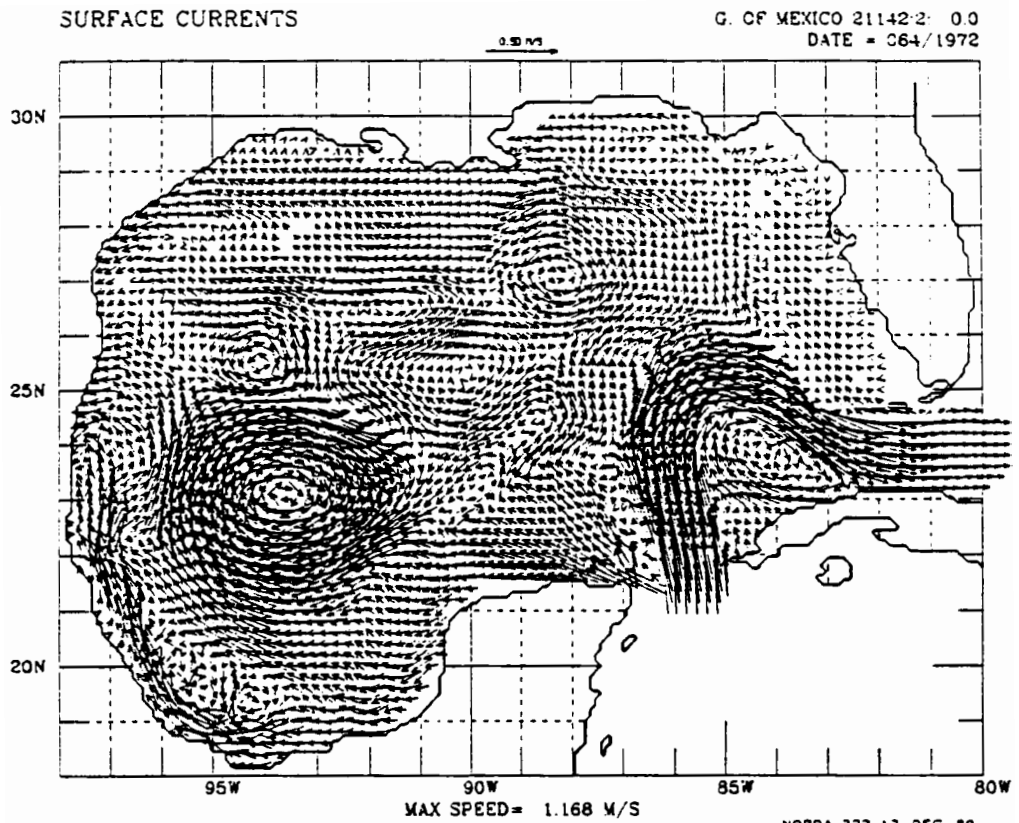


FIGURE 145

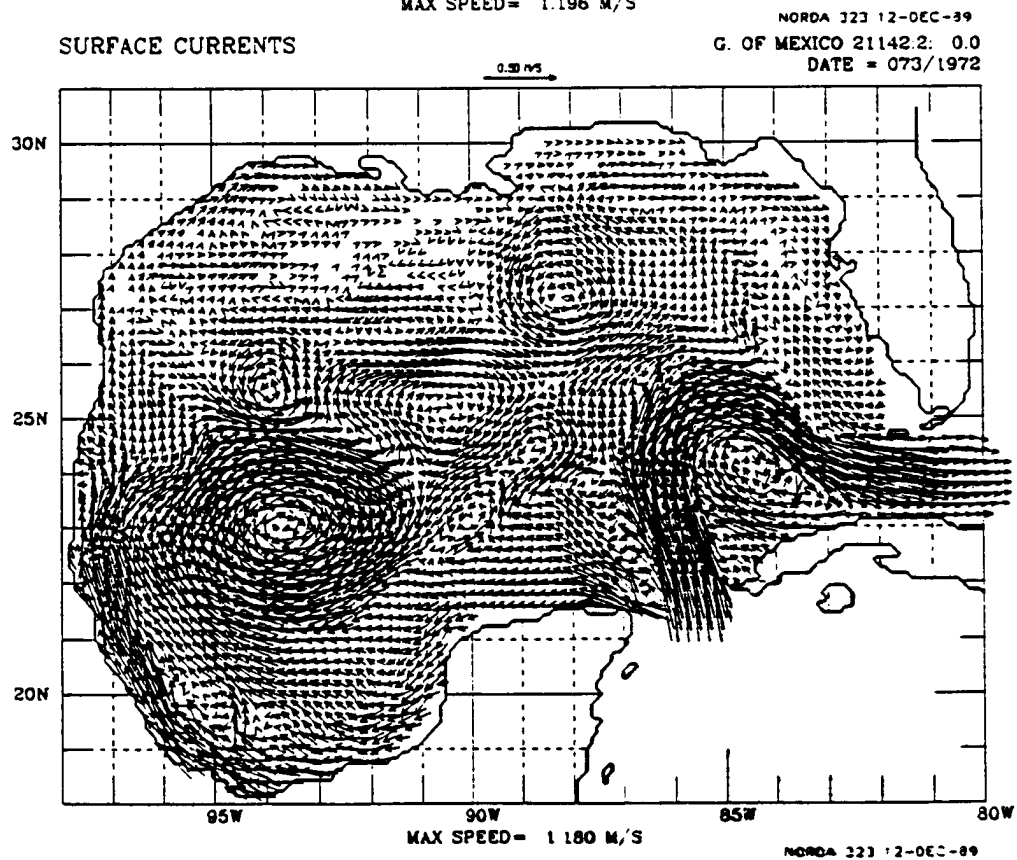
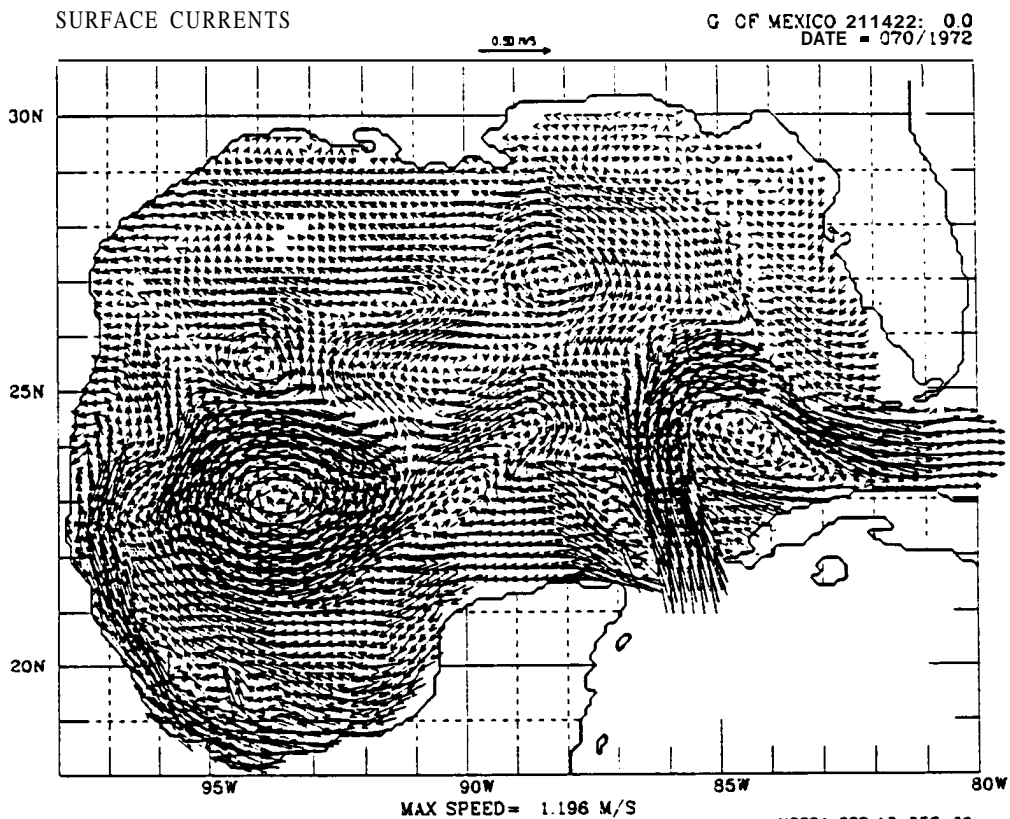


FIGURE 146

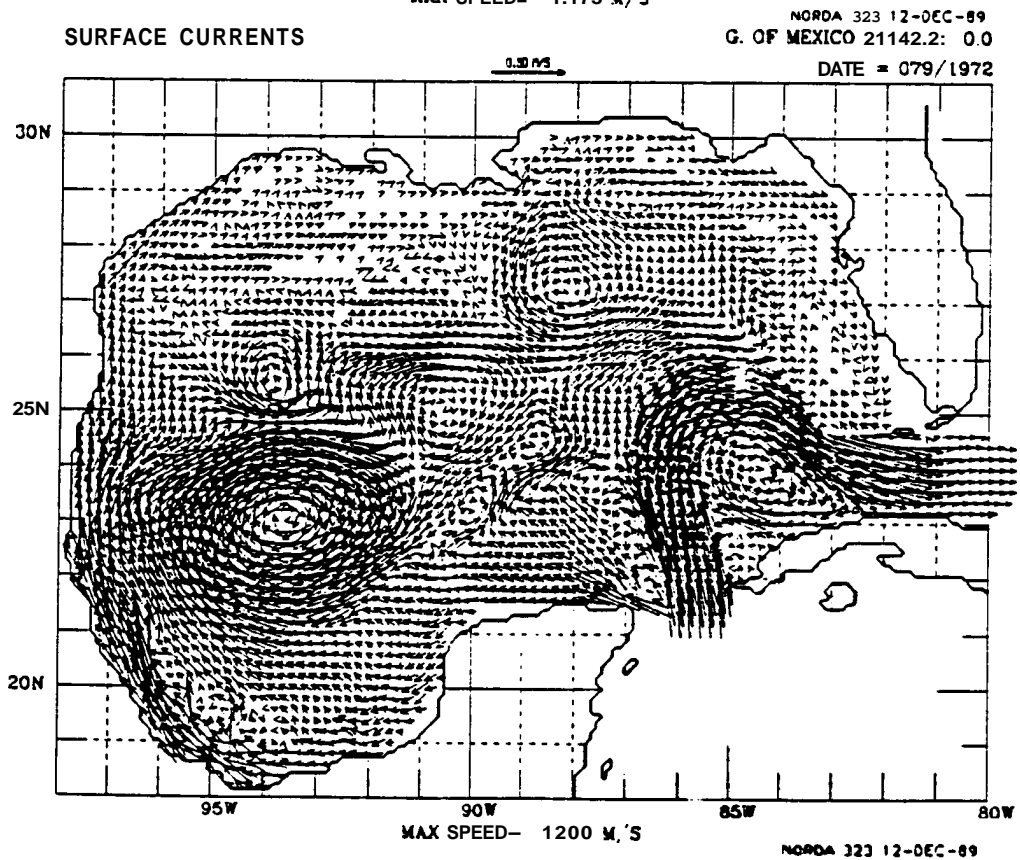
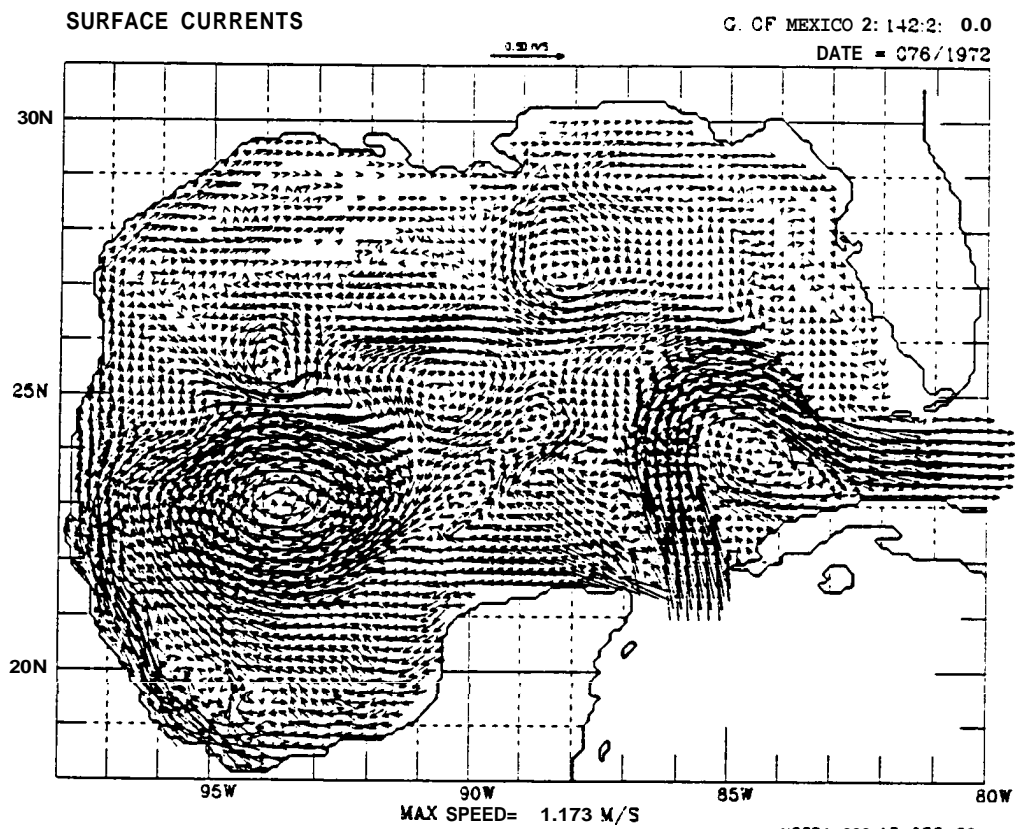
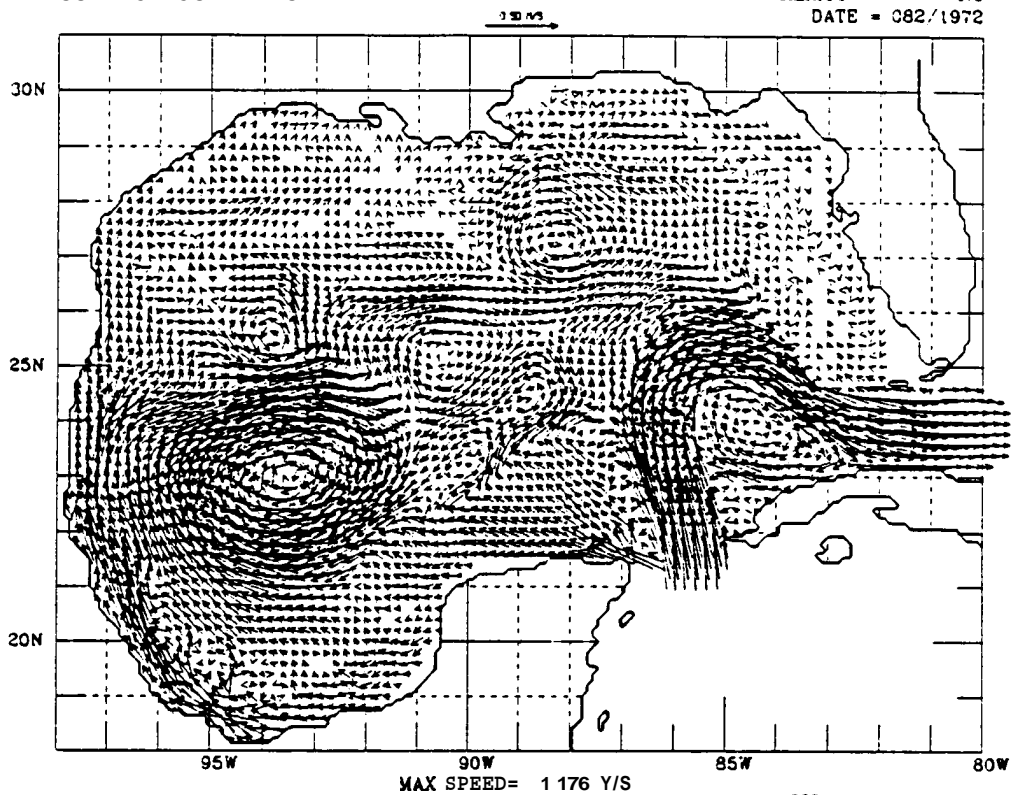


FIGURE 147

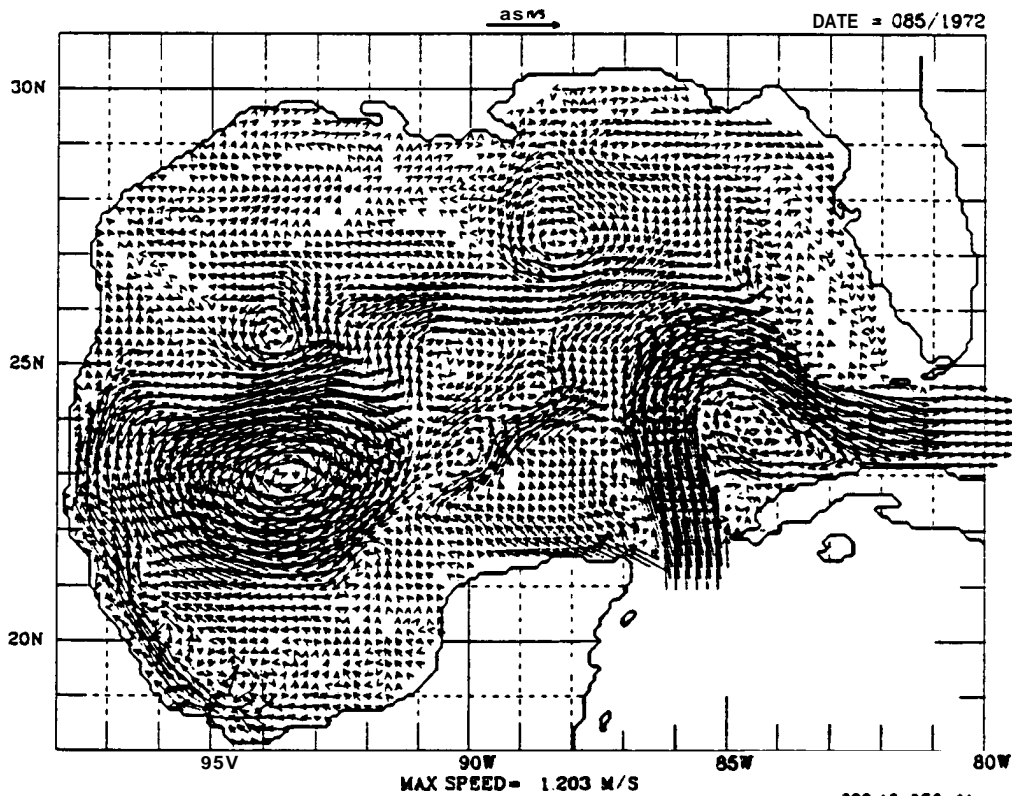
SURFACE CURRENTS

G. OF MEXICO 21142.2: 0.0
DATE = 082/1972



SURFACE CURRENTS

NORDA 323 12-DEC-89
G. Of MEXICO 21142.2: 0.0
DATE = 085/1972

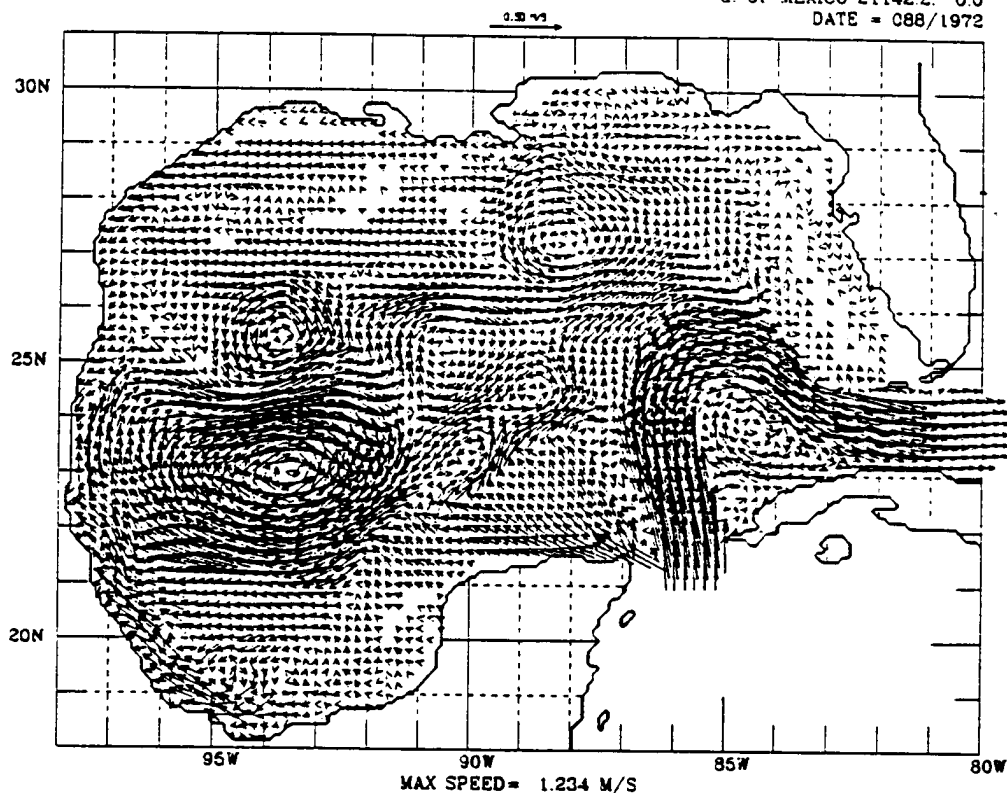


323 12-DEC-89

FIGURE 148

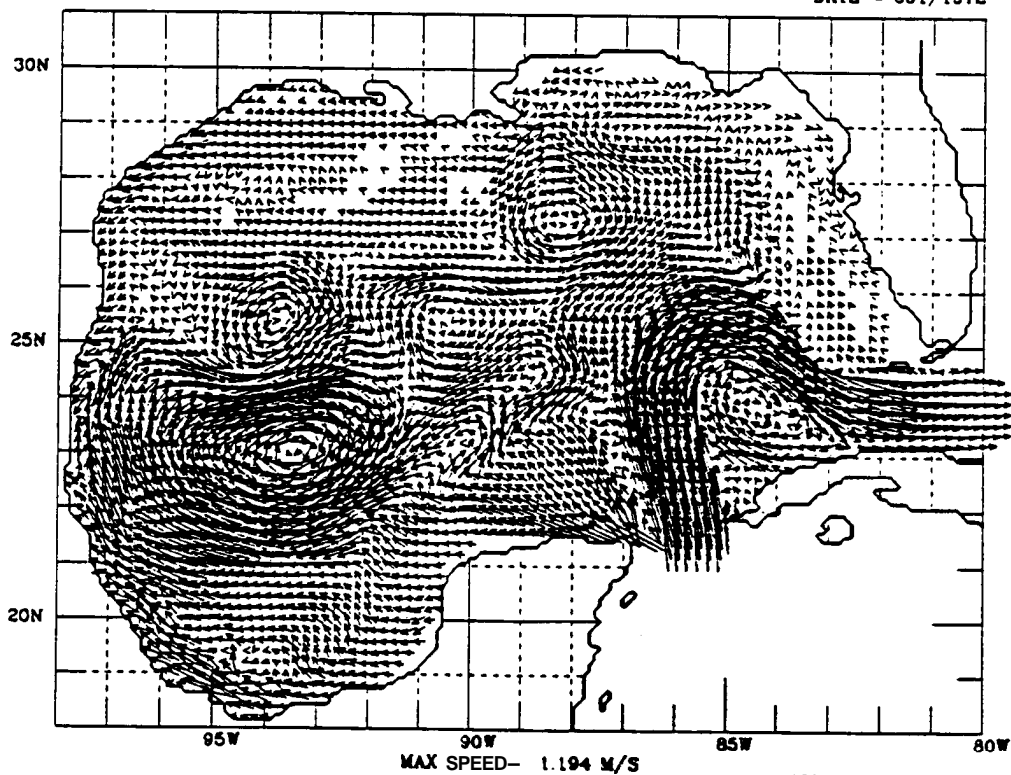
SURFACE CURRENTS

G. OF MEXICO 21142:2: 0.0
DATE = 088/1972



SURFACE CURRENTS

NORDA 323 12-DEC-89
G. OF MEXICO 21142:2: 0.0
DATE = 091/1972

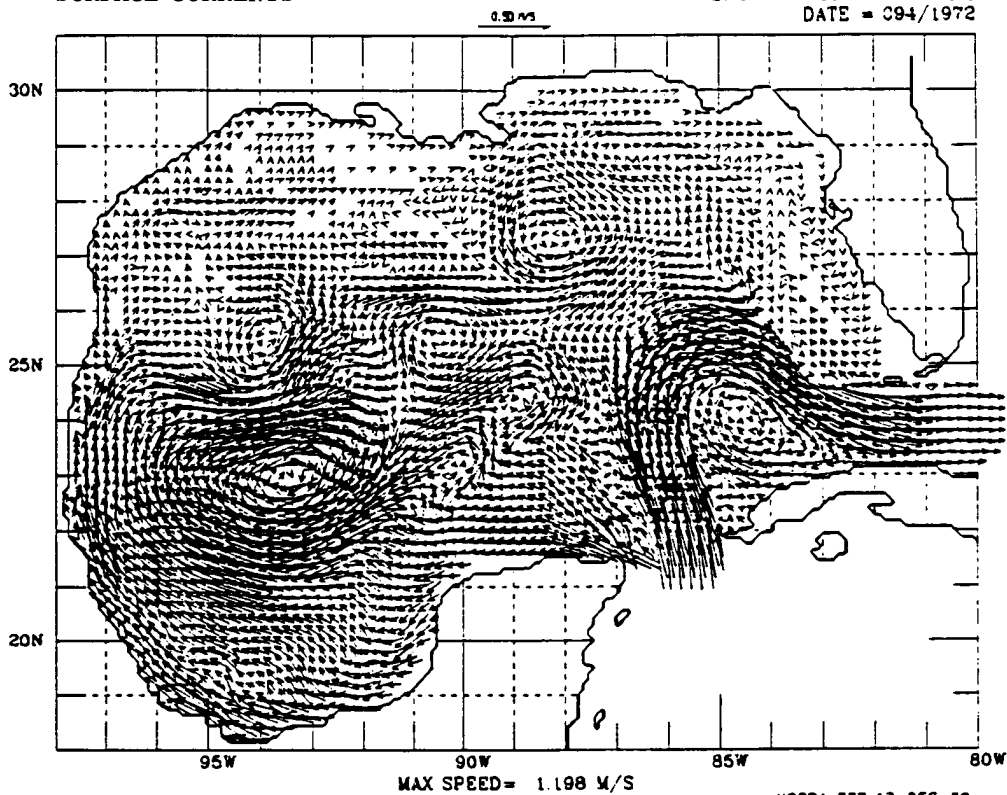


NORDA 323 12-DEC-89

FIGURE 149

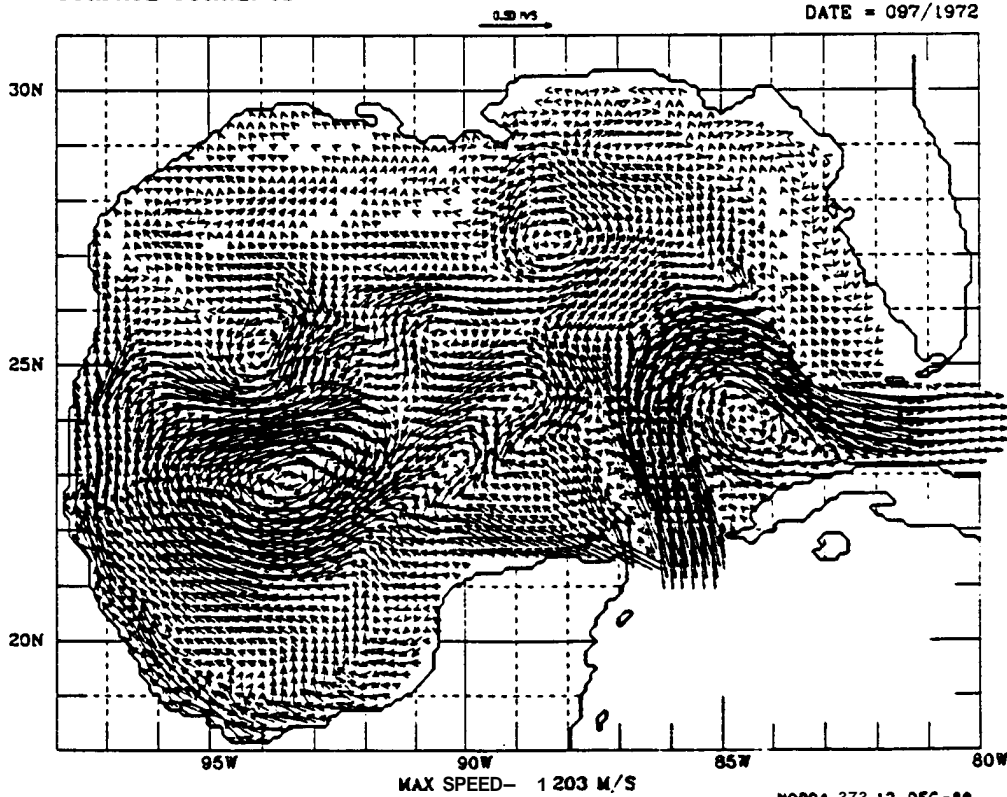
SURFACE CURRENTS

G. OF MEXICO 21142.2: 0.3
DATE = 094/1972



SURFACE CURRENTS

NORDA 323 12-DEC-89
G. OF MEXICO 21142.2: 0.3
DATE = 097/1972



NORDA 373 12-DEC-89

FIGURE 150

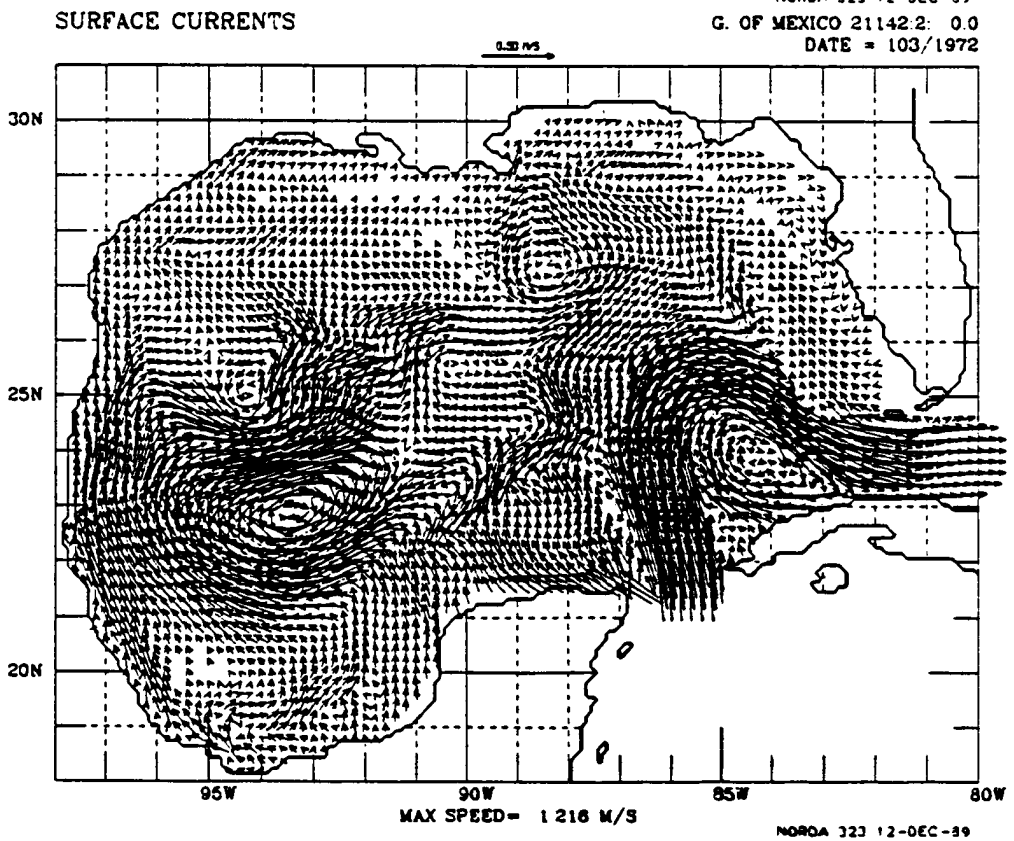
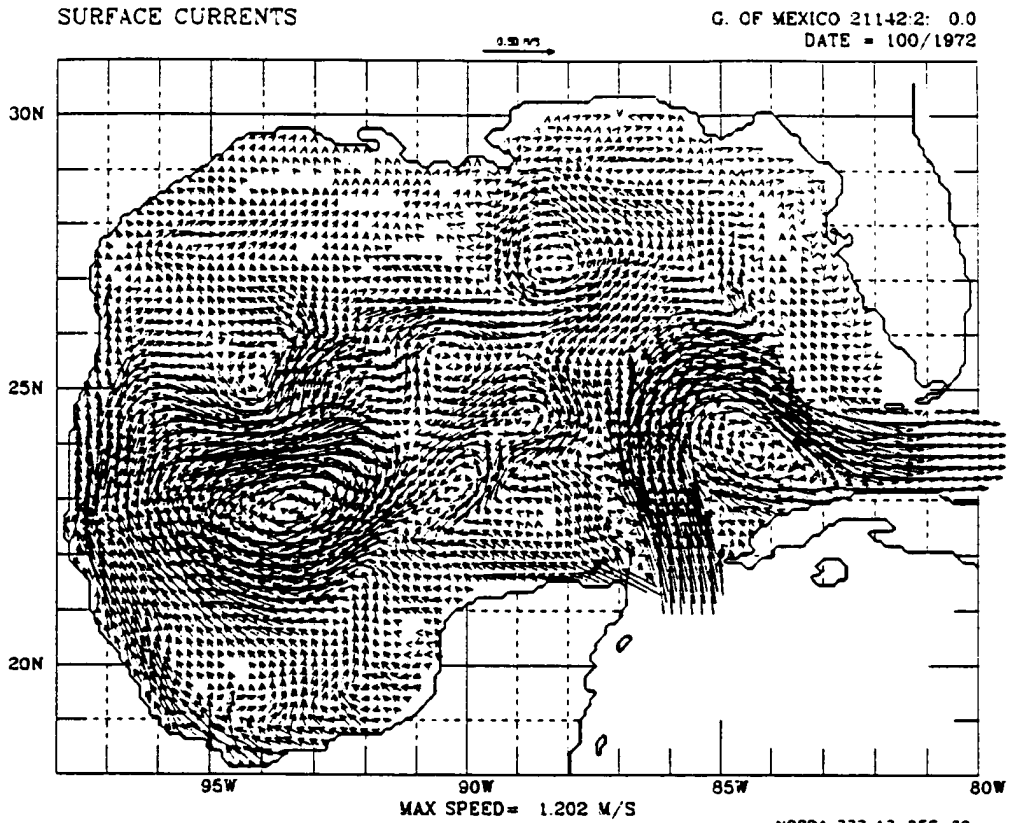
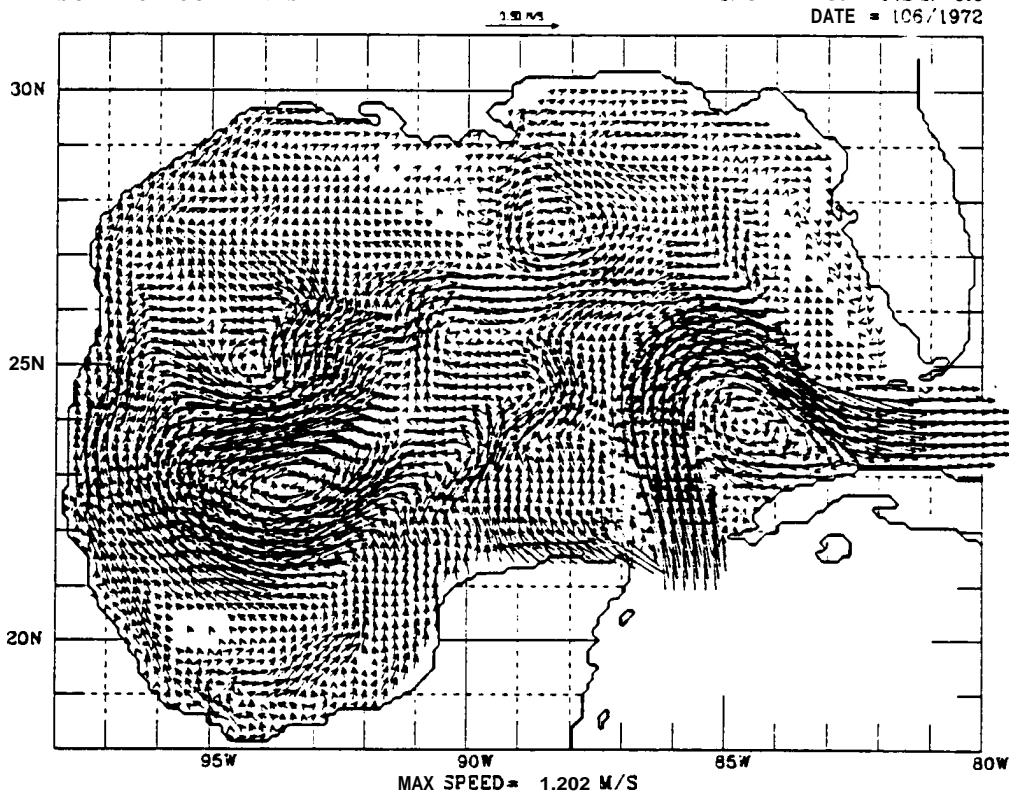


FIGURE 151

SURFACE CURRENTS

G. OF MEXICO 21142-2: 0.0
DATE = 106/1972



SURFACE CURRENTS

NORDA 323 12-DEC-89
G. OF MEXICO 21142 2 0.0
DATE = 109/1972

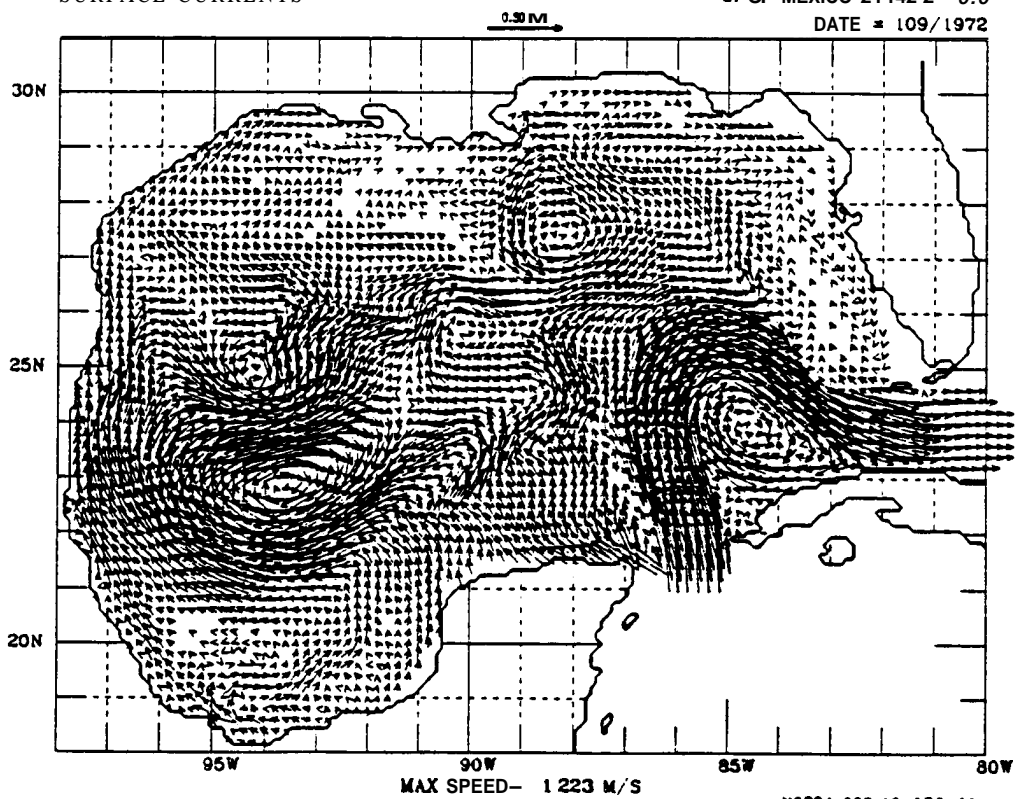
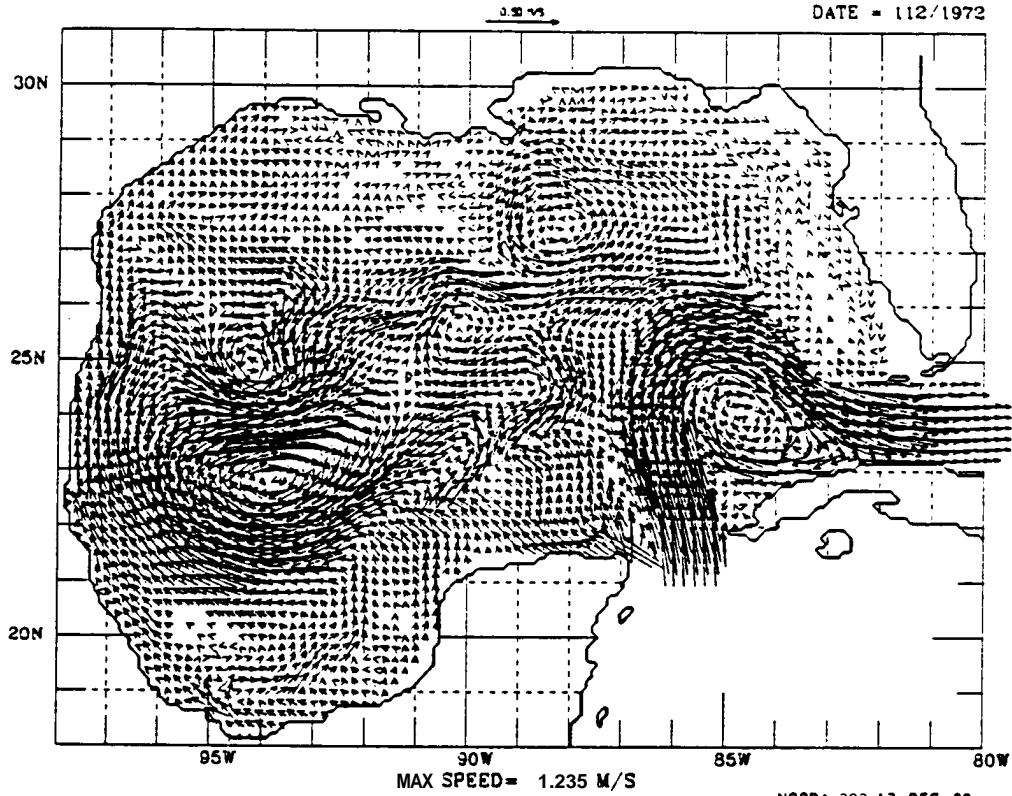


FIGURE 152

SURFACE CURRENTS

G. OF MEXICO 21142.2: 0.0
DATE = 112/1972



SURFACE CURRENTS

NORDA 323 12-DEC-89
G. OF MEXICO 21142.2: 0.0
DATE = 115/1972

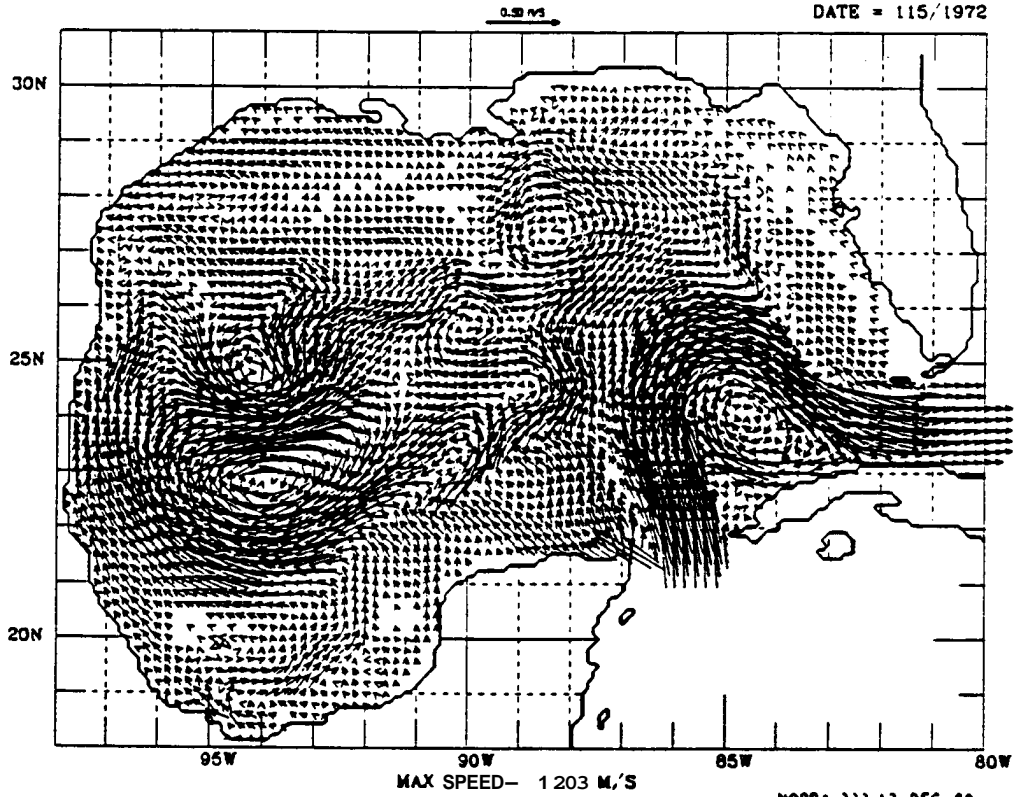


FIGURE 153

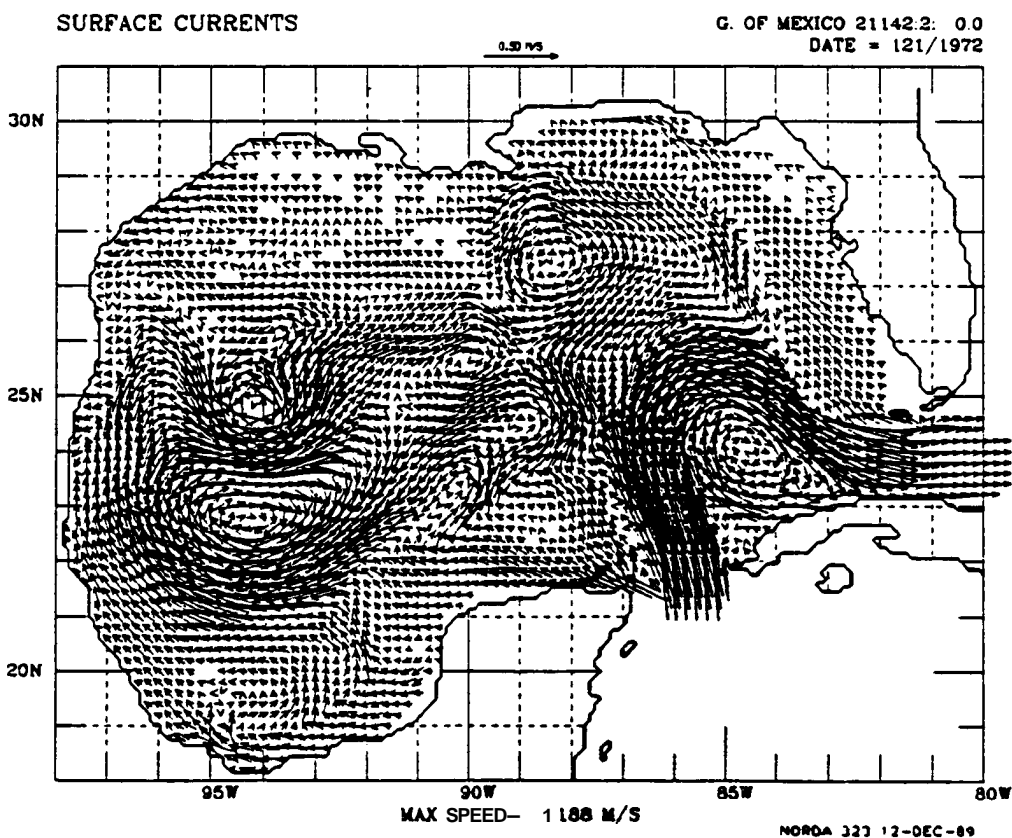
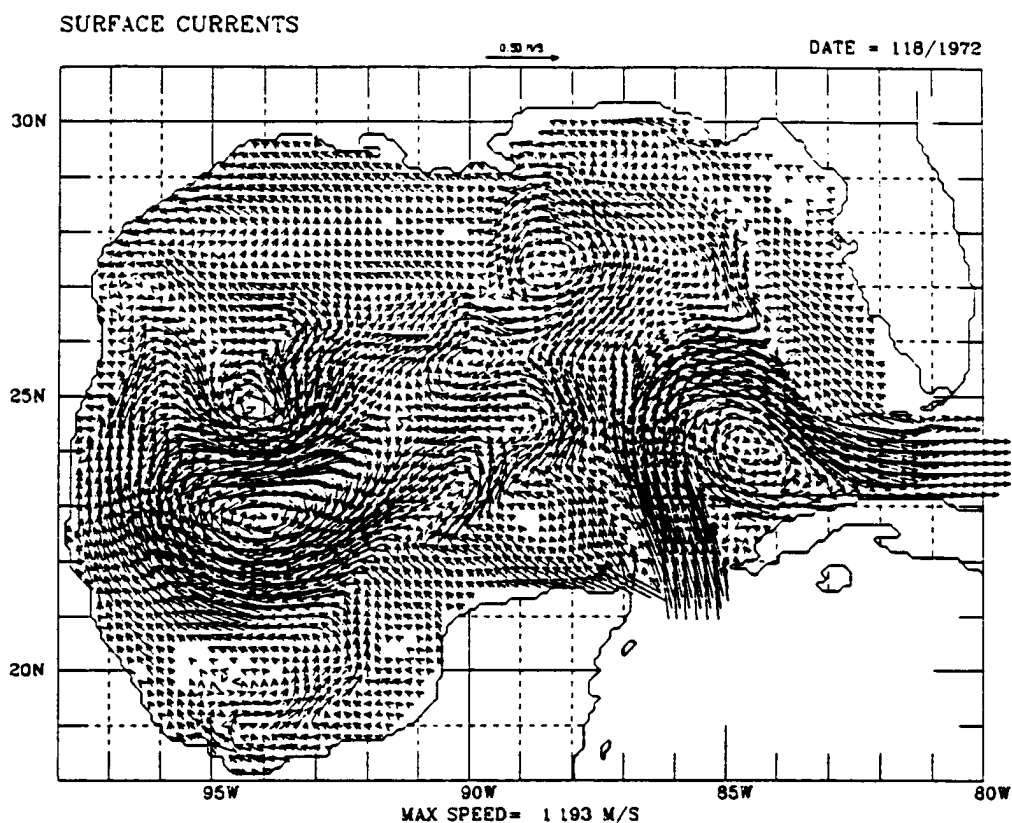
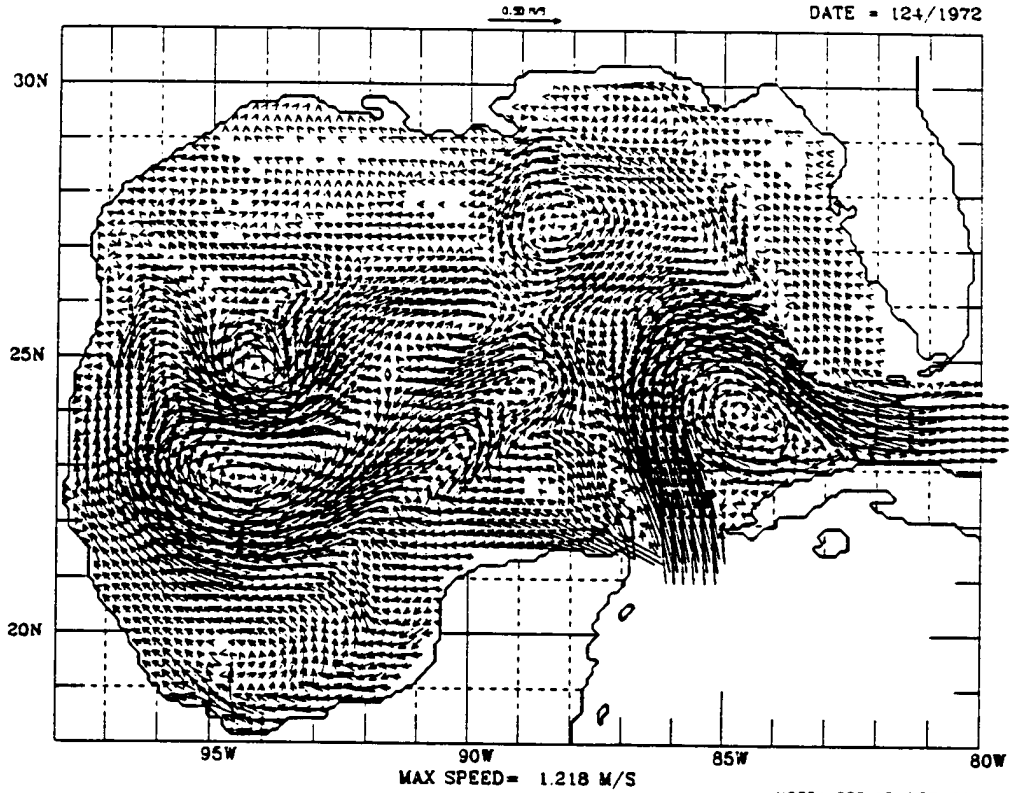


FIGURE 154

SURFACE CURRENTS

G. OF MEXICO 21142.2: 0.0
DATE = 124/1972



SURFACE CURRENTS

NORDA 323 12-DEC-89
G. OF MEXICO 21142.2: 0.0
DATE = 127/1972

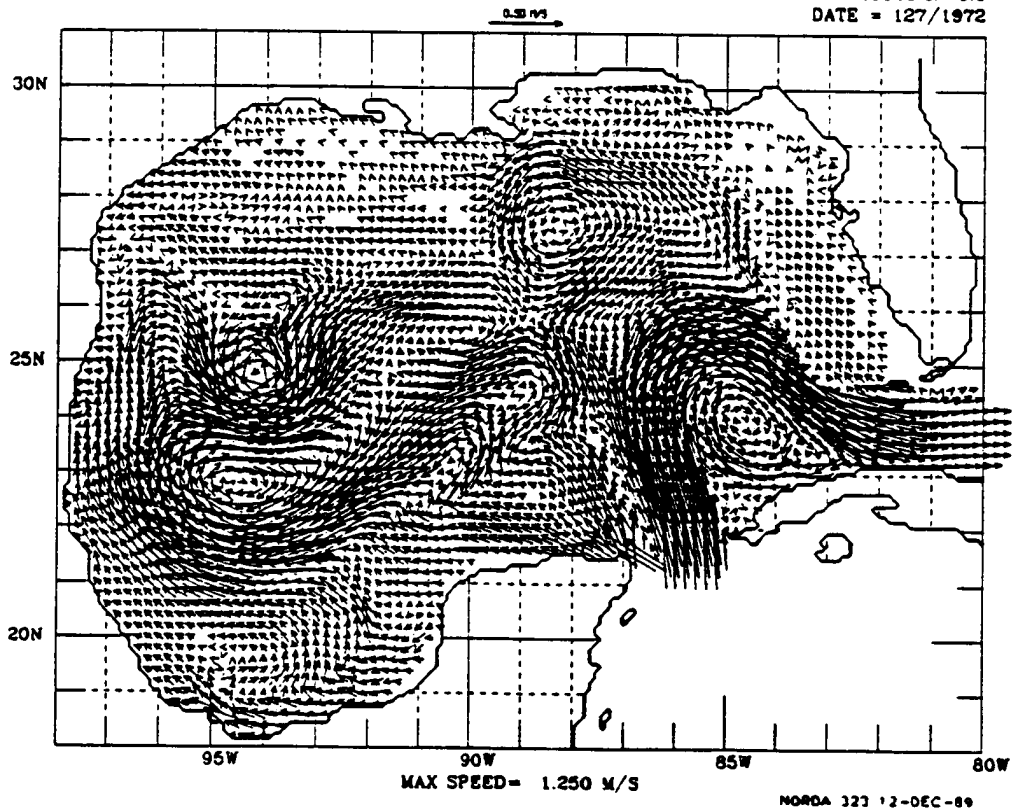
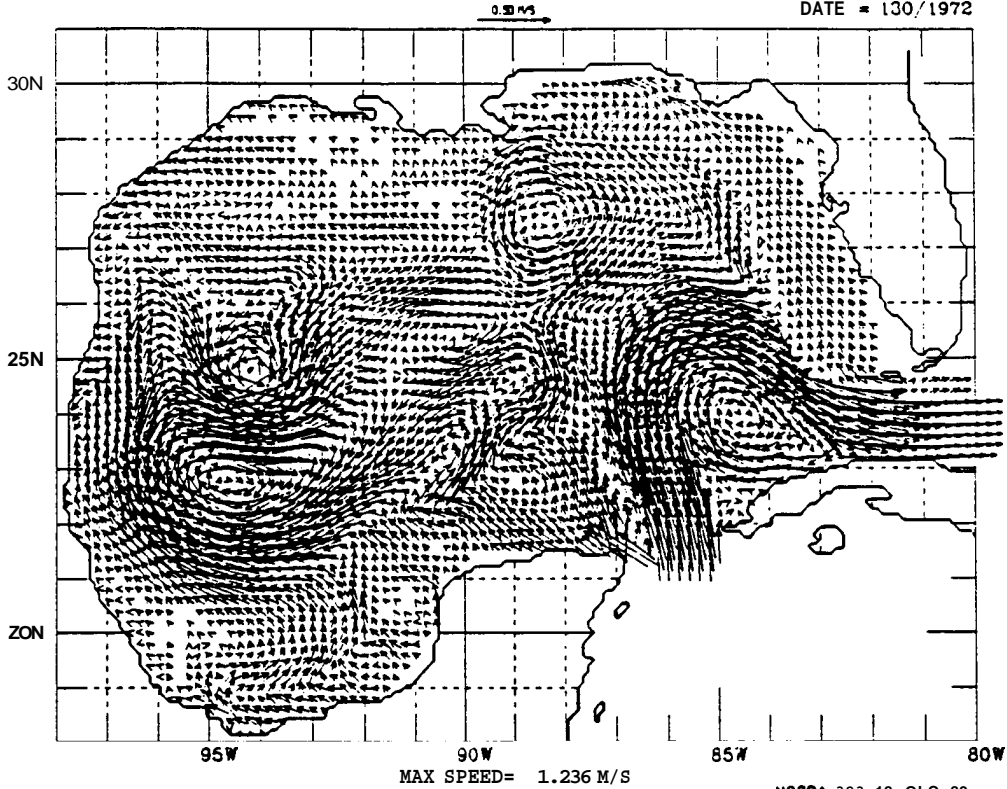


FIGURE 155

SURFACE CURRENTS

G. OF MEXICO 21142.2: 0.0
DATE = 130/1972



SURFACE CURRENTS

NORDA 323 12-OLC-89
G. OF MEXICO 21142.2: 0.0
DATE = 133/1972

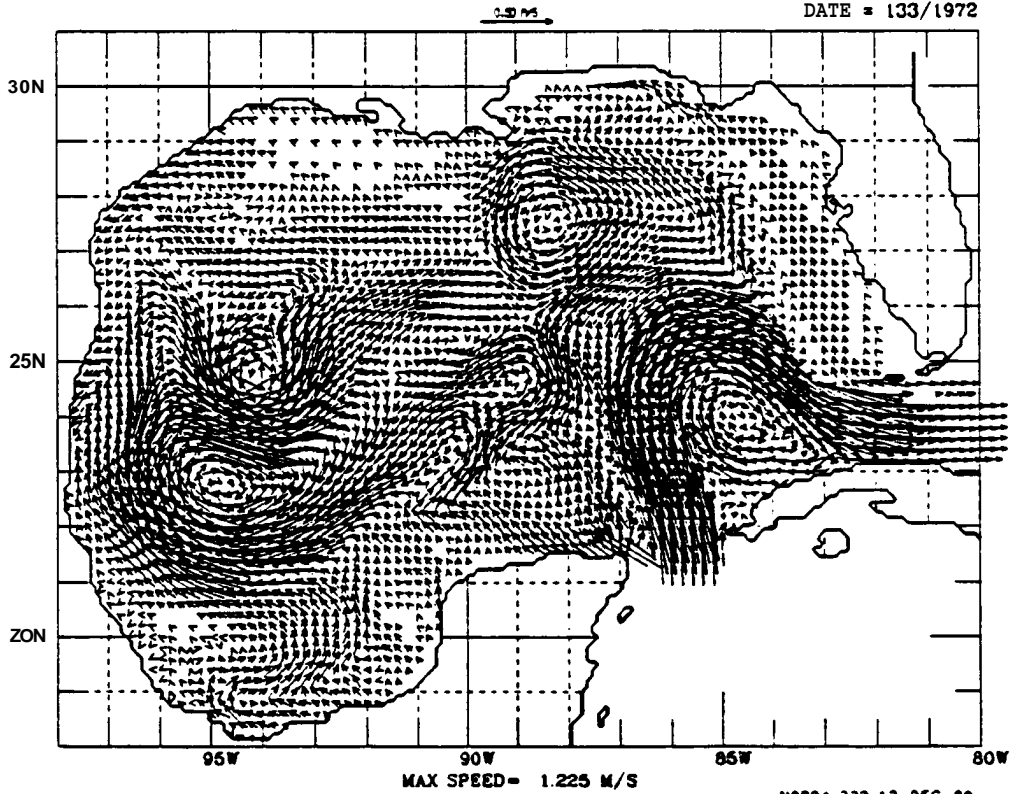
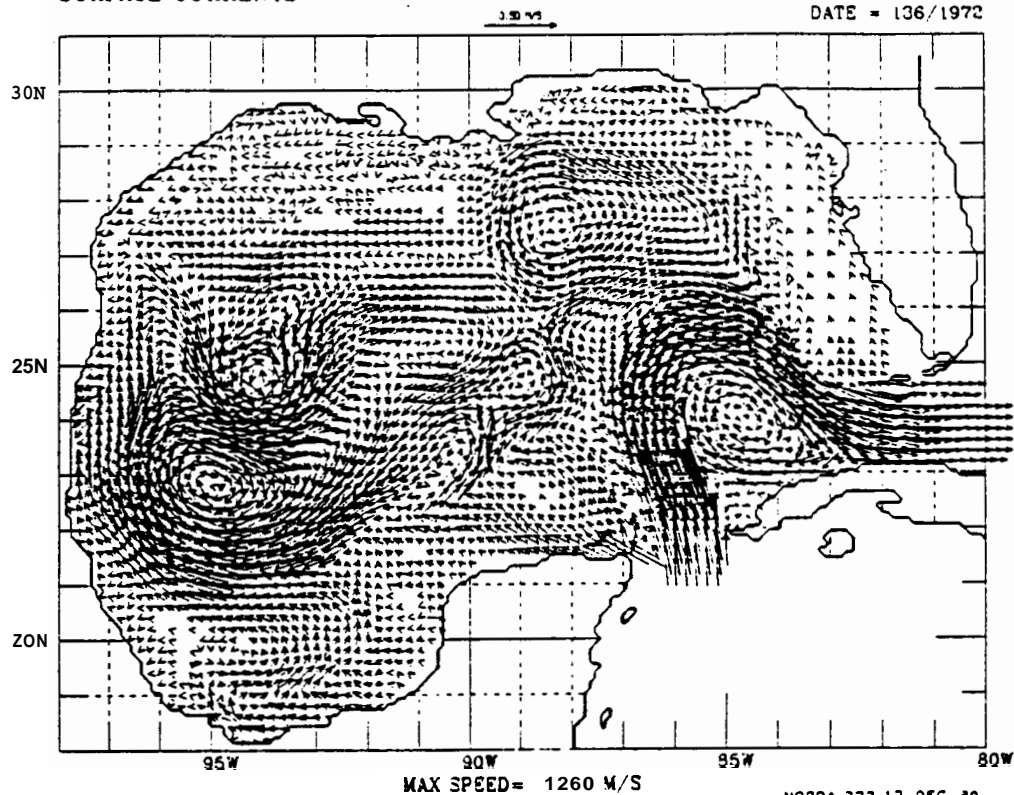


FIGURE 156

SURFACE CURRENTS

G. OF MEXICO 21142.2: 0.0
DATE = 136/1972



SURFACE CURRENTS

G. OF MEXICO 21142.2: 0.0
DATE = 139/1972

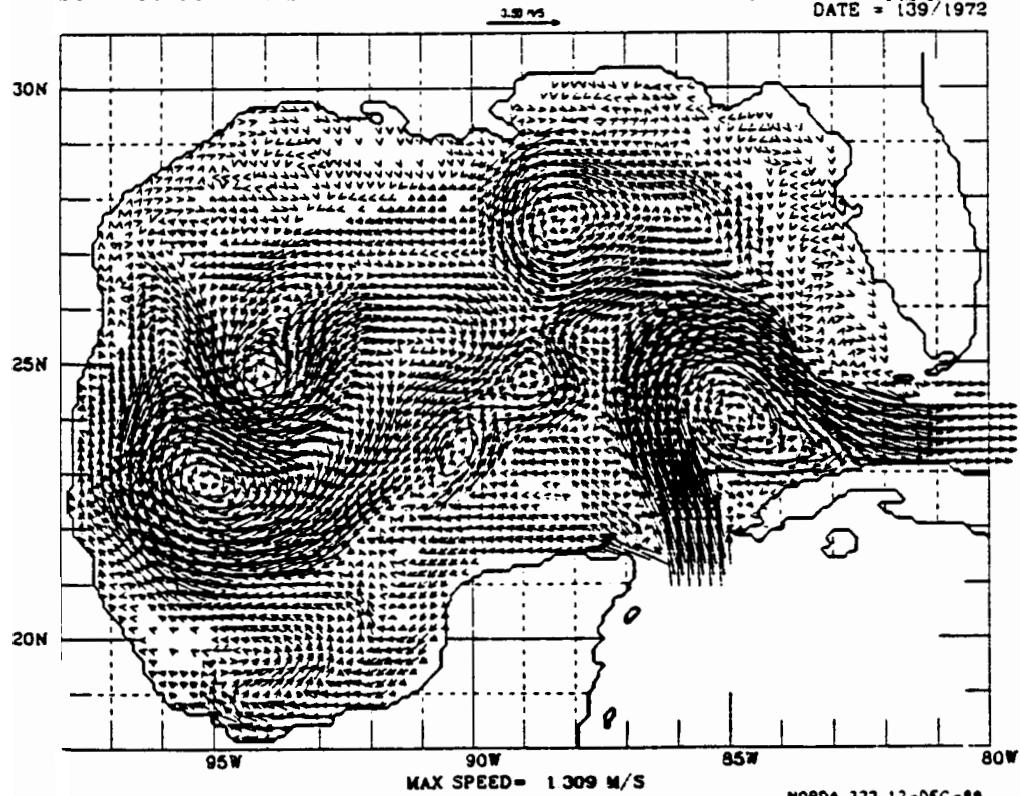
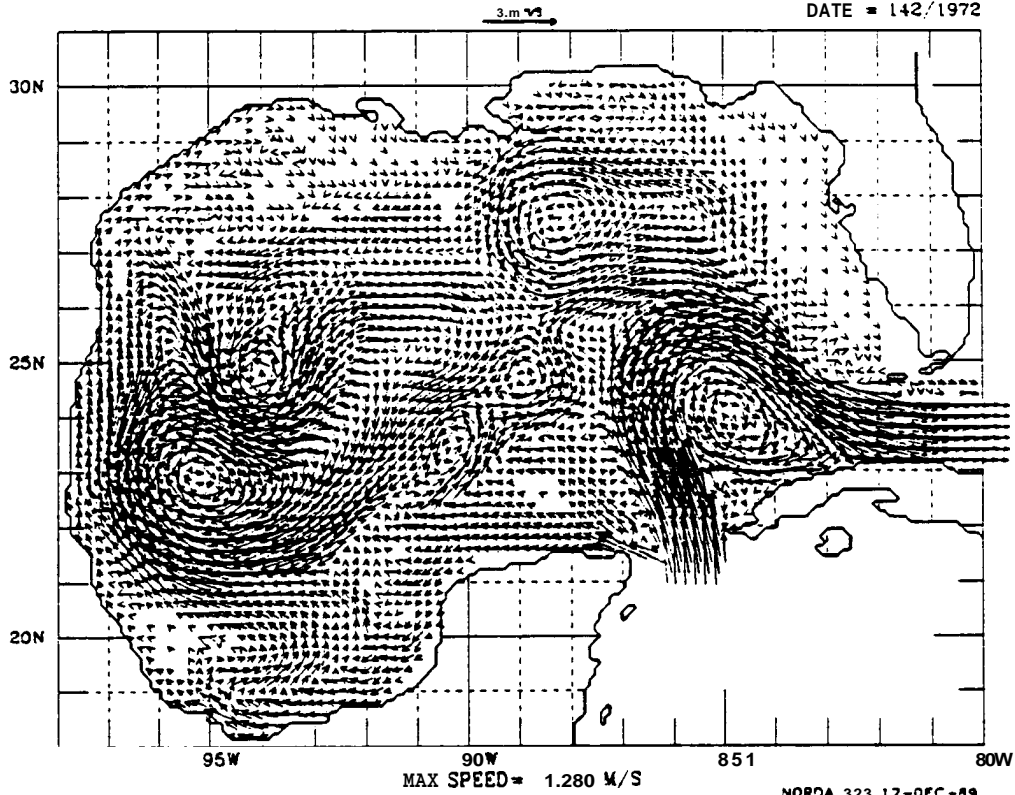


FIGURE 157

SURFACE CURRENTS

G. OF MEXICO 21142-2: 0.0
DATE = 142/1972



SURFACE CURRENTS

C. OF MEXICO 21142-2: 0.0
DATE = 145/1972

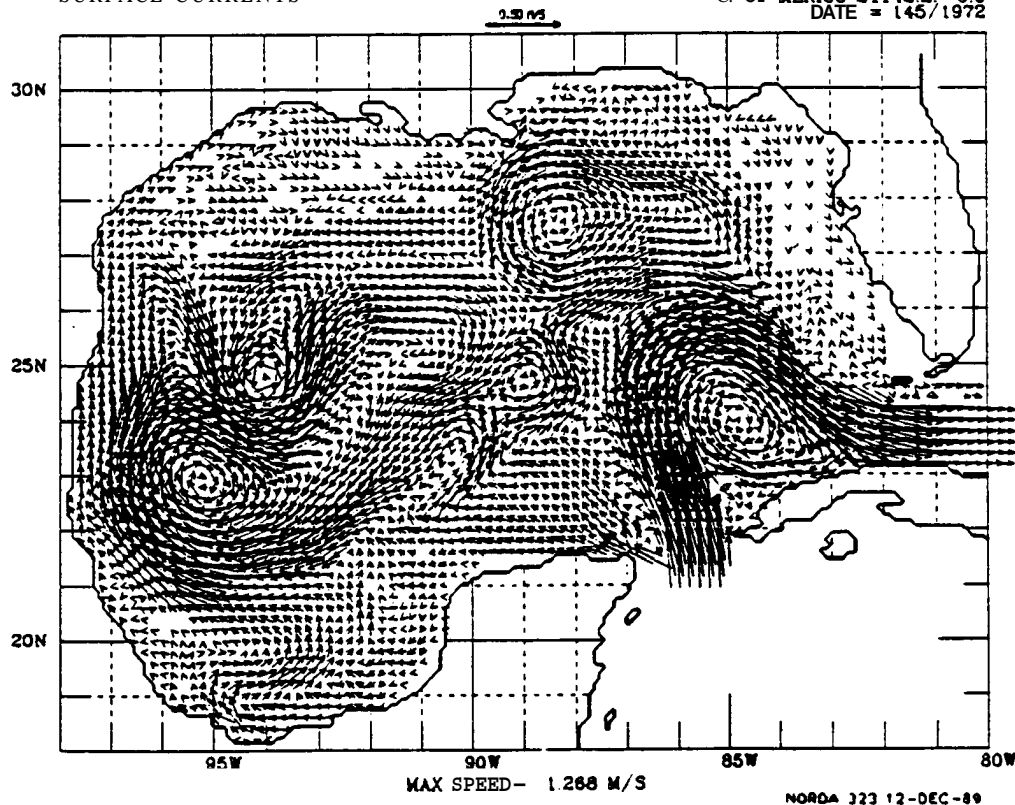
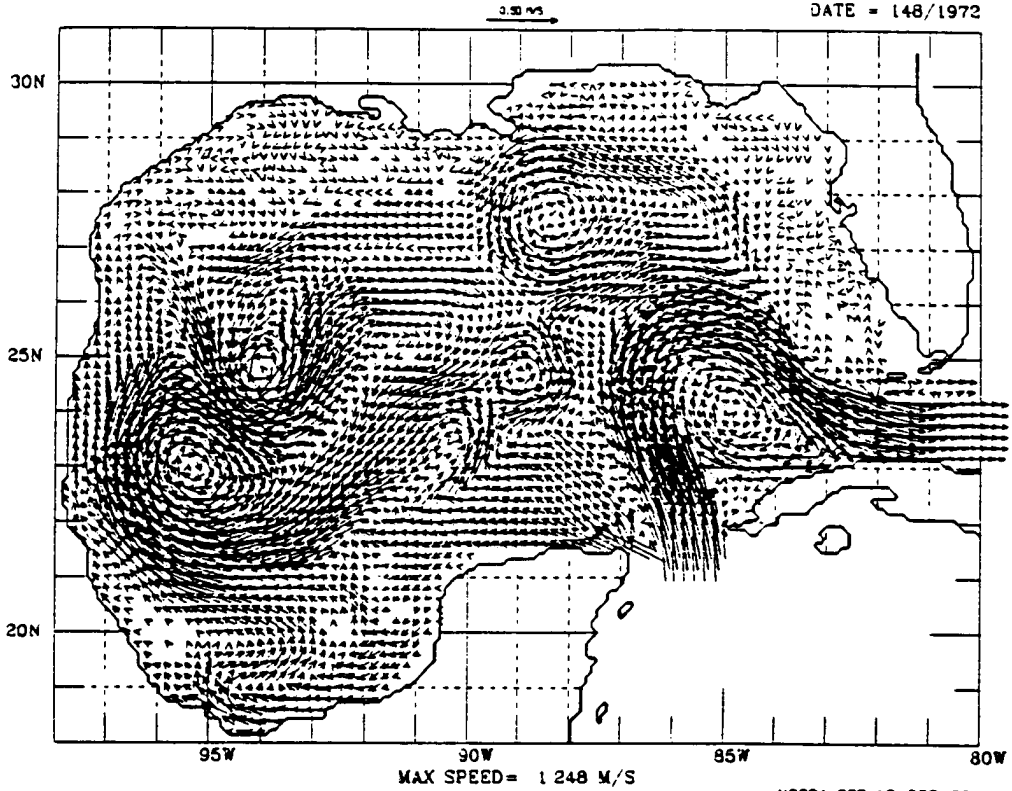


FIGURE 158

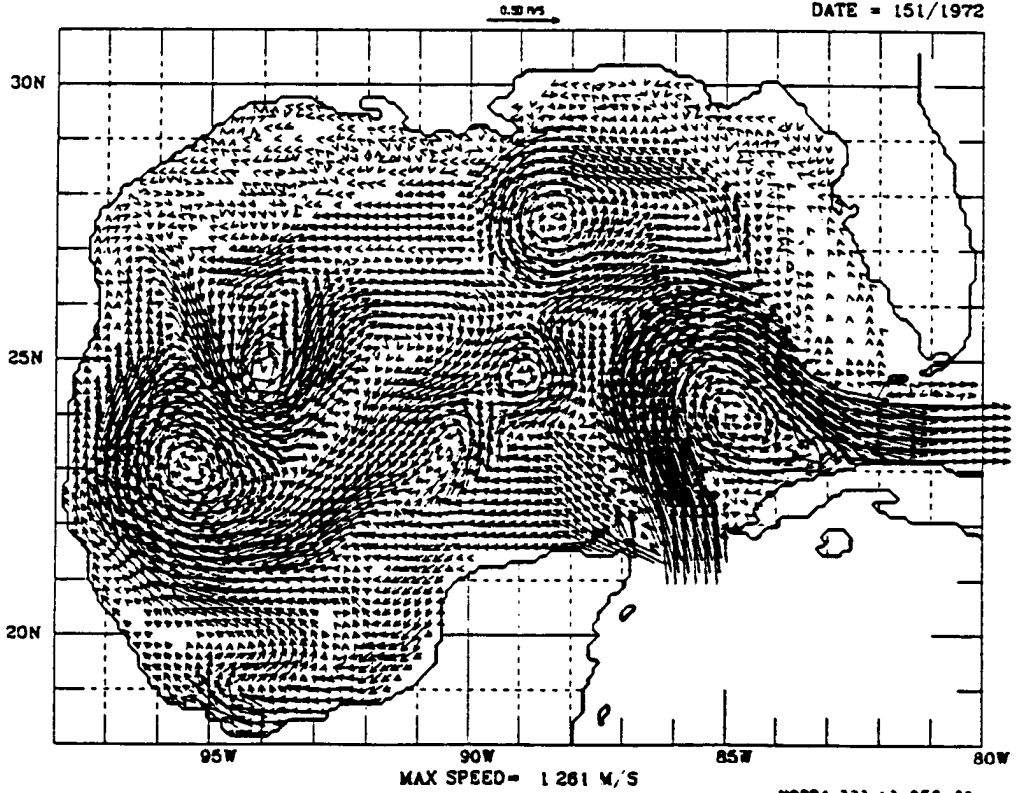
SURFACE CURRENTS

G. OF MEXICO 211422: 0.0
DATE = 148/1972



SURFACE CURRENTS

NORDA 323 12-DEC-89
G. OF MEXICO 211422: 0.0
DATE = 151/1972



NORDA 323 12-DEC-89

FIGURE 159

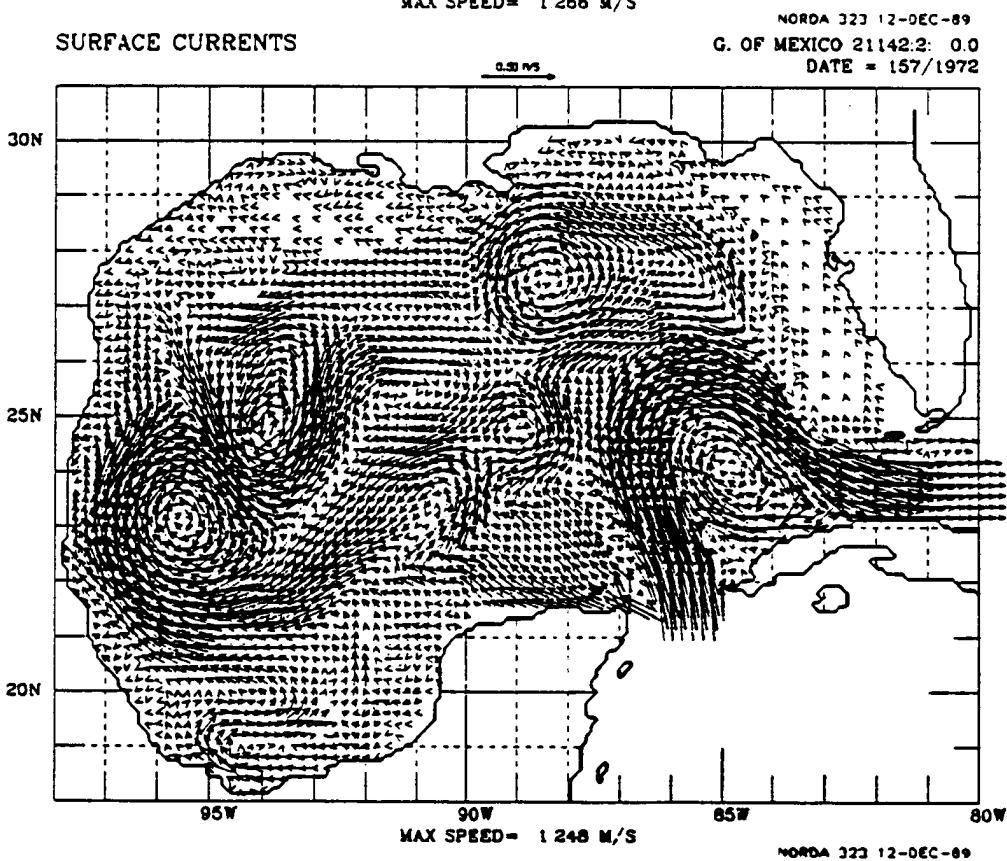
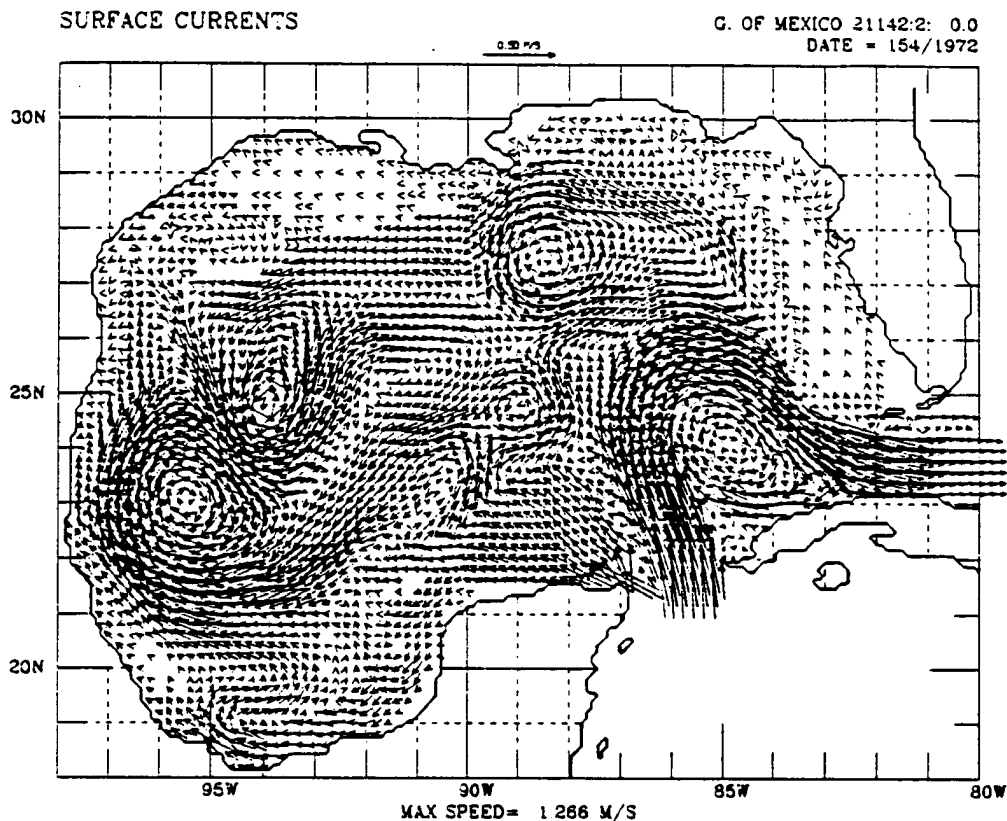


FIGURE 160

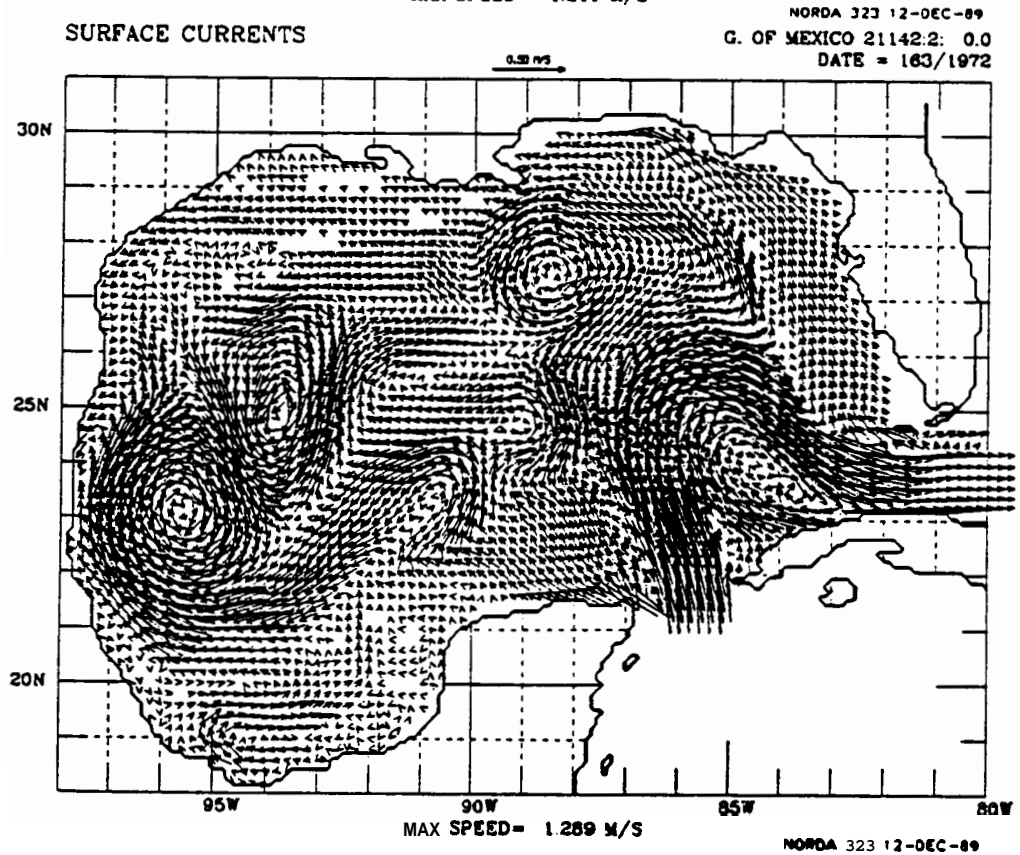
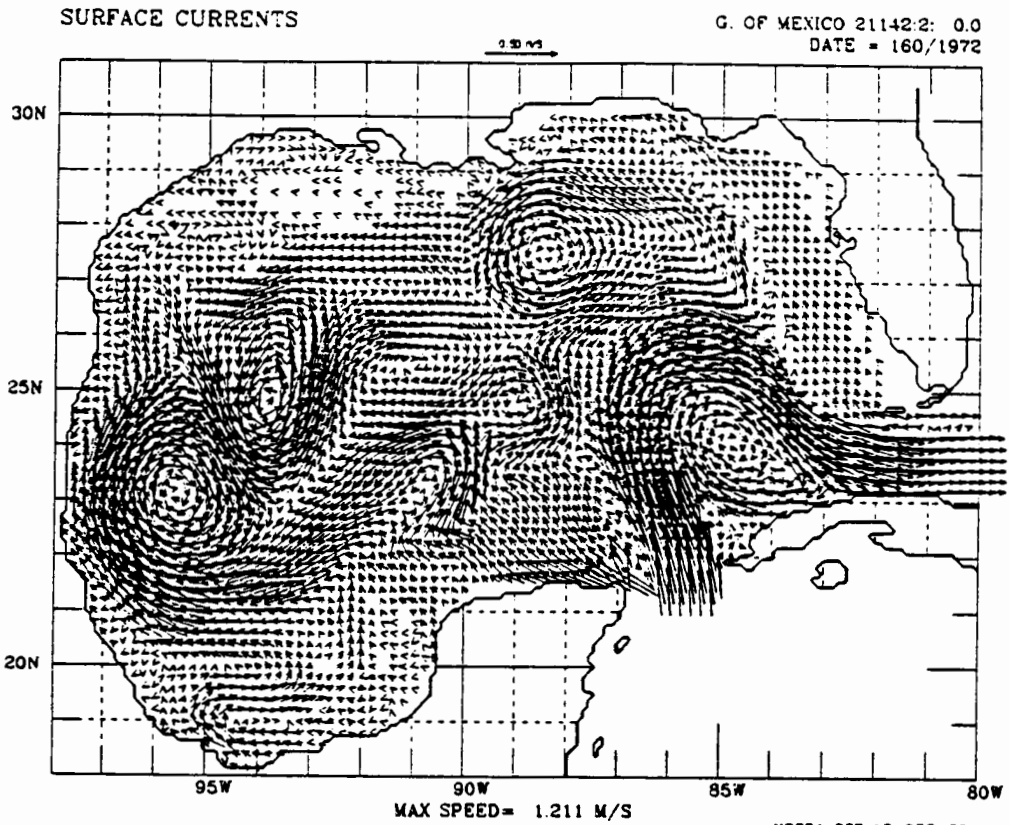
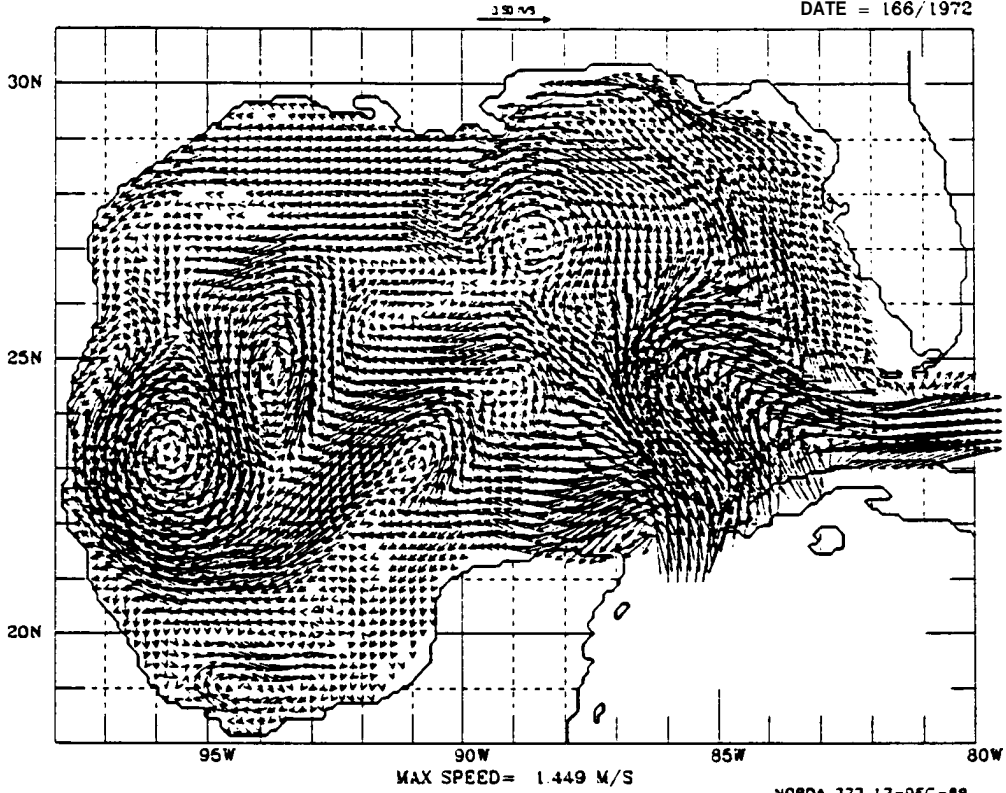


FIGURE 161

SURFACE CURRENTS

G. OF MEXICO 21142.2: 0 0
DATE = 166/1972



SURFACE CURRENTS

NORDA 323 12-DEC-89
G. OF MEXICO 21142.2: 0 0
DATE = 169/1972

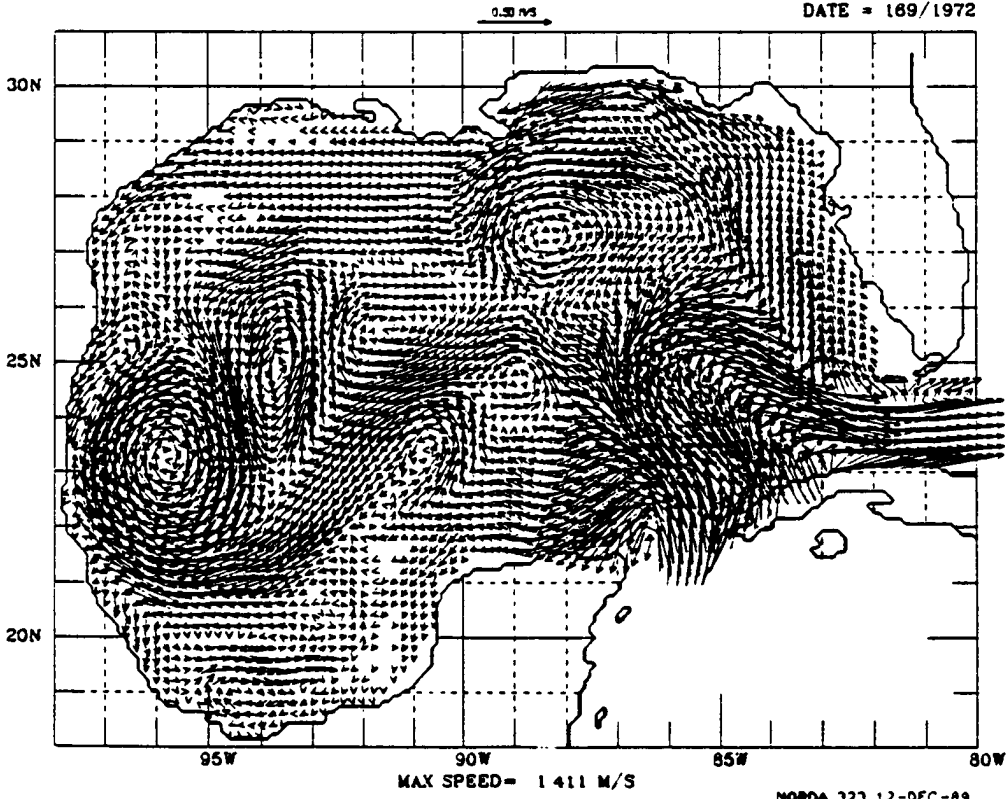
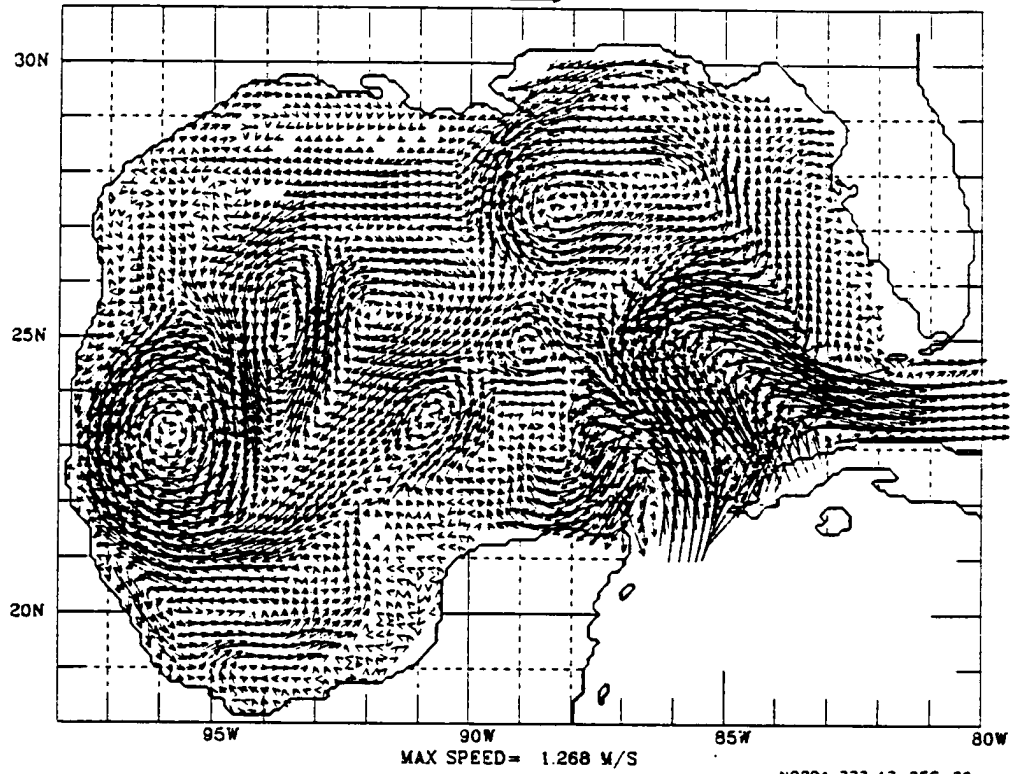


FIGURE 162

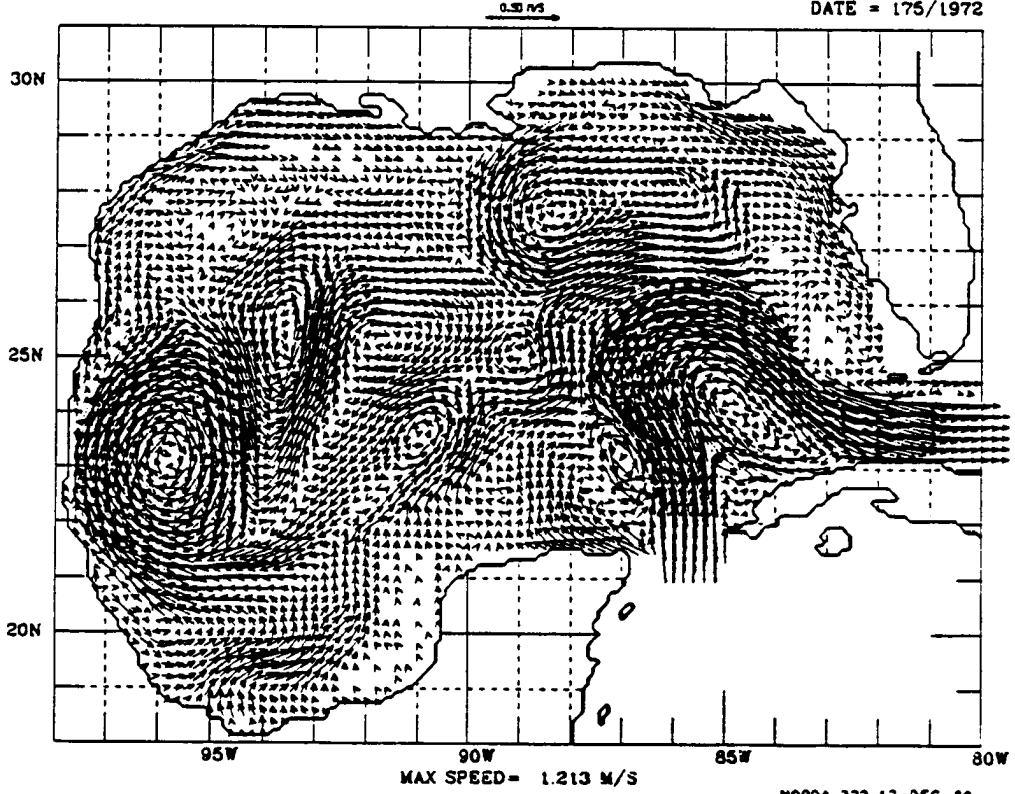
SURFACE CURRENTS

G. OF MEXICO 21142.2: 0.0
DATE = 172/1972



SURFACE CURRENTS

NORDA 323 12-DEC-89
G. OF MEXICO 21142.2: 0.0
DATE = 175/1972



NORDA 323 12-DEC-89

FIGURE 163

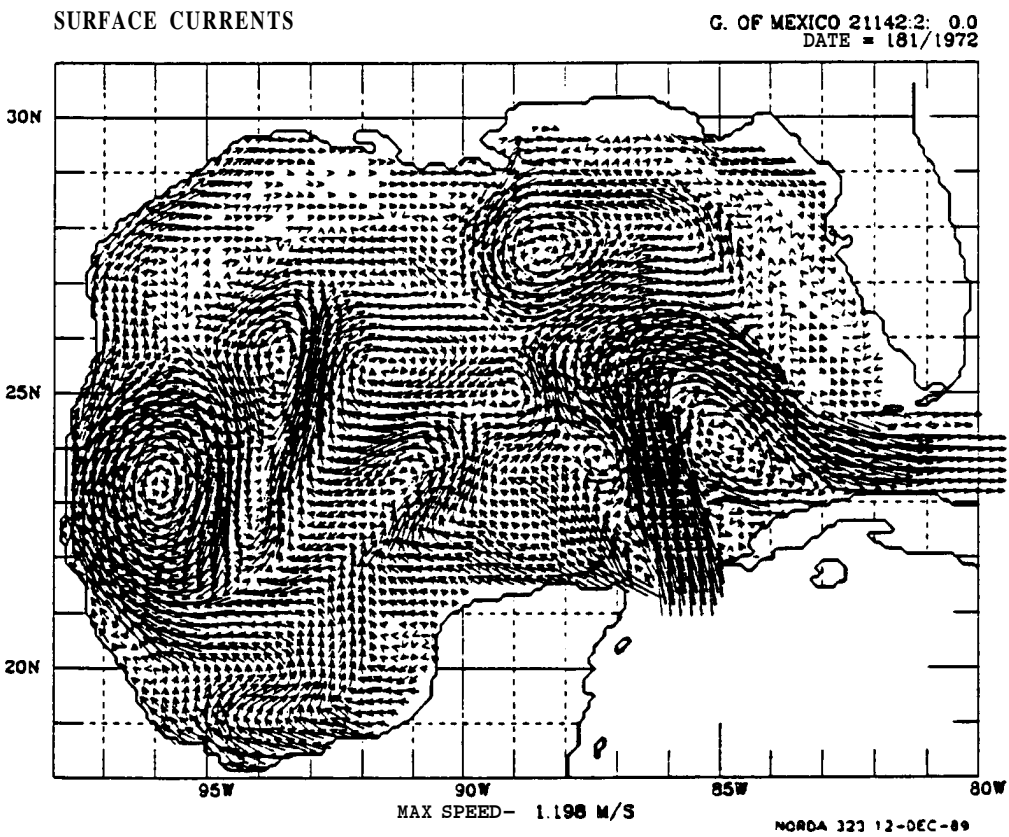
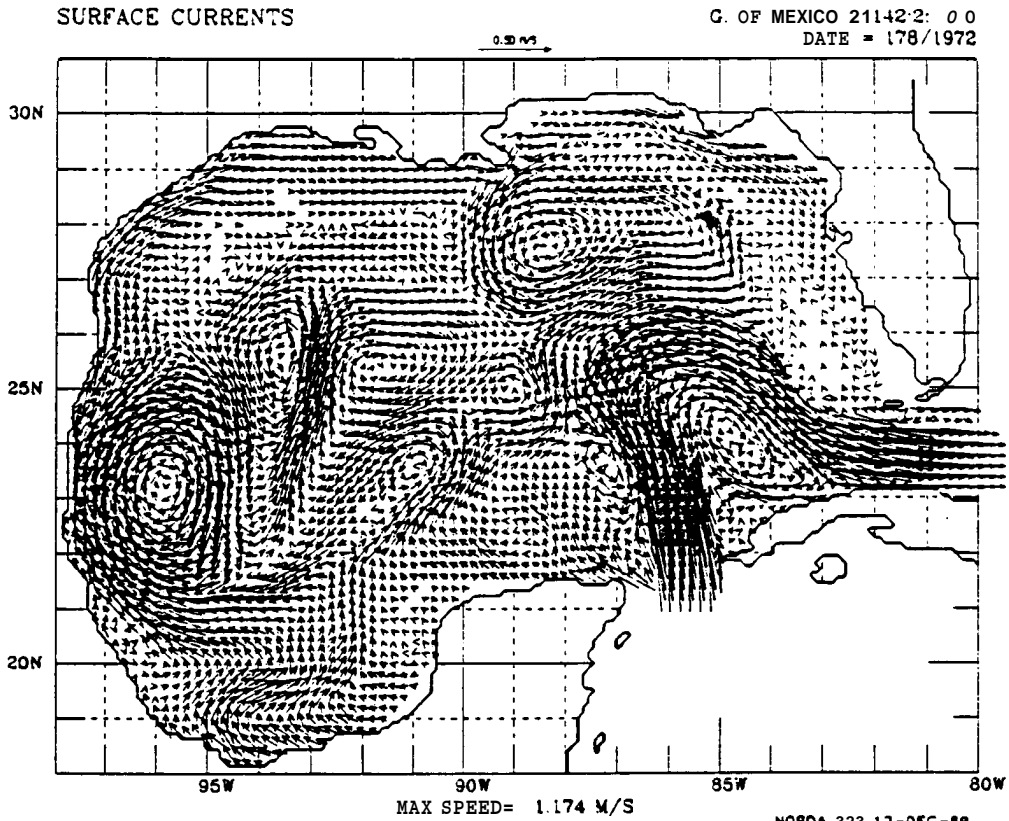
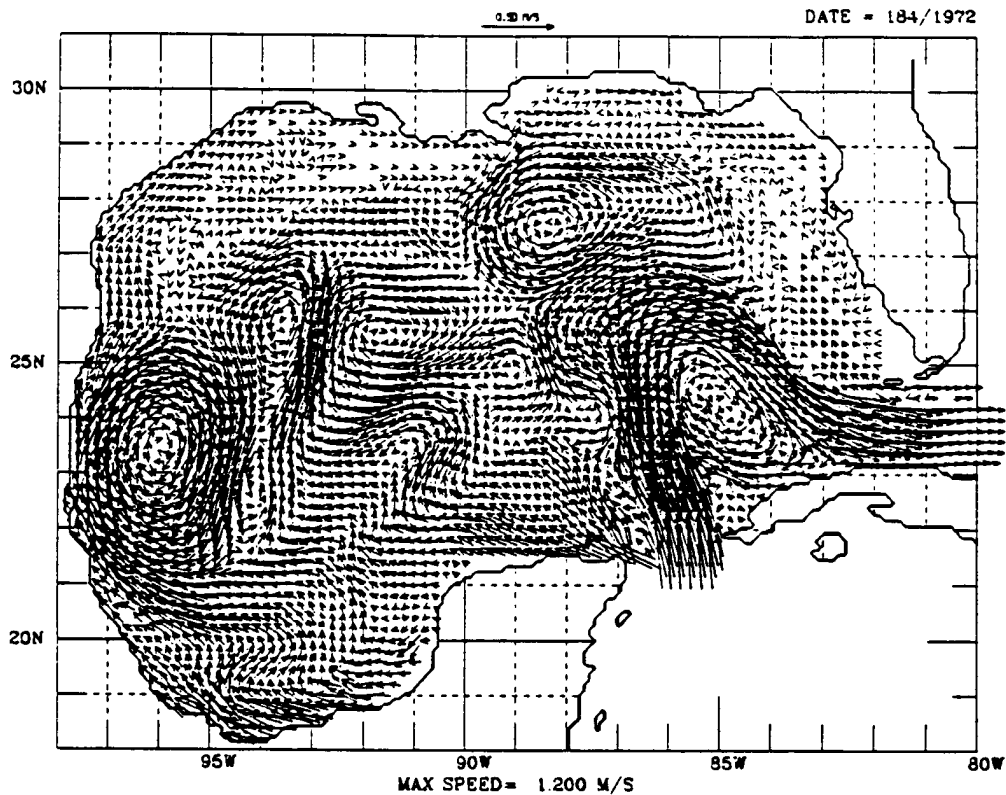


FIGURE 164

SURFACE CURRENTS

G. OF MEXICO 21142:2: 0.0
DATE = 184/1972



SURFACE CURRENTS

NORDA 323 12-DEC-89
G. OF MEXICO 21142:2: 0.0
DATE = 187/1972

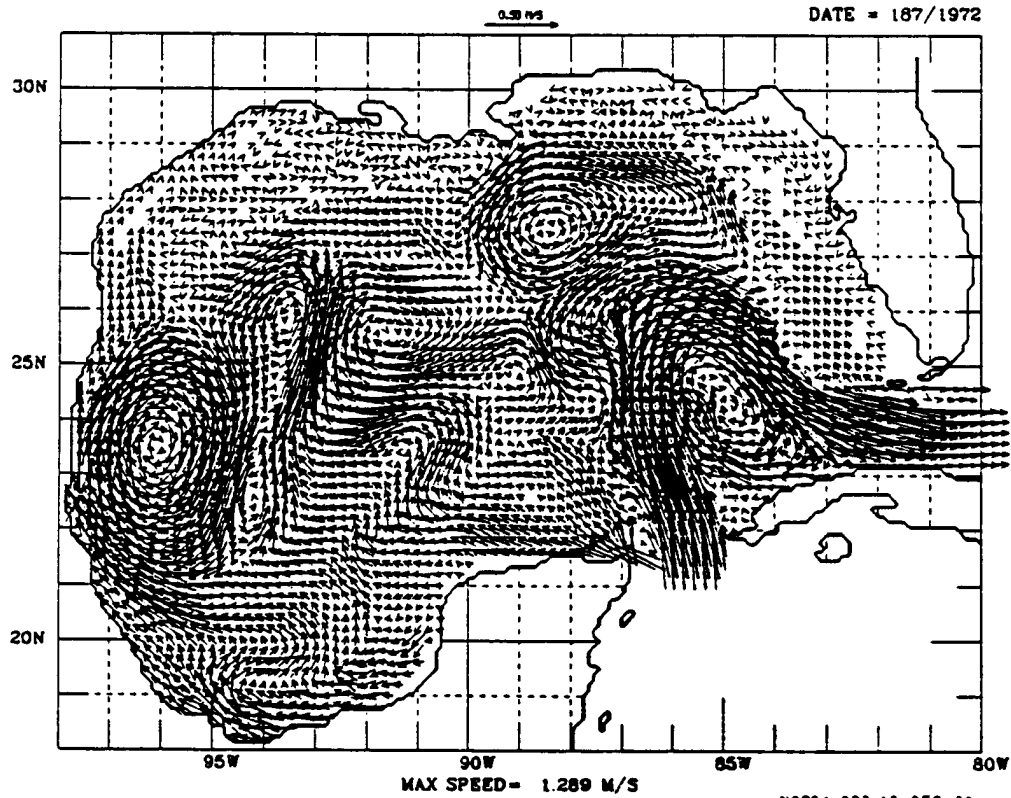


FIGURE 165

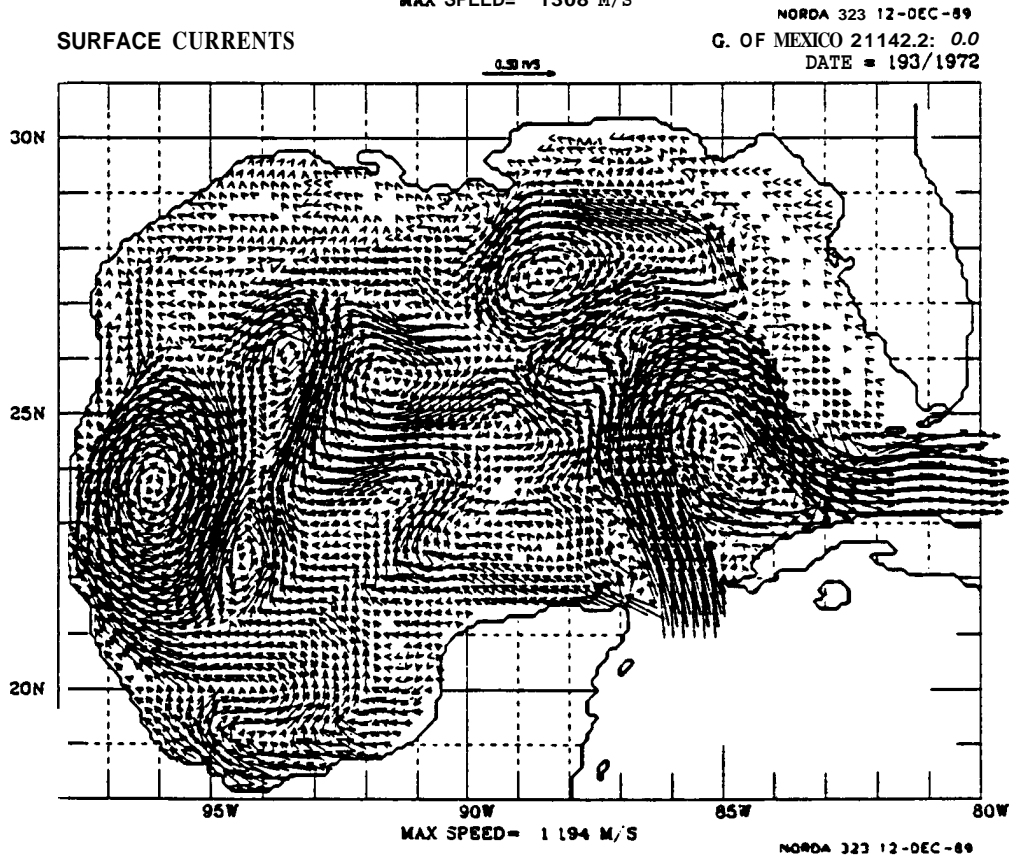
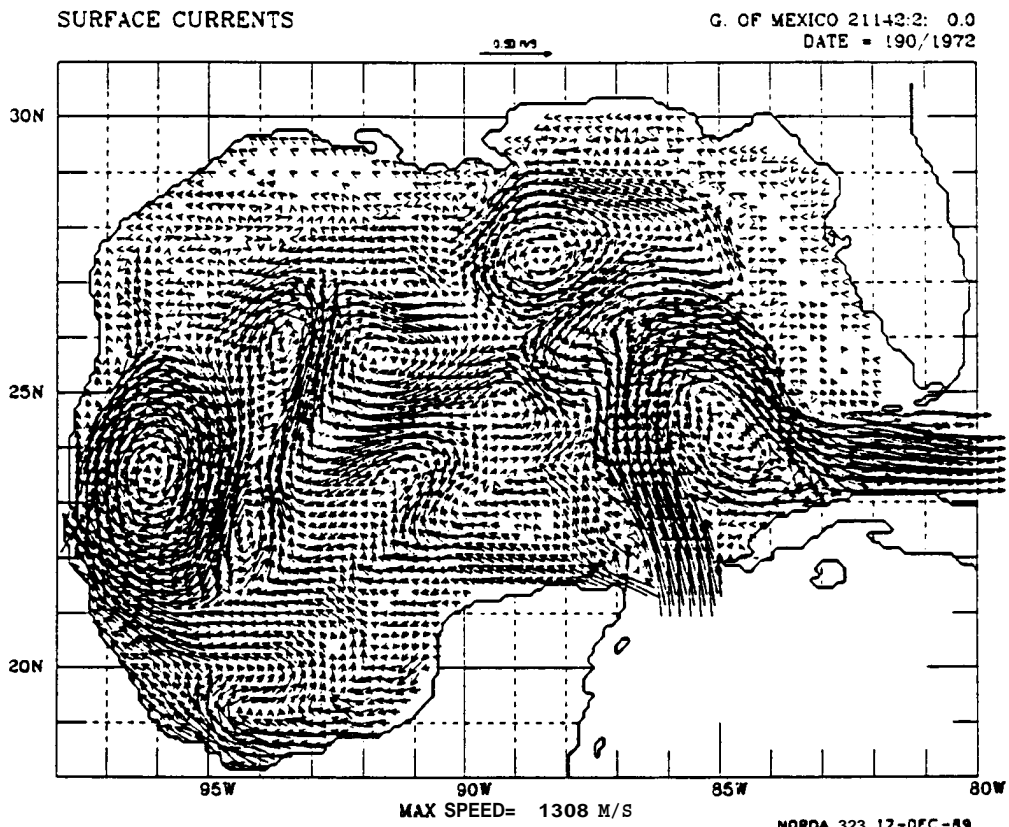


FIGURE 166

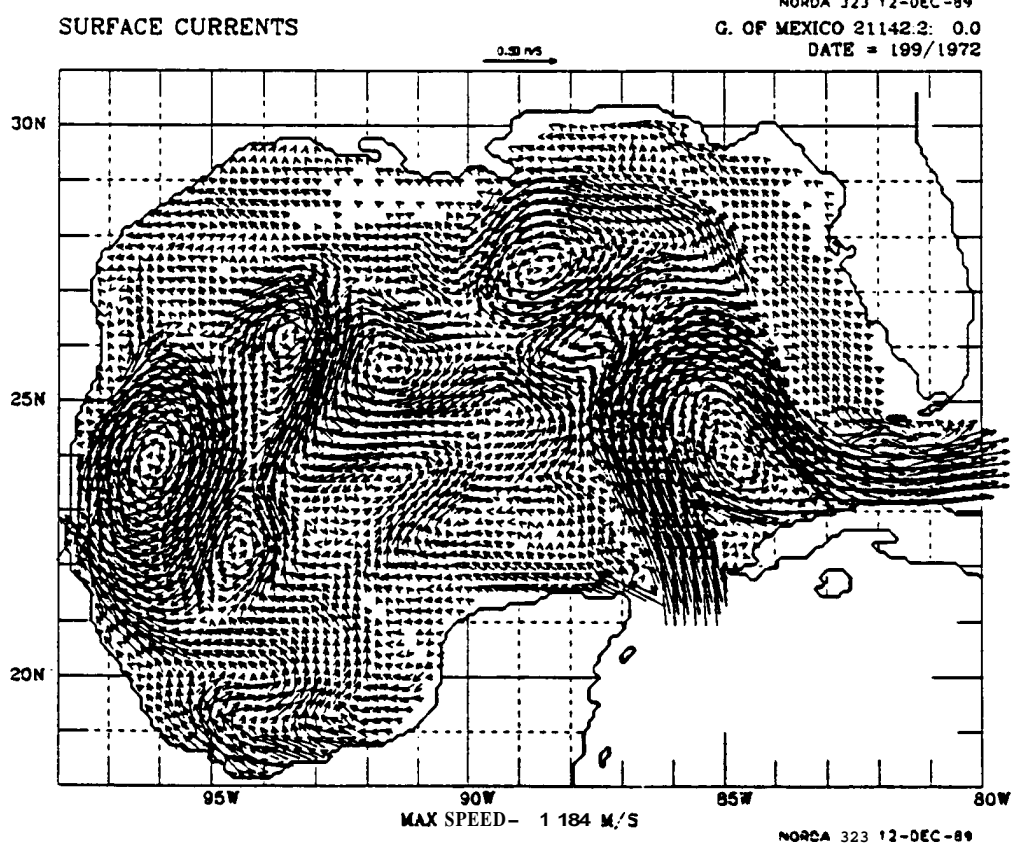
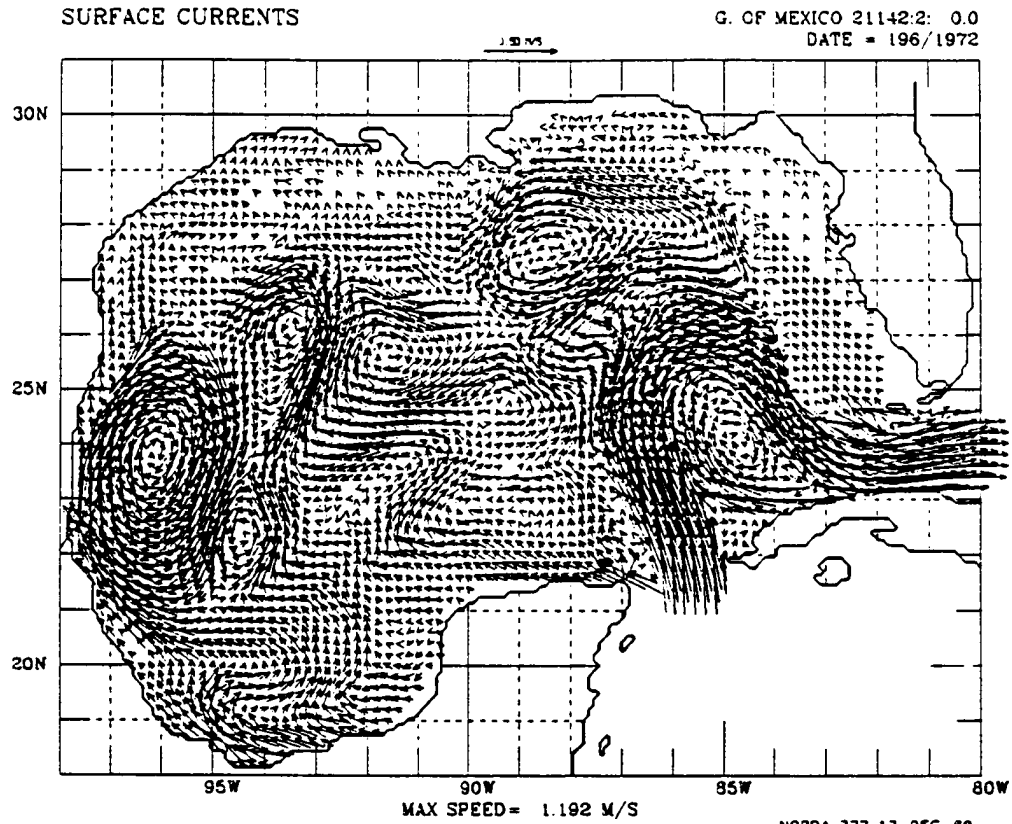
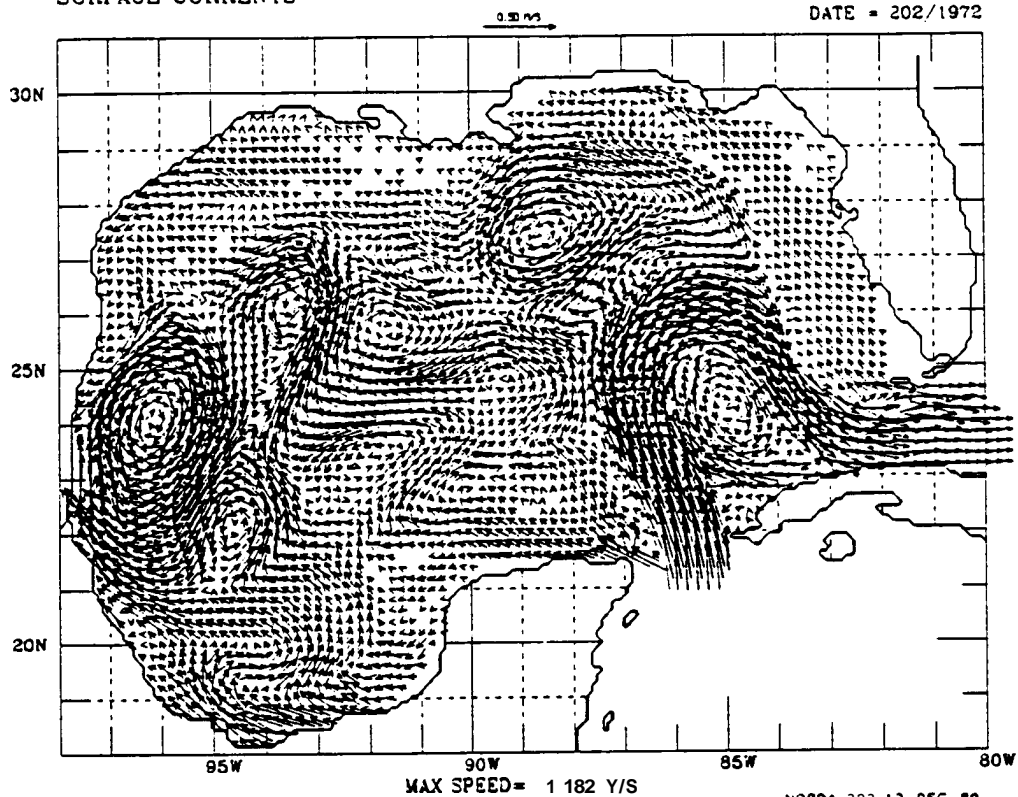


FIGURE 167

SURFACE CURRENTS

G. OF MEXICO 21142:2: 0.0
DATE = 202/1972



SURFACE CURRENTS

NORDA 323 12-DEC-89
G. OF MEXICO 21112:2: 0.0
DATE = 205/1972

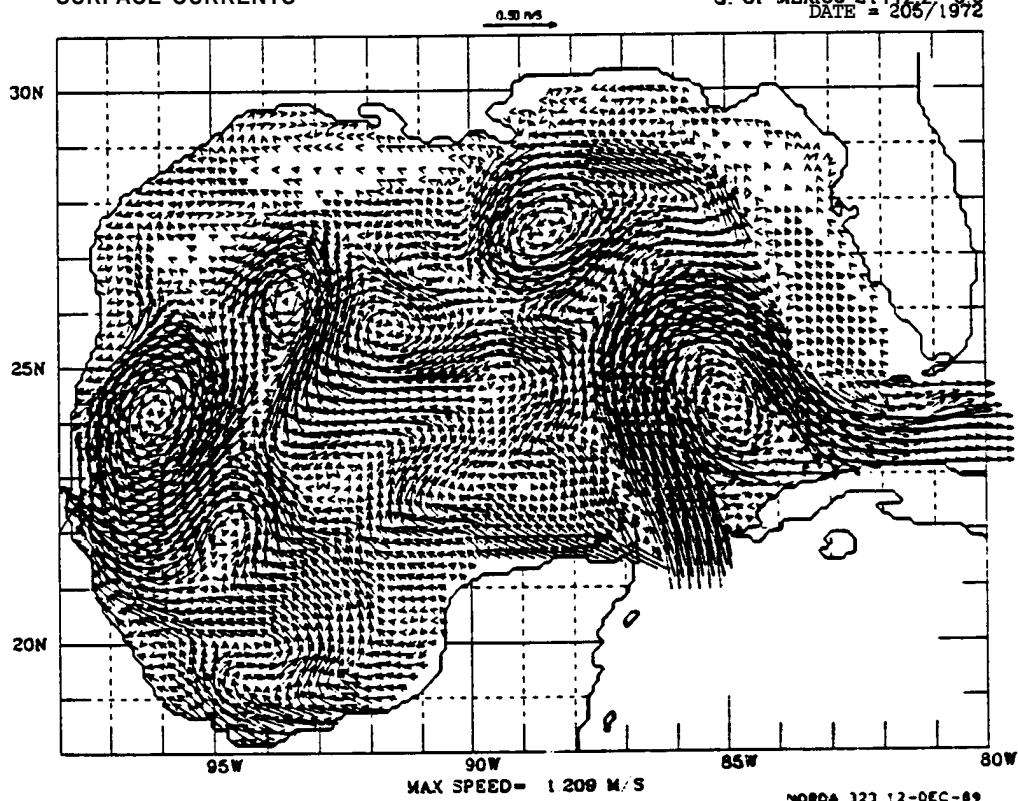
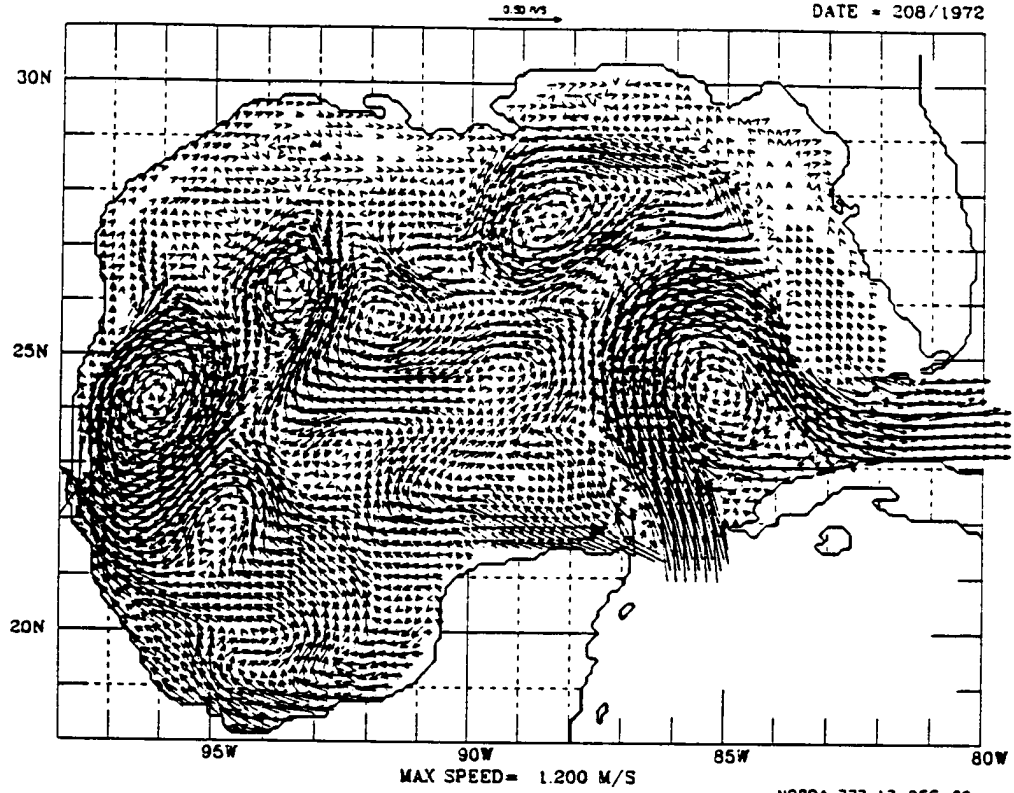


FIGURE 168

SURFACE CURRENTS

G. OF MEXICO 21142:2: 0.0
DATE = 208/1972



SURFACE CURRENTS

NORDA 323 12-DEC-89
G. OF MEXICO 21142:2: 0.0
DATE = 211/1972

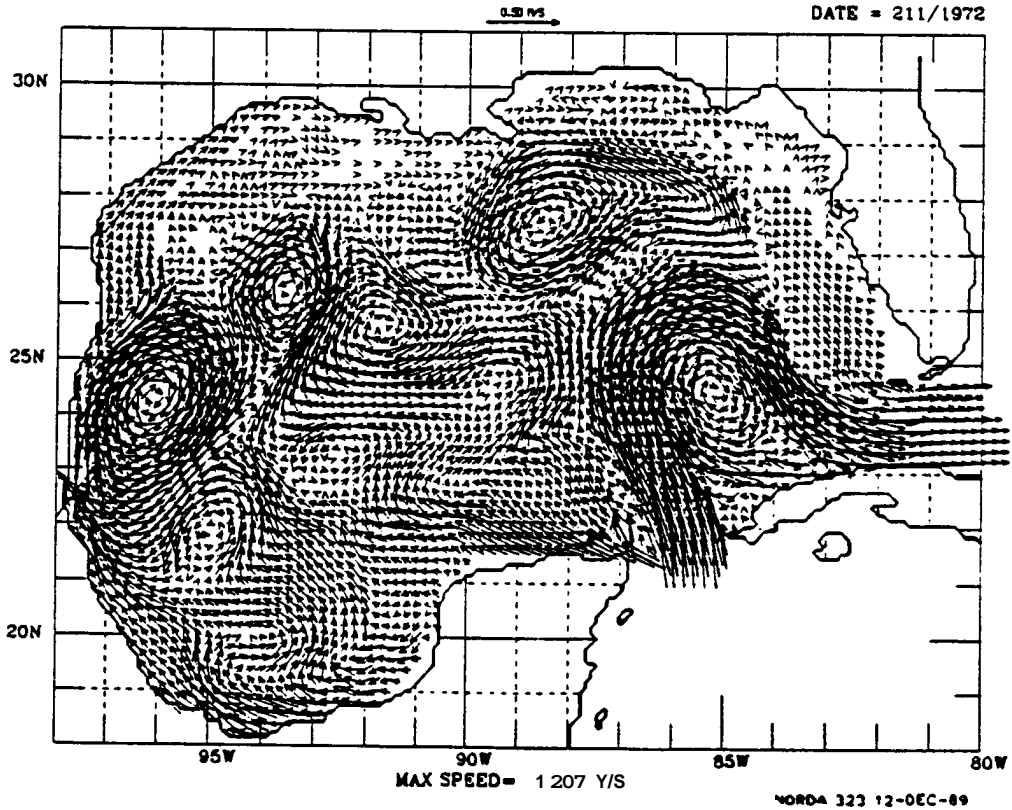
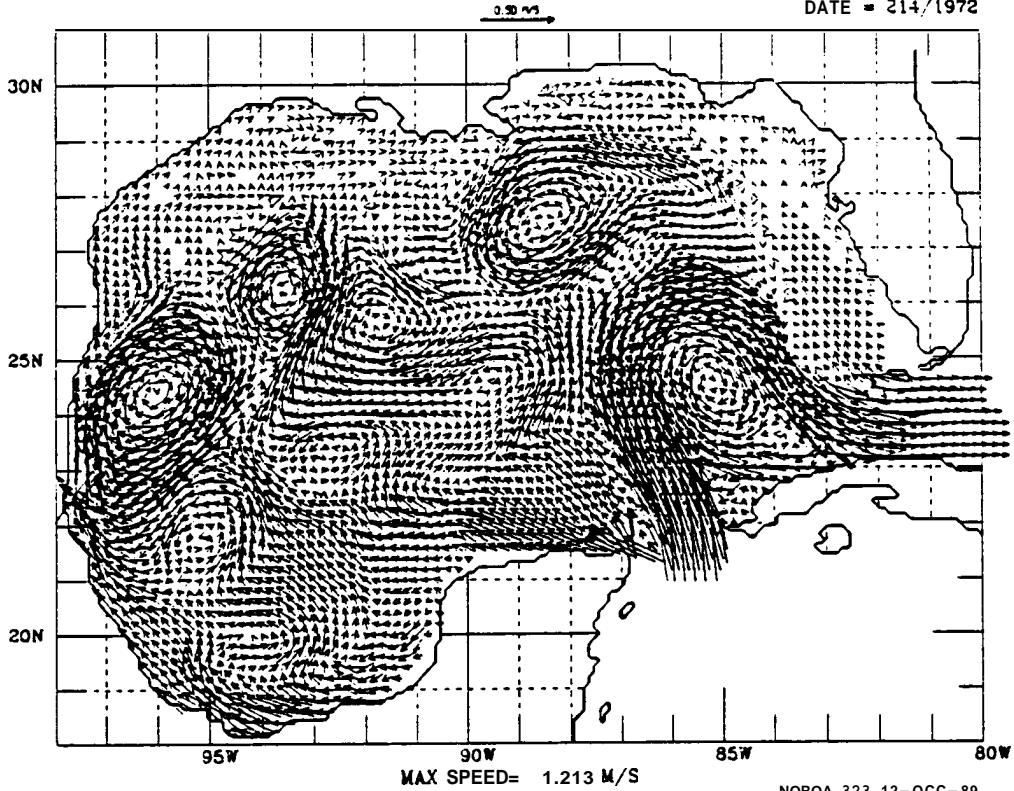


FIGURE 169

SURFACE CURRENTS

G. OF MEXICO 21142.2: 0.0
DATE = 214/1972



SURFACE CURRENTS

G. OF MEXICO 21142.2: 0.0
DATE = 217/1972

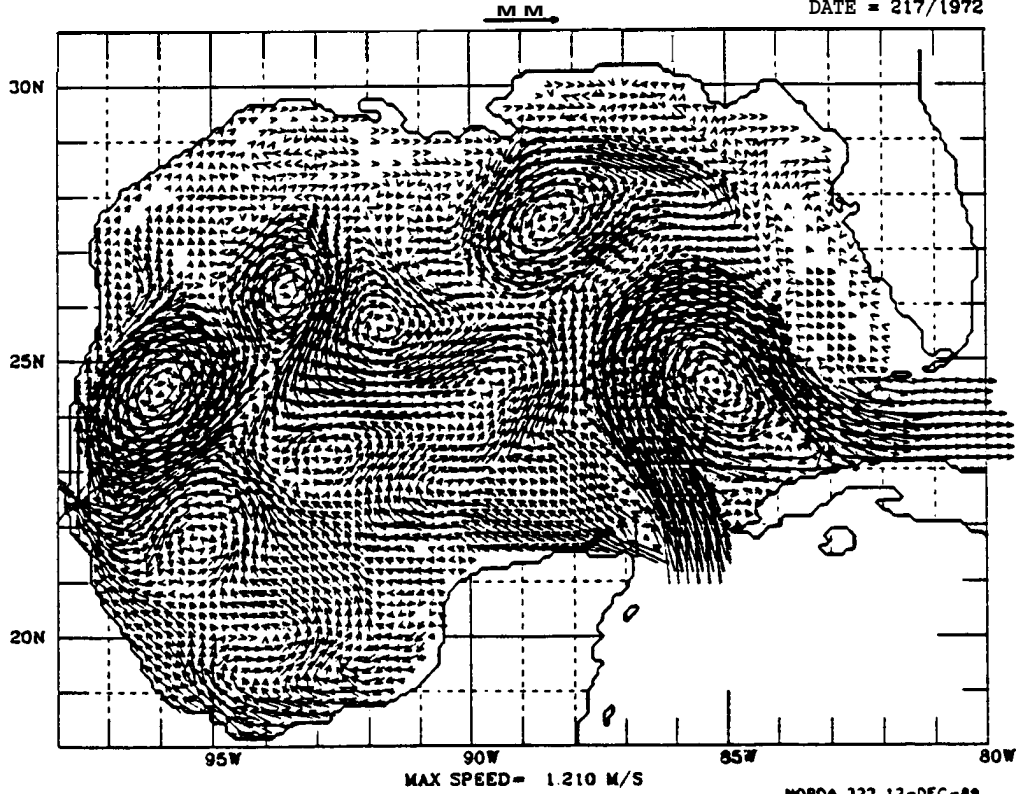
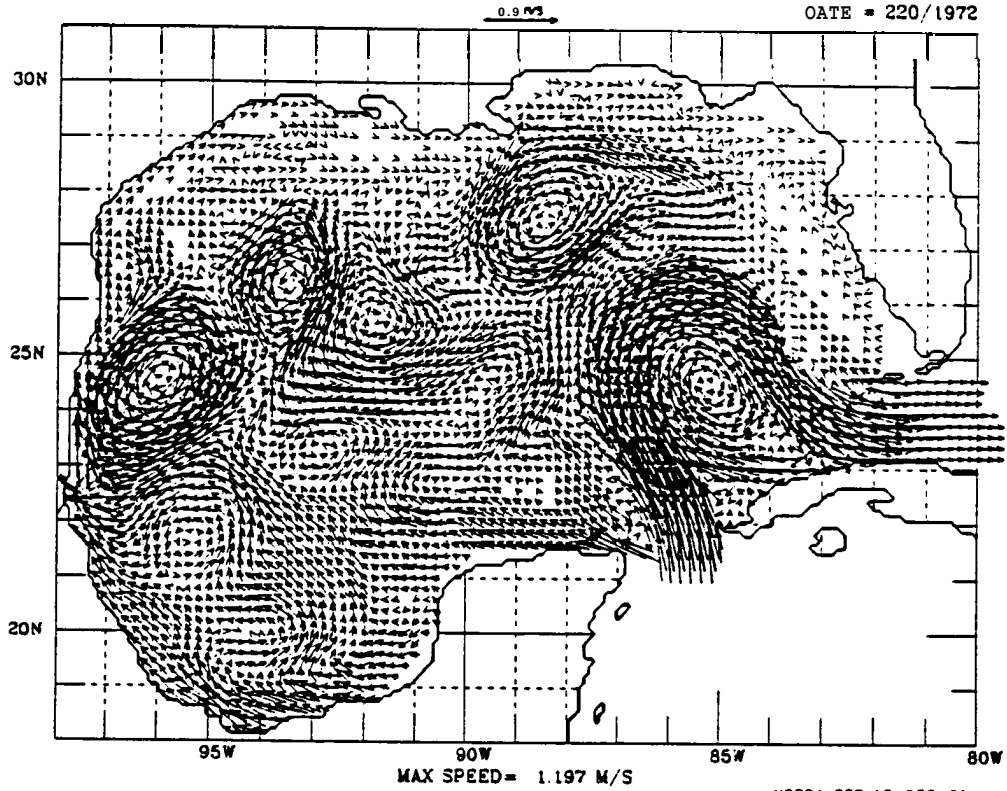


FIGURE 170

SURFACE CURRENTS

G. OF MEXICO 21142.2: 0.0

DATE = 220/1972



SURFACE CURRENTS

NORDA 323 12-DEC-89

G. OF MEXICO 21142.2: 0.0

DATE = 223/1972

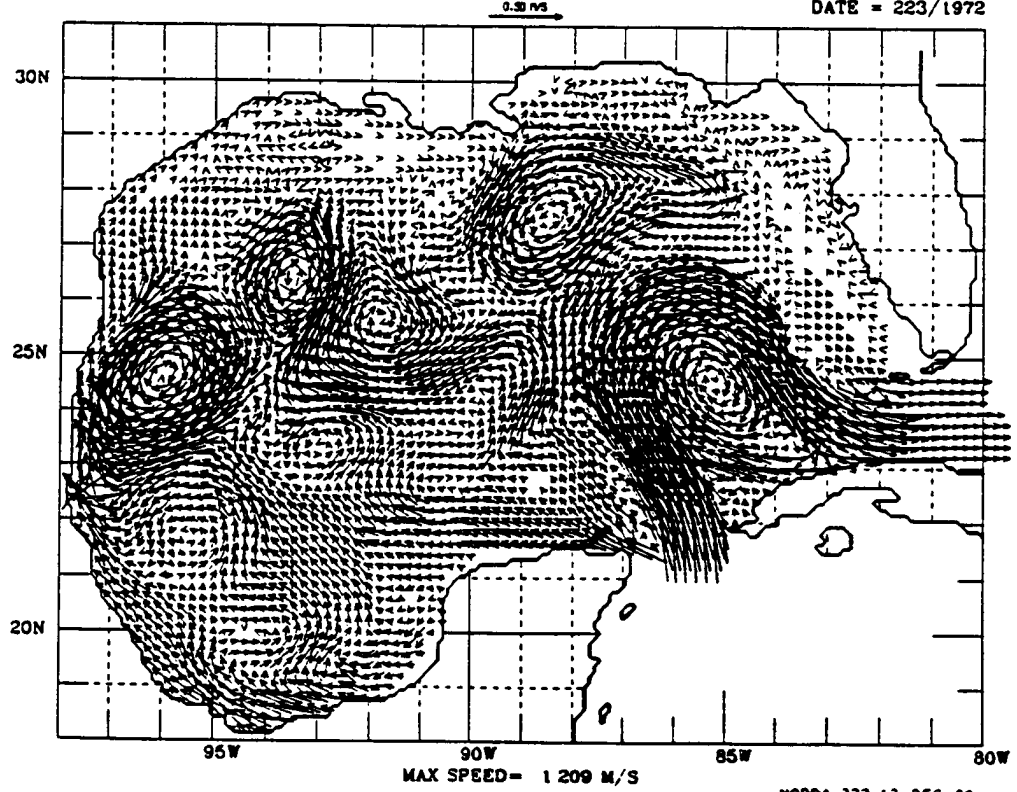
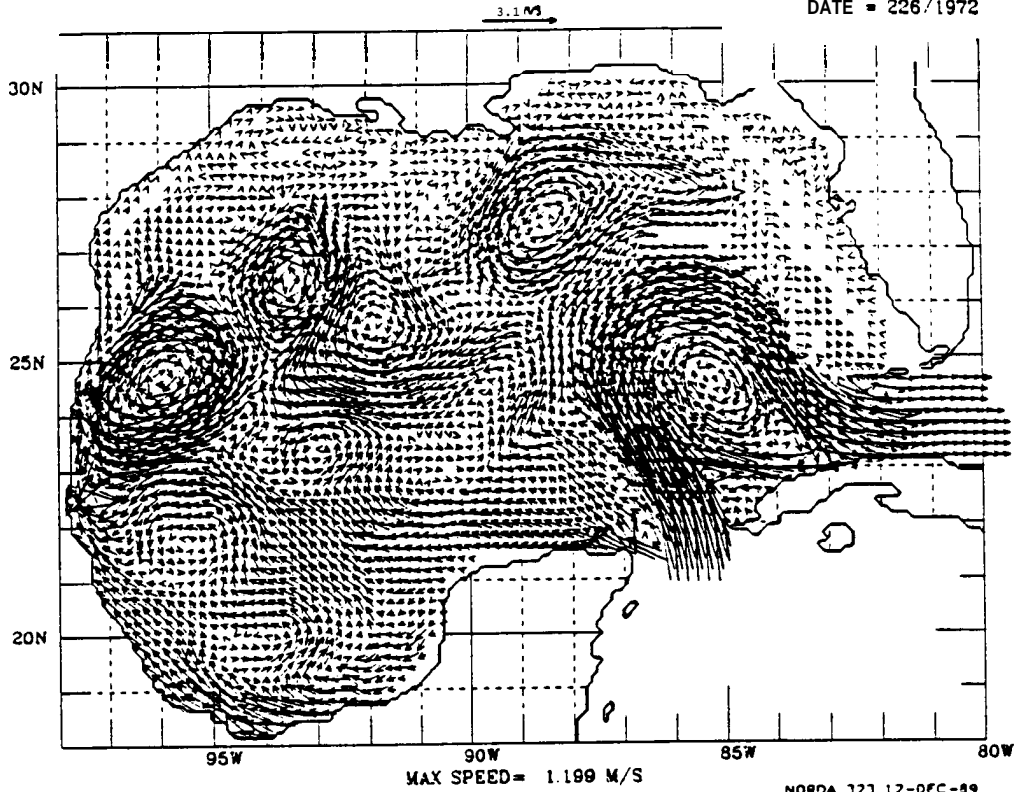


FIGURE 171

SURFACE CURRENTS

G. OF MEXICO 21142.2: 0.0
DATE = 226/1972



SURFACE CURRENTS

NORDA 323 12-DEC-89
G. OF MEXICO 21142.2: 0.0
DATE = 229/1972

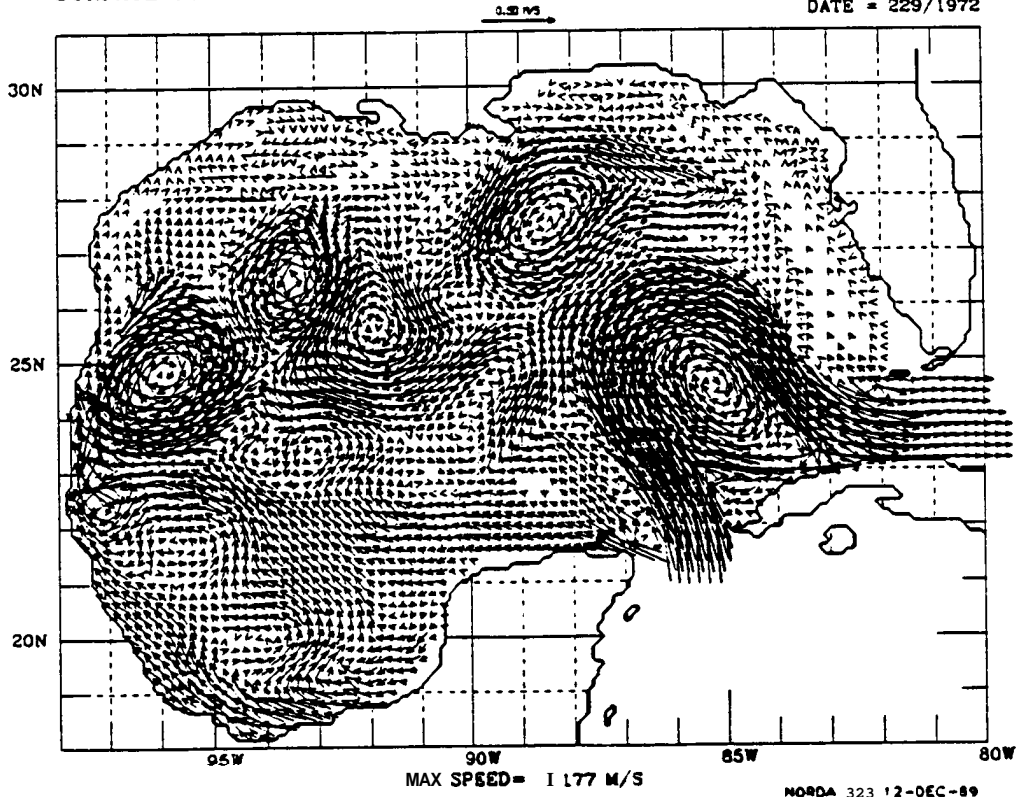


FIGURE 172

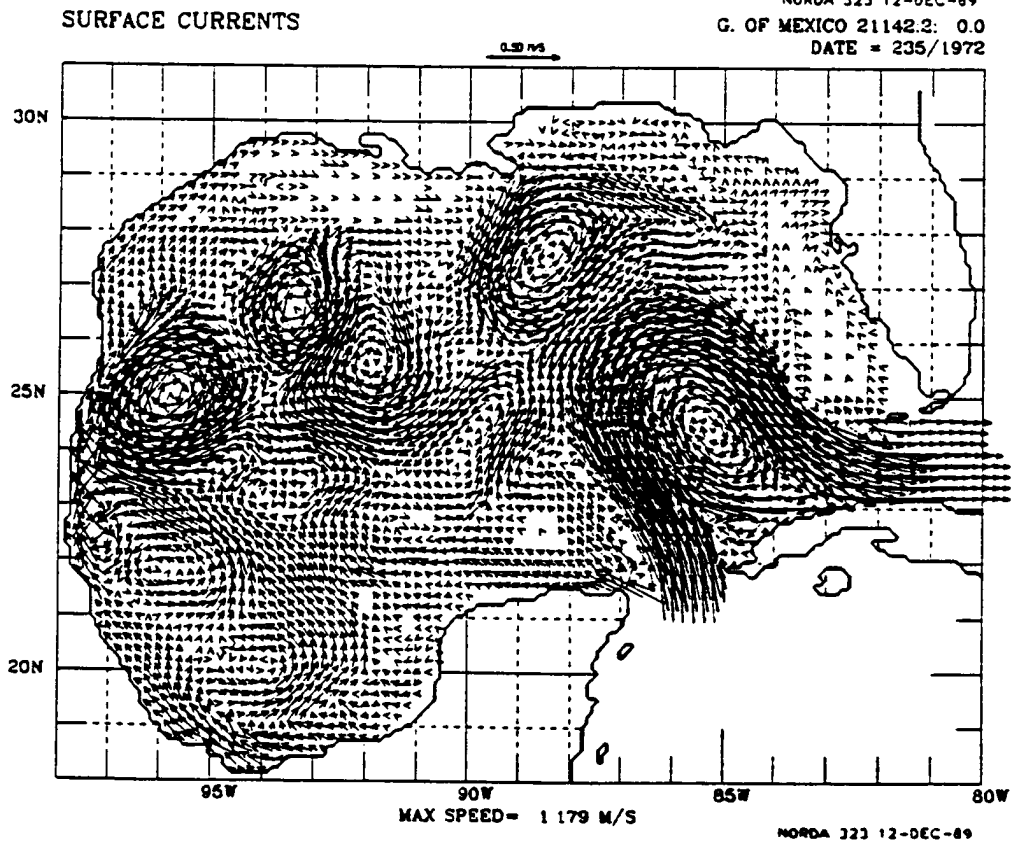
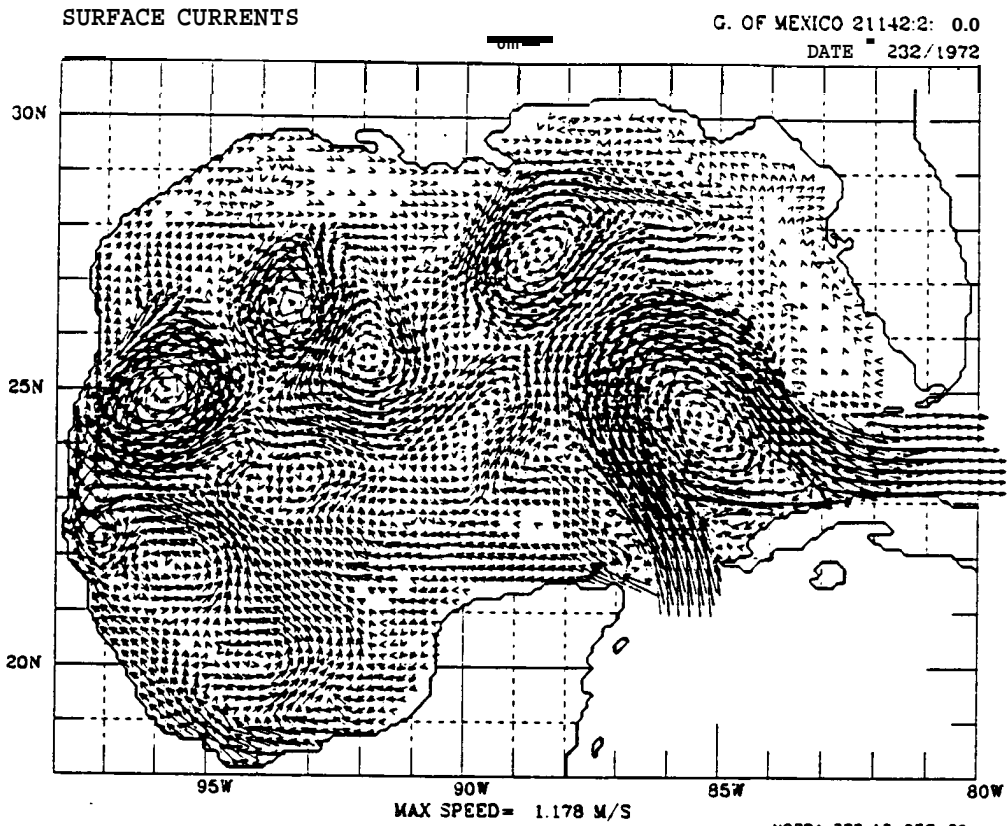
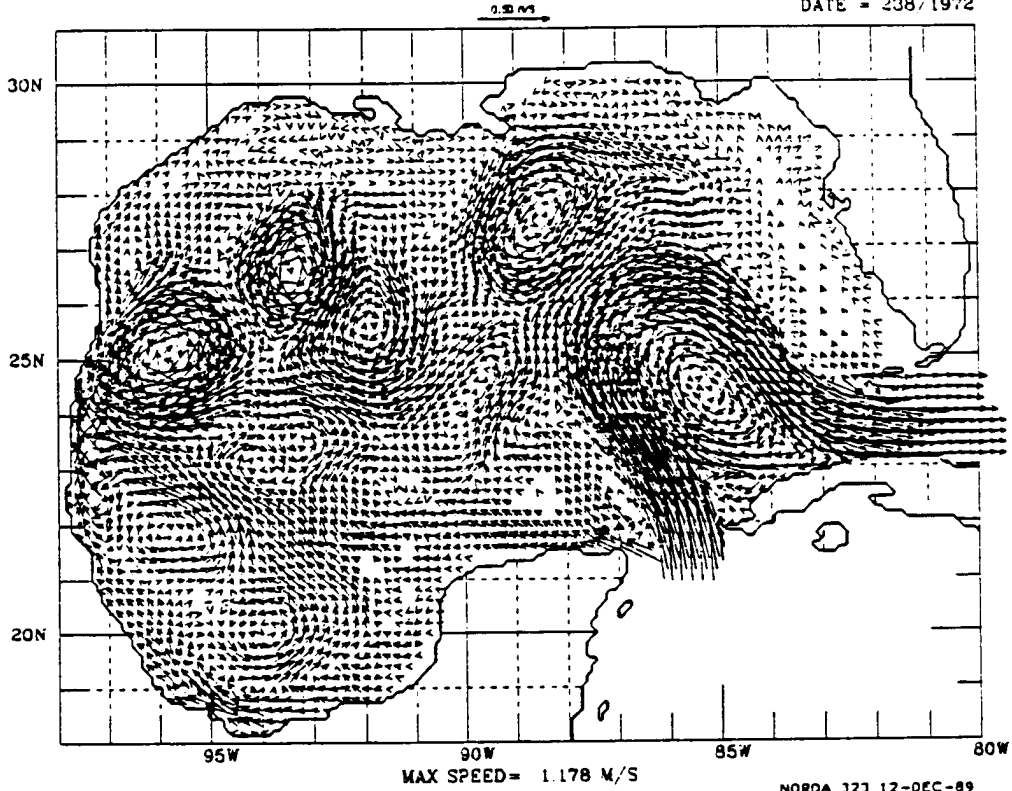


FIGURE 173

SURFACE CURRENTS

G. OF MEXICO 21142.2: 0.0
DATE = 238/1972



SURFACE CURRENTS

NOROA 323 12-DEC-89
G. OF MEXICO 21142.2: 0.0
DATE = 241/1972

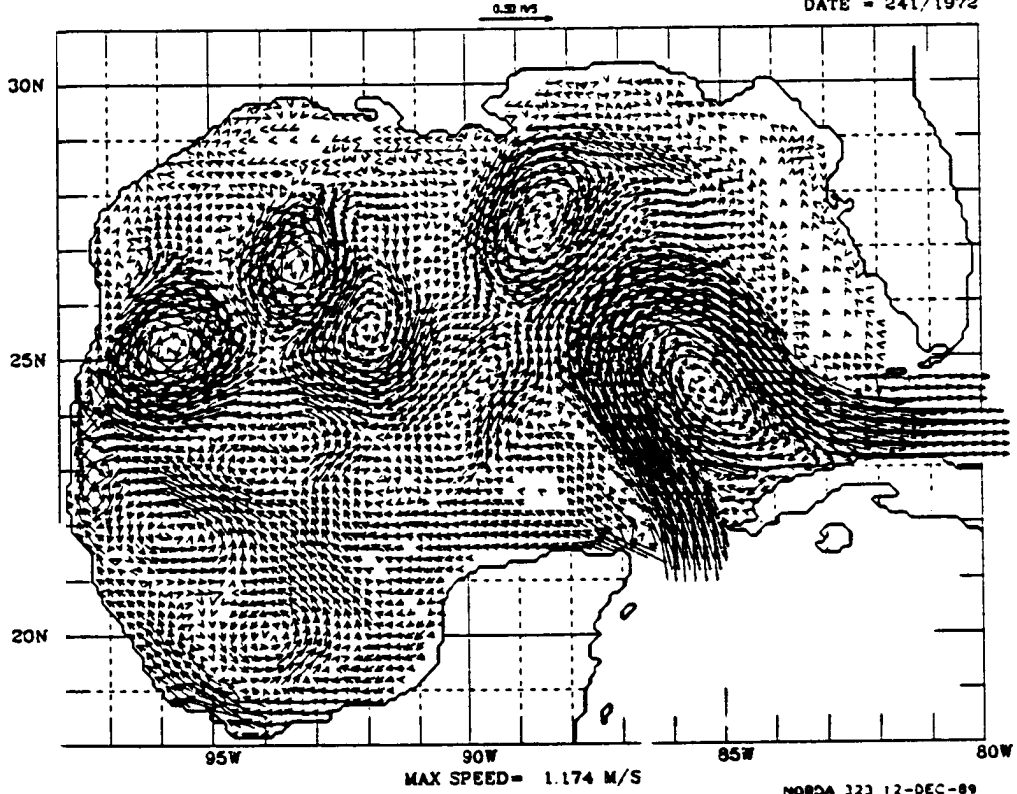
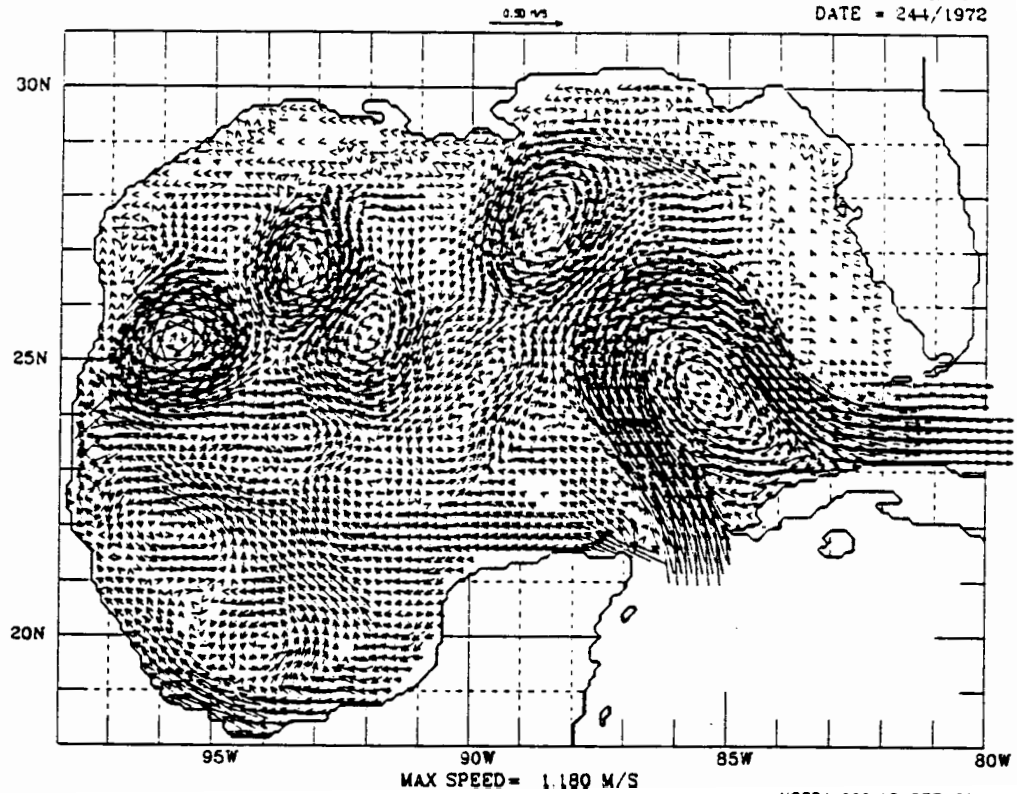


FIGURE 174

SURFACE CURRENTS

G. OF MEXICO 21142:2: 0.0
DATE = 244/1972



SURFACE CURRENTS

NORDA 323 12-DEC-89
G. OF MEXICO 21142:2: 0.0
DATE = 247/1972

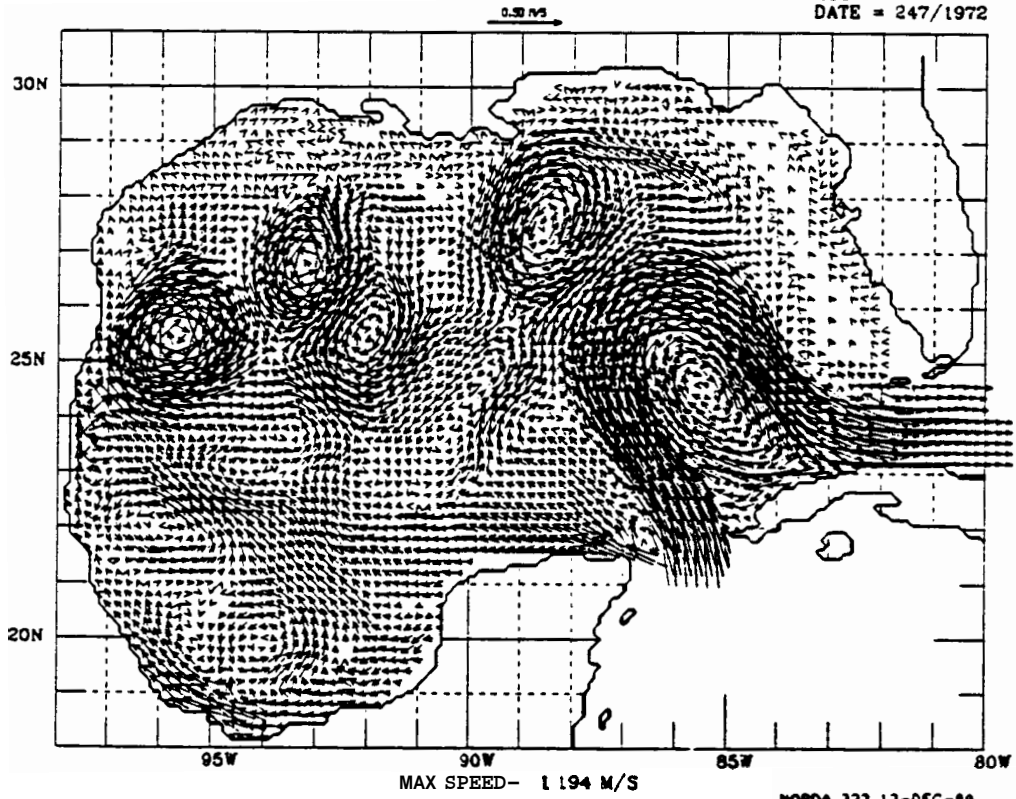


FIGURE 175

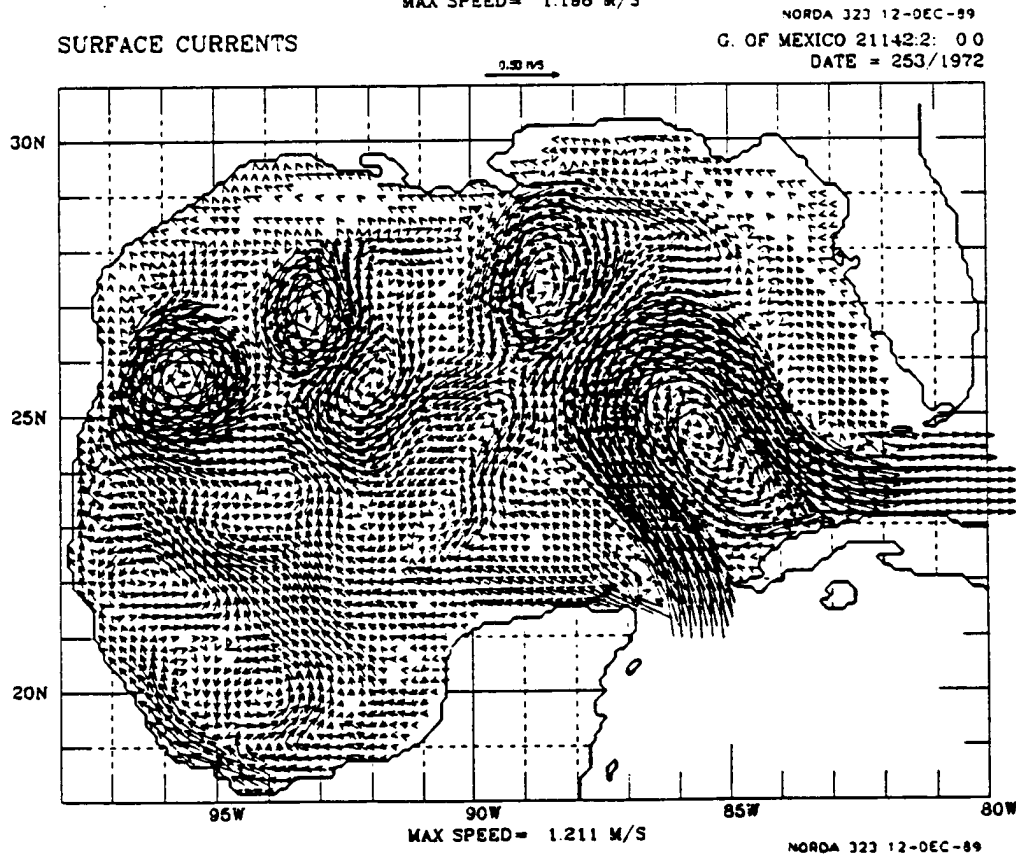
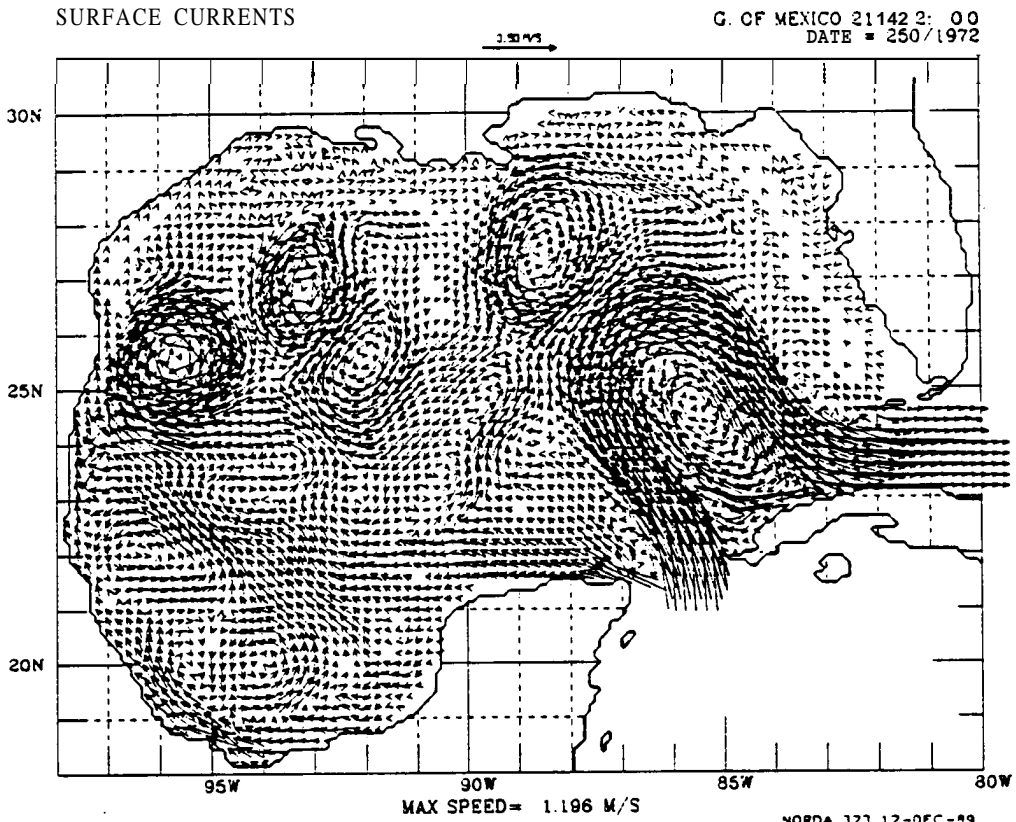


FIGURE 176

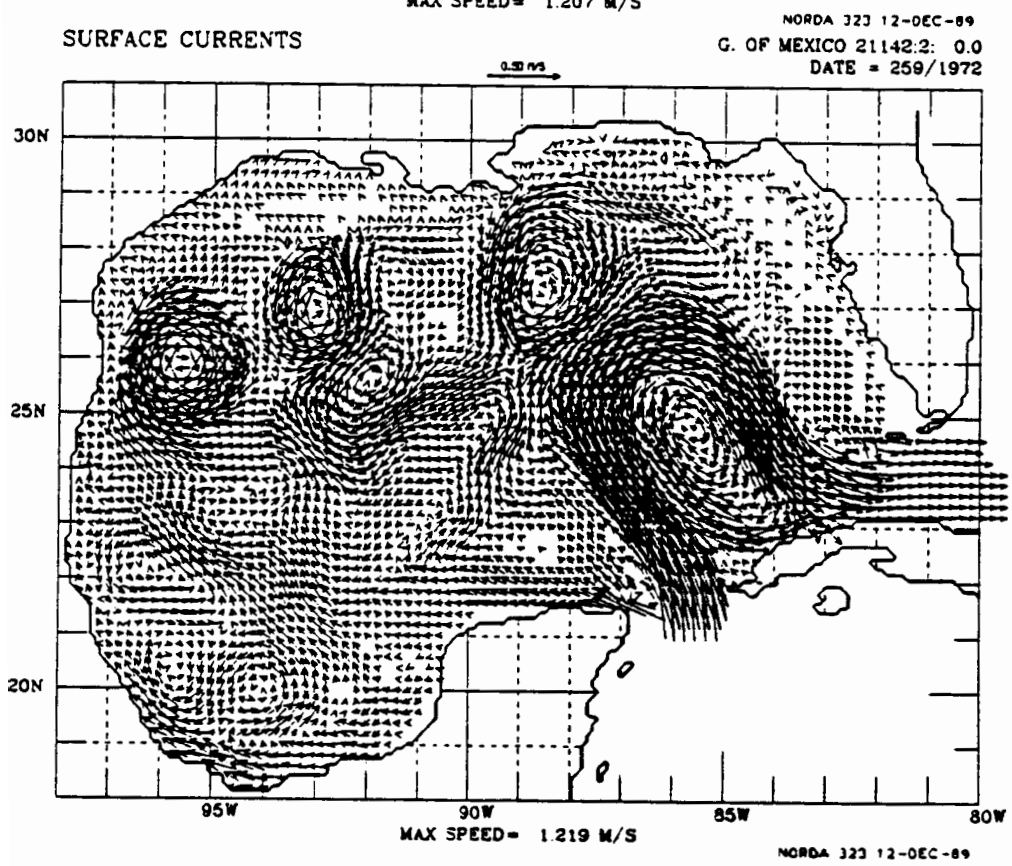
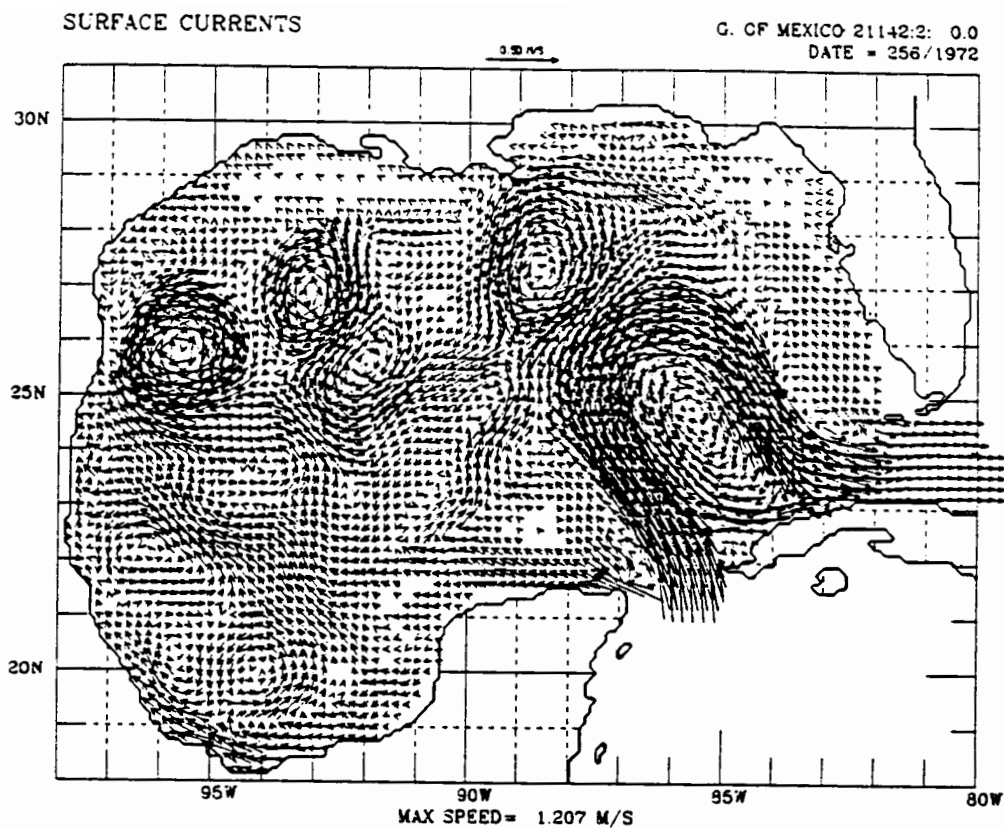


FIGURE 177

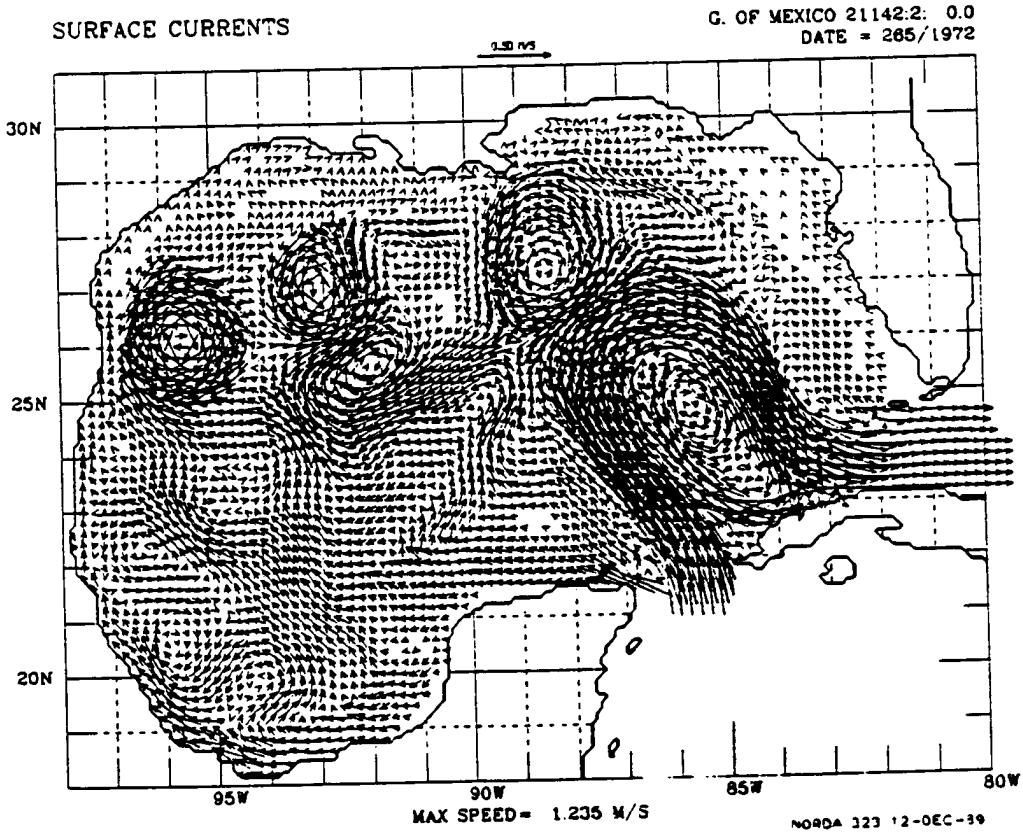
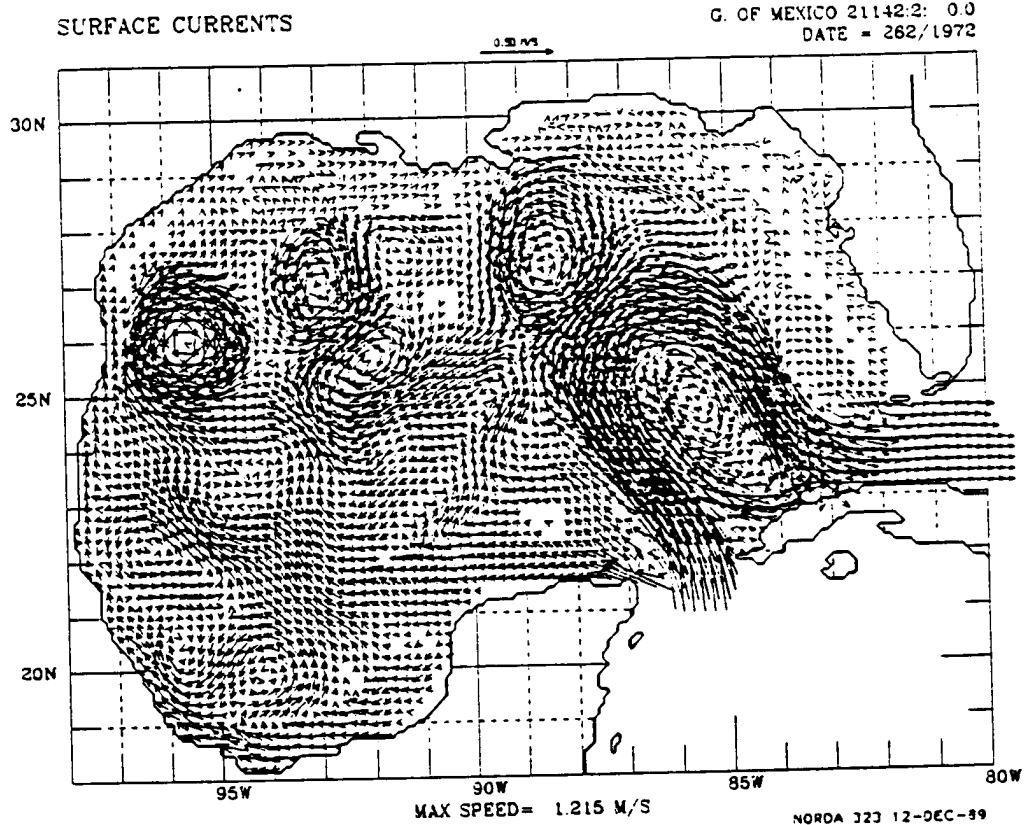


FIGURE 178

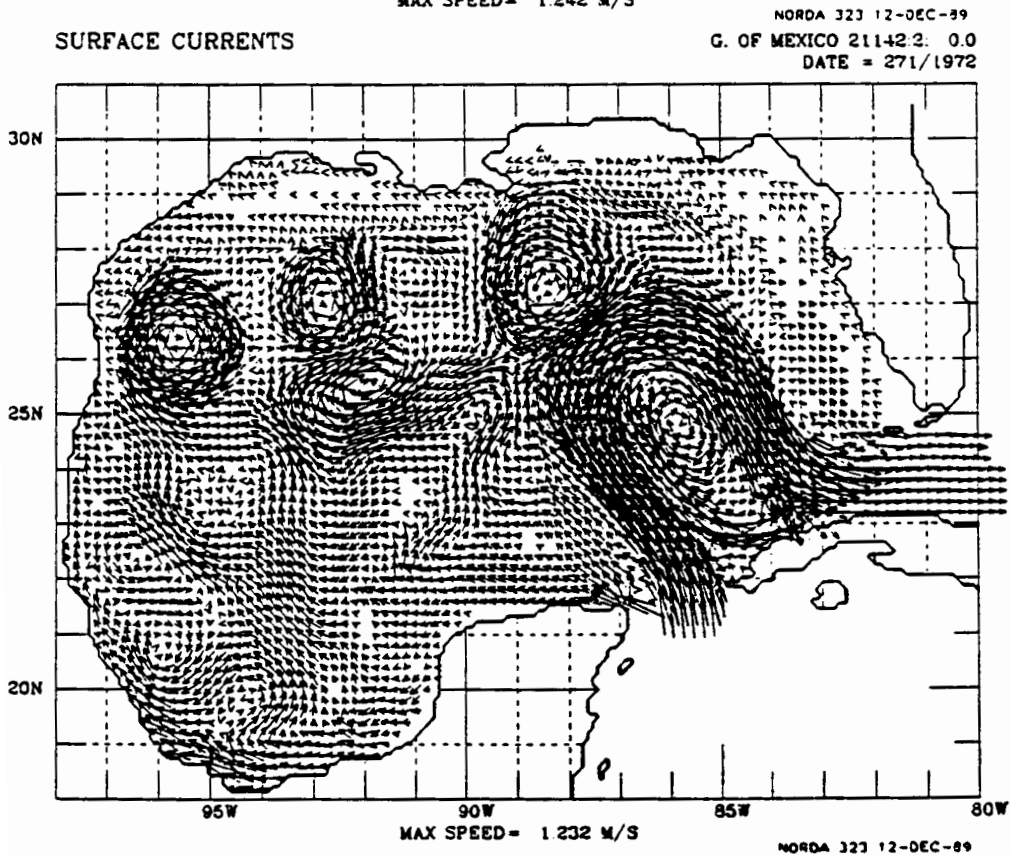
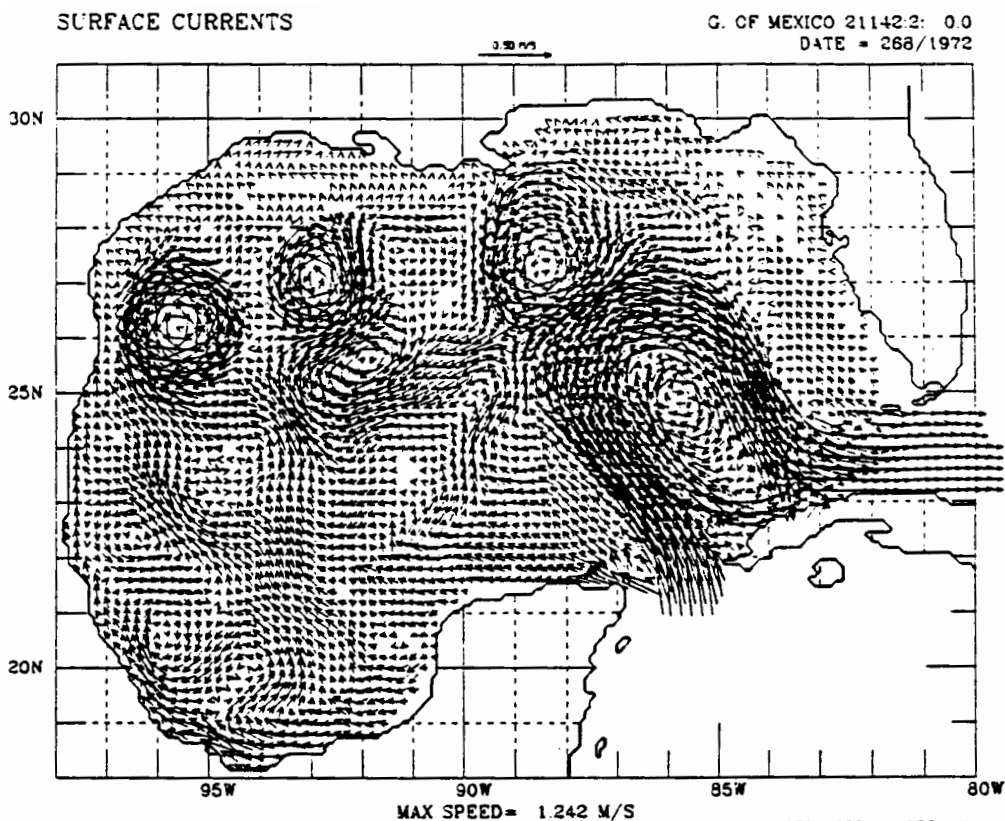
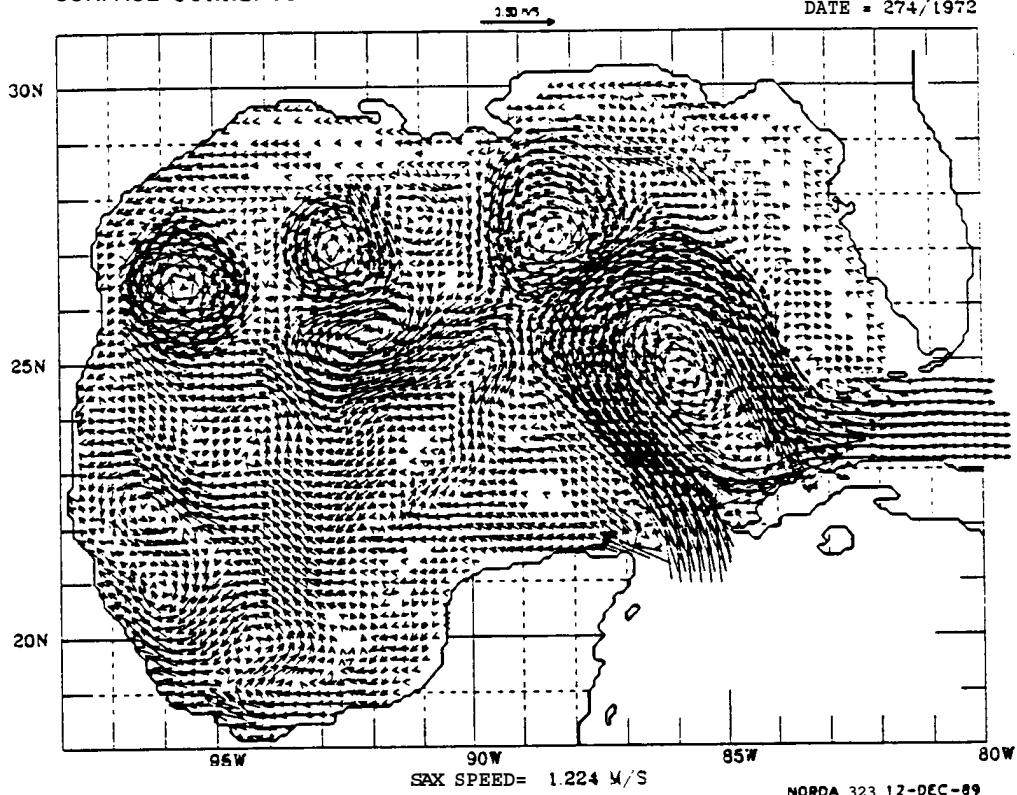


FIGURE 179

SURFACE CURRENTS

G. OF MEXICO 21142.2: 0.3
DATE = 274/1972



SURFACE CURRENTS

C. OF MEXICO 21142.2: 0.0
DATE = 277/1972

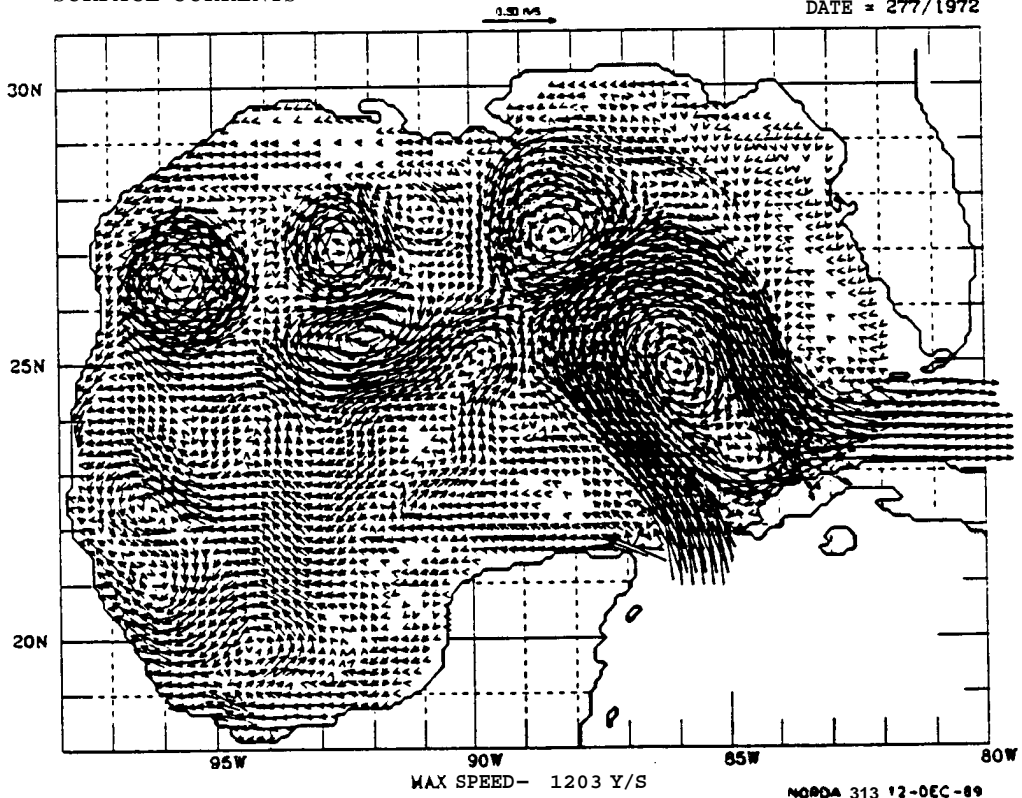
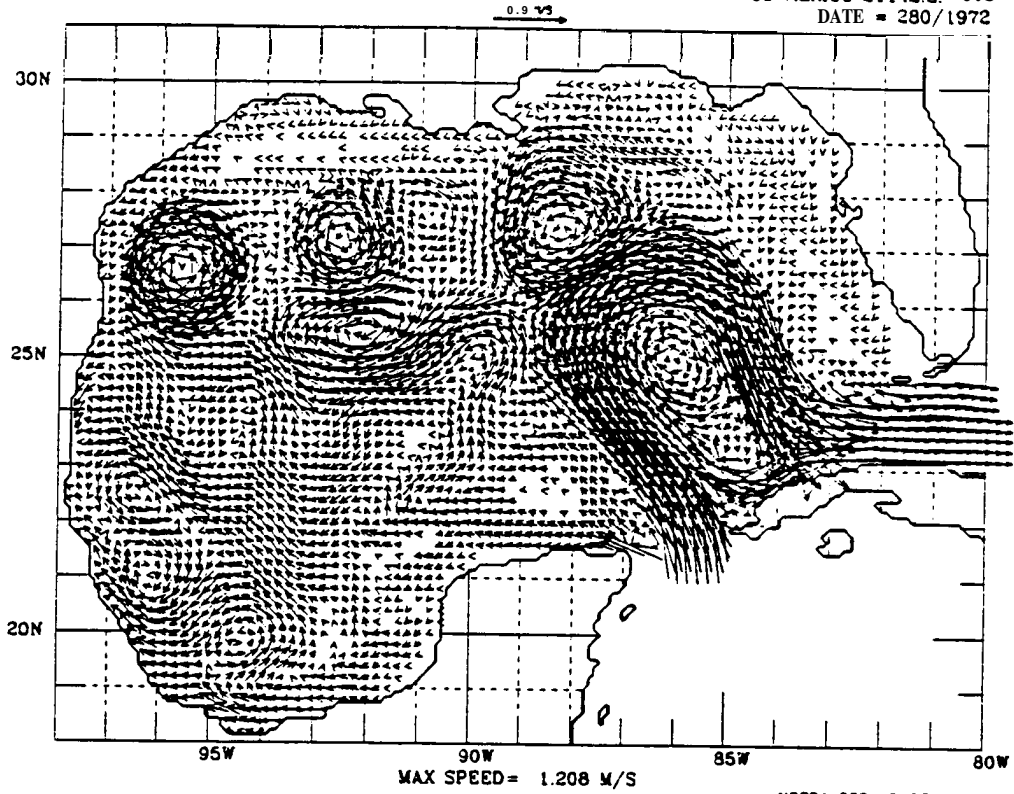


FIGURE 180

SURFACE CURRENTS

G. OF MEXICO 21142.2: 0.3
DATE = 280/1972



SURFACE CURRENTS

NORDA 323 12-DEC-89
G. OF MEXICO 21142.2: 0.0
DATE = 283/1972

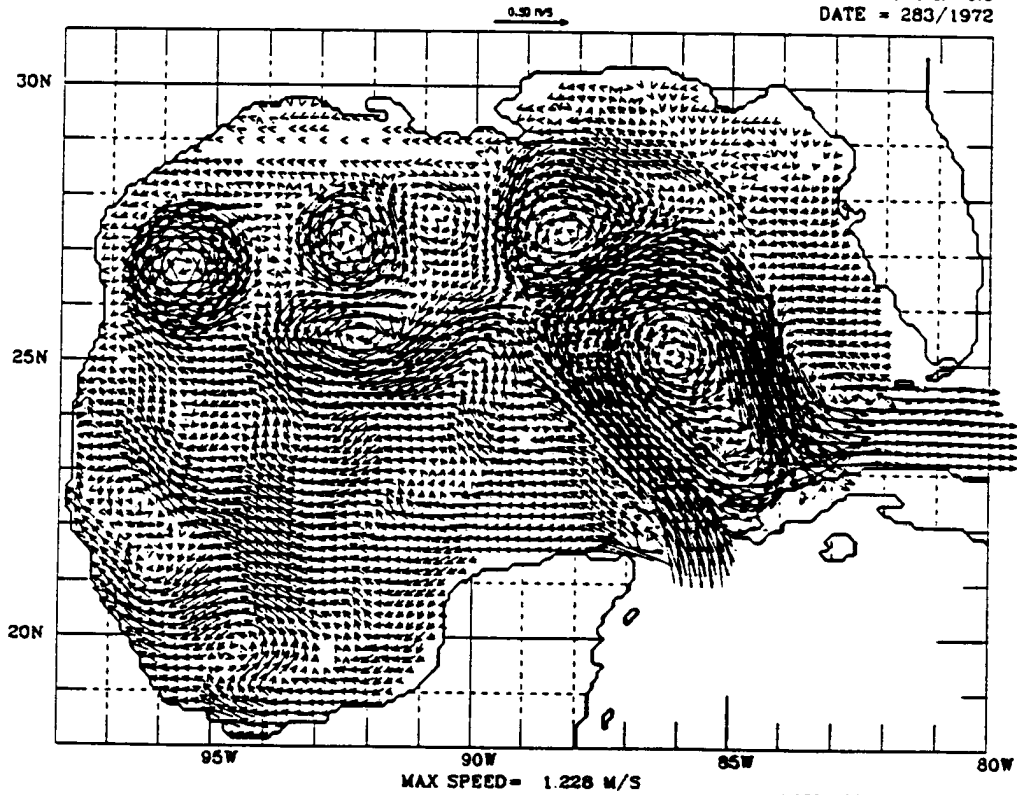


FIGURE 181

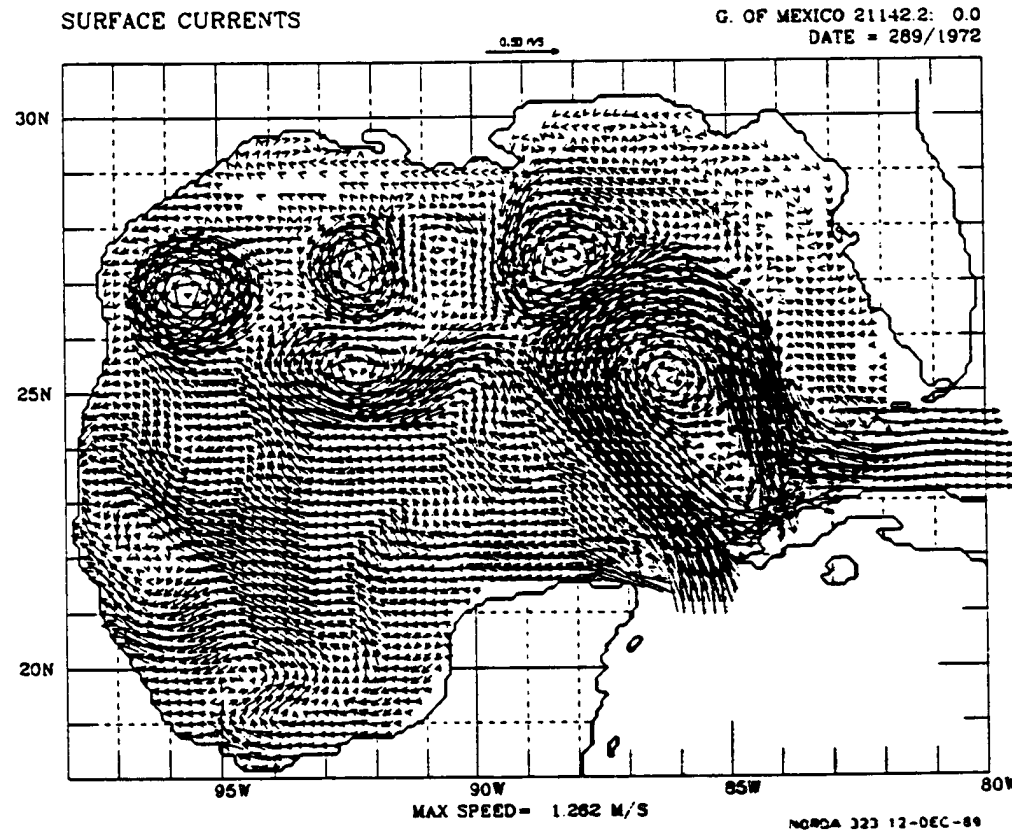
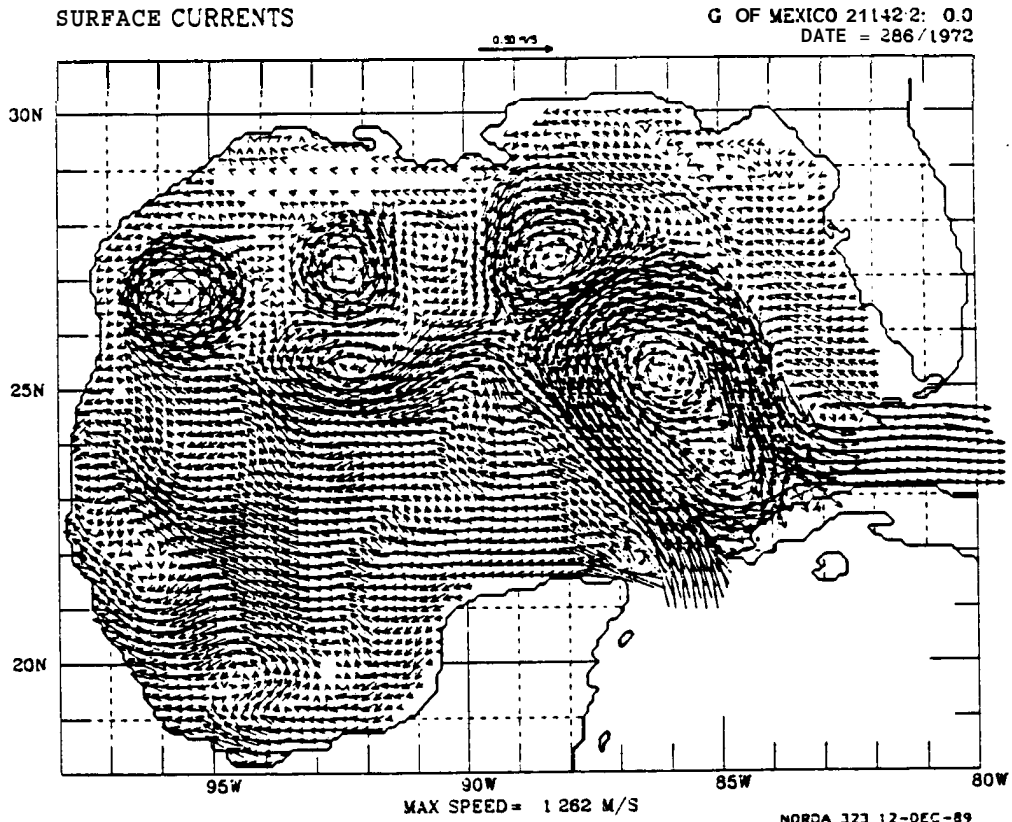


FIGURE 182

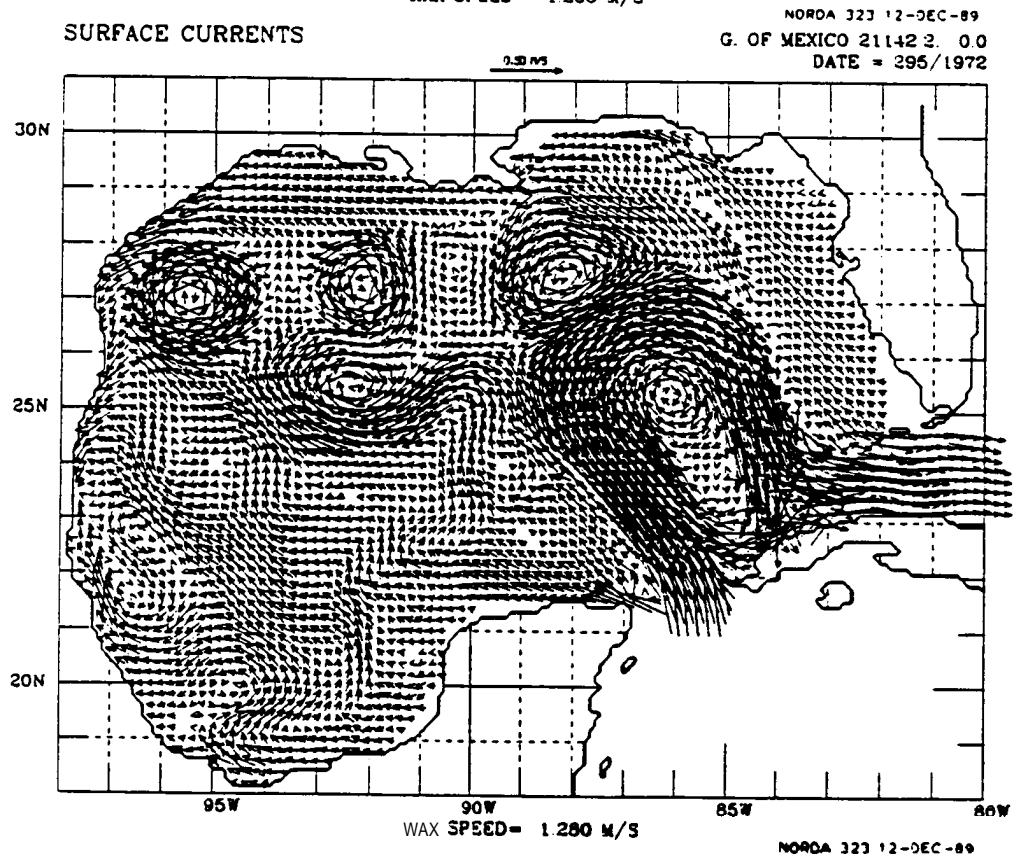
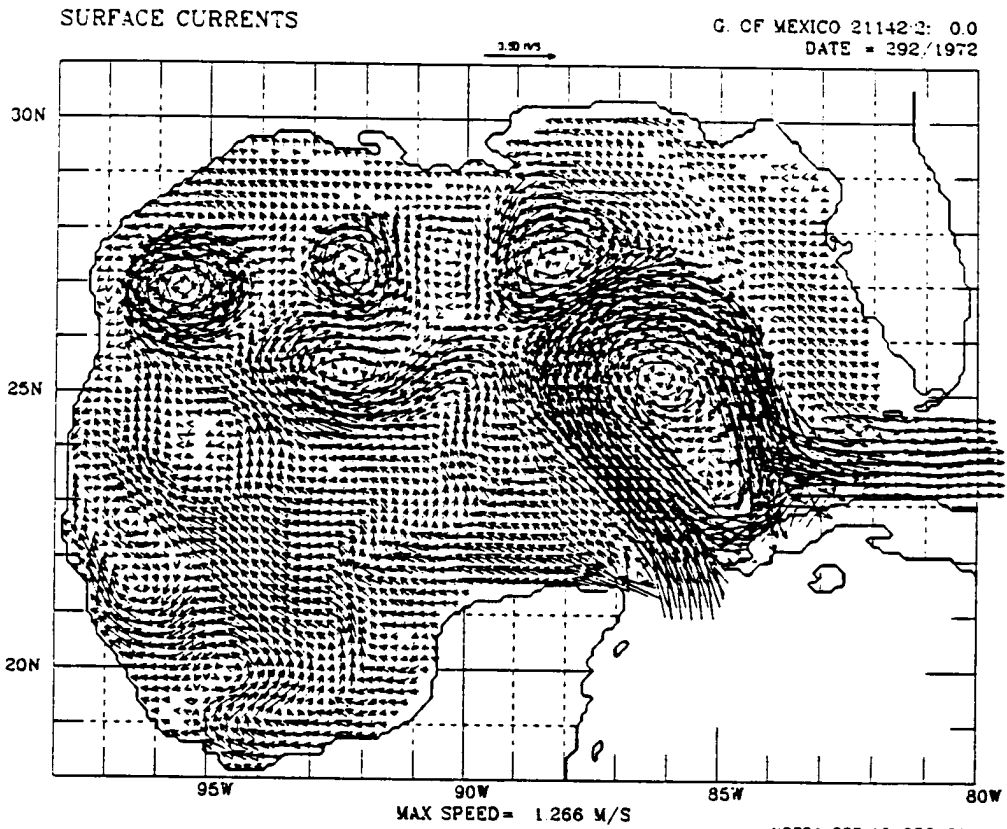
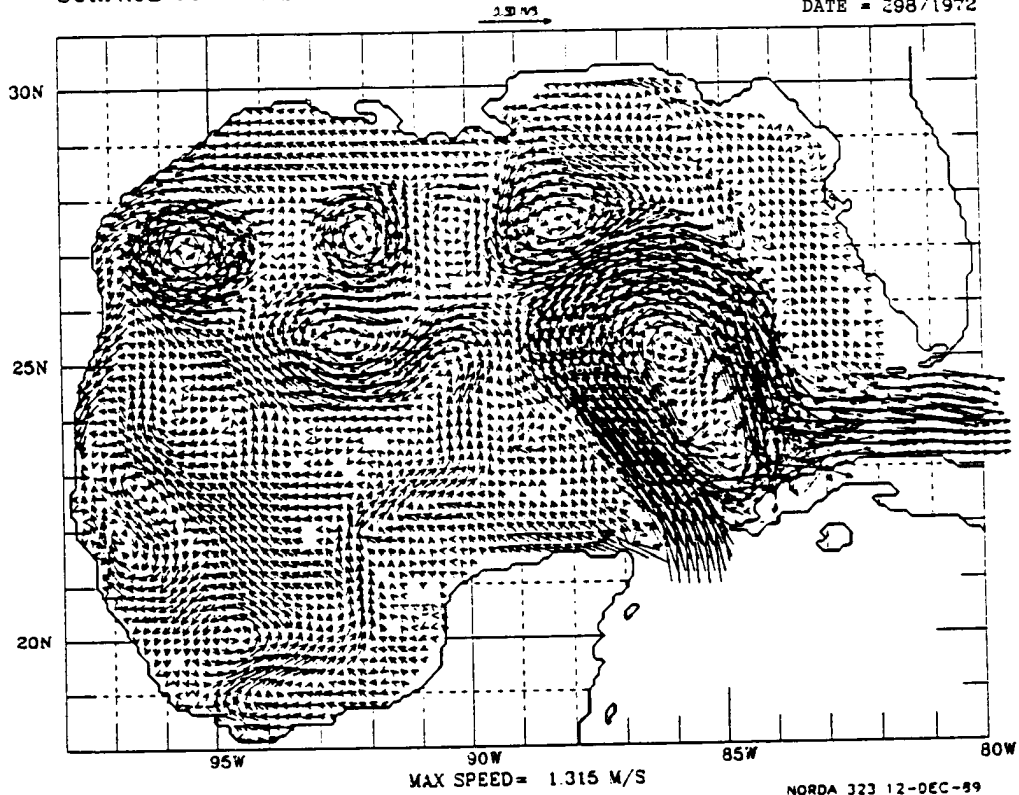


FIGURE 183

SURFACE CURRENTS

G. OF MEXICO 21142.2: 0.0
DATE = 298/1972



SURFACE CURRENTS

G. OF MEXICO 21142.2: 0.0
DATE = 301/1972

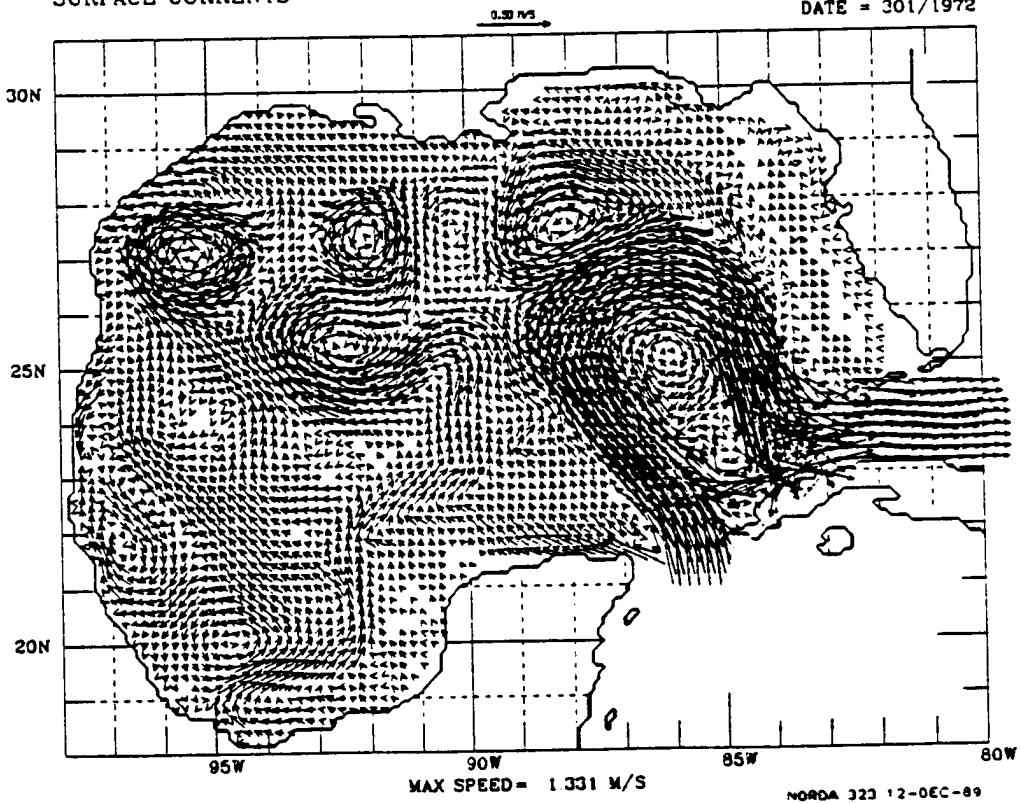
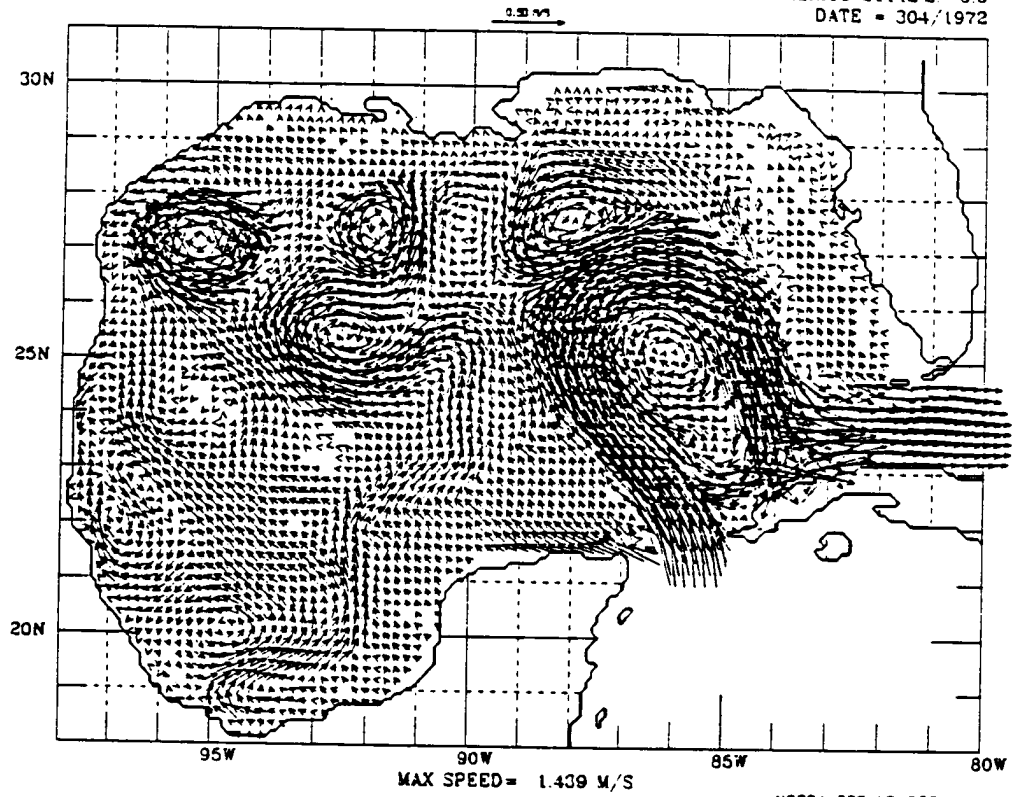


FIGURE 184

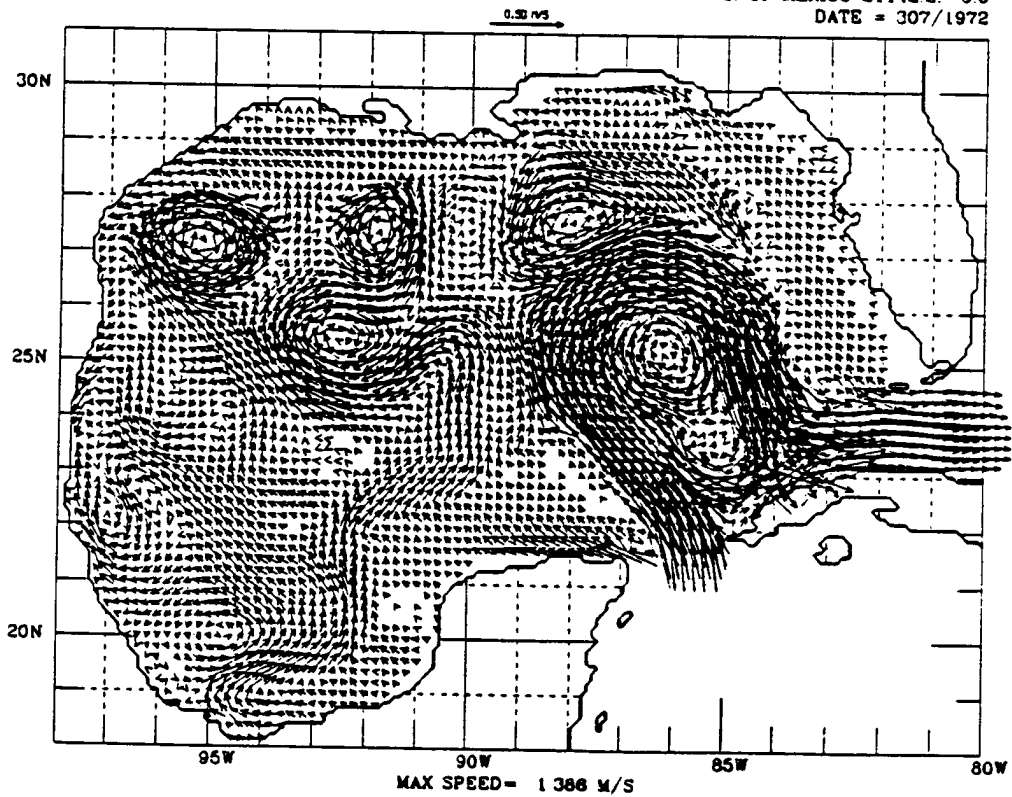
SURFACE CURRENTS

G. OF MEXICO 21142.2: 0.0
DATE = 304/1972



SURFACE CURRENTS

NORDA 323 12-DEC-89
G. OF MEXICO 21142.2: 0.0
DATE = 307/1972



NORDA 323 12-DEC-89

FIGURE 185

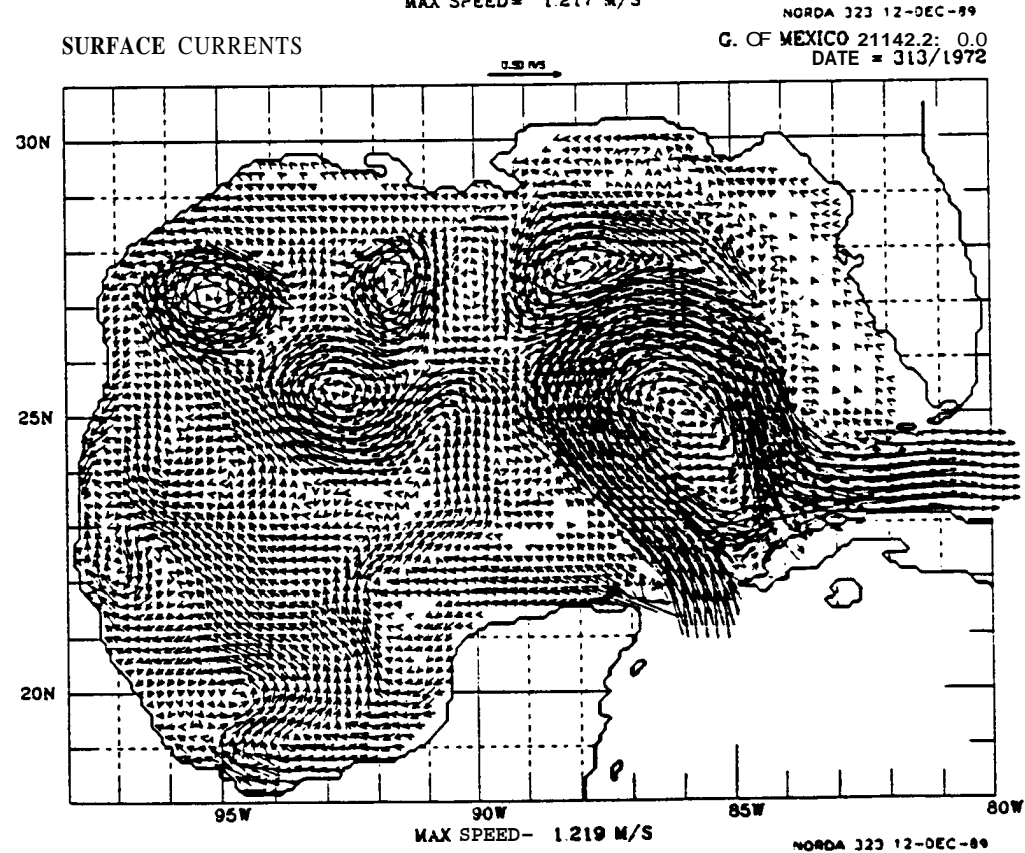
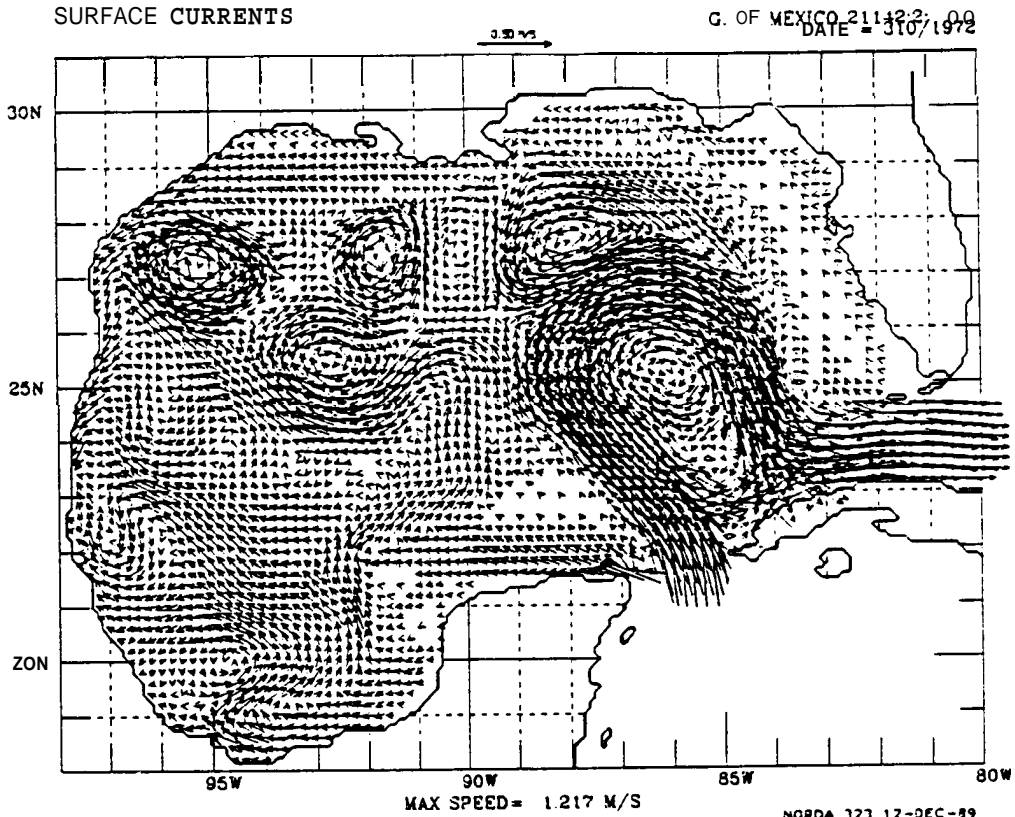
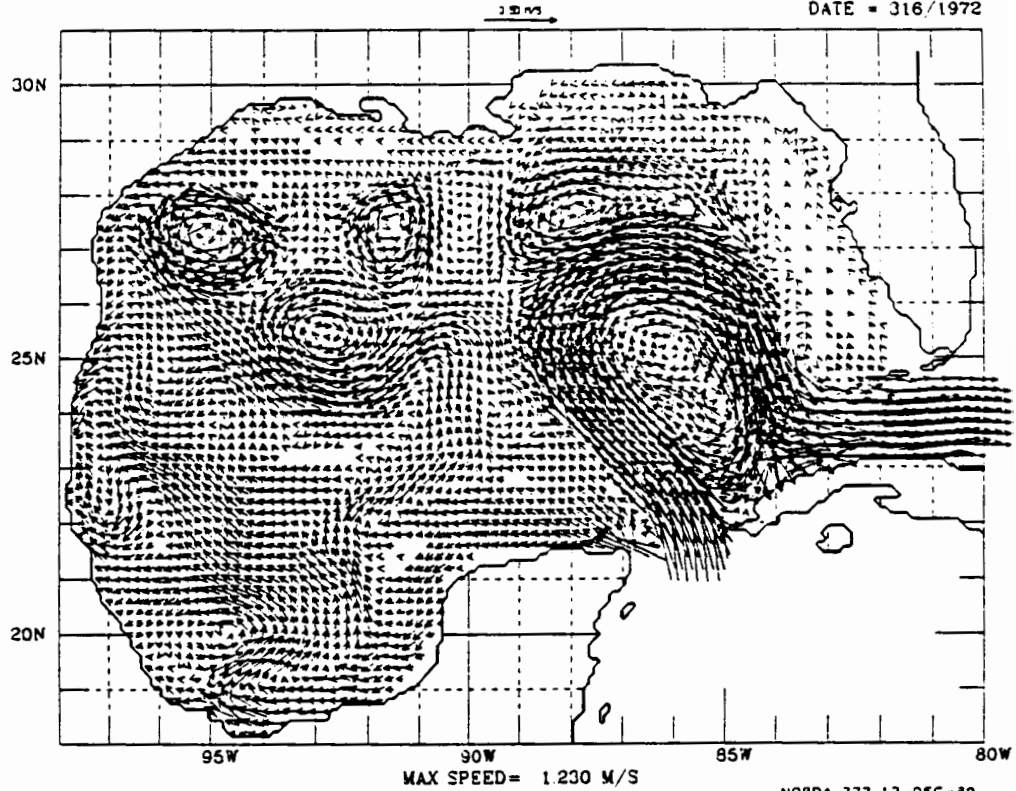


FIGURE 186

SURFACE CURRENTS

G. OF MEXICO 21142-2: 0.0
DATE = 316/1972



SURFACE CURRENTS

NORDA 323 12-DEC-89
G. OF MEXICO 21142-2: 0.0
DATE = 319/1972

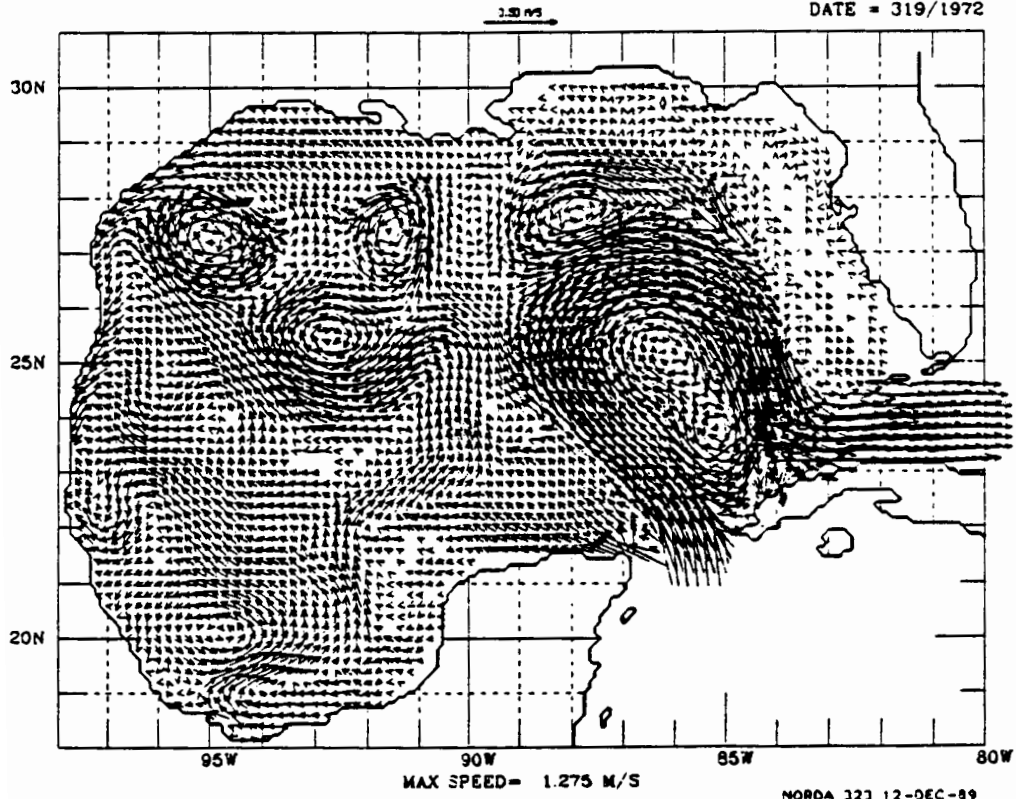
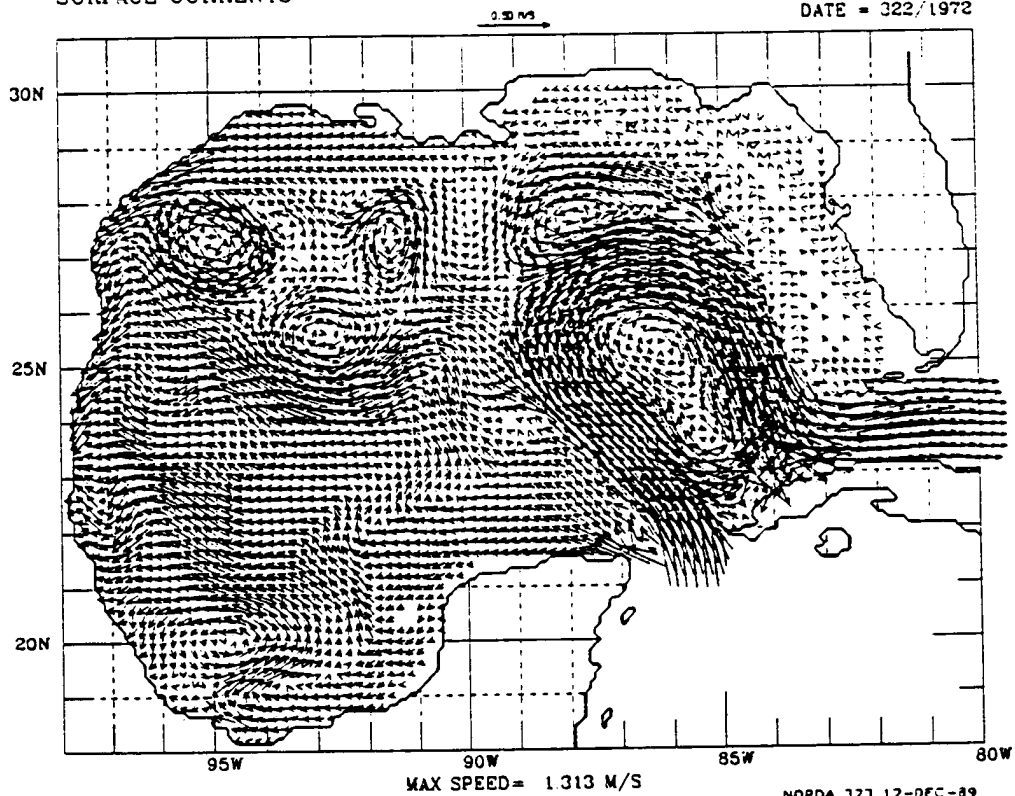


FIGURE 187

SURFACE CURRENTS

G. OF MEXICO 21142.2: 0.0
DATE = 322/1972



SURFACE CURRENTS

G. OF MEXICO 21142.2: 0.0
DATE = 325/1972

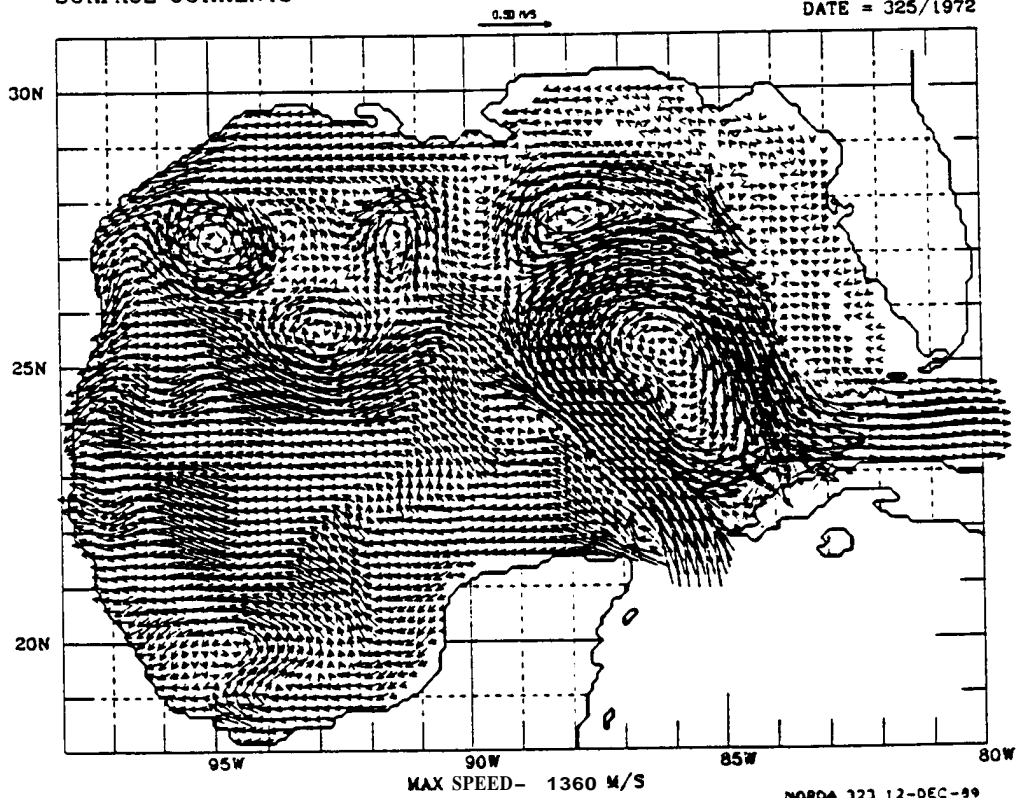


FIGURE 188

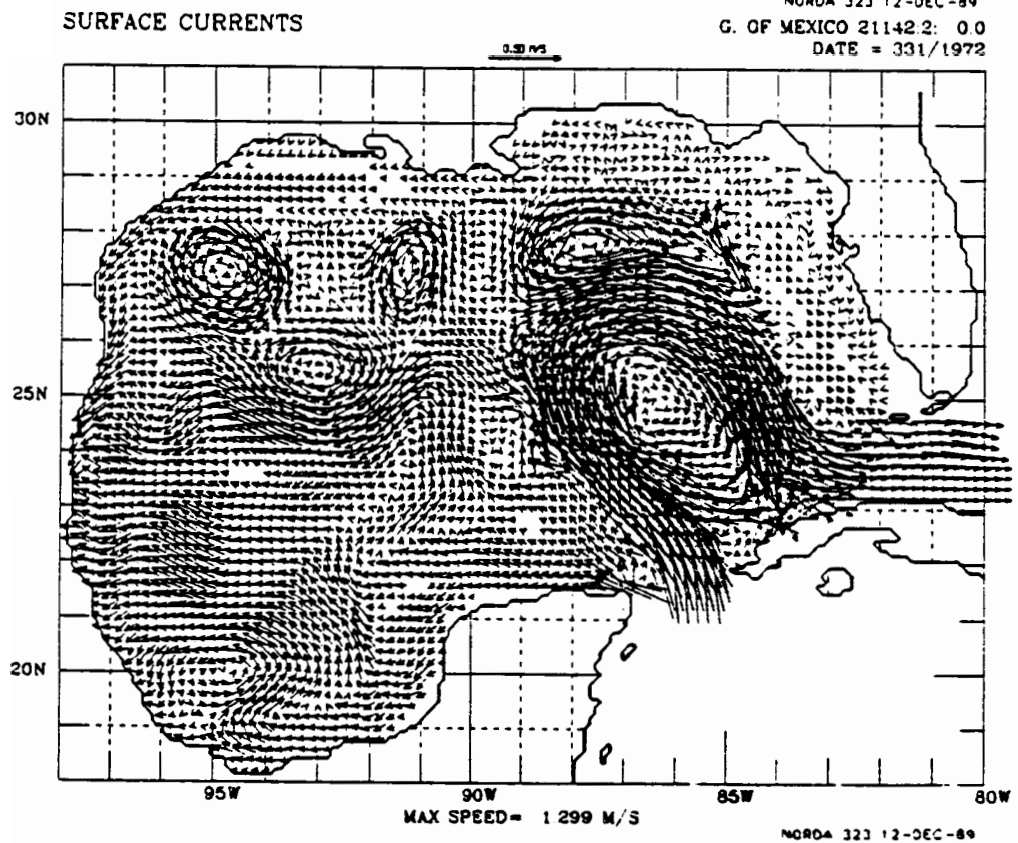
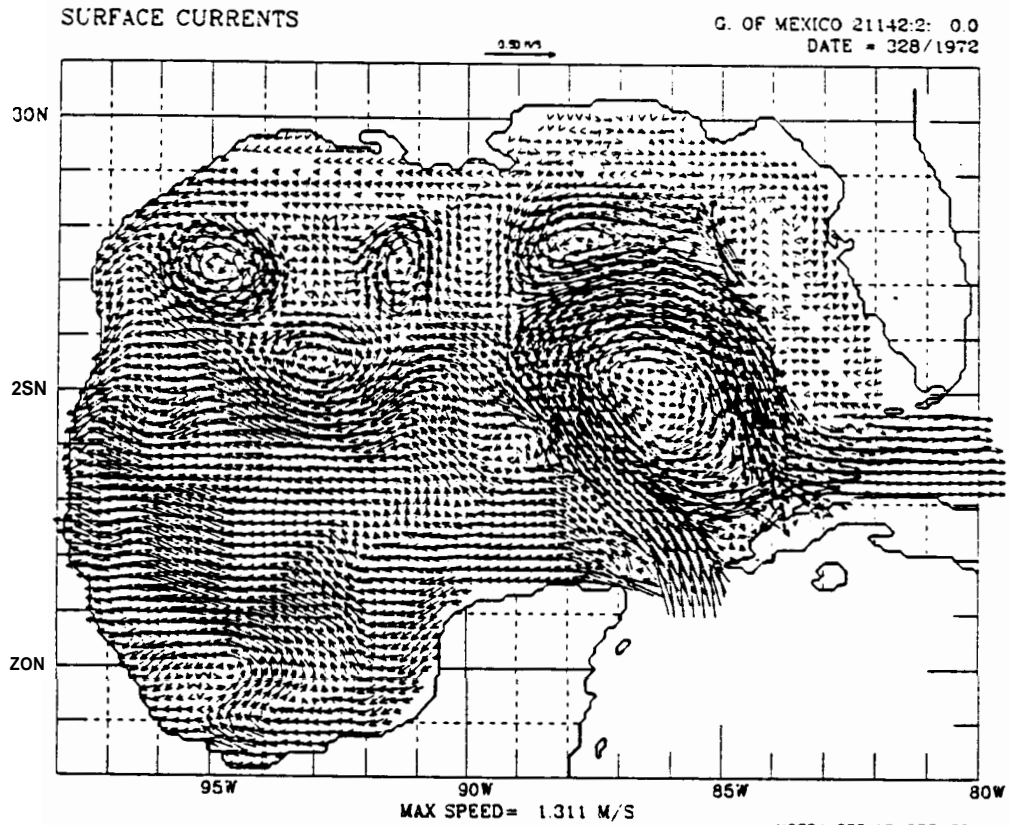
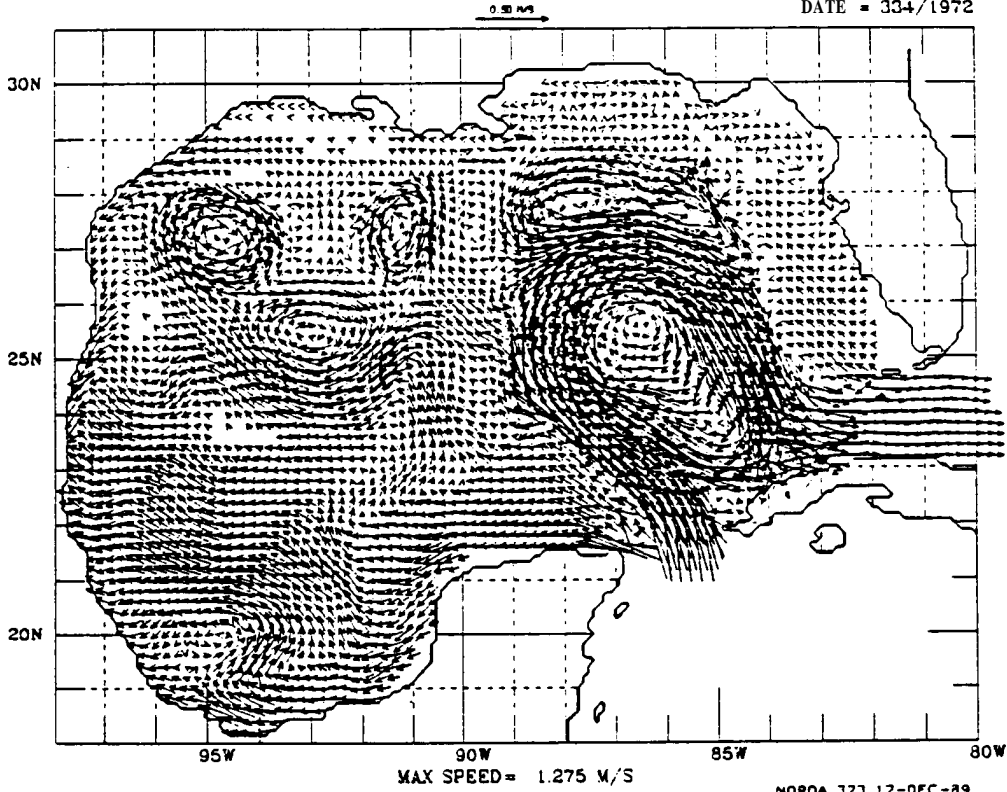


FIGURE 189

SURFACE CURRENTS

G. OF MEXICO 21142:2: 03
DATE = 334/1972



SURFACE CURRENTS

G. OF MEXICO 21142:2: 00
DATE = 337/1972

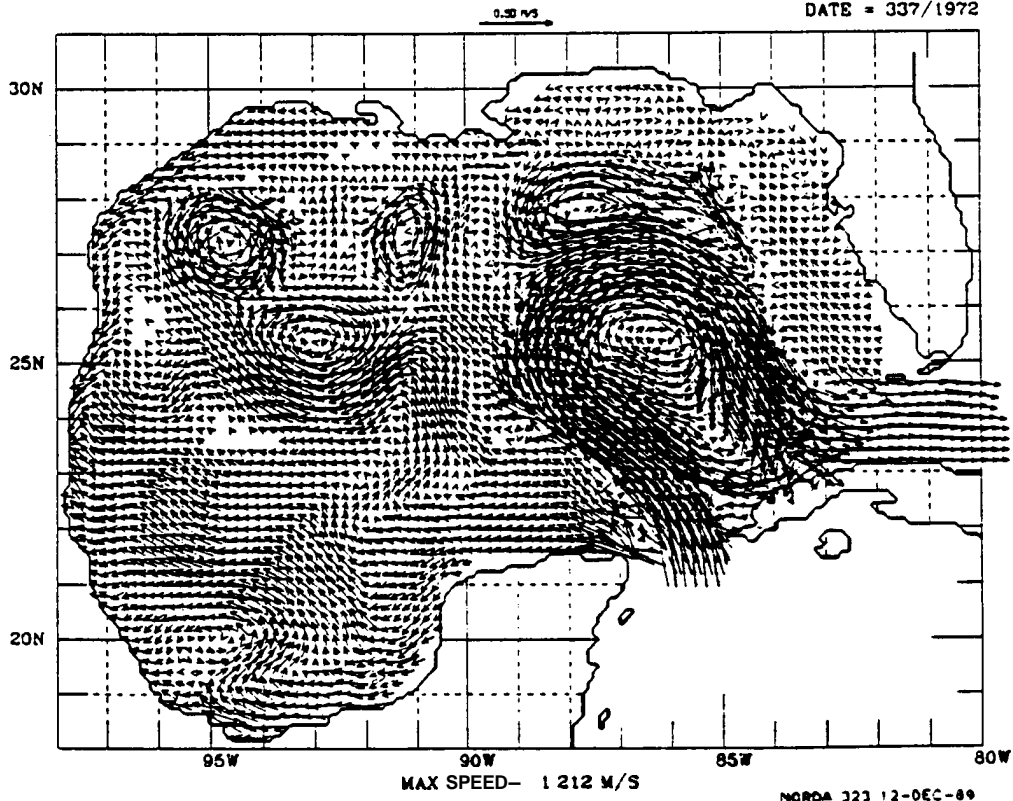


FIGURE 190

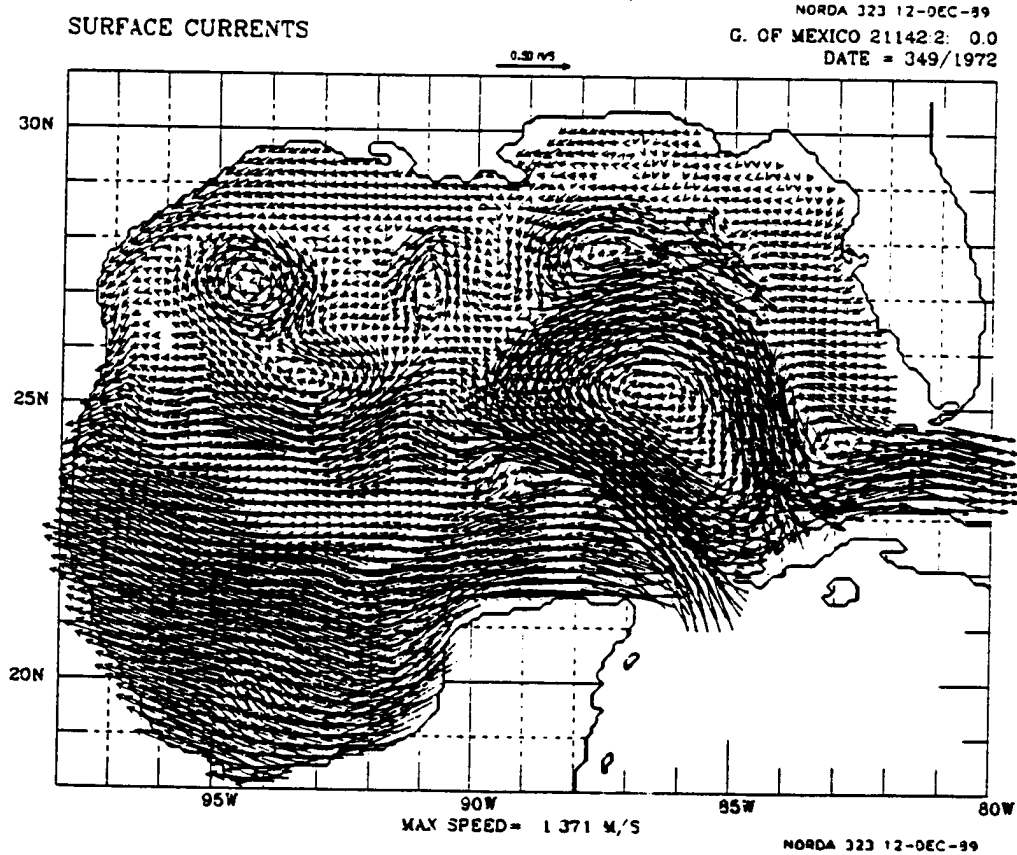
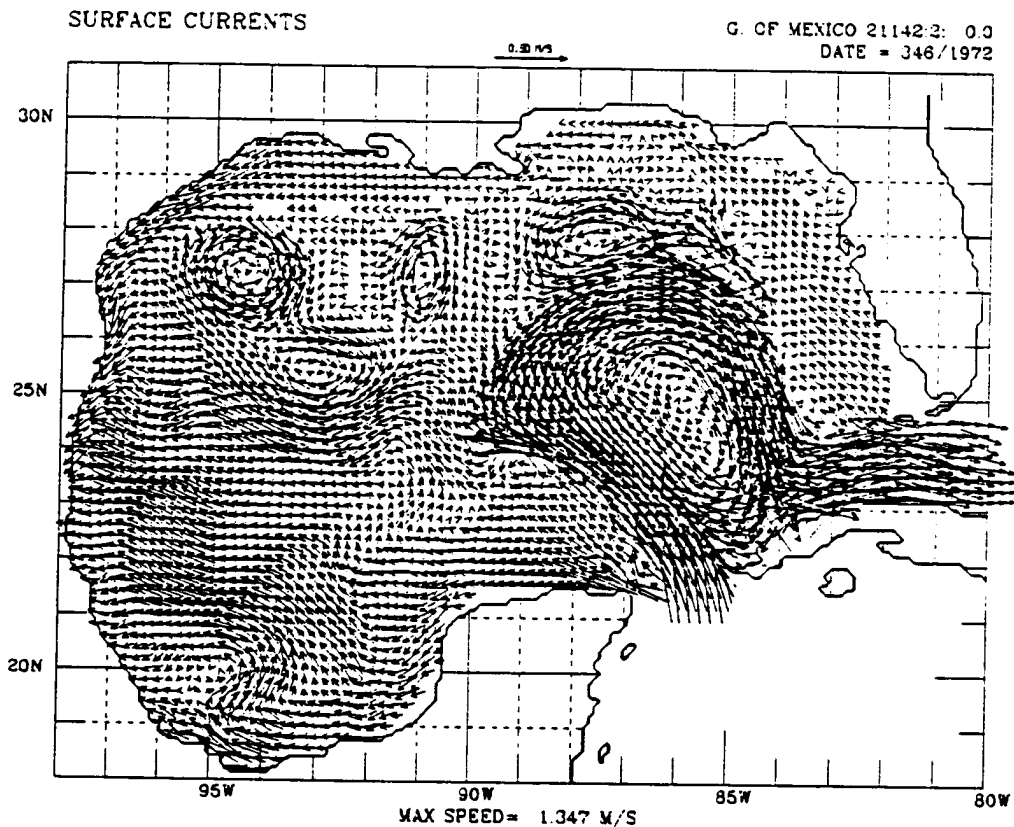


FIGURE 191

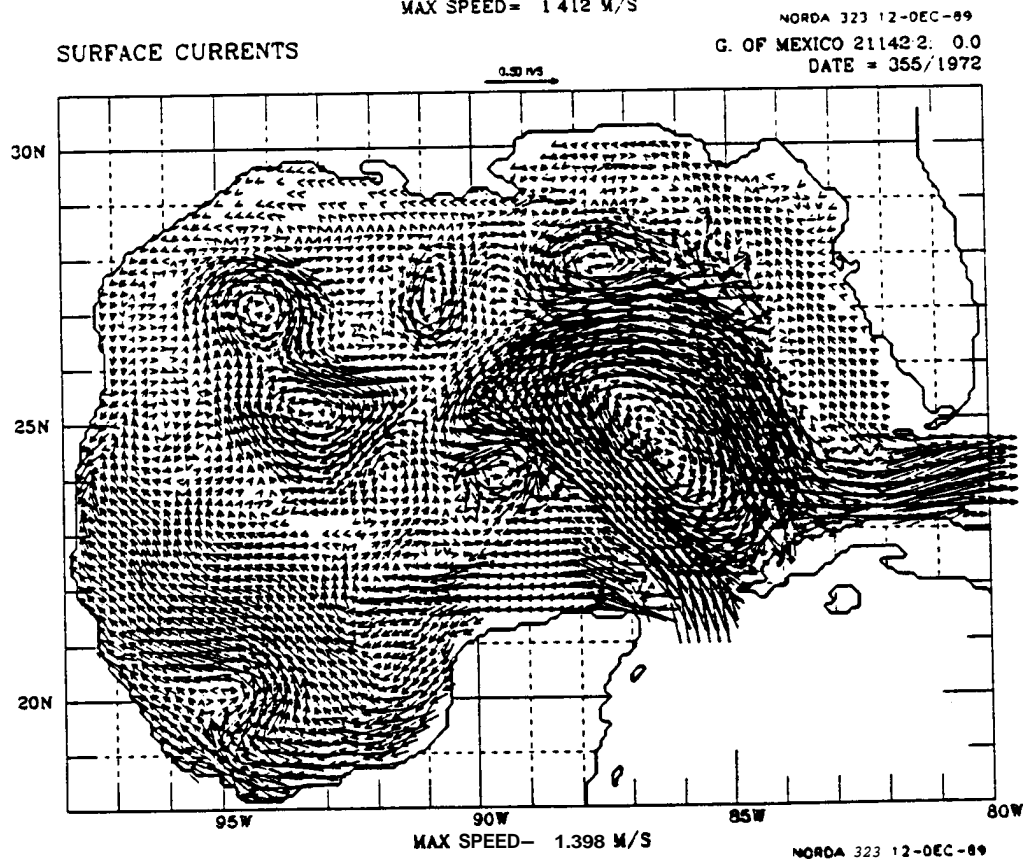
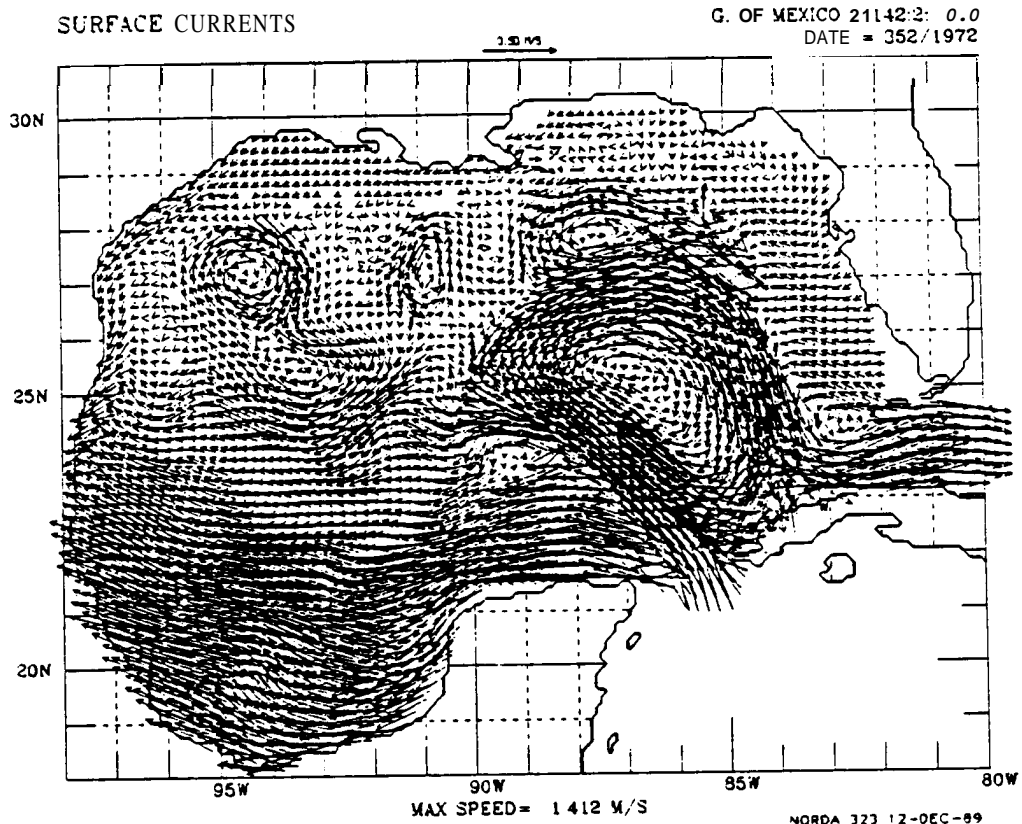
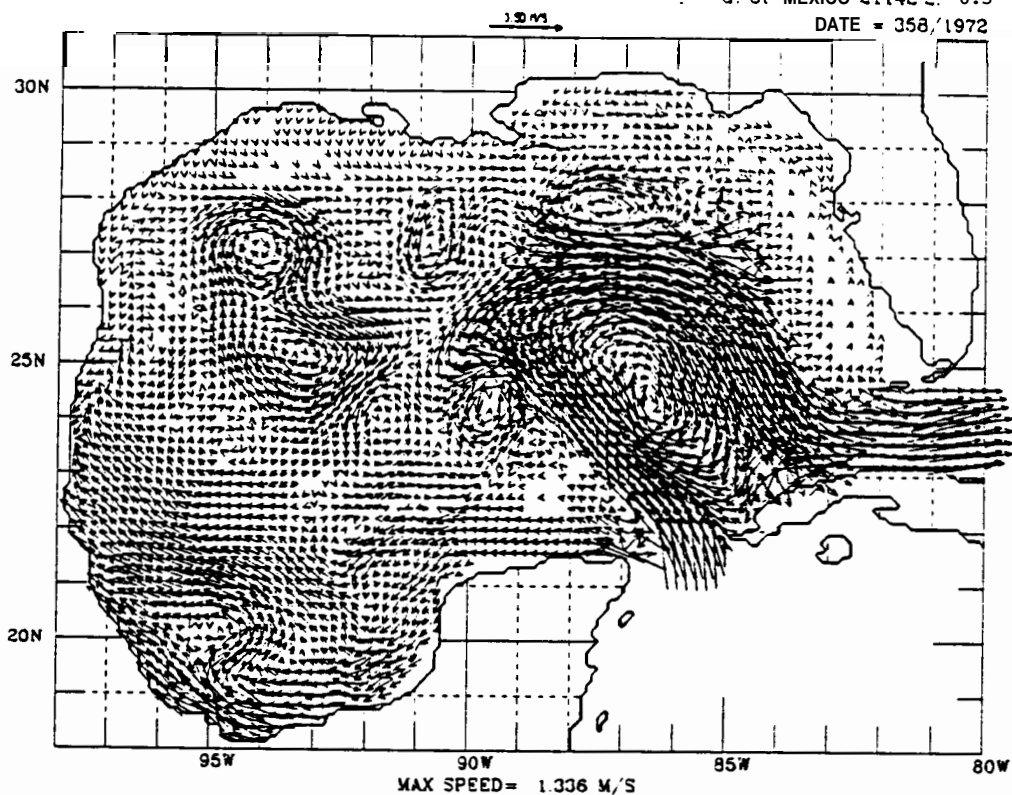


FIGURE 192

SURFACE CURRENTS

G. OF MEXICO 21142-2: 0.3

DATE = 358/1972



SURFACE CURRENTS

NORDA 323 12-DEC-89

G. OF MEXICO 21142-2: 0.0

DATE = 381/1972

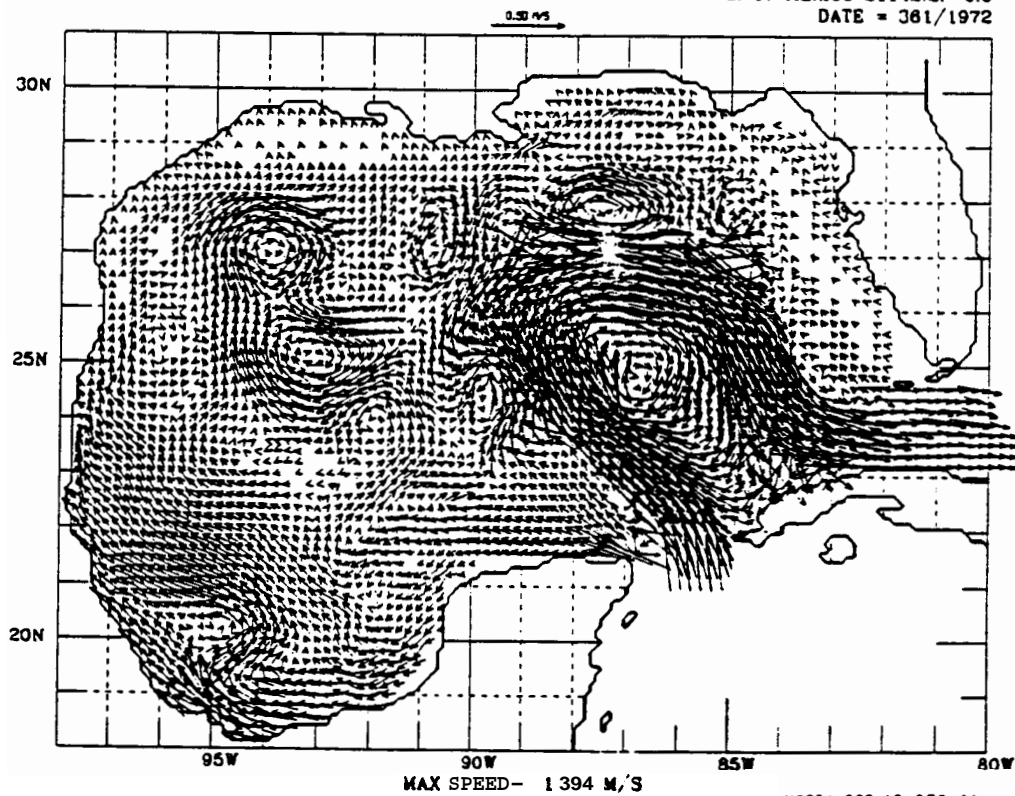
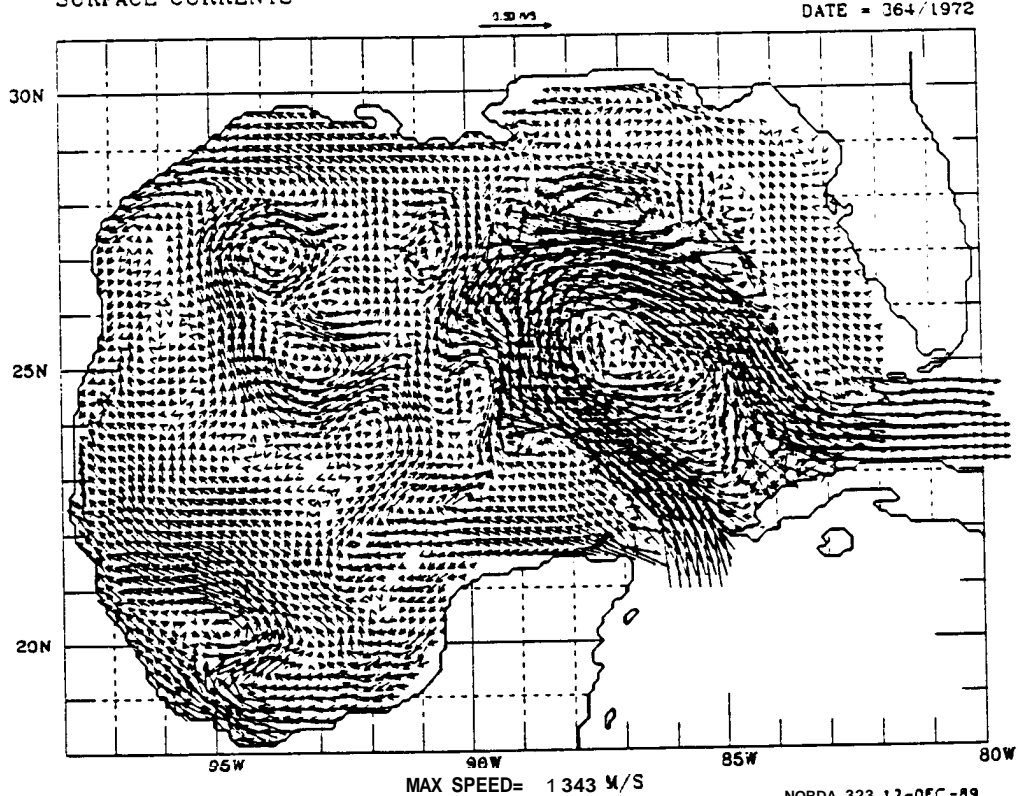


FIGURE 193

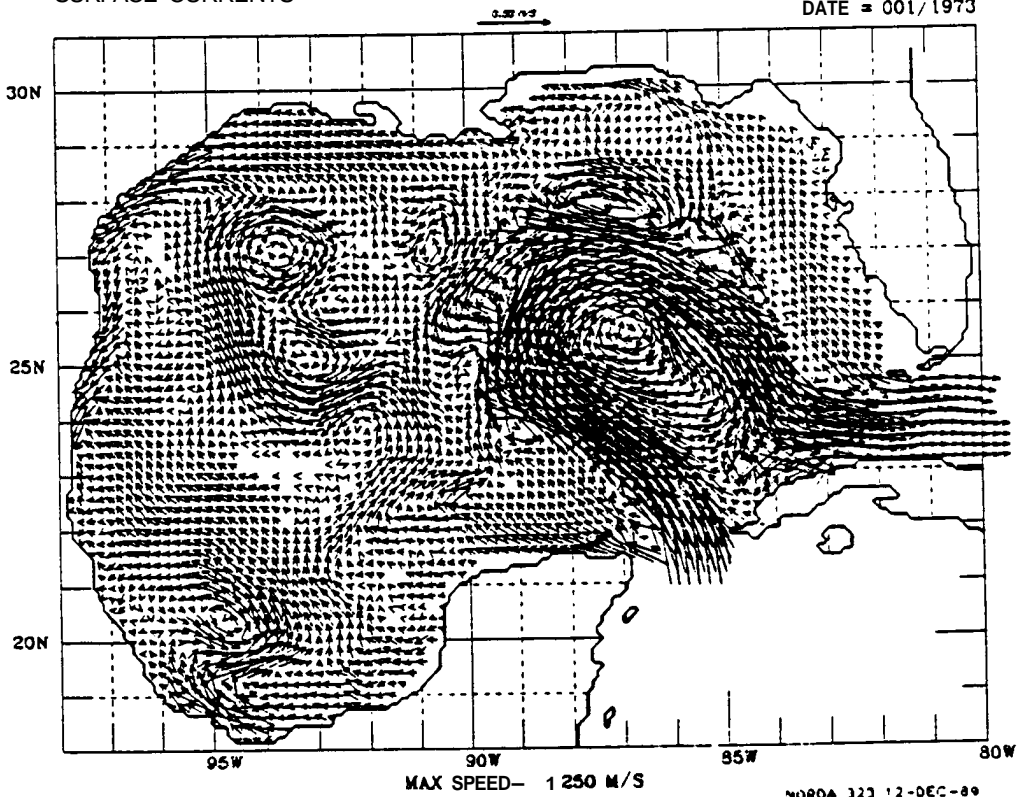
SURFACE CURRENTS

G. OF MEXICO 21142.2: 0.0
DATE = 364/1972



SURFACE CURRENTS

NORDA 323 12-DEC-89
G. OF MEXICO 21142.2: 0.0
DATE = 001/1973



to use a layered model in the Gulf, it should probably look first to flux-corrected transport techniques for producing improved simulations; however, such a project would also have the option of using several other **kinds** of ocean models that did not use layers in the vertical.

The final geostrophic surface currents (**L2+L1**) and surface currents (**L2+L1+P**) from this study provide a vastly improved realization of Gulf circulation than the existing alternatives; however, there are several limitations in the system design that suggest better simulations may be possible, such as the following approaches:

- The most obvious limitation of the deep water circulation is that the simulation's typical Loop Current eddy shedding period, at about two years, is twice as long as the generally-accepted average period for the Gulf. Other two-layer simulations have had shorter eddy shedding **periods**, but were less suitable for merging with the one-layer results.
- The transport through the Yucatan Straits was held constant in both magnitude and profile throughout all the simulations. The only possible source for a detailed long-term time series of currents through the Straits would be a numerical model of the entire North Atlantic forced by observed winds. The effects of variations in flow through the Yucatan Straits on Gulf circulation are not known; if they are indeed important, then a time series of this kind would be very useful for future models of the Gulf.
- A better simulation of shelf circulation could almost certainly be obtained by using a model designed specifically for that purpose.
- The validity of blending two simulations at all is open to question.

The most important model-related question for future field measurement programs is the nature and the degree of interaction between on- and off-shelf circulation. It might be that such a program would demonstrate that on- and off-shelf circulation can indeed be treated separately without significantly degrading simulation skill. At the very least it would quantify the **kinds** of interactions a model, or suite of models, must have to produce better simulations.

It is probably not possible to produce long-term simulations of the deep water circulation in any section of Gulf of Mexico without modeling the entire Gulf at a horizontal resolution of at least 25 km. Too little is known about the interactions between on- and off-shelf circulation to be confident that simulations that decouple these regimes can, even in principle, capture all the important variations in the current field. Therefore, the ideal long-term simulation in the Gulf would come from a model of the entire Gulf of Mexico or perhaps a system of tightly coupled models of the Gulf that demonstrated simulation skill in both the deep **water** and on the shelf. The problem with this approach is that the vertical scales and, to a lesser extent, the horizontal scales

required to model on- and off-shelf processes are entirely different. It is extremely difficult to include both sets of scales and the transition between them in one model at the same time. There are no models that have demonstrated the ability to do this successfully in any comparable oceanic region and there are only a few model designs that might, theoretically, be able to do so given sufficient resources.

On the horizon, there is an alternative to simulations of any kind. In the atmosphere the best source of wind fields **are** the prediction centers that produce atmospheric forecasts every day. Any **long-term** forecast sequences will provide better statistics than a long-term numerical simulation of the atmosphere. Similarly a **long-term** sequence of ocean forecasts would be superior to any simulation of the Gulf. The routine forecasting of ocean currents on the scales necessary for good statistics in the Gulf of Mexico should be a reality by 1994. These forecasts will immediately provide a valuable source of verification data for numerical simulations and will entirely supplant the need for simulations within 10 years of their introduction.

VI. REFERENCES

- Bleck, R., C. Rooth, and D.B. Boudra, "Wind-Driven **Spinup** in Eddy-Resolving Ocean Models Formulated in Isopycnic and Isobaric Coordinates," Rosenstiel School of Marine and Atmos. Sc., University of Miami, FL, 1983.
- Book, D.L., J.P. Boris, and S.T. **Zalesak**, "Flux-Corrected Transport" in D.L. Book (ed), Finite Difference Techniques for **Vectorized** Fluid Dynamics Calculations, Springer-Verlag, 1981.
- Cooper, C. and J.D. Thompson, Hurricane-Generated Currents on the Outer Continental Shelf 1 - Model Formulation and Verification, J. Geophys. Res. Vol. 94, pp.12513-12539, 1989.
- Hurlburt, H.E. and J.D. Thompson, A Numerical Study of Loop **Current** Intrusions and Eddy Shedding, J. Phys. Oceanogr. Vol. 10, pp.1611-1651, 1980.
- JAYCOR, Gulf of Mexico Circulation Modeling Study, JAYCOR Proposal Number 8206-83 to Minerals Management Service, **1983**.
- Leipper, D.F., A Sequence of Current Patterns in the Gulf of Mexico, J. Geophys. Res. 75, pp.637-657, 1970.
- O'Brien**, J.J., A Two-Dimensional Model of the Wind-Driven North Pacific, Investigation Pesguera, 35, pp.331-349, 1971.
- Rhodes, R.C., J.D. Thompson, and A.J. **Wallcraft**, Navy **Corrected** Geostrophic Wind Set for the Gulf of Mexico, NORDA Tech. Note 310, 1986.
- Rhodes, R.C., J.D. Thompson, and A.J. Wallcraft, Buoy-Calibrated Winds over the Gulf of Mexico, J. Atmos. and Oceanic Tech., Vol. 6, pp.608-623, 1989
- Robinson, M.K., Atlas of Monthly Mean Sea Surface and Subsurface Temperature and Depth of the Top of the Thermocline - Gulf of Mexico and Caribbean Sea, Scripps Institute of Oceanography, Reference No. 73-8, 1973.
- Samuels, W.B., N.E. Huang, and D.E. Amstutz, An **Oilspill** Trajectory Analysis Model with a Variable Wind Deflection Angle, Ocean Engineering Vol. 9, pp.347-360, **1982**.
- Science Applications International Corporation, Gulf of Mexico Physical Oceanography Program Final Report: Years 1 and 2, Volume II - Technical Report, OCS **Report/MMS**, U.S. Department of the Interior, Minerals Management Service, Gulf of Mexico OCS Regional Office, New Orleans, LA, 1986.
- Thompson, J.D., The Coastal Upwelling Cycle on a Beta-Plane Hydrodynamics and Thermodynamics, **CUEA** Technical Report No. 22, Florida State University, 1974.
- Vukovitch, F.M. and G.A. Maul, Cyclonic Eddies in the Eastern Gulf of Mexico, J. Phys. Oceanogr., 1984.
- Wallcraft, A.J., Gulf of Mexico Circulation Modeling **Study**, Year 1, Progress Report by JAYCOR for the Minerals Management Service, Gulf of Mexico **OCS** Region, New Orleans, LA, Contract No. **14-12-0001-30073**, 1984.
- Wallcraft, A.J., Gulf of Mexico Circulation Modeling Study, Year 1, Progress Report by JAYCOR for the Minerals Management Service, Gulf of Mexico OCS Region, New Orleans, LA, Contract No. **14-12-0001-30073**, 1986.

As the Nation's principal conservation agency, the Department of the Interior has responsibility for most of our nationally owned public lands and natural resources. The includes fostering the wisest use of our land and water resources, protecting our fish and wildlife, preserving the environmental and cultural-values of our national parks and historical places, and providing for the enjoyment of life through outdoor recreation. The Department assesses our energy and mineral resources and works to assure that their development is in the best interest of all our people. The Department also has a major responsibility for American Indian reservation communities and for people who live in Island Territories under U.S. Administration.

